EVOLUTION OF POSTEMBRYONIC DEVELOPMENT

EDITED BY: Nico Posnien, Patrícia Beldade and Fernando Casares
PUBLISHED IN: Frontiers in Ecology and Evolution and
Frontiers in Cell and Developmental Biology

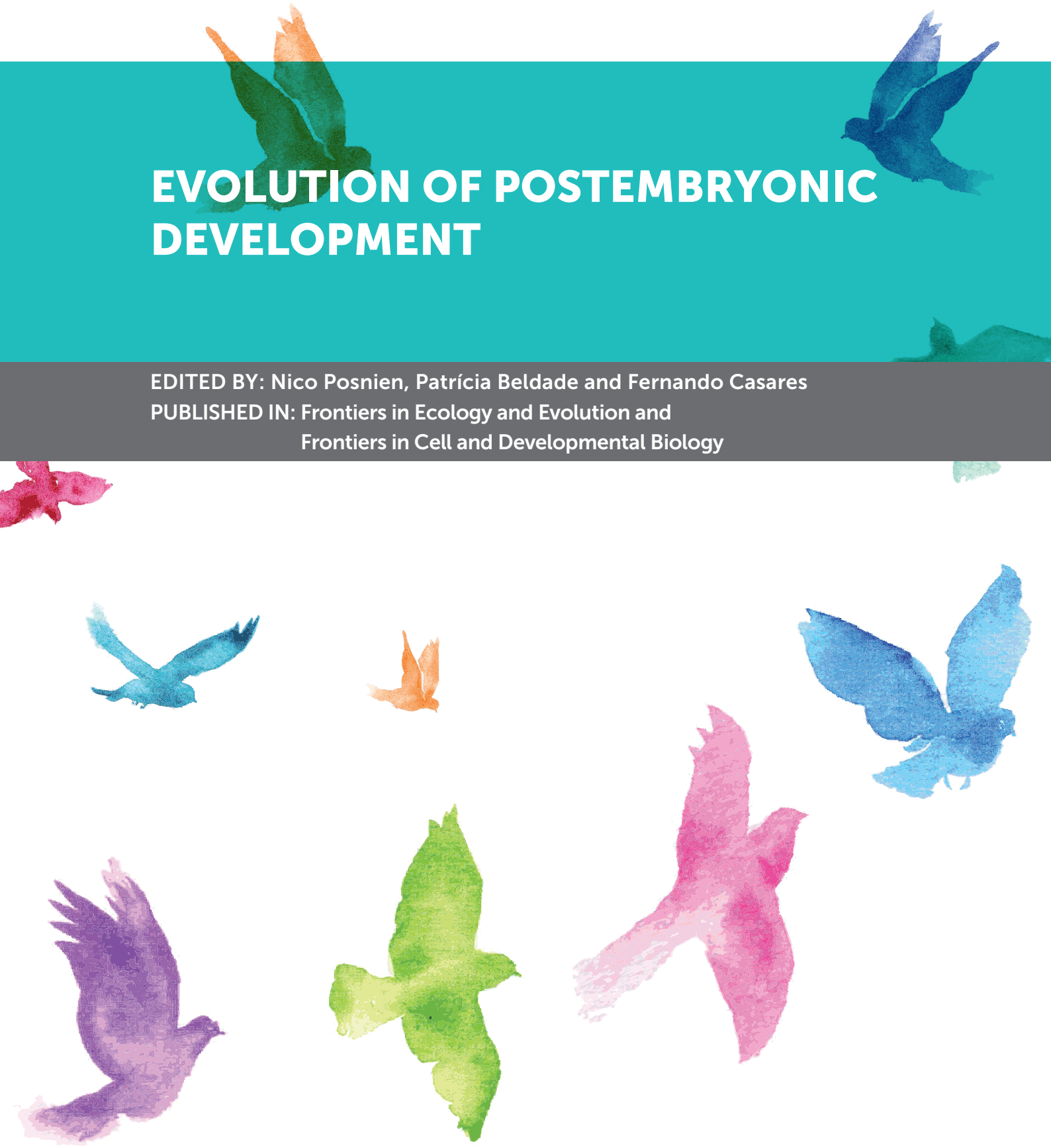

frontiers Research Topics

frontiers

ISSN 1664-8714
ISBN 978-2-88974-480-0
DOI 10.3389/978-2-88974-480-0

About Frontiers

Frontiers is more than just an open-access publisher of scholarly articles: it is a pioneering approach to the world of academia, radically improving the way scholarly research is managed. The grand vision of Frontiers is a world where all people have an equal opportunity to seek, share and generate knowledge. Frontiers provides immediate and permanent online open access to all its publications, but this alone is not enough to realize our grand goals.

Frontiers Journal Series

The Frontiers Journal Series is a multi-tier and interdisciplinary set of open-access, online journals, promising a paradigm shift from the current review, selection and dissemination processes in academic publishing. All Frontiers journals are driven by researchers for researchers; therefore, they constitute a service to the scholarly community. At the same time, the Frontiers Journal Series operates on a revolutionary invention, the tiered publishing system, initially addressing specific communities of scholars, and gradually climbing up to broader public understanding, thus serving the interests of the lay society, too.

Dedication to Quality

Each Frontiers article is a landmark of the highest quality, thanks to genuinely collaborative interactions between authors and review editors, who include some of the world's best academicians. Research must be certified by peers before entering a stream of knowledge that may eventually reach the public - and shape society; therefore, Frontiers only applies the most rigorous and unbiased reviews.
Frontiers revolutionizes research publishing by freely delivering the most outstanding research, evaluated with no bias from both the academic and social point of view. By applying the most advanced information technologies, Frontiers is catapulting scholarly publishing into a new generation.

What are Frontiers Research Topics?

Frontiers Research Topics are very popular trademarks of the Frontiers Journals Series: they are collections of at least ten articles, all centered on a particular subject. With their unique mix of varied contributions from Original Research to Review Articles, Frontiers Research Topics unify the most influential researchers, the latest key findings and historical advances in a hot research area! Find out more on how to host your own Frontiers Research Topic or contribute to one as an author by contacting the Frontiers Editorial Office: frontiersin.org/about/contact

EVOLUTION OF POSTEMBRYONIC DEVELOPMENT

Topic Editors:
Nico Posnien, University of Göttingen, Germany
Patrícia Beldade, University of Lisbon, Portugal
Fernando Casares, Andalusian Center for Development Biology, Spanish National Research Council (CSIC), Spain

Citation: Posnien, N., Beldade, P., Casares, F., eds. (2022). Evolution of Postembryonic Development. Lausanne: Frontiers Media SA.
doi: 10.3389/978-2-88974-480-0

Table of Contents

frontiers in Ecology and Evolution

EDITORIAL
published: 24 February 2022
doi: 10.3389/fevo.2022.859670

Editorial: Evolution of Postembryonic Development

Nico Posnien[1]*, *Patrícia Beldade*[2] *and Fernando Casares*[3]

[1] *Department of Developmental Biology, Göttingen Center for Molecular Biosciences (GZMB), Johann-Friedrich-Blumenbach-Institute of Zoology and Anthropology, University Göttingen, Göttingen, Germany,* [2] *Faculty of Sciences, Centre for Ecology, Evolution, and Environmental Changes, University of Lisbon, Lisbon, Portugal,* [3] *Andalusian Center for Development Biology (CABD), Spanish National Research Council (CSIC), Universidad Pablo de Olavide, Seville, Spain*

Keywords: evolution and development, postembryonic development, comparative genomics and transcriptomics, geometric morphometrics, genetics, metamorphosis, hormonal control

Editorial on the Research Topic

Evolution of Postembryonic Development

INTRODUCTION

Adult traits, such as morphology, physiology and behavior are defined during embryonic and postembryonic development, and the diversification of such traits is a result of changes in developmental programs. In organisms with direct development, selection on adult traits will result in changes in genes and processes involved in embryonic development. In contrast, in organisms that undergo metamorphosis (e.g., holometabolous insects) or grow throughout their entire life (e.g., crustaceans), variation in adult traits can result from changes in different life stages. Investigating the proximal and ultimate mechanisms shaping postembryonic development is an exciting endeavor that has been boosted by a series of technological advances. For example, recent advances in sequencing (e.g., transcriptomics, genomics) and genetic engineering (e.g., CRISPR/Cas9, RNAi) technologies allow going beyond well-established model organisms to enhance our understanding of how biological diversity is generated. Major innovations in imaging technologies and mathematical frameworks (e.g., Geometric Morphometrics) to describe complex morphological features further enable researchers to study postembryonic developmental processes on a mechanistic and quantitative level.

This Research Topic on "*Evolution of Postembryonic Development*" contributes primary data articles, perspectives and reviews, which collectively highlight the technical and conceptional challenges and opportunities in studying developmental process beyond embryonic stages. All contributions focus on the impact of variation in postembryonic development on variation in adult traits at evolutionary and individual scales (i.e., plasticity).

MANY DEVELOPMENTAL PROCESSES CAN ONLY BE STUDIED IN POSTEMBRYONIC STAGES

Many developmental processes are restricted to postembryonic stages and thus require the analysis of later stages of an organism's life history. For instance, Beer and Helfrich-Förster present novel insights into the development of the circadian clock. They document a temporal shift in the formation of the cell types responsible for circadian behaviors which are already present and fully functional in newly eclosed non-social (i.e., solitary) bees, but only develop during adult stages in a social bee. Similarly, parts of the nervous system and muscles develop during

OPEN ACCESS

Edited and reviewed by:
Mark A. Elgar,
The University of Melbourne, Australia

***Correspondence:**
Nico Posnien
nposnie@gwdg.de

Specialty section:
This article was submitted to Evolutionary Developmental Biology, a section of the journal Frontiers in Ecology and Evolution

Received: *24 January 2022*
Accepted: *03 February 2022*
Published: *24 February 2022*

Citation:
Posnien N, Beldade P and Casares F (2022) Editorial: Evolution of Postembryonic Development. Front. Ecol. Evol. 10:859670. doi: 10.3389/fevo.2022.859670

larval stages in ribbon worms (Nemertea), a small phylum of worm-shaped, mostly marine Lophotrochozoans. von Döhren presents comparative data on larval nervous system and muscle development in these worms. While the postembryonic development of the FMRFamide-like nervous system seems to be conserved among the studied species, the author observed highly variable development of the body wall musculature. Also, the beautiful color patterns and eye spots of butterfly and moth wings are the result of postembryonic developmental processes. Tendolkar et al. generated CRISPR/Cas9 mediated somatic *Ultrabithorax* knock-out clones in three species to study the impact of loss of function of this Hox gene on adult fore- and hindwing morphology. The data confirmed a role of Ultrabithorax in defining hindwing identity and effects on various aspects of wing morphology, such as scale derivatives, color patterns, eyespots, and wing structure. The authors conclude that Ultrabithorax has pleiotropic functions during postembryonic wing development, compatible with a micromanaging role of this Hox gene.

PLASTICITY OF POSTEMBRYONIC DEVELOPMENT

Developmental processes are affected by environmental cues resulting in plastic responses. Reis et al. applied geometric morphometrics to study plasticity in wing shape, as well as size and shape relationships in three Diptera species. The size and shape of fly wings is defined during postembryonic development in wing imaginal discs. Controlled variation in rearing temperature and larval density resulted in conserved and species-specific changes in wing size and shape, which is discussed in the context of different mating behaviors of the three fly species. May et al. demonstrate in *Drosophila melanogaster* that the larval diet has a major impact on adult gene expression. Intriguingly, different larval food compositions affected males and females differently. While genes affected by larval diet are related to reproduction processes in females, gene expression in males is related to nutrient sensing and metabolic processes. The authors raise the important question about whether and how these gene expression differences relate to the fitness of young adults.

METAMORPHOSIS AND SEXUAL MATURATION ARE POSTEMBRYONIC PROCESSES IN INSECTS

Metamorphosis and sexual maturation are key postembryonic processes in insects. Gegner et al. revealed extensive modulation of gene expression during metamorphosis in the tobacco hornworm *Manduca sexta*. They show that about half of the genes in the genome are differentially expressed between late larval and adult stages. Intriguingly, part of this transcriptomic remodeling is associated with epigenetic methylation marks that may have an impact on chromatin architecture through histone modification mechanisms. Various hormones and receptors regulate postembryonic molts and the onset of metamorphosis. Korb et al. studied the effect of juvenile hormone induction on postembryonic molts in termites and linked morphological variants to effects on juvenile hormone related gene expression. Their data confirms a previously suggested model proposing that juvenile hormone levels between postembryonic molts contribute to morphological diversity in termites. Taubenheim et al. provide a comprehensive review of the function and evolution of nuclear receptors, such as steroid receptors and thyroid receptors in vertebrates and ecdysone receptors in insects, which coordinate key postembryonic developmental transitions. The authors argue that future research should focus on how nuclear receptors integrate intrinsic and extrinsic environmental cues to control developmental transitions and they suggest that a broad taxonomic sampling with a special emphasis on early branching bilaterians and cnidarians is a promising route.

CHALLENGES OF CURRENT VIEWS AND FUTURE DIRECTIONS

In their Mini Review, Fusco and Minelli summarize findings from the fossil record, comparative morphology of extant taxa and gene expression studies in the context of segment addition after embryonic stages are completed (i.e., anamorphosis). Based on these data, they conclude that in many cases a clear distinction between embryonic and postembryonic stages is not as straightforward as previously thought. To understand the evolution of skeletal development and to reveal developmental modularity, ossification sequences are extensively studied in vertebrates. Rose discusses potential caveats of using these methods in amphibians and he calls for more integrative approaches that also include physiology and behavioral insights. White et al. summarize the current knowledge about sutures, fibrous joints that separate the cranial bones in mammals. These sutures play important roles during skull development, and they are also important for the function of skull bones, such as joint mobility during feeding. The authors argue that a thorough understanding of the evolution of adult skull morphology in mammals must integrate data on the development and function of sutures.

CONCLUSIONS

The articles collected in this Research Topic highlight the importance of postembryonic developmental processes for a comprehensive understanding of the evolution of development and the mechanisms underlying phenotypic diversity present in nature. The breadth of methods applied range from thorough morphological descriptions to the integration of next generation sequencing data and therefore provide an excellent roadmap for future studies. It will be exciting to expand the interdisciplinary experimental toolkit to apply it to as many organisms as possible to reveal common and diverse aspects of postembryonic development.

AUTHOR CONTRIBUTIONS

All authors co-edited the Research Topic and contributed to the article. The submitted version of this editorial is approved by all authors.

ACKNOWLEDGMENTS

We want to thank all authors who contributed their exciting data, thoughts, and ideas to this Research Topic. Thanks go to the Frontiers Editorial team that has been helpful throughout the process. Finally, special thanks to the external peer reviewers who invested considerable time to provide constructive feedback on the manuscripts in this issue.

Conflict of Interest: The authors declare that the research was conducted in the absence of any commercial or financial relationships that could be construed as a potential conflict of interest.

frontiers in Cell and Developmental Biology

ORIGINAL RESEARCH
published: 12 November 2020
doi: 10.3389/fcell.2020.581323

Post-embryonic Development of the Circadian Clock Seems to Correlate With Social Life Style in Bees

Katharina Beer and Charlotte Helfrich-Förster*

Department of Neurobiology and Genetics, Biocenter, University of Würzburg, Würzburg, Germany

Social life style can influence many aspects of an animal's daily life, but it has not yet been clarified, whether development of the circadian clock in social and solitary living bees differs. In a comparative study, with the social honey bee, *Apis mellifera*, and the solitary mason bee, *Osmia bicornis*, we now found indications for a differentially timed clock development in social and solitary bees. Newly emerged solitary bees showed rhythmic locomotion right away and the number of neurons in the brain that produce the clock component pigment-dispersing factor (PDF) did not change during aging of the adult solitary bee. Honey bees on the other hand, showed no circadian locomotion directly after emergence and the neuronal clock network continued to grow after emergence. Social bees appear to emerge at an early developmental stage at which the circadian clock is still immature, but bees are already able to fulfill in-hive tasks.

Keywords: social, honey bee, solitary bee, circadian clock, activity rhythm, neuronal network, development

OPEN ACCESS

Edited by:
Patrícia Beldade, University of Lisbon, Portugal

Reviewed by:
Mirko Pegoraro, Liverpool John Moores University, United Kingdom
Mathias Francois Wernet, Freie Universität Berlin, Germany

****Correspondence:***
Katharina Beer
Katharina.beer@uni-wuerzburg.de

Specialty section:
This article was submitted to Evolutionary Developmental Biology, a section of the journal Frontiers in Cell and Developmental Biology

Received: *08 July 2020*
Accepted: *21 October 2020*
Published: *12 November 2020*

Citation:
Beer K and Helfrich-Förster C (2020) Post-embryonic Development of the Circadian Clock Seems to Correlate With Social Life Style in Bees. Front. Cell Dev. Biol. 8:581323. doi: 10.3389/fcell.2020.581323

INTRODUCTION

Social interactions are known to influence behavioral rhythms in different animals (Sharma et al., 2004; Favreau et al., 2009; Eban-Rothschild and Bloch, 2012). Nevertheless, it is largely unexplored how social life style shapes the circadian system of animals.

The European honey bee, *Apis mellifera*, is an important model organism to study the impact of sociality on the circadian clock (Bloch, 2010; Eban-Rothschild and Bloch, 2012; Beer and Bloch, 2020). The honey bee displays the highest form of sociality known in insects, called eusociality. It is defined by (1) cooperative brood care (2) overlapping generations in one colony, and (3) reproductive division of labor with several sterile workers and one or a few fecund colony members (Winston, 1987; Michener, 2000). Honey bee colonies usually consist of one queen that reproduces with the male bees (drones) and several thousand worker bees, which take care of the colony. They do this in an age dependent manner, meaning that younger bees take care of the brood and older bees perform tasks like attending the queen, nest building and guarding (Free, 1965; Seeley, 1982; Robinson et al., 1989, 2005). The last stage in their life is becoming a forager bee.

The circadian clock plays an essential role for honey bee survival: forager bees show daily rhythms in flight times and a remarkable time memory, allowing them to synchronize with the most rewarding flowering times of the day (Kleber, 1935; Moore, 2001). Furthermore, the bees need their circadian clock for sun compass orientation (Lindauer, 1960).

The molecular basis of the circadian clock consists of transcriptional/translational feedback loops in the brain that drive circadian rhythms in behavior and physiology (Dunlap, 1999; Bloch, 2010). One of the major neuropeptides that controls rhythmic behavior in insects is pigment-dispersing factor (PDF) (Shafer and Yao, 2014; Beer et al., 2018). The neurons expressing PDF are part of the honey bee clock and build a complex network that connects the clock with brain centers

controlling locomotion, complex behaviors and the endocrine system (Fuchikawa et al., 2017; Beer et al., 2018).

As in other animals, the circadian clock of the honey bee "free-runs" with an endogenous period of circa 24 h in the absence of environmental time cues (Zeitgebers) (Edery, 2000). It is synchronized to the 24-h day by environmental light and temperature cycles and by social cues from the colony (Frisch and Koeniger, 1994). Social cues can even dominate the other Zeitgebers, demonstrating the profound impact of social life style on the honey bee's circadian clock (Beer et al., 2016; Fuchikawa et al., 2016). Social cues from the colony are furthermore beneficial for clock development in individual bees (Eban-Rothschild et al., 2012; Beer et al., 2016). Young bees that perform nursing tasks are arrhythmic and active around the clock, a behavior, which is believed to support rapid colony development (Moore et al., 1998; Bloch and Robinson, 2001; Bloch et al., 2013). Signals from the colony appear to help these nurse bees to mature and become rhythmic foragers: young bees kept isolated from the colony take longer to develop behavioral circadian rhythms than bees that have been in social contact (Eban-Rothschild et al., 2012; Beer et al., 2016). Most importantly, the circadian clock and the honey bee's behavior is highly plastic and strongly influenced by social cues, because foraging bees can revert to nursing without rhythms and young bees can start foraging prematurely with daily activity rhythms (Bloch and Robinson, 2001). All this depends on the needs of the colony.

In contrast to the honey bee, most other bee species pursue a solitary life style (Michener, 2000). The red mason bee, *Osmia bicornis*, is a generalist pollinator native to Europe, which lately has received increasing attention as a highly promising species for pollination services (Garibaldi et al., 2013; Sedivy and Dorn, 2014). As solitary bees, they do not show reproductive labor division and the young bees are not born in the safety of a bee hive, but emerge in spring from small nests, in which they overwintered in diapause (Raw, 1972). They have to cope with daily environmental changes right after emergence, which requires a fully matured circadian system. In our study, we hypothesized that the honey bee takes advantage of the social colony environment and emerges with an immature circadian clock compared to the clock system of the solitary bee. If this were to be the case, we expected that:

(I) Solitary bees display circadian behavior right after emergence, but honey bees do not.
(II) The clock network in the brain of honey bees shows continued maturation after the bee's emergence in contrast to the clock network in solitary bees.

MATERIALS AND METHODS

Honey bees: Honey bee colonies, species *A. mellifera*, subspecies *carnica*, were kept at the University of Würzburg, Department of Animal Ecology and Tropical Biology. Queens were inseminated by multiple drones. Standard beekeeping methods were applied with bees kept in field colonies consisting of approximately 35,000–40,000 bees.

Solitary bees: Cocoons of solitary bees, species *O. bicornis*, were purchased at a commercial beekeeper (WAB-Mauerbienenzucht, Konstanz) in autumn (2014, 2015, and 2016) and stored at 4°C and 60% temperature and humidity (RH) until the start of the experiments in the following spring.

We tested our hypothesis of an immature circadian system in the honey bee via a behavioral assay of monitoring locomotion after emergence of the social honey bees and the solitary mason bees. Furthermore, insect brain tissues of different developmental stages in the bees were stained via immunofluorescence to visualize the development of the clock neuronal network.

Circadian Rhythm Onset in Bee Behavior

In a set of behavior experiments, we assessed if the ontogeny of circadian rhythms in activity during post-emergence development of *O. bicornis* differs from the one in *A. mellifera*.

Monitoring Locomotion

Brood combs of *A. mellifera* colonies were kept overnight in a climate chamber [constant darkness (DD), 20°C, 60% RH, DD] and newly emerged female worker honey bees were collected for the behavioral experiments under dim red light. We introduced newly emerged bees into an infrared (IR)-beam based activity monitoring system (LAM-system, TriKinetics Inc., Waltham, MA United States) and monitored their locomotion under constant conditions (DD and RH; for details see **Table 1**). In an additional treatment, we monitored locomotion of newly emerged honey bees that were separated by a double mesh wire from a miniature bee colony next to the monitoring system. The miniature colony consisted of a brood comb (open and closed brood) with approximately 1,000 bees (hive bees and foragers) on it. Queen pheromone (Bee Boost with queen mandibular pheromone) substituted a real queen to reduce stress caused by removing the bees from the hive and their queen. We added this treatment, because the social contact to the colony increases survival of the honey bees in the set up (Beer et al., 2016). In three further trials, we introduced cocoons of *O. bicornis* into the monitoring tubes and monitored their locomotion after their emergence under constant environmental conditions (DD and RH; see **Table 1**). We monitored bee activity for as long as they lived in the set up, which was 3–45 days. We performed our experiments at temperatures, which young honey bees and solitary bees may experience in nature (Fahrenholz et al., 1989; Strohm et al., 2002). We decided to submit the honey bees to 30°C, which is a bit lower than the core hive temperature, because there were also forager bees in the miniature colony present that are typically not found in the hive center (Seeley, 1982; Klein et al., 2014). *O. bicornis* bees seem to favor temperatures of 20°C (or above) for emergence (Beer et al., 2019). Therefore, we performed the solitary bee experiments at approximately 20 and 25°C. We chose two different temperatures, because the mason bee is submitted to stronger temperature fluctuations than the honey bee in the thermoregulated hive, but we avoided extreme temperature conditions. The bees (honey bees and solitary bees) have never been exposed to light or oscillating temperature.

TABLE 1 | Rhythms in locomotor activity of newly emerged individuals of social (*A. mellifera*) and solitary (*O. bicornis*) bees.

	Apis 1	***Apis 2***	***Osmia 1***	***Osmia 2***	***Osmia 3***
Environmental conditions	30°C, 60% RH	30°C, 60% RH	20°C, 60% RH	19.2°C, 60% RH	25°C, 45% RH
N (male)	–	–	8	10	13
Rhythmic males	–	–	8	8	12
Percent of rhythmic males	–	–	100%	80%	92%
N (female)	15	25	9	40	7
Rhythmic females	0	0	9	26	7
Percent of rhythmic females	0%	0%	100%	65%	100%
Percent of rhythmic individuals	0%	0%	100%	68%	95%
p-value	<0.001	<0.001	<0.001	<0.05	<0.001

Environmental conditions, sample size, and absolute number as well as percentage of rhythmic individuals of five different experiments (Apis 1 and 2 with A. mellifera and Osmia 1–3 with O. bicornis). We monitored the activity of bees in experiments Apis 1 and Osmia 1–3 individually without any contact to other bees. In experiment Apis 2 locomotor activity of individual bees was monitored, which had social contact to a mini honey bee colony. In experiment Osmia 3 monitor tubes with two different diameters (16 and 25 mm) were used. There are significantly more arrhythmic individuals in the honey bee experiments and significantly more rhythmic individuals in the Osmia experiments (p-values and binomial test).

Data Analysis

The activity data was registered in counts (beam crosses) per minute in the TriKinetics system and evaluated with ActogramJ software plugin for ImageJ (Schmid et al., 2011) (Fiji ImageJ Version 1.49, Wayne Rasband, National Institutes of Health, Bethesda, MD, United States). We evaluated rhythmicity in locomotion only for bees that showed activity for at least three consecutive days in the analysis. Circadian rhythmicity during the first 2 days after emergence of the bees was determined by eye (detection of a circadian pattern of activity in the actogram; e.g., re-occurring activity at more or less the same time for consecutive days), because available statistical tests for periodicity are often not precise enough when only a few days are evaluated (Refinetti et al., 2007). Statistical analysis was conducted in R (R version 3.2.2) using R stats package.

Immunocytochemistry in the Clock Network of Bees

Honey bees were sampled after they were raised by the colony. For this, we reintroduced newly emerged honey bees (overnight in an incubator at 35°C and 60% RH) into the colony after marking them with paint on the thorax and sampled the marked honey bees at specific ages. Solitary bees were submitted to daily cycles of fluctuating temperature and light conditions (12 h of 25°C and light and 12 h of 15°C and darkness) and kept all together until sampling in a big flight tent (size: 60 cm × 60 cm × 56 cm) that was equipped with sugar syrup (APIinvert®, Südzucker, Mannheim, Germany), pollen, and water *ad libitum* as well as tubes for providing hiding places and clay. We performed sampling in all groups of bees always at the same time of the day, which resembled the subjective morning (Zeitgeber time 0–1.5).

Staining Clock Neurons in Bee Brains

Bees were demobilized on ice, decapitated and a window was cut into the cuticle of the frontal head. Heads were then fixed in 4% PFA in PBST (0.1% Triton) for 3–4 h on a shaker. All washing and incubation steps were performed on a shaker at lowest speed setting. After washing the heads in PBS three times (10 min each), brains were dissected in PBS and washed again three times in PBS. Samples were stored in 100% methanol until all differently aged bees were sampled (step wise dehydration and rehydration in methanol/ PBS solution: 0, 30, 50, 70, 90, and 100%, each 10 min). We added an additional fixation step with Zamboni's fixative over night at 4°C to reduce the background staining in the whole mount brains. Brains were washed three times in PBS and incubated in sodium citrate buffer (10 mM, pH 8.5) at 80°C in an antigen retrieval step. Afterward we washed the brains 10 times in PBS, two times in PBST (0.5%), one time in PBST (2%) and one time in PBST (0.5%) and pre-incubated in 5% NGS-PBST (0.5%) at 4°C overnight. The brains were then incubated in 1:3,000 anti-β-Pigment Dispersing Hormone (PDH) antibody solution [in 5% NGS-PBST (0.5%)] and 0.02% NaN_3 for 6 days at 4°C and 1 day at RT. PDH antibody recognizes the PDF peptide in various insects, including hymenoptera (Bloch et al., 2003; Weiss et al., 2009; Fuchikawa et al., 2017; Beer et al., 2018; Kay et al., 2018). The brains were washed six times in PBST (0.5%), incubated in the secondary antibody solution [1:200 Alexa Flour 635 goat anti rabbit in 5% NGS-PBST (0.5%)] and then washed again [three times in PBST (0.5%) and three times in PBS], before we mounted them in mounting medium for fluorescence (Vectashield, Vector laboratories, Burlingame, CA, United States). We mounted the brains between two microscope cover glasses with spacers in mounting medium for fluorescence, which prevented the tissue from being crushed.

Data Analysis

Immunocytochemistry data was analyzed with a Leica TCS SPE confocal microscope (Leica microsystems, Wetzlar, Germany) equipped with 10×/0.30 CS ACS APO and 20×/0.60 IMM CORR ACS APO objectives. Brains were scanned sequentially in stacks (Leica Application Suite Advanced Fluorescence 2.7.3.9723, Leica Microsystems, Mannheim, Germany). Samples of one experiment were processed with the same settings and obtained confocal pictures (resolution 1024 × 1024) were further processed in Fiji ImageJ (Version 1.49, Wayne Rasband, National

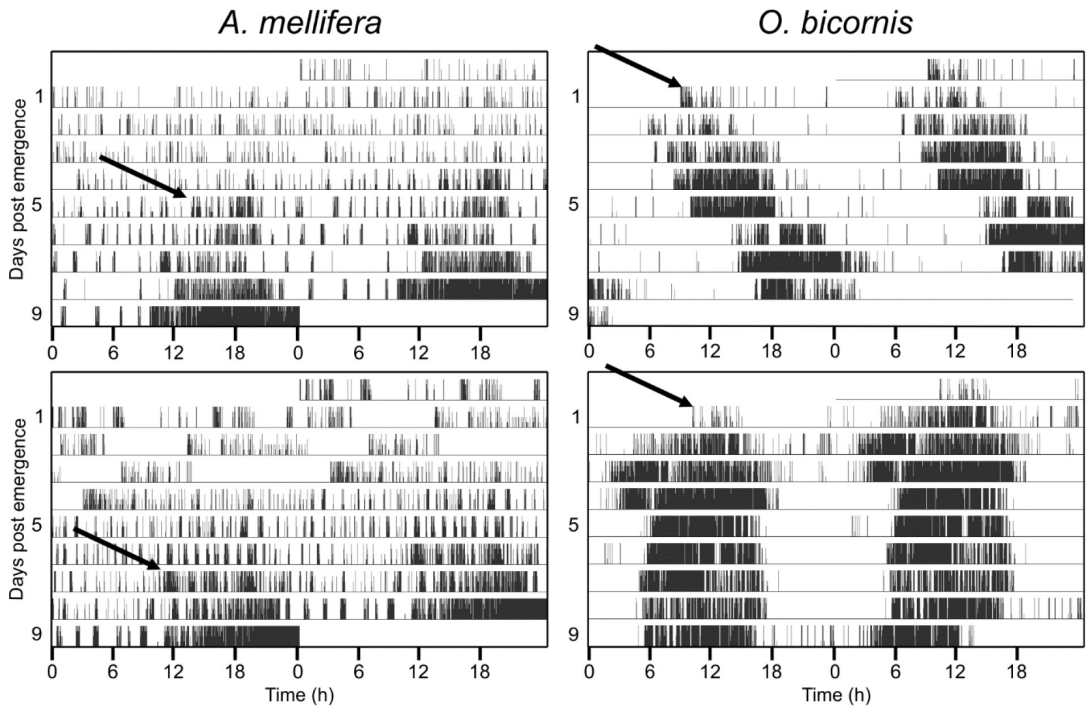

FIGURE 1 | Ontogeny of circadian activity rhythms in social (*A. mellifera*) and solitary (*O. bicornis*) bees. Four example actograms for the monitored activity in *A. mellifera* and *O. bicornis*. Actograms are double plotted, showing two consecutive days in a row, in order to better visualize the circadian pattern in activity rhythms. The honey bee *A. mellifera* never shows circadian activity during the first few days. In the example actograms, the honey bees start to exhibit circadian rhythmicity from the fifth day (upper panel) and seventh day (lower panel) onward (arrows). The solitary bees (*O. bicornis*) show circadian activity right after emergence from their cocoon (arrows in the right actograms).

Institutes of Health, Bethesda, MD, United States). Quantification of cell number was done by counting stained cells in both hemispheres and then averaging for the brain. Subsequently, brightness and contrast were adjusted in the figures displayed in the results section. Statistical analysis was conducted in R (R version 3.2.2) using R stats package.

RESULTS

Circadian Rhythms in Locomotion of Newly Emerged Bees

None of the honey bees in our experiments exhibited circadian rhythms during the first 2 days after their emergence (**Figure 1**). On the contrary, most of the solitary *Osmia* bees (mean for all experiments ± STE: 88% ± 0.1) showed circadian rhythmicity in their activity right after their emergence and this was the case under different temperature conditions and for both sexes (Exact binomial test and $p < 0.05$) (**Figure 1** and **Table 1**). The few individuals that did not show strong rhythmicity died only a few days after their emergence.

PDF Network Staining in Bees of Different Ages

The PDF-immunostaining of pre- and post-emerged bees of different ages showed that, in honey bees, the number of PDF neurons steadily increased with age (Kruskal Wallis rank sum test: 19.3, $df = 4$, $p < 0.01$; *post-hoc* test: pairwise comparison using Wilcoxon rank sum test) (**Figure 2**, left graph). In contrast, we could not detect such increment in *Osmia*, and the PDF cell number was approximately 14–15 neurons per hemisphere for all ages (**Figure 2**, right panels). Although we could see a slight increase in the PDF cell number from 2-day old mason bees to older mason bees (**Figure 2**, right graph) this turned out to be not significant (Kruskal Wallis rank sum test; *post-hoc* test: pairwise comparison using Wilcoxon rank sum test). Interestingly, in the two-day-old honey bee brains, the PDF cell bodies cluster closer together than it is the case in the older honey bees and *Osmia* of all ages (**Figure 2**, second row).

DISCUSSION

Our study indicates that the circadian clock system in newly emerged honey bees is immature at two levels: (I) behavioral output of the bee clock and (II) anatomy of the brain clock. While the neuronal honey bee clock network continues to grow moderately, but significantly after emergence (either due to continued cytogenesis or expression of PDF in more neurons in aged bees), the number of clock cells expressing PDF in solitary bees does not increase after the time point of emergence. This indicates that the circadian system of the solitary bees was mature

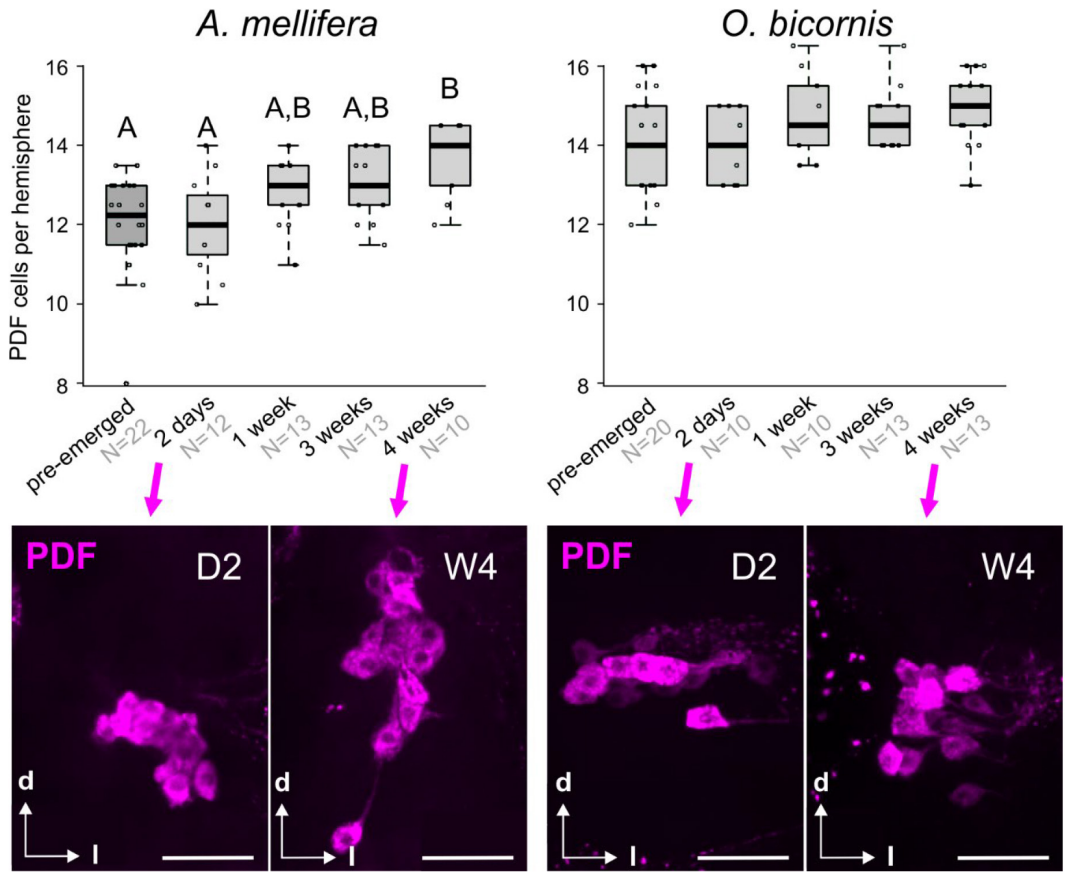

FIGURE 2 | Post-emergence development of the clock neuronal network in social bees (*A. mellifera*) and solitary bees (*O. bicornis*). Top row: The graphs display the number of PDF cells per brain hemisphere (boxplots with data points) in differently aged *A. mellifera* (left) and *O. bicornis* (right) bees. "Pre-emerged" means bees were sampled approximately 2–3 days before the bees would have emerged. In honey bees, pupal stages P7 and P9 are equivalents to pre-emerged *O. bicornis* bees, because these would have also emerged 2–3 days after sampling (the cell numbers of pre-emerged *A. mellifera* are calculated from a different unpublished experiment). Different letters indicate statistical difference in cell number. Sample sizes are indicated in light gray with the sample group. Second row: example pictures of PDF cell clusters (magenta) in *A. mellifera* (left) and *O. bicornis* (right) bees for the ages of 2 days (D2) and 4 weeks (W4). Scale bar: 50 μm.

at emergence, while that of the honey bees was immature. Our behavioral experiments confirm this assumption, because young solitary bees show rhythmic behavior right after emergence, while young honey bees remain behaviorally arrhythmic for some days.

Timing of Circadian Onset of Behavioral Rhythms Is Delayed in Adult Honey Bees

Several earlier studies suggested an important role of the social lifestyle of honey bees in circadian behavior and the normal development of the circadian system (Bloch and Robinson, 2001; Eban-Rothschild et al., 2012; Beer et al., 2016; Fuchikawa et al., 2016). Several studies discovered that the social environment plays an important role in the ontogenetic process of circadian behavior and bees kept in a colony environment during early adulthood could already exhibit circadian rhythms in locomotion at the age of 2 days (Eban-Rothschild et al., 2012; Beer et al., 2016; Fuchikawa et al., 2016). Recently, it has been shown that temperature plays a pivotal role in the ontogeny of circadian activity rhythms as well. Bees kept at 35°C, which corresponds to the core hive temperature, for the first 24 h of their life display rhythms already at the age of 1–2 days while the bees kept at typical laboratory temperatures of 25°C need a few days longer (Giannoni-Guzman, 2016; Nagari et al., 2017). This is not surprising, because the correct temperature is important for a normal brain development and affects behavioral performance in the adult bee (Tautz et al., 2003; Groh et al., 2004; Jones et al., 2005). The honey bee brain further matures during adulthood, which is indicated by an age-dependent plasticity in mushroom bodies (Farris et al., 2001; Groh and Meinertzhagen, 2010). In our experiments (performed at 30°C), all honeybees needed more than 2 days until they exhibited circadian rhythms in locomotion, with or without social contact to a mini-colony. This ontogeny of circadian rhythms is slightly later than reported in the above mentioned studies, that showed circadian ontogeny in young honeybees at the age of 2 days or earlier, when kept under social contact or hive temperature (Eban-Rothschild et al., 2012; Beer et al., 2016; Fuchikawa et al., 2016; Giannoni-Guzman, 2016; Nagari et al., 2017). Nevertheless, our results comply with other behavioral studies indicating that the circadian system is not

fully matured in newly emerged honey bees (Moore et al., 1998; Toma et al., 2000; Bloch et al., 2001; Eban-Rothschild et al., 2012; Beer et al., 2016; Giannoni-Guzman, 2016). Maturation speed in young honey bees thereby seems to depend on at least two factors: temperature and colony environment (possibly indirectly because of colony thermoregulation).

The solitary mason bee on the other hand shows circadian rhythms in locomotion right after emergence, which led us to the conclusion that the circadian system of this bee is fully matured at emergence. In contrast to the honey bee, temperature seemed to have no effect on the ontogeny of rhythmicity in solitary bees and most bees were rhythmic in both temperature treatments, which adds to our interpretation that development is largely finished at the time point of emergence of solitary bees compared to honey bees. Similarly, newly emerged fruit flies and tsetse flies, as examples of other holometabolic insects, also showed circadian behavior in locomotion (Brady, 1988; Sehgal et al., 1992).

PDF Neurons of the Honey Bee Clock Are Not Fully Developed at the Time of Emergence

We found that the number of neurons expressing PDF increased moderately but significantly after honey bee emergence, which supports our hypothesis of an immature circadian clock in newly emerged honey bees. Similarly, Bloch et al. (2003) reported that the number of clock protein PERIOD (PER) expressing cells in the brain of foragers is higher than in the brain of nurses (Bloch et al., 2003). In spite of the fact that the molecular circadian clock ticks already in nurses (Fuchikawa et al., 2017), this early clock appears immature. For example, *per* mRNA levels are higher in forager brains than in nurses and show circadian cycling only in foragers, while in nurse bee brains, per transcript levels are not rhythmically produced (Toma et al., 2000; Bloch et al., 2004). The lack of cycling or cycling with a diminished amplitude of clock gene transcripts in nurse bees was later proven to be task related and consistent with the lack of rhythmic behavior in nursing bees (Shemesh et al., 2007, 2010). The growing clock network during aging of the adult honey bee, as we have observed it in our study, may promote the integration of new functions into the circadian system. It may be that the growing network also gains complexity during aging. Our recent analysis of the PDF network in nurses and foragers demonstrated that peptide levels oscillated with slightly different phases in different regions of forager brains, while they were highly synchronous in the brains of nurse bees (Beer et al., 2018). This indicates a higher level of complexity in the transfer of time-related information to brain areas with different functions in forager bees, which may relate to the complex tasks of foragers outside the hive. Interestingly, the number of positively stained PDF cell bodies stayed always high throughout the day in forager bees and was highest at the end of the subjective night/beginning of the subjective day in nurse bees (Beer et al., 2018). Therefore, we chose the subjective morning for quantification of the cell number in the differently aged bees in the here presented study. It is not clear, if the difference in cycling of PDF levels in different brain areas depends on developmental stage or task, but the maturation of the circadian clock seems to correlate with the age dependent polyethism in the honey bee. Due to the time dependent PDF peptide levels in PDF neuron arborizations observed in our recent study (Beer et al., 2018), we limited our analysis to counting PDF cell bodies, which was more consistent throughout different ages/tasks of the honey bee (at least for day times with high expression levels). Future studies, under controlled laboratory conditions and in the social hive environment, may dissect, which components of the honey bee clock are subjected to age- or task-related plasticity. Furthermore, the temperature dependency of clock system maturation in adult bees may be investigated also on the neuroanatomical level in the future.

Emergence With an Immature Circadian Clock as Trait of Social Life Style in the Honey Bee

Sociality has evolved in multiple groups, such as mammals (e.g., mole rats), insects (e.g., some bees, some wasps and ants) or even microorganisms, because of evolutionary benefits from group hunting, development of resistance against disease or predators and increased reproductive success (Alexander, 1974; Crespi, 2001). In bees, eusociality (full sociality) was found only in few bee species (e.g., *Apis* and *Melipona* species), but social behavior has been found in several other bee species in different nuances (e.g., primitively social bumble bees or facultatively social sweat bees) (Shell and Rehan, 2018). In case of the honey bee, improved colony defense is one clear benefit of sociality, but also the vast amount of offspring production in a colony (Breed et al., 1990).

We propose in our research another adaptation that accelerates colony growth: a differentially timed development in social and solitary bees that results in the emergence of social bees with an immature circadian system. This may provide an evolutionary advantage on both colony and individual level. Even with an immature circadian system, honey bees can survive being under the protection of a social community and they can undertake in-hive tasks in the colony. A mismatch of activity to daytime is not relevant for avoiding predators or foraging success, because the young honey bee is provisioned by the older foragers. An immature circadian clock may be even beneficial to the young honey bee, which takes care of the brood day and night, because honey bees have so far shown a lack of ill effects caused by arrhythmic behavior, while other animals are strongly affected (Bloch et al., 2013).

As we expected, the number of PDF neurons does not change during aging of the solitary bee in our study. This fits, like the activity rhythms in young solitary bees, to our hypothesis of an already fully matured circadian system in the newly emerged solitary mason bee. Similarly, Withers and co-authors found that *A. mellifera* showed continued brain development during aging, while *Osmia lignaria* did not (Withers et al., 2008). Proportions of mushroom bodies compared to Kenyon cell bodies in newly emerged *Osmia* were just as high as in foraging honey bees. Furthermore, the proportions did not change during aging in *Osmia*, while this was the case in *Apis* (Withers et al., 2008). Our findings point to a shift of emergence to an earlier developmental stage of the circadian system in the social honey bee as compared

to the solitary bee. It is certainly true, that there are other differences in the life style of *A. mellifera* and *O. bicornis* and we want to state clearly that a causal association of sociality and difference in clock development cannot be drawn from our results. For example, *O. bicornis* is a univoltine species, but *A. mellifera* produces several generations per year (Raw, 1972). Nevertheless, sociality appears to be the most striking difference in life style of these bees and other adaptations may have co-evolved with the specific life style, like for example the almost continuous reproduction in honey bee colonies.

We limited our investigation of clock development in bees to one social and one solitary species out of technical reasons. Especially the clock in solitary bee species is so far extremely little investigated and future studies may show, whether our findings can be generalized to other social and solitary bees. There are a few studies on circadian plasticity in other social hymenoptera. In bumblebees, which display primitive sociality, circadian plasticity in activity and number of PDF expressing neurons has been associated with body size and task rather than age (Yerushalmi et al., 2006; Weiss et al., 2009). For ants, a similar dependency of circadian rhythms on task, like in the honey bee, has been postulated: forager ants display rhythmic behavior and cycling levels of clock gene transcripts, which was not the case in nurse ants (Ingram et al., 2009; Fujioka et al., 2017). In addition, age-dependent modulations of the circadian clock have been reported in ants. Ingram and coauthors (Ingram et al., 2009) determined an increased level of overall per transcript in old foragers of the harvester ant species *Pogonomyrmex occidentalis*, which is reminiscent of the situation found in *A. mellifera* (Toma et al., 2000; Bloch et al., 2004; Abreu et al., 2018). The modulation of circadian behavior via contact to other colony members seems to play a role in rhythmic behavior of ants as well, because young ants in contact with old ants showed only weak behavioral rhythms (Fujioka et al., 2019). Interestingly, the clocks of different mammals, including humans, showed progressed maturation after birth like the honey bee (Rivkees, 2003; Weinert, 2005). This raises the question, whether social life style (in particular the protection of the colony) is a prerequisite for evolution of emergence with an immature circadian system, or the other way around or these traits rather co-evolved in honey bees (and possibly other eusocial hymenoptera like ants). Further studies are needed to dissect the evolutionary background of maturation processes of the circadian system in different animals.

Summarized, our comparative study demonstrates a differentially timed clock development of the social honey bee and the solitary mason bee. While the circadian system of the mason bee seems completely matured at emergence, the honey bee clock shows continued maturation after emergence. The early emergence with an immature circadian system benefits the colony community of the social bee and this adaptation of the honey bee clock may have evolved along with this species' social life style.

DATA AVAILABILITY STATEMENT

The raw data supporting the conclusions of this article will be made available by the authors, without undue reservation.

AUTHOR CONTRIBUTIONS

KB collected and analyzed the data and wrote the manuscript. CH-F and KB conceived the project. CH-F contributed funding and revised the manuscript. Both authors contributed to the article and approved the submitted version.

FUNDING

This research was funded by the German Research Foundation CRC 1047 "Insect Timing" (project A1). KB was furthermore supported by a grant of the German Excellence Initiative to the Graduate School of Life Sciences, University of Würzburg and the SCIENTIA career development program of the University of Würzburg. This publication was supported by the Open Access Publication Fund of the University of Wuerzburg.

ACKNOWLEDGMENTS

We want to thank Alina Peteranderl and Damiano Zanini for technical assistance in the laboratory. We also want to thank Mariela Schenk for her advice on keeping solitary bees inside the laboratory and Heinrich Dircksen for providing the PDH antibody.

REFERENCES

Abreu, F. C. P., Freitas, F. C. P., and Simões, Z. L. P. (2018). Circadian clock genes are differentially modulated during the daily cycles and chronological age in the social honeybee (*Apis mellifera*). *Apidologie* 49, 71–83. doi: 10.1007/s13592-017-0558-7

Alexander, R. D. (1974). The evolution of social behavior. *Annu. Rev. Ecol. Syst.* 5, 325–383.

Beer, K., and Bloch, G. (2020). Circadian plasticity in honey bees. *Biochemist* 42, 22–26. doi: 10.1042/bio04202002

Beer, K., Kolbe, E., Kahana, N. B., Yayon, N., Weiss, R., Menegazzi, P., et al. (2018). Pigment-dispersing factor-expressing neurons convey circadian information in the honey bee brain. *Open Biol.* 8:170224. doi: 10.1098/rsob.170224

Beer, K., Schenk, M., Helfrich-Förster, C., and Holzschuh, A. (2019). The circadian clock uses different environmental time cues to synchronize emergence and locomotion of the solitary bee *Osmia bicornis*. *Sci. Rep.* 9:17748.

Beer, K., Steffan-Dewenter, I., Härtel, S., and Helfrich-Förster, C. (2016). A new device for monitoring individual activity rhythms of honey bees reveals critical effects of the social environment on behavior. *J. Compar. Physiol. A* 202, 555–565. doi: 10.1007/s00359-016-1103-2

Bloch, G. (2010). The social clock of the honeybee. *J. Biol. Rhyth.* 25, 307–317. doi: 10.1177/0748730410380149

Bloch, G., Barnes, B. M., Gerkema, M. P., and Helm, B. (2013). Animal activity around the clock with no overt circadian rhythms: patterns, mechanisms and adaptive value. *Proc. R. Soc. B Biol. Sci.* 280, 1–9.

Bloch, G., and Robinson, G. E. (2001). Chronobiology: reversal of honey bee behavioural rhythms. *Nat. Brief Commun.* 410:1048.

Bloch, G., Rubinstein, C. D., and Robinson, G. E. (2004). *period* expression in the honey bee brain is developmentally regulated and not affected by light, flight experience, or colony type. *Insect Biochem. Mol. Biol.* 34, 879–891. doi: 10.1016/j.ibmb.2004.05.004

Bloch, G., Solomon, S. M., Robinson, G. E., and Fahrbach, S. E. (2003). Patterns of PERIOD and pigment-dispersing hormone immunoreactivity in the brain of the European honeybee (*Apis mellifera*): age- and time-related plasticity. *J. Compar. Neurol.* 464, 269–284. doi: 10.1002/cne.10778

Bloch, G., Toma, D. P., and Robinson, G. E. (2001). Behavioral rhythmicity, age, division of labor and period expression in the honey bee brain. *J. Biol. Rhyth.* 16, 444–456. doi: 10.1177/074873001129002123

Brady, J. (1988). Circadian ontogeny in the tsetse fly: a permanent major phase change after the first feed. *J. Insect Physiol.* 34, 743–749. doi: 10.1016/0022-1910(88)90147-3

Breed, M. D., Abel, P., Bleuze, T. J., and Denton, S. E. (1990). Thievery, home ranges, and nestmate recognition in *Ectatomma ruidum*. *Oecologia* 84, 117–121. doi: 10.1007/bf00665604

Crespi, B. J. (2001). The evolution of social behavior in microorganisms. *Trends Ecol. Evol.* 16, 178–183. doi: 10.1016/s0169-5347(01)02115-2

Dunlap, J. C. (1999). Molecular bases for circadian clocks. *Cell* 96, 271–290. doi: 10.1016/s0092-8674(00)80566-8

Eban-Rothschild, A., and Bloch, G. (2012). Social influences on circadian rhythms and sleep in insects. *Adv. Genet.* 77, 1–32. doi: 10.1016/b978-0-12-387687-4.00001-5

Eban-Rothschild, A., Shemesh, Y., and Bloch, G. (2012). The colony environment, but not direct contact with conspecifics, influences the development of circadian rhythms in honey bees. *J. Biol. Rhyth.* 27, 217–225. doi: 10.1177/0748730412440851

Edery, I. (2000). Circadian rhythms in a nutshell. *Physiol. Genom.* 3, 59–74. doi: 10.1152/physiolgenomics.2000.3.2.59

Fahrenholz, L., Lamprecht, I., and Schricker, B. (1989). Thermal investigations of a honey bee colony: thermoregulation of the hive during summer and winter and heat production of members of different bee castes. *J. Comp. Physiol. B* 159, 551–560. doi: 10.1007/bf00694379

Farris, S. M., Robinson, G. E., and Fahrbach, S. E. (2001). Experience- and age-related outgrowth of intrinsic neurons in the mushroom bodies of the adult worker honeybee. *J. Neurosci.* 21, 6395–6404. doi: 10.1523/jneurosci.21-16-06395.2001

Favreau, A., Richard-Yris, M.-A., Bertin, A., Houdelier, C., and Lumineau, S. (2009). Social influences on circadian behavioural rhythms in vertebrates. *Anim. Behav.* 77, 983–989. doi: 10.1016/j.anbehav.2009.01.004

Free, J. B. (1965). The allocation of duties among worker honeybees. *Symp. Zool. Soc.* 14, 39–59.

Frisch, B., and Koeniger, N. (1994). Social synchronization of the activity rhythms of honeybees within a colony. *Behav. Ecol. Sociobiol.* 35, 91–98. doi: 10.1007/s002650050074

Fuchikawa, T., Beer, K., Linke-Winnebeck, C., Ben-David, R., Kotowoy, A., Tsang, V. W. K., et al. (2017). Neuronal circadian clock protein oscillations are similar in behaviourally rhythmic forager honeybees and in arrhythmic nurses. *Open Biol.* 7:170047. doi: 10.1098/rsob.170047

Fuchikawa, T., Eban-Rothschild, A., Nagari, M., Shemesh, Y., and Bloch, G. (2016). Potent social synchronization can override photic entrainment of circadian rhythms. *Nat. Commun.* 7:11662.

Fujioka, H., Abe, M. S., Fuchikawa, T., Tsuji, K., Shimada, M., and Okada, Y. (2017). Ant circadian activity associated with brood care type. *Biol. Lett.* 13:20160743. doi: 10.1098/rsbl.2016.0743

Fujioka, H., Abe, M. S., and Okada, Y. (2019). Ant activity-rest rhythms vary with age and interaction frequencies of workers. *Behav. Ecol. Sociobiol.* 73:30.

Garibaldi, L. A., Steffan-Dewenter, I., Winfree, R., Aizen, M. A., Bommarco, R., Cunningham, S. A., et al. (2013). Wild pollinators enhance fruit set of crops regardless of honey bee abundance. *Sci. Rep.* 339, 1608–1611. doi: 10.1126/science.1230200

Giannoni-Guzman, M. A. (2016). *Individual Differences in Circadian and Behavioral Rhythms of Honey Bee Workers (Apis mellifera L.)*. Ph. D thesis, University of Puerto Rico, San Juan.

Groh, C., and Meinertzhagen, I. A. (2010). Brain plasticity in diptera and Hymenoptera. *Front. Biosci.* 2, 268–288. doi: 10.2741/s63

Groh, C., Tautz, J., and Rössler, W. (2004). Synaptic organization in the adult honey bee brain is influenced by brood-temperature control during pupal development. *Proc. Natl. Acad. Sci. U.S.A.* 101, 4268–4273. doi: 10.1073/pnas.0400773101

Ingram, K. K., Krummey, S., and LeRoux, M. (2009). Expression patterns of a circadian clock gene are associated with age-related polyethism in harvester ants, *Pogonomyrmex occidentalis*. *BMC Ecol.* 9:7. doi: 10.1186/1472-6785-9-7

Jones, J. C., Helliwell, P., Beekman, M., Maleszka, R., and Oldroyd, B. P. (2005). The effects of rearing temperature on developmental stability and learning and memory in the honey bee, *Apis mellifera*. *J. Compar. Physiol. A* 191, 1121–1129. doi: 10.1007/s00359-005-0035-z

Kay, J., Menegazzi, P., Mildner, S., Roces, F., and Helfrich-Förster, C. (2018). The circadian clock of the ant *Camponotus floridanus* is localized in dorsal and lateral neurons of the brain. *J. Biol. Rhyth.* 33, 255–271. doi: 10.1177/0748730418764738

Kleber, E. (1935). Hat das Zeitgedächtnis der bienen biologische bedeutung? *Zeitschr. Vergleichende Physiol.* 22, 221–262. doi: 10.1007/bf00586500

Klein, B. A., Stiegler, M., Klein, A., and Tautz, J. (2014). Mapping sleeping bees within their nest: spatial and temporal analysis of worker honey bee sleep. *PLoS One* 9:e102316. doi: 10.1371/journal.pone.0102316

Lindauer, M. (1960). Time-compensated sun orientation in bees. *Cold Spring Harb. Symp. Quant. Biol.* 25, 371–377. doi: 10.1101/sqb.1960.025.01.039

Michener, C. D. (2000). *The Bees of the World*. Baltimore, MD: The Johns Hopkins University Press.

Moore, D. (2001). Honey bee circadian clocks: behavioral control from individual workers to whole-colony rhythms. *J. Insect Physiol.* 47, 843–857. doi: 10.1016/s0022-1910(01)00057-9

Moore, D., Angel, J. E., Cheeseman, I. M., Fahrbach, S. E., and Robinson, G. E. (1998). Timekeeping in the honey bee colony: integration of circadian rhythms and division of labor. *Behav. Ecol. Sociobiol.* 43, 147–160. doi: 10.1007/s002650050476

Nagari, M., Szyszka, P., Galizia, G., and Bloch, G. (2017). Task-related phasing of circadian rhythms in antennal responsiveness to odorants and pheromones in honeybees. *J. Biol. Rhyth.* 32, 593–608. doi: 10.1177/0748730417733573

Raw, A. (1972). The biology of the solitary bee *Osmia rufa* (L.) (Megachilidae). *Trans. R. Ent. Soc. Lond.* 124, 213–229. doi: 10.1111/j.1365-2311.1972.tb00364.x

Refinetti, R., Cornélissen, G., and Halberg, F. (2007). Procedures for numerical analysis of circadian rhythms. *Biol. Rhythm Res.* 38, 275–325. doi: 10.1080/09291010600903692

Rivkees, S. A. (2003). Developing circadian rhythmicity in infants. *Pediatrics* 112, 373–381. doi: 10.1542/peds.112.2.373

Robinson, G. E., Grozinger, C. M., and Whitfield, C. W. (2005). Sociogenomics: social life in molecular terms. *Nat. Rev. Genet.* 6, 257–270. doi: 10.1038/nrg1575

Robinson, G. E., Page, R. E. Jr., Strambi, C., and Strambi, A. (1989). Hormonal and genetic control of behavioral integration in honey bee colonies. *Science* 246, 109–111. doi: 10.1126/science.246.4926.109

Schmid, B., Helfrich-Forster, C., and Yoshii, T. (2011). A new ImageJ plug-in "ActogramJ" for chronobiological analyses. *J. Biol. Rhyth.* 26, 464–467. doi: 10.1177/0748730411414264

Sedivy, C., and Dorn, S. (2014). Towards a sustainable management of bees of the subgenus *Osmia* (Megachilidae; Osmia) as fruit tree pollinators. *Apidologie* 45, 88–105. doi: 10.1007/s13592-013-0231-8

Seeley, T. D. (1982). Adaptive significance of the age polyethism schedule in honeybee colonies. *Behav. Ecol. Sociobiol.* 11, 287–293. doi: 10.1007/bf00299306

Sehgal, A., Price, J., and Young, M. (1992). Ontogeny of a biological clock in *Drosophila melanogaster*. *Proc. Natl. Acad. Sci. U.S.A.* 89, 1423–1427. doi: 10.1073/pnas.89.4.1423

Shafer, O. T., and Yao, Z. (2014). Pigment-dispersing factor signaling and circadian rhythms in insect locomotor activity. *Curr. Opin. Insect Sci.* 1, 73–80. doi: 10.1016/j.cois.2014.05.002

Sharma, V., Lone, S., Goel, A., and Chandrashekaran, M. K. (2004). Circadian consequences of social organization in the ant species *Camponotus compressus*. *Naturwissenschaften* 91, 386–390.

Shell, W. A., and Rehan, S. M. (2018). Behavioral and genetic mechanisms of social evolution: insights from incipiently and facultatively social bees. *Apidologie* 49, 13–30.

Shemesh, Y., Cohen, M., and Bloch, G. (2007). Natural plasticity in circadian rhythms is mediated by reorganization in the molecular clockwork in honeybees. *FASEB J.* 21, 2304–2311. doi: 10.1096/fj.06-8032com

Shemesh, Y., Eban-Rothschild, A., Cohen, M., and Bloch, G. (2010). Molecular dynamics and social regulation of context-dependent plasticity in the circadian clockwork of the honey bee. *J. Neurosci.* 30, 12517–12525. doi: 10.1523/jneurosci.1490-10.2010

Strohm, E., Daniels, H., Warmers, C., and Stoll, C. (2002). Nest provisioning and a possible cost of reproduction in the megachilid bee *Osmia rufa* studied by a new observation method. *Ethol. Ecol. Evol.* 14, 255–268. doi: 10.1080/08927014.2002.9522744

Tautz, J., Maier, S., Groh, C., Rössler, W., and Brockmann, A. (2003). Behavioral performance in adult honey bees is influenced by the temperature experienced during their pupal development. *Proc. Natl. Acad. Sci. U.S.A.* 100, 7343–7347. doi: 10.1073/pnas.1232346100

Toma, D. P., Bloch, G., Moore, D., and Robinson, G. E. (2000). Changes in *period* mRNA levels in the brain and division of labor in honey bee colonies. *Proc. Natl. Acad. Sci. U.S.A.* 97, 6914–6919. doi: 10.1073/pnas.97.12.6914

Weinert, D. (2005). Ontogenetic development of the mammalian circadian system. *Chronobiol. Intern.* 22, 179–205. doi: 10.1081/cbi-200053473

Weiss, R., Dov, A., Fahrbach, S. E., and Bloch, G. (2009). Body size-related variation in pigment dispersing factor-immunoreactivity in the brain of the bumblebee *Bombus terrestris* (Hymenoptera, Apidae). *J. Insect Physiol.* 55, 479–487. doi: 10.1016/j.jinsphys.2009.01.016

Winston, M. L. (1987). *The Biology of the Honey Bee*. Cambridge, MA: Cambridge University Press.

Withers, G. S., Day, N. F., Talbot, E. F., Dobson, H. E. M., and Wallace, C. S. (2008). Experience-dependent plasticity in the mushroom bodies of the solitary bee *Osmia lignaria* (Megachilidae). *Dev. Neurobiol.* 68, 73–82. doi: 10.1002/dneu.20574

Yerushalmi, S., Bodenhaimer, S., and Bloch, G. (2006). Developmentally determined attenuation in circadian rhythms links chronobiology to social organization in bees. *J. Exper. Biol.* 209, 1044–1051. doi: 10.1242/jeb.02125

Conflict of Interest: The authors declare that the research was conducted in the absence of any commercial or financial relationships that could be construed as a potential conflict of interest.

frontiers in Ecology and Evolution

MINI REVIEW
published: 28 January 2021
doi: 10.3389/fevo.2021.622482

The Development of Arthropod Segmentation Across the Embryonic/Post-embryonic Divide – An Evolutionary Perspective

Giuseppe Fusco and Alessandro Minelli*

Department of Biology, University of Padova, Padova, Italy

In many arthropods, the appearance of new segments and their differentiation are not completed by the end of embryogenesis but continue, in different form and degree, well after hatching, in some cases up to the last post-embryonic molt. Focusing on the segmentation process currently described as post-embryonic segment addition (or, anamorphosis), we revise here the current knowledge and discuss it in an evolutionary framework which involves data from fossils, comparative morphology of extant taxa and gene expression. We advise that for a better understanding of the developmental changes underlying the evolution of arthropod segmentation, some key concepts should be applied in a critical way. These include the notion of the segment as a body block and the idea that hatching represents a well-defined divide, shared by all arthropods, between two contrasting developmental phases, embryonic vs. post-embryonic. This eventually reveals the complexity of the developmental processes occurring across hatching, which can evolve in different directions and with a different pace, creating the observed vagueness of the embryonic/post-embryonic divide.

Keywords: anamorphosis, comparative analysis, development, evolvability, fossils, hatching, gene expression, phylogeny

OPEN ACCESS

Edited by:
Nico Posnien,
University of Göttingen, Germany

Reviewed by:
Ariel D. Chipman,
Hebrew University of Jerusalem, Israel
Anna Schoenauer,
Oxford Brookes University,
United Kingdom

****Correspondence:***
Giuseppe Fusco
giuseppe.fusco@unipd.it

Specialty section:
This article was submitted to Evolutionary Developmental Biology, a section of the journal Frontiers in Ecology and Evolution

Received: *28 October 2020*
Accepted: *06 January 2021*
Published: *28 January 2021*

Citation:
Fusco G and Minelli A (2021) The Development of Arthropod Segmentation Across the Embryonic/Post-embryonic Divide – An Evolutionary Perspective. Front. Ecol. Evol. 9:622482. doi: 10.3389/fevo.2021.622482

INTRODUCTION

In many arthropods, production and differentiation of new segments are not completed by the end of embryogenesis but continue, in different form and degree, well after hatching, in some cases up to the last post-embryonic molt.

The post-embryonic addition of new segments is called *anamorphosis* and the taxa that present this mode of development are said to exhibit *anamorphic development*. Alternative to this developmental mode is *epimorphic development*, where the number of segments remains constant throughout the whole post-embryonic life. Completing the spectrum of options for the ontogenetic variation in the number of segments, there is the much less common process of *desegmentation* (or *regressive segmentation*), where the number of segments decreases at some point of the post-embryonic development; this is limited to a few holometabolous insects (Minelli and Fusco, 2013). Post-embryonic segment addition is not necessarily limited to a reproductively immature condition or to a larval phase, when present.

Anamorphosis: Numbers and Modes

Segmentation is a combination of multiple developmental processes that span from the first expression of segmentation genes to the complete display of all the morphological features of a mature segmental body unit. Since segmental units undergo developmental patterning (which may involve size, shape, limb formation, etc.), the "segmental stage" at which a segment can be considered "laid down" is an arbitrary choice. For instance, in the anostracan crustacean *Artemia*, this was identified either with the "segmental stage c," at which the segment has the shape of a short cylinder (Weisz, 1946), or with the appearance of a stripe of Engrailed protein at the prospective posterior boundary of the segment (Williams et al., 2012).

For our comparative purposes, we count as developmental addition of a new segment the first morphological appearance of a segmental unit as traditionally recognized by descriptive morphology (not necessarily the same for all taxa), irrespective of how close it is to its final morphology (e.g., disregarding presence/absence of limb buds). We calculated a *degree of anamorphosis* as the percentage of segments that are added during post-embryonic life, from 0% in epimorphic taxa, to >95% in the longest millipedes (see **Supplementary Table 1** for details on segment count).

Independent from the degree of anamorphosis, three main *modes of anamorphosis* are recognized, as first proposed by Enghoff et al. (1993) for millipedes. In *euanamorphosis*, segment number increases at each molt throughout the whole post-embryonic life, to terminate only with the death of the animal. In *teloanamorphosis*, segment number also increases throughout the animal's life, but both the number of molts and the schedule of segment addition at each molt are fixed for a given species and sex. Finally, in *hemianamorphosis*, the post-embryonic development includes a first anamorphic phase, through a first batch of stages (instars) separated by molts, followed by an epimorphic phase where molts take place without further increase in the number of body segments.

TAXONOMIC SURVEY

Anamorphosis in Extant Arthropods

The distribution of anamorphosis and epimorphosis in the main groups is shown in **Figure 1** (reference to source data in **Supplementary Table 1**).

In Chelicerata, hemianamorphosis is found among the Pycnogonida, which are sister to all the other Chelicerata, the Euchelicerata; these are all epimorphic to the exclusion of the Acariformes. Within the Pycnogonida and Acariformes, a few lineages have independently evolved epimorphic development (Lindquist, 1984; Brenneis and Arango, 2019).

Most myriapod lineages are hemianamorphic. Epimorphic development only occurs in the centipede clade rightly named Epimorpha, which includes the Scolopendromorpha and Geophilomorpha. Euanamorphosis and teloanamorphosis are found among the Helminthomorpha millipedes exclusively, where both modes may have evolved once or several times independently (Miyazawa et al., 2014).

Within the Pancrustacea, hemianamorphosis is the most common developmental mode among the "crustacean" (non-Hexapoda) lineages, but epimorphic development has evolved in some lineages, in association with direct development, whereas teloanamorphosis has possibly evolved in Copepoda (Huys, 2014) and euanamorphosis in Remipedia (Koenemann et al., 2009). Within the Hexapoda, only the Protura are hemianamorphic, while the Collembola, Diplura, and Insecta are epimorphic.

Anamorphosis in Fossil Arthropods

Ontogenetic series are available for several fossil arthropods, both stem- and crown-group. Many of these show anamorphic development and hemianamorphosis seems to be the most common mode of segmentation among stem-group taxa (e.g., Fu et al., 2014, 2018). However, segmentation in these ancient forms also exhibits some distinctive features with respect to extant taxa. Many Phosphatocopina, interpreted either as stem-group Pancrustacea (Haug and Haug, 2015) or stem-group Mandibulata (Chipman and Edgecombe, 2019), were anamorphic with indirect development (Haug and Haug, 2015), hatching as so-called *head larva*. In contrast to modern anamorphic taxa, no segments were added with the first few molts, that is, anamorphosis was in some way delayed. Another peculiar feature of anamorphosis in these early forms was that, similar to trilobites, segments first emerged as dorsally non-articulated units forming a single shield, the pygidium. The most anterior pygidial segments developed articulation in successive stages, in a process that in trilobites is called *segment release*. Trilobita, variably assigned to stem-group arthropods, stem-group chelicerates or stem-group mandibulates (Giribet and Edgecombe, 2019), mostly developed hemianamorphically (Hughes et al., 2006). However, some Emuellidae, with more than 100 trunk segments as adults, were possibly euanamorphic (Paterson and Edgecombe, 2006), whereas Zhang and Clarkson (2009) made the case for an epimorphic eodiscoid species. Delayed anamorphosis might have characterized trilobite post-embryonic development as well. Evidence for an even earlier phase of cephalic segment addition (during the so-called phaselus stage, if this was actually a phase of trilobite ontogeny), is weak (Hughes et al., 2006).

Phylogenetic Patterns

Phylogenetic distribution of anamorphosis in extant taxa and information from extinct forms concur to indicate hemianamorphic development as the primitive condition in arthropods (Hughes et al., 2006; Minelli and Fusco, 2013; Miyazawa et al., 2014; Haug and Haug, 2015; Brenneis et al., 2017). Uncertainties on key nodes of arthropod phylogeny and incomplete information on post-embryonic segmentation in several taxa prevent a formal analysis of the evolution of this developmental character at the level of the whole clade. However, starting from the hypothesis of hemianamorphosis as the plesiomorphic condition and complementing the phylogenetic distribution of the character in **Figure 1** with some available information at lower taxonomic level, four different evolutionary transitions can be recognized.

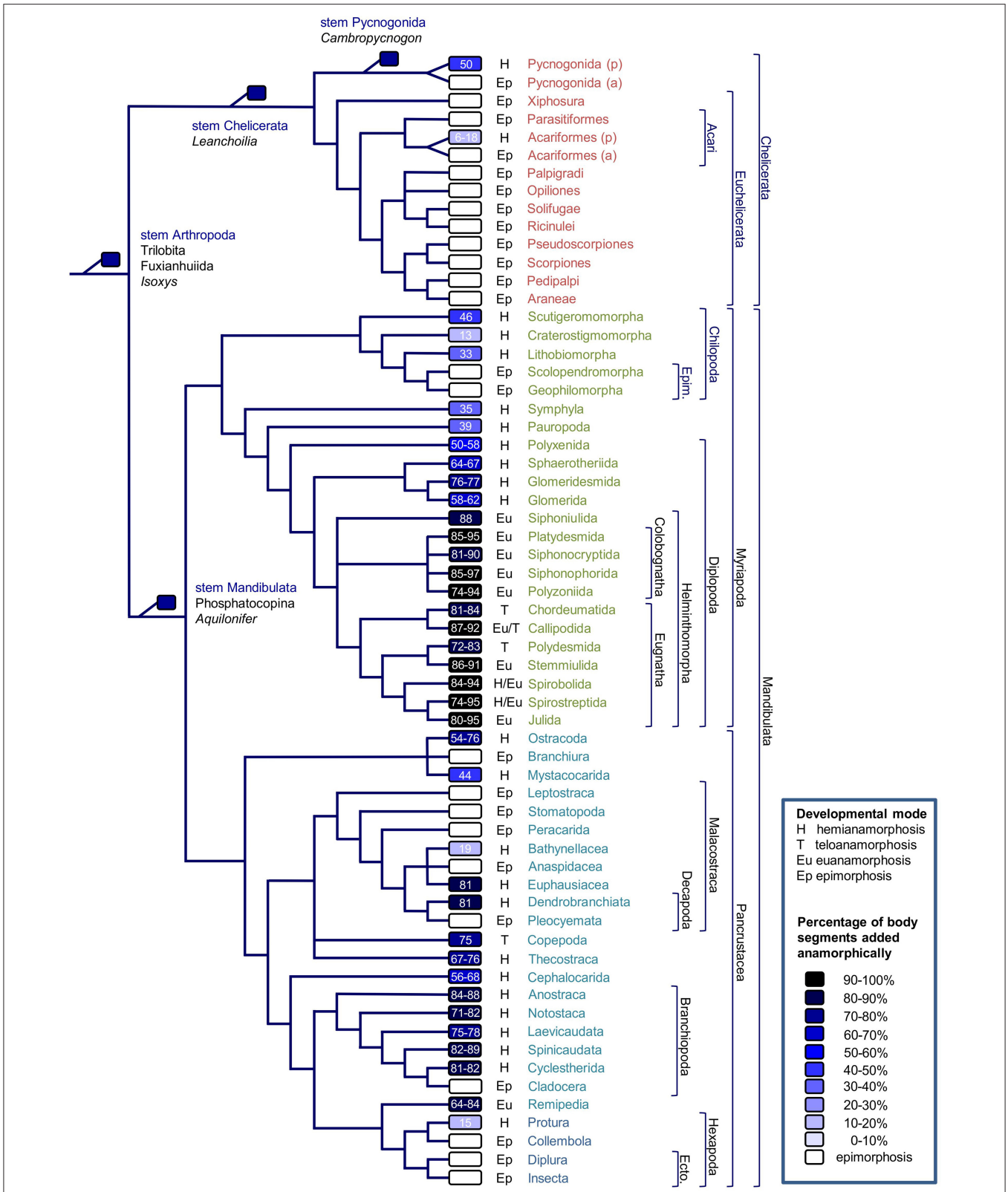

FIGURE 1 | Phylogenetic distribution of segmentation modes in arthropods. Phylogeny based on Giribet and Edgecombe (2019), Chipman and Edgecombe (2019) (fossils), Howard et al. (2020) (Chelicerata), Fernández et al. (2016) (Myriapoda), and Schwentner et al. (2018) (Branchiopoda and Malacostraca). p, plesiomorphic

(Continued)

FIGURE 1 | condition; a, apomorphic condition; H, hemianamorphosis; T, teloanamorphosis; Eu, eunanamorphosis; Ep, epimorphosis; Epim., Epimorpha; Ecto., Ectognatha. Color of boxes and figures inside each box (percentage of body segments added post-embryonically) express the degree of anamorphosis (quantified only for extant taxa). In case of variation at lower taxonomic level, data refers to the most common or to the hypothesized plesiomorphic condition in the taxon. Details in **Supplementary Table 1**.

(i) Partial embryonization of segmentation (less anamorphic segments), with a consequent reduction in the degree of anamorphosis, seems to have occurred frequently. Millipedes usually have four trunk segments at hatching, but several species from different clades (Polyzoniida, Platydesmida, Julida, Stemmiulida, Spirobolida) hatch with more, up to 38 segments (Minelli, 2015; **Supplementary Table 1**). In centipedes, interpretation of the phylogenetic pattern crucially depends on the identity of the taxon that is sister to Epimorpha, either Lithobiomorpha or Craterostigmomorpha. In the first case, mainly supported by molecular data, from the primitive condition represented by Scutigeromorpha, there would have been a conspicuous embryonization of segmentation in Craterostigmomorpha firstly, followed by an opposite change in Lithobiomorpha and complete embryonization in Geophilomorpha. In the second case, mainly supported by morphological data (other than segmentation mode), a progressive embryonization from Scutigeromorpha to Epimorpha would have occurred. Among crustaceans, from a primitive condition of hatching as a nauplius larva, many lineages have independently evolved shorter anamorphic development, hatching as a more advanced-stage larva (e.g., metanauplius in Cephalocarida and Mystacocarida). This cannot generally be interpreted as a systemic heterochronic change, because different aspects of segmentation (segment appearance, segment patterning, or limb formation) and development of larval features (autonomous nutrition, locomotion, muscular, and nervous systems) are not necessarily associated (Fritsch et al., 2013; Haug and Haug, 2015; Jirikowski et al., 2015). Segmental patterning can even progress in the opposite direction with respect to segment addition, i.e., from posterior to anterior (Minelli, 2003, p. 162).

(ii) Complete embryonization of segmentation (epimorphosis) has evolved several times independently: at least in one trilobite species (Zhang and Clarkson, 2009), in some lineages of Pycnogonida (Brenneis et al., 2017), in Euchelicerata, in Epimorpha among the centipedes, in several lineages of Malacostraca (but see below), in Cladocera and twice among the Hexapoda, i.e., in Collembola and Ectognatha. In some cases, this process is associated with the evolution of direct from indirect development (many crustaceans) and a shortening of the metameric trunk (e.g., Branchiura and Cladocera). However, the opposite is observed in Geophilomorpha, where epimorphosis is associated with the most segment-rich trunks among the arthropods. It must also be noted that epimorphosis can evolve from anamorphosis not only by embryonization of the addition of most posterior segments, but also from the suppression of the addition of those segments (*suppressed anamorphosis*), as suggested for some lineages of Acariformes (Bochkov, 2009; Bolton et al., 2017).

(iii) Partial de-embryonization of sequential segmentation from an anamorphic condition (more segments produced by anamorphosis), with a consequent increase in the degree of anamorphosis, is apparently less common. Stem-group Pancrustacea hatched as head larvae of five segments, whereas the primitive condition for crown-group Pancrustacea is thought to be a four-segment nauplius (Haug and Haug, 2015). According to Scholtz (2000), Euphausiacea and Dendrobranchiata would have evolved a "new" nauplius secondarily (and in parallel) from primitive Malacostraca with shorter anamorphosis, but this has been questioned more recently (Akther et al., 2015; see also below). In centipedes, if Lithobiomorpha are actually sister to Epimorpha (see above), the former would have extended anamorphosis from a shorter Craterostigmomorpha-like condition.

(iv) Partial de-embryonization of embryonic sequential segmentation from epimorphosis (*secondary anamorphosis*), seems to be even more rare, and putative cases are uncertain. In Pycnogonida, some Nymphonidae might have returned to anamorphosis (Brenneis et al., 2017), but uncertainties on the phylogeny of epimorphic pycnogonids do not allow to resolve this transition with confidence. If Euchelicerata are primitively epimorphic, Acariformes would have evolved anamorphosis secondarily. However, due to the persisting instability of phylogenetic hypotheses about the major clades of Euchelicerata (Giribet and Edgecombe, 2019), it is not unparsimonious to hypothesize that the Acariformes simply retained the plesiomorphic chelicerate condition (Bochkov, 2009; Bolton et al., 2017). The phylogeny in **Figure 1** would support epimorphosis as plesiomorphic for the Malacostraca, with secondary independent transition to anamorphosis in some derived taxa, compatible with the presence of a zoea-like larva as the plesiomorphic condition for the group (Jirikowski et al., 2015). However, in consideration of the similarities between the nauplii in anamorphic malacostracans and non-malacostracans and the differences in the direct development of epimorphic malacostracans, other authors have put forward the opposite hypothesis, i.e., the retention of the primitive condition of malacostracan anamorphic larval development in Bathynellacea, Euphausiacea, and Dendrobranchiata and its independent loss in the other malacostracan groups (Akther et al., 2015; Haug and Haug, 2015).

Anamophosis and epimorphosis are not fundamentally distinct developmental modes, the latter being only the lower extreme degree of the former. This is more than an arithmetic truism. In several clades, e.g., in decapod crustaceans, segment number is the same in anamorphic and epimorphic lineages. Among the most polymeric

epimorphic clade, the Geophilomorpha, Brena and Akam (2013) discovered a minimal leftover of anamorphosis in the species *Strigamia maritima*, where 2–3 terminal segments (out of 48–54 trunk segments) are added after hatching, during the first embryoid stages (see below). However, the opposite evolutionary transitions, embryonization vs. de-embryonization of segment formation, might not have the same evolvability, the former having apparently occurred more often than the latter.

Genetics of Anamorphosis

In anamorphic development, as well as in embryonic sequential segmentation, the new segments appear sequentially in anteroposterior progression from a subterminal region referred to as "segment addition zone" (SAZ; Janssen et al., 2010). This is also often referred to as the proliferative (or generative, or growth) zone, but SAZ is to be preferred because it makes no assumption of localized and continuous cell proliferation in the posterior of the body (Clark et al., 2019; see also Fusco, 2005). However, information about morphogenesis and gene expression associated with anamorphosis is scarce, and current investigations are mainly concerned with the evolution of embryonic simultaneous segmentation from embryonic sequential segmentation in insects.

Evidence of a conserved role of the segment polarity gene *engrailed* during anamorphosis was found in the anostracan crustaceans *Artemia* and *Thamnocephalus* (Manzanares et al., 1993; Constantinou et al., 2020), in the thecostracan crustacean *Sacculina* (Gibert et al., 2000) and in the centipede *Lithobius* (Bortolin et al., 2011).

The involvement of Notch signaling is increasingly emerging as a common feature of sequential segmentation throughout the Bilateria. Williams et al. (2012) showed that blocking Notch signaling causes a specific, repeatable effect on segmentation in *Artemia franciscana* and *Thamnocephalus platyurus*, although the observation that loss-of-function Notch phenotypes differ significantly across arthropods suggests some variation in the role of Notch in the regulation of sequential segmentation.

Despite the paucity of experimental data on the developmental genetics of anamorphosis, some indirect information can be obtained from comparative studies on embryonic segmentation. In a certain way, the evolutionary embryonization of anamorphosis can be seen as a natural experiment, where post-embryonic segmentation, a process not easily accessible to current molecular methodologies, is brought under the eye of the investigator. The extended similarities found in embryonic sequential segmentation in lineages that independently evolved either complete or partial embryonization of segmentation can perhaps indicate a common basic mechanism among lineages with different degree of anamorphosis up to epimorphosis. This could be based on the same clock-and-wavefront mechanism inferred from data on embryonic segmentation in a small number of model species, and hypothesized to be ancestral and conserved among arthropods (Clark et al., 2019).

ANAMORPHOSIS IN CONTEXT

Beyond the arbitrariness of what to count as the appearance of a new segment, the previous descriptions might suggest that anamorphosis is a well-defined phenomenon, and that its evolution can be confidently traced whenever reliable developmental and phylogenetic information is available. However, this is only a superficial view that can serve only broad comparative purposes. On a closer inspection, seeking for mechanistic explanations, anamorphosis remains surrounded by uncertainties that can be locally resolved only by overcoming the idealizations hidden in the traditional concepts of hatching, larva, and segment.

The Blurry Event of Hatching

It is not always the case that hatching separates embryonic from post-embryonic phases neatly. More or less embryo-like (embryoid) hatchlings are described for many arthropod groups, under a variety of taxon-specific terms (Minelli et al., 2006; Minelli and Fusco, 2013; Fritsch and Richter, 2015; Haug, 2020; **Supplementary Table 1**).

Focusing on taxonomic distribution and morphological and functional characteristics of these embryoid stages, three facts highlight the evolutionary flexibility of arthropod developmental schedules. First, conditions at hatching are often different between closely related taxa (e.g., in many spiders there is a pronymph with incompletely articulated appendages, but not in all). Second, this diversity is associated with a diversity in the number of molts the animal undergoes before and after the beginning of its active life. In most pterygote insects, three embryonic cuticles are shed before hatching, but only two in the cyclorrhaphous flies (Konopová and Zrzavý, 2005). Third, the condition at hatching is not necessarily correlated to segmentation schedule. For example, epimorphic hexapod hatchlings are anything between an active juvenile and a vermiform pronymph, while anamorphic myriapods hatch in conditions so different as the very active larva I of *Lithobius* and the motionless pupoid of *Pauropus* (Minelli et al., 2006).

Situated at one extreme of both embryonic and post-embryonic phases, where the methodologies used in the study of each phase are less effective, development around hatching time is little investigated, and recent work is disclosing unsuspected situations. For example, two embryoid stages were traditionally reported for the geophilomorph centipedes, whereas a recent closer scrutiny in *Strigamia maritima* revealed five stages (Brena, 2014).

The Multifaceted Larva

Many arthropods, in particular among the Pancrustacea, begin post-embryonic life as larvae. However, the term larva has been applied to immatures with very different, although non-mutually exclusive characteristics. These include forms that differ morphologically from the adult, have different ecological niches than the corresponding adult, or transform into an adult by a metamorphosis (see Haug (2020) for a detailed account), thus the qualification of development as either direct or indirect is somehow a matter of degree or requires qualitative specification

(e.g., for some intermediate cases Fritsch et al. (2013) introduced the term *pseudo-direct development*). The evolution of post-embryonic segmentation, although potentially independent from other developmental features of juvenile stages, can be found to be variably associated to larval evolution, as for instance when the evolution of direct development coincides with a transition to epimorphosis.

The Complex Segment

Description and comparative analysis of anamorphosis assume that we are dealing with unambiguously countable units, the segments. However, not all putatively segmental structures (especially those of internal anatomy) are in register, as they can have different period or phase. Thus, a more realistic depiction of arthropod body organization is obtained by dissociating the serial homology of individual periodic structures (e.g., legs or sclerites), or s*egmentation*, from the concept of the *segment as a body module* (e.g., Budd, 2001; Minelli and Fusco, 2004; Fusco, 2005, 2008; Fusco and Minelli, 2013; Hannibal and Patel, 2013). This accounts for the occurrence of so-called "segmental mismatch," i.e., the discordance between different segmental series within the same animal, and of a number of segmental abnormalities (Leśniewska et al., 2009), but also for the high disparity in arthropod segmental patterns. The study of anamorphosis cannot disregard the complexity and the disparity of the segmentation process (Minelli, 2020).

CONCLUSIONS

We advise that for a better understanding of the developmental changes underlying the evolution of arthropod segmentation, some key concepts should be applied in a critical way.

The putative embryonic/post-embryonic divide suffers the same shortcomings shown by the traditional periodization of development (articulation in temporal units for comparative purposes) within each of the two main phases of arthropod development (Minelli et al., 2006). During embryonic development, periodization can either be based on absolute time from egg laying, on the fraction of elapsed embryonic time, or with reference to a series of events such as blastoderm formation, gastrulation, etc. During post-embryonic development, periodization is mainly based on temporal units delimited by molts, generally referred to as stages or instars. In both phases, some developmental events are employed to give temporal order to other events, but there is no biological foundation for one series of events to be recognized as "ordinator" and all other events as "ordered." Periodization cannot be other than a relative framework, and the same is true for the passage from embryonic to post-embryonic life.

Evolutionary developmental biology seems to be over-preoccupied with boundaries, both in space (e.g., those between segments) and time (e.g., those between stages). However, these boundaries can easily hide both the continuity of many co-occurring developmental processes and the independence exhibited to a different degree by the same set of processes (Minelli et al., 2006). As an alternative, for instance, rather than defining embryonic development on the basis of its putative boundaries (fertilization, when the case, and hatching), it seems more sensible to define it based on "what it is," that is as a special context for early developmental events, characterized by the fact that the latter run protected by the body of a parent (or a host) or by a shell, that are stabilized in physical parameters, occur in relatively small-size living systems, are supplied with energy and materials from the parent, etc. None of these features is necessary, nor sufficient for defining the embryonic phase, and each one can change in evolution with different direction and pace, creating the observed vagueness of the embryonic/post-embryonic divide. From this stance, recurrent embryonization and (although less frequently) de-embryonization of segmentation in evolution reveal the robustness of the developmental processes involved, able to work in contexts so different as an embryo and an active animal, where in many cases these processes can go on for years.

Evolution is about change, and to study evolutionary change we need flexible conceptual frameworks and data formats.

AUTHOR CONTRIBUTIONS

Both authors listed have made a substantial, direct and intellectual contribution to the work, and approved it for publication.

ACKNOWLEDGMENTS

Jason Dunlop, Gregory D. Edgecombe, David A. Legg, Nigel C. Hughes, Jørgen Olesen, and Stefan Richter provided precious help in collecting and checking information on which the article is based. Jørgen Olesen, Stefan Richter, and the two reviewers provided useful comments on an earlier version of the ms.

SUPPLEMENTARY MATERIAL

The Supplementary Material for this article can be found online at: https://www.frontiersin.org/articles/10.3389/fevo.2021.622482/full#supplementary-material

REFERENCES

Akther, H., Agersted, M. D., and Olesen, J. (2015). Naupliar and metanaupliar development of *Thysanoessa raschii* (Malacostraca, Euphausiacea) from Godthåbsfjord, Greenland, with a reinstatement of the ancestral status of the free-living nauplius in malacostracan evolution. *PLoS ONE* 10:e0141955. doi: 10.1371/journal.pone.0141955

Bochkov, A. V. (2009). A review of mites of the parvorder Eleutherengona (Acariformes: Prostigmata) – permanent parasites of mammals. *Acarina* 1, 1–149.

Bolton, S. J., Chetverikov, P. E., and Klompen, H. (2017). Morphological support for a clade comprising two vermiform mite lineages: Eriophyoidea (Acariformes) and Nematalycidae (Acariformes). *Syst. Appl. Acarol.* 22, 1096–1131. doi: 10.11158/saa.22.8.2

Bortolin, F., Benna, C., and Fusco, G. (2011). Gene expression during post-embryonic segmentation in the centipede *Lithobius peregrinus* (Chilopoda, Lithobiomorpha). *Dev. Genes Evol.* 221, 105–111 doi: 10.1007/s00427-011-0359-3

Brena, C. (2014). The embryoid development of *Strigamia maritima* and its bearing on post-embryonic segmentation of geophilomorph centipedes. *Front. Zool.* 11:58. doi: 10.1186/s12983-014-0058-9

Brena, C., and Akam, M. (2013). An analysis of segmentation dynamics throughout embryogenesis in the centipede *Strigamia maritima*. *BMC Biol.* 11:112. doi: 10.1186/1741-7007-11-112

Brenneis, G., and Arango, C. P. (2019). First description of epimorphic development in Antarctic Pallenopsidae (Arthropoda, Pycnogonida) with insights into the evolution of the four-articled sea spider cheliphore. *Zool. Lett.* 5:4. doi: 10.1186/s40851-018-0118-7

Brenneis, G., Bogomolova, E. V., Arango, C. P., and Krapp, F. (2017). From egg to no-body: an overview and revision of developmental pathways in the ancient arthropod lineage Pycnogonida. *Front. Zool.* 14:6. doi: 10.1186/s12983-017-0192-2

Budd, G. E. (2001). Why are arthropods segmented? *Evol. Dev.* 3, 332–342. doi: 10.1046/j.1525-142X.2001.01041.x

Chipman, A. D., and Edgecombe, G. D. (2019). Developing an integrated understanding of the evolution of arthropod segmentation using fossils and evo-devo. *Proc. R. Soc. B* 286:20191881. doi: 10.1098/rspb.2019.1881

Clark, E., Peel, A. D., and Akam, M. (2019). Arthropod segmentation. *Development* 146:dev170480. doi: 10.1242/dev.170480

Constantinou, S. J., Duan, N., Nagy, L. M., Chipman, A. D., and Williams, T. A. (2020). Elongation during segmentation shows axial variability, low mitotic rates, and synchronized cell cycle domains in the crustacean, *Thamnocephalus platyurus*. *Evodevo* 11:1. doi: 10.1186/s13227-020-0147-0

Enghoff, H., Dohle, W., and Blower, J. G. (1993). Anamorphosis in millipedes (Diplopoda) – the present state of knowledge with some developmental and phylogenetic considerations. *Zool. J. Linn. Soc.* 109, 103–234. doi: 10.1111/j.1096-3642.1993.tb00305.x

Fernández, R., Edgecombe, G. D., and Giribet, G. (2016). Exploring phylogenetic relationships within Myriapoda and the effects of matrix composition and occupancy on phylogenomic reconstruction. *Syst. Biol.* 65, 871–889. doi: 10.1093/sysbio/syw041

Fritsch, M., Bininda-Emonds, O. P., and Richter, S. (2013). Unraveling the origin of Cladocera by identifying heterochrony in the developmental sequences of Branchiopoda. *Front. Zool.* 10:35. doi: 10.1186/1742-9994-10-35

Fritsch, M., and Richter, S. (2015). How the cladoceran heterogonic life cycle evolved — insights from gamogenetic reproduction and direct development in Cyclestherida. *Evol. Dev.* 17, 356–366. doi: 10.1111/ede.12163

Fu, D., Ortega-Hernández, J., Daley, A. C., Zhang, X., and Shu, D. (2018). Anamorphic development and extended parental care in a 520 million-year-old stem-group euarthropod from China. *BMC Evol. Biol.* 18:147. doi: 10.1186/s12862-018-1262-6

Fu, D., Zhang, X., Budd, G. E., Liu, W., and Pand, X. (2014). Ontogeny and dimorphism of *Isoxys auritus* (Arthropoda) from the Early Cambrian Chengjiang biota, South China. *Gondwana Res.* 25, 975–982. doi: 10.1016/j.gr.2013.06.007

Fusco, G. (2005). Trunk segment numbers and sequential segmentation in myriapods. *Evol. Dev.* 7, 608–617. doi: 10.1111/j.1525-142X.2005.05064.x

Fusco, G. (2008). "Morphological nomenclature, between patterns and processes: segments and segmentation as a paradigmatic case," in *Updating the Linnaean Heritage: Names as Tools for Thinking about Animals and Plants*, eds A. Minelli, L. Bonato, and G. Fusco (Auckland: Zootaxa 1950, Magnolia Press), 96–102. doi: 10.11646/zootaxa.1950.1.9

Fusco, G., and Minelli, A. (2013). "Arthropod segmentation and tagmosis," in *Arthropod Biology and Evolution. Molecules, Development, Morphology*, eds A. Minelli, G. Boxshall, and G. Fusco (Berlin Heidelberg: Springer), 197–221. doi: 10.1007/978-3-662-45798-6_9

Gibert, J.-M., Mouchel-Vielh, E., Quéinnec, E., and Deutsch, J. S. (2000). Barnacle duplicate *engrailed* genes: divergent expression patterns and evidence for a vestigial abdomen. *Evol. Dev.* 2, 1–9. doi: 10.1046/j.1525-142x.2000.00059.x

Giribet, G., and Edgecombe, G. D. (2019). The phylogeny and evolutionary history of arthropods. *Curr. Biol.* 29, R592–R602. doi: 10.1016/j.cub.2019.04.057

Hannibal, R. L., and Patel, N. H. (2013). What is a segment? *Evodevo* 4:35. doi: 10.1186/2041-9139-4-35

Haug, J. T. (2020). Why the term "larva" is ambiguous, or what makes a larva? *Acta Zool.* 101, 167–188. doi: 10.1111/azo.12283

Haug, J. T., and Haug, C. (2015). "Crustacea": comparative aspects of larval development," in *Evolutionary Developmental Biology of Invertebrates 4: Ecdysozoa II: Crustacea*, ed A. Wanninger (Wien: Springer), 1–37. doi: 10.1007/978-3-7091-1853-5_1

Howard, R. J., Puttick, M. N., Edgecombe, G. D., and Lozano-Fernandez, J. (2020). Arachnid monophyly: morphological, palaeontological and molecular support for a single terrestrialization within Chelicerata. *Arthropod Struct. Dev.* 59:100997. doi: 10.1016/j.asd.2020.100997

Hughes, N. C., Minelli, A., and Fusco, G. (2006). The ontogeny of trilobite segmentation: a comparative approach. *Paleobiology* 32, 602–627. doi: 10.1666/06017.1

Huys, R. (2014). "Copepoda," in *Atlas of Crustacean Larvae*, eds J. W. Martin, J. Olesen, and J. T. Høeg (Baltimore: The Johns Hopkins University Press), 144–163.

Janssen, R., Le Gouar, M., Pechmann, M., Poulin, F., Bolognesi, R., Schwager, E. E., et al. (2010). Conservation, loss, and redeployment of Wnt ligands in protostomes: implications for understanding the evolution of segment formation. *BMC Evol. Biol.* 10:374. doi: 10.1186/1471-2148-10-374

Jirikowski, G. J., Wolff, C., and Richter, S. (2015). Evolution of eumalacostracan development – new insights into loss and reacquisition of larval stages revealed by heterochrony analysis. *Evodevo* 6:4. doi: 10.1186/2041-9139-6-4

Koenemann, S., Olesen, J., Alwes, F., Iliffe, T. M., Hoenemann, M., Ungerer, P., et al. (2009). The post-embryonic development of Remipedia (Crustacea)—additional results and new insights. *Dev. Genes Evol.* 219, 131–145. doi: 10.1007/s00427-009-0273-0

Konopová, B., and Zrzavý, J. (2005). Ultrastructure, development, and homology of insect embryonic cuticles. *J. Morphol.* 264, 339–362. doi: 10.1002/jmor.10338

Leśniewska, M., Bonato, L., Minelli, A., and Fusco, G. (2009). Trunk anomalies in the centipede *Stigmatogaster subterranea* provide insight into late-embryonic segmentation. *Arthropod Struct. Dev.* 38, 417–426. doi: 10.1016/j.asd.2009.05.001

Lindquist, E. E. (1984). "Current theories on the evolution of major groups of Acari and on their relationship with other groups of Arachnida, with consequent implications for their classification," in *Acarology. Proceedings of the 6th International Congess of Acarology*, eds D. A. Griffiths and C. E. Bowman (Chichester: Ellis Horwood), 28–62.

Manzanares, M., Marco, R., and Garesse, R. (1993). Genomic organization and developmental pattern of expression of the *engrailed* gene from the brine shrimp *Artemia*. *Development* 118, 1209–1219.

Minelli, A. (2003). *The Development of Animal Form*. Cambridge: Cambridge University Press. doi: 10.1017/CBO9780511541476

Minelli, A. (2020). Arthropod segments and segmentation – lessons from myriapods, and open questions. *Opusc. Zool. Budapest* 51, 7–21. doi: 10.18348/opzool.2020.S2.7

Minelli, A. (ed). (2015). *Treatise on Zoology— Anatomy, Taxonomy, Biology. The Myriapoda, Vol 2*. Leiden: Brill. doi: 10.1163/9789004188273

Minelli, A., Brena, C., Deflorian, G., Maruzzo, D., and Fusco, G. (2006). From embryo to adult. Beyond the conventional periodization of arthropod development. *Dev. Genes Evol.* 216, 373–383. doi: 10.1007/s00427-006-0075-6

Minelli, A., and Fusco, G. (2004). Evo-devo perspectives on segmentation: model organisms and beyond. *Trends Ecol. Evol.* 19, 423–429. doi: 10.1016/j.tree.2004.06.007

Minelli, A., and Fusco, G. (2013). "Arthropod post-embryonic development," in *Arthropod Biology and Evolution.* Molecules, Development, Morphology, eds A. Minelli, G. Boxshall, and G. Fusco (Berlin Heidelberg: Springer), 91–122. doi: 10.1007/978-3-662-45798-6_5

Miyazawa, H., Ueda, C., Yahata, K., and Zhu, Z.-H. (2014). Molecular phylogeny of Myriapoda provides insights into evolutionary patterns of the mode in post-embryonic development. *Sci. Rep.* 4:4127. doi: 10.1038/srep04127

Paterson, J. R., and Edgecombe, G. D. (2006). The Early Cambrian trilobite family Emuellidae Pocock, 1970: systematic position and revision of Australian species. *J. Paleontol.* 80, 496–513. doi: 10.1666/0022-3360(2006)80[496:TECTFE]2.0.CO;2

Scholtz, G. (2000). Evolution of the nauplius stage in malacostracan crustaceans. *J. Zool. Syst. Evol. Res.* 38, 175–187. doi: 10.1046/j.1439-0469.2000.383151.x

Schwentner, M., Richter, S., Rogers, D. C., and Giribet, G. (2018). Tetraconatan phylogeny with special focus on Malacostraca and Branchiopoda: highlighting the strength of taxon-specific matrices in phylogenomics. *Proc. R. Soc. B Biol. Sci.* 285:20181524. doi: 10.1098/rspb.2018.1524

Weisz, P. B. (1946). The space-time pattern of segment formation in *Artemia salina*. *Biol. Bull.* 91, 119–140. doi: 10.2307/1538255

Williams, T., Blachuta, B., Hegna, T. A., and Nagy, L. M. (2012). Decoupling elongation and segmentation: Notch involvement in anostracan crustacean segmentation. *Evol. Dev.* 14, 372–382. doi: 10.1111/j.1525-142X.2012.00555.x

Zhang, X.-G., and Clarkson, E. N. K. (2009). Trunk segmentation of Cambrian eodiscoid trilobites. *Evol. Dev.* 11, 312–317. doi: 10.1111/j.1525-142X.2009.00333.x

Conflict of Interest: The authors declare that the research was conducted in the absence of any commercial or financial relationships that could be construed as a potential conflict of interest.

frontiers in Ecology and Evolution

PERSPECTIVE
published: 01 February 2021
doi: 10.3389/fevo.2021.620971

Amphibian Hormones, Calcium Physiology, Bone Weight, and Lung Use Call for a More Inclusive Approach to Understanding Ossification Sequence Evolution

*Christopher S. Rose**

Biology Department, James Madison University, Harrisonburg, VA, United States

Skeleton plays a huge role in understanding how vertebrate animals have diversified in phylogeny, ecology and behavior. Recent evo-devo research has used ossification sequences to compare skeletal development among major groups, to identify conserved and labile aspects of a sequence within a group, to derive ancestral and modal sequences, and to look for modularity based on embryonic origin and type of bone. However, questions remain about how to detect and order bone appearances, the adaptive significance of ossification sequences and their relationship to adult function, and the utility of categorizing bones by embryonic origin and type. Also, the singular focus on bone appearances and the omission of other tissues and behavioral, ecological and life history events limit the relevance of such analyses. Amphibians accentuate these concerns because of their highly specialized biphasic life histories and the exceptionally late timing, and high variability of their ossification sequences. Amphibians demonstrate a need for a whole-animal, whole-ontogeny approach that integrates the entire ossification process with physiology, behavior and ecology. I discuss evidence and hypotheses for how hormone mediation and calcium physiology might elicit non-adaptive variability in ossification sequence, and for adaptive strategies to partition larval habitats using bone to offset the buoyancy created by lung use. I also argue that understanding plasticity in ossification requires shifting focus away from embryonic development and adult function, and toward postembryonic mechanisms of regulating skeletal growth, especially ones that respond directly to midlife environments and behaviors.

Keywords: amphibians, bone, skeleton, thyroid hormone, metamorphosis, ossification sequence, plasticity, variability

OPEN ACCESS

Edited by:
Fernando Casares, Andalusian Center for Developmental Biology (CABD), Spain

Reviewed by:
Ivan Gomez-Mestre, Estación Biológica de Doñana (EBD), Spain
Alexander Schreiber, St. Lawrence University, United States

***Correspondence:**
Christopher S. Rose
rosecs@jmu.edu

Specialty section:
This article was submitted to Evolutionary Developmental Biology, a section of the journal Frontiers in Ecology and Evolution

Received: *24 October 2020*
Accepted: *11 January 2021*
Published: *01 February 2021*

Citation:
Rose CS (2021) Amphibian Hormones, Calcium Physiology, Bone Weight, and Lung Use Call for a More Inclusive Approach to Understanding Ossification Sequence Evolution. Front. Ecol. Evol. 9:620971. doi: 10.3389/fevo.2021.620971

INTRODUCTION

Ossification sequence, meaning the order by which bones appear in a species, has recently become the subject of much evo-devo study and phylogenetic analysis. Amphibians feature prominently in this research owing to the large number of species for which these data have been collected (over 60 at last count) and their biphasic life cycles, which entail dramatic transformations in morphology and behavior midway through life and have supported remarkable behavioral and

ecological diversification. While summarizing this research is beyond the scope of this paper, amphibians stand apart from other vertebrates for having exceptionally variable and late-occurring bone formation, as well as highly plastic rates of larval growth and development and high ranges in larval period. The goals here are 1. to summarize caveats about collecting and using ossification sequence data, 2. to use frogs and salamanders to question the prevailing adult function- and embryogeny-based approaches for interpreting ossification sequences, and 3. to present hypotheses and evidence that advocate for a new "whole-animal, whole-ontogeny" approach to understand the developmental and evolutionary significances of these data.

CAVEATS ABOUT COLLECTING AND INTERPRETING OSSIFICATION SEQUENCES

Determining when exactly a bone appears depends on how it is visualized, which has been done typically in Alizarin red-stained, glycerin-cleared whole mounts. Sectioned specimens (Hanken and Hall, 1988a) and calcein-stained whole mounts (Schreiber, 2006) can give earlier results, and micro-computed tomography (μCT) gives comparable results (Polachowski and Werneburg, 2013), but with the advantages of producing digital 3D images, and being faster, less size-limited and nondestructive, though caution must be taken to not dry out small specimens. However, μCT fails to resolve cartilage and small bones (Werneburg et al., 2015), and early appearing bones and portions of otherwise stained bones can also fail to stain with Alizarin red (Rieppel, 1993a; Cubbage and Mabee, 1996; Mabee and Trendler, 1996; Mitgutsch et al., 2011). One explanation for no staining is that the bone is still osteoid or not yet mineralized. Another is dissolution of the mineral by storage in formalin or by prior use of an acidic cartilage stain (Wagemans and Vandewalle, 2001; Grünbaum et al., 2003; Walker and Kimmel, 2007; Werneburg et al., 2015). Dissolution is more likely in specimens stored long term, especially in unbuffered or unstably buffered 10% formalin (Markle, 1984), or in 10% formaldehyde, as reported in one study reviewed for this paper. Distinguishing between the two requires fresh material that has been fixed for hours and not months or years, skipping the cartilage stain for some specimens or using a neutral stain (Walker and Kimmel, 2007; Ma et al., 2019), and using a stain for bone that detects calcium (von Kossa, Alizarin red, calcein) and not just matrix protein.

Obtaining a well-resolved ossification sequence depends not only on having a large number of specimens that represent a complete ontogenetic series, but on how specimens are ordered. Commonly used metrics are developmental stage, which is based on external morphological changes; body size (length or weight), which measures growth; and chronological age, which could be relative to fertilization, oviposition, hatching or birth. A fourth, physiological age, remains hypothetical as it requires finding a molecular marker that shows a constant rate of measurable change throughout life, and not just adulthood (Reiss, 1989; Austad, 1993; Strauss, 1999). Having a metric as well as multiple specimens for each stage, size, or age allows one to identify ranges of appearance, i.e., from the lowest stage/size/age at which a bone is first present in one or more specimens to the lowest stage/size/age at which that bone is present in all specimens. The convention for reporting ossification sequences is to use the former (Sheil et al., 2014). However, while staging systems are invaluable for the developmental biology of model organisms, comparative studies are often hindered by the absence of universal staging systems, meaning a sequence of external changes that are general enough and conserved enough in their relative timing to apply to all members of a major group of vertebrates, let alone to all vertebrates. Also, age is often not available for field collected and museum specimens, and even if age and size are both available, intraspecific variation in growth or developmental rates makes it difficult to use either metric to resolve an ossification sequence (Mabee and Trendler, 1996). The lack of a universal metric for gauging postembryonic progress is not surprising given the capacity for environmental factors and natural selection to dissociate traits at most, if not all, phenotypic levels (molecular, morphological, and growth).

Thus, the relatively recent idea to treat bone appearances relative to each other, either in pairs (Mabee and Trendler, 1996; Smith, 1997; Velhagen, 1997; Jeffery et al., 2005) or from first to last (Strauss, 1990; Germain and Laurin, 2009; Harrington et al., 2013), opened the door for many kinds of evo-devo analyses (Yeh, 2002; Sánchez-Villagra et al., 2008; Germain and Laurin, 2009; Maxwell et al., 2010; Weisbecker and Mitgutsch, 2010; Harrington et al., 2013; Koyabu et al., 2014; Werneburg et al., 2015). It became possible to identify heterochronic shifts in suites of characters between major groups of vertebrates as well as timing differences within a major group between modules of bones defined by function, developmental type or origin. It also became possible to experiment with ossification sequence data in creating phylogenies, and to use molecular based phylogenies for major groups to expose the conserved and labile components of their sequences, to estimate the phylogenetic signal of a sequence (meaning the impact of phylogenetic affinity on its evolution), and to derive ancestral or modal ossification sequences.

However, treating bone appearances relative *only* to each other also has its methodological constraints. The omission of everything that is not a bone appearance precludes one from distinguishing between small and large differences in timing of bone appearance. Also, the likelihood of finding intra- and interspecific differences in sequence as well as the significance of a difference varies not only with the number of bones involved and how closely they appear relative to each other, but with the relative length of the ossification period. This means the length of time over which bones appear relative to the portion of postembryonic life when the bony skeleton has developed to the point of actually contributing to fitness. Though a pioneering study of ossification sequences included key events in muscle, central nervous system and later bone development (Smith, 1997), most subsequent analyses have omitted important life history events such as hatching or birth, the onsets of exogenous feeding and metamorphosis, and changes in musculoskeletal function, behavior and ecology. Such features could serve as useful markers in developmental, ecological and phylogenetic

comparisons, and broaden the utility of such studies to more areas of biology.

HOW ARE AMPHIBIAN OSSIFICATION SEQUENCES SPECIAL?

As it is difficult to compare sequences across vertebrates, I will briefly review the ossification periods of the major non-amphibian groups as background for discussing amphibian ossification periods and sequences.

Studies on turtles, lizards, alligators, snakes, one dinosaur, altricial and precocial birds, and placental mammals show that most amniotes acquire all or almost all bones before hatching or birth (Rieppel, 1993a,b, 1994; Smith, 1997; Nunn and Smith, 1998; Sánchez-Villagra, 2002; Maxwell, 2008; Sánchez-Villagra et al., 2008; Maxwell and Larsson, 2009; Maxwell et al., 2010; Hautier et al., 2011; Mitgutsch et al., 2011; Polachowski and Werneburg, 2013; Koyabu et al., 2014; Werneburg et al., 2015; Chapelle et al., 2020). Marsupial mammals differ in acquiring three cranial bones for feeding a day or two before birth and the others by the end of the first quarter of pouch life (Smith, 1997; Nunn and Smith, 1998) The most complete studies for teleost fish show ossification starting right after hatching (and chondrification), and continuing for several weeks while the yolk is consumed (Cubbage and Mabee, 1996; Mabee and Trendler, 1996; Gluckmann et al., 1999; Wagemans and Vandewalle, 2001). Flatfish differ in that some (Brewster, 1987; Ma et al., 2019), but not all (Wagemans and Vandewalle, 2001; Schreiber, 2006) species delay most or all bone appearances to the onset of eye migration, at around 3 weeks post hatching. Basal actinopterygian fish and lungfish extend bone appearances past the yolk sac stage, and in the case of bichirs and two lungfish to the stage of external gill loss, at 6–8 weeks post hatching (Agar, 1906; Pehrson, 1940, 1944, 1949, 1958; Jollie, 1980, 1984a,b,c; Bartsch et al., 1997). All major groups have relatively conserved ossification sequences, coupled with small amounts of intraspecific variation and interspecific variation among closely related species, and a few timing shifts that can be correlated with other traits, e.g., the supraoccipital appearing earlier in larger brained mammals (Koyabu et al., 2014) and compressed ossification periods in rapidly developing mammals (Smith, 1997).

Amphibians ossification periods usually extend past metamorphosis, which generally occurs within 1 or 2 years of hatching, but can be as early as eight days and 6 weeks post-hatching in frogs and salamanders respectively, and as late as 4 and 5 years in these groups (Blanchard, 1923; Bruce, 1980, 1988; Newman, 1989; Petranka, 1998; Bury and Adams, 1999). Salamanders, which are carnivorous as both larvae and adults, acquire bones for feeding around the time of hatching, and others in mid to late larval stages and metamorphosis (Rose, 2003a). The most variable in timing are the maxilla, nasal and septomaxilla, which can appear before or during metamorphosis (Rose, 1996). In contrast, frogs, which typically have herbivorous larvae, are marked by late starts for ossification, and highly variable ossification sequences. The first three bones, usually the exoccipital, parasphenoid, and frontoparietal (**Figure 1**), can be acquired at an early larval stage (Haas and Richards, 1998; Senevirathne et al., 2017), midlarval stage (Wild, 1997, 1999), during metamorphosis (Maglia, 2003), and afterwards (Trueb, 1966). One species acquires its first 10 cranial bones in larval stages (Haas, 1999), whereas another acquires its first two in late metamorphosis, and the next 16 in juvenile growth (Trueb, 1966). Functionally important bones like the premaxilla, maxilla, angulosplenial, dentary, and nasal (**Figure 1**) can appear in tadpoles (Trueb and Hanken, 1992), froglets (Trueb, 1966; Gaudin, 1973), or in between (Maglia, 2003). Such variability defies easy characterization and draws into question the meaning of a modal or average ossification period or sequence for frogs.

HOW IS THE REST OF AMPHIBIAN DEVELOPMENT SPECIAL?

Ossification sequences are particularly easy to document and compare for metamorphosing amphibians because much of their postembryonic development is highly conserved. Most metamorphosing frogs exhibit very similar sequences of conspicuous change in the mouth, limbs, and tail, as well as of remodeling throughout the head and body (Fabrezi et al., 2010; Fabrezi, 2011), muscles (Alley, 1989; Fabrezi et al., 2014), gut (Schreiber et al., 2005; Ishizuya-Oka and Shi, 2007; Fabrezi et al., 2010), and skin (Fox, 1985; Lannoo, 1987; Regueira et al., 2016). Salamanders exhibit a less derived, less encompassing sequence of changes that differs from frogs externally by tail retention and earlier and more variable timing of hind limb development. The conservation of external changes allowed the creation of almost universal developmental staging systems for frogs (Gosner, 1960) and salamanders (Glücksohn, 1931; Rugh, 1962; Iwasawa and Kera, 1980; Norman, 1985; Shi and Boucaut, 1995) that extend from fertilization to the end of metamorphosis. The Gosner system for frogs, which consolidates two earlier systems (Taylor and Kollros, 1946; Limbaugh and Volpe, 1957), has been applied to almost all metamorphosing species studied so far (Altig and Johnston, 1989; Altig and McDiarmid, 2015), albeit with slight modifications for ones with exceptional larval growth (Moore and Townsend, 2003; Fabrezi et al., 2009). A similar, more detailed system for *Xenopus* and other pipids (Nieuwkoop and Faber, 1956) recognizes minor variability in the timing of external and internal characters, and points out the most reliable characters to use.

The conserved postembryonic development of amphibians derives from reliance upon one primary mediator, thyroid hormone (TH). TH production in frogs starts in early larval stages and increases through to metamorphosis (Etkin, 1935; Dodd and Dodd, 1976; White and Nicoll, 1981; Rose, 1999; Yaoita, 2019). The rise in plasma TH activates postembryonic changes through a combination of intracellular processes in tissues throughout the body that collectively determine if, when, and how each tissue and, for bone appearances, each population of precursor cells respond to TH (Gilbert et al., 1996; Shi, 2000). These processes include cytoplasmic enzymes converting T4 to the more active form, T3, and both to

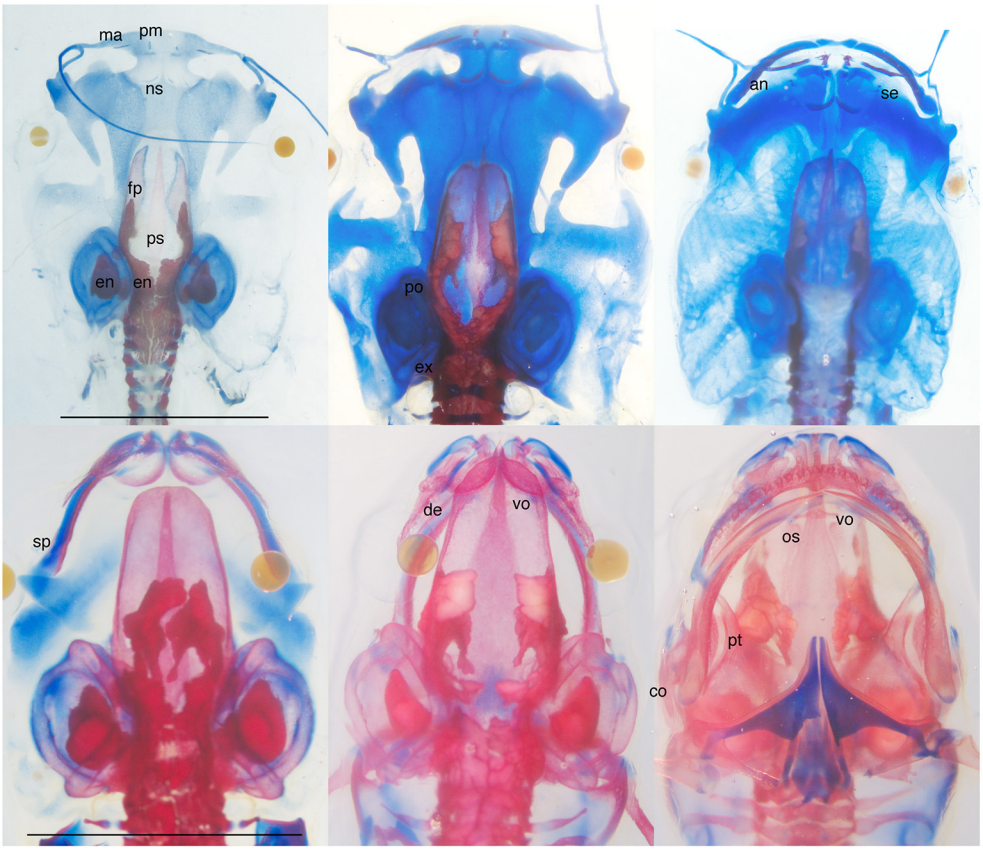

FIGURE 1 | Skeletally stained *Xenopus laevis* at larval (top L to R, NF stages 56, 57, 59) and metamorphic (bottom L to R, NF 63, 65, 66) stages; bottom right is a ventral view, others are dorsal views; NF 56 and 58 specimens have lower jaw and hyobranchial skeletons removed; blue is cartilage and red is bone; scale bars are 5 mm. Cranial bones appear as faintly stained thin plates (ps and fp), small splints (pm, ma, ns, se, sp, de, vo, an), and small zones of replacement (ex, os, po), and progress gradually and directly toward their adult shapes and sizes. The major changes in skull architecture (shrinkage of the snout, nasal capsule formation, lower jaw lengthening, and shape change, posterior rotation of the jaw suspension) occur in cartilage between NF 59 and 66. They make the head narrower and more pointed, the braincase overlap with the nasal capsule, the snout protrude beyond the jaw, and the corner of the mouth move from in front of the eye to behind the eye. Whereas the braincase roof is closed by the end of metamorphosis (NF 66), the dentary and angulosplenial remain separate in the lower jaw as do the facial processes of premaxilla and maxilla in the snout. Endolymphatic deposits, which have white interiors and are irregularly shaped and distributed within the braincase, ear capsule, and vertebral canal, appear before the first bone and persist after metamorphosis. Bone labels are placed next to bone rudiments and on top of larger bones; an, angular part of angulosplenial; **co**, columella; de, dentary; en; endolymphatic deposits; **ex**, exoccipital; fp, frontoparietal; ma, maxilla; ns, nasal; **op**, operculum; **os**, orbitosphenoid; ps, parasphenoid; pm, premaxilla; **po**, prootic; pt, pterygoid; se, septomaxilla; sp, splenial part of angulosplenial; vo, vomer; bold fonted bones are endochrondral; not shown are the quadrate and squamosal; the angular, pterygoid, prootic, and columella as rudiments; and the quadratojugal, which appears after NF 66.

nonactive forms (Becker et al., 1997; Brown, 2005), regulation of TH receptor gene expression (Yaoita and Brown, 1990), interactions of TH with other hormones (Tata et al., 1991; Sachs and Buchholz, 2019; Sterner et al., 2020), and changes in TH-regulated gene expression (Buckbinder and Brown, 1992; Berry et al., 1998). Though these processes work together to control when and how tissues respond to TH, the tradition of referring to early tissue responses, which are activated at lower plasma TH levels, as being more sensitive to TH remains useful for discussing evolutionary changes in developmental timing. Whereas whole-body evolutionary trends like direct development and paedomorphosis likely involve changes in both TH production and TH sensitivity, the persistence of largely conserved postembryonic patterns among metamorphosing frogs and salamanders strongly suggests that heterochronic changes in individual tissue responses like bone appearances result largely from changes in TH sensitivity.

WHAT CURRENT APPROACHES DO NOT TELL US ABOUT OSSIFICATION SEQUENCE EVOLUTION

Current efforts to understand evolutionary variation and modularity in ossification sequences are rooted in the historical traditions of functional and developmental morphology (alternative terms are externalist or adaptationist, and internalist) (Gould and Lewontin, 1979; Alberch, 1980, 1989; Hildebrand

et al., 1985; Gould, 1986; Rieppel, 1988; Ashley-Ross and Gillis, 2002). The functional approach emphasizes the selective pressures that are directed at individual bones and bone regions to accommodate mechanical stress as the animal attains its adult size and functions (Trueb, 1993; Mabee and Trendler, 1996; Wagemans and Vandewalle, 2001; Simon and Marroig, 2017). The developmental approach emphasizes the influences on adult morphology that are imparted by the embryonic history of cells and tissues, e.g., cranial neural crest versus paraxial mesoderm and anterior versus posterior crest origins, and dermal vs. endochondral or perichondral bone formation (Hallgrímsson et al., 2009; Koyabu et al., 2014; Simon and Marroig, 2017; Felice and Goswami, 2018). While the two viewpoints fuel highly productive research programs, they leave unanswered several important questions about adult functions, embryonic influences, and whether both are sufficient to explain evolutionary patterns in ossification sequences.

A fundamental question for understanding the functional significance of ossification sequences is when does bone strength matter to the point that bone development is shaped by selection. Unlike other vertebrates, amphibians acquire many bones as fully differentiated animals that are already using their cartilage skeletons for feeding, breathing, support and locomotion. Their dermal bones typically appear as single grains of mineralized tissue alongside cylindrical cartilages like the lower jaw and jaw suspension or as multiple diffuse grains that coalesce in open spaces in the roof, floor and wall of the nasal capsule and braincase (**Figure 1**, Lebedkina, 1960a,b, 1964, 1968, 2004; Smirnov and Vassilieva, 2009). But when does a bone rudiment that gradually elongates along a cartilage or expands above a sense organ or brain start to impact fitness? A bony splint might be expected to allow the portion of cartilage adjacent to it to resist deformation. However, this would shift load to adjoining cartilage not adjacent to bone and increase its likelihood of deformation, especially in parts close to joints. Also, given the strength and weight differences between bone and cartilage, bone rudiments growing adjacent to cartilage might detract from the latter's ability to distribute load, as well as increase the energy required for its movement. The first stage at which one might expect dermal bone strength to definitely enhance fitness is when single elements articulate or fuse with each other to form a bony framework whose response to loading supercedes that of cartilage and unconnected bone rudiments. Examples would be the solidification of dermal bones in the regions of the mandible, palate and jaw suspension, and the abutting of left and right roofing bones to complete a cranial vault. Such configurations are usually not attained in frogs until the end of metamorphosis or later (**Figure 2**).

Also, amphibian metamorphosis marks one of the biggest postembryonic transformations in musculoskeletal function and structure in vertebrates and the changes in breathing and feeding behavior that define the metamorphic period are underlain by major changes in cartilage regions of the skull, particularly the lower jaw, jaw suspension, palate, nasal capsule, and hyobranchium (**Figure 1**, Rose and Reiss, 1993; Rose et al., 2015). The period of transformation is also one of high vulnerability and mortality, implying there is strong selection to keep the changes as brief and as coordinated as possible (Wassersug and Sperry, 1977; Wassersug and Hoff, 1982). That many bones appear outside of this period, that almost all bone rudiments develop directly to their adult size and shape (**Figure 1**)—only the salamander vomer and coronoid attain shapes designed specifically for larval functions—and that the major functional transformations at metamorphosis are effected more in cartilage than in bone underscores the primacy of cartilage in the origin and diversification of amphibian metamorphosis (Rose, 2014b). These points also accentuate the conclusion drawn from other vertebrates that timing of bone appearance is not strongly tied to, and therefore not predictive of, onset of bone function in load bearing (Mabee and Trendler, 1996; Maxwell, 2008; Maxwell and Larsson, 2009).

From a developmental perspective, the decision to analyze sequences of *only* bone appearances presupposes that the mechanisms controlling timing of bone appearance are somehow distinct from those controlling the timing of other tissue changes, and even that bone appearances are developmentally interdependent. The same could be said for grouping bone appearances into modules based on embryonic origin of the skeletal precursor cells or mode of bone formation. Yet, despite many postulations to the contrary, there has been no developmental evidence or mechanism proposed so far for how the appearance of one or more bones might activate, enable, inhibit, or otherwise affect the appearance of other bones. Endochondral and perichondral bone appearances obviously require the presence of pre-existing cartilage. The former also requires vascularization to supply the cells required for cartilage resorption and bone deposition, although cartilage cells transforming directly into bone cells remains a possibility (Ishizeki et al., 2010), as does bone cells transforming into secondary cartilage cells (Woronowicz and Schneider, 2019). All dermal bone appearances require interaction with epithelia, and certain bones interact with specific epithelia, e.g., lateral line organs in fish and amphibians and the nasolacrimal duct in amphibians, and possibly also with cartilage (Hall and Hanken, 1985; Rose and Reiss, 1993; Richman et al., 2006; Wada et al., 2010). Cartilage serving as a scaffold for dermal bone condensation is suggested by bones forming normally next to cartilage in ectopic grafts of facial primordia (Richman et al., 2006) and TH-induced bones appearing out of order alongside precociously induced nasal cartilage (Rose, 1995, 1996). That certain amphibian bones additionally rely upon thyroid hormone (discussed below) would imply that they also depend upon the establishment of a functioning circulatory system and thyroid gland.

Also, skeletal cell condensation and differentiation are the products of gene regulatory networks that involve bone- and cartilage-specific transcription factors and signaling pathways, and play out to similar ends in precursor cell populations that vary in size, shape, location, and embryonic origin (Hanken and Gross, 2005; Richman et al., 2006; Hall et al., 2014; Jandzik et al., 2014, 2015; Gilbert and Barresi, 2016; Schneider, 2018; Woronowicz and Schneider, 2019). Other than TH mediation and the dermal bone interactions mentioned above, there is no *a priori* reasoning for why gene regulatory networks or

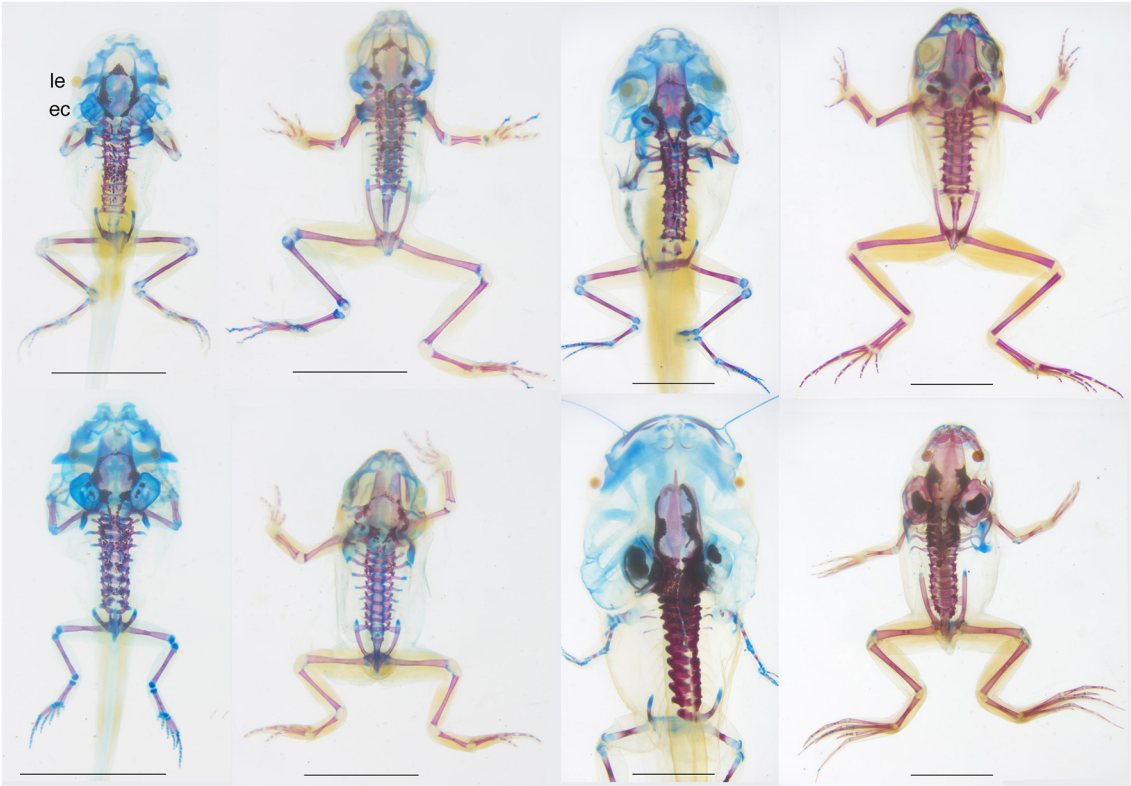

FIGURE 2 | Dorsal views of skeletally stained specimens of four species of frogs, from top left to bottom right, *Pseudacris crucifer* (Hylidae), *Lithobates sylvatica* (Ranidae), *Anaxyrus fowleri* (Bufonidae), and *Xenopus laevis* (Pipidae) showing interspecific differences in bone size and shape in mature tadpoles (left) and recent postmetamorphs (right), i.e., at the start and end of the cartilage remodeling described in **Figure 1** (GS 40-41 and GS 46 for the first three species; NF 59 and 66 for the fourth species). Mature tadpoles of all four species have endolymphatic deposits, one or more dermal bones lining the braincase, all vertebrae and rib ossifications, and all limb long bones and girdle bones excluding carpals and tarsals. Differences include the absence of the parasphenoid in *Anaxyrus*, the small size of limb bones in *Xenopus*, more bone rudiments in the snout of *Xenopus*, and narrow, widely separated frontoparietals in *Pseudacris*. Recent metamorphs all show general increases in cranial ossification; the braincase roof remains open and the ear capsule and snout remain poorly ossified in in *Pseudacris* and *Anaxyrus,* and *Xenopus* appears the most ossified of the four. ec, ear capsule; le, lens of eye. Scale bars are 5 mm. All specimens were collected and/or raised, prepared and DNA barcoded by the author using standard techniques, Virginia state collecting permits and AICUC approved protocols.

cell history would predispose certain bones or groups of bones to appear earlier or later than others. On the other hand, there are functional and physiological reasons for why certain bones appear when they do. The finding from across vertebrates (Mabee and Trendler, 1996; Wagemans and Vandewalle, 2001; Yeh, 2002; Maxwell et al., 2010; Koyabu et al., 2014; Ollonen et al., 2018) that dermal bones tend to appear earlier than endochondral bones need not reflect a developmental constraint (Koyabu et al., 2014). It could be simply that endochondral bones are not, and never have been, directly involved in the onset of feeding and breathing, and that the cartilage skeleton that precedes them in life (and probably evolution) suffices for support and locomotion in the aquatic environments occupied by amniote embryos and anamniote hatchlings and early larvae. Similarly, the late appearances of cranial bones in frogs and flatfish point to the sufficiency of a mostly cartilage skeleton for feeding and breathing throughout the larval period. Indeed, the supra- and infrarostral cartilages of tadpoles suffice for rasping algae and mouth closing even in the largest tadpoles (Alcalde and Barg, 2006; Downie et al., 2009a,b; Fabrezi and Goldberg, 2009). Also, delaying cranial bone appearances and growth to metamorphosis or afterwards allows for major reshaping of the skull without the physiological expense of having to resorb bone that has been shaped specifically for larval functions.

HOW ENVIRONMENTAL FACTORS IMPACT AMPHIBIAN OSSIFICATION SEQUENCES

Environmental factors can directly affect timing of bone appearances in both adaptive and non-adaptive ways. An example of adaptive plasticity is fin bone appearances being accelerated in a teleost raised in fast water (Cloutier et al., 2010). This implies that the gene regulatory networks for bone appearance can be configured epigenetically to activate cartilage replacement directly in response to mechanical stress, and that there is either a cost to early bone appearance or an adaptive advantage to later bone appearance; otherwise the early timing would become fixed genetically.

The most extreme case of variable bone appearances known for amphibians involves *Ascaphus truei*, a frog that spends 1–4 years as a tadpole sucking onto rocks in fast flowing mountain streams in temperate forests (Brown, 1990; Bury and Adams, 1999). Two of its three earliest bones (parasphenoid and frontoparietal) appear across a range of 11 Gosner stages, from the beginning of hind limb differentiation and growth at GS 30 to the beginning of metamorphosis at GS 41 (Moore and Townsend, 2003). Though the specimens were stored in formalin for about 20 years prior to Alizarin red staining, the authors took care to identify unstained bones. As 11 of the 14 other cranial bones appear across smaller ranges of stages, the number of possible ossification sequences exhibited by this species is immense. That a similar amount of variability was found in three populations from different parts of the species range argues for little, if any, adaptive significance to the exact stage of larval bone appearance. This conclusion is supported by studies on six distantly related species that report small ranges in all bone appearances for lab-raised animals, meaning that individuals are usually siblings, environmental and fixation conditions are controlled, and sources of variability are limited to differences in growth and developmental rates and feeding behavior (Kemp and Hoyt, 1969; Gaudin, 1978; Hanken and Hall, 1984; Smirnov, 1992; Trueb and Hanken, 1992; Haas, 1999). These differences, which could be genetic or induced by conspecifics (Wilbur and Collins, 1973), are indeed sufficient to produce variation in ossification sequence with lasting effects on adult bone shape (Smirnov, 1992).

HOW TH MEDIATION IMPACTS AMPHIBIAN OSSIFICATION SEQUENCES

Since larval growth and developmental rates can vary independently of each other (Alford and Harris, 1988; Rose, 2005; Gomez-Mestre et al., 2010), whether both parameters can affect timing of bone appearance and ossification sequence remains unclear. However, some plasticity in early bone appearances might be expected as a non-adaptive consequence of being hormonally regulated. The earliest frog bones, which also appear to be the most variable, first arise around Gosner stage 30 (or Nieuwkoop Faber stage 53), which is the earliest stage at which plasma TH has been detected in frogs by radioimmunoassays (Leloup and Buscaglia, 1977; Miyauchi et al., 1977; Regard et al., 1978; Mondou and Kaltenbach, 1979; Suzuki and Suzuki, 1981; Weil, 1986). GS 30 is also approximately when frog postembryonic development is believed to become TH mediated, since tissues at earlier stages can be accelerated by exogenous TH, but not delayed by TH inhibitors or thyroid gland inactivation (Allen, 1918; Terry, 1918; Brown, 2005; Kerney et al., 2010; Smirnov and Vassilieva, 2014; Rose and Cahill, 2019). By the same criteria, the onset of TH mediation in salamander ossification occurs between mid and late larval stages (Smirnov et al., 2020). Cells that condense and mineralize around GS 30 might be expected to show accelerated or delayed activation due to the high plasticity in amphibian growth and developmental rates (Rose, 2005, 2014a), and the exceptionally low TH involved in their activation. The plasma T4 of larval frogs, when first detected near the start of metamorphosis, is at 0.3–0.6 nM (which is just above the detectable limit of the tests), and peaks in mid or late metamorphosis at 6–13 nM (references above). This contrasts with larval fish, whose plasma TH levels are typically above 20 nM, and amniotes near hatching or birth whose levels can be over 100 nM (Rose, 2003b). Also, all amphibian studies that measured single individuals found some with non-detectable TH at all larval and metamorphic stages. Thus, the TH signal of larval frogs is inherently low and variable, and the earliest and lowest part of the signal might be further destabilized by environmental fluctuations that switch the animal back and forth between development and growth. The bones that respond to the early signal also appear to be inherently variable based on their tendency to appear in variable order (Hanken and Hall, 1988b) and from a variable number of ossification centers (Smirnov and Vassilieva, 2009) when induced at a constant TH level. Whether mediation by TH makes amphibians uniquely susceptible to variably timed bone appearances depends on the extent to which other vertebrates rely upon circulating factors to mediate bone condensation in a concentration-dependent fashion. One might expect less variability from condensation events in embryogenesis that are mediated only by locally secreted paracrine factors.

HOW CALCIUM PHYSIOLOGY IMPACTS AMPHIBIAN OSSIFICATION SEQUENCES

Another source of plasticity in the appearance and growth of bone involves the availability of calcium and the utilization of mineral reserves. Frogs, which generally do not eat during metamorphosis or resorb bones, appear to draw the calcium required for their metamorphic bone appearances and growth from exceptionally large calcium carbonate deposits that are built up in the endolymphatic sacs, braincase, and anterior vertebral canal during larval growth (**Figures 1**, **2**, Pilkington and Simkiss, 1966). Indeed, quantification of calcium, phosphate, and carbonate levels shows that as a ranid tadpole develops, it first deposits calcium carbonate as endolymphatic deposits, and then shifts to depositing calcium phosphate as bone as it approaches metamorphosis. Metamorphosis is characterized by both bone deposition and calcium carbonate resorption, implying that calcium mobilized from the carbonate reserves is redeposited as bone. A slight decrease in calcium content overall suggests that the calcium reserve is more than sufficient to supply the bone deposition (Pilkington and Simkiss, 1966). Both the calcium carbonate and bone deposits are larger in tadpoles raised in calcium-enriched water, and animals deprived of calcium do not grow bone during metamorphosis despite losing calcium carbonate. How such plasticity would impact skeletal anatomy and ultimately fitness would depend not only on calcium availability, but on how larval bone appearances are spaced relative to each other and to the buildup and dissolution of carbonate reserves.

How early mineral deposition affects later bone formation could also be influenced indirectly by environment as evidenced

by early appearing bones growing larger in tadpoles with extended larval periods (Smirnov, 1992). In other words, bone deposition can proceed unabated in existing bones during growth and developmental slow-downs that delay the appearance of later arising bones. This suggests that ossification in tadpoles involves at least three separate rate-controlling mechanisms. TH appears to regulate, albeit with some variability, when bones appear relative to other tissue changes; bone growth is presumably regulated by the same circulating factors that keep most tissues on their species-specific growth curves despite differences in body size; and mineral deposition and resorption are regulated to allow the body to accumulate and mobilize calcium in different ways at different stages of life. The resilience of the third control mechanism to environmental factors that slow development and growth raises new hypotheses for why late appearing bones can become exceptionally small (Wake, 1980) or lost altogether (Trueb, 1985) in amphibian evolution. More generally, as other vertebrates also store and mobilize endolymphatic calcium carbonate (Polachowski and Werneburg, 2013), the pathways and environmental factors regulating calcium utilization present an altogether new front for exploring how ossification periods and sequences are shaped by differences in larval environment and growth trajectory, and how plasticity in the early part of a sequence impacts later ossification and adult morphology.

HOW LUNG USE MIGHT IMPACT AMPHIBIAN OSSIFICATION SEQUENCES

When and where bone accumulates in the body might be adaptive in how bone weight rather than bone strength contributes to tadpole breathing, feeding, and locomotion. This derives from amphibian larvae having not one, but four respiratory organs: lungs, gills, skin, and the buccopharyngeal epithelium. The additional organs make lung use essentially optional for larval respiration, and while some amphibians have lost lungs altogether (Rose and James, 2013), others fall on a spectrum of larval lung use, with the extremes showing conspicuous differences in ossification, feeding and locomotion.

At one extreme, *Xenopus* tadpoles are suspension feeders that stay in the water column, and start lung breathing immediately after hatching (Rose and James, 2013). Their large lungs remain undivided, do little gas exchange under normal conditions (Burggren and West, 1982; Feder and Wassersug, 1984), and are not essential for life (Rose and James, 2013). Indeed, tadpoles denied access to air will metamorphose and live for years without inflating their lungs, and they can initiate lung use and resume lung development at any point in tadpole life (Rose and James, 2013). *Xenopus* tadpoles mostly likely use lungs to provide buoyancy as an energy saving measure for midwater living. The buoyancy is offset by beating a vertically flexed tail (Rose et al., 2018) and bone formation that starts at mid larval stages and produces a relatively well-ossified head and trunk by the start of metamorphosis (**Figures 1**, **2**, Sedra and Michael, 1957; Trueb and Hanken, 1992). *Xenopus* tadpoles reduce activity to avoid predators (Kruger et al., 2019), but rarely settle on the bottom unless they have been air-deprived (Rose and James, 2013). *Xenopus* tadpoles thus appear committed to midwater living, and their lungs and larval bones collectively support a head-down, tail-up swimming posture.

At the other extreme, toad tadpoles have tiny lung buds that are not inflated until metamorphosis (Wassersug and Seibert, 1975). They spend much of their time feeding and lying on the bottom (Tejedo, 1993), and often fall to the bottom rather than actively swimming there (Rose, pers. obs.). Since toads do not modify their tail size, shape or color in response to predators (Benard and Fordyce, 2003), their delayed lung use supports benthic living and avoiding the water column where they are more prone to predation (Tejedo, 1993). Toads also have late ossification, especially in the skull, which acquires most bones during and after metamorphosis (Gaudin, 1978; Gómez et al., 2017; **Figure 2**, Dunlap and Sanchiz, 1996). An ossified trunk and unossified head means a more posterior center of gravity and less forward momentum when swimming, which would facilitate rapid, passive settlement and immobility as an escape response. At the same time, differences in larval ossification are likely to have consequence for the onset of postmetamorphic locomotion. Whereas *Pseudacris* treefrogs jump to and from horizontal and vertical surfaces the moment they leave the water, *Anaxyrus* toads are noticeably less agile, appearing to learn to walk before they learn to jump (Rose, pers. obs., Wassersug and Sperry, 1977). How larval lung use and bone appearances have co-evolved to support different styles of larval swimming and feeding, and early juvenile movement and habitat use (Altig and Johnston, 1989; Bruce et al., 1994) represents another avenue for analyzing ossification sequences that emphasizes midlife adaptation over embryonic influence and adult function.

TOWARD A MORE INCLUSIVE APPROACH FOR UNDERSTANDING THE EVOLUTION OF OSSIFICATION

The two prevailing perspectives in evolutionary morphology are forward- and backward-looking in that one views early development through the lens of functional demands imposed by adulthood, and the other views adult morphology through the lens of embryonic events that influence postembryonic development. By virtue of their exceptional lateness, variability and plasticity, amphibian ossification sequences defy an explanation based strictly on governance by embryonic processes and compliance with adult functional demands. In addition to the two perspectives, amphibians call for a third, more "in-the-moment" perspective to embrace the interplay among environment, behavior, and physiology that directly shapes growth and development after embryogeny and before adulthood. This means implicitly a whole-animal approach that integrates bone appearances with other developmental events and traits such as using carbonate deposits as mineral reserves and lungs for buoyancy. It also means a whole-ontogeny approach that recognizes intermediate life history stages as being informative of how organisms diversify *regardless of* their impact on adult form and function. This would apply to all vertebrates and not just those whose larval and post-metamorphic bodies

have already been shown to evolve independently of each other (Sherratt et al., 2017).

Both modern (Polachowski and Werneburg, 2013; Simon and Marroig, 2017) and classical (Miller, 1923; Tchernavin, 1938) studies of vertebrate skeletons have proposed that differences in bone growth explain more of the adult skeleton than differences in timing of bone appearance or bone origin. There has been ample research on how bone and cartilage growth is affected by mechanical stress for mammals and birds (Murray, 1936; Herring, 1993; Hall, 2005), but relatively little for anamniotes, especially ones with biphasic development. We are beginning to understand the cellular mechanisms that regulate skeletal shape during growth (Vandenberg et al., 2012; Rose, 2014b; Kaucka et al., 2017; Pinet et al., 2019) and that produce interspecific differences in long bone (Farnum et al., 2008; Cooper et al., 2013) and dermal bone shapes (Slater et al., 2009). We have yet to investigate how plasticity in skeletal growth is regulated by the environmental, behavioral, and physiological factors discussed here and elsewhere (Aubret and Shine, 2009; Serrat, 2014). Thanks to big data approaches, our knowledge of both the gene regulatory networks underlying embryonic morphogenesis and the evolutionary patterns exhibited by adult skeletons is expanding at phenomenal rates. At the same time, it is important to recall not only that "ontogeny [and not just embryogeny] creates phylogeny" (Garstang, 1922), but that the cellular, behavioral and physiological processes which create morphological differences play out over entire ontogenies and can be impacted directly by environment.

DATA AVAILABILITY STATEMENT

The original contributions presented in the study are included in the article/supplementary material, further inquiries can be directed to the corresponding author/s.

ETHICS STATEMENT

The animal study was reviewed and approved by IACUC, James Madison University Office of Research Integrity.

AUTHOR CONTRIBUTIONS

The author confirms being the sole contributor of this work and has approved it for publication.

FUNDING

This research was supported by the Biology Department, James Madison University.

REFERENCES

Agar, W. E. (1906). The development of the skull and visceral arches in *Lepidosiren* and *Protopterus*. *Trans. Roy. Soc. Edinburgh* 45, 49–64. doi: 10.1017/S0080456800011637

Alberch, P. (1980). Ontogenesis and morphological diversification. *Amer. Zool.* 20, 653–667. doi: 10.1093/icb/20.4.653

Alberch, P. (1989). The logic of monsters: evidence for internal constraint in development and evolution. *Geobios Mémoire Spécial* 12, 21–57. doi: 10.1016/S0016-6995(89)80006-3

Alcalde, L., and Barg, M. (2006). Chondrocranium and cranial muscle morphology in *Lysapsus* and *Pseudis* tadpoles (Anura: Hylidae: Hylinae). *Acta Zoolog.* 87, 91–100. doi: 10.1111/j.1463-6395.2006.00205.x

Alford, R. A., and Harris, R. N. (1988). Effects of larval growth history on anuran metamorphosis. *Amer. Nat.* 131, 91–106. doi: 10.1086/284775

Allen, B. M. (1918). The results of thyroid removal in the larvae of *Rana pipiens*. *J. Exp. Zool. A Ecol. Genetics Physiol.* 24, 499–519. doi: 10.1002/jez.1400240303

Alley, K. E. (1989). Myofiber turnover is used to retrofit frog jaw muscles during metamorphosis. *Amer. J. Anat.* 184, 1–12. doi: 10.1002/aja.1001840102

Altig, R., and Johnston, G. F. (1989). Guilds of anuran larvae: relationships among developmental modes, morphologies, and habitats. *Herpetol. Monogr.* 3, 81–109. doi: 10.2307/1466987

Altig, R., and McDiarmid, R. W. (2015). *Handbook of Larval Amphibians of the United States and Canada*. Ithaca, NY: Cornell University Press. doi: 10.7591/9780801456084

Ashley-Ross, M. A., and Gillis, G. B. (2002). A brief history of vertebrate functional morphology. *Int. Comp. Biol.* 42, 183–189. doi: 10.1093/icb/42.2.183

Aubret, F., and Shine, R. (2009). Genetic assimilation and the postcolonization erosion of phenotypic plasticity in island tiger snakes. *Curr. Biol.* 19, 1932–1936. doi: 10.1016/j.cub.2009.09.061

Austad, S. N. (1993). Retarded senescence in an insular population of virginia opossums (*Didelphis virginiana*). *J. Zool.* 229, 695–708. doi: 10.1111/j.1469-7998.1993.tb02665.x

Bartsch, P., Gemballa, S., and Piotrowski, T. (1997). The embryonic and larval development of *Polypterus senegalus cuvier*, 1829: its staging with reference to external and skeletal features, behaviour and locomotory habits. *Acta Zoolog.* 78, 309–328. doi: 10.1111/j.1463-6395.1997.tb01014.x

Becker, K. B., Stephens, K. C., Davey, J. C., Schneider, M. J., and Galton, V. A. (1997). The type 2 and type 3 iodothyronine deiodinases play important roles in coordinating development in *Rana catesbeiana* tadpoles. *Endocrinology* 138, 2989–2997. doi: 10.1210/endo.138.7.5272

Benard, M. F., and Fordyce, J. A. (2003). Are induced defenses costly? Consequences of predator-induced defenses in western toads, *Bufo boreas*. *Ecology* 84, 68–78. doi: 10.1890/0012-9658(2003)084[0068:AIDCCO]2.0.CO;2

Berry, D. L., Rose, C. S., Remo, B. F., and Brown, D. D. (1998). The expression pattern of thyroid hormone response genes in remodeling tadpole tissues defines distinct growth and resorption gene expression programs. *Dev. Biol.* 203, 24–35. doi: 10.1006/dbio.1998.8975

Blanchard, F. N. (1923). The life-history of the four-toed salamander. *Amer. Nat.* 57, 262–268. doi: 10.1086/279920

Brewster, B. (1987). Eye migration and cranial development during flatfish metamorphosis: a reappraisal (Teleostei: Pleuronectiformes). *J. Fish Biol.* 31, 805–833. doi: 10.1111/j.1095-8649.1987.tb05281.x

Brown, D. D. (2005). The role of deiodinases in amphibian metamorphosis. *Thyroid* 15, 815–821. doi: 10.1089/thy.2005.15.815

Brown, H. A. (1990). Morphological variation and age-class determination in overwintering tadpoles of the tailed frog, *Ascaphus truei*. *J. Zool.* 220, 171–184. doi: 10.1111/j.1469-7998.1990.tb04301.x

Bruce, R. C. (1980). A model of the larval period of the spring salamander, *Gyrinophilus porphyriticus* based on size-frequency distributions. *Herpetologica* 36, 78–86.

Bruce, R. C. (1988). Life history variation in the salamander *Desmognathus quadramaculatus*. *Herpetologica* 44, 218–227.

Bruce, R. C., Beachy, C. K., Lenzo, P. G., Pronych, S. P., and Wassersug, R. J. (1994). Effects of lung reduction on rheotactic performance in amphibian larvae. *J. Exp. Zool.* 268, 377–380. doi: 10.1002/jez.1402680506

Buckbinder, L., and Brown, D. D. (1992). Thyroid hormone-induced gene expression changes in the developing frog limb. *J. Biol. Chem.* 267, 25786–25791. doi: 10.1016/S0021-9258(18)35678-3

Burggren, W. W., and West, N. H. (1982). Changing respiratory importance of gills, lungs and skin during metamorphosis in the bullfrog *Rana catesbeiana*. *Respir. Physiol.* 47, 151–164. doi: 10.1016/0034-5687(82)90108-6

Bury, R. B., and Adams, M. J. (1999). Variation in age at metamorphosis across a latitudinal gradient for the tailed frog, ascaphus truei. *Herpetologica* 55, 283–291.

Chapelle, K. E. J., Fernandez, V., and Choiniere, J. N. (2020). Conserved in-ovo cranial ossification sequences of extant saurians allow estimation of embryonic dinosaur developmental stages. *Sci. Rep.* 10:4224. doi: 10.1038/s41598-020-60292-z

Cloutier, R., Caron, A., Grünbaum, T., and Le François, N. R. (2010). Effect of water velocity on the timing of skeletogenesis in the arctic charr, *Salvelinus alpinus* (salmoniformes: Teleostei): an empirical case of developmental plasticity. *Int. J. Zool.* 2010:470546 doi: 10.1155/2010/470546

Cooper, K. L., Oh, S., Sung, Y., Dasari, R. R., Kirschner, M. W., and Tabin, C. J. (2013). Multiple phases of chondrocyte enlargement underlie differences in skeletal proportions. *Nature* 495, 375–378. doi: 10.1038/nature11940

Cubbage, C. C., and Mabee, P. M. (1996). Development of the cranium and paired fins in the zebrafish *Danio rerio* (Ostariophysi, Cyprinidae). *J. Morphol.* 229, 121–160. doi: 10.1002/(SICI)1097-4687(199608)229:2<121::AID-JMOR1>3.0.CO;2-4

Dodd, M. H. I., and Dodd, J. M. (1976). "The biology of metamorphosis," in *Physiology of the Amphibia*, ed B. Lofts (New York, NY: Academic Press), 467–599. doi: 10.1016/B978-0-12-455403-0.50015-3

Downie, J. R., Ramnarine, I., Sams, K., and Walsh, P. T. (2009a). The paradoxical frog pseudis paradoxa: larval habitat, growth and metamorphosis. *Herpetol. J.* 19, 11–19.

Downie, J. R., Sams, K., and Walsh, P. T. (2009b). The paradoxical frog *Pseudis paradoxa*: larval anatomical characteristics, including gonadal maturation. *Herpetol. J.* 19, 1–10.

Dunlap, K. D., and Sanchiz, B. (1996). Temporal dissociation between the development of the cranial appendicular skeletons in *Bufo bufo* (Amphibia: Bufonidae). *Herpetol* 30, 506–513. doi: 10.2307/1565693

Etkin, W. (1935). The mechanisms of anuran metamorphosis: 1. Thyroxine concentration and the metamorphic pattern. *J. Exp. Zool.* 71, 317–340. doi: 10.1002/jez.1400710208

Fabrezi, M. (2011). Heterochrony in growth and development in anurans from the chaco of south america. *Evol. Biol.* 38, 390–411. doi: 10.1007/s11692-011-9128-5

Fabrezi, M., and Goldberg, J. (2009). Heterochrony during skeletal development of *Pseudis platensis* (Anura, Hylidae) and the early offset of skeleton development and growth. *J. Morphol.* 270, 205–220. doi: 10.1002/jmor.10680

Fabrezi, M., Manzano, A. S., Abdala, V., and Lobo, F. (2014). Anuran locomotion: ontogeny and morphological variation of a distinctive set of muscles. *Evol. Biol.* 41, 308–326. doi: 10.1007/s11692-014-9270-y

Fabrezi, M., Quinzio, S. I., and Goldberg, J. (2009). Giant tadpole and delayed metamorphosis of *Pseudis platensis gallardo*, 1961 (Anura, Hylidae). *J. Herpetol.* 43, 228–243. doi: 10.1670/08-028R3.1

Fabrezi, M., Quinzio, S. I., and Goldberg, J. (2010). The ontogeny of *Pseudis platensis* (Anura, Hylidae): heterochrony and the effects of larval development on postmetamorphic life. *J. Morphol.* 271, 496–510. doi: 10.1002/jmor.10815

Farnum, C. E., Tinsley, M., and Hermanson, J. W. (2008). Forelimb versus hindlimb skeletal development in the big brown bat, *Eptesicus fuscus*: functional divergence is reflected in chondrocytic performance in autopodial growth plates. *Cells Tissues Organ.* 187, 35–47. doi: 10.1159/000109962

Feder, M. E., and Wassersug, R. J. (1984). Aerial versus aquatic oxygen consumption in larvae of the clawed frog, *Xenopus laevis*. *J. Exp. Biol.* 108, 231–245.

Felice, R. N., and Goswami, A. (2018). Developmental origins of mosaic evolution in the avian cranium. *PNAS* 115:555. doi: 10.1073/pnas.1716437115

Fox, H. (1985). "Changes in amphibian skin during larval development and metamorphosis," in *Metamorphosis*, ed M. Balls and M. Bownes (Oxford: Clarendon Press), 221–259.

Garstang, W. (1922). The theory of recapitulation: a critical re-statement of the biogenetic law. *Zool. J. Linnean Soc. London* 35, 81–101. doi: 10.1111/j.1096-3642.1922.tb00464.x

Gaudin, A. J. (1973). The development of the skull in the pacific tree frog, *Hyla regilla*. *Herpetologica* 29, 205–218.

Gaudin, A. J. (1978). The sequence of cranial ossification in the california toad, *Bufo boreas* (Amphibia, Anura, Bufonidae). *J. Herpetol.* 12, 309–318. doi: 10.2307/1563611

Germain, D., and Laurin, M. (2009). Evolution of ossification sequences in salamanders and urodele origins assessed through event-pairing and new methods. *Evol. Dev.* 11, 170–190. doi: 10.1111/j.1525-142X.2009.00318.x

Gilbert, L. I., Tata, J. R., and Atkinson, B. G. (1996). *Metamorphosis: Postembryonic Reprogramming of Gene Expression in Amphibian and Insect Cells*. San Diego: Academic Press.

Gilbert, S. F., and Barresi, M. J. F. (2016). *Developmental Biology*. Sunderland, MA: Sinauer Assoc., Inc.

Gluckmann, I., Huriaux, F., Focant, B., and Vandewalle, P. (1999). Postembryonic development of the cephalic skeleton in *Dicentrarchus labrax* (Pisces, Perciformes, Serranidae). *Bull. Marine Sci.* 65, 11–36.

Glücksohn, S. (1931). Äussere entwicklung der extremitäten und stadieneinteilung der larvenperiode von *Triton taeniatus leyd. Und Triton cristatus laur. Wilhelm Roux' Archiv fur Entwicklungsmechanik der Organismen* 125, 341–405. doi: 10.1007/BF00576359

Gómez, R., l,. O., Regueira, E., O'Donohoe, M. E. A., and Hermida, G. N. (2017). Delayed osteogenesis and calcification in a large true toad with a comparative survey of the timing of skeletal ossification in anurans. *Zool. Anzeiger* 267, 101–110. doi: 10.1016/j.jcz.2017.03.002

Gomez-Mestre, I., Saccoccio, V. L., Iijima, T., Collins, E. M., Rosenthal, G. G., and Warkentin, K. M. (2010). The shape of things to come: linking developmental plasticity to post-metamorphic morphology in anurans. *J. Evol. Biol.* 23, 1364–1373. doi: 10.1111/j.1420-9101.2010.02016.x

Gosner, K. (1960). A simplified table for staging anuran embryos and larvae with notes on identification. *Herpetologica* 16, 183–190.

Gould, S. J. (1986). Archetype and adaptation. *Nat. History* 10, 16–27.

Gould, S. J., and Lewontin, R. C. (1979). The spandrels of San Marco and the panglossian paradigm: a critique of the adaptationist programme. *Proc. R. Soc. Lond. B.* 205, 581–598. doi: 10.1098/rspb.1979.0086

Grünbaum, T., Cloutier, R., and Dumont, P. (2003). "Congruence between chondrification and ossification sequences during caudal skeleton development: a moxostomatini case study," in *The big fish bang. Proceedings of the 26th annual larval fish conference*, ed H. I. Browman and A. B. Skiftesvik (Bergen, Norway: Institute of Marine Research, Postboks), 161–176.

Haas, A. (1999). Larval and metamorphic skeletal development in the fast-developing frog *Pyxicephalus adspersus* (anura, ranidae). *Zoomorphology* 119, 23–35. doi: 10.1007/s004350050078

Haas, A., and Richards, S. J. (1998). Correlations of cranial morphology, ecology, and evolution in australian suctorial tadpoles of the genera *Litoria* and *Nyctimystes* (Amphibia: Anura: Hylidae: Pelodryadinae). *J. Morphol.* 238, 109–141. doi: 10.1002/(SICI)1097-4687(199811)238:2<109::AID-JMOR1>3.0.CO;2-#

Hall, B. K. (2005). *Bones and Cartilage, Developmental and Evolutionary Skeletal Biology*. San Diego: Elsevier Academic Press. doi: 10.1016/B978-0-12-319060-4.50065-8

Hall, B. K., and Hanken, J. (1985). "Forward," in *The Development of the Vertebrate Skull* (Oxford: Oxford University Press), vii–xxviii.

Hall, J., Jheon, A. H., Ealba, E. L., Eames, B. F., Butcher, K. D., Mak, S. S., et al. (2014). Evolution of a developmental mechanism: species-specific regulation of the cell cycle and the timing of events during craniofacial osteogenesis. *Dev. Biol.* 385, 380–395. doi: 10.1016/j.ydbio.2013.11.011

Hallgrímsson, B., Jamniczky, H., Young, N. M., Rolian, C., Parsons, T. E., Boughner, J. C., et al. (2009). Deciphering the palimpsest: studying the relationship between morphological integration and phenotypic covariation. *Evol. Biol.* 36, 355–376. doi: 10.1007/s11692-009-9076-5

Hanken, J., and Gross, J. B. (2005). Evolution of cranial development and the role of neural crest: insights from amphibians. *J. Anat.*207, 437–446. doi: 10.1111/j.1469-7580.2005.00481.x

Hanken, J., and Hall, B. K. (1984). Variation and timing of the cranial ossification sequence of the oriental fire-bellied toad, *Bombina orientalis* (Amphibia, Discoglossidae). *J. Morphol.* 182, 245–255. doi: 10.1002/jmor.1051820302

Hanken, J., and Hall, B. K. (1988a). Skull development during anuran metamorphosis: I. Early development of the first three bones to form–the

exoccipital, the parasphenoid, and the frontoparietal. *J. Morphol.* 195, 247–256. doi: 10.1002/jmor.1051950303

Hanken, J., and Hall, B. K. (1988b). Skull development during anuran metamorphosis. II. Role of thyroid hormone in osteogenesis. *Anat. Embryol.* 178, 219–227. doi: 10.1007/BF00318225

Harrington, S. M., Harrison, L. B., and Sheil, C. A. (2013). Ossification sequence heterochrony among amphibians. *Evol. Dev.* 15, 344–364. doi: 10.1111/ede.12043

Hautier, L., Weisbecker, V., Goswami, A., Knight, F., Kardjilov, N., and Asher, R. J. (2011). Skeletal ossification and sequence heterochrony in xenarthran evolution. *Evol. Dev.* 13, 460–476. doi: 10.1111/j.1525-142X.2011.00503.x

Herring, S. W. (1993). "Epigenetic and functional influences on skull growth," in *The Skull*, ed J. Hanken and B. K. Hall (Chicago: University of Chicago Press), 153–206.

Hildebrand, M., Bramble, D. M., Liem, K. F., and Wake, D. B. (1985). *Functional Vertebrate Morphology*. Cambridge, MA: Harvard University Press.

Ishizeki, K., Kagiya, T., Fujiwara, N., Otsu, K., and Harada, H. (2010). Biological significance of site-specific transformation of chondrocytes in mouse meckel's cartilage. *J. Oral Biosci.* 52, 136–142. doi: 10.1016/S1349-0079(10)80042-8

Ishizuya-Oka, A., and Shi, Y. B. (2007). Regulation of adult intestinal epithelial stem cell development by thyroid hormone during *Xenopus laevis* metamorphosis. *Dev. Dyn.* 236, 3358–3368. doi: 10.1002/dvdy.21291

Iwasawa, H., and Kera, Y. (1980). Normal stages of development of the japanese lungless salamander, onychodactylus japonicus (houttuyn). *Jap. J. Herpetol* 8, 73–89. doi: 10.5358/hsj1972.8.3_73

Jandzik, D., Garnett, A. T., Square, T. A., Cattell, M. V., Yu, J. K., and Medeiros, D. M. (2015). Evolution of the new vertebrate head by co-option of an ancient chordate skeletal tissue. *Nature* 518, 534–537. doi: 10.1038/nature14000

Jandzik, D., Hawkins, M. B., Cattell, M. V., Cerny, R., Square, T. A., and Medeiros, D. M. (2014). Roles for fgf in lamprey pharyngeal pouch formation and skeletogenesis highlight ancestral functions in the vertebrate head. *Development* 141, 629–638. doi: 10.1242/dev.097261

Jeffery, J. E., Bininda-Emonds, O. R. P., Coates, M. I., and Richardson, M. K. (2005). A new technique for identifying sequence heterochrony. *Systemat. Biol.* 54, 230–240. doi: 10.1080/10635150590923227

Jollie, M. (1980). Development of head and pectoral fin girdle skeleton and scales in *Acipenser*. *Copeia* 1980, 226–249. doi: 10.2307/1444000

Jollie, M. (1984a). Development of cranial and pectoral girdle bones of *Lepisosteus* with a note on scales. *Copeia* 476–502. doi: 10.2307/1445204

Jollie, M. (1984b). Development of the head and pectoral skeleton of *Amia* with a note on scales. *Gegenbaurs morphologisches Jahrbuch* 130, 315–351.

Jollie, M. (1984c). Development of the head and pectoral skeleton of *Polypterus* with a note on scales (pisces: Actinoptergii). *J. Zool.* 204, 469–507. doi: 10.1111/j.1469-7998.1984.tb02382.x

Kaucka, M., Zikmund, T., Tesarova, M., Gyllborg, D., Hellander, A., Jaros, J., et al. (2017). Oriented clonal cell dynamics enables accurate growth and shaping of vertebrate cartilage. *eLife* 6:25902. doi: 10.7554/eLife.25902

Kemp, N. E., and Hoyt, J. A. (1969). Sequence of ossification in the skeleton of growing and metamorphosing tadpoles of *Rana pipiens*. *J. Morphol.* 129, 415–444. doi: 10.1002/jmor.1051290404

Kerney, R., Wassersug, R., and Hall, B. K. (2010). Skeletal advance and arrest in giant non-metamorphosing african clawed frog tadpoles (*Xenopus laevis: Daudin*). *J. Anat.* 216, 132–143. doi: 10.1111/j.1469-7580.2009.01176.x

Koyabu, D., Werneburg, I., Morimoto, N., Zollikofer, C. P. E., Forasiepi, A. M., Endo, H., et al. (2014). Mammalian skull heterochrony reveals modular evolution and a link between cranial development and brain size. *Nat. Commun.* 5:3625. doi: 10.1038/ncomms4625

Kruger, N., Measey, J., Herrel, A., and Secondi, J. (2019). Anti-predator strategies of the invasive african clawed frog, *Xenopus laevis*, to native and invasive predators in western france. *Aquat. Invasions* 14, 433–443. doi: 10.3391/ai.2019.14.3.03

Lannoo, M. J. (1987). Neuromast topography in anuran amphibians. *J. Morphol.* 191, 115–129. doi: 10.1002/jmor.1051910203

Lebedkina, N. S. (1960a). Development of the bones of the palatal arch in the caudate amphibia. *Doklady* 131, 218–220.

Lebedkina, N. S. (1960b). Development of the parasphenoid in the caudate amphibia. *Doklady* 133, 539–542.

Lebedkina, N. S. (1964). Development of the nasal bones in the caudate amphibia. *Doklady* 159, 787–790.

Lebedkina, N. S. (1968). "The development of bones in the skull roof of amphibia," in *Current Problems of Lower Vertebrate Phylogeny*, ed T. Orvig (Stockholm: Interscience Publ.), 317–329.

Lebedkina, N. S. (2004). *Evolution of the Amphibian Skull Sophia*. Bulgaria: Pensoft.

Leloup, J., and Buscaglia, M. (1977). La triiodothyronine, hormone de la métamorphose des amphibiens. *Comptes Rendus des séances de l'Academie des Sciences, Série D* 284, 2261–2263.

Limbaugh, B. A., and Volpe, E. P. (1957). Early development of the gulf coast toad, *Bufo valliceps* wiegmann. *Amer. Museum Novitates* 1842, 1–32.

Ma, Q., Liu, S. F., Wang, X. X., Xiang, Z. L., and Zhuang, Z. M. (2019). Skeletal development of the chondrocranium in the tongue sole *Cynoglossus semilaevis* (Pleuronectiformes: Cynoglossidae). *J. Fish Biol.* 94, 223–230. doi: 10.1111/jfb.13870

Mabee, P. M., and Trendler, T. A. (1996). Development of the cranium and paired fins in *Betta splendens* (Teleostei: Percomorpha): intraspecific variation and interspecific comparisons. *J. Morphol.* 227, 249–287. doi: 10.1002/(SICI)1097-4687(199603)227:3<249::AID-JMOR1>3.0.CO;2-1

Maglia, A. M. (2003). Skeletal development of *Pelobates cultripes* and a comparison of the osteogenesis of pelobatid frogs (anura: Pelobatidae). *Nat. Hist. Museum Univ. Kansas Sci. Pap.* 30, 1–13. doi: 10.5962/bhl.title.10142

Markle, D. F. (1984). Phosphate buffered formalin for long term preservation of formalin fixed ichthyoplankton. *Copeia* 1984, 525–528. doi: 10.2307/1445208

Maxwell, E. E. (2008). Ossification sequence of the avian order anseriformes, with comparison to other precocial birds. *J. Morphol.* 269, 1095–1113. doi: 10.1002/jmor.10644

Maxwell, E. E., Harrison, L. B., and Larsson, H. C. E. (2010). Assessing the phylogenetic utility of sequence heterochrony: evolution of avian ossification sequences as a case study. *Zoology* 113, 57–66. doi: 10.1016/j.zool.2009.06.002

Maxwell, E. E., and Larsson, H. C. E. (2009). Comparative ossification sequence and skeletal development of the postcranium of palaeognathous birds (aves: Palaeognathae). *Zool. J. Linnean Soc.* 157, 169–196. doi: 10.1111/j.1096-3642.2009.00533.x

Miller, G. S. (1923). The telescoping of the cetacean skull (with eight plates). *Smithson. Miscellan. Collect.* 76, 1–68.

Mitgutsch, C., Wimmer, C., Sánchez-Villagra, M. R., Hahnloser, R., and Schneider, R. A. (2011). Timing of ossification in duck, quail, and zebra finch: lntraspecific variation, heterochronies, and life history evolution. *Zool. Sci.* 28, 491–500. doi: 10.2108/zsj.28.491

Miyauchi, H., LaRochelle, F. T. Jr., Suzuki, M., Freeman, M., and Frieden, E. (1977). Studies on thyroid hormones and their binding in bullfrog tadpole plasma during metamorphosis. *Gen. Comp. Endocrinol.* 33, 254–266. doi: 10.1016/0016-6480(77)90250-7

Mondou, P. M., and Kaltenbach, J. C. (1979). Thyroxine concentrations in blood serum and pericardial fluid of metamorphosing tadpoles and of adult frogs. *Gen. Comp. Endocrinol.* 39, 343–349. doi: 10.1016/0016-6480(79)90131-X

Moore, M. K., and Townsend, V. R. Jr. (2003). Intraspecific variation in cranial ossification in the tailed frog, ascaphus truei. *J. Herpetol.* 37, 714–717. doi: 10.1670/246-01N

Murray, P. D. F. (1936). *Bones. A Study of the Development and Structure of the Vertebrate Skeleton*. Cambridge: Cambridge University Press.

Newman, R. A. (1989). Developmental plasticity of *Scaphiopus couchii* tadpoles in an unpredictable environment. *Ecology* 70, 1775–1787. doi: 10.2307/1938111

Nieuwkoop, P. D., and Faber, J. (1956). *Normal table of Xenopus laevis (daudin). A systematical and chronological survey of the development from the fertilized egg till the end of metamorphosis*. Amsterdam: North-Holland Publishing Company.

Norman, M. F. (1985). A practical method for staging metamorphis in the tiger salamander *Ambystoma tigrinum*. *Anat. Rec.* 211, 102–109. doi: 10.1002/ar.1092110115

Nunn, C. L., and Smith, K. K. (1998). Statistical analyses of developmental sequences: the craniofacial region in marsupial and placental mammals. *Amer. Natur.* 152, 82–101. doi: 10.1086/286151

Ollonen, J., Da Silva, F. O., Mahlow, K., and Di-Poï, N. (2018). Skull development, ossification pattern, and adult shape in the emerging lizard model organism

Pogona vitticeps: a comparative analysis with other squamates. *Front. Physiol.* 9:278. doi: 10.3389/fphys.2018.00278

Pehrson, T. (1940). The development of dermal bones in the skull of *Amia calva*. *Acta Zool.* 21, 1–50. doi: 10.1111/j.1463-6395.1940.tb00338.x

Pehrson, T. (1944). Some observations on the development and morphology of the dermal bones in the skull of *Acipenser* and *Polyodon*. *Acta Zool.* 25, 27–48. doi: 10.1111/j.1463-6395.1944.tb00343.x

Pehrson, T. (1949). The ontogeny of the lateral line system in the head of dipnoans. *Acta Zool.* 30, 153–182. doi: 10.1111/j.1463-6395.1949.tb00505.x

Pehrson, T. (1958). The early ontogeny of the sensory lines and the dermal skull in *Polypterus*. *Acta Zool.* 39, 241–258. doi: 10.1111/j.1463-6395.1958.tb00387.x

Petranka, J. W. (1998). *Salamanders of the United States and Canada*. Washington: Smithsonian Institution Press.

Pilkington, J. B., and Simkiss, K. (1966). The mobilization of the calcium carbonate deposits in the endolymphatic sacs of metamorphosing frogs. *J. Exp. Biol.* 45:329.

Pinet, K., Deolankar, M., Leung, B., and McLaughlin, K. A. (2019). Adaptive correction of craniofacial defects in pre-metamorphic *Xenopus laevis* tadpoles involves thyroid hormone-independent tissue remodeling. *Development* 146:dev175893. doi: 10.1242/dev.175893

Polachowski, K. M., and Werneburg, I. (2013). Late embryos and bony skull development in *Bothropoides jararaca* (Srpentes, Viperidae). *Zoology* 116, 36–63. doi: 10.1016/j.zool.2012.07.003

Regard, E., Taurog, A., and Nakashima, T. (1978). Plasma thyroxine and triiodothyronine levels in spontaneously metamorphosing *Rana catesbeiana* tadpoles and in adult anuran amphibia. *Endocrinology* 102, 674–684. doi: 10.1210/endo-102-3-674

Regueira, E., Dávila, C., and Hermida, G. N. (2016). Morphological changes in skin glands during development in *Rhinella arenarum* (Anura: Bufonidae). *Anat. Rec.* 299, 141–156. doi: 10.1002/ar.23284

Reiss, J. O. (1989). The meaning of developmental time: a metric for comparative embryology. *Amer. Nat.* 134, 170–189. doi: 10.1086/284974

Richman, J. M., Buchtová, M., and Boughner, J. C. (2006). Comparative ontogeny and phylogeny of the upper jaw skeleton in amniotes. *Dev. Dyn.* 235, 1230–1243. doi: 10.1002/dvdy.20716

Rieppel, O. (1988). *Fundamentals of Comparative Biology*. Basel: Birkhauser Verlag.

Rieppel, O. (1993a). Studies on skeleton formation in reptiles: patterns of ossification in the skeleton of *Chelydra serpentina* (Reptilia, Testudines). *J. Zool.* 231, 487–509. doi: 10.1111/j.1469-7998.1993.tb01933.x

Rieppel, O. (1993b). Studies on skeleton formation in reptiles. V. Patterns of ossification in the skeleton of *Alligator mississippiensis* daudin (*Reptilia, Crocodylia*). *Zool. J. Linnean Soc.* 109, 301–325. doi: 10.1111/j.1096-3642.1993.tb02537.x

Rieppel, O. (1994). Studies on skeleton formation in reptiles: patterns of ossification in the skeleton of *Lacerta agilis exigua eichwald* (Reptilia, Squamata). *J Herpetol.* 28, 145–153. doi: 10.2307/1564613

Rose, C. S. (1995). Skeletal morphogenesis in the urodele skull: III. Effect of hormone dosage in TH-induced remodelling. *J. Morphol.* 223, 243–261. doi: 10.1002/jmor.1052230303

Rose, C. S. (1996). An endocrine-based model for developmental and morphogenetic diversification in metamorphic and paedomorphic urodeles. *J. Zool.* 239, 253–284. doi: 10.1111/j.1469-7998.1996.tb05451.x

Rose, C. S. (1999). "Hormonal control in larval development and evolution—Amphibians," in *The Origin and Evolution of Larval Forms*, eds B. K. Hall and M. H. Wake (San Diego: Academic Press), 167–216. doi: 10.1016/B978-012730935-4/50007-9

Rose, C. S. (2003a). "The developmental morphology of salamander skulls," in *Amphibian Biology, vol. 5. Osteology*, eds H. Heatwole and M. Davies (Chipping Norton, Australia: Surrey Beatty and Son Pty. Ltd.), 1686–1783.

Rose, C. S. (2003b). "Thyroid hormone-mediated development in vertebrates: What makes frogs unique?" in *Environment, Development and Evolution*, eds G. B. Müller, B. K. Hall and R. D. Pearson (Boston: MIT), 197–237.

Rose, C. S. (2005). Integrating ecology and developmental biology to explain the timing of frog metamorphosis. *TREE* 20, 129–134. doi: 10.1016/j.tree.2005.01.005

Rose, C. S. (2014a). Caging, but not air deprivation, slows tadpole growth and development in the amphibian *Xenopus laevis*. *J. Exp. Zool. A Ecol. Genetics Physiol.* 321, 365–375. doi: 10.1002/jez.1867

Rose, C. S. (2014b). The importance of cartilage to amphibian development and evolution. *Int. J. Dev. Biol.* 58, 917–927. doi: 10.1387/ijdb.150053cr

Rose, C. S., Aleagha, O., Modolo, C., and Hoguet, N. (2018). Xenopus tails are unique in combining whip-like lateral undulations and vertical extension and flexion. *Int. Comp. Biol.* 58:E409.

Rose, C. S., and Cahill, J. W. (2019). How thyroid hormones and their inhibitors affect cartilage growth and shape in the frog xenopus laevis. *J. Anat.* 234, 89–105. doi: 10.1111/joa.12897

Rose, C. S., and James, B. (2013). Plasticity of lung development in the amphibian, *Xenopus laevis*. *Biol. Open* 2, 1324–1335. doi: 10.1242/bio.20133772

Rose, C. S., Murawinski, D., and Horne, V. (2015). Deconstructing cartilage shape and size into contributions from embryogenesis, metamorphosis, and tadpole and frog growth. *J. Anat.* 226, 575–595. doi: 10.1111/joa.12303

Rose, C. S., and Reiss, J. O. (1993). "Metamorphosis and the vertebrate skull: ontogenetic patterns and developmental mechanisms," in *The Skull*, eds J. Hanken and B. K. Hall (Chicago: University of Chicago Press), 289–346.

Rugh, R. (1962). *Experimental Embryology Techniques and Procedures*. Minneapolis, MN: Burgess Publishing Co. doi: 10.5962/bhl.title.6412

Sachs, L. M., and Buchholz, D. R. (2019). Insufficiency of thyroid hormone in frog metamorphosis and the role of glucocorticoids. *Front. Endocrinol.* 10:287. doi: 10.3389/fendo.2019.00287

Sánchez-Villagra, M. R. (2002). Comparative patterns of postcranial ontogeny in therian mammals: an analysis of relative timing of ossification events. *J. Exp. Zool.* 294, 264–273. doi: 10.1002/jez.10147

Sánchez-Villagra, M. R., Goswami, A., Weisbecker, V., Mock, O., and Kuratani, S. (2008). Conserved relative timing of cranial ossification patterns in early mammalian evolution. *Evol. Dev.* 10, 519–530. doi: 10.1111/j.1525-142X.2008.00267.x

Schneider, R. A. (2018). Neural crest and the origin of species-specific pattern. *Genesis* 56, 1–33. doi: 10.1002/dvg.23219

Schreiber, A. M. (2006). Asymmetric craniofacial remodeling and lateralized behavior in larval flatfish. *J. Exp. Biol.* 209, 610–621. doi: 10.1242/jeb.02056

Schreiber, A. M., Cai, L., and Brown, D. D. (2005). Remodeling of the intestine during metamorphosis of *Xenopus laevis*. *PNAS* 102, 3720–3725. doi: 10.1073/pnas.0409868102

Sedra, S. N., and Michael, M. I. (1957). The development of the skull, visceral arches, larynx and visceral muscles of the south african clawed toad, *Xenopus laevis* (daudin) during the process of metamorphosis (from stage 55 to stage 66). *Verhandelingen der Koninklijke Nederlandse Akademie van Wetenschappen, Afdeling Natuurkunde. Tweede Reeks* 51, 1–80.

Senevirathne, G., Kerney, R., and Meegaskumbura, M. (2017). Comparative postembryonic skeletal ontogeny in two sister lineages of old world tree frogs (Rhacophoridae: *Taruga, polypedates*). *PLoS ONE* 12:167939. doi: 10.1371/journal.pone.0167939

Serrat, M. A. (2014). Environmental temperature impact on bone and cartilage growth. *Comp. Physiol.* 4, 621–655. doi: 10.1002/cphy.c130023

Sheil, C. A., Jorgensen, M., Tulenko, F., and Harrington, S. (2014). Variation in timing of ossification affects inferred heterochrony of cranial bones in lissamphibia. *Evol. Dev.* 16, 292–305. doi: 10.1111/ede.12092

Sherratt, E., Vidal-García, M., Anstis, M., and Keogh, J. S. (2017). Adult frogs and tadpoles have different macroevolutionary patterns across the australian continent. *Nat. Ecol. Evol.* 1, 1385–1391. doi: 10.1038/s41559-017-0268-6

Shi, D., and Boucaut, J. (1995). The chronological development of the urodele amphibian *Pleurodeles waltl* (*michah*). *Int. J. Dev. Biol.* 39, 427–441.

Shi, Y.-B. (2000). *Amphibian Metamorphosis: From Morphology to Molecular Biology*. New York, NY: John Wiley & Sons.

Simon, M. N., and Marroig, G. (2017). Evolution of a complex phenotype with biphasic ontogeny: contribution of development versus function and climatic variation to skull modularity in toads. *Ecol. Evol.* 7, 10752–10769. doi: 10.1002/ece3.3592

Slater, B. J., Liu, K. J., Kwan, M. D., Quarto, N., and Longaker, M. T. (2009). Cranial osteogenesis and suture morphology in *Xenopus laevis*: a unique model system for studying craniofacial development. *PLoS ONE* 4:e3914. doi: 10.1371/journal.pone.0003914

Smirnov, S. V. (1992). The influence of variation in larval period on adult cranial diversity in *Pelobates fuscus* (Anura: Pelobatidae). *J. Zool.* 226, 601–612. doi: 10.1111/j.1469-7998.1992.tb07503.x

Smirnov, S. V., Merkulova, K. M., and Vassilieva, A. B. (2020). Skull development in the iberian newt, *Pleurodeles waltl* (Salamandridae: Caudata: Amphibia): timing, sequence, variations, and thyroid hormone mediation of bone appearance. *J. Anatomy* 237, 543–555. doi: 10.1111/joa.13210

Smirnov, S. V., and Vassilieva, A. B. (2009). Number of ossification centers in the anuran cranial bones depends upon the rate of development: experimental evidence. *Russian J. Herptol.* 16, 167–176.

Smirnov, S. V., and Vassilieva, A. B. (2014). Thyroid hormones in the skeletogenesis and accessory sources of endogenous hormones in *Xenopus laevis* (Amphibia; Anura) ontogeny: experimental evidence. *Doklady Biol. Sci.* 455, 136–138. doi: 10.1134/S0012496614020185

Smith, K. K. (1997). Comparative patterns of craniofacial development in eutherian and metatherian mammals. *Evolution* 51, 1663–1678. doi: 10.1111/j.1558-5646.1997.tb01489.x

Sterner, Z. R., Shewade, L. H., Mertz, K. M., Sturgeon, S. M., and Buchholz, D. R. (2020). Glucocorticoid receptor is required for survival through metamorphosis in the frog *Xenopus tropicalis*. *Gen. Comp. Endocrinol.* 291:113419. doi: 10.1016/j.ygcen.2020.113419

Strauss, R. E. (1990). Heterochronic variation in the developmental timing of cranial ossifications in poeciliid fishes (Cyprinodontiformes). *Evolution* 44, 1558–1567. doi: 10.1111/j.1558-5646.1990.tb03846.x

Strauss, R. E. (1999). Brain-tissue accumulation of fluorescent age pigments in four poeciliid fishes (Cyprinodontiformes) and the estimation of "biological age." *Growth Dev. Aging* 63, 151–170.

Suzuki, S., and Suzuki, M. (1981). Changes in thyroidal and plasma Iodine compounds during and after metamorphosis of the bullfrog, *Rana catesbeiana*. *Gen. Comp. Endocrinol.* 45, 74–81. doi: 10.1016/0016-6480(81)90171-4

Tata, J. R., Kawahara, A., and Baker, B. S. (1991). Prolactin inhibits both thyroid hormone-induced morphogenesis and cell death in cultured amphibian larval tissues. *Dev. Biol.* 146, 72–80. doi: 10.1016/0012-1606(91)90447-B

Taylor, A. C., and Kollros, J. J. (1946). Stages in the normal development of *Rana pipiens* larvae. *Anat. Rec.* 94, 7–23. doi: 10.1002/ar.1090940103

Tchernavin, V. (1938). Changes in the salmon skull. *Trans. Zool. Soc. London* 24, 103–184. doi: 10.1111/j.1096-3642.1938.tb00390.x

Tejedo, M. (1993). Size-dependent vulnerability and behavioral responses of tadpoles of two anuran species to beetle larvae predators. *Herpetologica* 49, 287–294.

Terry, G. S. (1918). Effects of the extirpation of the thyroid gland upon ossification in *Rana pipiens*. *J. Exp. Zool.* 24, 567–587. doi: 10.1002/jez.1400240306

Trueb, L. (1966). Morphology and development of the skull in the frog *Hyla septentrionalis*. *Copeia* 1966, 562–573. doi: 10.2307/1441083

Trueb, L. (1985). A summary of osteocranial development in anurans with notes on the sequence of cranial ossification in *Rhinophrynus dorsalis* (Anura: Pipoidea: Rhinophrynidae). *S. African J. Sci.* 81, 181–185.

Trueb, L. (1993). "Patterns of cranial diversity among the lissamphibia," in *The Skull* eds J. Hanken and B. K. Hall (Chicago: University of Chicago Press), 255–343.

Trueb, L., and Hanken, J. (1992). Skeletal development in *Xenopus laevis* (Anura: Pipidae). *J. Morphol.* 214, 1–41. doi: 10.1002/jmor.1052140102

Vandenberg, L. N., Adams, D. S., and Levin, M. (2012). Normalized shape and location of perturbed craniofacial structures in the xenopus tadpole reveal an innate ability to achieve correct morphology. *Dev. Dyn.* 241, 863–878. doi: 10.1002/dvdy.23770

Velhagen, W. A. Jr. (1997). Analyzing developmental sequences using sequence units. *System. Biol.* 46, 204–210. doi: 10.1093/sysbio/46.1.204

Wada, H., Ghysen, A., Satou, C., Higashijima, S.-,i., Kawakami, K., Hamaguchi, S., et al. (2010). Dermal morphogenesis controls lateral line patterning during postembryonic development of teleost fish. *Dev. Biol.* 340, 583–594. doi: 10.1016/j.ydbio.2010.02.017

Wagemans, F., and Vandewalle, P. (2001). Development of the bony skull in common sole: brief survey of morpho-functional aspects of ossification sequence. *J. Fish Biol.* 59, 1350–1369. doi: 10.1111/j.1095-8649.2001.tb00197.x

Wake, D. B. (1980). Evidence of heterochronic evolution: a nasal bone in the olympic salamander, *Rhyacotriton olympicus*. *J. Herpetol.* 14, 292–295. doi: 10.2307/1563553

Walker, M. B., and Kimmel, C. B. (2007). A two-color acid-free cartilage and bone stain for zebrafish larvae. *Biotech. Histochem.* 82, 23–28. doi: 10.1080/10520290701333558

Wassersug, R. J., and Hoff, K. (1982). "Developmental changes in the orientation of the anuran jaw suspension," in *Evolutionary Biology*, eds M. K. Hecht, B. Wallace and G. T. Prance (New York, NY: Plenum), 223–246. doi: 10.1007/978-1-4615-6968-8_5

Wassersug, R. J., and Seibert, E. A. (1975). Behavioral responses of amphibian larvae to variation in dissolved oxygen. *Copeia* 1975, 86–103. doi: 10.2307/1442410

Wassersug, R. J., and Sperry, D. G. (1977). The relationship of locomotion to differential predation of *Pseudacris triseriata* (Anura: Hylidae). *Ecology* 58, 830–839. doi: 10.2307/1936218

Weil, M. R. (1986). Changes in plasma thyroxine levels during and after spontaneous metamorphosis in a natural population of the green frog, *Rana clamitans*. *Gen. Comp. Endocrinol.* 62, 8–12. doi: 10.1016/0016-6480(86)90088-2

Weisbecker, V., and Mitgutsch, C. (2010). A large-scale survey of heterochrony in anuran cranial ossification patterns. *J. Zool. Systematics Evolut. Res.* 48, 332–347. doi: 10.1111/j.1439-0469.2010.00570.x

Werneburg, I., Polachowski, K. M., and Hutchinson, M. N. (2015). Bony skull development in the argus monitor (Squamata, Varanidae, *Varanus panoptes*) with comments on developmental timing and adult anatomy. *Zoology* 118, 255–280. doi: 10.1016/j.zool.2015.02.004

White, B. A., and Nicoll, C. S. (1981). "Hormonal control of amphibian metamorphosis," in *Metamorphosis: A Problem in Developmental Biology*, eds L. I. Gilbert and E. Frieden (New York, NY: Plenum Press), 363–396. doi: 10.1007/978-1-4613-3246-6_11

Wilbur, H. M., and Collins, J. P. (1973). Ecological aspects of amphibian metamorphosis. *Science* 182, 1305–1314. doi: 10.1126/science.182.4119.1305

Wild, E. R. (1997). Description of the adult skeleton and developmental osteology of the hyperossified horned frog, *Ceratophrys cornuta* (Anura: Leptodactylidae). *J. Morphol.* 232, 169–206. doi: 10.1002/(SICI)1097-4687(199705)232:2<169::AID-JMOR4>3.0.CO;2-5

Wild, E. R. (1999). Description of the chondrocranium and osteogenesis of the chacoan burrowing frog, *Chacophrys pierotti* (Anura: Leptodactylidae). *J. Morphol.* 242, 229–246. doi: 10.1002/(SICI)1097-4687(199912)242:3<229::AID-JMOR3>3.0.CO;2-N

Woronowicz, K. C., and Schneider, R. A. (2019). Molecular and cellular mechanisms underlying the evolution of form and function in the amniote jaw. *EvoDevo* 10:8. doi: 10.1186/s13227-019-0131-8

Yaoita, Y. (2019). Tail resorption during metamorphosis in *Xenopus* tadpoles. *Front. Endocrinol.* 10:143. doi: 10.3389/fendo.2019.00143

Yaoita, Y., and Brown, D. D. (1990). A correlation of thyroid hormone receptor gene expression with amphibian metamorphosis. *Genes Dev.* 4, 1917–1924. doi: 10.1101/gad.4.11.1917

Yeh, J. (2002). The evolution of development: two portraits of skull ossification in pipoid frogs. *Evolution* 56, 2484–2498. doi: 10.1111/j.0014-3820.2002.tb00173.x

Conflict of Interest: The author declares that the research was conducted in the absence of any commercial or financial relationships that could be construed as a potential conflict of interest.

frontiers in Ecology and Evolution

ORIGINAL RESEARCH
published: 03 March 2021
doi: 10.3389/fevo.2021.619594

How Can Termites Achieve Their Unparalleled Postembryonic Developmental Plasticity? A Test for the Role of Intermolt-Specific High Juvenile Hormone Titers

Judith Korb[1], Carolin Greiner[2], Marion Foget[2] and Adrian Geiler[1]*

[1] Behavioural Biology, University of Osnabrück, Osnabrück, Germany, [2] Evolutionary Biology and Ecology, University of Freiburg, Freiburg, Germany

Termites are "social cockroaches" and amongst the most phenotypically plastic insects. The different castes (i.e., two types of reproductives, workers, and soldiers) within termite societies are all encoded by a single genome and present the result of differential postembryonic development. Besides the default progressive development into winged sexuals of solitary hemimetabolous insects, termites have two postembryonic, non-terminal molts (stationary and regressive; i.e., molts associated, respectively, with no change or reduction of size/morphological differentiation) which allow them to retain workers, and two terminal developmental types to become soldiers and replacement reproductives. Despite this unique plasticity, especially the mechanisms underlying the non-terminal development are poorly understood. In 1982, Nijhout and Wheeler proposed a model how this diversity might have evolved. They proposed that varying juvenile hormone (JH) titers at the start, mid-phase, and end of each intermolt period account for the developmental diversity. We tested this rarely addressed model in the lower termite *Cryptotermes secundus* using phase-specific pharmacological manipulations of JH titers. Our results partially support the Nijhout and Wheeler model. These data are supplemented with gene expression studies of JH-related genes that characterize different postembryonic developmental trajectories. Our study provides new insights into the evolution of the unique postembryonic developmental plasticity of termites that constitutes the foundation of their social life.

Keywords: developmental plasticity, social insect, juvenile hormone, molt, methoprene, JH epoxidase, krüppel-homolog 1

OPEN ACCESS

Edited by:
Fernando Casares, Andalusian Center for Development Biology (CABD), Spain

Reviewed by:
Bertrand Fouks, University of Münster, Germany
Vincent Debat, Muséum National d'Histoire Naturelle, France

****Correspondence:***
Judith Korb
judith.korb@biologie.uni-freiburg.de

Specialty section:
This article was submitted to Evolutionary Developmental Biology, a section of the journal Frontiers in Ecology and Evolution

Received: *20 October 2020*
Accepted: *09 February 2021*
Published: *03 March 2021*

Citation:
Korb J, Greiner C, Foget M and Geiler A (2021) How Can Termites Achieve Their Unparalleled Postembryonic Developmental Plasticity? A Test for the Role of Intermolt-Specific High Juvenile Hormone Titers. Front. Ecol. Evol. 9:619594. doi: 10.3389/fevo.2021.619594

INTRODUCTION

Termites (Infraorder: Isoptera) are unparalleled when it comes to developmental plasticity in insects which is the basis of their caste system (Noirot, 1990; Roisin, 2000; Korb and Hartfelder, 2008; Roisin and Korb, 2011; Korb and Thorne, 2017). Like in all eusocial insects, their colonies are characterized by overlapping generations and a reproducing caste, the queens (and in termites, also kings), and non-reproducing workers that generally perform tasks like brood care and foraging

(**Figure 1**). Due to their different ancestry, termites as "social cockroaches" (Inward et al., 2007) have a hemimetabolous development, while eusocial Hymenoptera (ants, bees, and wasps) belong to the holometabolous insects. In line, the workers of eusocial Hymenoptera are imaginal stages, while those of termites are immature instars, which can be arrested in their development in some lineages (Noirot, 1990; Roisin, 2000; Korb and Hartfelder, 2008; Roisin and Korb, 2011).

The highest developmental plasticity is observed in the two lower termite families Archotermopsidae (dampwood termites) and Kalotermitidae (drywood termites) as all eggs hatching within a colony appear totipotent to perform all molting types (Roisin, 2000; Roisin and Korb, 2011). These wood-dwelling termites (one-piece nesting, sensu Abe, 1987) nest in a single piece of wood that serves as food and shelter and which workers never leave to forage outside. Here the functional workers (ontogenetically also defined as "pseudergates *sensu lato*"; for simplicity, we will refer to them as "workers" in the following) are totipotent immatures that can develop into three terminal castes (Noirot and Pasteels, 1987; Noirot, 1990; Roisin, 2000; Korb and Hartfelder, 2008; Roisin and Korb, 2011; **Figure 1**). First, they can develop via one to several nymphal instars (instars with wingbuds) into winged sexuals that disperse and found a new colony. Second, they can become sterile soldiers via a presoldier instar. Third, they can develop with a single (sometimes two) molt/s into neotenic (replacement) reproductives that reproduce within the natal nest, especially when the current reproductives die or are unhealthy. The soldiers and neotenic reproductives are synapomorphies which distinguish termites from their subsocial sister taxon, the *Cryptocercus* woodroaches (Noirot and Pasteels, 1987; Noirot, 1990; Roisin, 2000; Korb and Hartfelder, 2008). This "progressive" development that finally results in terminal castes is complemented by two additional molting types that "allow" immatures staying as workers in the nest (**Figure 1**): (i) stationary molts during which individuals molt without any change of size or morphology, and (ii) regressive molts which are associated with reduction of size and/or developmental traits (especially wing buds). While stationary molts also occur in "solitary" cockroaches (Bell et al., 2007), regressive molts are unique to termites. This makes termites examples of unparalleled postembryonic developmental diversity. Developmental details (e.g., in the number of nymphal instars) can differ between species (Roisin and Korb, 2011). Development is regulated by hormones. In insects there are two major morphogenic hormones known to control development: juvenile hormone (JH) and ecdysone (e.g., Nijhout, 1994; Gilbert, 2012).

How can interactions between just two morphogenic hormones produce such diversity in molting types? Like in most insects, JHIII is the only JH moiety produced by termite corpora allata and detected in hemolymph (Lanzrein et al., 1985; Park and Raina, 2004; Brent et al., 2005; Yagi et al., 2005; Cornette et al., 2008). Based on seminal termite research in the 1950's and 60's (summarized in Lüscher, 1974b; Lenz, 1976), Nijhout and Wheeler (1982) developed a model (NW-model hereafter) to explain the developmental diversity in termites. They proposed three JH sensitive phases during an intermolt period (i.e., the time between two consecutive molts) which determine the subsequent molting type of a "lower termite" worker (**Figure 2**). These three phases occur at the start (phase 1), during mid-phase (phase 2), and toward the end (phase 3) of an intermolt period and they control, respectively, sexual reproductive traits, non-sexual adult traits (e.g., eyes and wings), and soldier traits (for more details see **Figure 2**). According to NW-model, a worker that develops progressively into a nymphal instar, and finally into a winged imago, is proposed to have low JH titers throughout all three sensitive phases (**Figure 2**). Continuously high JH titers characterize presoldier-soldier differentiation (**Figure 2**). Development of neotenic replacement reproductives requires low JH titers at the start of an intermolt period that increase later. As neotenic molts have shortened intermolt periods (Springhetti, 1972; Lüscher, 1974b; Hoffmann and Korb, 2011), they molt before the third sensitive phase (**Figure 2**). Finally, the reverse pattern with first high, then low JH titers is suggested to characterize individuals that remain immature workers. This last proposition does not distinguish between stationary and regressive molts. In addition, Lüscher (1956) and Springhetti (1969) suggested that regressive molts are associated with (constantly) high JH titers and that high JH titers during nymphal stages prevent development of termite workers into sexuals.

Except for the terminal molts into soldiers (see recent reviews: Miura and Scharf, 2011; Watanabe et al., 2014; Korb, 2015) and partly neotenic reproductives (Elliott and Stay, 2008; reviewed in: Korb, 2015), the NW-model remains largely untested. Very few studies addressed differences between progressive, stationary and regressive postembryonic development; these studies provide some evidence that progressive development is associated low JH titers (Lüscher, 1974b; Cornette et al., 2008; Korb et al., 2009, Korb et al., 2012). We systematically manipulated JH titers during all three phases of an intermolt period in nymphal instars of the wood-dwelling, drywood termite *Cryptotermes secundus* Hill (Kalotermitidae) to determine the influence of JH on development. These data are supplemented with gene expression studies of JH-related genes that are supposed to be associated with postembryonic developmental trajectories.

C. secundus is well suited to do these experiments. The developmental trajectories of the totipotent workers, comprising older larval, and nymphal instars, are well known (Korb and Katrantzis, 2004; Korb et al., 2009, Korb et al., 2012). *C. secundus* has three worker larval and five nymphal instars and except for the 4th, penultimate nymphal instar the intermolt period lasts about 2 months (Korb and Katrantzis, 2004; Korb et al., 2009, Korb et al., 2012). All instars can develop progressively and stationary (including nymphs); regressive development is possible for all instars, except the first and second larval instar. All instars that can develop regressively, can also develop into soldiers and neotenic replacement reproductives (Korb and Katrantzis, 2004; Hoffmann and Korb, 2011). Progressive development from 1st to 5th nymphal instar is associated with decreasing hemolymph JH titers and regressive molts have been hypothesized to be linked with high JH titers (Korb et al., 2009). However, during an intermolt period JH titers vary considerably

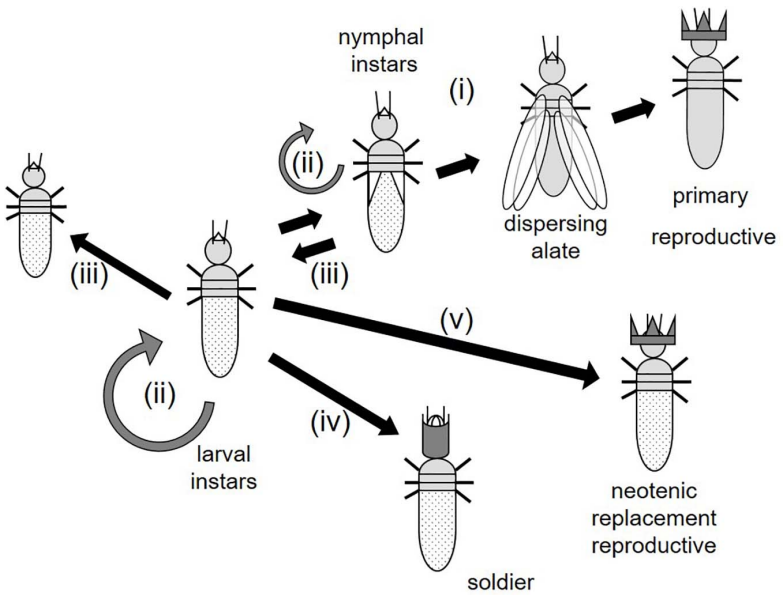

FIGURE 1 | Developmental plasticity of wood-dwelling termites. Immatures (larval and nymphal instars) can (i) develop progressively via several nymphal instars into winged sexuals (alates) that disperse and found a nest as primary reproductives, (ii) remain in the same instar by doing stationary molts (gray circles), (iii) develop regressively into an "earlier" instar, (iv) develop into a soldier, or (v) a neotenic replacement reproductive. For further information, see text. Adapted from Korb et al. (2012).

(Korb et al., 2012) and it is unclear whether and how different phases account for different molting types.

We tested the importance of JH in determining development by phase-specific manipulations using the JH analogon methoprene. Methoprene is a stable JH analogon that has been used successful in several experiments to induce soldier development in termites, generally in soldierless groups (e.g., Tarver et al., 2012; Maekawa et al., 2014). We did our experiments with complete colonies, including soldiers and reproductives. This is important in order to separate a social effect due to the presence/absence of castes from the endocrine effect of varying JH titers (Watanabe et al., 2014; Korb and Bellés, 2017). This is not possible with dish-assays that consist of workers only.

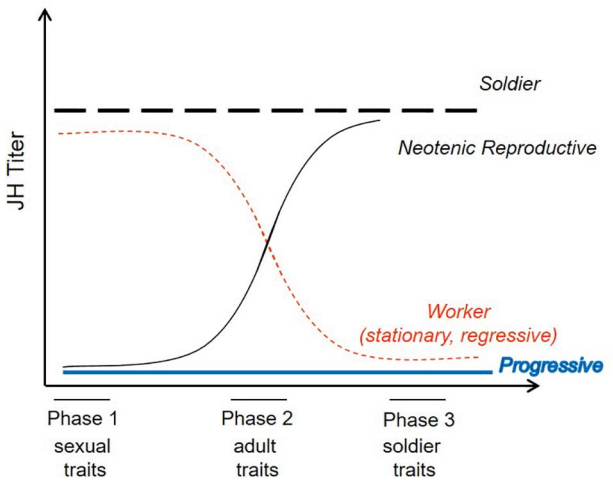

FIGURE 2 | Model proposed by Nijhout and Wheeler (1982) to explain the endocrine regulation of molting types in termites. JH titers during three sensitive periods (phases) between two consecutive molts determine the subsequent molting type of a termite worker. Continuously high or low titers result, respectively, in presoldier/soldier differentiation or progressive development toward winged imagoes. Titers that vary during the intermolt period account for neotenic and continued worker development. For further information, see text. Adapted from Nijhout and Wheeler (1982).

MATERIALS AND METHODS

Collection and Maintenance of Termites

Complete *Cryptotermes secundus* colonies were collected from *Ceriops tagal* trees in the mangrove area near Darwin (NT, Australia; 12°30′S 131°00′E) as described elsewhere (Korb and Lenz, 2004). Colonies were set up in standardized *Pinus radiata* wood blocks adjusted to colony size, providing abundant resource conditions (1 termite: about 10 cm^3 wood; for details see Korb and Lenz, 2004). Colonies were transferred to Germany and kept in climate chambers (12 h day/night cycle, 28°C, 70% relative humidity). Under these conditions, colony development as well as molting types and developmental trajectories of individuals in relocated lab colonies are indistinguishable from relocated colonies kept in the field (Korb and Katrantzis, 2004).

Preparation of Experimental Colonies

In order to follow individual development, wood blocks were split in Germany and their colonies were transferred into a drilled chamber of a new abundant-food wood block, which

allowed monitoring of individuals (for details see: Korb and Schmidinger, 2004). To prevent the termites from disappearing into the wood, newly dug tunnels were blocked with soft paper. Wood chips and humid filter paper was provided as additional food and water supply.

All our experiments were done with complete colonies including soldiers and workers. "Artificial" groups consisting of workers only are often used in similar studies. However, such worker groups are less appropriate because they lack important social interactions leading to artificial results. Thus, it is for instance known that the absence of castes influence development of individuals (e.g., Lüscher, 1974b; Lenz, 1976; Korb and Katrantzis, 2004; Maekawa et al., 2012; Watanabe et al., 2014). Our set-up also prevented neotenic and soldier differentiation which is triggered in *C. secundus* by the absence of the corresponding caste (Korb et al., 2003; Hoffmann and Korb, 2011). All colonies used in this experiment were a maximum of 2 years in the laboratory when the experiments were performed. To avoid seasonal differences all experiments were done between April and August when nymphal development takes place (Korb and Katrantzis, 2004).

For individual identification, workers were arbitrarily selected and marked with an individual color code of enamel paint (Revell, Germany) on the abdomen and/or thorax. Individuals were checked at least four times per week throughout the duration of the experiment to ensure they retained their markings.

Before a molt, individuals become whitish and translucent. These individuals were separated for the length of the molt. Their developmental stage was classified into instars according to wing bud shape and size before and after the molt (for more details see: Korb and Katrantzis, 2004) to identify molting types.

Endocrine Experiment

In order to do phase-specific manipulations we had to follow single individuals over extended periods (generally about 3–5 months). Freshly marked individuals were followed until their next molt which defined the start of the subsequent intermolt period. We performed three sets of experiments that addressed, respectively, phase 1, 2, and 3 of the intermolt period. Accordingly, we treated nymphal instars within the next 2 days after the molt (phase 1), 4 weeks after the molt (phase 2), or before the subsequent molt (indicated by their whitish and translucent appearance, which occurs 3–6 days before the next molt) (phase 3). After treatment all individuals were monitored until their next molt to determine subsequent, experimentally affected molting types.

The manipulations of JH titers consisted in topical application of the JH analogon, methoprene (99%, Sigma-Aldrich, Germany) (2 μl of 1 μg methoprene/10 μl acetone solution) on nymphs. Untreated nymphs served as controls (for a test of potential solvent effects, see next section "Supplementary Experiments and Rational for Set-Ups"). In total, we marked and followed over 1,000 individuals of which we could record the development of 870 individuals (control: 792, 15 colonies; methoprene treated individuals: phase 1: 51 individuals from five colonies; phase 2: 12 individuals from four colonies; phase 3: 15 individuals from to two colonies) from a total of 26 different colonies (see **Supplementary Data Set 1**). Individuals of the different treatments always originated from different colonies. Despite intensive efforts of monitoring all individuals at least four times a week, we were unable to follow over 50% of the treated individuals until the end of our experiments because they lost their individual identifying marks during the months-long duration of this experiment. As *C. secundus* has small colonies of generally less than 200 individuals (Korb and Lenz, 2004; Korb and Schneider, 2007) (here between 53 and 215 individuals), we were able to record the development of a considerable fraction of individuals within each colony.

Supplementary Experiments and Rational for Set-Ups

We did several supplementary experiments to test the suitability of methods. First, we compared the development between acetone (solvent) and untreated individuals. It showed that acetone does not seem to affect a nymphs subsequent molting type compared to untreated individuals (chi^2 contingency analysis: $N_{acetone} = 44$, $N_{untreated} = 792$, $\chi^2_{2,836} = 3.12$, $P = 0.210$). Second, we tested the suitability of methoprene to emulate effects of increased JH titers. We chose a concentration of 2 μl of 1 μg methoprene/10 μl acetone solution per nymph based on former studies (Tarver et al., 2012; Maekawa et al., 2014), taking into account body size differences between species. This separate experiment showed that the mortality rate of methoprene-treated nymphs using these concentrations did not differ significantly from those of control individuals (survival untreated: 72%, survival methoprene: 88%; chi^2 contingency analysis: $N_{methoprene} = 17$, $N_{untreated} = 25$, $\chi^2_{1,42} = 1.58$, $P = 0.208$). This experiment covered a period until, and including, the next molt of an individual; most mortality occurred during molting when the animals are separated from the colony. Finally, we tested whether such a methoprene treatment results in an upregulation of JH signaling as increased JH titers do. Note, methoprene is an JH analogon and not JH, hence its titers cannot be determined using methods such as radio-immunoassays that measure JH directly. Therefore, we measured gene expression of genes involved in JH signaling by performing quantitative realtime PCR (qRT-PCR) experiment (see next section "qRT-PCR"). We quantified the expression of *Kr-h1* (*Krüppel-homolog 1*, *CsecKr-h1*), which is an early response gene upregulated under high JH titers in insects (e.g., Bellés et al., 2005; Bellés and Santos, 2014; Jindra et al., 2015). Additionally, we tested genes supposed to be involved in JH biosynthesis: two JH epoxidases (P450-15A1; *CsecJH epoxidase1* and *CsecJH epoxidase2*) and the supposed two JH receptor genes, *CsecMet* (*Methoprene-tolerant*) and *CsecTai* (*Taiman*) (for more details on genes and methods, see below) (Harrison et al., 2018; Jongepier et al., 2018). If methoprene treatment functions efficiently, these four JH biosynthesis genes should not be affected by methoprene treatment. As expected, none of the genes associated with JH biosynthesis was affected by our methoprene treatment (Kruskal Wallis tests: always $P > 0.305$) but *CsecKr-h1* was significantly upregulated in methoprene-treated individuals compared to untreated and acetone treated individuals (Kruskal Wallis test:

$\chi^2_{2,30}$ = 7.51, P = 0.023, Dunn-Bonferroni *Post hoc* tests: $N_{untreated}$ = 19, $N_{acetone}$ = 5, $N_{methoprene}$ = 6; untreated vs. methoprene: $z = -2.52$, P = 0.035; acetone vs. methoprene: $z = -2.36$, P = 0.055; untreated vs. acetone: z = 0.50, P = 1.00). These results show that our methoprene treatment specifically up-regulated JH signaling and that acetone did not have a similar JH effect.

qRT-PCR

To obtain insights into JH titers and genetic mechanisms underlying postembryonic development, we performed qRT-PCR experiments of selected genes expressed in the head and thorax that are known to be associated with JH signaling in other insects, including cockroaches (e.g., Bellés et al., 2005; Bellés and Santos, 2014; Jindra et al., 2015):

(i) *CsecKr-h1*, the *C. secundus* 1:1 ortholog of the early response gene of JH signaling in the fruit fly *D. melanogaster Kr-h1*;
(ii) two JH epoxidases (P450-15A genes), *CsecJH epoxidase1* and *CsecJH epoxidase2*; these two genes have been identified as an ortholog and a paralog of the *D. melanogaster JH epoxidase* that synthesize JH (Harrison et al., 2018; Jongepier et al., 2018). As we do not know which of both genes has the same function in *C. secundus*, we tested both genes.
(iii) *CsecMet*, a 1:1 ortholog of the gene *Methoprene-tolerant* (*met*) of the cockroach *Blattella germanica* whose protein functions as receptor of JH (Jindra et al., 2015);
(iv) *CsecTai*, a 1:1 ortholog of the *B. germanica* gene *Taiman* (*Tai*) which encodes a protein that dimerizises with Met upon JH binding (Jindra et al., 2015). The resulting JH-Met-Tai complex then induces transcription of the early response gene *Kr-h1* in *B. germanica* and other insects (Jindra et al., 2015).

qRT-PCR was performed as described elsewhere (Elsner et al., 2018). In short, total RNA of head and thorax was extracted according to the peqGOLD TriFast protocol as described in Elsner et al. (2018). RNA concentration and purity were measured with a Nanodrop 2000c (peqLab) and the RNA was diluted to 25 ng/µl with nuclease-free H_2O. Reverse transcription and qRT-PCR were performed with a LightCycler 96 (Roche) using the QuantiTect SYBR Green RT-PCR Kit (Qiagen). We used a reaction volume of 25 µl. After reverse transcription for 1,800 s at 50°C and an initial activation for 900 s at 95°C, 50 amplification cycles were run. These consisted of 15 s of denaturation at 95°C, 30 s of annealing at 62°C, and 70 s of extension at 72°C. This was followed by a melting step with 10 s at 95°C, 60 s at 65°C, and 1 s at 97°C, followed by a cooling step for 30 s at 37°C. We checked the amplification and melting curves to ensure target specificity. We used *18S rRNA* to normalize expression, as it was previously established to be stable expressed in termites (Weil et al., 2007). Three technical replicates per gene and sample were done. For primer sequences see **Supplementary Table S1**.

Using this approach (i) we tested whether methropene results in increased JH signaling (see above), (ii) we inferred the JH titers before and after a molt, and (iii) we associated molting types (progressive, stationary, regressive) with JH related gene expression and JH titers after a molt. Note, it is impossible to determine gene expression before a molt and link it with the potential subsequent molting type as one cannot predict how an individual would have molted if one would not have killed it for gene expression analysis.

For these experiments, we used another set of 17 *C. secundus* colonies. The experimental procedure was identical to that described in "Endocrine manipulations." All gene expression data are provided as **Supplementary Data Set 2**.

Statistical Analyses

Endocrine Experiment

To test whether an increase in JH signaling influenced developmental trajectories of nymphs, we compared the frequency of molting types (i.e., the number how often a molting type occurred) after methoprene treatment with those of control individuals. Colony identity affected molting type frequencies. Hence, we performed generalized mixed models with multinomial error distributions and "treatment" as fixed factor and "colony ID" as random factor to control for colony effects. All models differed significantly compared to a null model (see section "Results"). With *post hoc* tests we compared changes in frequencies relative to the proportion of regressive molts. To do this, we applied the Satterthwaite approach which is especially useful if the data are unbalanced like in our case where we had more control than treated individuals. All analyses were done separately for each phase to identify which phase is crucial for affecting developmental trajectories.

Gene Expression Studies

For none of the five studied genes, gene expression was affected by colony identity (Kruskal-Wallis tests: always $P > 0.100$). Hence, we analyzed gene expression data with Mann Whitney-U-tests (before vs. after molt) or Kruskal Wallis-tests (all other analyses) and applied FDR correction for multiple testing.

All statistical analyses were performed using IBM SPSS 26 and all tests were two-tailed.

RESULTS

Effect of Methoprene on Molting Type Frequencies

During the study period, untreated, control nymphs mainly performed stationary molts (360 molts, 45.5%), followed by progressive (280 molts, 35.4%) and regressive molts (152 molts, 19.2%) (**Figure 3**).

Increased JH signaling induced by methoprene treatment resulted during all three phases in altered molting types. Methoprene treatment directly after a molt (phase 1) significantly changed molting type frequencies [$F_{(2,\ 839)}$ = 13.56, $P < 0.001$] with more regressive and less progressive molts compared to control individuals (**Figure 3**). *Post hoc* testing revealed that compared to the frequency of regressive molts, the number of progressive molts significantly decreased, while those of stationary molts was unaffected (progressive vs. regressive:

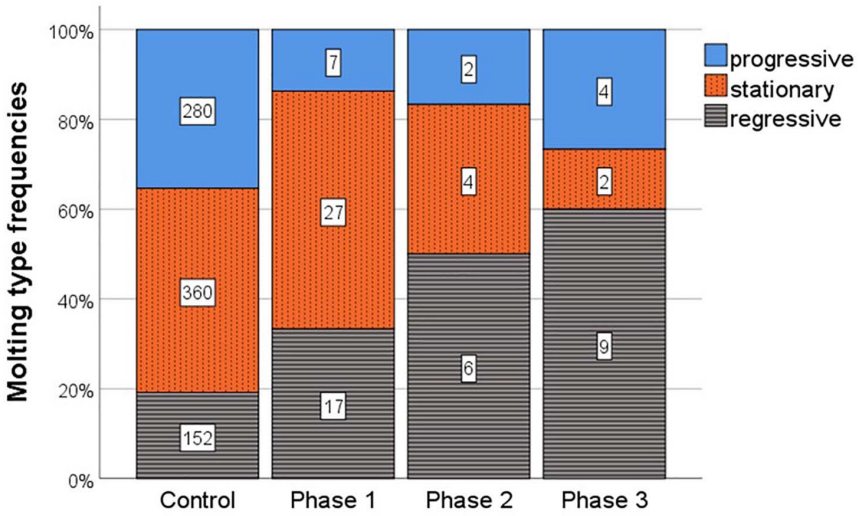

FIGURE 3 | Molting type frequencies (i.e., number of each type of molt) after induction of JH signaling with methoprene during three phases of the intermolt period and in untreated control individuals. Shown are the frequencies of progressive (blue, filled), stationary (orange, dotted vertical stripes), and regressive (gray/black, horizontal stripes) molting types. Numbers inside bar show absolute numbers of each type of molt, the *y*-axis represents this as relative proportions.

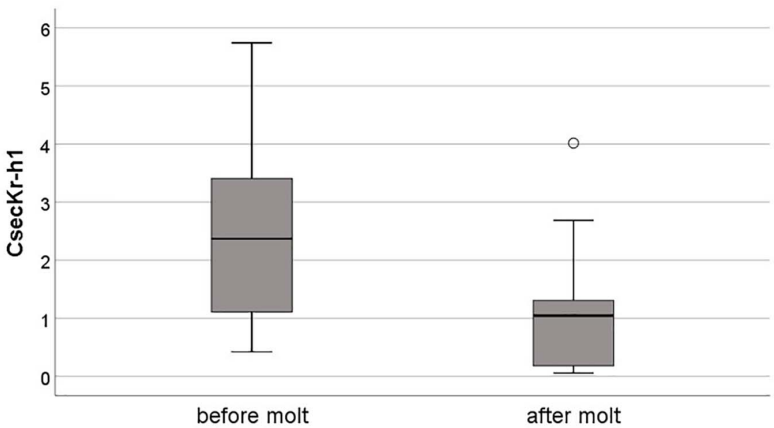

FIGURE 4 | Relative expression of the *CsecKr-h1* before and after a molt in untreated individuals. The expression of this early response gene of JH signaling was significantly higher before than after a molt. Shown are boxplots with median, quartiles, minimal and maximal values, and outliers (open circle), the later are cases that have values at least three times the height of the boxes.

$t = -5.13$, $P < 0.001$; stationary vs. regressive: $t = -1.23$, $P = 0.218$).

Also methoprene treatment during mid-phase of the molting period (phase 2) resulted in significantly altered molting type frequencies [$F_{(2,\ 800)} = 7.75$, $P < 0.001$], again with more regressive and less progressive molts, while the proportion of stationary molts slightly declined (**Figure 3**). In line, compared to the frequency of regressive molts, the number of progressive molts was significantly reduced and there was a trend that stationary molts also declined (progressive vs. regressive: $t = -2.08$, $P < 0.001$; stationary vs. regressive: $t = -1.94$, $P = 0.052$).

Methoprene treatment directly before a molt (phase 3) also changed molting type frequencies significantly [$F_{(2,\ 802)} = 134.67$, $P < 0.001$], with an increase in regressive molts and fewer progressive as well as stationary molts (**Figure 3**). Compared to the frequency of regressive molts, the frequency of progressive molts as well as stationary molts significantly declined (progressive vs. regressive: $t = -4.80$, $P < 0.001$; progressive vs. stationary: $t = -3.00$, $P = 0.003$) (**Figure 3**).

We did not observe neotenic- or pre-/soldier development, as expected when using complete colonies in which the presence of the corresponding castes inhibits terminal differentiation.

Expression of JH-Related Genes

Comparing the expression of JH-related gene before (phase 3) and after a molt (phase 1) revealed no significant differences (Mann-Whitney U-test: always $P > 0.270$; for more details

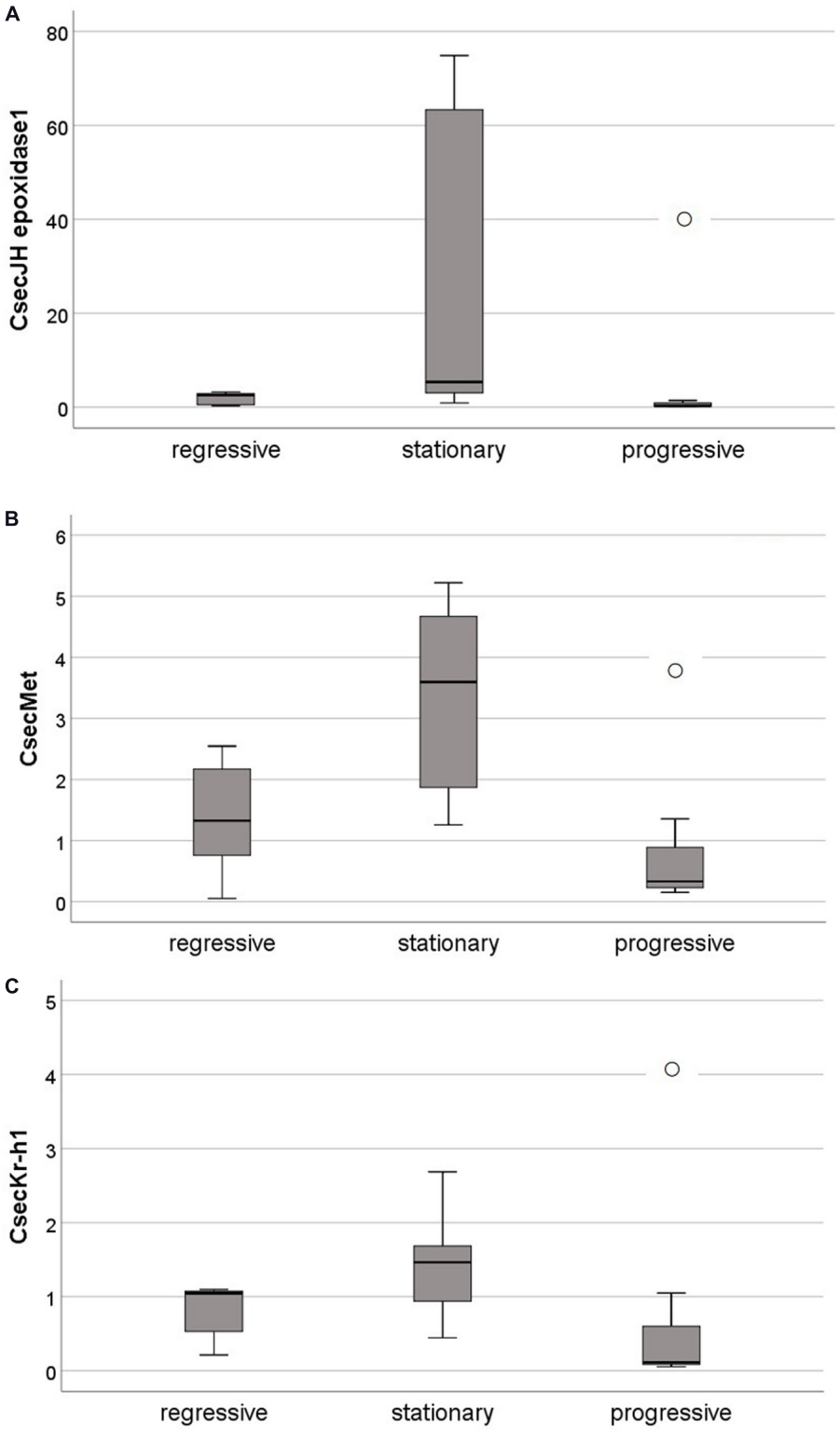

FIGURE 5 | Relative expression of genes related to JH biosynthesis and JH signaling after a molt, in relation to molting types. All shown genes were significantly (by trend for *CsecKr-h1*) higher expressed after stationary than progressive and regressive molts. **(A)** *CsecJH epoxidase1*, a genes supposed to catalyze the last step of JH biosynthesis. **(B)** *CsecMet*, the 1:1 ortholog of *met* from the cockroach *Blattella germanica* whose protein functions as receptor of JH. **(C)** *CsecKr-h1,* the 1:1 ortholog of *Kr-h1* in *D. melanogaster* and *B. germanica* which functions as early response gene of JH signaling. Shown are boxplots with median, quartiles, minimal and maximal values, and outliers (open circle), the later are cases that have values at least three times the height of the boxes.

see **Supplementary Table S2** and **Supplementary Figure S1**), except for *CsecKr-h1* which was higher expressed before than after a molt ($N_{before\ molt}$ = 22, $N_{after\ molt}$ = 19, U = 78.00, P = 0.001) (**Figure 4**). This indicates that JH production did not differ but that JH signaling was higher before than after a molt.

After a molt, gene expression did not differ between molting types for the genes *CsecJH epoxidase2* and *CsecTai* (Kruskal Wallis tests: always $P > 0.800$; for more details see **Supplementary Table S3** and **Supplementary Figure S2**). Yet, *CsecJH epoxidase1* and *CsecMet* expression differed significantly between molting types, and *CsecKr-h1* by trend (*CsecJH epoxidase1*: $\chi^2_{2,19}$ = 8.16, P = 0.017; *CsecMet*: $\chi^2_{2,19}$ = 7.24, P = 0.027; *CsecKr-h1*: $\chi^2_{2,19}$ = 5.88, P = 0.053) (**Figure 5**). All three genes had their highest expression after stationary molts (**Figure 5**), indicating that JH production as well as signaling are up-regulated after a stationary molt.

DISCUSSION

Our results suggest that hemolymph JH titers during all phases are crucial in determining the developmental trajectory of *C. secundus* nymphs. Increasing JH signaling with methoprene always influenced molting type frequencies compared to untreated control individuals (**Figure 3**). As a caveat, it should be noted that we did not test the methoprene treated individuals against solvent treated individual in our phase-specific experiment. Yet, we found no solvent (acetone) effect on molting types in our supplementary experiments.

During all phases an increase in JH signaling resulted in an elevated proportion of regressive molts. During all phases this was at the cost of progressive molts which became less common (**Figure 3**). Starting in phase 2, also the number of stationary molts decreased, while they slightly—but not significantly—increased during phase 1. Our results imply that (i) high JH titers, regardless of the intermolt period, favor regressive development, (ii) progressive development is associated with low—or at least not high—JH titers during all phases of the intermolt period, and (iii) stationary molts seem to be less influenced by varying JH titers during the first phase (i.e., directly after the molt) but they also require rather low titers thereafter, especially before the next molt.

We adjusted our methoprene concentrations to what was used before in termite studies (see Methods). Yet, we cannot completely rule out that we observed a pharmacological rather than a physiological effect due to emulating artificially high JH titers. If this was the case, postembryonic developmental plasticity could not be explained by varying JH titers during the intermolt period as the NW model predicted. Given the evidence that exists that varying JH titers are associated with different developmental trajectories in termites in general (reviewed in Korb, 2015; for soldiers: Miura and Scharf, 2011) and the fact that our results are in line with a former study that found an association of high JH titers with regressive molts in *C. secundus* (Korb et al., 2009), we think that it is unlikely that we produced highly artificial results in our study.

Updating the NW Model to Explain Termite's Development Plasticity

Our data confirmed the NW model and former suggestions in that progressive molts require rather low JH titers throughout the molting period (Springhetti, 1969; Nijhout and Wheeler, 1982; Korb et al., 2009; Korb and Bellés, 2017; **Figures 2**, **6**). In line, average JH titers decline in *C. secundus* (Korb et al., 2009) as well as *Hodotermes sjostedti* (Cornette et al., 2008) with progressive development along the nymphal-alate line.

The NW model did not explicitly mention regressive molts. Yet, it suggested that individuals that remain immature workers—which comprises regressive and stationary molts—are characterized by first high, then low JH titers (**Figure 2**). This corresponds with our results for the stationary molts which seem to require low JH signaling during phase 3 (**Figure 3**). However, the NW model's suggestion that low JH titers toward the end of the intermolt period characterize individuals that remain immatures, is not in line with our findings that regressive molts were induced by high JH signaling during phase 3 (**Figure 3**). Yet, our results correspond with previous hypotheses (Lüscher, 1956, 1974b; Springhetti, 1969) and first evidence (Korb et al., 2009) that regressive molts are the results of high JH titers throughout the intermolt period.

According to the NW model as well as several experimental studies using JH analoga and *in vitro* measurements (e.g., Elliott and Stay, 2008; for recent reviews see: Miura and Scharf, 2011; Watanabe et al., 2014; Korb, 2015), high JH titers lead to soldier development. This seems to contrast with our results that they elicit regressive molts. However, presoldier/soldier development

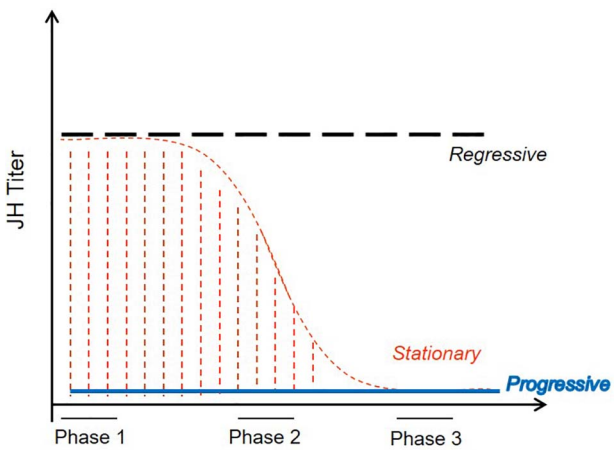

FIGURE 6 | According to current results, revised model to explain the unparalleled diversity of postembryonic, non-terminal developmental trajectories of wood-dwelling termites. High JH titers throughout the intermolt period increase the likelihood of regressive development (black, broken line). Progressive molts (blue, continuous line) require low JH titers throughout the intermolt period. Stationary molts (orange, dotted line), by contrast, can have medium-high JH titers during phase 1 but require increasing low JH titers thereafter. The presence of reproductives and soldiers prevent terminal molts into the corresponding castes. For further information, see text.

generally require an absence of the soldiers which prevent the differentiation of further soldiers (e.g., Castle, 1934; Lüscher, 1974a; Haverty and Howard, 1981; Lefeuve and Bordereau, 1984; Henderson, 1998; Korb et al., 2003; Park and Raina, 2005; Tarver et al., 2010; Miura and Scharf, 2011; Watanabe et al., 2011, 2014; for few exception see Lenz, 1976; Hrdy et al., 2006).

Our experiments were done with complete colonies, including soldiers, and soldiers inhibit soldier differentiation in *C. secundus* (Korb et al., 2003; Roux and Korb, 2004). Thus, high JH signaling in the presence of soldiers seems to trigger regressive molts while it may lead to soldier differentiation in the absence of soldiers. This corresponds to a recently proposed model for the evolution of termite developmental plasticity based on "shared endocrinology" between postembryonic, non-terminal and terminal molts derived from a cockroach ancestor (Korb and Bellés, 2017). According to this model, JH titers in combination with social interactions could explain termite plasticity. High JH titers in the presence of soldiers result in regressive molts, while presoldier/soldier development is induced when soldiers are lacking. Correspondingly, constantly low JH titers trigger either progressive postembryonic development or a terminal neotenic molt, depending on the presence and absence of reproductives, respectively. In our experiment, the presence of reproductives prevented neotenic differentiation in *C. secundus* as it does in other Kalotermitidae (e.g., Grassé and Noirot, 1946; Lüscher, 1952; Lüscher, 1974b; Lenz, 1976; Hoffmann and Korb, 2011; for a recent review see: Korb, 2015). This model of shared endocrinology is in line with several recent studies which also stress the importance of social interactions in explaining phenotypic plasticity in termites (e.g., Tarver et al., 2010; Watanabe et al., 2014; Oguchi et al., 2020).

What Next?

Our study is the first that explicitly tested the NW model by phase-specific endocrine manipulations which led to a revision of the NW model and it improved our understanding of unparalleled diversity of postembryonic development in termites (**Figure 6**). Yet, it has some caveats that should be addressed in further studies. The sample sizes were relatively small for the later phase manipulations compared to the control treatment. However, we found statistical support for changes caused by methoprene treatment, which suggests that the effects were large. Additional studies, including also other species, should test the robustness of our results. Such investigations should most suitably use acetone (solvent) treated individuals as control. In our supplementary experiments, we found no evidence that acetone had an effect on molting types. Neither the direct comparison of molting types with untreated individuals revealed significant differences nor our gene expression experiment suggested an effect of acetone on JH signalling in workers. More studies could substantiate our results.

Our studies gives directions for future research by identifying a number of specific questions: How does JH-related gene expression vary during the different phases? We determined it for phase 1 and found that it varies and that it seems affected by the preceding molting type. As a consequence, does a preceding molting type influence the direction of the subsequent molt and hence does a sequential pattern of molting types emerge? We have some preliminary data (unpublished) that this seems not to be the case. Are there any predictors of an individual's upcoming molting type? This appears as one of the most urgent quests to unravel the molecular mechanisms underlying the different developmental trajectories. Our study opened a new door by performing intermolt/phase-specific manipulations of JH signaling, which have not been done before. By doing so, it revealed new insights into the puzzle how termites can achieve their extraordinary diversity of postembryonic developmental plasticity, with a "standard" endocrine toolkit.

DATA AVAILABILITY STATEMENT

All data are uploaded as **Supplementary Material**, which we have updated and which are attached.

AUTHOR CONTRIBUTIONS

JK conceptualized and designed the experiments, analyzed the data, and wrote the manuscript. CG and MF performed endocrine experiments and analyzed the data. AG performed qPCR experiments and analyzed the data. All authors read the manuscript and approved publication of the manuscript.

FUNDING

This work was supported by the Deutsche Forschungsgemeinschaft (DFG) (KO1895/6 and KO1895/20-1).

ACKNOWLEDGMENTS

We thank Parks and Wildlife Commission, Northern Territory, and Environment Australia for permission to collect (permits 26851 and 30073) and export (permits WT2007-4154 and WT2008-4184) the termites; Charles Darwin University (Australia), and especially S. Garnett and the Horticulture and Aquaculture team, for providing logistic support during termite collection; Katharina Hoffmann for help in collecting termites and performing experiments, the editor FC for providing the opportunity to submit this work and two reviewers for helpful comments on the manuscript. The study was conducted according to the Nagoya protocol.

SUPPLEMENTARY MATERIAL

The Supplementary Material for this article can be found online at: https://www.frontiersin.org/articles/10.3389/fevo.2021.619594/full#supplementary-material

REFERENCES

Abe, T. (1987). "Evolution of life types in termites," in *Evolution and Coadaptation in Biotic Communities*, eds S. Kawano, J. H. Connell, and T. Hidaka (Tokyo: University of Tokyo Press), 125–148.

Bell, W. J., Roth, L. M., and Nalepa, C. A. (2007). *Cockroaches: Ecology, Behavior, and Natural History*. Baltimore, MD: The Johns Hopkins University Press.

Bellés, X., Martín, D., and Piulachs, M.-D. (2005). The mevalonate pathway and the synthesis of juvenile hormone in insects. *Annu. Rev. Entomol.* 50, 181–199. doi: 10.1146/annurev.ento.50.071803.130356

Bellés, X., and Santos, C. G. (2014). The MEKRE93 (Methoprene tolerant-Krüppel homolog 1-E93) pathway in the regulation of insect metamorphosis, and the homology of the pupal stage. *Insect Biochem. Mol. Biol.* 52, 60–68. doi: 10.1016/j.ibmb.2014.06.009

Brent, C. S., Schal, C., and Vargo, E. L. (2005). Endocrine changes in maturing primary queens of *Zootermopsis angusticollis*. *J. Insect Physiol.* 51, 1200–1209. doi: 10.1016/j.jinsphys.2005.06.009

Castle, G. B. (1934). "The damp-wood termite of the Western United States, genus *Zootermopsis* (formerly, *Termopsis*)," in *Termites and Termite Control*, ed. G. A. Kofoid (Berkeley, CA: University of California Press), 273–310.

Cornette, R., Gotoh, H., Koshikawa, S., and Miura, T. (2008). Juvenile hormone titers and caste differentiation in the damp-wood termite *Hodotermopsis sjostedti* (Isoptera, Termopsidae). *J. Insect Physiol.* 54, 922–930. doi: 10.1016/j.jinsphys.2008.04.017

Elliott, K. L., and Stay, B. (2008). Changes in juvenile hormone synthesis in the termite *Reticulitermes flavipes* during development of soldiers and neotenic reproductives from groups of isolated workers. *J. Insect Physiol.* 54, 492–500. doi: 10.1016/j.jinsphys.2007.11.008

Elsner, D., Meusemann, K., and Korb, J. (2018). Longevity and transposon defense, the case of termite reproductives. *Proc. Natl. Acad. Sci. U.S.A.* 115, 5504–5509. doi: 10.1073/pnas.1804046115

Gilbert, L. I. (2012). *Insect Endocrinology*. London: Academic Press.

Grassé, P. P., and Noirot, C. (1946). La production des sexués néoteniques chez le termite á cou jaune (*Calotermes flavicollis*): inhibition germinale et inhibition somatique. *Compt. Rend. Acad. Sci.* 223, 869–871.

Harrison, M. C., Jongepier, E., Robertson, H. M., Arning, N., Bitard-Feildel, T., Chao, H., et al. (2018). Hemimetabolous genomes reveal molecular basis of termite eusociality. *Nat. Ecol. Evol.* 2, 557–566. doi: 10.1038/s41559-017-0459-1

Haverty, M. I., and Howard, R. W. (1981). Production of soldiers and maintenance of soldier proportions by laboratory experimental groups of *Reticulitermes flavipes* (Kollar) and *Reticulitermes virginicus* (Banks) (Isoptera: Rhinotermitidae). *Insectes Soc.* 28, 32–39. doi: 10.1007/bf02223620

Henderson, G. (1998). "Primer pheromones and possible soldier caste influence on the evolution of sociality in lower termites," in *Phermone Communication in Social Insects*, eds R. K. Vander Meer, M. D. Breed, K. E. Espelie, and M. L. Winston (Boulder, CO: Westview Press), 314–330. doi: 10.1201/9780429301575-13

Hoffmann, K., and Korb, J. (2011). Is there conflict over direct reproduction in lower termite colonies? *Anim. Behav.* 81, 265–274. doi: 10.1016/j.anbehav.2010.10.017

Hrdy, I., Kuldová, J., Hanus, R., and Wimmer, Z. (2006). Juvenile hormone III, hydroprene and a juvenogen as soldier caste differentiation regulators in three *Reticulitermes* species: potential of juvenile hormone analogues in termite control. *Pest Manag. Sci.* 62, 848–854. doi: 10.1002/ps.1244

Inward, D., Beccaloni, G., and Eggleton, P. (2007). Death of an order: a comprehensive molecular phylogenetic study confirms that termites are eusocial cockroaches. *Biol. Lett.* 3, 331–335. doi: 10.1098/rsbl.2007.0102

Jindra, M., Belles, X., and Shinoda, T. (2015). Molecular basis of juvenile hormone signaling. *Curr. Opin. Insect Sci.* 11, 39–46. doi: 10.1016/j.cois.2015.08.004

Jongepier, E., Kemena, C., Lopez-Ezquerra, A., Bellés, X., Bornberg-Bauer, E., and Korb, J. (2018). Remodeling of the juvenile hormone pathway through caste-biased gene expression and positive selection along a gradient of termite eusociality. *J. Exp. Zool. B Mol. Dev. Evol.* 330, 296–304. doi: 10.1002/jez.b.22805

Korb, J. (2015). "Juvenile hormone, a central regulator of termite caste polyphenism," in *Advances in Insect Physiology 48: Physiology, Behavior, and Genomics of Social Insects*, eds C. Kent and A. Zayed (Oxford: Elsevier), 131–161.

Korb, J., and Bellés, X. (2017). Juvenile hormone and hemimetabolan eusociality: a comparison of cockroaches with termites. *Curr. Opin. Insect Sci.* 22, 109–116. doi: 10.1016/j.cois.2017.06.002

Korb, J., and Hartfelder, K. (2008). Life history and development – a framework for understanding the ample developmental plasticity in lower termites. *Biol. Rev. Camb. Philos. Soc.* 83, 295–313.

Korb, J., Hoffmann, K., and Hartfelder, K. (2009). Endocrine signatures underlying plasticity in postembryonic development of a lower termite, *Cryptotermes secundus* (Kalotermitidae). *Evol. Dev.* 11, 269–277. doi: 10.1111/j.1525-142x.2009.00329.x

Korb, J., Hoffmann, K., and Hartfelder, K. (2012). Molting dynamics and juvenile hormone titer profiles in the nymphal stages of a lower termite, *Cryptotermes secundus* (Kalotermitidae) – signatures of developmental plasticity. *J. Insect Physiol.* 58, 376–383. doi: 10.1016/j.jinsphys.2011.12.016

Korb, J., and Katrantzis, S. (2004). Influence of environmental conditions on the expression of the sexual dispersal phenotype in a lower termite: implications for the evolution of workers in termites. *Evol. Dev.* 6, 342–352. doi: 10.1111/j.1525-142x.2004.04042.x

Korb, J., and Lenz, M. (2004). Reproductive decision-making in the termite, *Cryptotermes secundus* (Kalotermitidae), under variable food conditions. *Behav. Ecol.* 15, 390–395. doi: 10.1093/beheco/arh033

Korb, J., Roux, E., and Lenz, M. (2003). Proximate factors influencing soldier development in the basal termite *Cryptotermes secundus* (Hill). *Insectes Soc.* 50, 299–303. doi: 10.1007/s00040-003-0674-4

Korb, J., and Schmidinger, S. (2004). Help or disperse? Cooperation in termites influenced by food conditions. *Behav. Ecol. Sociobiol.* 56, 89–95. doi: 10.1007/s00265-004-0757-x

Korb, J., and Schneider, K. (2007). Does kin structure explain the occurrence of workers in a lower termite? *Evol. Ecol.* 21, 817–828. doi: 10.1007/s10682-006-9153-5

Korb, J., and Thorne, B. (2017). "Sociality in termites," in *Comparative Social Evolution*, eds D. R. Rubenstein and P. Abbot (Cambridge: Cambridge University Press), 124–153.

Lanzrein, B., Gentinetta, V., and Fehr, R. (1985). "Titres of juvenile hormone and ecdysteroids in reproductives and eggs of *Macrotermes michaelseni*: relation to caste determination?," in *Caste Differentiation in Social Insects*, eds J. A. L. Watson, B. M. Okot-Kotber, and C. Noirot (Oxford: Pergamon Press), 307–328. doi: 10.1016/b978-0-08-030783-1.50027-6

Lefeuve, P., and Bordereau, C. (1984). Soldier formation regulated by a primer pheromone from the soldier frontal gland in a higher termite, *Nasutitermes lujae*. *Proc. Natl. Acad. Sci. U.S.A.* 81, 7665–7668. doi: 10.1073/pnas.81.23.7665

Lenz, M. (1976). "The dependence of hormone effects in termite caste determination on external factors," in *Phase and Caste Determination in Insects - Endocrine Aspects*, ed. M. Lüscher (Oxford: Pergamon Press), 73–89. doi: 10.1016/b978-0-08-021256-2.50012-1

Lüscher, M. (1952). Die Produktion und Elimination von Ersatzgeschlechtstieren bei der Termite *Kalotermes flavicollis* (Fabr.). *Zeitschrift vergl. Physiol.* 34, 123–141.

Lüscher, M. (1956). Die Entstehung von Ersatzgeschlechtstieren bei der Termite *Kalotermes flavicollis* (Fabr.). *Insectes Soc.* 3, 119–128. doi: 10.1007/bf02230672

Lüscher, M. (1974a). Die Kompetenz zur Soldatenbildung bei Larven (Pseudergaten) der Termite *Zootermopsis angusticollis*. *Rev. Suisse Zool.* 81, 711–714.

Lüscher, M. (1974b). "Kasten und Kastendifferenzierung bei niederen Termiten," in *Sozialpolymorphismus bei Insekten*, ed. G. H. Schmidt (Stuttgart: Wissenschaftliche Verlagsgesellschaft), 694–739.

Maekawa, K., Hayashi, Y., Lee, T., and Lo, N. (2014). Presoldier differentiation of Australian termite species induced by juvenile hormone analogues. *Austral Entomol.* 53, 138–143. doi: 10.1111/aen.12060

Maekawa, K., Nakamura, S., and Watanabe, D. (2012). Termite soldier differentiation in incipient colonies is related to parental proctodeal trophallactic behavior. *Zoolog. Sci.* 29, 213–217. doi: 10.2108/zsj.29.213

Miura, T., and Scharf, M. E. (2011). "Molecular basis underlying caste differentiation in termites," in *Biology of Termites: A Modern Synthesis*, eds D. E. Bignell, Y. Roisin, and N. Lo (London: Springer Press), 211–254. doi: 10.1007/978-90-481-3977-4_9

Nijhout, H. F. (1994). *Insect Hormones*. Princeton, NJ: Princeton University Press.

Nijhout, H. F., and Wheeler, D. E. (1982). Juvenile hormone and the physiological basis of insect polyphenisms. *Q. Rev. Biol.* 57, 109–133. doi: 10.1086/412671

Noirot, C. (1990). "Sexual castes and reproductive strategies in termites," in *An Evolutionary Approach to Castes and Reproduction*, ed. W. Engels (Berlin: Springer Verlag), 5–35. doi: 10.1007/978-3-642-74490-7_3

Noirot, C., and Pasteels, J. M. (1987). Ontogenic development and evolution of the worker caste in termites. *Experientia* 43, 851–860. doi: 10.1007/bf01951642

Oguchi, K., Sugime, Y., Shimoji, H., Hayashi, Y., and Miura, T. (2020). Male neotenic reproductives accelerate additional differentiation of female reproductives by lowering JH titer in termites. *Sci. Rep.* 10:9435.

Park, Y. I., and Raina, A. K. (2004). Juvenile hormone III titers and regulation of soldier caste in *Coptotermes formosanus* (Isoptera: Rhinotermitidae). *J. Insect Physiol.* 50, 561–566. doi: 10.1016/j.jinsphys.2004.04.002

Park, Y. I., and Raina, A. K. (2005). Regulation of juvenile hormone titers by soldiers in the Formosan subterranean termite *Coptotermes formosanus*. *J. Insect Physiol.* 51, 385–391. doi: 10.1016/j.jinsphys.2005.02.001

Roisin, Y. (2000). "Diversity and evolution of caste patterns," in *Termites: Evolution, Sociality, Symbioses, Ecology*, eds T. Abe, D. E. Bignell, and M. Higashi (Dordrecht: Kluwer Academic Publishers), 95–119. doi: 10.1007/978-94-017-3223-9_5

Roisin, Y., and Korb, J. (2011). "Social organisation and the status of workers in termites," in *Biology of Termites: A Modern Synthesis*, eds D. E. Bignell, Y. Roisin, and N. Lo (London: Springer), 133–164. doi: 10.1007/978-90-481-3977-4_6

Roux, E. A., and Korb, J. (2004). Evolution of eusociality and the soldier caste in termites: a validation of the intrinsic benefit hypothesis. *J. Evol. Biol.* 17, 869–875. doi: 10.1111/j.1420-9101.2004.00727.x

Springhetti, A. (1969). Il controllo sociale della differenziazione degli alati in *Kalotermes flavicollis* Fabr. (Isoptera). *Ann. Univ. Ferrara Sez III Biol. Anim.* 3, 73–96.

Springhetti, A. (1972). The competence of *Kalotermes flavicollis* F. (Isoptera) pseudergates to differentiate into soldiers. *Monit. Zool. Ital.* 6, 97–111.

Tarver, M. R., Florane, C., Zhang, D., Grimm, C., and Lax, A. R. (2012). Methoprene and temperature effects on caste differentiation and protein composition in the Formosan subterranean termite *Coptotermes fomosanus*. *J. Insect Sci.* 12:e18.

Tarver, M. R., Zhou, X. G., and Scharf, M. E. (2010). Socio-environmental and endocrine influences on developmental and caste-regulatory gene expression in the eusocial termite *Reticulitermes flavipes*. *BMC Mol. Biol.* 11:e28. doi: 10.1186/1471-2199-11-28

Watanabe, D., Gotoh, H., Miura, T., and Maekawa, K. (2011). Soldier presence suppressed presoldier differentiation through a rapid decrease of JH in the termite *Reticulitermes speratus*. *J. Insect Physiol.* 57, 791–795. doi: 10.1016/j.jinsphys.2011.03.005

Watanabe, D., Gotoh, H., Miura, T., and Maekawa, K. (2014). Social interactions affecting caste development through physiological actions in termites. *Front. Physiol.* 5:e127. doi: 10.3389/fphys.2014.00127

Weil, T., Rehli, M., and Korb, J. (2007). Molecular basis for the reproductive division of labour in a lower termite. *BMC Genomics* 8:e198. doi: 10.1186/1471-2164-8-198

Yagi, K. J., Kwok, R., Chan, K. K., Setter, R. R., Myles, T. G., Tobe, S. S., et al. (2005). Phe-Gly-Leu-amide allatostatin in the termite *Reticulitermes flavipes*: content in brain and corpus allatum and effect on juvenile hormone synthesis. *J. Insect Physiol.* 51, 357–365. doi: 10.1016/j.jinsphys.2004.12.006

Conflict of Interest: The authors declare that the research was conducted in the absence of any commercial or financial relationships that could be construed as a potential conflict of interest.

frontiers in Ecology and Evolution

ORIGINAL RESEARCH
published: 08 March 2021
doi: 10.3389/fevo.2021.624306

The Transcriptome in Transition: Global Gene Expression Profiles of Young Adult Fruit Flies Depend More Strongly on Developmental Than Adult Diet

Christina M. May[1†‡], Erik B. Van den Akker[2,3,4†‡] and Bas J. Zwaan[1]*

[1] Laboratory of Genetics, Department of Plant Sciences, Wageningen University, Wageningen, Netherlands, [2] Leiden Computational Biology Center, Department of Biomedical Data Sciences, Leiden University Medical Center, Leiden, Netherlands, [3] Molecular Epidemiology, Department of Biomedical Data Sciences, Leiden University Medical Center, Leiden, Netherlands, [4] Pattern Recognition & Bioinformatics, Delft University of Technology, Delft, Netherlands

OPEN ACCESS

Edited by:
Nico Posnien,
University of Göttingen, Germany

Reviewed by:
Sonja Grath,
Ludwig Maximilian University of Munich, Germany
Neda Barghi,
University of Veterinary Medicine Vienna, Austria

***Correspondence:**
Bas J. Zwaan
bas.zwaan@wur.nl
orcid.org/0000-0002-8221-4998

[†] These authors share first authorship

[‡]ORCID:
Christina M. May
orcid.org/0000-0003-2691-505X
Erik B. Van den Akker
orcid.org/0000-0002-7693-0728

Specialty section:
This article was submitted to Evolutionary Developmental Biology, a section of the journal Frontiers in Ecology and Evolution

Received: 31 October 2020
Accepted: 12 February 2021
Published: 08 March 2021

Citation:
May CM, Van den Akker EB and Zwaan BJ (2021) The Transcriptome in Transition: Global Gene Expression Profiles of Young Adult Fruit Flies Depend More Strongly on Developmental Than Adult Diet. Front. Ecol. Evol. 9:624306. doi: 10.3389/fevo.2021.624306

Developmental diet is known to exert long-term effects on adult phenotypes in many animal species as well as disease risk in humans, purportedly mediated through long-term changes in gene expression. However, there are few studies linking developmental diet to adult gene expression. Here, we use a full-factorial design to address how three different larval and adult diets interact to affect gene expression in 1-day-old adult fruit flies (*Drosophila melanogaster*) of both sexes. We found that the largest contributor to transcriptional variation in young adult flies is larval, and not adult diet, particularly in females. We further characterized gene expression variation by applying weighted gene correlation network analysis (WGCNA) to identify modules of co-expressed genes. In adult female flies, the caloric content of the larval diet associated with two strongly negatively correlated modules, one of which was highly enriched for reproduction-related processes. This suggests that gene expression in young adult female flies is in large part related to investment into reproduction-related processes, and that the level of expression is affected by dietary conditions during development. In males, most modules had expression patterns independent of developmental or adult diet. However, the modules that did correlate with larval and/or adult dietary regimes related primarily to nutrient sensing and metabolic functions, and contained genes highly expressed in the gut and fat body. The gut and fat body are among the most important nutrient sensing tissues, and are also the only tissues known to avoid histolysis during pupation. This suggests that correlations between larval diet and gene expression in male flies may be mediated by the carry-over of these tissues into young adulthood. Our results show that developmental diet can have profound effects on gene expression in early life and warrant future research into how they correlate with actual fitness related traits in early adulthood.

Keywords: phenotypic plasticity, transcriptomics, diet, development, nutrition, *Drosophila melanogaster*

INTRODUCTION

Developmental diet can exert long-term effects on adult phenotypes and disease risk (Schlichting and Pigliucci, 1998). For example, human and rodent studies have demonstrated that inadequate developmental diet can increase the risk of heart disease, obesity, stroke, and hypertension in adulthood (reviewed in Bruce and Hanson, 2010; Burdge and Lillycrop, 2010; Langley-Evans, 2015). Several evolutionary theories have been proposed to explain the mechanisms underlying this link including the silver spoon hypothesis, the developmental programming hypothesis, and the predictive adaptive response (PAR) hypothesis (reviewed in Lindström, 1999; Monaghan, 2008). The silver spoon hypothesis proposes that sub-optimal developmental conditions directly constrain overall adult size or quality, resulting in decreased fitness across adult environments (e.g., Emlen, 1997; Lanet and Maurange, 2014), while the developmental programming hypothesis extends this idea and suggests that the negative effects of sub-optimal development conditions will be more pronounced the more the developmental and adult environment differ (Fernandez-Twinn and Ozanne, 2006). Finally, the PAR hypothesis goes one step further and proposes that the developmental environment can serve as a cue anticipating the adult environment, allowing individuals to adjust their phenotypes during development to "match" their predicted adult conditions. However, when these predictions are incorrect a mismatch occurs, resulting in an increased risk of metabolic disease (Ravelli et al., 1998; Gluckman and Hanson, 2004; Gluckman et al., 2007; Bateson et al., 2014).

Regardless of the mechanism, developmental influences on adult phenotypes are expected to result in gene-expression changes at the level of the whole organism (Burdge et al., 2007; Burdge and Lillycrop, 2010). Yet, despite the widespread incidence of variation in the quality of the developmental environment, relatively few studies have addressed the extent to which developmental diet influences gene expression in adulthood. In rats, the adult offspring of protein-restricted mothers have altered expression of metabolic genes (Bertram et al., 2001; Maloney et al., 2003; Lillycrop et al., 2005), while high protein larval diets in fruit flies affect immune gene expression in young adults (Fellous and Lazzaro, 2010). We have previously shown that subtle effects of developmental diet on the transcriptome persist into middle- and old-age in fruit flies (May and Zwaan, 2017), and that the expression of particular ribosome, transcription, and translation-related genes correlate with observed patterns of lifespan and fecundity across diets (May and Zwaan, 2017). However, to our knowledge, no study has addressed the global effect of developmental diet on the transcriptome in early life, nor if and how it depends on the adult environment.

Here, we use the fruit fly, *Drosophila melanogaster,* to determine to what extent developmental diet affects whole-body, whole-genome, gene expression in 1-day old adult male and female flies, and how this interacts with adult dietary conditions. We chose 1-day old flies in order to establish a baseline effect of developmental diet on adult gene-expression. We first assess broad-scale patterns of expression variation as obtained from principle component analysis (PCA). Subsequently, we use weighted gene correlation network analysis (WGCNA v1.69. Langfelder and Horvath, 2008) to identify modules of genes whose expression is affected by larval and/or adult dietary conditions. We chose to focus on gene co-expression modules as these more accurately reflect the nature of genes as components of hierarchically structured regulatory networks (Zhang and Horvath, 2005). As such, co-expression often reflects co-regulation (Allocco et al., 2004), or tissue-specific function (Boutanaev et al., 2002) and can provide more biologically meaningful insights as compared to single-gene analysis (e.g., Oldham et al., 2006; Hilliard et al., 2012; Xue et al., 2013). After identifying modules of co-expressed genes affected by dietary conditions, we annotate the modules using several external databases and address whether there is evidence for specific functions [gene ontology (GO)], tissue-specific roles (FlyAtlas and FlyGut databases), or co-regulation of the modules by specific transcription factors (TFs) (DroID Database).

We find that both larval and adult diet affect the whole-body transcriptome of young adults, however, the effect of larval diet is considerably larger than that of adult diet, especially in females. In females, larval diet primarily affects relative expression of reproduction vs non-reproduction related processes, while in males, larval diet modulates the expression of modules associated with nutrient sensing and metabolic functions, containing genes highly expressed in the gut and fat body. This suggests that there is scope for long-term effects of developmental conditions on adult gene expression. We discuss the results in the context of theories and hypotheses linking early life conditions to late life health as they relate to epigenetic mechanisms.

MATERIALS AND METHODS

Fly Stocks and Experimental Design

We used the laboratory stock population described in May et al. (2015). This population was derived from six wild populations collected across Europe in 2006. To ensure equal representation of existing genetic variation, the populations were subjected to four rounds of crossing to generate the final population, This population has been maintained in the laboratory for more than 60 generations under standard laboratory conditions: 25°C, 65% humidity, 12:12 h light:dark cycle, 14 day generation time, and a standard diet (1SY) of 100 grams sugar, 70 grams yeast, 20 grams agar, 15 mL nipagin, and 3 mL propionic acid per liter of water. We modified the sugar (S) and yeast (Y) content of our standard laboratory diet (1SY) by 0.25 times and 2.5 times, respectively to obtain three diets (0.25SY, 1SY, and 2.5SY) spanning a 10-fold range of sugar and yeast concentrations. For the experiment, we raised larvae on these three diets at a density of 100 eggs per vial (6 mL medium) and immediately after eclosion randomly distributed the resulting adults across these three diets again in a full factorial design (**Supplementary Figure 1**). To obtain virgin flies we sexed the adults immediately after the cuticle had hardened (∼3 h post eclosion) and maintained them at a density of 10 adults per vial. Twenty-four hours post-eclosion, we flash froze the flies in groups of five using liquid nitrogen.

RNA Extraction, Hybridization, and Data Pre-processing

We extracted RNA from four replicates per combination of sex, larval diet, and adult diet (4 replicates × 2 sexes × 3 larval diets × 3 adult diets = 72 arrays), using the Machery Nagel Nucleospin II kit (Machery and Nagel). For each sample we homogenized five whole flies together in order to minimize the effect of random variation between individuals. Biotin labeling, cRNA synthesis, hybridization to Affymetrix Drosophila 2.0 GeneChips and array readouts were performed by ServiceXS[1].

Prior to analysis we excluded ten female and four male arrays from analysis due to either evidence of mating (5 female samples) or outlier status as defined by WGCNA (z.k. score > 2.5; Horvath, 2011). Excluded arrays were randomly distributed across the nine treatment groups. Subsequently we performed background adjustment, quantile normalization and summarization using the robust multi-array average (RMA) algorithm (Irizarry et al., 2003). When normalizing males and females together, 96% of the variation in expression was due to sex, so we normalized male and female samples separately to emphasize the effects of larval and adult diet rather than ubiquitous and well-documented sex-specific differences (e.g., Ayroles et al., 2009). We performed all subsequent analysis steps separately for each sex. To gain an understanding of the broad patterns of variation in the data we applied principal components analysis to the normalized expression data (PCA; Pearson 1901). The data quality check and all other analyses were performed using R (version 4.0.3) and Bioconductor (v1.30.10; Gentleman et al. 2004).

Data Analysis

Weighted Gene Correlation Network Analysis

We applied WGCNA to the normalized expression data for each sex. We used signed modules and applied the recommended default settings for detection of signed modules (Zhang and Horvath, 2005). WGCNA first determines expression correlations for all pairs of genes and weights them by the connection strength. These correlations are then clustered using hierarchical clustering, and modules are defined as branches of the clustering tree. The expression profile of each module can be summarized by its eigengene (E), which is defined as the first principal component of the expression matrix. The eigengene can be thought of as a weighted average expression profile and thus for a particular sample, the value of its eigengene is representative of the overall expression of the module (Langfelder and Horvath, 2008). For each module, eigengenes can be compared across samples to detect significant correlations between treatments and module eigengenes (i.e., expression). By convention, modules are named by colors, with unassigned genes grouped together in the "gray" module. Implementation of WGCNA is freely available in the WGCNA R package (v1.69., Langfelder and Horvath, 2008).

Module Annotation

We applied several additional analysis steps to biologically characterize the modules. First, for each module we fitted an analysis of variance (ANOVA) model that partitions the variance in module eigengene expression explained by larval diet (L), adult diet (A), and their interaction (L by A). We set a false discovery rate (FDR) threshold of 0.001 (Benjamini and Hochberg, 1995) and focused the remaining analysis on the modules that showed a significant effect of dietary treatment on their eigengene value.

We next submitted the probe list associated with each module to DAVID (Database for Annotation, Visualization and Integrated Discovery; Huang et al., 2008) for GO enrichment analysis focusing on GO FAT terms. GO FAT terms exclude broader GO terms and eliminate term redundancy. We adjusted *p*-values using the linear step-up method of Benjamini and Hochberg (1995) to correct for multiple comparisons. To facilitate interpretation, we submitted lists of more than 20 terms to the REVIGO online tool which uses semantic similarity to reduce large lists of terms to a representative subset of terms (REduce and VIsualize Gene Ontology: Supek et al., 2011).

We used two external databases: FlyAtlas (Chintapalli et al., 2007) and FlyGut (Buchon et al., 2013) to address whether modules showed evidence of tissue-specific expression profiles. FlyAtlas contains tissue-specific gene expression data for both larval and adult tissues of the fruit fly, while FlyGut contains region-specific expression patterns in the gut. For each of our modules, we calculated the median expression across all of its probes in each tissue available in the FlyAtlas database and in each gut region available in the FlyGut database.

We used the Drosophila Interactions Database (DroID; Murali et al., 2010) to address whether there was evidence that modules were co-regulated by certain TFs. DroID is a merged dataset of empirically validated interactions between TFs and genes from the "Regulatory Element Database for Drosophila and other insects" (REDfly; Halfon et al., 2008) and "model organism ENCyclopedia Of DNA Elements" databases (modENCODE; Roy et al., 2010). We first filtered the data set to exclude TFs that are known to interact with less than five genes. We then performed a Fisher's exact test to identify modules enriched for genes regulated by the same TFs. We considered a module enriched for probes binding a certain TF at an odds-ratio of greater than 1.5-fold and *p*-value of <0.05, although at this threshold, not all interactions remained significant after applying the Bonferroni correction for multiple testing (Neyman and Pearson, 1928). Source code and links to data for all analyses are available at https://github.com/transcriptome-in-transition/Transcriptome-in-transition.

RESULTS

Larval Diet Dominates Global Gene Expression Patterns in Young Adults

The first principal component in both sexes (PC1) is driven by larval diet (females: **Figure 1A**; males: **Figure 1B**). The proportion of variation explained is much higher in females than in males (females: 43%, males: 13%), suggesting female gene expression is more strongly dependent on larval conditions. In both sexes, PC1 separates flies raised on the 0.25SY and 1SY diets as larvae, while those raised on 2.5SY fall in between (females: **Figure 1C**, males: **Figure 1D**). PC2, by contrast, appears

[1]www.servicexs.com

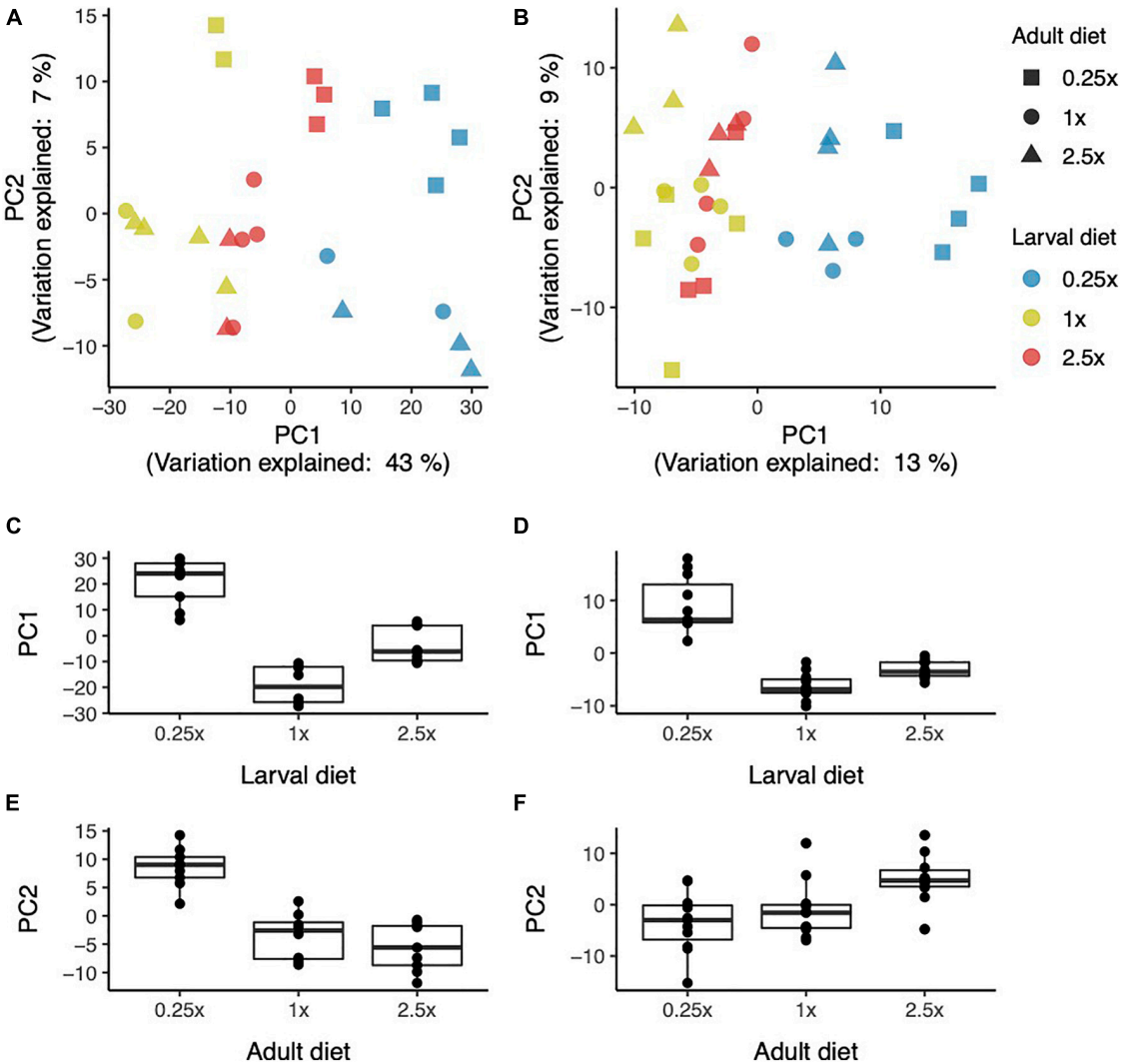

FIGURE 1 | Principle component analysis of global gene expression. PC1 vs. PC2 in females **(A)** and males **(B)**. Larval diet vs. PC1 in females **(C)** and males **(D)** and adult diet vs. PC2 in females **(E)** and males **(F)**.

to reflect more subtle effects of adult diet in both sexes. In females, PC2 separates flies transferred to the 0.25SY diet as adults from the rest, suggesting a rapid transcriptional response to this dietary condition (**Figure 1E**). In males, PC2 appears to separate flies transferred to the 2.5SY diet as adults from the rest (**Figure 1F**). Additional PC's did not explain more than 5% of variation individually and did not show clear effects of diet, suggesting that any additional effects are too subtle to be detected at the global level.

Sex-Specific Differences in Module Size and Membership

As an alternative to PCA, we also identified modules of co-expressed genes using WGCNA. In females, WGCNA identified two very large co-expression modules: blue (5,509 probes) and turquoise (5,695 probes) while the gray module (7,565) contained genes not assigned to a module. The eigengenes of the blue and turquoise modules were nearly perfectly anti-correlated ($r^2 = -0.96$, $n = 26$, $p < 0.0001$; **Figure 2A**), thus increased expression of one module implies decreased expression of the other. We could identify only subtle tissue specific effects for these two modules (**Figures 3A–C**): a relatively high expression in the larval central nervous system (CNS) for the turquoise module (and low for blue; **Figure 3A**), and higher expression in the adult ovary for the turquoise module (and thus low for blue; **Figure 3B**).

In males, we identified 22 co-expression modules ranging in size from 41 to 3,805 probes (**Figure 2B**). A total of 15,082 probes (80% of total) were assigned to a module while 3,687 probes were unassigned (gray module). Nearly all modules possessed significant GO annotation and enrichment for binding of specific TFs (**Supplementary File 1**), as well as distinct tissue-specific expression profiles in the FlyAtlas and FlyGut databases (**Figures 3D–F**) suggesting that WGCNA was able to identify

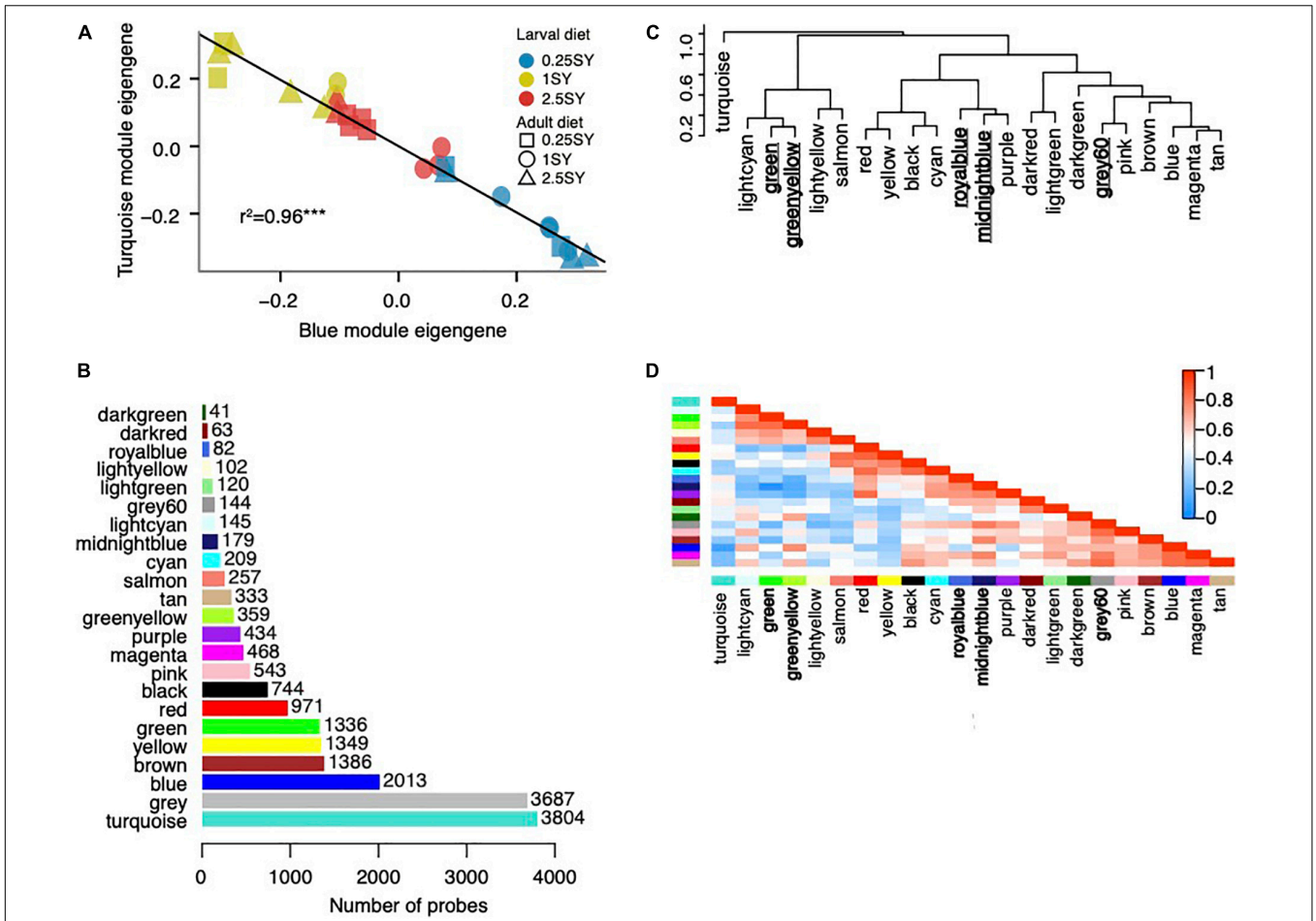

FIGURE 2 | Modules detected by WGCNA. **(A)** Module eigengenes of the female blue module plotted against eigengenes of the female turquoise module. Eigengenes of the two modules are nearly perfectly negatively correlated ($r^2 = 0.96$). **(B)** Module sizes in males. **(C)** Hierarchical clustering dendrogram of male module eigengenes (labeled by their colors). **(D)** Heatmap plot of the adjacencies in the eigengene network. Each row and column in the heatmap corresponds to one module eigengene (labeled by color). A value of 1 (red) represents high adjacency (perfect positive correlation), while 0 (blue) represents low adjacency (perfect negative correlation). Modules with high adjacency tend to have similar tissue-specific expression profiles in the FlyAtlas and FlyGut datasets. For both sexes, the "gray" module contains probes that were unassigned to a module.

biologically relevant groups of co-expressed genes. For example, the salmon, red, yellow, black, and cyan modules contain genes whose expression is restricted to the adult testes and wandering larval fat body in external databases (**Figures 3D,E**). These two pieces of external information are consistent with each other, as the testes are embedded within the wandering fat body during larval development (Gärtner et al., 2014).

We next assessed which modules were affected by larval or adult diet. ANOVA analysis of module eigengenes showed that the expression of both female modules and five out of 22 male modules were affected by dietary conditions (**Table 1**), thus we focus our remaining analysis on these modules.

Gene Expression in Young Adult Females Is Driven by Larval Diet

In females, the eigengene value of both modules (i.e., expression) was strongly dependent on larval diet (**Table 1**). In both modules, the 0.25SY and 1SY-raised flies form the two extremes of expression, while the 2.5SY-raised flies fall in between (**Figures 4A,B**), similar to the differences observed for the PCA analysis (**Figure 1**). The blue module is up-regulated in 0.25SY raised flies (**Figure 4A**), and the turquoise module is down-regulated (**Figure 4B**), consistent with the tight negative correlation of the module eigengene values (**Figure 2A**). Furthermore, the blue module also shows increased expression in flies transferred to the 0.25SY diet as adults, suggesting a rapid transcriptional response in the same direction as the effect of larval diet (**Figure 4A**).

Both modules have extensive GO enrichment (Blue module: 373 terms; Turquoise module: 564 terms; **Supplementary File 1**). Summarization with REVIGO (Supek et al., 2011) shows the blue module (up-regulated in 0.25SY) is enriched for a broad spectrum of terms including mesoderm development, detection of external stimuli, leg and limb morphogenesis, energy derivation by oxidation of organic compounds, and generation of precursor

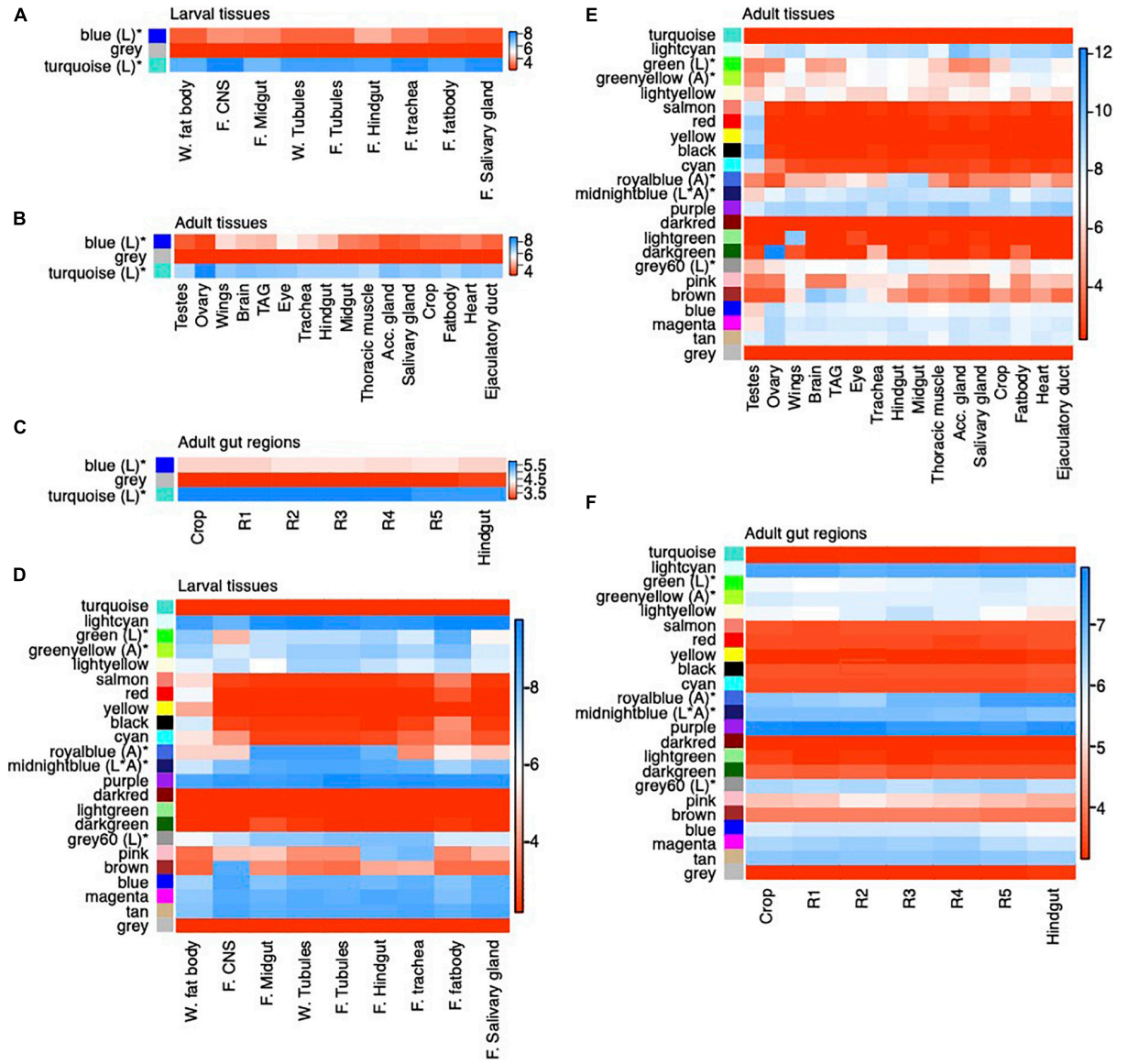

FIGURE 3 | Heatmaps of module median expression in the FlyAtlas and FlyGut tissue-specific gene expression databases. Median expression of female modules per tissue in **(A)** larval tissues in FlyAtlas, **(B)** adult tissues in FlyAtlas and **(C)** across gut regions in FlyGut. Median expression of male modules per tissue in **(D)** larval tissues in FlyAtlas, **(E)** adult tissues in FlyAtlas, and **(F)** across gut regions in FlyGut. W: wandering, F: feeding, CNS: central nervous system, Acc. gland: accessory gland. For larval tissues "W." refers to tissues collected during the wandering larval stage (late third instar) and "F." refers to tissues collected while third instar larvae were still feeding. For FlyGut data **(C,F)** R1 through R5 refer to five sequential regions of the gut which are delineated by the combination of an anatomical constriction between one region and the next, changes in histology and changes in gene expression (Buchon et al., 2013). Modules are shown in the same order as they appear in the hierarchical clustering dendrogram. Modules whose expression is affected by larval or adult diet are indicated by a "*" and annotated with whether they are affected by larval diet (L), adult diet (A), or their interaction (L*A).

metabolites and energy (**Figure 5A**), while the turquoise module (down-regulated in 0.25SY) is annotated with terms related to cell division, cell cycle, oogenesis and reproduction (**Figure 5B**).

The turquoise module has relatively high overall expression across tissues (**Figures 3A,C**), and is particularly highly expressed in the adult ovary (**Figure 3B**), consistent with its enrichment for cell cycle and reproduction related GO terms, while the blue module has relatively low median expression overall (**Figures 3A,C**) and in the ovary in particular (**Figure 3B**), consistent with its lack of reproduction and cell-cycle related GO terms. Assessment of enrichment of TF binding probes found enrichment for 19 TFs in the turquoise module, but none in the blue module (**Table 2**). These 19 TFs show similar tissue-specific transcription patterns to the turquoise module overall (i.e., they are highly expressed in general, and especially in the ovary; **Supplementary File 2a,c**) and also share very similar GO annotation with the turquoise module, with 89 of the 92 terms enriched for the TF list also enriched in the turquoise

TABLE 1 | *q*-values for per-module ANOVAs assessing the effect of larval diet (L), adult diet (A), and their interaction (L*A) on module eigengene values.

	q-value		
Module	**Larval diet (L)**	**Adult diet (L)**	**L*A**
Female			
Blue*	<0.001	0.024	0.490
Turquoise*	<0.001	0.320	0.680
Gray	0.690	0.035	0.680
Male			
Turquoise	0.720	0.440	0.073
Lightcyan	0.440	0.021	0.160
Green*	<0.001	0.011	0.110
Greenyellow*	0.011	<0.001	0.760
Lightyellow	0.043	0.230	0.730
Salmon	0.021	0.440	0.600
Red	0.440	0.036	0.150
Yellow	0.160	0.210	0.440
Black	0.140	0.720	0.210
Cyan	0.300	0.290	0.160
Royalblue*	0.051	<0.001	0.790
Midnightblue*	<0.001	<0.001	<0.001
Purple	0.078	0.074	0.440
Darkred	0.011	0.360	0.500
Lightgreen	0.022	0.410	0.810
Darkgreen	0.410	0.033	0.760
Gray60*	<0.001	0.003	0.440
Pink	0.021	0.240	0.240
Brown	0.005	0.730	0.083
Blue	0.530	0.079	0.530
Magenta	0.120	0.710	0.600
Tan	0.130	0.400	0.700
Gray	0.720	0.180	0.570

Modules with q-values below the FDR-corrected significance cut-off (0.001) are indicated by a "."*

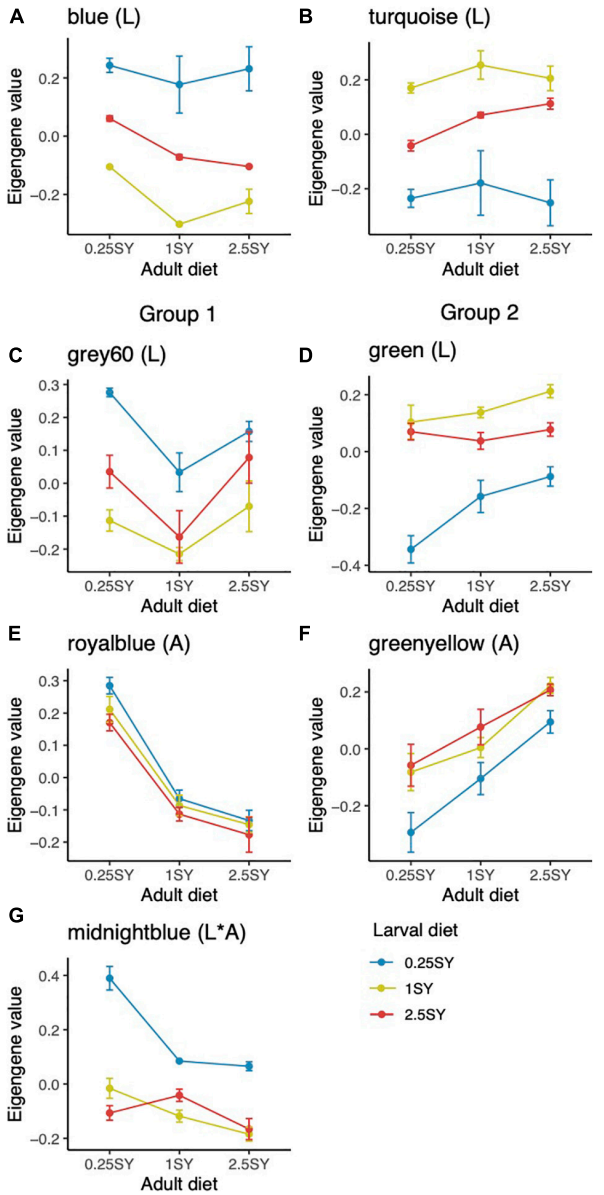

FIGURE 4 | Module eigengene (expression) values across larval (colors) and adult (*x*-axis) diets. Module eigengenes of blue **(A)** and turquoise **(B)** female modules. Both modules are significantly affected by larval diet. Module eigengenes of gray60 **(C)** and green **(D)** male modules. The eigengene values of both modules are significantly affected by larval diet. Module eigengenes of royal blue **(E)** and green yellow **(F)** male modules. The eigengene values of both modules are significantly affected by adult diet. **(G)** Module eigengenes of the midnight blue module. Expression of the midnight blue module is significantly affected by the interaction between larval and adult diet. Male modules can be divided into two groups based on their expression correlation: Group 1 **(C,E,G)** and Group 2 **(D,F)**. Within a group eigengene expression is highly correlated, but across groups, eigengene expressions are negatively correlated. All error bars are 95% C.I's.

module. Furthermore, REVIGO summary of these 92 terms shows a similar emphasis on reproduction, oogenesis, and early embryonic development (**Supplementary File 2d**).

Overall, these findings suggest that larval diet drives relative investment into reproduction and cell-cycle related processes (turquoise) *versus* non-reproduction related processes (blue) in young adult females. The low calorie 0.25SY larval (and to some extent adult) diet shifts the balance toward higher expression of the blue, non-reproduction related module, while the 1SY larval diet does the opposite.

Male Modules Fall Into Two Distinct Groups With Roughly Inverse Expression Profiles

In males, we found a significant effect of diet in five out of 22 modules (**Table 1**). Thus, in contrast to females, a significant proportion of gene expression in young males is independent of dietary conditions, as was suggested by the principal component analysis (**Figure 1B**). Of the five modules, two were affected by larval diet (gray60, green), two by adult diet (royal blue, green yellow), and one by their interaction (midnight blue). The modules could be broadly divided into two

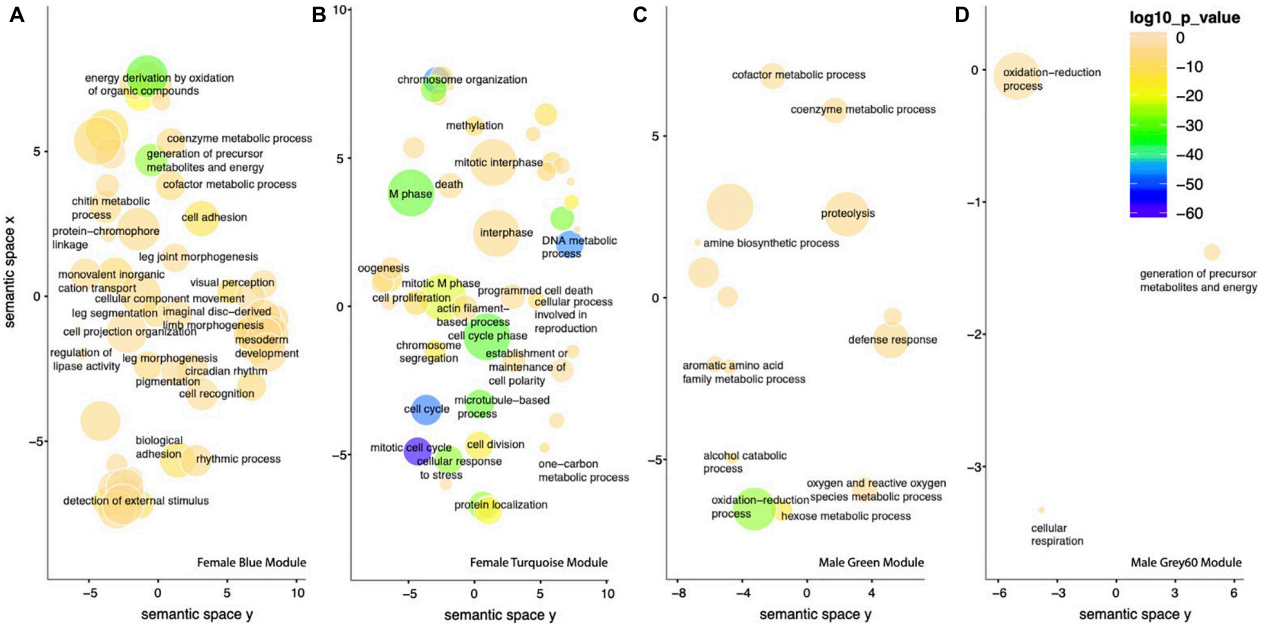

FIGURE 5 | Summarization of module GO annotation using REVIGO. Representative GO terms summarizing **(A)** the 373 GO terms significantly associated with the blue female module, **(B)** the 564 GO terms associated with the turquoise female module, **(C)** the 75 GO terms associated with the green male module, and **(D)** the 21 terms associated with the gray60 male module. Each scatterplot shows the cluster representatives (i.e., terms remaining after the redundancy reduction) in a two dimensional space derived by applying multidimensional scaling to a matrix of the GO terms' semantic similarities. Bubble size indicates the frequency of the GO term in the underlying GO database; more general terms have larger bubbles. Bubble color indicates the significance of the enrichment in the DAVID analysis (log10 *p*-value).

groups whose eigengenes were highly positively correlated within groups, but negatively correlated across groups (Group 1: gray60, royalblue and midnight blue; Group 2: green and greenyellow; **Figures 2C,D**). Modules within a group tend to have similar expression profiles (**Figures 4C,G**) and tissue specific expression levels (**Figures 3D,F**) while across groups, these two metrics are roughly inverse.

The modules in Group 1 are most highly expressed in flies either raised on (gray60, midnight blue) or transferred to (royal blue, midnight blue) the 0.25SY diet (**Figures 4C,E,G**). The midnight blue module shows an interaction between these two effects as it is up-regulated in flies raised on the 0.25SY larval diet, but this effect is especially pronounced when combined with transfer to the 0.25SY adult diet (**Figure 4G**). The modules in Group 2 are down-regulated in flies raised on (green) or transferred to (green–yellow) the 0.25SY diet (**Figures 4D,F**). For the two modules affected by larval diet (gray60, green), flies raised on the 2.5SY diet have intermediate expression between 0.25SY and 1SY raised flies, similar to the pattern observed for the modules affected by larval diet in female flies (**Figures 4C,D**). For the two modules affected by adult diet (royal blue, green yellow) the effect of adult diet tends to be linear, thus expression either decreases (green yellow) or increases (royal blue) with increasing adult diet (**Figures 4E,F**). For the interacting module, midnight blue, there is no consistent difference between the flies raised on or transferred to the 1SY and 2.5SY diet, suggesting that this module is driven by changes in expression particular to experiencing the 0.25SY diet, especially when experienced during both development and early adulthood (**Figure 4G**).

Gene Oncology Analysis Identifies Enrichment for Nutrient Sensing and Metabolic Genes in Males

Each of the five modules are enriched for GO terms (**Supplementary File 1**). The two modules affected by larval diet, gray60, and green, possess the most extensive annotation. The gray60 module, up-regulated in flies raised on the 0.25SY larval diet (**Figure 4C**), is enriched for 21 terms, and REVIGO summary of these identifies three main functional categories: oxidation-reduction process, generation of precursor metabolites and energy, and cellular respiration (**Figure 5D**). The green module, which is down-regulated in 0.25SY raised flies (**Figure 4D**), is significantly enriched for 75 terms related to metabolism (hexose metabolic process, amine biosynthetic process, cofactor metabolic process *et cetera*) and defense response (**Figure 5C**). By contrast, the two modules affected by adult diet possess relatively little annotation: the royal blue module, which is strongly up-regulated in flies transferred to the 0.25SY adult diet (**Figure 4E**), is solely enriched for the term alkaline phosphatase activity and contains five out of the 13 putative *Drosophila* alkaline phosphatases. The green–yellow module, whose expression increases linearly with increasing adult diet (**Figure 4F**), is annotated with the two general terms proteolysis and peptidase activity. These terms are also enriched in the green module,

which falls in the same group. Finally, the midnight blue module is annotated with the general terms "response to nutrients" and "response to extracellular stimulus."

Of the 101 GO terms enriched in all five male modules, none overlapped with the terms enriched for the female turquoise reproduction and cell-cycle related module, but nearly 60% (58/101) overlapped with the female blue module. This suggests that the response to diet in males is not directly related to (female) reproduction and cell-cycle related processes, and furthermore, processes that show more subtle regulation in males are subsumed in females into the blue "non-reproduction" module.

Male Modules Show Two Distinct Tissue-Specific Expression Profiles

In addition to having correlated eigengenes (**Figure 2D**), tissue specific expression profiles are also correlated within groups (**Figures 3D,F**). In larval tissues in FlyAtlas, the Group 2 modules (green, green yellow) which are down-regulated in response to 0.25SY larval or adult diet are highly expressed overall, and they are most highly expressed in the feeding and wandering fat body (**Figure 3D**). By contrast, the Group 1 modules, which are up-regulated in response to 0.25SY larval or adult diet show generally high expression across tissues, particularly in the midgut, hindgut and malpighian tubules, but have their lowest expression in the feeding and wandering fat body (**Figure 3D**). Expression of the royal blue module in particular is restricted to the midgut, hindgut and malpighian tubules in FlyAtlas. In adult tissues of FlyAtlas, the Group 2 modules (green and green yellow) show generally lower expression than in larval tissues, but are most highly expressed in the fat body, heart and trachea (**Figure 3E**). The Group 1 modules are also generally less highly expressed in adult tissues than in larval tissues. Expression of the royal blue module in adult tissues is also constrained to the hindgut and midgut similar to its expression in larval tissues (**Figure 3E**). The gray60 module shows a similar pattern, while the midnight blue module shows expression across all tissues, but a slight tendency for higher expression in the crop (**Figure 3E**). Furthermore, two of the three modules (midnight blue, gray60) have their lowest expression in the adult fat body (**Figure 3E**). Finally, we looked at expression in the FlyGut database (**Figure 3F**). Consistent with their relatively high expression in gut tissues, the Group 1 modules are relatively highly expressed across gut regions, while the Group 2 modules show intermediate expression. It is noteworthy that the royal blue module, whose expression is most strongly restricted to the gut and malpighian tubules, contains five of 13 known alkaline phosphatases (APH; Pletcher et al., 2005), which are known to be expressed almost exclusively in the midgut and malpighian tubules (Yang et al., 2000). ALPs respond strongly to changes in available nutrition (Pletcher et al., 2002, 2005; Landis et al., 2004) and play roles in phosphate uptake and in secretory processes in epithelia (Cabrero et al., 2004). By contrast, the green module (Group 2) is annotated with terms related to metabolism (hexose metabolic process, amine biosynthetic process, cofactor metabolic process) and defense response, canonical functions of the insect fat body (Arrese and Soulages, 2010; Zhang and Xi, 2015).

TABLE 2 | Transcription-factor binding enrichments per module.

Module	TF	OR	*p*-value	*q*-value	# module	# TF	Overlap
Female							
Turquoise	BEAF-32	1.54	<0.0001	<0.0001	4,771	6,597	4,200
	CBP	1.79	<0.0001	<0.0001	4,771	1,291	953
	cnc	1.54	<0.0001	<0.0001	4,771	440	279
	disco	1.53	<0.0001	<0.0001	4,771	1,481	938
	E2f2	1.54	<0.0001	<0.0001	4,771	2,251	1,436
	GATAe	1.60	<0.0001	<0.0001	4,771	647	428
	jumu	1.82	<0.0001	<0.0001	4,771	920	690
	kn	1.52	<0.0001	<0.0001	4,771	497	312
	lin-52	1.53	<0.0001	<0.0001	4,771	2,161	1,366
	Med	1.52	<0.0001	<0.0001	4,771	4,974	3,116
	mip120	1.61	<0.0001	<0.0001	4,771	4,943	3,286
	Myb	1.55	<0.0001	<0.0001	4,771	5,589	3,583
	pho	1.56	<0.0001	<0.0001	4,771	2,978	1,921
	phol	1.64	<0.0001	<0.0001	4,771	3,713	2,508
	Snr1	1.82	<0.0001	<0.0001	4,771	289	217
	TfIIB	1.67	<0.0001	<0.0001	4,771	2,661	1,835
	trx	1.52	<0.0001	<0.0001	4,771	6,591	4,137
	ttk	1.75	<0.0001	<0.0001	4,771	453	328
	Ubx	1.72	<0.0001	<0.0001	4,771	2,251	1,603
Male							
Royalblue	bap	6.87	0.004	0.027	70	96	4
	bin	2.48	0.016	0.087	70	598	9
Midnightblue	bap	3.21	0.042	0.179	150	96	4
	bin	2.06	0.011	0.062	150	598	16
	disco	1.56	0.033	0.149	150	1,481	30
	Dsp1	1.69	0.009	0.056	150	1,455	32
	E(z)	1.72	0.007	0.048	150	1,521	34
	gro	1.65	0.035	0.155	150	1,024	22
	hkb	1.68	0.020	0.107	150	1,236	27
	Mef2	1.77	0.003	0.023	150	1,699	39
	NELF-B	2.13	0.002	0.013	150	869	24
	Nelf-E	1.78	0.047	0.195	150	606	14
	slp1	1.84	0.026	0.125	150	669	16
Gray60	inv	1.72	0.050	0.205	127	897	17
	run	1.95	0.024	0.119	127	654	14
Greenyellow	gsb-n	1.64	0.022	0.111	309	594	26
	NELF-B	1.59	0.014	0.079	309	869	37
	tin	1.80	0.024	0.121	309	374	18

Results of the hyper-geometric test for enrichment of probes known to bind particular transcription factors (TFs) per sex and module. For each significant TF we include the odds ratio (OR), the p-value and the FDR corrected q-value, the number of genes in the module (# module), the number of probes known to interact with the TF (# TF), and the number of probes overlapping between the module and the probes modulated by the TF (Overlap). We set a significance cut-off at OR > 1.5 and p-value < 0.05. The full set of tests for all modules and all TFs can be found in ***Supplementary File 1****.*

Transcription Factor Enrichment of Key Male Modules

The Group 1 modules which were up-regulated in response to 0.25SY larval or adult diet were each enriched for probes

binding TFs known to be involved in gut development (**Table 2**), which is consistent with their tissue-specific expression profiles. Both the royal blue and midnight blue modules were enriched for probes binding two related TFs (**Table 2**): *bagpipe (bap)* and *biniou (bin)*. Both of these TFs are important regulators of the development of the visceral musculature of the midgut (Azpiazu and Frasch, 1993; Zaffran et al., 2001). The midnight blue module was also enriched for nine additional TFs (**Table 2**) which are enriched for GO terms related to mesoderm development/morphogenesis, heart development, formation of the primary germ layer, and regulation of transcription from RNA polymerase II (**Supplementary File 2e**). Finally, the gray60 module was enriched for the TFs *runt* and *invected* (**Table 2**), both of which are important in the embryonic development of the hindgut (Iwaki and Lengyel, 2002; Nam et al., 2002).

Of the Group 2 modules, which were down-regulated in response to 0.25SY larval or adult diet, only the green yellow module was enriched for TF binding (**Table 2**). It was enriched for three seemingly unrelated TFs (**Table 2**): *gooseberry-neuro (gsb-n)*, *Negative Elongation Factor Complex Member B (NELF-B)*, and *tinman (tin)*. *gsb-n* is known to play an important role in the patterning of the CNS (He and Noll, 2013) while *NELF-B* is a component of the NELF complex which negatively regulates the elongation of transcription by RNA II polymerase (Wu et al., 2005). *tinman* is essential to the development of visceral and cardiac mesoderm during development (Azpiazu and Frasch, 1993).

DISCUSSION

Here, we show that both larval and adult diet affect the whole-body transcriptome of young adults, however, the effect of larval diet is considerably larger than that of adult diet, especially in females. Thus flies do not begin life with a clean slate, but rather, retain a considerable legacy of their developmental conditions in their whole-body transcriptome, setting the stage not only for early life (life history) differences in phenotypic trait values, but also for potential long-term effects of developmental diet on adult gene expression and late-life phenotypes. Indeed, we previously analyzed data from flies raised in the same experiment that were allowed to survive to middle- and old-age (May and Zwaan, 2017). At these time points, larval diet explained less than 5% of gene expression variation. Furthermore, there is little overlap between the tissues and processes affected here and those affected later in life. This suggests that while the effects observed here are substantial, they are largely lost and may be more strongly related to ensuring fitness in early life. Such early-life effects of "post-embryonic" development may be unique to species with completely distinct developmental stages, as in the fruit fly. In that respect, it is notable that that the genes affected by larval diet in males are highly expressed in the larval gut, fat body and malpighian tubules, tissues that are known to avoid complete histolysis during pupation and development into adulthood (Riddiford, 1993; Klapper, 2000; Nelliot et al., 2006; Aguila et al., 2007, 2013), suggesting a true physiological link between "post-embryonic" development and early adulthood.

Larval Diet and Young-Adult Gene Expression Are Not Linearly Correlated

We found that development on the 2.5SY larval diet, rather than leading to the most extreme expression, actually lead to intermediate expression in both sexes (**Figures 1A,B**). Therefore, there is no linear correlation between available calories during development and global gene expression profiles in young adults. We have previously shown that the effects of these diets on larval phenotypes follows a similar pattern: flies raised on the 0.25SY larval diet develop slower and are smaller as adults, while flies raised on the 2.5SY larval diet are intermediate between 0.25SY and 1SY (May et al., 2015). This suggests that both the 0.25SY and 2.5SY larval diet may reflect sub-optimal developmental conditions, and that this is reflected in the relative similarity of their gene expression profiles. Interestingly, the long-term phenotypic effects of the larval diets follow a different pattern: as caloric content of the larval diet increases, adult lifespan and fecundity decreases (May et al., 2015). Thus, the global patterns of gene expression patterns at the beginning of adult life do not appear to translate to patterns of variation in lifespan or fecundity. So, while it is clear that the developmental nutritional environment is reflected to a large extent in whole-body gene expression early in life, this effect is much smaller late in life and this variation is likely causally related to adult life history and fitness-related traits for only a small number of genes (May and Zwaan, 2017). Indeed, we have argued before (May and Zwaan, 2017), that "developmental imprints" on gene expression (or other epigenetic marks) are more likely to be "ghosts of development past" than the result of evolved mechanisms as suggested by hypotheses such as the predictive-adaptive-responses (c.f., Van Den Heuvel et al., 2016).

Larval Diet Determines Degree of Reproduction-Related Gene Expression in Young Females

Female fruit flies begin life primed for egg-laying and reproduction, being both most receptive to mating and most fecund within the first week of life (Sgrò and Partridge, 2000; Fricke et al., 2013). We show here that this immediate drive for reproduction is clearly visible in the transcriptome; while in males we could identify many different co-expression modules, the female transcriptome could only be broken down into two highly negatively correlated modules, one highly related to reproduction related processes (turquoise module) and the other not (blue module). Furthermore, the relative expression of the two modules was strongly dependent on larval diet. This suggests that, (i) at the beginning of life, there is scope for a large effect of developmental diet on reproductive output, and (ii) that developmental diet can also have long-term effects on the transcriptome, a prerequisite for each of the hypotheses that link development to adult late-life phenotypes (e.g., silver spoon, developmental programming, and PAR).

There are several plausible mechanisms by which larval diet may affect the extent of reproduction related gene expression. First, larval diet may determine the overall energy available to reproduction. In fruit flies, larval-derived carbon is known

to contribute to egg production in the first week of adult life (Min et al., 2006), and furthermore, considerable energy for early reproduction comes from the larval fat body (Aguila et al., 2013) which dissociates during pupation and persists into early adulthood as free-floating fat cells (Nelliot et al., 2006; Aguila et al., 2007, 2013). Thus, the 0.25SY larval diet may simply decrease the relative size of energy stores, and in so doing decrease overall reproduction related expression. However, such an effect is not likely to persist, as the larval fat body dissociates and after 1 week larval-derived carbon is no longer detectable in eggs (Min et al., 2006). Alternatively, larval diet may affect the relative size of reproductive tissues. Ovariole number is set during development, and females raised on nutritionally poor larval diets often have fewer ovarioles as adults, putting an upper limit on their potential fecundity (Hodin and Riddiford, 2000; Tu and Tatar, 2003). Thus, it is also plausible that the 0.25SY larval diet leads to fewer ovarioles, and a concomitant decrease in overall fecundity and reproduction related gene expression. However, given the (non-significant) trend toward decreased expression of the turquoise module observed in flies transferred to the poor larval diet as adults (whose ovariole number is set), ovariole number alone is unlikely to account for the entire response. This assessment is borne out by the observation that females resulting from larvae raised on poor-calorie food actually have increased early and total life fecundity (May et al., 2015; May and Zwaan, 2017). Another possibility is that ovary size has been affected by larval diet. In contrast to ovariole number, ovary size retains plasticity into adulthood and is not permanently set during development (Poças et al., 2020), however, larval diet does affect the overall size of the ovaries at the beginning of adulthood (Hodin and Riddiford, 2000; Tu and Tatar, 2003). This may also result in the observed differences in reproduction related gene expression. Further work looking at the expression of the individual tissues may further help to elucidate whether allometric changes, or changes in gene expression regulation *per se* underlie the observed differences.

Male Responses to Diet

In contrast to females, male gene expression could be decomposed into a substantially larger number of co-expression modules, most of which were unaffected by dietary conditions. For the modules that were affected by diet, GO annotation showed that they were primarily annotated with terms related to metabolism and nutrient sensing, and furthermore, while they overlapped considerably with the female blue "non-reproduction" module, they did not overlap at all with the female turquoise "reproduction-related" module. This suggests a much smaller role for diet in reproduction related processes in males and indicates that processes that show more subtle regulation in males are subsumed into the dichotomy of "reproduction" versus "non-reproduction" related gene expression in females. In general, these patterns and our interpretation aligns well with the much lower direct costs to reproduction in males than in females (i.e., sperm is much less "costly" than eggs).

It is becoming increasingly clear that some tissues are not histolysed during metamorphosis in *D. melanogaster*, but rather persist into adulthood. These tissues include the visceral musculature of the gut (Klapper, 2000), the larval fat body (Nelliot et al., 2006; Aguila et al., 2007, 2013), and the malpighian tubules (Riddiford, 1993). Thus, one intriguing hypothesis for the relatively high expression of the male modules affected by larval diet in these tissues is that they simply represent the carry-over of these tissues from development into adulthood, and that the size and/or the regulation of the tissue has been affected by larval diet. For example, the green module, which is highly expressed in the larval fat body, is strongly down-regulated in flies raised on the 0.25SY larval diet, suggesting that they may have accumulated less fat during development. The modules affected by adult diet then could reflect modifications of the expression of these "carried over" tissues to adapt to the current adult conditions. For example, the green yellow module, which is also highly expressed in the larval fat body (but with less specificity than the green module), is strongly down-regulated in flies transferred to the 0.25SY adult diet. Because the adult fat body only forms several days after eclosion (Hoshizaki et al., 1995; Aguila et al., 2007), one hypothesis suggested by the annotation of proteolysis and peptidase activity of this module is that the green yellow module may relate to the breakdown of the larval fat body, and that this process depends on the adult dietary conditions. It has been shown that inhibition of programmed cell death (PCD) of the larval fat body in adults increases starvation resistance (Aguila et al., 2007), thus it seems plausible that PCD of the larval fat body may also be inhibited in response to poor adult dietary conditions, and up-regulated in plentiful adult conditions where stores can easily be replenished. The two modules affected by adult diet and highly expressed in the gut (royal blue, midnight blue) may reflect the adaptation of the visceral musculature to adult dietary conditions, or adaptation of other regions of the gut. Regional patterning of the Drosophila gut is not complete until approximately 3 days after eclosion (Buchon et al., 2013), thus early adulthood may provide an optimal time to adjust the gut to prevailing dietary conditions. This opens up the possibility that long-term phenotypic effects would not be the direct result of variation in gene expression (or other epigenetic marks) at the time these phenotypes are assessed, but rather the result of structural tissue remodeling as part of post-embryonic development driven by early-life gene expression variation. This warrants a closer look at allometric variation in explaining the link between developmental perturbation and adult phenotypes, in addition to measuring molecular marks of epigenetic effects such as gene expression, DNA methylation, or histone modifications (c.f., May and Zwaan, 2017).

The question then remains: why do we not observe any evidence for a role of the gut or fat body in females? This can either be because there is no such effect in females, or because we are unable to detect it. The latter explanation is simpler: because of the effect of reproduction on the female transcriptome is so large, more subtle changes may be obscured, especially at the level of the whole-body transcriptome. However, the former explanation is also plausible. Regan et al. (2016) showed that the male and female gut of Drosophila are fundamentally different, and that these differences may underlie observed differences between the sexes in the lifespan response to adult diet. Thus, the male and female gut may also respond differently

to developmental and early adult diet. Furthermore, the female gut retains extensive plasticity in adult life, showing extensive remodeling in response to mating for instance (Reiff et al., 2015). Thus, there may be no incentive for females to "remodel" their gut early in life, as we hypothesize may be the case in males.

CONCLUSION

Here, we show that developmental diet continues to affect the whole-body transcriptome of young adult flies, especially females. This finding is relevant for the potential of the flies to respond to early life environments and their capacity for reproduction. Moreover, there is scope for long-term effects of developmental diet on gene expression, which is necessary for all hypothesized mechanisms that link developmental conditions to late-life health and disease. In females, larval diet modulates the relative expression levels of reproduction *versus* non-reproduction related genes, while in males a large portion of the transcriptome is unaffected by dietary conditions, suggesting a lesser role for both larval and adult diet in affecting gene expression. The modules affected by diet in males relate primarily to nutrient sensing and metabolism and show no evidence of the reproduction and cell-cycle related processes identified in females, however, their expression in external tissue specific data sets suggests a role for the gut and fat body in mediating the effects of diet in males. Given the oft-cited hypothesis that long-term phenotypic effects of developmental diet may be mediated by changes in gene expression, these findings suggest that such effects are possible, and furthermore, at least in *Drosophila*, are likely to be largely sex specific.

DATA AVAILABILITY STATEMENT

The original contributions presented in the study are publicly available. This data can be found here: GEO repository, accession number: GSE101882 (https://www.ncbi.nlm.nih.gov/geo/query/acc.cgi?acc=GSE101882), and all code in the github repository (https://github.com/transcriptome-in-transition/Transcriptome-in-transition).

AUTHOR CONTRIBUTIONS

CM and BZ designed the experiment. CM performed the experiments. EV and CM analyzed the data. CM, EV, and BZ wrote, edited, and approved the manuscript. All authors contributed to the article and approved the submitted version.

FUNDING

This work was supported by the European Union's FP6 Program (Network of Excellence LifeSpan FP6/036894) and the EU's FP7 Program (IDEAL FP7/2007-2011/259679).

ACKNOWLEDGMENTS

We would like to thank Dennie Helmink, Marijke Slakhorst, and Bertha Koopmanschap (†) for help with fly rearing and the set-up of the experiment. We would also like to thank Fons Debets and Jelle Zandveld for helpful discussions on the experimental design and interpretation of the results.

SUPPLEMENTARY MATERIAL

The Supplementary Material for this article can be found online at: https://www.frontiersin.org/articles/10.3389/fevo.2021.624306/full#supplementary-material

Supplementary Figure 1 | Experimental design. Eggs developed from larvae to adults under three diets, 0.25SY, 1SY, and 2.5SY, that differed only in their concentrations of sugar and yeast. Emerging adults were immediately divided across these same three diets resulting in a total of nine different treatment groups. Flies were collected for gene expression analysis 24 h after eclosion as adults. Adapted with permission from May and Zwaan (2017).

Supplementary File 1 | Module membership, GO enrichment and TF enrichment. Excel File containing module membership of all probes for both sexes (Tab 1), significant GO terms for each module (Tab 2) and results of the hypergeometric test for transcription factor enrichment for each TF in each module (Tab 3).

Supplementary File 2 | Expression and annotation of enriched transcription factors. Expression profiles of TFs enriched per module in **(a)** adult FlyAtlas data, **(b)** FlyGut regions, and **(c)** larval FlyAtlas data. REVIGO analysis of GO terms associated with TFs enriched in **(e)** the female turquoise module and **(f)** the male midnight blue module. For panels **(e)** and **(f)**, each scatterplot shows the cluster representatives (i.e., terms remaining after the redundancy reduction) in a two dimensional space derived by applying multidimensional scaling to a matrix of the GO terms' semantic similarities. Bubble size indicates the frequency of the GO term in the underlying GO database; more general terms have larger bubbles. Bubble color indicates the significance of the enrichment in the DAVID analysis (log10 *p*-value).

REFERENCES

Aguila, J. R., Hoshizaki, D. K., and Gibbs, A. G. (2013). Contribution of larval nutrition to adult reproduction in *Drosophila melanogaster*. *J. Exp. Biol.* 216, 399–406. doi: 10.1242/jeb.078311

Aguila, J. R., Suszko, J., Gibbs, A. G., and Hoshizaki, D. K. (2007). The role of larval fat cells in adult *Drosophila melanogaster*. *J. Exp. Biol.* 210, 956–963. doi: 10.1242/jeb.001586

Allocco, D. J., Kohane, I. S., and Butte, A. J. (2004). Quantifying the relationship between co-expression, co-regulation and gene function. *BMC Bioinformatics* 5:18. doi: 10.1186/1471-2105-5-18

Arrese, E. L., and Soulages, J. L. (2010). Insect fat body: energy, metabolism, and regulation. *Ann. Rev. Entomol.* 55, 207–225. doi: 10.1146/annurev-ento-112408-085356

Ayroles, J. F., Carbone, M. A., Stone, E. A., Jordan, K. W., Lyman, R. F., Magwire, M. M., et al. (2009). Systems genetics of complex traits in *Drosophila melanogaster*. *Nat. Genet.* 41, 299–307. doi: 10.1038/ng.332

Azpiazu, N., and Frasch, M. (1993). Tinman and bagpipe: two homeo box genes that determine cell fates in the dorsal mesoderm of drosophila. *Genes Dev.* 7, 1325–1340. doi: 10.1101/gad.7.7b.1325

Bateson, P., Gluckman, P., and Hanson, M. (2014). The biology of developmental plasticity and the predictive adaptive response

hypothesis. *J. Physiol.* 592, 2357–2368. doi: 10.1113/jphysiol.2014.271460

Benjamini, Y., and Hochberg, Y. (1995). Controlling the false discovery rate: a practical and powerful approach to multiple testing. *J. Royal Stat. Soc. Series B* 57, 289–300. doi: 10.1111/j.2517-6161.1995.tb02031.x

Bertram, C., Trowern, A., Copin, N., Jackson, A., and Whorwood, C. (2001). The maternal diet during pregnancy programs altered expression of the glucocorticoid receptor and type 2 11β-hydroxysteroid dehydrogenase: potential molecular mechanisms underlying the programming of hypertension in utero 1. *Endocrinology* 142, 2841–2853. doi: 10.1210/endo.142.7.8238

Boutanaev, A. M., Kalmykova, A. I., Shevelyov, Y. Y., and Nurminsky, D. I. (2002). Large clusters of co-expressed genes in the drosophila genome. *Nature* 420, 666–669. doi: 10.1038/nature01216

Bruce, K. D., and Hanson, M. A. (2010). The developmental origins, mechanisms, and implications of metabolic syndrome. *J. Nutr.* 140, 648–652. doi: 10.3945/jn.109.111179

Buchon, N., Osman, D., David, F. P., Fang, H. Y., Boquete, J. P., Deplancke, B., et al. (2013). Morphological and molecular characterization of adult midgut compartmentalization in drosophila. *Cell. Rep.* 3, 1725–1738. doi: 10.1016/j.celrep.2013.04.001

Burdge, G. C., Hanson, M. A., Slater-Jefferies, J. L., and Lillycrop, K. A. (2007). Epigenetic regulation of transcription: a mechanism for inducing variations in phenotype (fetal programming) by differences in nutrition during early life? *Br. J. Nutr.* 97, 1036–1046. doi: 10.1017/S0007114507682920

Burdge, G. C., and Lillycrop, K. A. (2010). Nutrition, epigenetics, and developmental plasticity: implications for understanding human disease. *Ann. Rev. Nutr.* 30, 315–339. doi: 10.1146/annurev.nutr.012809.104751

Cabrero, P., Pollock, V. P., Davies, S. A., and Dow, J. A. T. (2004). A conserved domain of alkaline phosphatase expression in the malpighian tubules of dipteran insects. *J. Exp. Biol.* 207, 3299–3305. doi: 10.1242/jeb.01156

Chintapalli, R. V., Wang, J., and Dow, J. A. T. (2007). Using FlyAtlas to identify better *Drosophila melanogaster* models of human disease. *Nat. Genet.* 39, 715–720. doi: 10.1038/ng2049

Emlen, D. J. (1997). Diet alters male horn allometry in the beetle *Onthophagus acuminatus* (Coleoptera: Scarabaeidae). *Proc. Biol. Sci.* 264, 567–574. doi: 10.1098/rspb.1997.0081

Fellous, S., and Lazzaro, B. P. (2010). Larval food quality affects adult (but not larval) immune gene expression independent of effects on general condition. *Mol. Ecol.* 19, 1462–1468. doi: 10.1111/j.1365-294X.2010.04567.x

Fernandez-Twinn, D. S., and Ozanne, S. E. (2006). Mechanisms by which poor early growth programs type-2 diabetes, obesity and the metabolic syndrome. *Physiol. Behav.* 88, 234–243. doi: 10.1016/j.physbeh.2006.05.039

Fricke, C., Green, D., Mills, W. E., and Chapman, T. (2013). Age-dependent female responses to a male ejaculate signal alter demographic opportunities for selection. *Proc. Biol. Sci.* 280:20130428. doi: 10.1098/rspb.2013.0428

Gärtner, S. M. K., Rathke, C., Renkawitz-Pohl, R., and Awe, S. (2014). Ex vivo culture of Drosophila pupal testis and single male germ-line cysts: dissection, imaging, and pharmacological treatment. *J. Vis. Exp.* 91:51868. doi: 10.3791/51868

Gluckman, P. D., and Hanson, M. A. (2004). The developmental origins of the metabolic syndrome. *Trends Endocrinol. Metab.* 15, 183–187. doi: 10.1016/j.tem.2004.03.002

Gluckman, P. D., Hanson, M. A., and Beedle, A. S. (2007). Early life events and their consequences for later disease: a life history and evolutionary perspective. *Am. J. Hum. Biol.* 19, 1–19. doi: 10.1002/ajhb.20590

Halfon, M. S., Gallo, S. M., and Bergman, C. M. (2008). REDfly 2.0: an integrated database of cis-regulatory modules and transcription factor binding sites in drosophila. *Nucleic Acids Res.* 36, D594–D598. doi: 10.1093/nar/gkm876

He, H., and Noll, M. (2013). Differential and redundant functions of gooseberry and gooseberry neuro in the central nervous system and segmentation of the drosophila embryo. *Dev. Biol.* 382, 209–223. doi: 10.1016/j.ydbio.2013.05.017

Hilliard, A. T., Miller, J. E., Fraley, E. R., Horvath, S., and White, S. A. (2012). Molecular microcircuitry underlies functional specification in a basal ganglia circuit dedicated to vocal learning. *Neuron* 73, 537–552. doi: 10.1016/j.neuron.2012.01.005

Hodin, J., and Riddiford, L. M. (2000). Different mechanisms underlie phenotypic plasticity and interspecifc variation for a reproductive character in drosophilids (insecta: diptera). *Evolution* 54, 1638–1653. doi: 10.1111/j.0014-3820.2000.tb00708.x

Horvath, S. (2011). *Weighted network analysis: applications in genomics and systems biology*. Berlin, Germany: Springer Science & Business Media. doi: 10.1007/978-1-4419-8819-5

Hoshizaki, D. K., Lunz, R., Johnson, W., and Ghosh, M. (1995). Identification of fat-cell enhancer activity in drosophila melanogaster using P-element enhancer traps. *Genome* 38, 497–506. doi: 10.1139/g95-065

Huang, D. W., Sherman, B. T., and Lempicki, R. A. (2008). Systematic and integrative analysis of large gene lists using DAVID bioinformatics resources. *Nat. Protocols* 4, 44–57. doi: 10.1038/nprot.2008.211

Irizarry, R. A., Hobbs, B., Collin, F., Beazer-Barclay, Y. D., Antonellis, K. J., Scherf, U., et al. (2003). Exploration, normalization, and summaries of high density oligonucleotide array probe level data. *Biostatistics* 4, 249–264. doi: 10.1093/biostatistics/4.2.249

Iwaki, D. D., and Lengyel, J. A. (2002). A Delta–Notch signaling border regulated by engrailed/invected repression specifies boundary cells in the drosophila hindgut. *Mech. Dev.* 114, 71–84. doi: 10.1016/S0925-4773(02)00061-8

Klapper, R. (2000). The longitudinal visceral musculature of drosophila melanogaster persists through metamorphosis. *Mech. Dev.* 95, 47–54. doi: 10.1016/S0925-4773(00)00328-2

Landis, G., Abdueva, D., Skvortsov, D., Yang, J., Rabin, B., Carrick, J., et al. (2004). Similar gene expression patterns characterize aging and oxidative stress in Drosophila melanogaster. *Proc. Natl. Acad. Sci. U S A.* 101, 7663–7668. doi: 10.1073/pnas.0307605101

Lanet, E., and Maurange, C. (2014). Building a brain under nutritional restriction: insights on sparing and plasticity from drosophila studies. *Front. Physiol.* 5:117. doi: 10.3389/fphys.2014.00117

Langfelder, P., and Horvath, S. (2008). WGCNA: an R package for weighted correlation network analysis. *BMC Bioinformatics* 9:559. doi: 10.1186/1471-2105-9-559

Langley-Evans, S. C. (2015). Nutrition in early life and the programming of adult disease: a review. *J. Hum. Nutr. Diet* 28, 1–14. doi: 10.1111/jhn.12212

Lillycrop, K. A., Phillips, E. S., Jackson, A. A., Hanson, M. A., and Burdge, G. C. (2005). Dietary protein restriction of pregnant rats induces and folic acid supplementation prevents epigenetic modification of hepatic gene expression in the offspring. *J. Nutr.* 135, 1382–1386. doi: 10.1093/jn/135.6.1382

Lindström, J. (1999). Early development and fitness in birds and mammals. *Trends Ecol. Evol.* 14, 343–348. doi: 10.1016/S0169-5347(99)01639-0

Maloney, C. A., Gosby, A. K., Phuyal, J. L., Denyer, G. S., Bryson, J. M., and Caterson, I. D. (2003). Site-specific changes in the expression of fat-partitioning genes in weanling rats exposed to a low-protein diet in utero. *Obesity Res.* 11, 461–468. doi: 10.1038/oby.2003.63

May, C. M., Doroszuk, A., and Zwaan, B. J. (2015). The effect of developmental nutrition on life span and fecundity depends on the adult reproductive environment in drosophila melanogaster. *Ecol. Evol.* 5, 1156–1168. doi: 10.1002/ece3.1389

May, C. M., and Zwaan, B. J. (2017). Relating past and present diet to phenotypic and transcriptomic variation in the fruit fly. *BMC Genom.* 18:640. doi: 10.1186/s12864-017-3968-z

Min, K.-J., Hogan, M. F., Tatar, M., and O'brien, D. M. (2006). Resource allocation to reproduction and soma in drosophila: a stable isotope analysis of carbon from dietary sugar. *J. Insect Physiol.* 52, 763–770. doi: 10.1016/j.jinsphys.2006.04.004

Monaghan, P. (2008). Early growth conditions, phenotypic development and environmental change. *Philos. Trans. R Soc. Lond B Biol. Sci.* 363, 1635–1645. doi: 10.1098/rstb.2007.0011

Murali, T., Pacifico, S., Yu, J., Guest, S., Roberts, G. G., and Finley, R. L. (2010). DroID 2011: a comprehensive, integrated resource for protein, transcription factor, RNA and gene interactions for drosophila. *Nucleic Acids Res.* 39, 736–743. doi: 10.1093/nar/gkq1092

Nam, S., Jin, Y.-H., Li, Q.-L., Lee, K.-Y., Jeong, G.-B., Ito, Y., et al. (2002). Expression pattern, regulation, and biological role of runt domain transcription factor, run, in caenorhabditis elegans. *Mol. Cell. Biol.* 22, 547–554. doi: 10.1128/MCB.22.2.547-554.2002

Nelliot, A., Bond, N., and Hoshizaki, D. K. (2006). Fat-body remodeling in drosophila melanogaster. *Genesis* 44, 396–400. doi: 10.1002/dvg.20229

Neyman, J., and Pearson, E. S. (1928). On the use and interpretation of certain test criteria for purposes of statistical inference: part I. *Biometrika* 20, 175–240. doi: 10.1093/biomet/20A.1-2.175

Oldham, M. C., Horvath, S., and Geschwind, D. H. (2006). Conservation and evolution of gene coexpression networks in human and chimpanzee brains. *Proc. Natl. Acad. Sci.* 103, 17973–17978. doi: 10.1073/pnas.0605938103

Pletcher, S., Macdonald, S., Marguerie, R., Certa, U., Stearns, S., Goldstein, D., et al. (2002). Genome-wide transcript profiles in aging and calorically restricted drosophila melanogaster. *Curr. Biol.* 12, 712–723. doi: 10.1016/S0960-9822(02)00808-4

Pletcher, S. D., Libert, S., and Skorupa, D. (2005). Flies and their golden apples: the effect of dietary restriction on drosophila aging and age-dependent gene expression. *Ageing Res. Rev.* 4, 451–480. doi: 10.1016/j.arr.2005.06.007

Poças, G. M., Crosbie, A. E., and Mirth, C. K. (2020). When does diet matter? the roles of larval and adult nutrition in regulating adult size traits in drosophila melanogaster. *J. Insect Physiol.* 2020:104051. doi: 10.1016/j.jinsphys.2020.104051

Ravelli, A. C. J., Van Der Meulen, J. H. P., Michels, R. P. J., Osmond, C., Barker, D. J. P., Hales, C. N., et al. (1998). Glucose tolerance in adults after prenatal exposure to famine. *Lancet* 351, 173–177. doi: 10.1016/S0140-6736(97)07244-9

Regan, J. C., Khericha, M., Dobson, A. J., Bolukbasi, E., Rattanavirotkul, N., and Partridge, L. (2016). Sex difference in pathology of the ageing gut mediates the greater response of female lifespan to dietary restriction. *eLife* 5:e10956. doi: 10.7554/eLife.10956

Reiff, T., Jacobson, J., Cognigni, P., Antonello, Z., Ballesta, E., Tan, K. J., et al. (2015). Endocrine remodelling of the adult intestine sustains reproduction in drosophila. *Elife* 4:e06930. doi: 10.7554/eLife.06930.012

Riddiford, L. M. (1993). Hormones and drosophila development. *Dev. Drosophila Melanogaster* 2, 899–939.

Roy, S., Ernst, J., Kharchenko, P. V., Kheradpour, P., Negre, N., Eaton, M. L., et al. (2010). Identification of functional elements and regulatory circuits by drosophila modencode. *Science* 330, 1787–1797. doi: 10.1126/science.1198374

Schlichting, C., and Pigliucci, M. (1998). *Phenotypic Evolution: A Reaction Norm Perspective*. Sunderland, MA: Sinauer.

Sgrò, C. M., and Partridge, L. (2000). Evolutionary responses of the life history of wild-caught drosophila melanogaster to two standard methods of laboratory culture. *Am. Nat.* 156, 341–353. doi: 10.1086/303394

Supek, F., Bošnjak, M., Škunca, N., and Šmuc, T. (2011). REVIGO summarizes and visualizes long lists of gene ontology terms. *PloS One* 6:e21800. doi: 10.1371/journal.pone.0021800

Tu, M. P., and Tatar, M. (2003). Juvenile diet restriction and the aging and reproduction of adult drosophila melanogaster. *Aging Cell.* 2, 327–333. doi: 10.1046/j.1474-9728.2003.00064.x

Van Den Heuvel, J., English, S., and Uller, T. (2016). Disposable soma theory and the evolution of maternal effects on ageing. *PLoS One* 11:e0145544. doi: 10.1371/journal.pone.0145544

Wu, C.-H., Lee, C., Fan, R., Smith, M. J., Yamaguchi, Y., Handa, H., et al. (2005). Molecular characterization of drosophila NELF. *Nucleic Acids Res.* 33, 1269–1279. doi: 10.1093/nar/gki274

Xue, Z., Huang, K., Cai, C., Cai, L., Jiang, C.-Y., Feng, Y., et al. (2013). Genetic programs in human and mouse early embryos revealed by single-cell RNA[thinsp]sequencing. *Nature* 500, 593–597. doi: 10.1038/nature12364

Yang, M. Y., Wang, Z., Macpherson, M., Dow, J. A., and Kaiser, K. (2000). A novel Drosophila alkaline phosphatase specific to the ellipsoid body of the adult brain and the lower malpighian (renal) tubule. *Genetics* 154, 285–297.

Zaffran, S., Küchler, A., Lee, H.-H., and Frasch, M. (2001). biniou (FoxF), a central component in a regulatory network controlling visceral mesoderm development and midgut morphogenesis in drosophila. *Genes Dev.* 15, 2900–2915.

Zhang, B., and Horvath, S. (2005). A general framework for weighted gene co-expression network analysis. *Stat. Appl. Genet. Mol. Biol.* 4:7. doi: 10.2202/1544-6115.1128

Zhang, Y., and Xi, Y. (2015). Fat body development and its function in energy storage and nutrient sensing in drosophila melanogaster. *J. Tissue Sci. Engin.* 6:141.

Conflict of Interest: The authors declare that the research was conducted in the absence of any commercial or financial relationships that could be construed as a potential conflict of interest.

frontiers in Ecology and Evolution

ORIGINAL RESEARCH
published: 11 March 2021
doi: 10.3389/fevo.2021.646281

Complete Metamorphosis in *Manduca sexta* Involves Specific Changes in DNA Methylation Patterns

Jasmin Gegner[1], *Heiko Vogel*[2], *André Billion*[1], *Frank Förster*[3]* *and Andreas Vilcinskas*[1,4]*

[1] Branch for Bioresources, Fraunhofer Institute for Molecular Biology and Applied Ecology IME, Gießen, Germany, [2] Department of Entomology, Max-Planck Institute for Chemical Ecology, Jena, Germany, [3] Bioinformatics and Systems Biology, Justus-Liebig-University of Gießen, Gießen, Germany, [4] Institute for Insect Biotechnology, Department of Applied Entomology, Justus-Liebig-University of Gießen, Gießen, Germany

The transition between morphologically distinct phenotypes during complete metamorphosis in holometabolous insects is accompanied by fundamental transcriptional reprogramming. Using the tobacco hornworm (*Manduca sexta*), a powerful model for the analysis of insect evolution and development, we conducted a genome-wide comparative analysis of gene expression and DNA methylation in caterpillars and adults to determine whether complete metamorphosis has an epigenetic basis in this species. Bisulfite sequencing indicated a generally low level of DNA methylation with a unimodal $CpG_{O/E}$ distribution. Expression analysis revealed that 24 % of all known *M. sexta* genes (3.729) were upregulated in last-instar larvae relative to the adult moth, whereas 26 % (4.077) were downregulated. We also identified 4.946 loci and 4.960 regions showing stage-specific differential methylation. Interestingly, genes encoding histone acetyltransferases and histone deacetylases were differentially methylated in the larvae and adults, indicating there is crosstalk between different epigenetic mechanisms. The distinct sets of methylated genes in *M. sexta* larvae and adults suggest that complete metamorphosis involves epigenetic modifications associated with profound transcriptional reprogramming, involving approximately half of all the genes in this species.

Keywords: ***Manduca sexta*, metamorphosis, epigenetics, DNA-methylation, differential gene expression, development**

OPEN ACCESS

Edited by:
Nico Posnien,
University of Göttingen, Germany

Reviewed by:
Michael Kanost,
Kansas State University, United States
Yuichiro Suzuki,
Wellesley College, United States

***Correspondence:**
Andreas Vilcinskas
andreas.vilcinskas@agrar.uni-giessen.de
Frank Förster
frank.foerster@computational.bio.uni-giessen.de

Specialty section:
This article was submitted to Evolutionary Developmental Biology, a section of the journal Frontiers in Ecology and Evolution

Received: *25 December 2020*
Accepted: *08 February 2021*
Published: *11 March 2021*

Citation:
Gegner J, Vogel H, Billion A, Förster F and Vilcinskas A (2021) Complete Metamorphosis in Manduca sexta *Involves Specific Changes in DNA Methylation Patterns. Front. Ecol. Evol. 9:646281. doi: 10.3389/fevo.2021.646281*

1. INTRODUCTION

Transformation from one morphologically distinct phenotype to another during development is known as metamorphosis. The complete metamorphosis of holometabolous insects involves a pupal stage, during which larval tissues and organs are remodeled and/or replaced by the structures required in the imagoes. A fundamental question in developmental biology is how the same genome can generate morphologically and ecologically distinct phenotypes, such as the caterpillars, pupae, and imagoes in the order Lepidoptera. Many if not all developmental processes involve the orchestrated large-scale transcriptional reprogramming of genes. We therefore postulate that the metamorphosis of holometabolous insect larvae into adults involves fundamental changes in gene expression, and that epigenetic mechanisms may be involved in this process. Epigenetics

can explain the phenotypic diversity of insect larvae, pupae, and adults sharing a common genome because such mechanisms globally modulate gene expression rather than altering the DNA sequence (Belles, 2017; Glastad et al., 2019).

There are three major epigenetic mechanisms, one of which is the expression of microRNAs. These short, non-coding RNAs (18–24 bp) operate at the post-transcriptional level to inhibit the translation of specific mRNAs by base-pairing with the untranslated regions or occasionally the coding region (Asgari, 2013; Hussain and Asgari, 2014). Individual microRNAs can regulate the expression of single genes or hundreds of genes. The role of microRNAs in the regulation of complete metamorphosis in holometabolous insects is well-established (Belles, 2017; Ylla et al., 2017). The first microRNAs that are differentially expressed during lepidopteran metamorphosis have been identified in the greater wax moth *Galleria mellonella* (Mukherjee and Vilcinskas, 2014).

The two other principal epigenetic mechanisms regulate transcriptional initiation. The first is the acetylation and deacetylation of histones by enzymes with opposing activities, thus controlling the ability of transcription factors to access chromatin and initiate gene expression. The addition of acetyl groups to histones is mediated by histone acetyltransferases (HATs), which enhance access to DNA by loosening the chromatin, whereas the removal of acetyl groups by histone deacetylases (HDACs) has the opposite effect and therefore causes gene silencing (Marks et al., 2003). We have previously shown that histone acetylation/deacetylation modulates gene expression during the complete metamorphosis of *G. mellonella* (Mukherjee et al., 2012). The involvement of both histone modification and microRNAs in this process provides evidence for cross-talk between different epigenetic mechanisms (Mukherjee and Vilcinskas, 2014).

The final major epigenetic mechanism is DNA methylation (Glastad et al., 2019). The addition of a methyl group to a cytosine residue in the dinucleotide sequence CpG results in the formation of 5-methylcytosine, which retains the base-pairing specificity of the unmodified nucleoside but influences its interactions with regulatory proteins. The transfer of methyl groups to DNA is mediated by evolutionarily-conserved enzymes collectively known as DNA methyltransferases (DNMTs). These can be divided further into maintenance methyltransferases (DNMT1), which complete the symmetrical methylation marks on newly-replicated DNA by recognizing the hemimethylated sequences inherited from each parent, and *de novo* methyltransferases (DNMT3), which establish new methylation marks on unmethylated DNA (Bestor, 2000; Klose and Bird, 2006). In insects, DNMT1 is evolutionarily conserved and widely distributed whereas DNMT3 is restricted to some species (Bewick et al., 2017). Despite the apparent loss of DNMT3 in the order Lepidoptera, these insects have functional methylation systems (Provataris et al., 2018). Indeed, the DNA of holometabolous insects is methylated, although typically only in exon sequences (Provataris et al., 2018).

Here, we tested the hypothesis that metamorphosis-related transcriptional reprogramming in the lepidopteran model species *M. sexta* involves DNA methylation. We carried out a genome-wide comparative analysis of gene expression and DNA methylation in caterpillars and adults, and identified correlations between stage-specific genes and methylation marks, including marks affecting genes involved in other epigenetic processes.

Our data provide insight into the potential role of epigenetic modifications of complete metamorphosis of holometabolous insects.

2. RESULTS

2.1. Methylation in *Manduca sexta*

Comparing DNA methylation in different developmental stages in *M. sexta*, the mean mapping efficiency for Bismark mapping for paired end mapping was 45.6 % and could be increased to 57.2 % due to the following single end mapping (**Supplementary Table 1**). The HISAT2 mean mapping for transcriptome sequencing results was 67.6 % (**Supplementary Table 1**).

The overall level of DNA methylation in each sample (L1—3, A1—3) was 0.18–0.48 %, but when focusing on specific positions (found in two out of three larvae or adults) the level of DNA methylation was much lower (0.05 %), as shown in **Supplementary Material** (**Supplementary Table 2**). To gain more insight into the methylated sites in the *M. sexta* genome, we compared the positions based on the sequence context (CpG, CHG, or CHH) and the sample type (larvae, adults, or both). This showed that the CpG context was the most prominent (62 % of all methylated sites) compared to CHG at 6 % and CHH at 32 % (**Figure 1A** and **Supplementary Table 3**). The positions were almost equally distributed in all three samples: 28 % in larvae, 37 % in adults, and 35 % in both (**Figure 1B** and **Supplementary Table 3**). The normalized CpG content ($CpG_{O/E}$) revealed a unimodal distribution (**Figure 2**). Given the relatively large number of methylated positions in the sequence contexts CHG and CHH (**Figure 1A**), we carried out a global analysis of differential methylation in *M. sexta* (CX) rather than focusing on CpG, CHG or CHH methylation alone. We identified 4946 differentially methylated loci (DMLs) and 4960 differentially methylated regions (DMRs) in total. These were classified according to their genomic location as belonging to the gene body (gb), regulatory region (rr), or intergenic region (ir). Interestingly, metamorphosis was accompanied by a significant shift in the location of DMLs and DMRs, resulting in an increase in the number of methylated sites in gene bodies at the expense of sites especially in the intergenic regions, whereas the number of methylated sites in regulatory regions was almost the same in both developmental stages (**Figure 3** and **Supplementary Table 4**).

2.2. Differential Gene Expression

The annotated *M. sexta* genome sequence contains 15.542 genes (Kanost et al., 2016a,b,c). We compared the expression profiles of all these genes in larvae and adults, and found that about half of them were either not expressed at detectable levels during either stage (n.d., 35 %) or showed no evidence of significant differential expression (n.s., 15 %). The remaining genes were either

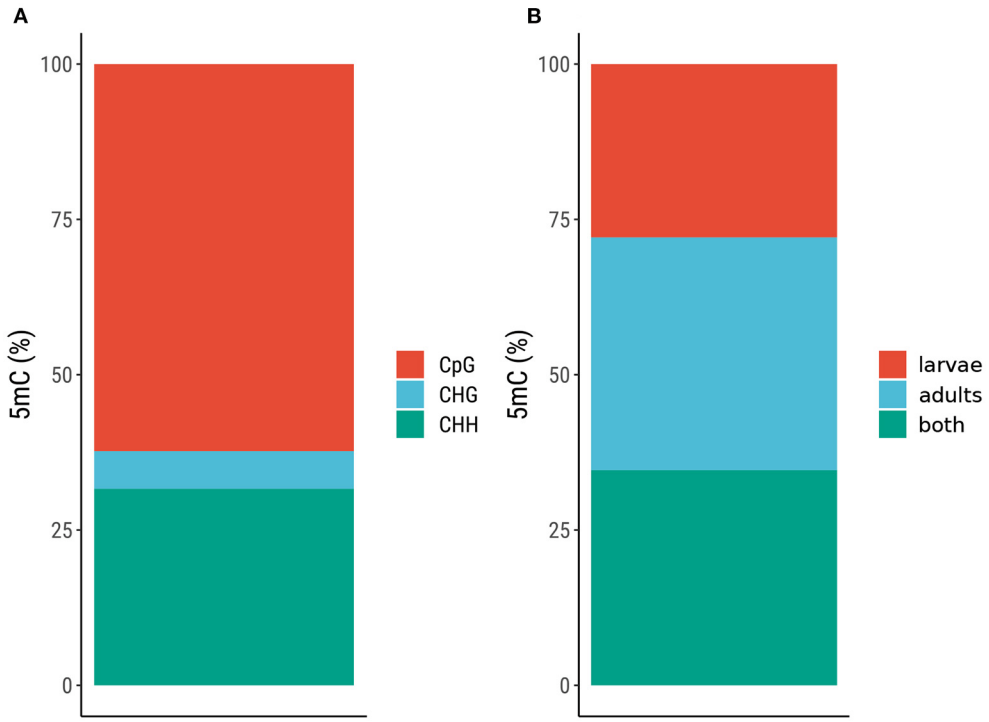

FIGURE 1 | Distribution of 5′-methylcytosine (5mC) in the genome of *Manduca sexta*. **(A)** Classification by sequence context. **(B)** Distribution across different life stages (larvae and adults).

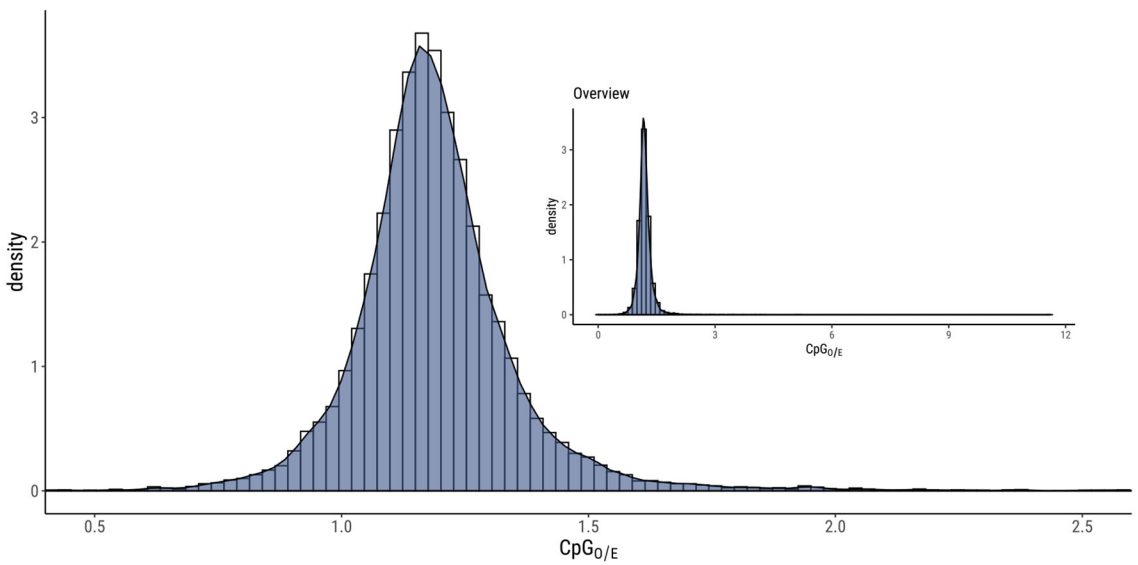

FIGURE 2 | CpG$_{O/E}$ analysis of *Manduca sexta* showing a unimodal distribution, which represents a low rate of C to T transitions in the sequence context CpG and therefore indicates a generally low level of CpG methylation.

upregulated (24 %) or downregulated (26 %) in larvae compared to imagoes (**Supplementary Table 5**). Gene ontology enrichment analysis revealed eight functional categories with stage-specific over-representation, seven of which were related to reproduction and one involved in sensory perception (**Supplementary Table 6**).

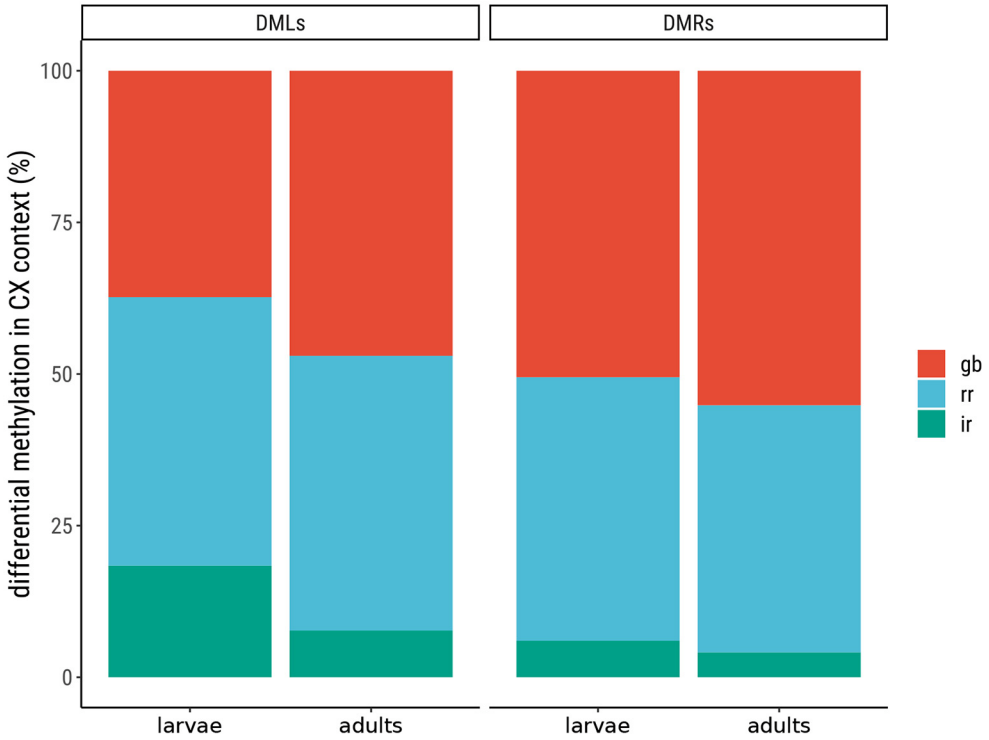

FIGURE 3 | Differential methylation in *Manduca sexta* according to genomic location. The differentially methylated loci (DMLs) and differentially methylated regions (DMRs) are classified by their location in the gene body (gb), regulatory region (rr), or intergenic region (ir).

2.3. Correlation Between Differential Methylation and Gene Expression

To investigate the correlation between differential methylation and gene expression, we selected all genes expressed at detectable levels at one or both developmental stages that also contained DMLs or DMRs (without distinguishing between the type of methylated site). Given the possibility that genes might overlap with multiple DMLs or DMRs, we also distinguished between genes that were exclusively methylated in the larvae or adults (L_5mC or A_5mC), methylated more extensively but not exclusively in the larvae or imagoes (pL_5mC or pA_5mC), and those methylated to the same extent in larvae and adults (mixed). As shown in **Table 1**, most of the differentially expressed genes showed no evidence of methylation (74 %). After this, the most abundant categories were the exclusively differentially methylated genes (L_5mC 14 % and A_5mC 10 %). Only a small proportion of the genes were assigned to the mixed, pL_5mC, and pA_5mC categories.

For the investigation of a potential correlation between methylation pattern and expression status, we analyzed the log fold change for all differential expressed genes in dependency of their methylation status. With an exception of pL_5mC all medians for log fold changes are negative and indicate a down regulation of the gene expression. For pL_5mC this trend is reversed and the median of the log fold changes is positive and represents an up regulation (**Figure 4**).

2.4. Genes of Interest

To understand the functional implications of the correlation between gene expression and DNA methylation during metamorphosis, we focused on 850 *M. sexta* genes representing eight different functional categories: chitin metabolism, detoxification, immunity, epigenetic modification, juvenile hormone/ecdysone signaling, chorion proteins, and vitellogenin (**Supplementary Table 7**). The genes coding for chorion proteins and vitellogenin showed no evidence of differential methylation. Where differential methylation was detected, in general there was no correlation between gene expression levels and the degree of DNA methylation at each developmental stage (**Table 2** and **Supplementary Table 8**). For example, seven genes encoding chitin-binding proteins were higher expressed in larvae, three of which were hypermethylated in larvae and four hypermethylated in imagoes. However, one exceptional case was the immunity-related gene Atg8 (Msex2.12227), which produces two separate transcripts encoding protein isoforms involved in autophagy. Transcript Msex2.12227-RA was upregulated in larvae relative to adults, whereas transcript Msex2.12227-RB was downregulated. The genomic region for that gene contain three differentially methylated regions: two hypermethylated in adults covering both transcripts and one hypermethylated in larvae exclusive covering the transcript Msex2.12227-RA. We also identified genes with roles in histone acetylation/deacetylation that were upregulated in imagoes and generally hypermethylated in the larvae, with the exception of one HDAC gene that hypermethylated in adults.

TABLE 1 | Classification of gene expression based on differential methylation analysis.

	Up		Down		Not significant		All	
A_5mC	307	(3.0 %)	427	(4.2 %)	241	(2.4 %)	975	(9.6 %)
pA_5mC	21	(0.2 %)	25	(0.2 %)	22	(0.2 %)	68	(0.7 %)
L_5mC	480	(4.8 %)	577	(5.7 %)	344	(3.4 %)	1401	(13.9 %)
pL_5mC	29	(0.3 %)	12	(0.1 %)	20	(0.2 %)	61	(0.6 %)
Mixed	39	(0.4 %)	70	(0.7 %)	40	(0.4 %)	149	(1.5 %)
Not differentially methylated	2.853	(28.2 %)	2.966	(29.4 %)	1632	(16.2 %)	7451	(73.7 %)

Genes are either upregulated (higher expression in larvae than adults), downregulated (higher expression in adults than larvae) or not significant (expressed at similar levels at both stages). For each gene, the methylation status was assigned as (probably) higher methylation in adults (p)A_5mC, (probably) higher methylation in larvae (p)L_5mC, mixed methylation signature with equal methylation counts higher in adults and larvae, or not differentially methylated.

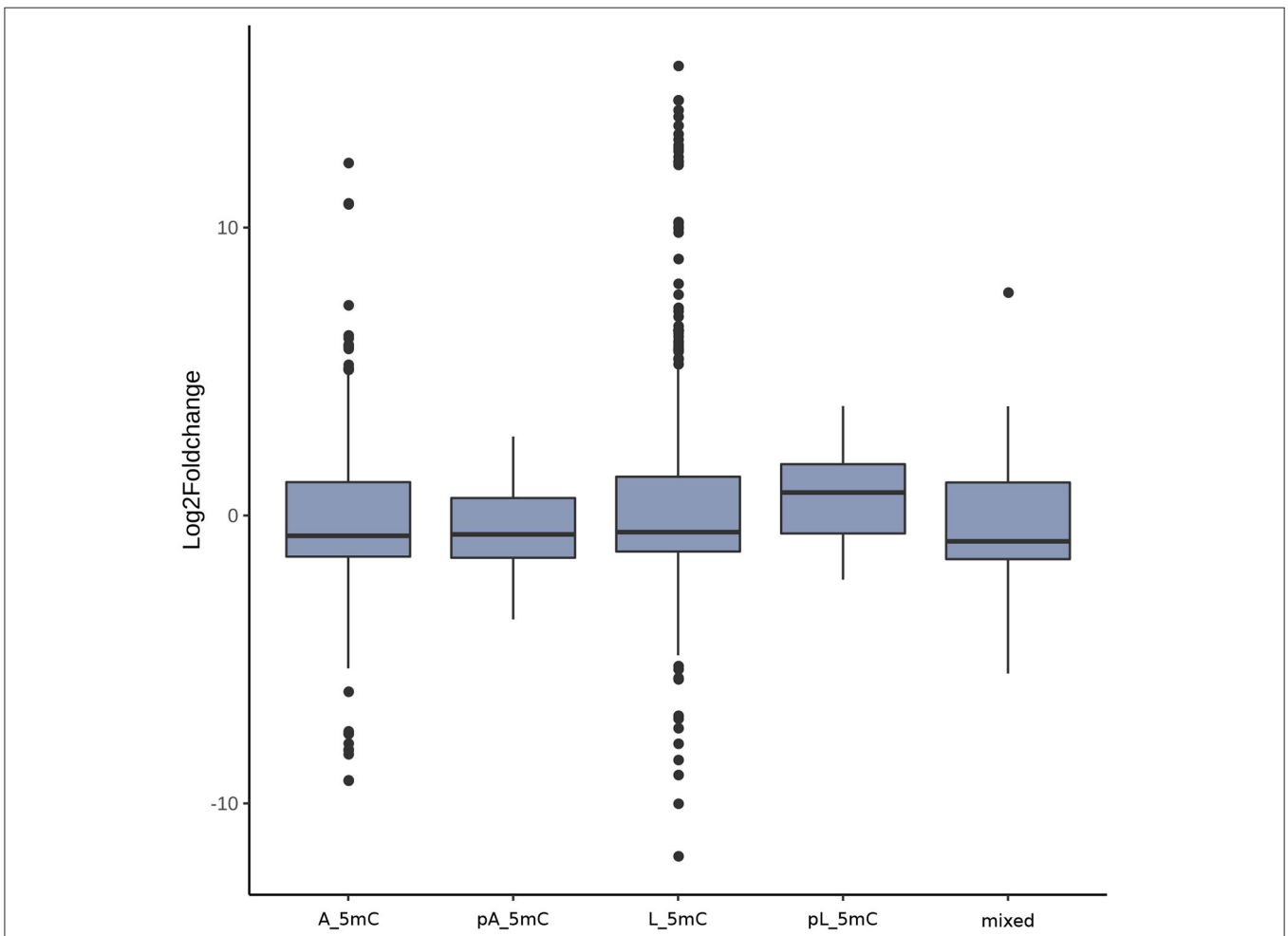

FIGURE 4 | Correlation between gene expression (log2 fold change) and the different possible groups based on methylation status per gene. The methylation status of each gene was defined as mixed, for equal numbers of methylated loci and regions in larvae and adults, as higher methylation in larvae (L_5mC) or higher methylation in adults (A_5mC) where methylation was exclusively state-specific, or as probably higher methylation in larvae (pL_5mC) or probably higher methylation in adults (pA_5mC) for loci/regions methylated in both samples but with a preference for one stage over the other.

3. DISCUSSION

DNA methylation is involved in the regulation of many physiological and developmental processes in insects, but its role in metamorphosis has not been investigated in detail. Previous studies have shown that the transcriptional reprogramming that accompanies metamorphosis is associated with other forms of epigenetic regulation, specifically microRNA expression and the acetylation/deacetylation of histones (Mukherjee et al., 2012; Mukherjee and Vilcinskas, 2014).

TABLE 2 | Summary of differential gene expression and methylation patterns in genes of interest.

Differential methylation	*N* (up)	*N* (down)	*N* (n.s.)	Gene set
L_5mC	5	0	0	
pL_5mC	0	0	0	
A_5mC	5	0	1	Chitin metabolism
pA_5mC	0	0	0	
Mixed	0	0	0	
L_5mC	5	2	1	
pL_5mC	1	0	0	
A_5mC	3	6	2	Detoxification
pA_5mC	0	0	0	
Mixed	1	0	0	
L_5mC	0	2	0	
pL_5mC	0	1	0	
A_5mC	0	1	0	Epigenetic modification
pA_5mC	0	0	0	
Mixed	0	0	0	
L_5mC	11	12	4	
pL_5mC	1	0	0	
A_5mC	9	6	3	Immune response
pA_5mC	0	0	0	
Mixed	0	3	0	
L_5mC	1	0	1	
pL_5mC	0	0	0	
A_5mC	0	0	0	Juvenile hormone and ecdysone regulated pathways
pA_5mC	0	0	0	
Mixed	0	0	0	

Number (N) of upregulated, downregulated (down), and not significantly differentially expressed (n.s.) genes are listed according to the type of differential methylation: higher methylation in larvae (L_5mC), probably higher methylation in larvae (pL_5mC), higher methylation in adults (A_5mC), probably higher methylation in adults (pA_5mC), or equal amount of differential methylated regions (mixed).

Therefore, we investigated the relationship between genomic DNA methylation and developmentally-regulated gene expression during metamorphosis in the model lepidopteran species *M. sexta*.

Initially we measured the general prevalence of DNA methylation in the *M. sexta* genome and found that the overall level of methylation was low. This is in line with recent findings in other holometabolous insects, which tend to have lower levels of DNA methylation in exons in comparison to hemimetabolous insects (Provataris et al., 2018). Accordingly, $CpG_{O/E}$ analysis revealed a unimodal distribution which indicates a limited degree of C to T transitions over evolutionary timescales, consistent with a low level of CpG methylation (Provataris et al., 2018). Similar unimodal distributions have been reported in the silkworm *Bombyx mori*, the red flour beetle *Tribolium castaneum*, and the large milkweed bug *Oncopeltus fasciatus* (Bewick et al., 2017) as well as the mosquito *Anopheles gambiae* (Bewick et al., 2017). Two different distributions in one specimen were found in the ant species *Camponotus floridanus* and *Harpegnathos saltator*, which also show low DNA methylation levels. While CpG dinucleotides have a bimodal distribution, the CHH and CHG context showed a unimodal one (Bonasio et al., 2012). In contrast, the honeybee *Apis mellifera* features a bimodal $CpG_{O/E}$ distribution reflecting DNA methylation associated with differential gene expression in different bee castes (Elango et al., 2009). However, positive correlation between gene expression and cytosines located in CpG context in species with a unimodal $CpG_{O/E}$ and low methylation levels, like it was observed for *T. castaneum* (Song et al., 2017). Consequently, the sparse DNA methylation in *M. sexta* does not exclude the possibility of a role during complete metamorphosis. We therefore expanded our comparative analysis of DNA methylation in larvae and adults beyond the $CpG_{O/E}$ distribution to include the separate analysis of sites located in gene bodies, regulatory regions, and intergenic regions. This revealed that both stages showed preponderance for DMLs and DMRs in the gene body. Nevertheless, a significant shift during metamorphosis was detected with a greater proportion of gene body sites in the adult moths primarily at the expense of intergenic sites, which were more prevalent in the larvae. The number of sites in gene regulatory regions remained almost steady throughout development. These observations are in contrast with the report of Song et al. (2017) showing that more than 80 % of the methylated cytosine residues in *T. castaneum* are almost entirely restricted to intergenic regions (Song et al., 2017).

We were particularly interested to probe the relationship between differential methylation and differential gene expression during metamorphosis in *M. sexta*. We found that almost half of all genes were differentially expressed, the remainder either are expressed at similar levels in both larvae and adults or not expressed at detectable levels in either stage. There was little overall correlation between the methylation patterns and gene expression profiles, but there were a small number of striking correlations for highly relevant genes. One of the differentially methylated genes in *M. sexta* encoded chitin synthase 2. In *B. mori* a gene from the same class is also differentially methylated during development, with the methylation mark being erased from the promoter in the adult allowing its expression in the wings (Xu et al., 2018). We also observed a correlation between expression and methylation for two different transcripts of the atg8, which is involved in autophagy. Isoform RA was upregulated in larvae and the corresponding genomic region was potentially hypermethylated in imagoes, whereas isoform RB was downregulated in larvae and the corresponding genomic region was exclusively hypermethylated in the adults. Similarly, *G. mellonella* Atg8 is induced during metamorphosis, with the increasing abundance of the transcript and protein suggesting a role in midgut transformation (Khoa and Takeda, 2012). Combined with our findings, the data suggest that DNA methylation contributes to the regulation of Atg8 during metamorphosis in the Lepidoptera. Juvenile hormone and ecdysone are particularly important regulators in insect development, and the corresponding genes were recently found to be regulated by histone acetylation and deacetylation (Roy and Palli, 2018). We therefore focused on the corresponding *M. sexta* genes, but only two of these were differentially methylated genes and there was no relationship with the observed expression

profiles. The absence of a link between DNA methylation and juvenile hormone has also been demonstrated in honeybees (Cardoso-Junior et al., 2018). The latter study also showed that DNA hypomethylation led to an increase in vitellogenin expression, which is important for reproduction. In contrast, DNA hypomethylation in the brown planthopper *Nilaparvata lugens* caused a loss of fecundity (Zhang et al., 2015). In *M. sexta*, we found no evidence that genes encoding chorion proteins or vitellogenin were differentially methylated, suggesting they are not regulated directly by this epigenetic mechanism.

The expression of differentially methylated genes related to the RNA interference pathway declined during the transition from larvae to imagoes, suggesting that RNA-dependent regulation may play a more prominent role in *M. sexta* larvae than adults. We identified few differentially methylated genes involved in detoxification and immunity-related functions, but interestingly we found that some genes with roles in histone acetylation/deacetylation were upregulated in adults and generally hypermethylated in the larvae, with the exception of one HDAC gene that hypermethylated in imagoes. This indicates there is crosstalk between different epigenetic mechanisms and that histone modification may work in concert with DNA methylation during metamorphosis in *M. sexta*. Similarly, we found that the specific inhibition of HATs in *G. mellonella* delays pupation whereas the inhibition of HDACs leads to precocious pupation and accelerated development (Mukherjee et al., 2012). Given that the opposing activities of HATs and HDACs are tightly regulated, we conclude that differential methylation of the corresponding genes has the potential to contribute to the epigenetic regulation of transcriptional reprogramming during metamorphosis in *M. sexta* and other lepidopterans. Furthermore, histone acetylation and deacetylation in *T. castaneum* influence the production of juvenile hormone (Roy and Palli, 2018). Thus, our findings suggest that DNA methylation could indirectly regulate the juvenile hormone system.

Metamorphosis in the oyster *Crassostrea gigas* is accompanied by changes in the methylation status of exons, introns, promoters, repeats and transposons, including the increased methylation of exons at the expense of introns, which contrasts with our findings in *M. sexta* (Riviere et al., 2017). The same study revealed that, regardless of the level of methylation, the pattern of methylation within genes is associated with transcriptional regulation. Another recent study revealed that the model cephalochordate *Amphioxus lanceolatum* has also low levels of CpG methylation, but this nevertheless is involved in the regulation of metamorphosis (Marletaz et al., 2018). Changes in DNA methylation patterns therefore have the capability to accompany metamorphosis in all organisms that contain methylated cytosines, but there is immense diversity in terms of the methylation targets: gene bodies, regulatory regions, and intergenic regions. Even low levels of methylation can help to regulate the transcriptional reprograming that occurs during metamorphosis in holometabolous animals, potentially in an indirect manner involving other epigenetic mechanisms. We have provided the first evidence that DNA methylation is potentially involved in the complete metamorphosis of *M. sexta*, a model lepidopteran.

4. METHODS

4.1. Sample Preparation

Samples were taken from our in-house *M. sexta* stock, which was reared as previously described (Gegner et al., 2019). We selected three female L5 during their feeding stage (2–3 days after molting) and three female adults 2–3 days after their eclosion. Individual insects were frozen and ground in liquid nitrogen. RNA was isolated from 50 mg of ground tissue of one animal using the Direct-zol RNA MiniPrep Kit (ZymoResearch) including DNA digestion according to the manufacturer's recommendations. Sample quantity and purity were assessed using a NanoDrop ND-1000 UV/Vis spectrophotometer (Thermo Fisher Scientific) and the integrity was verified using an Agilent 2100 Bioanalyzer and a RNA 6000 Nano Kit (Agilent Technologies). DNA was extracted from equal amounts of tissue from the same individual using the Genomic-tip 20/G and Genomic DNA Buffer Set (Qiagen) according to the manufacturer's protocol. RNA-Seq using poly(A)+ enriched RNA fragmented to an average of 250 bp and bisulfite sequencing were carried out using the Illumina 2000 HiSeq2500 platform at GATC Biotech (Eurofins Genomics) based on single samples of 2 µg RNA or 1 µg DNA, respectively. Sample preparation for Bisulfite and RNA sequencing was performed by GATC Biotech using their in house protocols.

4.2. Raw Read Processing and Methylation Analysis

Sequence data were processed using GNU parallel v20141022 (Tange, 2011). The quality of the raw and processed reads was controlled using FastQC v0.11.7 (Andrews, 2010). Sequences were trimmed using Trim Galore v0.4.5 (Krueger, 2012) based on FastQC v0.11.7 and Cutadapt v1.9.1 (Martin, 2011). The software was combined into a Docker Trim Galore image (Förster, 2018i) tagged v0.4.5.1. Trim Galore was executed for each Fastq file pair using the following parameters: `-retain_unpaired -paired -fastqc_args -nogroup -noextract -outdir QC/after_trimming' -gzip -length 20 -quality 20 -fastqc`.

The *M. sexta* draft genome sequence (Kanost et al., 2016b) was used as a reference (Kanost et al., 2016a,b,c). Reads were mapped by paired-end mapping in Bismark v0.15.0 (Krueger and Andrews, 2011) using Bowtie2 v2.3.4.1 with default settings (Langmead and Salzberg, 2012). The software was combined into a Bismark Docker image (Förster, 2018a) tagged v0.15.0. Unmapped reads were remapped separately by single-end mapping, and all mapped reads were deduplicated using the Perl script `deduplicate_bismark_alignment_output.pl` from Bismark software package. Positions of one biological sample with coverage > 10 and $\geq$ 10% methylated cytosine residues were defined as methylated (Wang et al., 2013). If positions were called methylated in two out of three biological samples per developmental stage, they were defined as methylated within that stage. Differential methylation analysis

was processed using DSS v2.26.0 (Wu et al., 2013, 2015; Feng et al., 2014; Park and Wu, 2016) in R v3.4.4 (R Development Core Team, 2020) with default settings and an unspecified cytosine context (CX). The *p*-value threshold was set to 0.001 for differentially methylated loci and to 0.01 for differentially methylated regions. The DSS installation was combined into a DSS Docker image (Förster, 2018c) and tagged v2.28.0.

4.3. Characterization of Methylated Regions

The original genome annotation file contained only some annotations for 5′ and 3′ untranslated regions (UTRs). Therefore, the complete file was re-analyzed and annotations for 5′ and 3′ UTRs were added to the transcript annotation, if the coding region was shorter than the complete transcript. The genome was sectioned into three sequence categories: gene bodies (gb: exons, introns, 5′ and 3′ UTRs), regulatory regions (rr: sequences 2 kbp beyond the UTRs), and intergenic regions (ir). DMLs and DMRs were characterized by their location in the genome and the expression of any genes. These results were summarized per gene and the methylation status of each gene was defined as mixed, for equal numbers of methylated loci and regions in larvae and imagoes, as higher methylation in larvae (L_5mC) or higher methylation in adults (A_5mC) where methylation was exclusively state-specific, or as probably higher methylation in larvae (pL_5mC) or probably higher methylation in adults (pA_5mC) for loci/regions methylated in both samples but with a preference for one stage over the other.

4.4. RNA Raw Read Processing and Differential Expression Analysis

Quality control measures, including the filtering of high-quality reads based on fastq file scores, the removal of reads containing primer/adapter sequences, and trimming of the read length, were carried out using CLC Genomics Workbench v8.1 (Qiagen Bioinformatics, 2018). Predicted transcript sequences in the *M. sexta* draft genome (Kanost et al., 2016a) sequence were downloaded from (Kanost et al., 2016c) and matched to our RNA-Seq data using HISAT2 v2.1.0 (Kim et al., 2015). The software was combined into a HISAT2 Docker image (Förster, 2018d) and tagged v2.1.0. The resulting SAM files were converted into BAM files using samtools v1.9 (Li et al., 2009). The BAM files were processed by stringtie v1.3.4d (Pertea et al., 2015, 2016) to generate count information for each transcript and sample. Stringtie includes the script `prepDE.py` which was used to prepare the mapping counts for the differential expression analysis. Docker images are available containing samtools (Förster, 2018g) and stringtie (Förster, 2018h), tagged v1.9 and v1.3.4d, respectively.

Differential expression analysis was performed using DESeq2 v1.14.1 (Love et al., 2014) for GNU R v3.4.4, which is available as a Docker image (Förster, 2018b) tagged v1.14.1. All transcripts with normalized count sums of < 1.000 across all samples were defined as not detected (n.d.). Transcripts with adjusted $p \geq 0.05$ showed no significant differential expression profiles (n.s.). Where the adjusted *p*-values were < 0.05, a log2 fold change < 0 reflected the upregulation of the corresponding gene in larvae compared to imagoes whereas a log2 fold change > 0 reflected the downregulation of that gene in larvae compared to adults. Genes were classified as modulated when the expression of at least one transcript was upregulated or downregulated. If the same gene was simultaneously represented by upregulated and downregulated transcripts, the expression class was defined by the mRNA with the highest raw mean value.

4.5. $CpG_{O/E}$ Analysis

The normalized CpG dinucleotide content was used as a proxy for the presence of DNA methylation because methylated cytosine residues are prone to spontaneous deamination into thymine, leading to a gradual decline in the prevalence of CpG dinucleotides, a phenomenon known as CpG depletion (Provataris et al., 2018). Based on the published gene set, $CpG_{O/E}$ analysis was performed according to Bird (1980). We used the script `cpgoe.pl` with the gene annotation file and the draft genome scaffolds as inputs.

4.6. Gene Set (Re-)annotation

The original *M. sexta* gene set was re-annotated using InterproScan v5.27-66.0 (Jones et al., 2014), including separately-licensed versions of TMHMM v2.0c (Sonnhammer et al., 1998; Krogh et al., 2001), SignalP v4.1 (Petersen et al., 2011), and Phobius v1.01 (Kall et al., 2004). A Docker image (Förster, 2018e) comprising the installation of InterproScan and all the additional publicly available software is tagged v5.27.66. Separately-licensed software was added to the running Docker container as volume.

4.7. Gene Ontology Enrichment

Gene ontology terms were obtained by InterproScan reannotation, and gene enrichment analysis was carried out using ontologizer v2.1 (Bauer et al., 2008). The docker image providing the software installation (Förster, 2018f) was tagged as v2.1. The required `go.obo` file (Ashburner et al., 2000; The Gene Ontology, Consortium, 2019) was downloaded from (The Gene Ontology, Consortium, 2018).

4.8. Genes of Interest

We analyzed 850 genes of interest to determine their methylation status and expression profile. We selected genes involved in chitin metabolism (65), detoxification (255), immunity (411), epigenetic modification (22), and juvenile hormone/ecdysone signaling (15), as well as those encoding chorion proteins (79) or vitellogenin (3) (Palli et al., 1992; Segraves and Woldin, 1993; Fujiwara et al., 1995; Hiruma et al., 1995; Jindra et al., 1996, 1997; Zhou et al., 1998a,b; Weller et al., 2001; Stilwell et al., 2003; Dubrovskaya et al., 2004; Cao et al., 2015a,b; Tetreau et al., 2015a,b; Kanost et al., 2016a). A full list is available in **Supplementary Material** (**Supplementary Table 7**).

DATA AVAILABILITY STATEMENT

The datasets presented in this study can be found in online repositories. The names of the repository/repositories and

accession number(s) can be found below: https://www.ncbi.nlm.nih.gov/, PRJNA517460.

AUTHOR CONTRIBUTIONS

JG and FF contributed to analysis and interpretation of data. HV, AB, and AV designed the study. AV inspired the study and acquired funding. All authors contributed to the drafting of the manuscript and gave their final approval.

FUNDING

AV acknowledges generous funding by the Hessen State Ministry of Higher Education, Research and the Arts (HMWK) via the LOEWE Centers Insect Biotechnology and Bioresources and Translational Biodiversity Genomics. HV acknowledges funding by the Max Planck Gesellschaft.

ACKNOWLEDGMENTS

We thank Richard M. Twyman for editing the manuscript.

SUPPLEMENTARY MATERIAL

The Supplementary Material for this article can be found online at: https://www.frontiersin.org/articles/10.3389/fevo.2021.646281/full#supplementary-material

REFERENCES

Andrews, S. (2010). *FastQC: A Quality Control Tool for High Throughput Sequence Data*. Available online at: http://www.bioinformatics.babraham.ac.uk/projects/fastqc

Asgari, S. (2013). MicroRNA functions in insects. *Insect Biochem. Mol. Biol.* 43, 388–397. doi: 10.1016/j.ibmb.2012.10.005

Ashburner, M., Ball, C. A., Blake, J. A., Botstein, D., Butler, H., Cherry, J. M., et al. (2000). Gene ontology: tool for the unification of biology. The Gene Ontology Consortium. *Nat. Genet.* 25, 25–29. doi: 10.1038/75556

Bauer, S., Grossmann, S., Vingron, M., and Robinson, P. N. (2008). Ontologizer 2.0-a multifunctional tool for GO term enrichment analysis and data exploration. *Bioinformatics* 24, 1650–1651. doi: 10.1093/bioinformatics/btn250

Belles, X. (2017). MicroRNAs and the evolution of insect metamorphosis. *Annu. Rev. Entomol.* 62, 111–125. doi: 10.1146/annurev-ento-031616-034925

Bestor, T. H. (2000). The DNA methyltransferases of mammals. *Hum. Mol. Genet.* 9, 2395–2402. doi: 10.1093/hmg/9.16.2395

Bewick, A. J., Vogel, K. J., Moore, A. J., and Schmitz, R. J. (2017). Evolution of DNA methylation across insects. *Mol. Biol. Evol.* 34, 654–665. doi: 10.1093/molbev/msw264

Bird, A. P. (1980). DNA methylation and the frequency of CpG in animal DNA. *Nucleic Acids Res.* 8, 1499–1504. doi: 10.1093/nar/8.7.1499

Bonasio, R., Li, Q., Lian, J., Mutti, N. S., Jin, L., Zhao, H., et al. (2012). Genome-wide and caste-specific DNA methylomes of the ants *Camponotus floridanus* and *Harpegnathos saltator*. *Curr. Biol.* 22, 1755–1764. doi: 10.1016/j.cub.2012.07.042

Cao, X., He, Y., Hu, Y., Wang, Y., Chen, Y. R., Bryant, B., et al. (2015a). The immune signaling pathways of *Manduca sexta*. *Insect Biochem. Mol. Biol.* 62, 64–74. doi: 10.1016/j.ibmb.2015.03.006

Cao, X., He, Y., Hu, Y., Zhang, X., Wang, Y., Zou, Z., et al. (2015b). Sequence conservation, phylogenetic relationships, and expression profiles of nondigestive serine proteases and serine protease homologs in *Manduca sexta*. *Insect Biochem. Mol. Biol.* 62, 51–63. doi: 10.1016/j.ibmb.2014.10.006

Cardoso-Junior, C. A. M., Guidugli-Lazzarini, K. R., and Hartfelder, K. (2018). DNA methylation affects the lifespan of honey bee (*Apis mellifera* L.) workers - Evidence for a regulatory module that involves vitellogenin expression but is independent of juvenile hormone function. *Insect Biochem. Mol. Biol.* 92, 21–29. doi: 10.1016/j.ibmb.2017.11.005

Dubrovskaya, V. A., Berger, E. M., and Dubrovsky, E. B. (2004). Juvenile hormone regulation of the E75 nuclear receptor is conserved in Diptera and Lepidoptera. *Gene* 340, 171–177. doi: 10.1016/j.gene.2004.07.022

Elango, N., Hunt, B. G., Goodisman, M. A., and Yi, S. V. (2009). DNA methylation is widespread and associated with differential gene expression in castes of the honeybee, *Apis mellifera*. *Proc. Natl. Acad. Sci. U.S.A.* 106, 11206–11211. doi: 10.1073/pnas.0900301106

Feng, H., Conneely, K. N., and Wu, H. (2014). A Bayesian hierarchical model to detect differentially methylated loci from single nucleotide resolution sequencing data. *Nucleic Acids Res.* 42:e69. doi: 10.1093/nar/gku154

Förster, F. (2018a). *Bismark Docker Image*. Dockerhub. Available online at: https://hub.docker.com/r/greatfireball/ime_bismark

Förster, F. (2018b). *DESeq2 Docker Image*. Dockerhub. Available online at: https://hub.docker.com/r/greatfireball/ime_deseq2

Förster, F. (2018c). *DSS Docker Image*. Dockerhub. Available online at: https://hub.docker.com/r/greatfireball/ime_dss

Förster, F. (2018d). *Hisat2 Docker Image*. Dockerhub. Available online at: https://hub.docker.com/r/greatfireball/ime_hisat2

Förster, F. (2018e). *InterProScan Docker Image*. Dockerhub. Available online at: https://hub.docker.com/r/greatfireball/ime_interproscan

Förster, F. (2018f). *Ontologizer Docker Image*. Dockerhub. Available online at: https://hub.docker.com/r/greatfireball/ime_ontologizer

Förster, F. (2018g). *Samtools Docker Image*. Dockerhub. Available online at: https://hub.docker.com/r/greatfireball/ime_samtools

Förster, F. (2018h). *Stringtie Docker Image*. Dockerhub. Available online at: https://hub.docker.com/r/greatfireball/ime_stringtie

Förster, F. (2018i). *TrimGalore Docker Image*. Dockerhub. Available online at: https://hub.docker.com/r/imetools/trimgalore

Förster, F. (2019). *Digital Supplemental Source Code*. Zenodo. doi: 10.5281/zenodo.2548594

Fujiwara, H., Jindra, M., Newitt, R., Palli, S. R., Hiruma, K., and Riddiford, L. M. (1995). Cloning of an ecdysone receptor homolog from *Manduca sexta* and the developmental profile of its mRNA in wings. *Insect Biochem. Mol. Biol.* 25, 845–856. doi: 10.1016/0965-1748(95)00023-O

Gegner, J., Baudach, A., Mukherjee, K., Halitschke, R., Vogel, H., and Vilcinskas, A. (2019). Epigenetic mechanisms are involved in sex-specific trans-generational immune priming in the lepidopteran model host *Manduca sexta*. *Front. Physiol.* 10:137. doi: 10.3389/fphys.2019.00137

Glastad, K. M., Hunt, B. G., and Goodisman, M. A. D. (2019). Epigenetics in insects: genome regulation and the generation of phenotypic diversity. *Annu. Rev. Entomol.* 64, 185–203. doi: 10.1146/annurev-ento-011118-111914

Hiruma, K., Carter, M. S., and Riddiford, L. M. (1995). Characterization of the dopa decarboxylase gene of *Manduca sexta* and its suppression by 20-hydroxyecdysone. *Dev. Biol.* 169, 195–209. doi: 10.1006/dbio.1995.1137

Hussain, M., and Asgari, S. (2014). MicroRNAs as mediators of insect host-pathogen interactions and immunity. *J. Insect Physiol.* 70, 151–158. doi: 10.1016/j.jinsphys.2014.08.003

Jindra, M., Huang, J. Y., Malone, F., Asahina, M., and Riddiford, L. M. (1997). Identification and mRNA developmental profiles of two ultraspiracle isoforms in the epidermis and wings of *Manduca sexta*. *Insect Mol. Biol.* 6, 41–53. doi: 10.1046/j.1365-2583.1997.00153.x

Jindra, M., Malone, F., Hiruma, K., and Riddiford, L. M. (1996). Developmental profiles and ecdysteroid regulation of the mRNAs for two ecdysone receptor isoforms in the epidermis and wings of the tobacco hornworm, *Manduca sexta*. *Dev. Biol.* 180, 258–272. doi: 10.1006/dbio.1996.0299

Jones, P., Binns, D., Chang, H. Y., Fraser, M., Li, W., McAnulla, C., et al. (2014). InterProScan 5: genome-scale protein function classification. *Bioinformatics* 30, 1236–1240. doi: 10.1093/bioinformatics/btu031

Kall, L., Krogh, A., and Sonnhammer, E. L. (2004). A combined transmembrane topology and signal peptide prediction method. *J. Mol. Biol.* 338, 1027–1036. doi: 10.1016/j.jmb.2004.03.016

Kanost, M. R., Arrese, E. L., Cao, X., Chen, Y. R., Chellapilla, S., Goldsmith, M. R., et al. (2016a). Multifaceted biological insights from a draft genome sequence of the tobacco hornworm moth, *Manduca sexta*. *Insect Biochem. Mol. Biol.* 76, 118–147. doi: 10.1016/j.ibmb.2016.07.005

Kanost, M. R., Arrese, E. L., Cao, X., Chen, Y. R., Chellapilla, S., Goldsmith, M. R., et al. (2016b). *Manduca sexta Genome Sequence*. Available online at: https://i5k.nal.usda.gov/data/Arthropoda/mansex-%28Manduca_sexta%29/Current%20Genome%20Assembly/1.Genome%20Assembly/Manduca_sexta_v1.0/Scaffolds/

Kanost, M. R., Arrese, E. L., Cao, X., Chen, Y. R., Chellapilla, S., Goldsmith, M. R., et al. (2016c). *Manduca sexta Genome Annotation*. Available online at: https://i5k.nal.usda.gov/data/Arthropoda/mansex-(Manduca_sexta)/Current%20Genome%20Assembly/2.Official%20or%20Primary%20Gene%20Set/OGS2.0/ms_ogs_transcripts.fa

Khoa, D. B., and Takeda, M. (2012). Expression of autophagy 8 (Atg8) and its role in the midgut and other organs of the greater wax moth, *Galleria mellonella*, during metamorphic remodelling and under starvation. *Insect Mol. Biol.* 21, 473–487. doi: 10.1111/j.1365-2583.2012.01152.x

Kim, D., Langmead, B., and Salzberg, S. L. (2015). HISAT: a fast spliced aligner with low memory requirements. *Nat. Methods* 12, 357–360. doi: 10.1038/nmeth.3317

Klose, R. J., and Bird, A. P. (2006). Genomic DNA methylation: the mark and its mediators. *Trends Biochem. Sci.* 31, 89–97. doi: 10.1016/j.tibs.2005.12.008

Krogh, A., Larsson, B., von Heijne, G., and Sonnhammer, E. L. (2001). Predicting transmembrane protein topology with a hidden Markov model: application to complete genomes. *J. Mol. Biol.* 305, 567–580. doi: 10.1006/jmbi.2000.4315

Krueger, F. (2012). Trim Galore: *A Wrapper Tool Around Cutadapt and FastQC*. Available online at: http://www.bioinformatics.babraham.ac.uk/projects/trim_galore

Krueger, F., and Andrews, S. R. (2011). Bismark: a flexible aligner and methylation caller for Bisulfite-Seq applications. *Bioinformatics* 27, 1571–1572. doi: 10.1093/bioinformatics/btr167

Langmead, B., and Salzberg, S. L. (2012). Fast gapped-read alignment with Bowtie 2. *Nat. Methods* 9, 357–359. doi: 10.1038/nmeth.1923

Li, H., Handsaker, B., Wysoker, A., Fennell, T., Ruan, J., Homer, N., et al. (2009). The sequence alignment/map format and SAMtools. *Bioinformatics* 25, 2078–2079. doi: 10.1093/bioinformatics/btp352

Love, M. I., Huber, W., and Anders, S. (2014). Moderated estimation of fold change and dispersion for RNA-seq data with DESeq2. *Genome Biol.* 15:550. doi: 10.1186/s13059-014-0550-8

Marks, P. A., Miller, T., and Richon, V. M. (2003). Histone deacetylases. *Curr. Opin. Pharmacol.* 3, 344–351. doi: 10.1016/S1471-4892(03)00084-5

Marletaz, F., Firbas, P. N., Maeso, I., Tena, J. J., Bogdanovic, O., Perry, M., et al. (2018). *Amphioxus* functional genomics and the origins of vertebrate gene regulation. *Nature* 564, 64–70. doi: 10.1038/s41586-018-0734-6

Martin, M. (2011). Cutadapt removes adapter sequences from high-throughput sequencing reads. *EMBnet J.* 17:10. doi: 10.14806/ej.17.1.200

Mukherjee, K., Fischer, R., and Vilcinskas, A. (2012). Histone acetylation mediates epigenetic regulation of transcriptional reprogramming in insects during metamorphosis, wounding and infection. *Front. Zool.* 9:25. doi: 10.1186/1742-9994-9-25

Mukherjee, K., and Vilcinskas, A. (2014). Development and immunity-related microRNAs of the lepidopteran model host *Galleria mellonella*. *BMC Genomics* 15:705. doi: 10.1186/1471-2164-15-705

Palli, S. R., Hiruma, K., and Riddiford, L. M. (1992). An ecdysteroid-inducible *Manduca* gene similar to the *Drosophila* DHR3 gene, a member of the steroid hormone receptor superfamily. *Dev. Biol.* 150, 306–318. doi: 10.1016/0012-1606(92)90244-B

Park, Y., and Wu, H. (2016). Differential methylation analysis for BS-seq data under general experimental design. *Bioinformatics* 32, 1446–1453. doi: 10.1093/bioinformatics/btw026

Pertea, M., Kim, D., Pertea, G. M., Leek, J. T., and Salzberg, S. L. (2016). Transcript-level expression analysis of RNA-seq experiments with HISAT, StringTie and Ballgown. *Nat. Protoc.* 11, 1650–1667. doi: 10.1038/nprot.2016.095

Pertea, M., Pertea, G. M., Antonescu, C. M., Chang, T. C., Mendell, J. T., and Salzberg, S. L. (2015). StringTie enables improved reconstruction of a transcriptome from RNA-seq reads. *Nat. Biotechnol.* 33, 290–295. doi: 10.1038/nbt.3122

Petersen, T. N., Brunak, S., von Heijne, G., and Nielsen, H. (2011). SignalP 4.0: discriminating signal peptides from transmembrane regions. *Nat. Methods* 8, 785–786. doi: 10.1038/nmeth.1701

Provataris, P., Meusemann, K., Niehuis, O., Grath, S., and Misof, B. (2018). Signatures of DNA methylation across insects suggest reduced DNA methylation levels in holometabola. *Genome Biol. Evol.* 10, 1185–1197. doi: 10.1093/gbe/evy066

Qiagen Bioinformatics (2018). *CLCWorkbench*. Available online at: http://www.clcbio.com

R Core Team (2020). R: *A Language and Environment for Statistical Computing. R Foundation for Statistical Computing*. Vienna. Available online at: https://www.R-project.org/

Riviere, G., He, Y., Tecchio, S., Crowell, E., Gras, M., Sourdaine, P., et al. (2017). Dynamics of DNA methylomes underlie oyster development. *PLoS Genet.* 13:e1006807. doi: 10.1371/journal.pgen.1006807

Roy, A., and Palli, S. R. (2018). Epigenetic modifications acetylation and deacetylation play important roles in juvenile hormone action. *BMC Genomics* 19:934. doi: 10.1186/s12864-018-5323-4

Segraves, W. A., and Woldin, C. (1993). The E75 gene of *Manduca sexta* and comparison with its *Drosophila* homolog. *Insect Biochem Mol. Biol.* 23, 91–97. doi: 10.1016/0965-1748(93)90086-8

Song, X., Huang, F., Liu, J., Li, C., Gao, S., Wu, W., et al. (2017). Genome-wide DNA methylomes from discrete developmental stages reveal the predominance of non-CpG methylation in *Tribolium castaneum*. *DNA Res.* 24, 445–457. doi: 10.1093/dnares/dsx016

Sonnhammer, E. L., von Heijne, G., and Krogh, A. (1998). A hidden Markov model for predicting transmembrane helices in protein sequences. *Proc. Int. Conf. Intell. Syst. Mol. Biol.* 6, 175–182.

Stilwell, G. E., Nelson, C. A., Weller, J., Cui, H., Hiruma, K., Truman, J. W., et al. (2003). E74 exhibits stage-specific hormonal regulation in the epidermis of the tobacco hornworm, *Manduca sexta*. *Dev. Biol.* 258, 76–90. doi: 10.1016/S0012-1606(03)00105-2

Tange, O. (2011). GNU parallel - the command-line power tool. *USENIX Magaz.* 36, 42–47. doi: 10.5281/zenodo.16303

Tetreau, G., Cao, X., Chen, Y. R., Muthukrishnan, S., Jiang, H., Blissard, G. W., et al. (2015a). Overview of chitin metabolism enzymes in *Manduca sexta*: identification, domain organization, phylogenetic analysis and gene expression. *Insect Biochem. Mol. Biol.* 62, 114–126. doi: 10.1016/j.ibmb.2015.01.006

Tetreau, G., Dittmer, N. T., Cao, X., Agrawal, S., Chen, Y. R., Muthukrishnan, S., et al. (2015b). Analysis of chitin-binding proteins from *Manduca sexta* provides new insights into evolution of peritrophin A-type chitin-binding domains in insects. *Insect Biochem. Mol. Biol.* 62, 127–141. doi: 10.1016/j.ibmb.2014.12.002

The Gene Ontology Consortium (2018). Available online at: http://geneontology.org/page/download-ontology

The Gene Ontology Consortium (2019). The Gene Ontology Resource: 20 years and still GOing strong. *Nucleic Acids Res.* 47, D330–D338. doi: 10.1093/nar/gky1055

Wang, X., Wheeler, D., Avery, A., Rago, A., Choi, J. H., Colbourne, J. K., et al. (2013). Function and evolution of DNA methylation in *Nasonia vitripennis*. *PLoS Genet.* 9:e1003872. doi: 10.1371/journal.pgen.1003872

Weller, J., Sun, G. C., Zhou, B., Lan, Q., Hiruma, K., and Riddiford, L. M. (2001). Isolation and developmental expression of two nuclear receptors, MHR4 and betaFTZ-F1, in the tobacco hornworm, *Manduca sexta*. *Insect Biochem. Mol. Biol.* 31, 827–837. doi: 10.1016/S0965-1748(00)00188-0

Wu, H., Wang, C., and Wu, Z. (2013). A new shrinkage estimator for dispersion improves differential expression detection in RNA-seq data. *Biostatistics* 14, 232–243. doi: 10.1093/biostatistics/kxs033

Wu, H., Xu, T., Feng, H., Chen, L., Li, B., Yao, B., et al. (2015). Detection of differentially methylated regions from whole-genome bisulfite sequencing data without replicates. *Nucleic Acids Res.* 43:e141. doi: 10.1093/nar/gkv715

Xu, G., Zhang, J., Lyu, H., Song, Q., Feng, Q., Xiang, H., et al. (2018). DNA methylation mediates BmDeaf1-regulated tissue- and stage-specific expression of BmCHSA-2b in the silkworm, *Bombyx mori*. *Epigenet. Chromatin* 11:32. doi: 10.1186/s13072-018-0202-4

Ylla, G., Piulachs, M. D., and Belles, X. (2017). Comparative analysis of miRNA expression during the development of insects of different metamorphosis modes and germ-band types. *BMC Genomics* 18:774. doi: 10.1186/s12864-017-4177-5

Zhang, J., Xing, Y., Li, Y., Yin, C., Ge, C., and Li, F. (2015). DNA methyltransferases have an essential role in female fecundity in brown planthopper, *Nilaparvata lugens*. *Biochem. Biophys. Res. Commun*. 464, 83–88. doi: 10.1016/j.bbrc.2015.05.114

Zhou, B., Hiruma, K., Jindra, M., Shinoda, T., Segraves, W. A., Malone, F., et al. (1998a). Regulation of the transcription factor E75 by 20-hydroxyecdysone and juvenile hormone in the epidermis of the tobacco hornworm, *Manduca sexta*, during larval molting and metamorphosis. *Dev. Biol*. 193, 127–138. doi: 10.1006/dbio.1997.8798

Zhou, B., Hiruma, K., Shinoda, T., and Riddiford, L. M. (1998b). Juvenile hormone prevents ecdysteroid-induced expression of broad complex RNAs in the epidermis of the tobacco hornworm, *Manduca sexta*. Dev. Biol. 203, 233–244. doi: 10.1006/dbio.1998.9059

Conflict of Interest: The authors declare that the research was conducted in the absence of any commercial or financial relationships that could be construed as a potential conflict of interest.

frontiers in Ecology and Evolution

ORIGINAL RESEARCH
published: 18 March 2021
doi: 10.3389/fevo.2021.643661

Ultrabithorax Is a Micromanager of Hindwing Identity in Butterflies and Moths

Amruta Tendolkar[1†], Aaron F. Pomerantz[2,3†], Christa Heryanto[1†], Paul D. Shirk[4], Nipam H. Patel[3†] and Arnaud Martin[1†]*

[1] Department of Biological Sciences, The George Washington University, Washington, DC, United States, [2] Department Integrative Biology, University of California Berkeley, Berkeley, CA, United States, [3] Marine Biological Laboratory, Woods Hole, MA, United States, [4] USDA-ARS CMAVE IBBRU, Gainesville, FL, United States

OPEN ACCESS

Edited by:
Patrícia Beldade,
University of Lisbon, Portugal

Reviewed by:
Antonia Monteiro,
National University of Singapore, Singapore
Pedro Martinez,
University of Barcelona, Spain

***Correspondence:**
Arnaud Martin
arnaud@gwu.edu

†ORCID:
Amruta Tendolkar
orcid.org/0000-0002-8496-3669
Aaron F. Pomerantz
orcid.org/0000-0002-6412-9001
Christa Heryanto
orcid.org/0000-0002-9917-5710
Nipam H. Patel
orcid.org/0000-0003-4328-654X
Arnaud Martin
orcid.org/0000-0002-5980-2249

Specialty section:
This article was submitted to Evolutionary Developmental Biology, a section of the journal Frontiers in Ecology and Evolution

Received: 18 December 2020
Accepted: 26 February 2021
Published: 18 March 2021

Citation:
Tendolkar A, Pomerantz AF, Heryanto C, Shirk PD, Patel NH and Martin A (2021) Ultrabithorax Is a Micromanager of Hindwing Identity in Butterflies and Moths. Front. Ecol. Evol. 9:643661. doi: 10.3389/fevo.2021.643661

The forewings and hindwings of butterflies and moths (Lepidoptera) are differentiated from each other, with segment-specific morphologies and color patterns that mediate a wide range of functions in flight, signaling, and protection. The Hox gene *Ultrabithorax* (*Ubx*) is a master selector gene that differentiates metathoracic from mesothoracic identities across winged insects, and previous work has shown this role extends to at least some of the color patterns from the butterfly hindwing. Here we used CRISPR targeted mutagenesis to generate *Ubx* loss-of-function somatic mutations in two nymphalid butterflies (*Junonia coenia*, *Vanessa cardui*) and a pyralid moth (*Plodia interpunctella*). The resulting mosaic clones yielded hindwing-to-forewing transformations, showing *Ubx* is necessary for specifying many aspects of hindwing-specific identities, including scale morphologies, color patterns, and wing venation and structure. These homeotic phenotypes showed cell-autonomous, sharp transitions between mutant and non-mutant scales, except for clones that encroached into the border ocelli (eyespots) and resulted in composite and non-autonomous effects on eyespot ring determination. In the pyralid moth, homeotic clones converted the folding and depigmented hindwing into rigid and pigmented composites, affected the wing-coupling frenulum, and induced ectopic scent-scales in male androconia. These data confirm *Ubx* is a master selector of lepidopteran hindwing identity and suggest it acts on many gene regulatory networks involved in wing development and patterning.

Keywords: Hox genes, color patterns, evo-devo, CRISPR, wing evolution

INTRODUCTION

Hox genes are major players in the evolution of animal body plans, as they provide region-specific information to developing tissues that enables the specialization of body parts, including serial homologs that form the axial skeleton of vertebrates or the appendages of arthropods (Hughes and Kaufman, 2002; Pourquie, 2009). First identified and characterized in *Drosophila*, it has been shown that these genes are well conserved across metazoans, prompting a prolific effort to understand how Hox genes are embedded in the regulatory logic of development, and how they may mediate phenotypic change at evolutionary scales.

The diversity of insect wing configurations provides a good comparative system to tackle those questions. Wing appendage development occurs in the second and third thoracic segments (T2 and T3, *syn.* mesothorax and metathorax). The development of wing primordia includes segment-specific processes that give rise to marked functional differences, such as the T3 halteres of Diptera, the T2 protective shields of Coleoptera and Hemiptera (elytra, hemelytra), and the many examples of divergence in color pattern and flight functions between the T2/T3 wings of Lepidoptera (Williams and Carroll, 1993; Carroll, 1994; Jantzen and Eisner, 2008; Ohde et al., 2014; Tomoyasu et al., 2017). The homeotic selector gene *Ultrabithorax* (*Ubx*) is consistently expressed in the T3 but not in the T2 wing primordia of winged insects (Hughes and Kaufman, 2002; Tomoyasu, 2017), and instructs the differentiation of T3 relative to T2 wing derivatives. A complete loss of *Ubx* in the *Drosophila melanogaster* T3 imaginal disks replaces the halteres with an apparent second set of wings (Bender et al., 1983; Weatherbee et al., 1998; Hersh et al., 2007; Lipshitz, 2007; Pavlopoulos and Akam, 2011). This seminal discovery has led to detailed studies showing that *Ubx* represses forewing identity in the haltere disc, both through the transcriptional repression of wing genes and activation of haltere genes (Shashidhara et al., 1999; Crickmore and Mann, 2006; Mohit et al., 2006; Navas et al., 2006; Hersh et al., 2007; Makhijani et al., 2007). In conjunction with work in *Drosophila* legs and embryonic tissues, these data have established *Ubx* as a selector gene that specifies metathoracic structures from their *Ubx*-free homologs (Zandvakili et al., 2019).

This generic role of Ubx is supported in all insect wing systems for which functional data has been reported so far. RNAi knock-downs of *Ubx* in *Tribolium castaneum* (Tomoyasu et al., 2005, 2009), *Oncopeltus fasciatus* (Medved et al., 2015) and *Nilaparvata lugens* (Fu et al., 2020) all showed homeotic transformations of T3 wing tissue into a T2 identity. In Lepidoptera, two lines of evidence have confirmed the role of *Ubx* as a homeotic selector gene specifying T3/hindwing identity. A spontaneous mutation called *Hindsight*, isolated from a *Junonia coenia* laboratory colony, causes mosaic patches of forewing color pattern and scale identities on the ventral side of butterfly hindwings (Nijhout and Rountree, 1995; Weatherbee et al., 1999). It is unclear if *Hindsight* is caused by a mutation at the *Ubx* locus itself, but it induces dominant somatic clones that lack *Ubx* expression during development, and its restriction to the more posterior region of the T3 appendage is somewhat reminiscent of the *Postbithorax* and *bithoraxoid* alleles at the *Drosophila Ubx* locus, which result in clonal homeotic transformations of the posterior haltere (Adler, 1979, 1981). More recently, crispants (CRISPR/Cas9 somatic knock-outs) of *Ubx* in *Bicyclus anynana* revealed T3-to-T2 homeotic transformations on the hindwings (Matsuoka and Monteiro, 2020), where local homeotic shifts in scale types and pattern size mirrored the matching forewing condition. For instance, in *B. anynana*, silver scales are normally limited to the ventral posterior region of the forewings, and ectopic silver scales appeared in mutant hindwing clones that were restricted to the ventral posterior region. Likewise, eyespots that are present in the hindwing but are absent in forewings were reduced or missing upon mosaic KO, while conversely, eyespots that are prominent in the forewing were enlarged.

Overall, these butterfly wing data suggest that Ubx loss-of-function phenotypes vary across the wing (context-dependency), and that this Hox input is plugged into the differential control of a majority of hindwing-specific features. This includes homeotic shifts in both scale identities (e.g., a specific morphology and pigment) and in their pattern arrangement (e.g., eyespot size and color composition). Here we leveraged the diversity of lepidopteran wing traits to gain additional insights into the modalities of Ubx hindwing trait specification. Our study expanded the use of CRISPR *Ubx* mosaic knock-outs to two other nymphalid butterflies, *J. coenia* and *Vanessa cardui*, which display marked pattern organization and color differences between their two sets of wings, as well as in the pyralid moth *Plodia interpunctella*, a lepidopteran with folding and depigmented hindwings.

RESULTS

Cell-Autonomous Homeotic Effects of *Ubx* Loss-of-Function in *Junonia*

The nymphalid butterfly *J. coenia* shows marked forewing/hindwing (FW/HW) differences in the distribution and color of pattern elements (**Figure 1A**), including the Discalis stripes, the central symmetry system, eyespots (*s.s.* border ocelli), and the parafocal/marginal bands (Mazo-Vargas et al., 2017). Previously described homeotic clones from the *Hindsight* line affect those elements but are limited to the posterior compartment of the ventral hindwings. To formally test the role of *Ubx* in hindwing patterning in this species, we generated somatic loss-of-function mutants by injecting Cas9/sgRNA duplexes into syncytial embryos, targeting the *Ubx* coding sequence (**Table 1**, **Supplementary Figure 1**, and **Supplementary Table 1**). These experiments led to high-mortality rates at both embryonic and post-embryonic stages, but batches injected 3 h after egg-laying (AEL) showed enough mosaicism to allow survivors to reach adulthood. A total of 19 adult butterflies showed hindwing-to-forewing color pattern transformations, not only replicating the effects of *Hindsight* on the ventral posterior hindwings but also extending to the dorsal surface and to the anterior compartments (**Supplementary Figures 2–4**). Scales of the *J. coenia* ventral hindwing are normally serrated, contrasting with the rounded shape of their forewing homologs, which allows the delineation of homeotic clones, as in the *Hindsight* mutants (Nijhout and Rountree, 1995; Weatherbee et al., 1999). For all the pattern elements besides the eyespots, homeotic clones induced a color shift in a cell autonomous fashion, with mutant scale patches showing sharp demarcation from non-mutant scales (**Figure 1**). Those shifts in scale morphology were always accompanied by the acquisition of color states exactly matching the forewing state in the equivalent position. This is particularly evident in the induction of orange and black patterns known as the forewing Discalis elements in positions where in the wild type hindwing they are brown/beige (ventral) or absent (dorsal). Likewise, mutants show discrete

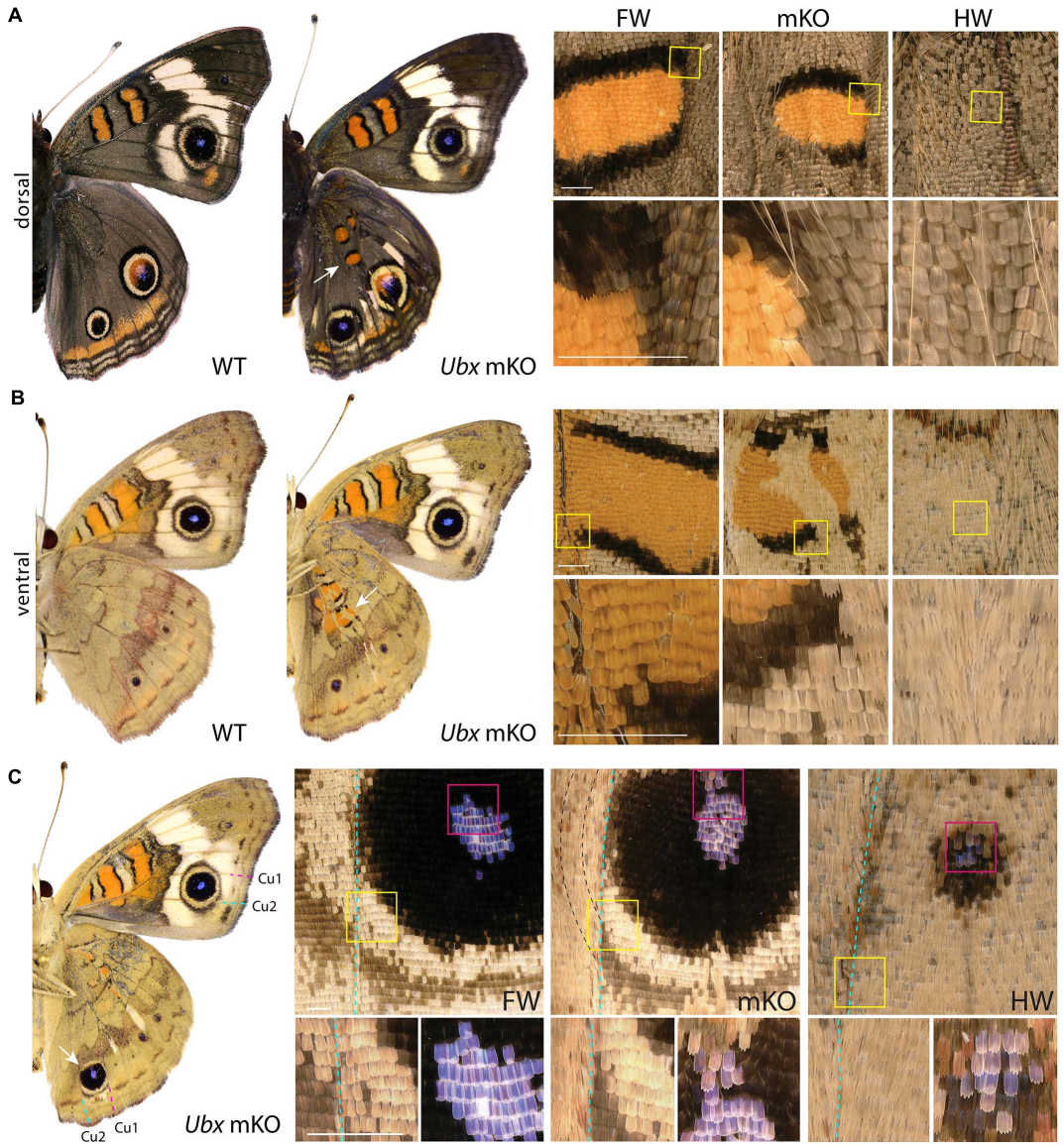

FIGURE 1 | *Ubx* mosaic knock-outs show homeotic transformations of hindwing color patterns in *J. coenia*. Insets depict homeotic hindwing (HW)-to-forewing (FW) mutant patterns [mosaic knock-out (mKO), center column]. **(A,B)** Dorsal and ventral views of WT and an example *Ubx* mKO *J. coenia*, with insets showing the Discalis I pattern element. **(C)** Example of a ventral Cu1-Cu2 eyespot homeosis; mutant cells stopped at the Cu2 vein (dashed line), and non-mutant cells across that clone failed to induce outer rings. Scale bars = 500 μm.

clones transposing the white band from the forewing onto the corresponding hindwing territories. Similar homeoses are conspicuous in the stripe systems that border the margin of the wings, where in wild type they are continuous, but in the mutant clones they are interrupted and absent. The positioning and outlining of the aforementioned patterns all depend on positional information derived from Wnt ligands in *Junonia* (Martin and Reed, 2014; Mazo-Vargas et al., 2017). Overall, these cell-autonomous effects suggest that the two wing sets deploy equivalent spatial information and that differences in color patterns are mostly due to differential interpretation and color fate induction.

Homeotic Effects of *Ubx* Mosaics on Eyespot Formation in *J. coenia*

Eyespots showed more complex and variegated effects than other pattern elements, depending on clone size, shape, and position. In *J. coenia*, the Cu1–Cu2 eyespot is particularly prominent in forewings (see **Figures 2A,B** for vein nomenclature). One *Ubx* mosaic knock-out induced the gain of a large eyespot in the hindwing Cu1–Cu2 region, almost reaching the size of its forewing homolog, but with its outer ring failing to cross the veins (**Figure 1C**). Scale shape shifts indicate that the mutant clone included the signaling focus and most of eyespot field, but did not cross the Cu1 and Cu2 veins, leading to an eyespot

TABLE 1 | Summary of CRISPR/Cas9 injection experiments.

Species	sgRNA name	Injection time (hrs) AEL	Final concentration (ng/μL) [Cas9: sgRNA]	Total injected (N)	L1 larvae	Egg hatching Rate (%)	Adults (total)	Adults with homeotic phenotype	Penetrance (% of adults)
Junonia coenia	Vc_sgRNA1	2–3	125: 75	251	0	0.0	0	0	–
		2–3	250: 125	155	0	0.0	0	0	–
		4–5	250: 125	66	15	22.7	–	3	–
		2.6–4	500: 250	306	64	21.0	–	2	–
		2–4.5	250: 125	–	–	–	–	–	–
		2.7–9	500: 250	111	29	26.1	–	6	–
	Jc_sgRNA1	2–4	250: 125	126	16	12.7	13	3	23.1
Vanessa cardui	Vc_sgRNA1	2–3.5	500: 250	108	49	45.4	23	3	13.1
		2–6	500: 250	135	109	80.7	29	3	10.4
	Vc_sgRNA2 and 3	2–4	250: 125	212	137	64.6	9	2	22.3
Plodia interpunctella	Pi_sgRNA1	0.1–1.6	333: 167	318	143	45.0	72	2	2.8
		1.6–2.6	333: 167	709	306	43.0	182	34	18.7
		2–3	500: 250	281	54	19.2	42	14	33.3

The number of hatchlings and adults (WT and mutant) obtained for different times and concentration of injections for the three species and penetrance of mutation per injection are reported.
Dashes: data missing.

trimmed from the sections of its outer rings that normally extend into the neighboring M3vCu1 and Cu2–A1 regions. Thus, WT cells from those two regions were not responsive to the neighboring effect of the modified eyespot and mutant cells, indicating cell autonomy in the determination of the outer rings. We also obtained mosaic eyespot phenotypes, and speculate here on a few salient cases. A small satellite eyespot appeared in the R5–M1 hindwing region – normally devoid of eyespots – likely by transposing the morphogenetic activity of the small white R5–M1 forewing eyespot (**Figure 2A**). Remarkably, the induced eyespot was not transformed, but instead formed a complete black outer ring, suggesting this area retained the competency of WT dorsal hindwing tissue. M1–M2 eyespots are large in WT hindwings and reduced or cryptic in forewings. We did not obtain clones clearly overlapping with its induction focus, which may have reduced them in the mutant context; however, several individuals showed elongated clones streaking through this pattern, and resulting in its truncation (**Figures 2B–D**). The inner, orange-pink-blue-black sections from those eyespots were disorganized, while their outer buff and black rings were truncated, again pointing at a cell-autonomous mode of induction. A similar effect was observed in a partially transformed Cu1–Cu2 eyespot that showed discontinuity in its rings (**Figure 2E**). Overall, those composite eyespot phenotypes highlight the complex dynamics of eyespot development, and suggest that the determination of outer rings respond differently to eyespot morphogens between the two wing sets.

Cell Autonomous Scale Morphology and Color Pattern Homeoses in *Vanessa* Hindwings

Next, we investigated the effects of Ubx mosaic knock-outs in *V. cardui*, another nymphalid butterfly. In *V. cardui*, injections earlier than 4 h AEL produced a low hatching rate at 250 ng/μL of sgRNA but a higher hatching rate at 125 ng/μL of sgRNA. The hatching rate was highest for injections done up to 6 h AEL at 250 ng/μL, however, penetrance was low (**Table 1**). A total of eight surviving adults showed hindwing-to-forewing homeosis, visible as shifts in scale morphology and color pattern organization (**Figure 3** and **Supplementary Figure 5**). As in *Junonia*, transformed hindwings showed cell autonomous homeotic shifts equivalent to a visible transposition of the color patterns from the matching forewing position. For instance, we observed the transformation of the ventral hindwing central symmetry system into pink and black patterns from the forewing (**Figures 3A–C**). The distal parafocal elements of *V. cardui* (Otaki, 2012; Abbasi and Marcus, 2015) are chevrons that vary in color (black in the forewing, blue in the hindwing), and the same mutant showed a composite chevron with the forewing-like black section showing a thicker and pointier shape (**Figure 3D**). As the WT blue section was unaffected by the neighboring clone, we extrapolate that this pattern identity shift relied on a cell autonomous conversion of the cells to a forewing fate. Other cell autonomous effects were prominent on the dorsal surfaces, as seen in clones showing both the loss of hair-like scales, and the transposition of forewing color patterns such as the Discalis black patterns of the forewing and their surrounding orange-pink scales (**Figures 3E–G**).

Variegated Effects of *Ubx* mKOs in *Vanessa* Eyespots

As in *Junonia*, mosaic knock-outs of *Ubx* varied in penetrance (percentage of mutant adults) and expressivity (clone size) depending on the injected stage interval and possibly the sgRNA dosage sequence. But more importantly they produced variegated effects in the eyespot field that depended on the affected vein compartment, on the nature of the WT pattern differences between the wing sets, and on clone size and

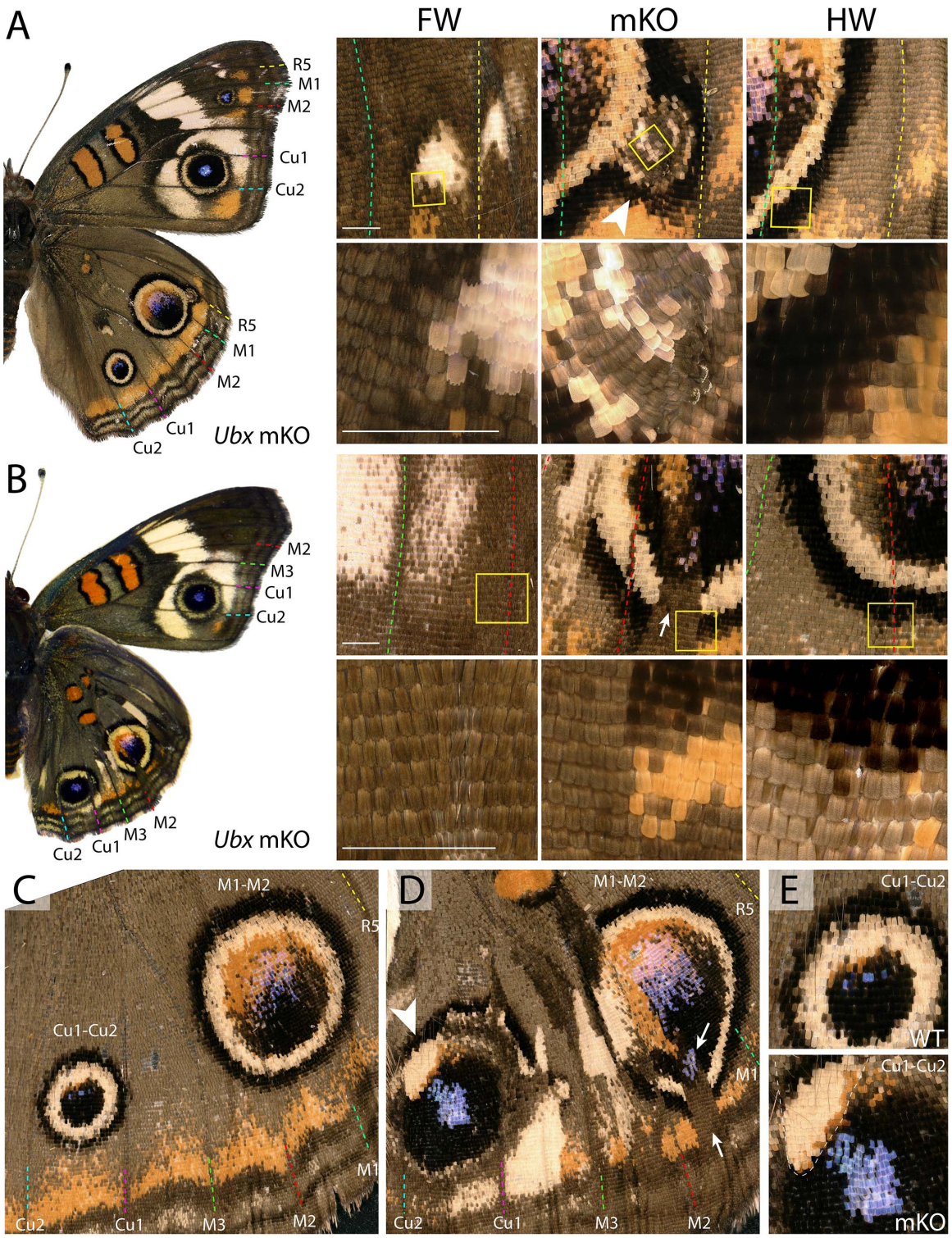

FIGURE 2 | Variegated effect of partial mKO in the *Junonia* eyespot fields. **(A)** Ectopic R5-M1 eyespot appearing as a satellite to a WT M1–M2 eyespot, and forming rings not observed in the forewing (arrowhead). Lower panel depicts magnification of yellow insets in the upper panels. **(B)** Mosaic mutant with a complete Cu1–Cu2 eyespot homeosis, and partial mutant clones in the M1–M2 eyespot (insets). Arrow: missing outer rings and orange distal parafocal element in a mutant clone. **(C)** Magnified view of a WT hindwing (inset in **E, upper panel**: Cu1–Cu2 eyespot) **(D)** Equivalent view of a mosaic KO with partial Cu1–Cu2 and M1–M2 eyespot phenotype. Arrow: missing outer rings and orange distal parafocal element in a mutant clone; arrowhead: residual outer rings in a WT clone. Inset in **(E, lower panel):** magnified view of the Cu1–Cu2 eyespot, with residual outer rings in wild-type tissue (upper left, dashed line). Scale bars = 500 μm.

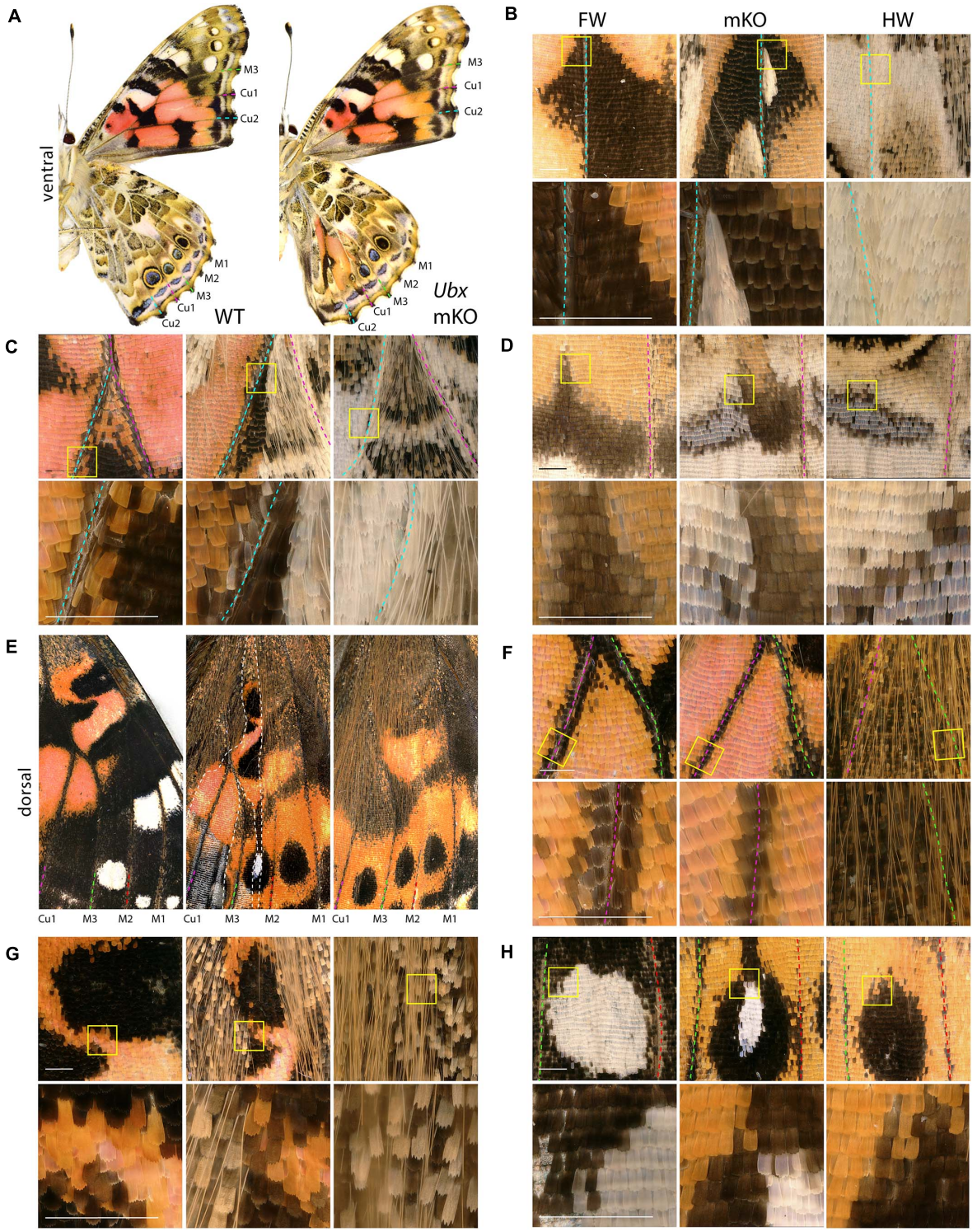

FIGURE 3 | Homeotic transformations of hindwing color patterns after *Ubx* mosaic knock-out in *V. cardui.* Panels **(B–H)** each show tripartite comparisons of positionally matched patterns from a forewing (left), a mutant hindwing (center), and a WT hindwing (right). Lower panel depicts magnification of yellow insets in the upper panel. **(A)** Ventral side of WT and an *Ubx* mKO individual in *V. cardui*, with magnified views in panels **(B)** (median Cu2), **(C)** (Cu1–Cu2 vein junction), and **(D)** (Cu1–Cu2 distal parafocal element). **(E)** Comparison of a dorsal forewing area, and the corresponding region of the mutant and WT hindwing, with an elongated mutant clone resulting in homeoses, as magnified in panels **(F)** (Cu1–M3 vein junction), **(G)** (Discalis II elements), and **(H)** (M2–M3 eyespot). The wildtype forewing in panel E was shrunk to 75% of its original length to adjust for allometric differences with the hindwings. Scale bars = 500 μm.

position. The forewing eyespots are limited to the R5–M1, M1–M2, and M2–M3 intravenous compartments in *Vanessa*. These three white eyespots are peculiar as they are the only ones known to express *WntA*, suggesting a recent co-option in this lineage (Martin and Reed, 2014; Mazo-Vargas et al., 2017). Interestingly, we found several occurrences of mutant hindwing eyespot foci acquiring a white color in those compartments, including in a visibly elongated clone that encroached right through the focus on the mutant dorsal side (**Figures 3E,H**, **4A–D**). On the ventral side, these three eyespots are bilaterally symmetric and white in the forewing, but radially symmetric with more color complexity in the hindwing, and mosaic knock-outs yielded predicted partial and complete transformations of the latter into the former (**Figures 4A,C,D**). Finally, we were surprised to observe a composite Cu1–Cu2 hindwing eyespot where most of the intravenous field took the orange/spotless identity of the forewing, as expected, but where a WT clone also left an eyespot remnant that included portions of the blue, black, and buff rings (**Figures 4E,F'**). This eyespot seems to have acted as its own signaling center, as suggested by a faded black ring in the mutant clone that radiates from its center (arrowhead in **Figure 4F'**). Thus, mosaic mutant eyespot field may displace the position of signaling centers and result in adjacent eyespots. The transformed tissue failed to recapitulate the ring organization observed across in the wild-type tissue, suggesting limited competency to respond to the satellite signaling activity. Together, these observations suggest that at least in the *V. cardui* Cu1–Cu2 space, *Ubx* is acting at two consecutive stages of eyespot development (Beldade and Monteiro, 2021): first it may be required of the correct positioning and induction of an eyespot signaling center, and later during the signaling phase, it may provide hindwing identity that is used for the integration of the signals into rings of the proper color and size.

Loss of *Ubx* Induces Ectopic Abdominal Legs

Among the survivors that were derived from a batch of 212 *V. cardui* eggs injected between 2 and 4 h, five larvae showed ectopic limbs on the first abdominal segment (A1) at the fifth instar stage. Those rudimentary limbs showed all three podomers observed in a T3 leg, but were shorter and smaller (**Figure 5**). These results are consistent with RNAi and spontaneous mutations in the silkworm and tobacco hornworm, which established Ubx as a suppressor of larval leg development in the A1–A2 segments (Zheng et al., 1999; Masumoto et al., 2009), and with the known role of Ubx in repressing thoracic appendage development in the abdomen of other insects (Hughes and Kaufman, 2002; Angelini et al., 2005; Mahfooz et al., 2007). The effect of sgRNA dosage and time of injection on the penetrance and expressivity of this phenotype were untested, but we note a high embryonic lethality of CRISPR injections performed prior to 3 h AEL (**Table 1**), suggesting the level of mosaicism needed for generating larval phenotypes is optimal in injections performed at 3–4 h AEL.

Ubx Permits the Morphological Specialization of Pyralid Hindwings

Spontaneous color pattern homeoses similar to *Hindsight* have been described in museum specimens spanning many lineages of butterflies and moths (Sibatani, 1980, 1983a,b). However, it is unknown if homeotic transformations can also affect other aspects of wing morphology, as in the more radically T2/T3 specialized appendages of *Drosophila* (wing/haltere) and *Tribolium* (elytra/wing). Phycitine moths of the Pyralidae family offer a level of wing specialization that is somewhat analogous to elytral wing plans. The forewings of Phycitinae are thick, concave, and elongate beyond the caudal end of the insect, thus providing protection to the animal while at rest, while, akin to beetles, hindwings are thin and folded at rest. The hindwing has a hook-like frenulum that locks into the retinaculum, a tuft of bristles at the base of the ventral forewing (Braun, 1924; Zaspel, 2016). This frenulo-retinacular wing coupling mechanically pulls the folded hindwing open, and synchronizes the wings during flight (Wootton, 2002). The dorsal forewing is pigmented, as the only surface exposed at rest, while the hindwing is lightly pigmented. Here we used the phycitine Indian Mealmoth (*P. interpunctella*) as a model system to investigate additional aspects of lepidopteran wing specialization. First, we confirmed that the UbdA antigen (anti-Ubx/abd-A FP6.87 monoclonal antibody) is absent from the forewing imaginal disks, and expressed throughout the hindwing, thus corroborating the hindwing-specific expression of *Ubx* described in other lepidopterans (Weatherbee et al., 1998; Tong et al., 2014; Prasad et al., 2016). Then, we generated Ubx mosaic knock-outs and observed homeotic clones on the hindwing that were most conspicuous as transpositions toward black-and-brown pigmented states on the dorsal side (**Figures 6A,B** and **Supplementary Figure 6**). Importantly, the most transformed hindwings were imperfectly folded, and we often noticed a kink in the positioning of the overlying forewing in the live emerged adults. These hindwings also showed visible transformation in their overall architecture, with a thicker anterior edge, and clones in the anal region that prevented the fan-like folding along the abdomen (**Figure 6C**). The hindwing-specific frenulum hook was malformed in several individuals. We failed to detect ectopic retinaculum on mutant hindwings, possibly because it derives from a small patch of transformed scales that was not reached in the mosaics we screened. Finally, male forewings possess a scent-producing apparatus at the base of the ventral costa, consisting of a costal fold and external tuft of hairs, that protects androconial scales known as hairpencils, and exposes them by eversion during courtship (Richards and Thomson, 1932; Grant, 1978). In mosaic KOs, we recovered two males with a hindwing that acquired an ectopic, fully developed set of hairpencils at its base, as well as a reduced external tuft in what appears to be a incomplete costal fold (**Figures 6C,D** and **Supplementary Figure 6D**). Upon descaling, mosaic KO hindwings revealed additional homeotic transformations of their vein organization (**Figure 6E**). The costal area was transformed to recreate the thicker leading edge of forewing, visible by the ectopic gain of radial veins. In the anal region, the CuP and A3 veins are specific

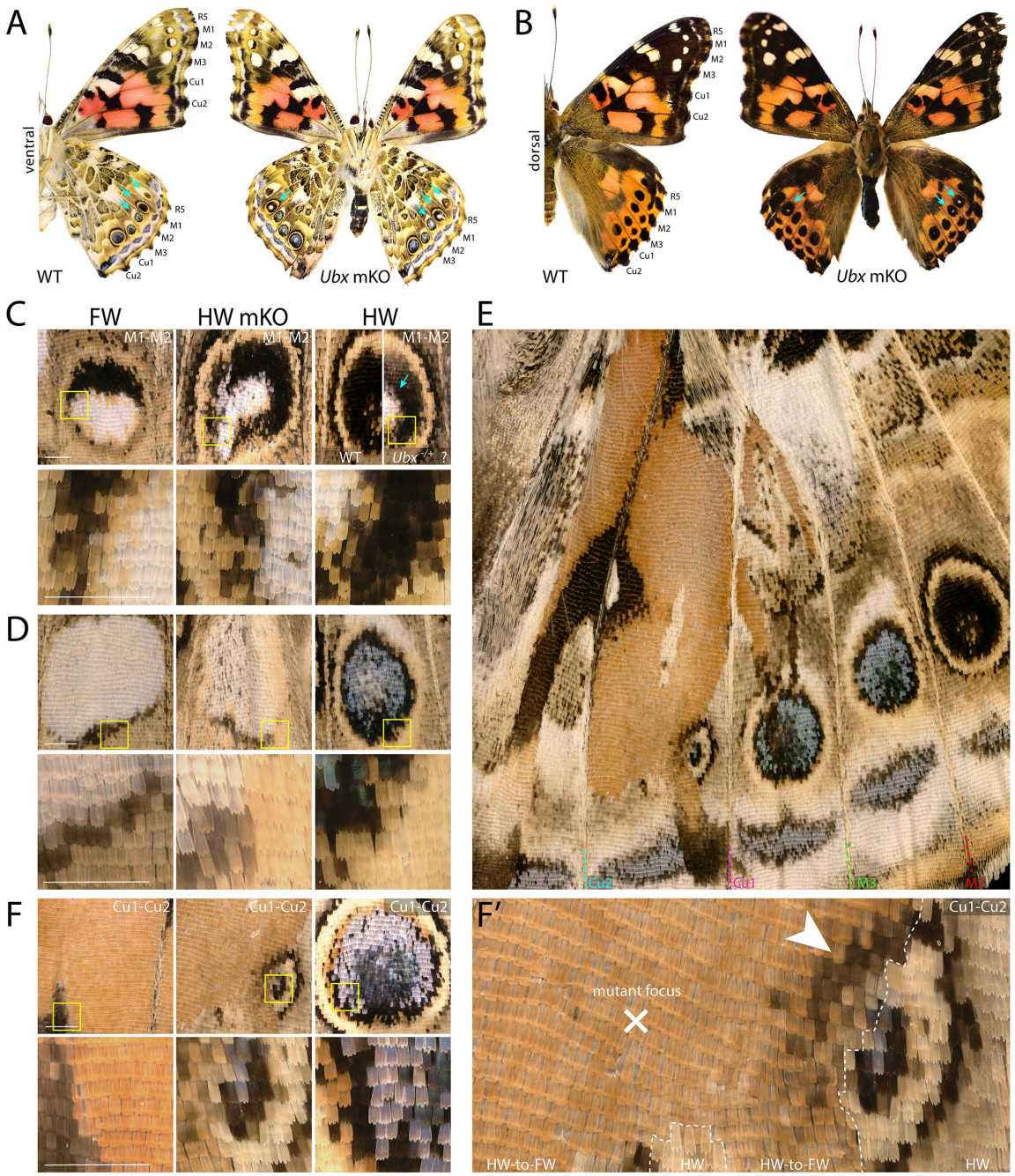

FIGURE 4 | Dominant-white, partial and complete replacement, and large truncation effects on *Vanessa* eyespots. **(A,B)** *Ubx* mKO individual with multiple hindwing eyespots showing ectopic white. White scales are prominent in the three WT forewing eyespots between R5 and M3, but normally absent from hindwings (arrows). **(C)** Magnified views featuring two mutant M1–M2 eyespots from panel A; center: homeotic transformation of the left side, the rest of the eyespot may be heterozygous-mutant due to the forewing-like white center; right: comparison of a putative heterozygous mKO and WT (uninjected) eyespots. **(D)** Complete homeosis of an M2–M3 eyespot. **(E–F')** Views at increasing magnification of truncated Cu1–Cu2. Most of the eyespot field is transformed, but unaffected tissue left an eyespot remnant that likely deployed its own signaling activity, as the partial induction of black rings in the mutant field implies (arrowhead). Panels **(A,C–F')**: ventral views. Scale bars = 500 μm.

to the WT hindwing and involved in the fan-like folding of this wing, but those veins were lost in mutant hindwings, here again adopting a forewing morphology (**Supplementary Figure 7**). Overall the pyralid data show that *Ubx* is not only required for hindwing depigmentation but also for the repression of forewing states, including secondary sexual structures involved in male courtship behavior, and vein architectures that influence wing shape, rigidity, and foldability.

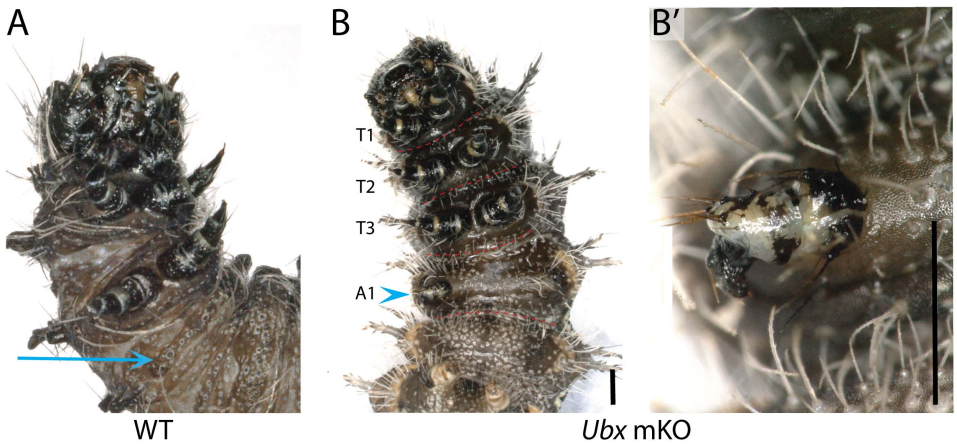

FIGURE 5 | Loss of Ubx produces ectopic abdominal legs. **(A)** WT fifth instar larva, ventral view; arrow: A1 ventral epithelium. **(B,B')** Partial limb (arrowhead, magnified in **B'**) on the A1 segment of a fifth instar *Vanessa cardui Ubx* mKO larva. Scale bars = 1000 μm.

DISCUSSION

Ubx Represses Leg Identity in A1

Ubx loss-of-function was deleterious throughout development, with few individuals reaching the adult stage. Previous mosaic knock-outs of the *WntA* gene, which show no embryonic or larval defects, can generate crispants with a mutant phenotype that extends to all the wing surfaces (Mazo-Vargas et al., 2017; Concha et al., 2019). This contrasts with the bulk of our *Ubx* wing phenotypes, which showed small wing clones and no complete hindwing transformation. Mosaicism was thus needed to generate viable adults, and as a corollary, our failure to observe certain clone sizes or locations can be due to a form of "survivorship bias." The observed lethality of those experiments is reminiscent of the low hatching rate of silkworm embryos injected with *Ubx* RNAi, perhaps due to the inferred role of *Ubx* in patterning the central nervous system (Warren et al., 1994; Zheng et al., 1999; Masumoto et al., 2009). As a visible manifestation of those functions in embryos and larvae, we observed *Ubx* crispant larvae exhibiting partially developed additional thoracic limbs on the A1 segment (**Figure 5**). These results are in line with a previous study that functionally characterized *Ubx* in *Bombyx mori* embryos through RNAi, suggesting it acts as a suppressor of leg development in the first abdominal segment (Masumoto et al., 2009). Homeotic mutants that map to the *Ubx/abd-A* region show deficient expressions of *Ubx,* and bear ectopic A1 (and occasionally A2) larval legs, have also been isolated in both *B. mori* and *Manduca sexta* (Ueno et al., 1995; Zheng et al., 1999; Tong et al., 2017). Previous data and our *Ubx* loss-of-function somatic mutations via CRISPR targeted mutagenesis thus indicate *Ubx* is a suppressor of A1 leg development. Importantly, the embryos of most insects including lepidopterans develop a transient A1 appendage, known as the pleuropod, which functions as a glandular organ involved in egg hatching (Konopová et al., 2020). Instead of blocking appendage development in A1, it is likely that *Ubx* is necessary for establishing the identity of the pleuropod appendage, and that ectopic A1 legs that have been observed in Hox perturbation experiments are pleuropod-to-leg homeoses (Lewis et al., 2000; Konopova and Akam, 2014).

Context-Dependency and Clonal Effects in Eyespot Homeoses

Previous studies have highlighted that mosaic wing homeoses perturb the eyespot determination system, and have discussed how effects can vary based on the placement of the clone and whether or not it encompasses a focal signaling center (Sibatani, 1980; Nijhout and Rountree, 1995; Weatherbee et al., 1999). As previously reported, our *Ubx* mosaic knock-outs as well as the ones reported in *Bicyclus* (Matsuoka and Monteiro, 2020) are consistent with those previous findings: a large homeotic clone overlapping with the putative eyespot center will result in a gain or reduction of eyespot development depending on the corresponding forewing state in this vein compartment. In general, hindwings and forewings seem to respond to the same morphogenetic signal (Nijhout and Rountree, 1995). As a possible exception, *Vanessa* shows a recent, forewing specific evolutionary acquisition of focal *WntA* in the developing eyespots (Mazo-Vargas et al., 2017), and we speculate that this transposed signal causes the induction of white foci in the mutant hindwings. When they do not intersect with the signaling center, mutant clones can also reveal color pattern discontinuities that are informative about eyespot signaling and color ring induction. Our data suggest the hindwing cells require *Ubx* in a cell autonomous fashion to induce outer black and buff eyespot rings, in the dorsal hindwing eyespots of *J. coenia*, and in the ventral *V. cardui* Cu1–Cu2 eyespot. In contrast, the inner ring or "core" of those eyespots (Iwata and Otaki, 2016) were disrupted in a more unpredictable way in *Junonia* mosaics: in clones that streaked through the vicinity of the M1–M2 eyespot focus, the core eyespot showed a disorganization of the color field rather than a reversion to the eyespot-free state of the corresponding forewing field. The current model of eyespot formation involves the definition of Distal-less (Dll)

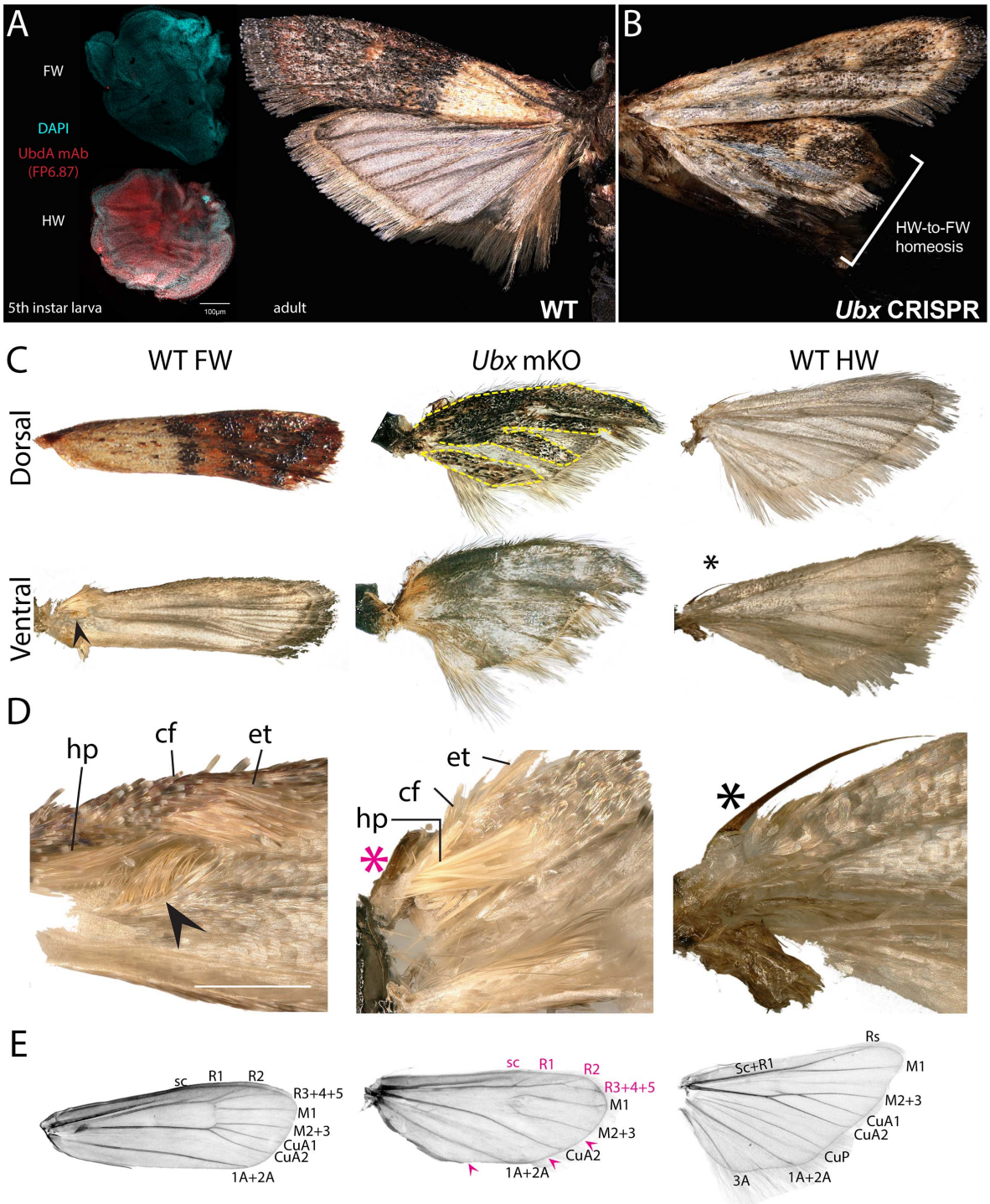

FIGURE 6 | Ubx controls hindwing specification in *Plodia.* **(A)** Left: Immunodetection of UbdA in fifth instar larval wing disks (FP6.87 mAb, red; DAPI, cyan). Right: wild-type *P. interpunctella* (dorsal view). **(B)** *Ubx* mKO individual with transformation in pigmentation and wing rigidity. **(C)** Dorsal and ventral surfaces of a WT forewing, *Ubx* mKO and WT hindwing from male specimens. The mutant hindwing takes a concave appearance, loses its posterior folds and shows transformed dorsal black/brown patterns with a forewing identity (dashed lines). **(D)** Magnified ventral view of the wing base. Wing coupling uses a frenulum (black asterisk) engaging into a retinaculum (arrowhead). Male forewings also possess an extendable scent apparatus. The *Ubx* crispant hindwing shows a defective frenulum (magenta) and an ectopic scent apparatus with fully developed hairpencils (hp); cf: costal fold; et: external tuft of hair. **(E)** Wing venation of a de-scaled adult female forewing, *Ubx* mKO and hindwing. The *Ubx* mosaic KO shows homeoses of anterior veins toward the forewing venation (magenta letters) and loss of a few veins (magenta arrowheads). Vein nomenclature adapted from the phycitine moth wing plan (Solis and Neunzig, 2017). Scale bars: A = 100 µm; D = 500 µm.

positive foci in the midvein spaces from fifth instar imaginal disks, which becomes a signaling center during early pupal stages, and establishes morphogen gradients or signals that pattern boundaries between the surrounding rings, directly or sequentially (Monteiro, 2015; Connahs et al., 2019; Iwata and Otaki, 2019). Besides its role in focus activation, Distal-less is also involved in the determination of the core eyespot (Brunetti et al., 2001; Monteiro et al., 2013). Ubx represses *Dll* in insect abdomens (Vachon et al., 1992; Angelini et al., 2005; Uhl et al., 2016), and in *Junonia* pupal eyespot rings (Weatherbee et al., 1999), implying that the core eyespot disorganization may be linked to a depression of Dll. This phenomenon may not hold true in in satyrid butterflies like *Bicyclus*, which express *Ubx* and *Antp* in the eyespot foci, and where *Ubx* gain-of-function experiments suggest Ubx acts as an activator of *Dll* (Tong et al., 2014; Matsuoka and Monteiro, 2020). Moving forward, a better understanding of the eyespot determination networks and of the levels of *Ubx* integration within them may help to better understand the different *Ubx* mutant clones, as well as possible differences between different nymphalid lineages (Tong et al., 2014; Matsuoka and Monteiro, 2020; Monteiro, 2020).

Ubx as a Micromanager of Metathoracic Wing Specialization

Ubx somatic mutagenesis consistently yielded complete homeotic transformation of hindwing states into their forewing positional homolog. This included identity T3-to-T2 shifts in scale derivatives (color scales, wing-coupling scales, male-specific androconia), color pattern arrangements, eyespot size, and wing structure. Thus, consistently with other insect wing systems (Tomoyasu et al., 2009; Pavlopoulos and Akam, 2011; Kaschula et al., 2018), lepidopteran *Ubx* seems to act as a multitasking master gene or "micromanager" (Akam, 1998) that is embedded in a multitude of gene regulatory networks during wing development. As previously reviewed (Tomoyasu, 2017), similar roles of *Ubx* as a metathoracic specifier have been identified in a variety of insects, and probably indicate a conserved function across Holometabola. It would be challenging but providential to study *Ubx* expression and function in insect lineages with alternative wing sets such as Strepsiptera (T2 halteres, T3 wings), or in basal winged insects such as dragonflies and mayflies. At the molecular level, a characterization of the regulation, transcriptional targets, and chromatin-level interactions of *Ubx* is underway in a variety of systems (McKay and Lieb, 2013; Prasad et al., 2016; Sánchez-Higueras et al., 2019; Diaz-de-la-Loza et al., 2020), and we expect similar approaches in lepidopterans to yield valuable insights on the evolutionary specialization of serial homologs.

MATERIALS AND METHODS

Rearing

Insect stock origins, rearing conditions, larval diets and oviposition plants are summarized in **Supplementary Table 2**. Both butterfly species were reared in plastic cups following a previously described procedure (Martin et al., 2020). For *J. coenia*, the agar-based diet was prepared using water boiled with dry ground leaves of the host plant *Plantago lanceolata*. The modified larval diet for *P. interpunctella* (Silhacek and Murphy, 2008) was made by mixing (w/w) 50% coarse wheat bran, 22% glycerol, 13% dextrose, 8% water, 5% brewer's yeast powder, and 2% canola oil.

Design of sgRNA Targets

Ubx sequences of *J. coenia* (AAL71873.1) and *V. tameamea* (XP_026485353.1) were obtained from NCBI and we used TBLASTN against the *J. coenia* genome (van der Burg et al., 2019), a *V. cardui* wing transcriptome (Connahs et al., 2016), and the *P. interpunctella* genome (Roberts et al., 2020) to obtain additional sequences. SgRNAs were designed against *Ubx* exon 1 in order to produce a frameshift mutation due to imperfect non-homologous end joining repair. The uniqueness of the guide was confirmed by performing a BLASTN against the available whole genome assemblies.

CRISPR Reagents

Cas9:sgRNA heteroduplexes were prepared as previously described (Martin et al., 2020). Before each experiment, frozen aliquots of 2.5 μL sgRNA (250 ng/μL or 333 ng/μL) and Cas9 (500 or 666 ng/μL) were mixed, incubated at room temperature for 10 min, and left on ice until injection.

Egg Collection and Micro-Injection

Butterfly eggs laid on host plant leaves were collected at controlled time intervals before injection. To soften the chorion, *J. coenia* eggs were washed for 1 min in 5% benzalkonium chloride, rinsed with autoclaved water and dried using a gentle flow of compressed air. Eggs from both butterfly species were arranged with the micropyle side facing up on double-sided tape and injected on the side following a previously described procedure (Martin et al., 2020). Post injection, butterfly eggs were rested in a humidity chamber at their respective rearing temperatures until hatching and addition of artificial diet. *P. interpunctella* adults were anaesthetized with CO_2 gas which triggers a release of freshly fertilized eggs. Eggs were collected and arranged horizontally on a parafilm strip for immediate injection in the posterior half, opposite to the micropyle. The egg injection wounds were sealed with cyanoacrylate glue and stored in a humidity chamber until hatching. All injections were performed using a compressed air micro-injection set-up and pulled borosilicate needles.

Imaging

Adult butterflies were pinned with the mutant side up (ventral side up for adults with mutant clones on both surfaces). Full-mount photographs of butterflies were taken either on a Nikon D5300 digital camera mounted with an AF-S VR MicroNikkor 105 mm f/2.8G lens and an 80-LED ring light, or on a Keyence VHX-5000 digital microscope at 50X on a VH-Z00T lens. The high resolution images of butterflies and the wing mounts of moths were taken at 100X, 300X or 600X, and 50X, respectively, on the Keyence VHX-5000 fitted with a VH-Z100T lens.

Immunofluorescence

Wing disks of *P. interpunctella* were dissected from fifth instar larvae that stopped feeding and had spun a silk chamber, fixed in 3.7% formaldehyde, and stained for immunolocalization of the UbdA epitope following a previously described procedure (Martin et al., 2020).

P. interpunctella Wing Descaling

Wings were dissected and washed by repeating consecutive immersions in 90% ethanol and 10% freshly prepared bleach. Descaled wings were washed in 1X PBS to remove debris, mounted with coverslips in 100% ethanol, and immediately imaged for green autofluorescence on an Olympus SZX2 fluorescent stereomicroscope. Photographs were post-processed in Adobe Photoshop for contrast adjustment and the generation of inverted gray images.

DATA AVAILABILITY STATEMENT

The datasets presented in this study can be found in online repositories. The names of the repository/repositories and accession number(s) can be found in the article/**Supplementary Material**.

AUTHOR CONTRIBUTIONS

AT, AFP, and CH conducted the research. PDS, NHP, and AM supervised the project. AT, AFP, and AM wrote the manuscript. All authors contributed to the article and approved the submitted version.

FUNDING

This work was supported by the NSF awards IOS-1656553 and IOS-1923147 to AM, and a GWU Packer Graduate Fellowship to AT.

ACKNOWLEDGMENTS

We thank Chris Day, Nora Wolcott, Emily Earls, Damien Gailly, Ling Sheng Loh, Joseph Hanly, and Richard Furlong for their assistance with micro-injections and insect rearing throughout this project, Joseph Hanly for proof-reading the manuscript, and the Insect Genetic Transformation Research Coordination Network led by David O'Brochta and Rob Harrell for stimulating the initiation of this project via the Peer-to-Peer training program.

SUPPLEMENTARY MATERIAL

The Supplementary Material for this article can be found online at: https://www.frontiersin.org/articles/10.3389/fevo.2021.643661/full#supplementary-material

REFERENCES

Abbasi, R., and Marcus, J. M. (2015). Color pattern evolution in Vanessa butterflies (Nymphalidae: Nymphalini): non-eyespot characters. *Evol. Dev.* 17, 63–81. doi: 10.1111/ede.12109

Adler, P. N. (1979). Position-specific interaction between cells of the imaginal wing and haltere discs of *Drosophila melanogaster*. *Dev. Biol.* 70, 262–267. doi: 10.1016/0012-1606(79)90023-X

Adler, P. N. (1981). Bithoraxoid, postbithorax, and the determination system of the haltere disk. *Dev. Biol.* 86, 157–169. doi: 10.1016/0012-1606(81)90326-2

Akam, M. (1998). Hox genes: from master genes to micromanagers. *Curr. Biol.* 8, R676–R678. doi: 10.1016/S0960-9822(98)70433-6

Angelini, D. R., Liu, P. Z., Hughes, C. L., and Kaufman, T. C. (2005). Hox gene function and interaction in the milkweed bug *Oncopeltus fasciatus* (Hemiptera). *Dev. Biol.* 287, 440–455. doi: 10.1016/j.ydbio.2005.08.010

Beldade, P., and Monteiro, A. (2021). Eco-evo-devo advances with butterfly eyespots. *Curr. Opin. Genet. Dev.* 69, 6–13.

Bender, W., Akam, M., Karch, F., Beachy, P. A., Peifer, M., Spierer, P., et al. (1983). Molecular genetics of the bithorax complex in *Drosophila melanogaster*. *Science* 221, 23–29. doi: 10.1126/science.221.4605.23

Braun, A. F. (1924). The frenulum and its retinaculum in the Lepidoptera. *Ann. Entomol. Soc. Am.* 17, 234–257. doi: 10.1093/aesa/17.3.234

Brunetti, C. R., Selegue, J. E., Monteiro, A., French, V., Brakefield, P. M., and Carroll, S. B. (2001). The generation and diversification of butterfly eyespot color patterns. *Curr. Biol.* 11, 1578–1585. doi: 10.1016/S0960-9822(01)00502-4

Carroll, S. B. (1994). Developmental regulatory mechanisms in the evolution of insect diversity. *Development* 1994, 217–223.

Concha, C., Wallbank, R. W. R., Hanly, J. J., Fenner, J., Livraghi, L., Rivera, E. S., et al. (2019). Interplay between developmental flexibility and determinism in the evolution of mimetic heliconius wing patterns. *Curr. Biol.* 29, 3996.e–4009.e. doi: 10.1016/j.cub.2019.10.010

Connahs, H., Rhen, T., and Simmons, R. B. (2016). Transcriptome analysis of the painted lady butterfly, *Vanessa cardui* during wing color pattern development. *BMC Genomics* 17:270. doi: 10.1186/s12864-016-2586-5

Connahs, H., Tlili, S., Creij, J., van Loo, T. Y. J., Banerjee, T. D., Saunders, T. E., et al. (2019). Activation of butterfly eyespots by Distal-less is consistent with a reaction-diffusion process. *Development* 146:dev169367. doi: 10.1242/dev.169367

Crickmore, M. A., and Mann, R. S. (2006). Hox control of organ size by regulation of morphogen production and mobility. *Science* 313, 63–68. doi: 10.1126/science.1128650

Diaz-de-la-Loza, M.-C., Loker, R., Mann, R. S., and Thompson, B. J. (2020). Control of tissue morphogenesis by the HOX gene Ultrabithorax. *Development* 147:dev184564. doi: 10.1242/dev.184564

Fu, S.-J., Zhang, J.-L., Chen, S.-J., Chen, H.-H., Liu, Y.-L., and Xu, H.-J. (2020). Functional analysis of Ultrabithorax in the wing-dimorphic planthopper *Nilaparvata lugens* (Stål, 1854) (Hemiptera: Delphacidae). *Gene* 737:144446. doi: 10.1016/j.gene.2020.144446

Grant, G. G. (1978). Morphology of the presumed male pheromone glands on the forewings of tortricid and phycitid moths. *Ann. Entomol. Soc. Am.* 71, 423–431. doi: 10.1093/aesa/71.3.423

Hersh, B. M., Nelson, C. E., Stoll, S. J., Norton, J. E., Albert, T. J., and Carroll, S. B. (2007). The UBX-regulated network in the haltere imaginal disc of D. melanogaster. *Dev. Biol.* 302, 717–727. doi: 10.1016/j.ydbio.2006.11.011

Hughes, C. L., and Kaufman, T. C. (2002). Hox genes and the evolution of the arthropod body plan1. *Evol. Dev.* 4, 459–499. doi: 10.1046/j.1525-142X.2002.02034.x

Iwata, M., and Otaki, J. M. (2016). Spatial patterns of correlated scale size and scale color in relation to color pattern elements in butterfly wings. *J. Insect Physiol.* 85, 32–45. doi: 10.1016/j.jinsphys.2015.11.013

Iwata, M., and Otaki, J. M. (2019). Insights into eyespot color-pattern formation mechanisms from color gradients, boundary scales, and rudimentary eyespots

in butterfly wings. *J. Insect Physiol.* 114, 68–82. doi: 10.1016/j.jinsphys.2019.02.009

Jantzen, B., and Eisner, T. (2008). Hindwings are unnecessary for flight but essential for execution of normal evasive flight in Lepidoptera. *PNAS* 105, 16636–16640. doi: 10.1073/pnas.0807223105

Kaschula, R., Pinho, S., and Alonso, C. R. (2018). MicroRNA-dependent regulation of hox gene expression sculpts fine-grain morphological patterns in a Drosophila appendage. *Development* 145:dev161133. doi: 10.1242/dev.161133

Konopova, B., and Akam, M. (2014). The hox genes Ultrabithorax and abdominal-A specify three different types of abdominal appendage in the springtail *Orchesella cincta* (Collembola). *EvoDevo* 5:2. doi: 10.1186/2041-9139-5-2

Konopová, B., Buchberger, E., and Crisp, A. (2020). Transcriptome of pleuropodia from locust embryos supports that these organs produce enzymes enabling the larva to hatch. *Front. Zool.* 17:4. doi: 10.1186/s12983-019-0349-2

Lewis, D. L., DeCamillis, M., and Bennett, R. L. (2000). Distinct roles of the homeotic genes Ubx and abd-A in beetle embryonic abdominal appendage development. *PNAS* 97, 4504–4509. doi: 10.1073/pnas.97.9.4504

Lipshitz, H. D. (2007). *Genes, Development and Cancer: The Life and Work of E. B. Lewis*. Dordrecht: Springer Netherlands.

Mahfooz, N., Turchyn, N., Mihajlovic, M., Hrycaj, S., and Popadić, A. (2007). Ubx regulates differential enlargement and diversification of insect hind legs. *PLoS One* 2:e866. doi: 10.1371/journal.pone.0000866

Makhijani, K., Kalyani, C., Srividya, T., and Shashidhara, L. S. (2007). Modulation of decapentaplegic gradient during haltere specification in Drosophila. *Dev. Biol.* 302, 243–255. doi: 10.1016/j.ydbio.2006.09.029

Martin, A., and Reed, R. D. (2014). Wnt signaling underlies evolution and development of the butterfly wing pattern symmetry systems. *Dev. Biol.* 395, 367–378. doi: 10.1016/j.ydbio.2014.08.031

Martin, A., Wolcott, N. S., and O'Connell, L. A. (2020). Bringing immersive science to undergraduate laboratory courses using CRISPR gene knockouts in frogs and butterflies. *J. Exp. Biol.* 223:jeb208793. doi: 10.1242/jeb.208793

Masumoto, M., Yaginuma, T., and Niimi, T. (2009). Functional analysis of Ultrabithorax in the silkworm, *Bombyx mori*, using RNAi. *Dev. Genes Evol.* 219, 437–444. doi: 10.1007/s00427-009-0305-9

Matsuoka, Y., and Monteiro, A. (2020). Hox genes are essential for the development of eyespots in *Bicyclus anynana* butterflies. *Genetics* 217:iyaa005. doi: 10.1093/genetics/iyaa005

Mazo-Vargas, A., Concha, C., Livraghi, L., Massardo, D., Wallbank, R. W. R., Zhang, L., et al. (2017). Macroevolutionary shifts of WntA function potentiate butterfly wing-pattern diversity. *Proc. Natl. Acad. Sci. U.S.A.* 114:10701. doi: 10.1073/pnas.1708149114

McKay, D. J., and Lieb, J. D. (2013). A common set of DNA regulatory elements shapes Drosophila appendages. *Dev. Cell* 27, 306–318. doi: 10.1016/j.devcel.2013.10.009

Medved, V., Marden, J. H., Fescemyer, H. W., Der, J. P., Liu, J., Mahfooz, N., et al. (2015). Origin and diversification of wings: insights from a neopteran insect. *PNAS* 112, 15946–15951. doi: 10.1073/pnas.1509517112

Mohit, P., Makhijani, K., Madhavi, M. B., Bharathi, V., Lal, A., Sirdesai, G., et al. (2006). Modulation of AP and DV signaling pathways by the homeotic gene Ultrabithorax during haltere development in Drosophila. *Dev. Biol.* 291, 356–367. doi: 10.1016/j.ydbio.2005.12.022

Monteiro, A. (2015). Origin, development, and evolution of butterfly eyespots. *Annu. Rev. Entomol.* 60, 253–271. doi: 10.1146/annurev-ento-010814-020942

Monteiro, A. (2020). Distinguishing serial homologs from novel traits: experimental limitations and ideas for improvements. *BioEssays* 43:e2000162. doi: 10.1002/bies.202000162

Monteiro, A., Chen, B., Ramos, D. M., Oliver, J. C., Tong, X., Guo, M., et al. (2013). Distal-less regulates eyespot patterns and melanization in Bicyclus butterflies. *J. Exp. Zool. B Mol. Dev. Evol.* 320, 321–331. doi: 10.1002/jez.b.22503

Navas, L. F., de Garaulet, D. L., and Sánchez-Herrero, E. (2006). The Ultrabithorax hox gene of Drosophila controls haltere size by regulating the Dpp pathway. *Development* 133, 4495–4506. doi: 10.1242/dev.02609

Nijhout, H. F., and Rountree, D. B. (1995). Pattern induction across a homeotic boundary in the wings of Precis coenia (Hbn.) (Lepidoptera: Nymphalidae). *Int. J. Insect Morphol. Embryol.* 24, 243–251. doi: 10.1016/0020-7322(95)00004-N

Ohde, T., Yaginuma, T., and Niimi, T. (2014). Wing serial homologs and the origin and evolution of the insect wing. *Zoology* 117, 93–94. doi: 10.1016/j.zool.2013.11.001

Otaki, J. M. (2012). Color pattern analysis of nymphalid butterfly wings: revision of the nymphalid groundplan. *Zoolog. Sci.* 29, 568–576. doi: 10.2108/zsj.29.568

Pavlopoulos, A., and Akam, M. (2011). Hox gene Ultrabithorax regulates distinct sets of target genes at successive stages of Drosophila haltere morphogenesis. *PNAS* 108, 2855–2860. doi: 10.1073/pnas.1015077108

Pourquie, O. (2009). *HOX Genes*, 1st Edn. 88. Available online at: https://www.elsevier.com/books/hox-genes/pourquie/978-0-12-374529-3 [Accessed November 24, 2020]

Prasad, N., Tarikere, S., Khanale, D., Habib, F., and Shashidhara, L. S. (2016). A comparative genomic analysis of targets of Hox protein Ultrabithorax amongst distant insect species. *Sci. Rep.* 6:27885. doi: 10.1038/srep27885

Richards, O. W., and Thomson, W. S. (1932). A contribution to the study of the genera Ephestia, Gn. (including Strymax, Dyar), and Plodia, Gn. (Lepidoptera, Phycitidae), with notes on parasites of the larvae. *Trans. R. Entomol. Soc. Lond.* 80, 169–247. doi: 10.1111/j.1365-2311.1932.tb03306.x

Roberts, K. E., Meaden, S., Sharpe, S., Kay, S., Doyle, T., Wilson, D., et al. (2020). Resource quality determines the evolution of resistance and its genetic basis. *Mol. Ecol.* 29, 4128–4142. doi: 10.1111/mec.15621

Sánchez-Higueras, C., Rastogi, C., Voutev, R., Bussemaker, H. J., Mann, R. S., and Hombría, J. C.-G. (2019). In vivo hox binding specificity revealed by systematic changes to a single cis regulatory module. *Nat. Commun.* 10:3597. doi: 10.1038/s41467-019-11416-1

Shashidhara, L. S., Agrawal, N., Bajpai, R., Bharathi, V., and Sinha, P. (1999). Negative regulation of dorsoventral signaling by the homeotic gene Ultrabithorax during haltere development in Drosophila. *Dev. Biol.* 212, 491–502. doi: 10.1006/dbio.1999.9341

Sibatani, A. (1980). Wing homoeosis in Lepidoptera: a survey. *Dev. Biol.* 79, 1–18. doi: 10.1016/0012-1606(80)90069-X

Sibatani, A. (1983a). A compilation of data on wing homoeosis in Lepidoptera. *J. Res. Lepid* 22, 1–46.

Sibatani, A. (1983b). Compilation of data on wing homoeosis on Lepidoptera: supplement I. *J. Res. Lepid* 22, 118–125.

Silhacek, D., and Murphy, C. (2008). Moisture content in a wheat germ diet and its effect on the growth of Plodia interpunctella (Hübner). *J. Stored Prod. Res.* 44, 36–40. doi: 10.1016/j.jspr.2006.03.004

Solis, M. A., and Neunzig, H. H. (2017). A new phycitine genus and species of a pourouma-feeding moth (Lepidoptera: Pyralidae) from Panama. *Proc. Entomol. Soc. Wash.* 119, 464–470.

Tomoyasu, Y. (2017). Ultrabithorax and the evolution of insect forewing/hindwing differentiation. *Curr. Opin. Insect Sci.* 19, 8–15. doi: 10.1016/j.cois.2016.10.007

Tomoyasu, Y., Arakane, Y., Kramer, K. J., and Denell, R. E. (2009). Repeated co-options of exoskeleton formation during wing-to-elytron evolution in beetles. *Curr. Biol.* 19, 2057–2065. doi: 10.1016/j.cub.2009.11.014

Tomoyasu, Y., Ohde, T., and Clark-Hachtel, C. (2017). What serial homologs can tell us about the origin of insect wings. *F1000Res* 6:268. doi: 10.12688/f1000research.10285.1

Tomoyasu, Y., Wheeler, S. R., and Denell, R. E. (2005). Ultrabithorax is required for membranous wing identity in the beetle *Tribolium castaneum*. *Nature* 433, 643–647. doi: 10.1038/nature03272

Tong, X., Fu, M. Y., Chen, P., Chen, L., Xiang, Z. H., Lu, C., et al. (2017). Ultrabithorax and abdominal-A specify the abdominal appendage in a dosage-dependent manner in silkworm, *Bombyx mori*. *Heredity* 118, 578–584. doi: 10.1038/hdy.2016.131

Tong, X., Hrycaj, S., Podlaha, O., Popadic, A., and Monteiro, A. (2014). Over-expression of Ultrabithorax alters embryonic body plan and wing patterns in the butterfly *Bicyclus anynana*. *Dev. Biol.* 394, 357–366. doi: 10.1016/j.ydbio.2014.08.020

Ueno, K., Toshifumi, N., and Suzuki, Y. (1995). "Roles of homeotic genes in the Bombyx body plan," in *Molecular Model Systems in the Lepidoptera*, eds A. S. Wilkins and M. R. Goldsmith (Cambridge: Cambridge University Press), 165–180.

Uhl, J. D., Zandvakili, A., and Gebelein, B. (2016). A hox transcription factor collective binds a highly conserved Distal-less cis-Regulatory module to generate robust transcriptional outcomes. *PLoS Genet.* 12:e1005981. doi: 10.1371/journal.pgen.1005981

Vachon, G., Cohen, B., Pfeifle, C., McGuffin, M. E., Botas, J., and Cohen, S. M. (1992). Homeotic genes of the bithorax complex repress limb development in

the abdomen of the Drosophila embryo through the target gene Distal-less. *Cell* 71, 437–450. doi: 10.1016/0092-8674(92)90513-C

van der Burg, K. R. L., Lewis, J. J., Martin, A., Nijhout, H. F., Danko, C. G., and Reed, R. D. (2019). Contrasting roles of transcription factors spineless and EcR in the highly dynamic chromatin landscape of butterfly wing metamorphosis. *Cell Reports* 27, 1027–1038.e3. doi: 10.1016/j.celrep.2019.03.092

Warren, R. W., Nagy, L., Selegue, J., Gates, J., and Carroll, S. (1994). Evolution of homeotic gene regulation and function in flies and butterflies. *Nature* 372, 458–461. doi: 10.1038/372458a0

Weatherbee, S. D., Halder, G., Kim, J., Hudson, A., and Carroll, S. (1998). Ultrabithorax regulates genes at several levels of the wing-patterning hierarchy to shape the development of the *Drosophila haltere*. *Genes Dev.* 12, 1474–1482. doi: 10.1101/gad.12.10.1474

Weatherbee, S. D., Nijhout, H. F., Grunert, L. W., Halder, G., Galant, R., Selegue, J., et al. (1999). Ultrabithorax function in butterfly wings and the evolution of insect wing patterns. *Curr. Biol.* 9, 109–115. doi: 10.1016/S0960-9822(99)80064-5

Williams, J. A., and Carroll, S. B. (1993). The origin, patterning and evolution of insect appendages. *BioEssays* 15, 567–577. doi: 10.1002/bies.950150902

Wootton, R. J. (2002). Design, function and evolution in the wings of holometabolous insects. *Zool. Scripta* 31, 31–40. doi: 10.1046/j.0300-3256.2001.00076.x

Zandvakili, A., Uhl, J. D., Campbell, I., Salomone, J., Song, Y. C., and Gebelein, B. (2019). The cis-regulatory logic underlying abdominal Hox-mediated repression versus activation of regulatory elements in *Drosophila*. *Dev. Biol.* 445, 226–236. doi: 10.1016/j.ydbio.2018.11.006

Zaspel, J. M. (2016). *The Insects: An Outline of Entomology*, 5th Edn. Oxford Academic:Oxford.

Zheng, Z., Khoo, A., Fambrough, D. Jr., Garza, L., and Booker, R. (1999). Homeotic gene expression in the wild-type and a homeotic mutant of the moth *Manduca sexta*. *Dev. Gene Evol.* 209, 460–472. doi: 10.1007/s004270050279

Conflict of Interest: The authors declare that the research was conducted in the absence of any commercial or financial relationships that could be construed as a potential conflict of interest.

frontiers in Cell and Developmental Biology

REVIEW
published: 26 March 2021
doi: 10.3389/fcell.2021.653579

The Intertwined Evolution and Development of Sutures and Cranial Morphology

Heather E. White[1,2,3], Anjali Goswami[1,3] and Abigail S. Tucker[2]*

[1] Department of Life Sciences, Natural History Museum, London, United Kingdom, [2] Centre for Craniofacial and Regenerative Biology, King's College London, London, United Kingdom, [3] Division of Biosciences, University College London, London, United Kingdom

Phenotypic variation across mammals is extensive and reflects their ecological diversification into a remarkable range of habitats on every continent and in every ocean. The skull performs many functions to enable each species to thrive within its unique ecological niche, from prey acquisition, feeding, sensory capture (supporting vision and hearing) to brain protection. Diversity of skull function is reflected by its complex and highly variable morphology. Cranial morphology can be quantified using geometric morphometric techniques to offer invaluable insights into evolutionary patterns, ecomorphology, development, taxonomy, and phylogenetics. Therefore, the skull is one of the best suited skeletal elements for developmental and evolutionary analyses. In contrast, less attention is dedicated to the fibrous sutural joints separating the cranial bones. Throughout postnatal craniofacial development, sutures function as sites of bone growth, accommodating expansion of a growing brain. As growth frontiers, cranial sutures are actively responsible for the size and shape of the cranial bones, with overall skull shape being altered by changes to both the level and time period of activity of a given cranial suture. In keeping with this, pathological premature closure of sutures postnatally causes profound misshaping of the skull (craniosynostosis). Beyond this crucial role, sutures also function postnatally to provide locomotive shock absorption, allow joint mobility during feeding, and, in later postnatal stages, suture fusion acts to protect the developed brain. All these sutural functions have a clear impact on overall cranial function, development and morphology, and highlight the importance that patterns of suture development have in shaping the diversity of cranial morphology across taxa. Here we focus on the mammalian cranial system and review the intrinsic relationship between suture development and morphology and cranial shape from an evolutionary developmental biology perspective, with a view to understanding the influence of sutures on evolutionary diversity. Future work integrating suture development into a comparative evolutionary framework will be instrumental to understanding how developmental mechanisms shaping sutures ultimately influence evolutionary diversity.

Keywords: suture, morphology, development, craniofacial, evolution, mammal, skull

OPEN ACCESS

Edited by:
Nico Posnien,
University of Göttingen, Germany

Reviewed by:
Borja Esteve-Altava,
Pompeu Fabra University, Spain
Julia Boughner,
University of Saskatchewan, Canada

****Correspondence:***
Heather E. White
h.white@nhm.ac.uk;
heather.white.17@ucl.ac.uk

Specialty section:
This article was submitted to Evolutionary Developmental Biology, a section of the journal Frontiers in Cell and Developmental Biology

Received: *14 January 2021*
Accepted: *08 March 2021*
Published: *26 March 2021*

Citation:
White HE, Goswami A and Tucker AS (2021) The Intertwined Evolution and Development of Sutures and Cranial Morphology. Front. Cell Dev. Biol. 9:653579. doi: 10.3389/fcell.2021.653579

AN INTRODUCTION TO SUTURES

Cranial diversity is shaped by the unique development and functional complexity of the skull. This diversity reflects vast ecological diversification present across vertebrates (McCurry et al., 2015; Arbour et al., 2019; Felice et al., 2019; Watanabe et al., 2019). The skull performs many functions enabling each species to thrive within their unique ecological niche, by supporting prey acquisition, feeding, and breathing, while protecting the brain and sensory organs to support sensory capture (i.e., vision and hearing). Across vertebrates, the adjacent cranial and facial bones are connected by fibrous joints, known as cranial sutures (Opperman, 2000). As joints, the term "suture" therefore encompasses both the fibrous connective tissue and the osteogenic expanding bone fronts connected by such fibres (Lenton et al., 2005).

Recent instrumental advances in geometric morphometric techniques have supported an extensive body of research considering the comparative morphology, functioning, and development of the skull (Stayton, 2005; Pierce et al., 2009; Brusatte et al., 2011; Foth et al., 2012; Esteve-Altava et al., 2013; Fabre et al., 2014; Lu et al., 2014; Parr et al., 2016; McCurry et al., 2017; Felice and Goswami, 2018; Heck et al., 2018; Bardua et al., 2019; Evans et al., 2019). In contrast, relatively little work focusses on the comparative morphology of cranial sutures (Kathe, 1999; Monteiro and Lessa, 2000; Byron, 2009; Buezas et al., 2017). Even less has work directly addressed the interrelationship between the skull and sutures (Richtsmeier et al., 2006; Heuzé et al., 2010; Esteve-Altava and Rasskin-Gutman, 2015), in particular in a comparative taxonomic framework (Richtsmeier et al., 2006; Heuzé et al., 2010; Esteve-Altava and Rasskin-Gutman, 2015). To highlight this difference, a Google Scholar search returned a 20-fold difference in the number of papers containing the keyword skull compared to those containing the keywords skull and sutures. The limited work addressing comparative suture morphology compared to the comprehensive analysis of cranial morphology, stems, in part, from the inherent natural complexity of sutures. For example, the open outlines of sutures (i.e., sutures do not exhibit a closed shape) can complicate comparative analysis of their morphology (Canfield and Anstey, 1981; Allen, 2006). Moreover, there is a distinct lack of well-defined homologous anatomical landmarks that can implemented for these non-osseous structures (Toussaint et al., 2021).

From an evolutionary perspective, sutures can broadly refer to any connections between hard tissue structures, including those found across both vertebrate and invertebrate clades. The earliest examples of such structures can be found in trilobites from the Cambrian (541–485 Ma) (Paterson and Edgecombe, 2006). Cranial examples, which are not homologous to the earlier examples found in trilobites and other extinct groups such as ammonoids are first observed in fossil fishes from the Ordovician (485–444 Ma) (Bryant, 1932). Such cranial sutures are common to all clades of vertebrates (Kathe, 1999; Clack, 2002; Rayfield, 2005; Markey et al., 2006; Curtis et al., 2013; Rager et al., 2014; Kammerer et al., 2015; Bailleul et al., 2016; Bailleul and Horner, 2016), including both extinct and extant mammals (Goswami et al., 2013; Rager et al., 2014). Whilst the sutures of trilobite exoskeletons and ammonoid shells are clearly not homologous to the cranial sutures of modern vertebrates, some interesting similarities have been proposed. For example, both types of sutures may have been shaped in response to external pressures. It is well known that vertebrate suture morphology responds to stresses imposed by behaviour and ecology (Jaslow and Biewener, 1995; Clack, 2002; Goswami et al., 2013; Buezas et al., 2017). It has similarly long been postulated that ammonoid shell suture morphology may also respond to ecological stresses such as hydrostatic pressure (Hewitt and Westermann, 2007), although there is controversy within the literature and this idea is still debated (Lemanis, 2020). Remarkably, these non-homologous sutures may have convergently evolved to respond to similar external pressures.

The major sutures of the mammalian cranial vault (**Figure 1**) form between: the paired frontal bones to create the interfrontal (metopic) suture; between the paired parietal bones to create the sagittal suture; between both frontal and parietal bones to form the paired coronal sutures; between the interparietal and two parietal bones to form the paired lambdoid sutures; and between both squamosal and parietal bones to form two squamosal sutures (shown in the mouse in **Figure 1**). Three sutures separate the neurocranium from the viscerocranium (**Figure 1**): the frontonasal suture forms between the nasal bone of the viscerocranium and the frontal bone of the neurocranium; the frontozygomatic suture forms between the zygomatic bone of the viscerocranium and the frontal bone of the neurocranium; the temporozygomatic suture forms between the zygomatic bone of the viscerocranium and the squamosal bone of the neurocranium (Hanken and Hall, 1993). The presence of these cranial sutures supports skull function.

It is worth noting here that not all joints of the skull are sutures. Sutures, as mentioned above, are fibrous joints forming between the membranous bones of the skull, whereas synchondroses form cartilaginous joints between the endochondral bones of the skull (Opperman et al., 2005). Whilst synchondroses differ developmentally from sutures, they function in a similar manner to facilitate the growth of cranial bones and thus have crucial roles during postnatal craniofacial development (Cendekiawan et al., 2010). In humans, synchondroses are recognised to be functionally important for enabling cranial base flexion to accommodate the increased brain volume (encephalization), whilst cranial base flexion in turn influences facial projection (Lesciotto and Richtsmeier, 2019). It is important to highlight here that many evolutionary studies commonly refer to synchondroses as sutures and thus use the term suture to broadly include both fibrous and cartilaginous joints.

Whilst sutures are present in the skulls of all vertebrates, suture development, morphology, complexity, and fusion patterns differ both within and across species. The phylogenetic distance between clades (e.g., birds and mammals) has resulted in alternative mechanisms of suture growth and fusion. For example, archosaurs have a greater diversity in the number of sutures present than mammals, in addition to using an entirely different mineralised tissue at the sutures themselves (Bailleul and Horner, 2016). Therefore, focussing on one vertebrate

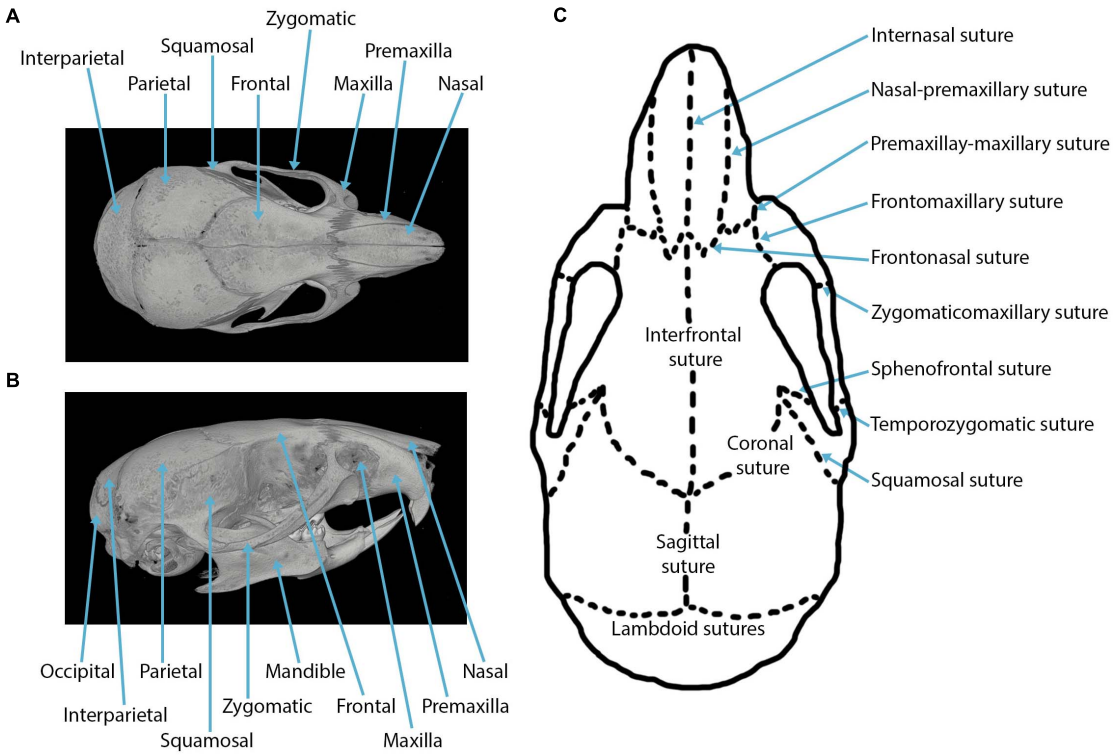

FIGURE 1 | Craniofacial anatomy: **(A)** dorsal view of a mouse skull depicting the cranial bones in a microCT reconstruction; **(B)** lateral view of a mouse skull depicting the cranial bones in a microCT reconstruction; **(C)** cranial sutures in the dorsal view.

clade minimises comparison challenges, such as differences in suture number and structure, allowing direct analysis of how suture morphology influences cranial morphology. Mammals are an optimal clade to study in order to understand the drivers of morphological variation and diversification due to their broad ecological diversification into a range of habitats on every continent and in every ocean, coupled with their variation in both cranial and suture morphology. Moreover, the mouse model is one of the most commonly used model systems within developmental biology research, meaning that applicable developmental data is readily available. Despite the variation in suture shape, the composition of the mature suture in mammals appears to be largely comparable across various mammalian species (Pritchard et al., 1956; Persson et al., 1978; Bailleul and Horner, 2016). Therefore, suggesting that the process and general principles of postnatal suture development are similar across mammalian taxa and that lessons from one species could be applied to others. This conserved structure could dictate the similar functioning of sutures across mammals, such as providing shock absorption (Moazen et al., 2009) and supporting mastication (Goswami et al., 2013). Collectively, mammals present an ideal system for studying the frontier between evolutionary and developmental biology.

Here, we review current knowledge on the interaction between suture development and morphology and cranial shape in mammals from an evolutionary developmental biology perspective, with a view to understanding suture development and its influence on evolutionary diversity. From several perspectives, it is clear that suture closure plays a role in shaping human cranial morphology. Pathology research suggests that the order of cranial suture fusion is instrumental in producing various craniofacial morphologies (Heuzé et al., 2010). Anthropological researchers have proposed the hypothesis of functional craniology (Moss and Young, 1960; Bruner, 2007) which has led to the notion that sutures are themselves crucial elements of the cranial functional network (Di leva et al., 2013). Theoretical morphological studies, implementing network models of the skull, have also highlighted the potential importance of suture closure timing in shaping the human skull form (Esteve-Altava and Rasskin-Gutman, 2015). Combined, these studies and others suggest a relationship between cranial form and suture morphology, fusion, and functioning. We have, therefore, compiled evidence from human pathology, mouse mutants, comparative anatomy, and evolutionary trends, to further develop our understanding of this interaction between suture development and morphology and mammalian cranial shape.

SUTURE MORPHOLOGY

Suture morphology has been studied on a number of levels, covering the microscopic morphological organisation of the fibres, the cross-sectional joint morphology, and the gross

morphology spanning the entire sutural length. It is well known that suture morphology and fusion adapt over time by responding to a number of pressures (Wilkie and Morriss-Kay, 2001; Clack, 2002; Byron, 2009; Buezas et al., 2017). Here, we refer to "suture fusion" as the closure of the suture, which is accompanied by the process of suture obliteration, whereas the term "patent suture" describes the sutures remaining open and unfused.

At the microscopic level, a dense network of Sharpey's fibres creating a matrix of connective tissue, consisting mainly of type 1 collagen, forms the fibrous sutural joint connection between two approaching bone fronts (Pritchard et al., 1956; Khonsari et al., 2013). The microscopic organisation of these fibres has been studied using various methods including confocal laser scanning, histology, and synchrotron X-ray microtomography, all of which identify a unique fibre orientation pattern for each suture locale. Sutures undergoing fusion, such as the interfrontal suture in the mouse, have been identified to have a highly organised lattice of Sharpey's fibres with new bone matrix deposition (Koskinen et al., 1976; Warren et al., 2008; Khonsari et al., 2013). In contrast, sutures that remain patent, such as the sagittal suture, have a random arrangement of fibres (Warren et al., 2008). In scenarios of a convex approaching bone front, fibres have been observed to present in a fan pattern (Khonsari et al., 2013). This variable fibre orientation across the sutures appears to be associated with minute growth, specific to the suture locale, thus producing a unique microscopic morphology at each suture (Koskinen et al., 1976). Moreover, the orientation of these Sharpey's fibres adapts throughout ontogeny creating a pattern that is specific to the growth at the suture locale (Koskinen et al., 1976). Over time, the fibrous connective tissue becomes increasingly organised, forming straighter collagen fibrils connecting the approaching bones (Zimmermann et al., 1998). At this microscopic level, a unique morphology can evidently be observed at each suture location.

Akin to any other mechanical joint, sutures present with different joint types (**Figure 2**). For sutures, the joint type is identified in the cross-section through the suture. In this cross-section, butt joints form end-to-end connections (**Figures 2A,E**), bevelled joints present with overlapping bone fronts (**Figure 2B**), and finger joints have interlocking and interdigitations (**Figures 2C,D**; Moss, 1957; Koskinen et al., 1976). Consequently, interdigitations are not a unique feature of gross suture morphology, but also exist across internal suture cross-sections, suggesting that complexity might be hidden from a superficial gross morphological view. The type of sutural joint is not thought to be predetermined, but instead thought to occur as a consequence of mechanical pressure from functional demands (Moss, 1957; Herring, 1972; Koskinen et al., 1976). Therefore, it is unsurprising that sutures start out as the simplest joint type, end-to-end joints, and throughout ontogeny develop to include other joint types which are modifications of this simple butt joint morphology (Moss, 1957).

The gross morphological scale captures the entire suture length and is outlined by the approaching bone fronts. At this gross scale, suture morphology is once again highly variable, with the same suture having a very different morphology even in relatively closely related species of mammal (**Figure 3**). Patterns span a range of morphologies, including straight, highly curved, looping, and interdigitated outlines (White et al., 2020). Interestingly, there is a strong association between the microscopic fibre organisation and the gross suture morphology (Khonsari et al., 2013). Mechanical constraints and pressures generated during sutural growth are thought to influence the fibre orientation which in turn shapes and modifies the developed gross suture morphology (Khonsari et al., 2013). Throughout ontogeny, gross suture morphology undergoes large morphological transformations, starting out as straight morphologies and developing to become highly interdigitated with complex patterns (Nicolay and Vaders, 2006; Curtis et al., 2014). In the mouse, such interdigitations are established at around 7 weeks postnatal, following sexual maturity and progress as growth continues to adulthood (3 months) (Miura et al., 2009).

In the developed suture, gross morphology varies between the sexes, from suture to suture, and across species. Sexual dimorphism of cranial sutures has been identified for certain species. Specifically, male wild sheep (*Ovis orientalis*) exhibit a greater degree of complexity in the facial sutures than females, which is thought to be a result of head-to-head fighting (Jaslow, 1989). Additionally, sutures in different cranial regions have been reported to have differing morphologies, with straight sutures identified in the facial region and interdigitated sutures within the braincase (Monteiro and Lessa, 2000). Finally, the level of sutural interdigitation, ranging from low to high, reflects interspecific variation at different taxonomic levels, within both genus (*Cebus*) and infraorder (Caviomorpha) (Byron, 2009; Buezas et al., 2017). Interspecific suture morphological variation likely implies the presence of heightened developmental variation. Several metrics have previously been proposed to quantify this gross morphological complexity of sutures, which have recently been compared on mammal sutures (White et al., 2020). Quantification of gross suture morphological complexity will enable the untangling of mechanisms driving the alterations in complexity. Nevertheless, this is complicated by the number of external factors involved in shaping suture morphology. Factors driving this gross suture variation have been attributed to a number of biological pressures, such as diet, behaviour, and ecology (Jaslow and Biewener, 1995; Herring and Teng, 2000; Monteiro and Lessa, 2000; Byron et al., 2004; Byron, 2009; Buezas et al., 2017), in addition to patterns of growth (Henderson et al., 2005) and trends toward increasing complexity over geologic time scales (Allen, 2006). Irrespective of the scale at which suture morphology has been studied (micro, cross-sectional, gross), a unique morphology specific to the suture locale can be observed. Whilst it is possible that suture phenotypic variation could be used to interpret information regarding the external stresses, deriving the specific pressure responsible for a suture phenotype, however, is difficult given the complexity of factors and stresses (development, sex, diet, ecology, and behaviour) proposed to be involved. As studies have only been conducted on a limited range of mammalian taxa to date, as discussed above, the need for comparative studies becomes ever more pertinent to help reveal evolutionary differences and stresses involved

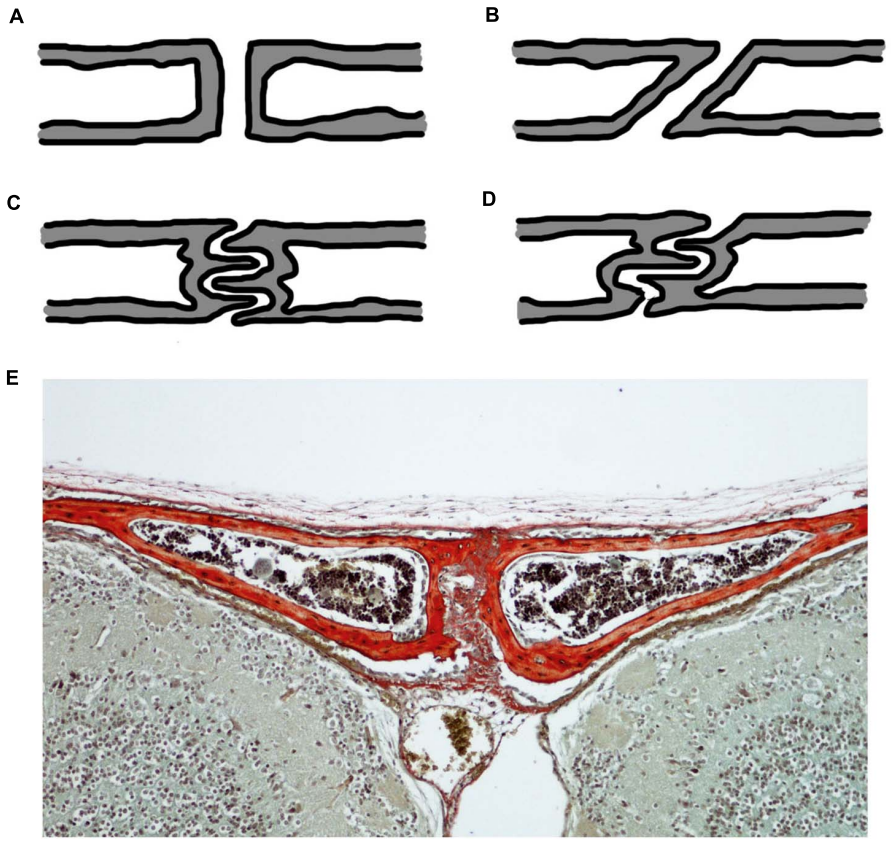

FIGURE 2 | Cross-sectional suture joint morphology: **(A)** butt joint; **(B)** bevelled joint; **(C)** finger joint at a butt end-to-end connection; **(D)** finger joint at an overlapping bevelled connection; **(E)** CD1 mouse trichrome stain at P20 showing the cross-section through the interfrontal suture with bone indicated in red reflecting the butt joint in **(A)**. Schematics **(A–D)** based on (Moss, 1957; Koskinen et al., 1976).

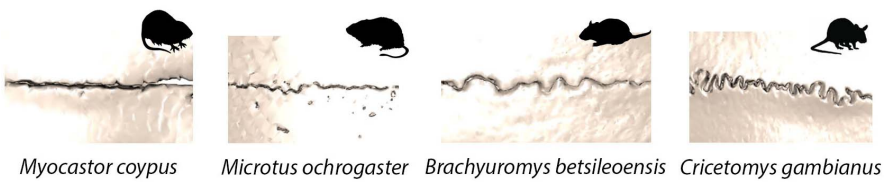

FIGURE 3 | Sagittal suture morphological variation in four species of rodent: *Myocastor coypus* (coypu); *Mircotus ochrogaster* (prairie vole); *Brachyuromys betsileoensis* (Betsileo short-tailed rat); *Cricetomys gambianus* (Gambian pouched rat).

in shaping the suture at the micro, cross-sectional and gross morphological scales.

THE IMPORTANCE OF SUTURES

As the major joints of the skull, sutures have a number of crucial functional roles. Each role supports the overall functioning of the cranium, highlighting a functional link between sutures and the skull.

Open sutures act as signalling centres to regulate the balance between proliferation of osteoblast precursors and osteogenic differentiation (Iseki et al., 1997; Zhou et al., 2000). Consequently, sutures are able to carry out one of their key functional roles, by acting as the major site of interstitial bone growth for the cranial bones of the skull (Baer, 1954; Opperman, 2000; Lana-Elola et al., 2007; Jin et al., 2016). During postnatal development, the suture mesenchyme provides a unique niche operating as a reservoir for mesenchymal stem cells (MSC), which are key to supporting cranial bone growth. Within the suture mesenchyme, lineage tracing experiments have identified Gli1+ cells to be the main MSC population (Zhao et al., 2015). These Gli1+ cells function to support the growth of all craniofacial bones (Zhao et al., 2015). Moreover, an Axin2 expressing cell population, identified more specifically within the midline suture mesenchyme, has also been associated with calvarial development (Maruyama et al., 2016).

A third population of similarly located Prx1 positive cells has also been recently identified (Wilk et al., 2017). As such, MSC populations within the suture mesenchyme enable the cranial bones to expand in a coordinated manner around the growing brain and can act as a reservoir of cells during homeostasis. Evidence for this interstitial bone growth role across evolutionary taxa, has been identified outside of mammals. In the zebrafish, studies suggest that patency is also necessary for maintaining a stem cell population at the suture locale required for cranial bone osteogenesis (Teng et al., 2018). Beyond bone growth, sutures also support cranial bone repair by providing a major source of stem cells (Doro et al., 2017). While the Gli1 population has been shown to have a role in homeostasis and repair (Zhao et al., 2015), the Axin2 population appears to represent a reserve population specifically activated during injury (Maruyama et al., 2016). Therefore, craniofacial bone homeostasis seems to be highly dependent upon this unique niche of sutural mesenchymal stem cells. It is possible, with much future work, that these stem cell populations could be harnessed to support craniofacial repair in patients, through the design of new therapies for future clinical implementations (Doro et al., 2017). Once closed, sutures appear to lose their MSC population. The Gli1+ population is lost at the site of the fused interfrontal suture in mice (Zhao et al., 2015), whilst there is a reduction in the Axin2 population at prematurely fused sutures in craniosynostosis patients (Di Pietro et al., 2020). Thus, suggesting that an open suture status is necessary for the suture to contain a reservoir of MSCs enabling it to function as a site of interstitial bone growth and support normal craniofacial development.

Sutures additionally function to allow skull movement. During birth, in humans, the sutures enable movement of the cranial bones, creating overlapping to ease the passage through the birth canal (Jin et al., 2016). This functional role of the sutures is likely to have greater significance in placental mammals than in monotremes or marsupials, since the short gestation period results in highly altricial young (Lillegraven et al., 1987; Nunn and Smith, 1998). Marsupials exhibit a lower level of closure than placentals, and sutures are reported to remain open throughout life (Rager et al., 2014). It is thus possible that variation in suture closure between placentals and marsupials may be indicative of differing postnatal functional roles, especially given the significance of suture fusion status in supporting postcranial bone growth (Zhao et al., 2015; Di Pietro et al., 2020).

Fused sutures, as well as open sutures, are both functionally important. Across placental mammals, sutures of the cranial vault and synchondroses of the cranial base generally close postnatally (Rager et al., 2014). Suture fusion provides protection to the developed brain. Interestingly, the sutures of the facial region of most placentals never fuse (Rager et al., 2014) and suggest additional functional roles for open sutures, such as an involvement in the masticatory process (Herring, 1972; Flores et al., 2006; Goswami et al., 2013). A modelling approach utilising finite element analysis (FEA) has indicated that stresses are mitigated in skulls with a higher number of open sutures, suggesting that sutures are essential for shock absorption and the redistribution of strain across the skull (Moazen et al., 2009). Therefore, strains that are produced during biting can be modified across the skull as a result of suture presence (Moazen et al., 2009). Strain at the suture is both greater than within the adjacent cranial bones and is dependent on the muscle activity during mastication (Herring and Teng, 2000). Moreover, sutures facilitate the process of feeding by providing compliant and elastic joint mobility within the skull (Herrel et al., 2000; Herring and Teng, 2000). In geckos, cranial kinesis, which is supported by the cranial sutures, offers the capability for a larger bite force (Herrel et al., 2000). It is possible this functional role of sutures observed in cranial kinesis of geckos is mimicked in mammals which also exhibit cranial kinesis, such as rabbits (Kraatz and Sherratt, 2016). Not only are sutures functionally important during feeding, but they also act as shock absorbers to absorb strains from other external inputs, such as fighting behaviours and locomotion (Curtis et al., 2013). Evidently, sutures have hugely important functional roles both across postnatal development and throughout an organism's life, all these roles support and contribute to the normal functioning of the skull.

The importance of proper suture functioning for maintaining normal craniofacial development across postnatal development is evidenced in examples of abnormal suture development and when sutural defects occur. Craniosynostosis describes a premature pathologic fusion of one or more sutures and was first coined by Otto (1830). The prevalence of craniosynostosis is estimated to be between 1 in 2,000 and 1 in 2,500 live births (Johnson and Wilkie, 2011), with an increasing rate of occurrence reported (Cornelissen et al., 2016). Molecular and developmental studies have highlighted the complex pathogenesis that underlines craniosynostosis and how this contributes to the multitude of craniofacial dysmorphologies arising from premature suture fusion (Flaherty et al., 2016).

Craniosynostosis can either present as syndromic or non-syndromic. It can also be classified as either primary or secondary (developmental disorder directly or indirectly targeting the suture), and simple or compound (one or multiple sutures involved) (Flaherty et al., 2016). Syndromic craniosynostosis is associated with a genetic abnormality which in turn interrupts various signalling pathways to produce a number of dysmorphologies. Of these dysmorphologies one of the defects is craniosynostosis (suture fusion), resulting in craniofacial abnormalities (Senarath-Yapa et al., 2012). Numerous mutations, disrupting a multitude of signalling pathways, have been associated with craniosynostosis (Flaherty et al., 2016). In contrast, non-syndromic craniosynostosis is the fusion of a cranial suture in the absence of trunk, limb or other dysmorphologies; it is the suture fusion that is the most pronounced phenotypic abnormality (Flaherty et al., 2016). Examples of syndromic craniosynostosis include: Antley-Bixler syndrome, Apert syndrome, Carpenter syndrome, Crouzon syndrome, Muenke syndrome, Pfeiffer syndrome, and Saethre-Chotzen syndrome (Wilkie and Morriss-Kay, 2001; Lenton et al., 2005). Of these syndromes, Muenke syndrome is the most common and presents with coronal suture synostosis (O'Hara et al., 2019). However, in non-syndromic craniosynostosis the sagittal suture as the most frequently affected (Kimonis et al., 2007; Flaherty et al., 2016). Aside from the coronal and sagittal

sutures, the interfrontal and lambdoid sutures are also commonly affected (Kimonis et al., 2007). In each of these examples, craniosynostosis of the suture has a resultant effect on the cranial morphology (Flaherty et al., 2016).

Morphological changes in the skull can also impact on the brain. In severe cases, brain expansion becomes limited or distorted from the alterations in cranial morphology leading to cognitive deficits (Shim et al., 2016). The reduction in cranial size induces a physiological increase in intracranial pressure, which creates a number of functional impairments, manifesting as visual impairments, deafness, and further cognitive deficits (Gault et al., 1992; Panchal and Uttchin, 2003), requiring surgical correction (Lenton et al., 2005; Slater et al., 2008). Craniosynostosis reveals a persistent co-adjustment between the brain and skull, which, with advancing research will better inform surgical interventions and more accurately predict outcomes (Lesciotto and Richtsmeier, 2019). More detail on premature suture fusion, the associated signalling pathways, and the resultant craniofacial dysmorphologies (craniosynostosis) are discussed in greater detail later in this review in order to consider whether sutures may act as targets for evolutionary change in cranial morphology. Nevertheless, it is evident that correct suture function is critical for normal craniofacial development and functioning.

SUTURE DEVELOPMENT

Understanding normal suture development is pertinent to our understanding of the significance of abnormal suture development from a pathological perspective. Moreover, an understanding of suture development allows for an appreciation of how developing sutures can act as targets for evolutionary change. Suture development has been studied using a wide array of animal models, including the mouse, rat, rabbit, sheep, frog, and zebrafish (Grova et al., 2012). Comparisons across these distantly related vertebrate clades can be complicated by variation in developmental timings, origins, and processes (Bailleul and Horner, 2016). Here, we focus on mouse sutural development, as murine sutures have been shown to share major similarities with other mammalian taxa, including humans (Grova et al., 2012; Rager et al., 2014), thus a considerable amount of work is available documenting mouse craniofacial development making it an ideal model system for studying suture development from a pathological perspective (Wilkie and Morriss-Kay, 2001). Moreover, given the similarities in mature suture composition across mammals, information pertaining to mouse suture development and function will also be useful for understanding the pattern of suture formation, fusion, and thus functioning in mammals (Pritchard et al., 1956; Bailleul and Horner, 2016). Where other animal models are integrated within the discussions below, this will be specified. For the purpose of this review, focus will be given to the development of the sutures within the cranial vault, due to the importance of cranial vault sutures in facilitating brain growth. More detailed discussions of suture development can be referred to in the literature (Opperman, 2000; Lenton et al., 2005; Flaherty et al., 2016).

During early embryogenesis, the mesenchyme that forms the basis for the vertebrate fetal head is derived from two different developmental origins, mesoderm and neural crest (Couly et al., 1993; Jiang et al., 2002; Le Douarin, 2012). The neural crest originates from the ectoderm and undergoes an epithelial-mesenchymal transition to form a migratory population of mesenchymal cells (Hay, 2005). The developed skull can be separated into the viscerocranium and the neurocranium. Aspects of each of these are derived from different developmental origins (**Figure 4**). The viscerocranium, which makes up the bones of the facial region, is produced exclusively by neural crest derived cells (Le Douarin, 1982; Jiang et al., 2002). In mammalian development, the cranial neural crest cells are localised in the first and second pharyngeal arches, which contribute to the formation of the viscerocranium (Chai et al., 2000). In contrast, the neurocranium, which includes the cranial regions protecting the brain (cranial vault and base), has been strongly debated in terms of its embryological origins. Avian developmental studies have opposingly identified that the neurocranium is derived either solely from neural crest (Couly et al., 1993), or from a combined neural crest and mesoderm origin (Le Lièvre, 1978; Noden, 1988). More recently, increasingly precise labelling techniques agree that the neurocranium is formed from both neural crest and mesoderm, with the frontal bone being of dual origin and the remainder of the neurocranium mesodermally derived (Evans and Noden, 2006). Mammalian developmental studies agree with the vast majority of avian research, which suggests that the neurocranium is comprised of bones derived from both neural crest and mesoderm origins (Jiang et al., 2002; McBratney-Owen et al., 2008; Le Douarin, 2012). The neurocranium can be subdivided into the cartilaginous aspect (chondrocranium) and the membranous aspect (dermatocranium), both of which consist of bones from both cellular origins. Lineage tracing experiments in the mouse using a Wnt1-Cre allele and Mesp1-Cre allele, to mark neural crest and mesoderm origins, respectively, have shown the that the neural crest-mesoderm interface lies within the neurocranium (Jiang et al., 2002; Yoshida et al., 2008; Maddin et al., 2016; Teng et al., 2019). This boundary falls between the neural crest derived frontal bones and the mesoderm derived parietal bones (**Figure 4**).

Sutures of the murine cranial vault (interfrontal, sagittal, coronal, lambdoid) often form directly at the interface between mesoderm and neural crest derived tissue (Jiang et al., 2002; Lenton et al., 2005). Not only do the sutures separate bones of differing embryological origin, but they are themselves derived from different origins (**Figure 4**). The neural crest-mesoderm boundary separating the neural crest derived frontal bones and mesodermal derived parietal bones in the mammalian skull has been pinpointed to the coronal suture (Maddin et al., 2016; Teng et al., 2019). Moreover, the mesenchyme of the coronal suture itself is of mesoderm origin, which means it forms a direct neural crest-mesodermal interface (Jiang et al., 2002). This interface is established in early stages of development, at E9.5, and later leads to the formation of the coronal suture (Jiang et al., 2002). In contrast, the sagittal suture separates the two mesodermal parietal bones, but creates a neural crest-mesoderm boundary as the suture mesenchyme is neural crest (Jiang et al., 2002;

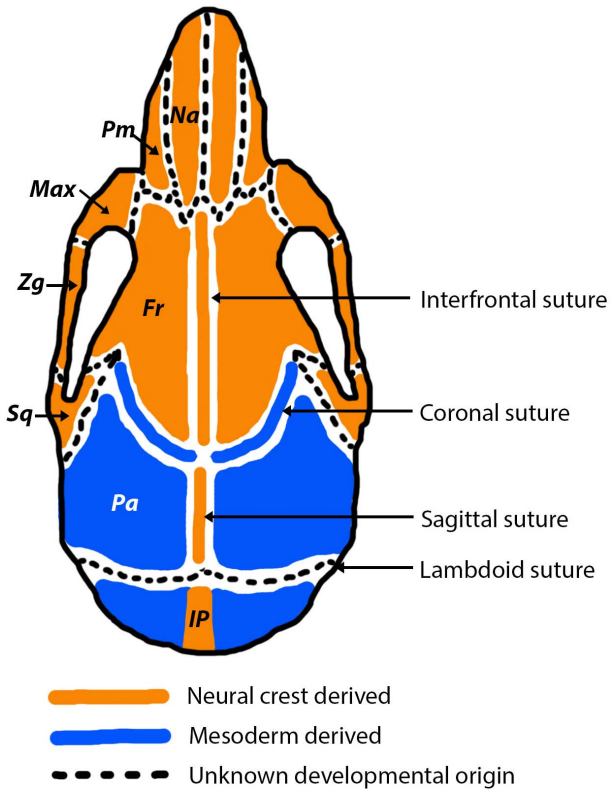

FIGURE 4 | Cranial bone and cranial suture developmental origins pictured in the adult mouse. Neural crest derived bones and sutures are depicted in orange and mesodermally derived bones and sutures are depicted in blue. In the early stages of development (E15.5-P0) the origins of the sutures are more nuanced, for example the sagittal and coronal sutures express a combination of mesoderm and neural crest derived cells (Doro et al., 2019). Abbreviations are as follows: Na, nasal; Pm, premaxilla; Max, maxilla; Zg, Zygomatic; Sq, squamosal; Fr, frontal; Pa, parietal; IP, interparietal.

Lenton et al., 2005). As a result of the neural crest-mesoderm boundaries, it has been speculated that the sagittal and coronal sutures have the greatest contributions to cranial growth, due to being present at the interface between the two tissue origins (neural crest and mesoderm) (Jiang et al., 2002). In contrast, the interfrontal and lambdoid sutures are not thought sit at an interface, but instead separate the neural crest derived frontal bones and the mesoderm derived parietal and interparietal bones, respectively. However, the origin of the lambdoid suture, like with many others, is unknown and therefore it is unclear if the lambdoid suture does sit at a neural crest-mesoderm interface (Lenton et al., 2005).

Following the appearance of a neural crest-mesoderm interface evident at E9.5 (Jiang et al., 2002), a cranial bone matrix is established at around E15 (Alberius and Friede, 1992). The cranial bones begin to grow and expand toward each other via both intramembranous and endochondral ossification, dependent on the bone. This process has been reported after 2 days of culture of E15.5 parietal bones and at E19 in the rat (Kim et al., 1998; Opperman, 2000). At this stage, each bone is widely separated by mesenchyme also referred to as the presumptive sutural matrix (Opperman et al., 1993; Opperman, 2000). Presumptive sutural matrix is formed at specific locales across the developing skull. For the coronal suture, as mentioned previously, this develops directly at the interface between neural crest and mesoderm (Jiang et al., 2002), whereas the other sutures of the cranial vault, form at anatomical landmarks of the underlying brain tissue. For example, the sagittal and interfrontal sutures develop at the midline between the cerebral hemispheres and olfactory lobes and the lambdoid suture develops between the cerebral hemispheres and the cerebellum (Morriss-Kay and Wilkie, 2005).

A significant part of suture development in the mouse occurs postnatally. After birth, the presumptive sutural matrix creating the gap between the approaching parietal bone fronts, at the location of the sagittal suture, distinctly reduces (P1) (Zimmermann et al., 1998). Within the mesenchyme of this presumptive sutural matrix the presence of blood vessels is evident. At this stage, a fibrous structure forms at the prospective mineralisation sites for the parietal bones. During the early stages of postnatal development of the suture, there is a clear a shift with the underlying mesenchyme forming fibrous connective tissue separating the bone margins (Markens, 1975; Zimmermann et al., 1998; Lenton et al., 2005). At P9 a homologous collagen matrix replaces the presumptive sutural matrix and forms a straight fibrous connective tissue by P14 (Zimmermann et al., 1998). The parietal bone plates surrounding the sagittal suture undergo a large thickening at the later stages of development (P14–20). As cranial expansion slows, at around P20 (P21 in the rat), following a reduction in the number of cells lining the bone fronts, the sutures become increasingly narrow to create mature sutures. At the mature suture, the previously approaching bones are connected by collagen fibrils of the fibrous connective tissue (Zimmermann et al., 1998; Opperman, 2000). The various sutures reach a matured state at different postnatal ages, variability is also observed across species. In the rat, as cranial expansion slows by P21, the coronal suture narrows to reach its fully formed developed state (Opperman et al., 1993). In the mouse, the sagittal suture forms by P20 and reaches maturity by P26–28 (Zimmermann et al., 1998). At these final stages of postnatal development, the collagen fibrils run continuously between the fibrous connective tissue of the suture into the bone to create a highly organised cross-striated bone structure (Zimmermann et al., 1998). As cranial expansion slows (P20–28) once the fibrous connective tissue of the sutures has formed, sutures become the primary site of craniofacial osteogenesis (Opperman, 2000; Luo et al., 2019). As the mature suture composition is similar across mammals (Pritchard et al., 1956; Persson et al., 1978; Bailleul and Horner, 2016), developmental information from the mouse is likely to be applicable across mammalian species and could result in similar suture functioning (Herrel et al., 2000; Moazen et al., 2009; Curtis et al., 2013; Goswami et al., 2013).

Once formed, the decision to keep a suture open (patent) or closed is essential for the coordinated growth of the cranial bones and brain. In the mouse, patency is seen throughout life for many sutures, including the sagittal, coronal and lambdoid sutures (Lenton et al., 2005). However, not all sutures remain

patent but instead undergo fusion in order to protect the developed brain. The only suture to undergo such fusion in the mouse is the interfrontal suture which fuses at around P7–12 (Bradley et al., 1996), occurring in the early stages of postnatal development prior to the point of sexual maturity. Across different species there appears to be a large degree of variation as to which sutures fuse and which remain patent (Rager et al., 2014). Interestingly, whilst the fusion of the interfrontal suture in mice is akin to that of humans, all other sutures in the human skull fuse in adulthood unlike the mouse (Weinzweig et al., 2003). Nevertheless, throughout the process of postnatal development sutures narrow, progressing from an open to near fused or fused status.

The commonality of suture fusion occurring in the late stages of postnatal skull development unites mammals and thus the mouse model in terms of their postnatal suture development (Rager et al., 2014; Esteve-Altava et al., 2020), and contrasts with some species of reptile where the sutures are thought to become increasingly patent across ontogeny (Bailleul et al., 2016). As suture patency is key to suture function, extending the life of an open suture would maintain the reservoir of mesenchymal stem cells at the suture enabling it to act as a site of bone growth, homeostasis, and repair for longer (Zhao et al., 2015), as well as providing shock absorption for longer across life (Moazen et al., 2009). Such functional roles are likely applicable across mammals, given that sutural stem cell populations necessary for interstitial cranial bone growth have been identified beyond mammalian species (Teng et al., 2018). Therefore, the transition of a suture from an open to a fused status, or vice versa, has the potential to impact the shape, size, and function of the associated cranial bones, which as a consequence could be a driver for evolutionary skull morphological change and variation across mammals.

WHAT CAN WE LEARN FROM A SUTURE?

Beyond their crucial roles during development and their functional importance, sutures are becoming increasingly powerful for understanding species ecology and life history across a number of vertebrates (**Figure 5**). As noted above, suture fusion and morphology are thought to respond to biomechanical stresses from the external environment, suggesting that sutural features and morphology may aid in the interpretation of functional pressures driving cranial form. The influence mechanical pressures have on shaping sutures, where external forces alter sutures from a butt joint morphology to a bevelled or finger joint or create a gross interdigitated morphology, means it may be possible, in the future, to interpret the diet, behaviour, ecology and mechanical stresses of an individual from the suture morphology (Moss, 1957; Oudhof, 1982; Kathe, 1999; Monteiro and Lessa, 2000; Clack, 2002; Nicolay and Vaders, 2006). As the complexity of mammal suture morphology is also thought to respond to biological pressures (Herring, 1972; Nicolay and Vaders, 2006), advances in morphometric techniques make it is possible to quantify and compare suture morphological complexity across a range of mammalian species (White et al., 2020). As such, we may be able to use suture morphology to better infer organismal biology and morphology alone. Current work has identified that harder diets and chisel-tooth digging of caviomorph rodents place greater demands on the sutures, thus increasing suture complexity (Buezas et al., 2017). In the rodents shown in **Figure 3**, the most complex suture is observed in *Cricetomys gambianus* (Gambian pouched rat). The differences seen here in suture complexity are likely to be due, in part, to the differences in muscle mass at the jaw joint in the different species, with larger muscles producing a higher bite force and in turn generating an increasingly complex suture morphology (Byron et al., 2004). Interestingly, the connective tissue within the mammalian sutural joint itself is also known to respond to biomechanical pressures, suggesting that the micro-scale morphology could similarly be used to shed light on localised functional pressures (Byron et al., 2004).

Suture closure patterns in addition to suture morphology, at all scales (macro/meso/micro), could similarly be used to understand external stresses acting on a species. Suture closure patterns have been reported to indicate locomotory strategies in several species of Hystricognathi rodents (Wilson and Sánchez-Villagra, 2009). Species of Hystricognathi rodents that presented with the highest level of overall suture closure did not follow the pattern of closure proposed by Krogman (1930) which is considered to be generally applicable to mammals (Chopra, 1957). The Krogman pattern of suture closure is as follows: vault, base, circum-meatal, palatal, facial, and cranio-facial. It is these species of Hystricognathi, deviating from the Krogman pattern of suture closure and exhibiting a greater level of suture closure, that displayed different locomotory patterns: subterranean (*Bathyergus suillus* and *Nannospalax ehrenbergi*) and arboreal (*Coendou spinosus*, *Coendou insidiosus*, and *Coendou prehensilis*). Suture fusion and morphological complexity appear to provide useful tools for interpreting external pressures, as a result of distortion occurring at the suture to such stresses.

Aside from the ability to shed light on external stresses, sutures can prove useful in understanding developmental timings, growth, ontogeny, and even be used to inform forensic and archaeological dating. During human childhood development, suture development and fusion status are used to follow development and growth (Goyal, 2020). Therefore, an in depth understanding of sutures would further assist in the medical ability to monitor normal cranial development. Sutures can also offer insights into growth rates and craniofacial growth patterns. Bone overlapping occurring within the cross-sectional plane of a suture has been reported to be associated with the growth rate of an individual, using the rat as a developmental model here, with overlapping bones reflecting periods of fast growth (Koskinen et al., 1976). Similarly, in Dinosauria, sutures can provide information about ontogeny, whereby fusion status is considered to be a good proxy for age (Sampson et al., 1997; Fujiwara and Takakuwa, 2011; Longrich and Field, 2012). Additionally, within the fields of archaeology and forensics, suture closure timings have been proposed as a viable option for determining age in humans (Key et al, 1994; Vodanović et al, 2011; Wood, 2015; Ubelaker and Khosrowshahi, 2019). Not only do multiple parameters pertaining to sutures have the capability

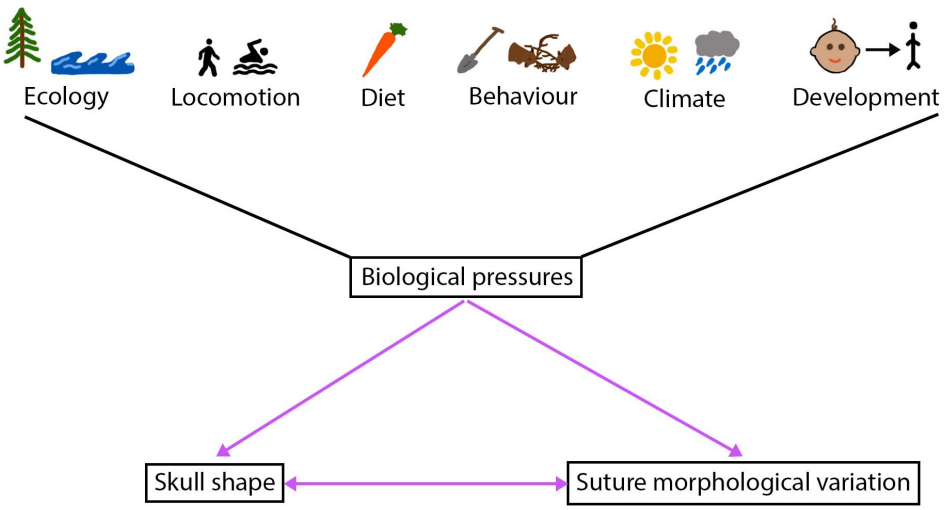

FIGURE 5 | The intertwined relationship between the cranial sutures and skull, a number of biological pressures shape this relationship.

of providing useful information and shedding light on the fields of evolutionary and developmental biology, but the possibilities extend far beyond these disciplines.

SUTURES AS TARGETS FOR EVOLUTIONARY CHANGE IN SKULL MORPHOLOGY

An abundance of information can evidently be taken from the morphology, complexity, fusion pattern, and development of sutures, without beginning to consider the impact such suture parameters have on mature cranial morphology. Nevertheless, suture functioning, development and fusion timing have been highlighted as crucial for supporting normal skull functioning, suggesting a key link between sutures and the skull, as discussed previously. This interdependence is further evidenced by alterations to suture fusion, morphology, and development which cause knock-on changes affecting the cranial form, thus pointing toward an integrated evolution of sutures and craniofacial morphology. Such a relationship, between sutures and skull form, can be explored across several scientific fields on multiple levels, from pathologies, to mouse model systems, to natural variation.

Given the importance sutures have in maintaining the normal development of craniofacial form, many questions arise surrounding what impact the timing, activity, and development of sutures has on mature skull morphology. Evidence from pathology is instrumental in untangling this relationship between sutures and skull shape, as abnormal suture development is often coupled with alterations to the craniofacial morphology. Premature suture fusion is known to result in craniofacial developmental defects, such as craniosynostosis; here, the cranial morphology is distorted in response to early suture fusion (Lenton et al., 2005; Flaherty et al., 2016). More specifically, suture fusion characterised by craniosynostosis causes an excessive cranial bone growth in the parallel axis and prevents expansion in the perpendicular axis, referred to as Virchow's concept (Virchow, 1851; Delashaw et al., 1999). Consequently, premature sagittal suture fusion produces a long and narrow skull morphology (scaphocephaly), whereas premature coronal suture fusion results in a broad and short cranial morphology (brachycephaly).

Interestingly, finite element analysis has been found to predict skull form following cranial reconstruction of clinically observed craniosynostosis (Malde et al., 2020). This modelling approach has huge implications for understanding craniofacial reconstruction techniques and thus for enhancing clinical remodelling surgery of craniosynostosis patients. Moreover, predictions based on Virchow's theory on suture fusion patterns and advances in modelling approaches could be used to understand patterns of cranial bone growth across ontogeny and possibly predict the mature craniofacial morphology across taxa (**Figure 6**). This relationship between suture closure and skull morphology becomes increasing complex when multiple suture synostoses are involved. Similarly, abnormal growth of the skull occurs in response to premature fusion of multiple sutures, although growth is stimulated and restricted in a multitude of directions. The skull is instead distorted into a trilobed structure with the overall dysmorphology referred to as the cloverleaf skull or Kleeblattschädel-deformity syndrome (Angle et al., 1967), with the coronal and lambdoid as the most common combination of sutures to fuse (Manjila et al., 2010). It appears evident that the abnormal pattern of suture development and fusion is responsible for encouraging growth in various planes, ultimately warping the skull morphology in a predictable manner based on the location and timing of suture fusion (**Figure 6**). In humans, not only could suture fusion patterns prove informative in predicting adult cranial morphology, but so too could suture complexity, with a greater complexity in the sagittal suture associated with an altered cranial morphology (lower and broader skull) (Skrzat et al., 2004).

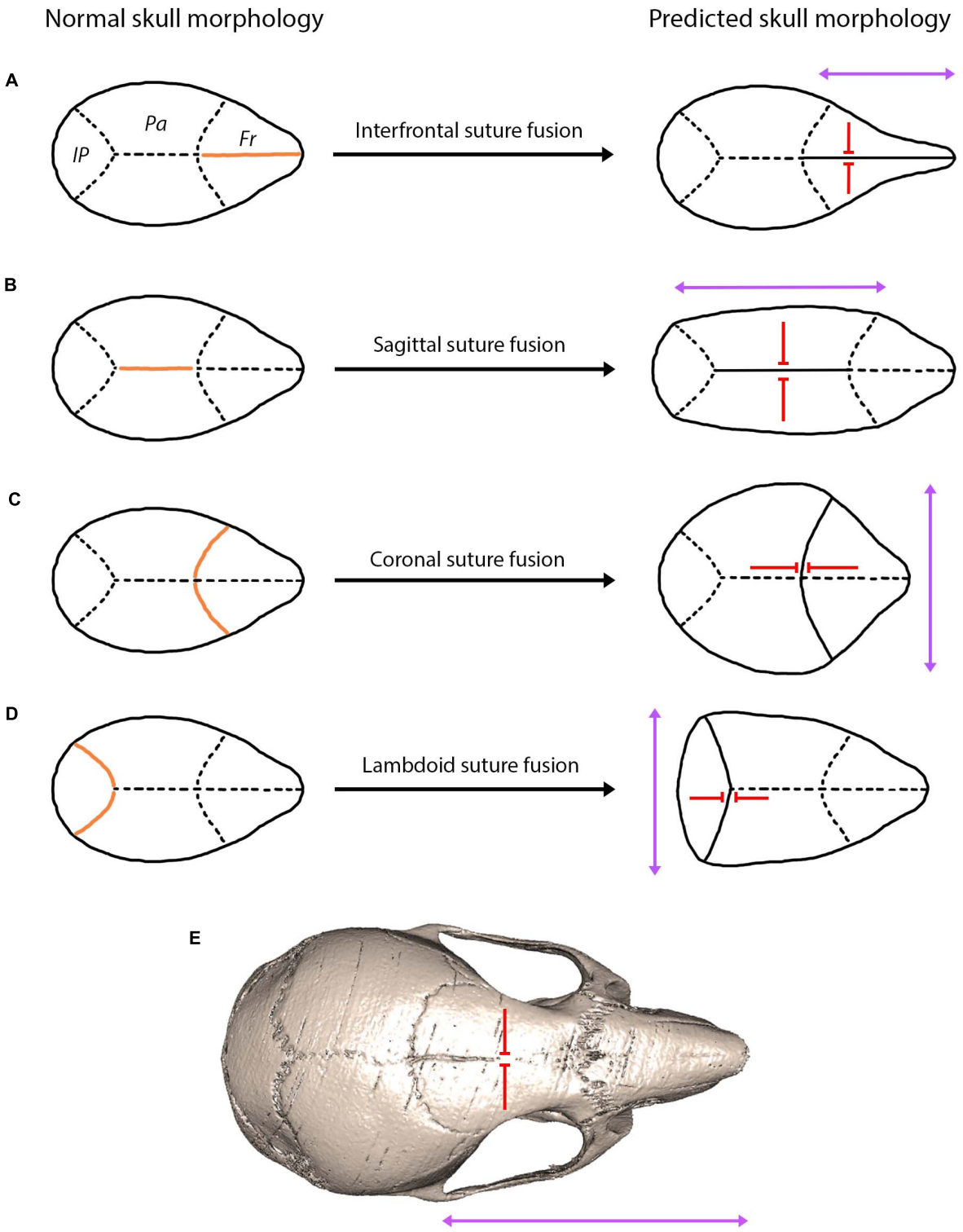

FIGURE 6 | A hypothesis showing the predicted skull morphology following suture fusion, based on the concept of growth occurring in the parallel axis to the fused suture with prevention of growth in the perpendicular axis (Virchow, 1851; Delashaw et al., 1999). Orange indicates the fused suture location, purple arrows indicate the direction of growth, red arrows indicate the direction growth is restricted: **(A)** fusion of the interfrontal suture produces a narrow and elongated skull in the facial region; **(B)** fusion of the sagittal suture produces a narrow and elongated skull in the cranial vault region; **(C)** fusion of the coronal suture produces a shorter and widened cranial vault; **(D)** fusion of the lambdoid suture produces a shorted and widened posterior cranial vault; **(E)** fusion of the interfrontal suture in the mouse using microCT indicates a narrow and elongated facial region similar to the prediction of **(A)**.

The link between suture closure and overall skull morphology is also highlighted in the field of developmental biology, through the use of mouse mutants where the pattern of suture patency can be disrupted by manipulating transcription factors and signalling pathways (Grova et al., 2012). Alterations to the developmental pathways result in abnormalities in suture fusion timing and drive a number of craniofacial dysmorphologies. A number of mouse models have been established for many of the craniosynostosis syndromes, allowing for an assessment of the interaction between suture fusion and skull morphology (Cornille et al., 2019; Lee et al., 2019). Mutations of the TWIST gene in heterozygous Twist (+/−) mouse mutants, result in premature fusion and an altered overall skull shape reflecting that of Saethre-Chotzen syndrome (el Ghouzzi et al., 1997). More specifically, haploinsufficiency of Twist1, using Twist1 (+/−) mouse mutants, results in coronal synostosis and in turn a widened skull in the left-right lateral direction with a shortening in its anterior-posterior length, similarly reflecting the phenotype of Saethre-Chotzen syndrome (Behr et al., 2011). Given the interaction between Twist and FGF, it is perhaps unsurprising that Ser250Trp substitutions in Fgfr2 using mouse mutant Fgfr2 (250/+) also lead to premature suture fusion (Chen et al., 2003). In the case of the Fgfr2 (250/+) mouse mutant, premature fusion of the coronal suture produces a phenotype mimicking that of Apert syndrome; where a dome-shaped skull morphology and significantly shortened skull in the anterior-posterior axis are observed (Chen et al., 2003). Resultant abnormalities in cranial morphology arising from alterations in suture fusion timings can severely impair craniofacial functioning, as well as creating physiological changes. As in patients with craniosynostosis, the mouse mutants highlight how premature suture fusion can influence the shape of the mature cranial morphology (**Figure 6**). However, a reduction or to delay in the suture fusion also plays a key role in shaping the skull. In the case of the OPG KO mouse model, an OPG deficiency created a reduced fusion of the interfrontal suture which was coupled with a shortened skull morphology in the anterior-posterior direction (brachycephaly) (Beederman et al., 2015). Evidence from mouse models suggests that sutures, irrespective of the closure status, can serve as targets for developmental changes that affect the overall cranial morphology.

Evidence from pathology and mouse mutants suggest that alterations to suture fusion and morphology have clear implications on the overall cranial morphology. With regard to natural variation, there is much less existing evidence linking the two together. Most papers focussing on sutures to date consider how patterns of suture closure are driven by mechanical and ecological factors across the major clades of animals (Kathe, 1999; Nicolay and Vaders, 2006; Bärmann and Sánchez-Villagra, 2012; Goswami et al., 2013), rather than addressing and considering what consequence suture closure patterns might have on skull shape. For example, in mammals, early fusion of facial sutures in *Pecari* species strengthens the facial region to aid feeding (Bärmann and Sánchez-Villagra, 2012). Such cranial demand and functioning vary across different clades which, in turn, are associated with differing patterns of suture fusion. An interesting example of this adaptive variation can be seen between birds and mammals. Cranial ossification in birds occurs relatively late, after which time the sutures fuse to protect the developed brain. Whereas, in mammals brain growth is extended across many years, in particular in larger mammals, and suture fusion occurs at a later stage in order to support the extended brain maturation period (Morriss-Kay, 2001).

Aside from reports of suture fusion timing involved in supporting cranial functioning, some evidence does exist to support a relationship between suture fusion and morphology, and the overall cranial morphology, across species. In species of *Pecari* (Artiodactyla), suture closure was found to correlate with adult cranial proportions, thus suggesting suture fusion creates a knock-on cranial shape change (Herring, 1974). The early fusing premaxillo-maxillary suture, in peccaries, is associated with a significant increase in palatal length. With the fusion of the middle intermaxillary suture, the palatal width increases in the molar region. This suture fusion and skull growth pattern continues to be the case for other cranial width measurements (distance between supraorbital foramina, anterior nasal width, vault width). Interestingly, this pattern of significant growth subsequent to suture fusion appears to be the case for skull width parameters, rather than skull length parameters, which instead remained largely stable (Herring, 1974). Focussing on mammals, an association between the degree of suture closure level and skull length has been identified within several species of hystricognathous rodents, with suture closure level negatively correlated to cranial length (Wilson and Sánchez-Villagra, 2009). However, it is common for papers to group together the level of suture closure across all suture sites within one specimen, by providing a score for the percentage of average sutural closure per specimen, thus calculating the influence of this average suture closure level on the overall cranial size (Wilson and Sánchez-Villagra, 2009). Grouping the sutures together in this manner to provide an average closure score, is likely to be less informative than considering specific correlations between suture closure and cranial growth patterns. This perhaps explains why the relationship between suture fusion and cranial growth remains so complex with no clear correlation identified (Herring, 1974).

An interesting case study of how suture morphology has helped to shape cranial morphology across evolutionary time, can be observed in Cetacea. Some of the greatest morphological changes in response to the environment observed in any mammalian skull are that of Cetacea. Evolution of telescoping and asymmetry within the cetacean skull have, respectively, facilitated breathing and echolocation enabling cetacean species to thrive within aquatic environments (Miller, 1923; Huggenberger et al., 2017). Telescoping is seen in both odontocetes (toothed whales) and mysticetes (baleen whales), although differs slightly between the clades (Miller, 1923). The phenomenon refers to a shift in the nasal position from the tip of the snout in ancient whales to the top of the head in modern whales. In odontocetes, this involved a posterior displacement and expansion of the premaxilla and maxilla, with extensive overlapping of the maxilla and frontal bones. These extreme changes in cranial morphology are thought to have occurred rapidly during the Oligocene (34–23 Ma) diversification of the modern clades of cetaceans (Churchill et al., 2018;

Coombs et al., 2020). During this period of rapid cranial shape change, overlapping at the sutures is thought to have played a central role, which has ultimately altered contact relationships in cetacean cranial bone morphology (Roston and Roth, 2019). In the telescoped areas, sutures are transformed to extreme morphologies; the overlapping bones mean that sutures must span large regions producing an extensive joining surface, also termed "horizontal sutures" (Gatesy et al., 2013). Many questions around telescoping still go unresolved, although it is thought the answers might lie with the sutures, thus stressing the importance of suture morphological changes in craniofacial evolution and development (Roston and Roth, 2019).

It is clear that there is an incredible amount of natural variation across both suture and skull morphology. Even within a single species, changes in cranial morphology can occur across a single year creating seasonal variability in cranial morphology, as reported in the common shrew and least weasels (Pucek, 1963; Dechmann et al., 2017). It is possible suture morphology could also exhibit seasonal fluctuations in-keeping with the cranial adaptations, particularly as sutures are thought to display plasticity to the environment (Roston and Roth, 2019). It has been suggested that cranial morphological changes occurring over evolutionary time could be coupled with alterations in gross suture morphology (Richtsmeier et al., 2006). From a wider evolutionary perspective, finite element analysis (FEA) has shown that sutures have a functional role in responding to and altering strain distribution across lizard skulls (Moazen et al., 2009; Jones et al., 2017). This points toward an ability for sutures to work collectively in adapting to and maintaining a threshold level of strain for bone maintenance across the skull, which in turn may impact the gross suture morphology. Within mammals, there is also a tremendous amount of interspecific variation in both the timing of suture fusion (Wilson and Sánchez-Villagra, 2009; Rager et al., 2014; del Castillo et al., 2015) and suture morphology (Byron, 2009; Buezas et al., 2017). Variation in the timing of suture fusion has been attributed to differing functional pressures and heterochrony (Wilson and Sánchez-Villagra, 2009; Goswami et al., 2013). Given the importance of suture fusion timing in determining craniofacial morphology in pathology and mouse mutants, suture fusion appears to be equally as important as suture morphology in shaping the mammalian skull morphological variation.

Previous work has identified a possible link between craniosynostosis and mammal skull morphological variation (Richtsmeier et al., 2006; Esteve-Altava and Rasskin-Gutman, 2015). As premature suture fusion is hypothesised to be a direct cause of craniosynostosis and, as such, cause modifications to the skull morphology, it is possible that craniosynostosis could act as model for mammal skull evolution (Richtsmeier et al., 2006). Anatomical network models analysing integration and modular organisation of the skull have since shown that craniosynostosis could offer developmental explanations for how changes in suture fusion could occur at a macroevolutionary scale (Esteve-Altava and Rasskin-Gutman, 2015). It has further been suggested that bone loss resulting in higher cranial complexity during development could translate to processes shaping the morphological evolution of the skull (Esteve-Altava et al., 2013). Such losses and bone fusions are thought to impact the skull morphology differently depending on the cranial bones targeted during developmental losses (Esteve-Altava et al., 2014). Within the specific system of mammals, it has been suggested that suture fusion, rather than bone loss, could be the dominant process driving the reduction of cranial bones through the evolutionary history of synapsids (including mammals and their ancestors), a trend referred to as Williston's law (Gregory et al., 1935; Sidor, 2001; Richtsmeier et al., 2006). This hypothesis requires further testing, although it is clear from multiple sources of evidence, including pathology, mouse mutants and evolutionary trends, that sutures play a key role in the development and evolution of the mature cranial morphology in mammals.

POSSIBLE MECHANISMS FOR EVOLUTIONARY CHANGE

The craniofacial variation observed across mammals could arise from evolutionary mechanisms acting on a number of signalling pathways that alter the development and fate of sutures. Multiple signalling pathways could be the target of evolutionary change, such as those which have been identified from multiple mouse models of craniosynostosis (Richtsmeier et al., 2006). During embryonic development, as the initial cranial bones expand and approach each other, it is thought that a gradient of signalling factors is created across the bones, leading to the initial formation of the presumptive sutural matrix (Opperman et al., 1993). However, it is unclear as to which signalling factors are responsible for this formation. Stabilisation of this newly formed presumptive suture is provided by signalling from the dura mater (Opperman et al., 1993). In the absence of a dura mater, sutures continue to form, suggesting that the initiation of suture formation occurs irrespective of dura mater signalling and thus signalling produced at the expanding bone fronts would be necessary for suture formation. This certainly seems to be the case for the sutures formed at anatomical landmarks of the underlying brain tissue (sagittal, interfrontal, and lambdoid). However, in the instance of the coronal suture which forms at the interface of mesoderm and neural crest derived cells, the transcription factor engrailed 1 (En1) is thought to regulate the neural crest and mesodermal cell movements, thus determining the position of the neural crest-mesoderm boundary, which is in turn required for the formation of the coronal suture (Deckelbaum et al., 2012). Moreover, Twist expression during embryonic development also seems to be necessary for the initiation and formation of the coronal suture (Johnson et al., 2000). At the point of appearance of the presumptive suture matrix, a number of growth and transcription factors are known to be present at the suture locale (presumptive suture matrix, underlying dura mater, and approaching bone fronts) including BMP-4, BMP-7, FGF-9 (growth factors), MSX1 and MSX2, and TWIST (transcription factors) (Opperman, 2000). Looking specifically at the Twist pathway, $Twist1^{+/-}$ mouse mutants, produce a reduction in the number of Gli1+ progenitor cells, suggesting there is a crucial link between the TWIST

transcription factor and the ability for the suture to act as a site of cranial bone growth (Zhao et al., 2015). As Gli1+ cells are one of the major mesenchymal stem cell populations within the suture mesenchyme that contribute to cranial bone growth, as with the mouse mutants, alterations to the Twist signalling pathway over evolution could have acted to generate craniofacial variation.

Similarly, to suture development, a number of signalling pathways are involved in determining the fate of suture fusion status (patent or fused). Given the significance of these signalling pathways associated with suture fusion status dictating the mature cranial morphology in pathology (craniosynostosis) and mouse models (Grova et al., 2012), such signalling pathways associated with are also likely to be key evolutionary targets for craniofacial morphological change. Sutural-dural interactions have been shown to be required for the maintenance of suture patency throughout postnatal development (Opperman et al., 1993; Roth et al., 1996). Absence of a dura mater instead favours cell proliferation and synthesis of a collagenous extracellular matrix responsible for premature osseous obliteration of the sutures (Opperman et al., 1998). The influence the dura mater has on the maintenance of suture patency and the determination of suture fusion timing is thought to be the result of a number of mediatory signalling factors rather the direct sutural-dural cell interactions (Opperman et al., 1995). Such signalling factors are later dominated by those from the osteogenic fronts (Kim et al., 1998). Variation in the absence or presence of signalling for a number of different factors including TGF-β, FGF, Twist, BMP, noggin, and Wnt collectively determine suture fate. To some extent, fusion of the interfrontal suture is determined by the presence of transforming growth factor (TGF)-β, whereas its absence prevents fusion from occurring (Mehrara et al., 2002). Fibroblast growth factor (FGF) signalling (Fgf1, Fgf2, Fgf3, Fgf4, Fgf9, and Fgf18) is not only necessary for the normal fusion of sutures but is also largely involved in premature suture fusion identified in craniosynostosis syndromes (Carlton et al., 1998; Rice et al., 1998; Greenwald et al., 2001; Lenton et al., 2005). A relationship between FGF and Twist signalling exists, whereby disruption of their interaction can lead to premature suture fusion (Rice et al., 2000). Overexpression of the transcription factor Msx2 enhances osteoblast differentiation thus leading again to premature suture fusion (Liu et al., 1999). Similarly, to TGF-β, bone morphogenetic protein (BMP) favours osteogenesis and thus its presence leads to the osseous obliteration of sutures (Warren et al., 2003). As the activity of BMP is controlled by noggin, whereby noggin activation inhibits BMP signalling, BMP can also be present in patent sutures as well as obliterated sutures. In contrast, the continuous activity of the canonical Wnt pathway is associated with maintaining patent sutures and its inhibition responsible for ossification and suture fusion (Behr et al., 2010, 2011). Differential modulation of this canonical Wnt pathway is thought to be responsible for the different fates of the interfrontal and sagittal sutures in the mouse (Behr et al., 2010). The ultimate fate of sutures is underpinned by the complex interaction of signalling factors released from various sites across the suture locale. Evolutionary interruption of such pathways could result in osseous obliteration of the suture in turn affecting suture function and the potential for cranial bone growth.

The patency and osseous obliteration of a suture is largely controlled by the bone remodelling activity of osteoclasts and osteoblasts. A balance between these bone remodelling cells (osteoclasts and osteoblasts) is required for suture homeostasis and the maintenance of a patent suture (Beederman et al., 2015). Given the role of osteoclasts and osteoblasts in determining suture fusion status in mammals, they have a crucial role in regulating the cranial bone growth capacity at the suture. Many of the signalling pathways discussed above for premature suture fusion, directly impact the balance between osteoblasts and osteoclasts, thus influencing the level of osteogenesis. As the bone forming cells, increased osteoblast activity has often been associated with a premature suture fusion whereby an increase in bone formation is observed at the fused suture (De Pollack et al., 1996). Alterations to a number of signalling factors are known to create perturbations to the bone remodelling process and have since been discovered to lead to changes in suture fusion status. FGF signalling is associated with osteoblast differentiation, if disrupted this is one of the critical pathways known to cause premature suture fusion (Rice et al., 2003). Perturbations in the RANK/RANKL/OPG pathway, which is associated with both osteoblast and osteoclast activity, have more recently been linked to alterations in cranial suture fusion, implying that osteoclasts may also play a critical role at the suture locale (Lee et al., 2011; Beederman et al., 2015). Osteoclast differentiation and activation through the RANK/RANKL interaction maintains suture patency (Lee et al., 2011). Osteoprotegerin (OPG) acts to block this interaction to instead favour osteoblast activity. Therefore, when OPG deficiency occurs, which supports osteoclast differentiation via RANK/RANKL signalling, suture patency is maintained (Beederman et al., 2015). Defects in osteoclast differentiation unsurprisingly are related to premature fusion (Kawata et al., 1998), which have been associated with a downregulation of RANK. In contrast, the presence of RANK appears to be key for the maintenance of suture patency, suggesting a correlation between RANK presence/absence and suture status (Lee et al., 2011). Suture fusion status is therefore unsurprisingly influenced by perturbations in the balance between bone forming osteoblasts and bone resorbing osteoclasts. The extent to which this perturbation impacts skull morphology could be largely dependent upon the timing at which sutural osseous obliteration occurs during ontogeny.

Homeostasis at the suture itself requires a complex interplay between osteoblasts and osteoclasts. We currently have very limited knowledge on this interaction at the suture locale compared to osteoblast and osteoclast involvement in bone homeostasis. Nevertheless, MSCs are thought to have a complex role in mediating the osteoblast-osteoclast interaction within the cranial suture (Guo et al., 2018), given the appropriate signalling MSCs undergo a transition toward an osteoblast fate, a transition that is reliant upon BMP-IHH signalling (Beederman et al., 2013; Guo et al., 2018). It is unsurprising, therefore, that BMP is also found at the fused suture locale given it favours the formation of bone forming cells (osteoblast) (Warren et al., 2003). As the

balance between the proliferation of osteoblast precursors and osteogenic differentiation is mediated at the suture, the bone remodelling process has a key involvement in the maintenance of suture patency, enabling the sutures themselves to serve as major signalling centres (Iseki et al., 1997; Zhou et al., 2000). This regulatory function, dictated by suture development and signalling pathways, allows the sutures to function as primary growth centres for the craniofacial bones (Opperman, 2000). Therefore, understanding normal suture development is key to understanding how large scale craniofacial morphological change could occur. Beyond the role of suture fusion, osteoclasts are also thought to be involved in the production of a waveform suture pattern, specifically the osteoclasts that have been identified at the approaching bone fronts (Byron, 2006). As is clear from evolutionary evidence in Cetacea (Roston and Roth, 2019) and from suture morphological diversity across mammals (Byron, 2009; Buezas et al., 2017), suture morphology appears to play a key role in shaping the evolutionary diversity of cranial morphology across mammals. Therefore, it is also possible that this suture morphological variation is controlled on the cellular scale, and thus could be adjusted through the signalling pathways mediating osteoclast activity to produce large scale craniofacial diversity.

It could be hypothesised that the large scale cranial morphological disparity observed across mammals (Goswami, 2006; Koyabu et al., 2014; Usui and Tokita, 2018) is shaped to some degree by the sutural variation, in terms of suture fusion status, developmental processes, and morphology. This variation could result from evolutionary alterations to signalling pathways which underlie suture development and fusion. Such a hypothesis appears to be largely supported by the evidence presented through pathology, mouse mutant models, and natural variation. Nevertheless, much work remains to fully understand the integrated evolution of craniofacial morphology and the adaptive landscape of suture morphology. A greater understanding of this relationship may also aid with future inference of species ecology and life history from suture morphology, fusion, and development and skull form (**Figure 5**).

CONCLUSIONS

An overwhelming body of research conducted within the fields of development and evolution focusses on the morphology of the skull, including individual skull bones or regions. In contrast, less attention is given to the fibrous sutural joints separating the cranial bones. In light of the ever advancing imaging and geometric morphometric techniques available in the evolutionary developmental biologist's toolkit, it is becoming increasingly possible to quantitatively and comparatively study sutures to address many of the outstanding questions regarding suture development, morphology, evolution, and importance. Suture development is critical for the normal development of the skull through the provision of interstitial bone growth sites, supporting homeostasis and facilitating repair. Synchronisation in developmental timing between suture formation and cranial bone tissue growth enables a coordinated expansion of the skull and brain. Functionally, sutures support feeding, provide shock absorption during locomotion, and accommodate brain growth. Thus, suture development and skull function are closely intertwined.

In this review, we highlight the importance of sutures, from a number of perspectives, such as morphology, complexity, fusion, and development, in not only supporting the overall functioning of the skull but also in shaping its mature morphology. Evidence from pathology, mutant mouse models, and natural variation, suggests that sutures may act as targets for change in craniofacial morphology, which likely contributes to some of the cranial variation observed across mammals and other vertebrates. While the vast majority of previous work on skull evolution almost entirely overlooks suture morphology and fusion, this review highlights the importance of studying suture morphology and fusion in parallel to skull morphology. As a result, it becomes increasingly important to rethink traditional evolutionary developmental biology questions which consider the skull in isolation. Future work integrating suture development into a comparative evolutionary framework will be instrumental in understanding how developmental mechanisms shaping suture morphology ultimately influences craniofacial form. As critical structures for skull development, function, and morphology, sutures are central to reconstructing the evolution of cranial diversity, but at present, are sorely understudied in evolutionary and developmental biology.

AUTHOR CONTRIBUTIONS

HW, AG, and AT designed the outline and aims for the review. HW performed the research necessary for the review and wrote the first draft of the manuscript. AG and AT provided insightful discussion, ideas, and guidance for additional research to produce the final manuscript, as well as contributed to the writing and reading of the final version. All authors approved the final version.

FUNDING

HW was supported by the Biotechnology and Biosciences Research Council through the London Interdisciplinary Doctoral Training Programme (BBSRC LIDo DTP) (grant no. BB/M009513/1). AT was supported by a Wellcome Trust Investigator Awards (102889/Z/13/Z). AG was supported by the European Research Council grant no. STG-2014–637171.

ACKNOWLEDGMENTS

We would like to thank the members of both the Goswami and Tucker labs for their interesting discussions at lab meetings, which have helped to shape this literature review. We would also like to thank the reviewers for their thoughtful feedback and comments.

REFERENCES

Alberius, P., and Friede, H. (1992). "Skull growth," in *Bone*, ed. B. K. Hall (Boca Raton, FL: CRC Press), 129–155.

Allen, E. G. (2006). New approaches to Fourier analysis of ammonoid sutures and other complex, open curves. *Paleobiology* 32, 299–315.

Angle, C. R., McIntire, M. S., and Moore, R. C. (1967). Cloverleaf Skull: kleeblattschädel-Deformity Syndrome. *Am. J. Dis. Child* 114, 198–202. doi: 10.1001/archpedi.1967.02090230128018

Arbour, J. H., Curtis, A. A., and Santana, S. E. (2019). Signatures of echolocation and dietary ecology in the adaptive evolution of skull shape in bats. *Nat. Commun.* 10:2036. doi: 10.1038/s41467-019-09951-y

Baer, M. J. (1954). Patterns of growth of the skull as revealed by vital staining. *Hum. Biol.* 26, 80–126.

Bailleul, A. M., and Horner, J. R. (2016). Comparative histology of some craniofacial sutures and skull-base synchondroses in non-avian dinosaurs and their extant phylogenetic bracket. *J. Anat.* 229, 252–285. doi: 10.1111/joa.12471

Bailleul, A. M., Scannella, J. B., Horner, J. R., and Evans, D. C. (2016). Fusion patterns in the skulls of modern archosaurs reveal that sutures are ambiguous maturity indicators for the Dinosauria. *PLoS One* 11:e0147687. doi: 10.1371/journal.pone.0147687

Bardua, C., Wilkinson, M., Gower, D. J., Sherratt, E., and Goswami, A. (2019). Morphological evolution and modularity of the caecilian skull. *BMC Evol. Biol.* 19:30. doi: 10.1186/s12862-018-1342-7

Bärmann, E. V., and Sánchez-Villagra, M. R. (2012). A phylogenetic study of late growth events in a mammalian evolutionary radiation: the cranial sutures of terrestrial artiodactyl mammals. *J. Mammal. Evol.* 19, 43–56. doi: 10.1007/s10914-011-9176-8

Beederman, M., Kim, S. H., Rogers, M. R., Lyon, S. M., He, T.-C., and Reid, R. R. (2015). OPG deficiency results in disruption of posterofrontal suture closure in mice: Implications in nonsyndromic craniosynostosis. *Plast. Reconstr. Surg.* 135, 990e–999e. doi: 10.1097/PRS.0000000000001284

Beederman, M., Lamplot, J. D., Nan, G., Wang, J., Liu, X., Yin, L., et al. (2013). BMP signaling in mesenchymal stem cell differentiation and bone formation. *J. Biomed. Sci. Eng.* 6, 32–52. doi: 10.4236/jbise.2013.68A1004

Behr, B., Longaker, M. T., and Quarto, N. (2010). Differential activation of canonical Wnt signaling determines cranial sutures fate: a novel mechanism for sagittal suture craniosynostosis. *Dev. Biol.* 344, 922–940. doi: 10.1016/j.ydbio.2010.06.009

Behr, B., Longaker, M. T., and Quarto, N. (2011). Craniosynostosis of coronal suture in twist1 mice occurs through endochondral ossification recapitulating the physiological closure of posterior frontal suture. *Front. Physiol.* 2:37. doi: 10.3389/fphys.2011.00037

Bradley, J. P., Levine, J. P., Blewett, C., Krummel, T., McCarthy, J. G., and Longaker, M. T. (1996). Studies in cranial suture biology: *in vitro* cranial suture fusion. *Cleft Palate Craniofac. J.* 33, 150–156. doi: 10.1597/1545-1569_1996_033_0150_sicsbv_2.3.co_2

Bruner, E. (2007). Cranial shape and size variation in human evolution: structural and functional perspectives. *Childs Nerv. Syst.* 23, 1357–1365. doi: 10.1007/s00381-007-0434-2

Brusatte, S. L., Sakamoto, M., Montanari, S., and Harcourt Smith, W. E. H. (2011). The evolution of cranial form and function in theropod dinosaurs: insights from geometric morphometrics. *J. Evol. Biol.* 25, 365–377. doi: 10.1111/j.1420-9101.2011.02427.x

Bryant, W. (1932). Lower devonian fishes of bear tooth butte, wyoming. *Proc. Am. Philos. Soc.* 71, 225–254.

Buezas, G., Becerra, F., and Vassallo, A. (2017). Cranial suture complexity in caviomorph rodents (Rodentia; Ctenohystrica). *J. Morphol.* 278, 1125–1136. doi: 10.1002/jmor.20699

Byron, C. D. (2006). Role of the osteoclast in cranial suture waveform patterning. *Anat. Rec. A Discov. Mol. Cell Evol. Biol.* 288, 552–563.

Byron, C. D. (2009). Cranial suture morphology and its relationship to diet in Cebus. *J. Hum. Evol.* 57, 649–655. doi: 10.1016/j.jhevol.2008.11.006

Byron, C. D., Borke, J., Yu, J., Pashley, D., Wingard, C. J., and Hamrick, M. (2004). Effects of increased muscle mass on mouse sagittal suture morphology and mechanics. *Anat. Rec. A Discov. Mol. Cell Evol. Biol.* 279A, 676–684. doi: 10.1002/ar.a.20055

Canfield, D. J., and Anstey, R. L. (1981). Harmonic analysis of cephalopod suture patterns. *Math. Geosci.* 13, 23–35. doi: 10.1007/BF01032007

Carlton, M. B., Colledge, W. H., and Evans, M. J. (1998). Crouzon-like craniofacial dysmorphology in the mouse is caused by an insertional mutation at the Fgf3/Fgf4 locus. *Dev. Dyn.* 212, 242–249. doi: 10.1002/(SICI)1097-0177(199806)212:2<242::AID-AJA8<3.0.CO;2-H

Cendekiawan, T., Wong, R. W. K., and Rabie, A. B. M. (2010). Relationships between cranial base synchondroses and craniofacial development: a review. *Open Anat. J.* 2, 67–75.

Chai, Y., Jiang, X., Ito, Y., Bringas, P. Jr., Han, J., Rowitch, D. H., et al. (2000). Fate of the mammalian cranial neural crest during tooth and mandibular morphogenesis. *Development* 127, 1671–1679.

Chen, L., Li, D., Li, C., Engel, A., and Deng, C.-X. (2003). A Ser252Trp [corrected] substitution in mouse fibroblast growth factor receptor 2 (Fgfr2) results in craniosynostosis. *Bone* 33, 169–178. doi: 10.1016/s8756-3282(03)00222-9

Chopra, S. R. K. (1957). The cranial suture closure in monkeys. *Proc. Zool. Soc. Lond.* 128, 67–112. doi: 10.1111/j.1096-3642.1957.tb00257.x

Churchill, M., Geisler, J., Beatty, B., and Goswami, A. (2018). Evolution of cranial telescoping in echolocating whales (Cetacea: Odontoceti), evolution. *Soc. Stud. Evol.* 72, 1092–1108. doi: 10.1111/evo.13480

Clack, J. A. (2002). The dermal skull roof of *Acanthostega gunnari*, an early tetrapod from the Late Devonian. *Trans. R. Soc. Edinb. Earth Sci.* 93, 17–33. doi: 10.1017/S0263593300000304

Coombs, E. J., Clavel, J., Park, T., Churchill, M., and Goswami, A. (2020). Wonky whales: the evolution of cranial asymmetry in cetaceans. *BMC Evol. Biol.* 18:86. doi: 10.1186/s12915-020-00805-4

Cornelissen, M., den Ottelander, B., Rizopoulos, B., van der Hulst, R., van der Molen, A. M., van der Horst, C., et al. (2016). Increase of prevalence of craniosynostosis. *J. Oral Maxilllofac. Surg.* 44, 1273–1279. doi: 10.1016/j.jcms.2016.07.007

Cornille, M., Dambroise, E., Komla-Ebri, D., Kaci, N., Biosse-Duplan, M., Di Rocco, F., et al. (2019). Animal models of craniosynostosis. *Neurochirurgie* 65, 202–209. doi: 10.1016/j.neuchi.2019.09.010

Couly, G. F., Coltey, P. M., and Le Douarin, N. M. (1993). The triple origin of skull in higher vertebrates: a study in quail-chick chimeras. *Development* 117, 409–429.

Curtis, N., Jones, M. E. H., Evans, S. E., O'Higgins, P., and Fagan, M. J. (2013). Cranial sutures work collectively to distribute strain throughout the reptile skull. *J. R. Soc. Interface* 10:20130442. doi: 10.1098/rsif.2013.0442

Curtis, N., Witzel, U., and Fagan, M. J. (2014). Development and three-dimensional morphology of the zygomaticotemporal suture in primate skulls. *Folia Primatol. (Basel)* 85, 77–87. doi: 10.1159/000357526

De Pollack, C., Renier, D., Hott, M., and Marie, P. J. (1996). Increased bone formation and osteoblastic cell phenotype in premature cranial suture ossification (craniosynostosis). *J. Bone Miner. Res.* 11, 401–407. doi: 10.1002/jbmr.5650110314

Dechmann, D. K. N., LaPoint, S., Dullin, C., Hertel, M., Taylor, J. R. E., Zub, K., et al. (2017). Profound seasonal shrinking and regrowth of the ossified braincase in phylogenetically distant mammals with similar life histories. *Sci. Rep.* 7:42443. doi: 10.1038/srep42443

Deckelbaum, R. A., Holmes, G., Zhao, Z., Tong, C., Basilico, C., and Loomis, C. A. (2012). Regulation of cranial morphogenesis and cell fate at the neural crest-mesoderm boundary by engrailed 1. *Development* 139, 1346–1358. doi: 10.1242/dev.076729

del Castillo, D. L., Flores, D. A., and Cappozzo, H. L. (2015). Cranial suture closure in the Franciscana Dolphin, *Pontoporia blainvillei* (Gervais and D'Orbigny, 1844). *Mastozool. Neotrop.* 22, 141–148.

Delashaw, J. B., Persing, J. A., Broaddus, W. C., and Jane, J. A. (1999). Cranial vault growth in craniosynostosis. *J. Neurosurg.* 70, 159–165. doi: 10.3171/jns.1989.70.2.0159

Di leva, A., Bruner, E., Davidson, J., Pisano, P., Haider, T., Stone, S. S., et al. (2013). Cranial sutures: a multidisciplinary review. *Childs Nerv. Syst.* 29, 893–905. doi: 10.1007/s00381-013-2061-4

Di Pietro, L., Barba, M., Prampolini, C., Ceccariglia, S., Frassanito, P., Vita, A., et al. (2020). GLI1 and AXIN2 are distinctive markers of human calvarial mesenchymal stromal cells in nonsyndromic craniosynostosis. *Int. J. Mol. Sci.* 21:4356. doi: 10.3390/ijms21124356

Doro, D. H., Grigoriadis, A. E., and Liu, K. J. (2017). Calvarial suture-derived stem cells and their contribution to cranial bone repair. *Front. Physiol.* 8:956. doi: 10.3389/fphys.2017.00956

Doro, D. H., Lui, A., Grigoriadis, A. E., and Liu, K. J. (2019). The osteogenic potential of the neural crest lineage may contribute to craniosynostosis. *Mol. Syndromol.* 10, 48–57. doi: 10.1159/000493106

el Ghouzzi, V., Le Merrer, M., Perrin-Schmitt, F., Lajeunie, E., Benit, P., Renier, D., et al. (1997). Mutations of the TWIST gene in the Saethre-Chotzen syndrome. *Nat. Genet.* 15, 42–46. doi: 10.1038/ng0197-42

Esteve-Altava, B., Barteri, F., Farré, X., Muntané, G., Pastor, J. F., and Navarro, A. (2020). Evolutionary phenome-genome analysis of cranial suture closure in mammals. *bioRxiv (Preprint)* doi: 10.1101/2020.06.15.148130

Esteve-Altava, B., Marugán-Lobón, J., Botella, H., and Rasskin-Gutman, D. (2013). Structural constraints in the evolution of the tetrapod skull complexity: williston's law revisited using network models. *Evol. Biol.* 40, 209–219. doi: 10.1007/s11692-012-9200-9

Esteve-Altava, B., Marugán-Lobón, J., Botella, H., and Rasskin-Gutman, D. (2014). Random loss and selective fusion of bones originate morphological complexity trends in tetrapod skull networks. *Evol. Biol.* 41, 52–61. doi: 10.1007/s11692-013-9245-4

Esteve-Altava, B., and Rasskin-Gutman, D. (2015). Evo-Devo insights from pathological networks: exploring craniosynostosis as a developmental mechanism for modularity and complexity in the human skull. *J. Antropol. Sci.* 93, 103–107. doi: 10.4436/JASS.93001

Evans, D. J., and Noden, D. M. (2006). Spatial relations between avian craniofacial neural crest and paraxial mesoderm cells. *Dev. Dyn.* 235, 1310–1325. doi: 10.1002/dvdy.20663

Evans, K., Vidal-Garcia, M., Tagliacollo, V., Taylor, S., and Fenolio, D. (2019). Bony Patchwork: mosaic patterns of evolution in the skull of electric fishes (Apteronotidae: Gymnotiformes). *Integr. Comp. Biol.* 59, 420–431. doi: 10.1093/icb/icz026

Fabre, A. C., Cornette, R., Huyghe, K., Andrade, D. V., and Herrel, A. (2014). Linear versus geometric morphometric approaches for the analysis of head shape dimorphism in lizards. *J. Morphol.* 275, 1016–1026. doi: 10.1002/jmor.20278

Felice, R. N., and Goswami, A. (2018). Developmental origins of mosaic evolution in the avian cranium. *Proc. Natl. Acad. Sci. U.S.A.* 113, 555–560. doi: 10.1073/pnas.1716437115

Felice, R. N., Tobias, J. A., Pigot, A. L., and Goswami, A. (2019). Dietary niche and the evolution of cranial morphology in birds. *Proc. R. Soc. B.* 286:20182677. doi: 10.1098/rspb.2018.2677

Flaherty, K., Singh, N., and Richtsmeier, J. T. (2016). Understanding craniosynostosis as a growth disorder. *Wiley Interdiscip. Rev. Dev. Biol.* 5, 429–459. doi: 10.1002/wdev.227

Flores, D. A., Giannini, N., and Abdala, F. (2006). Comparative postnatal ontogeny of the skull in the australidelphian metatherian *Dasyurus albopunctatus* (Marsupialia: Dasyuromorpha: Dasyuridae). *J. Morphol* 267, 426–440. doi: 10.1002/jmor.10420

Foth, C., Brusatte, S. L., and Butler, R. J. (2012). Do different disparity proxies converge on a common signal? Insights from the cranial morphometrics and evolutionary history of Pterosauria (Diapsida: Archosauria). *J. Evol. Biol.* 25, 904–915. doi: 10.1111/j.1420-9101.2012.02479.x

Fujiwara, S. I., and Takakuwa, Y. (2011). A sub-adult growth stage indicated in the degree of suture co-ossification in Triceratops. *Bull. Gunma Mus. Natu. His.* 15, 1–17.

Gatesy, J., Geisler, J. H., Chang, J., Buell, C., Berta, A., Meredith, R. W., et al. (2013). A phylogenetic blueprint for a modern whale. *Mol. Phylogenet. Evol.* 66, 479–506. doi: 10.1016/j.ympev.2012.10.012

Gault, D., Renier, D., Marchac, D., and Jones, B. (1992). Intracranial pressure and intracranial volume in children with craniosynostosis. *Plast. Reconstr. Surg.* 90, 377–381. doi: 10.1097/00006534-199209000-00003

Goswami, A. (2006). Cranial modularity shifts during mammalian evolution. *Am. Nat.* 168, 170–180. doi: 10.1086/505758

Goswami, A., Foley, L., and Weisbecker, V. (2013). Patterns and implications of extensive heterochrony in carnivoran cranial suture closure. *J. Evol. Biol.* 26, 1294–1306. doi: 10.1111/jeb.12127

Goyal, N. K. (2020). "The newborn infant," in *Nelson Textbook of Pediatrics*, 21st Edn, Chap. 113, eds R. M. Kliegman, J. W. St. Geme, N. J. Blum, S. S. Shah, R. C. Tasker, and K. M. Wilson (Philadelphia: Elsevier).

Greenwald, J. A., Mehrara, B. J., Spector, J. A., Warren, S. M., Fagenholz, P. J., Smith, L. P., et al. (2001). In vivo modulation of FGF biological activity alters cranial suture fate. *Am. J. Pathol.* 158, 441–452. doi: 10.1016/s0002-9440(10)63987-9

Gregory, W. K., Roigneau, M., Burr, E. R., Evans, G., Hellman, E., Jackson, F. A., et al. (1935). Williston's law relating to the evolution of skull bones in the vertebrates. *Am. J. Phys. Anthropol.* 20, 123–152.

Grova, M., Lo, D. D., Montoro, D., Hyun, J. S., Chung, M. T., Wan, D. C., et al. (2012). Animal models of cranial suture biology. *J. Craniofac. Surg.* 23, 1954–1958. doi: 10.1097/SCS.0b013e318258ba53

Guo, Y., Yuan, Y., Wu, L., Ho, T.-V., Jing, J., Sugii, H., et al. (2018). BMP-IHH-mediated interplay between mesenchymal stem cells and osteoclasts supports calvarial bone homeostasis and repair. *Bone Res.* 6:30. doi: 10.1038/s41413-018-0031-x

Hanken, J., and Hall, B. K. (1993). *The Skull*, Vol. 1-3. Chicago, IL: University of Chicago Press.

Hay, E. D. (2005). The mesenchymal cell, its role in the embryo, and the remarkable signaling mechanisms that create it. *Dev. Dyn.* 233, 706–720. doi: 10.1002/dvdy.20345

Heck, L., Wilson, L. A. B., Evin, A., Stange, M., and Sánchez-Villagra, M. R. (2018). Shape variation and modularity of skull and teeth in domesticated horses and wild equids. *Front. Zool.* 15:14. doi: 10.1186/s12983-018-0258-9

Henderson, J. H., Chang, L. Y., Song, H. M., Longaker, M. T., and Carter, D. R. (2005). Age-dependent properties and quasi-static strain in the rat sagittal suture. *J. Biomech.* 38, 2294–2301. doi: 10.1016/j.jbiomech.2004.07.037

Herrel, A., Aerts, P., and De Vree, F. (2000). Cranial kinesis in geckoes: functional implications. *J. Exp. Biol.* 203, 1415–1423.

Herring, S. W. (1972). Sutures: a tool in functional cranial analysis. *Acta Anat.* 83, 222–247. doi: 10.1159/000143860

Herring, S. W. (1974). A biometric study of suture fusion and skull growth in peccaries. *Anat. Embryol. (Berl)* 146, 167–180. doi: 10.1007/BF00315593

Herring, S. W., and Teng, S. (2000). Strain in the braincase and its sutures during function. *Am. J. Phys. Anthropol.* 112, 575–593. doi: 10.1002/1096-8644(200008)112:4<575::AID-AJPA10<3.0.CO;2-0

Heuzé, Y., Boyadjiev, S. A., Marsh, J. L., Kane, A. A., Cherkez, E., Boggan, J. E., et al. (2010). New insights into the relationship between suture closure and craniofacial dysmorphology in sagittal nonsyndromic craniosynostosis. *J. Anat.* 217, 85–96. doi: 10.1111/j.1469-7580.2010.01258.x

Hewitt, R. A., and Westermann, G. E. G. (2007). Mechanical significance of ammonoid septa with complex sutures. *Lethaia* 30, 205–212. doi: 10.1111/j.1502-3931.1997.tb00462.x

Huggenberger, S., Leidenberger, S., and Oelschläger, H. H. A. (2017). Asymmetry of the nasofacial skull in toothed whales (Odontoceti). *J. Zool.* 302, 15–23. doi: 10.1111/jzo.12425

Iseki, S., Wilkie, A. O., Heath, J. K., Ishimaru, T., Eto, K., and Morriss-Kay, G. M. (1997). Fgfr2 and osteopontin domains in the developing skull vault are mutually exclusive and can be altered by locally applied FGF2. *Development* 124, 3375–3384.

Jaslow, C. R. (1989). Sexual dimorphism of cranial suture complexity in wild sheep (*Ovis orientalis*). *Zool. J. Linn. Soc.* 95, 273–284. doi: 10.1111/j.1096-3642.1989.tb02312.x

Jaslow, C. R., and Biewener, A. A. (1995). Strain patterns in the horncores, cranial bones and sutures of goats (Capra hircus) during impact loading. *J. Zool.* 235, 193–210. doi: 10.1111/j.1469-7998.1995.tb05137.x

Jiang, X., Iseki, S., Maxson, R. E., Sucov, H. M., and Morriss-Kay, G. M. (2002). Tissue origins and interactions in the mammalian skull vault. *Dev. Biol.* 241, 106–116. doi: 10.1006/dbio.2001.0487

Jin, S.-W., Sim, K.-B., and Kim, S.-D. (2016). Development and growth of the normal cranial vault: an embryologic review. *J. Korean Neurosurg. Soc.* 59, 192–196. doi: 10.3340/jkns.2016.59.3.192

Johnson, D., Iseki, S., Wilkie, A. O., and Morriss-Kay, G. M. (2000). Expression patterns of Twist and Fgfr1, -2 and -3 in the developing mouse coronal suture suggest a key role for twist in suture initiation and biogenesis. *Mech. Dev.* 91, 341–345. doi: 10.1016/s0925-4773(99)00278-6

Johnson, D., and Wilkie, A. O. (2011). Craniosynostosis. *Eur. J. Hum. Genet.* 19, 369–376. doi: 10.1038/ejhg.2010.235

Jones, M. E. H., Gröning, F., Dutel, H., Sharp, A., Fagan, M. J., and Evans, S. E. (2017). The biomechanical role of the chondrocranium and sutures in a lizard cranium. *J. R. Soc. Interface* 14:20170637. doi: 10.1098/rsif.2017.0637

Kammerer, C. F., Angielczyk, K. D., and Fröbisch, J. (2015). Redescription of the geikiid Pelanomodon (Therapsida, Dicynodontia), with a reconsideration of 'Propelanomodon'. *J. Vertebr. Paleontol.* 36:e1030408. doi: 10.1080/02724634.2015.1030408

Kathe, W. (1999). Comparative morphology and functional interpretation of the sutures in the dermal skull roof of temnospondyl amphibians. *Zool. J. Linn. Soc.* 126, 1–40. doi: 10.1006/zjls.1997.0154

Kawata, T., Tokimasa, C., Fujita, T., Kawasoko, S., Kaku, M., Sugiyama, H., et al. (1998). Midpalatal suture of osteopetrotic (op/op) mice exhibits immature fusion. *Exp. Anim.* 47, 277–281. doi: 10.1538/expanim.47.277

Key, C. A., Aiello, L. C., and Molleson, T. (1994). Cranial suture closure and its implications for age estimation. *Int. J. Osteoarchaeol.* 4, 193–207. doi: 10.1002/oa.1390040304

Khonsari, R. H., Olivier, J., Vigneaux, P., Sanchez, S., Tafforeau, P., Ahlberg, P. E., et al. (2013). A mathematical model for mechanotransduction at the early steps of suture formation. *Proc. R. Soc. B* 280:20122670. doi: 10.1098/rspb.2012.2670

Kim, H. J., Rice, D. P., Kettunen, P. J., and Thesleff, I. (1998). FGF-, BMP- and Shh-mediated signalling pathways in the regulation of cranial suture morphogenesis and calvarial bone development. *Development* 125, 1241–1251.

Kimonis, V., Gold, J.-A., Hoffman, T. L., Panchal, J., and Boyadjiev, S. A. (2007). Genetics of craniosynostosis. *Semin. Pediatr. Neurol.* 14, 150–161. doi: 10.1016/j.spen.2007.08.008

Koskinen, L., Isotupa, K., and Koski, K. (1976). A note on craniofacial sutural growth. *Am. J. Phys. Anthropol.* 45, 511–516. doi: 10.1002/ajpa.1330450312

Koyabu, D., Werneburg, I., Morimoto, N., Zollikofer, C. P., Forasiepi, A. M., Endo, H., et al. (2014). Mammalian skull heterochrony reveals modular evolution and a link between cranial development and brain size. *Nat. Commun.* 5:3625. doi: 10.1038/ncomms4625

Kraatz, B., and Sherratt, E. (2016). Evolutionary morphology of the rabbit skull. *PeerJ.* 4:e2453. doi: 10.7717/peerj.2453

Krogman, W. M. (1930). Studies in growth changes in the skull and face of anthropoids. II. Ectocranial and endocranial suture closure in anthropoids and Old World Apes. *Am. J. Anat.* 46, 315–353. doi: 10.1002/aja.1000460206

Lana-Elola, E., Rice, R., Grigoriadis, A., and Rice, D. C. (2007). Cell fate specification during calvarial bone and suture development. *Dev. Biol.* 311, 335–346. doi: 10.1016/j.ydbio.2007.08.028

Le Lièvre, C. S. (1978). Participation of neural crest-derived cells in the genesis of the skull in birds. *J. Embryol. Exp. Morphol.* 47, 17–37.

Le Douarin, N. M. (1982). *The Neural Crest*. Cambridge: Cambridge University Press.

Le Douarin, N. M. (2012). Piecing together the vertebrate skull. *Development* 139, 4293–4296. doi: 10.1242/dev.085191

Lee, J. C., Spiguel, L., Shenaq, D. S., Zhong, M., Wietholt, C., He, T. C., et al. (2011). Role of RANK-RANKL-OPG axis in cranial suture homeostasis. *J. Craniofac. Surg.* 22, 699–705. doi: 10.1097/SCS.0b013e3182077fbd

Lee, K. K. L., Stanier, P., and Pauws, E. (2019). Mouse models of syndromic craniosynostosis. *Mol. Syndromol.* 10, 58–73. doi: 10.1159/000491004

Lemanis, R. (2020). The ammonite septum is not an adaptation to deep water: re-evaluating a centuries-old idea. *Proc. R. Soc. B* 287:20201919. doi: 10.1098/rspb.2020.1919

Lenton, L. M., Nacamuli, R. P., Wan, D. C., Helms, J. A., and Longaker, M. T. (2005). Cranial suture biology. *Curr. Top. Dev. Biol.* 66, 287–328. doi: 10.1016/S0070-2153(05)66009-7

Lesciotto, K. M., and Richtsmeier, J. T. (2019). Craniofacial skeletal response to encephalization: how do we know what we think we know? *Am. J. Phys. Anthropol.* 168, 27–46. doi: 10.1002/ajpa.23766

Lillegraven, J. A., Thompson, S. D., McNab, B. K., and Patton, J. L. (1987). The origin of eutherian mammals. *Biol. J. Linn. Soc.* 32, 281–336. doi: 10.1111/j.1095-8312.1987.tb00434.x

Liu, Y.-H., Tang, Z., Kundu, R. K., Wu, L., Luo, W., Zhu, D., et al. (1999). Msx2 gene dosage influences the number of proliferative osteogenic cells in the growth centers of the developing murine skull: a possible mechanism for MSX2-mediated craniosynostosis in humans. *Dev. Biol.* 205, 260–274. doi: 10.1006/dbio.1998.9114

Longrich, N. R., and Field, D. J. (2012). Torosaurus is not Triceratops: Ontogeny in chasmosaurine ceratopsids as a case study in dinosaur taxonomy. *PloS One* 7:e32623. doi: 10.1371/journal.pone.0032623

Lu, X., Ge, D., Xia, L., Huang, C., and Yang, Q. (2014). Geometric morphometric study of the skull shape diversification in Sciuridae (Mammalia. *Rodentia). Integr. Zool.* 9, 231–245. doi: 10.1111/1749-4877.12035

Luo, W., Yi, Y., Jing, D., Zhang, S., Men, Y., Ge, W.-P., et al. (2019). Investigation of postnatal craniofacial bone development with tissue clearing-based three-dimensional imaging. *Stem Cells Dev.* 28, 1310–1321. doi: 10.1089/scd.2019.0104

Maddin, H. C., Piekarski, N., Sefton, E. M., and Hanken, J. (2016). Homology of the cranial vault in birds: new insights based on embryonic fate-mapping and character analysis. *R. Soc. Open Sci.* 3:160356. doi: 10.1098/rsos.160356

Malde, O., Cross, C., Lim, C. L., Marghoub, A., Cunningham, M. L., Hopper, R. A., et al. (2020). Predicting calvarial morphology in sagittal craniosynostosis. *Sci. Rep.* 10:3. doi: 10.1038/s41598-019-55224-5

Manjila, S., Chim, H., Eisele, S., Chowdhry, S. A., Gosain, A. K., and Cohen, A. R. (2010). History of the Kleeblattschädel deformity: origin of concepts and evolution of management in the past 50 years. *Neurosurg. Focus* 29:E7. doi: 10.3171/2010.9.FOCUS10212

Markens, I. S. (1975). Embryonic development of the coronal suture in man and rat. *Acta Anat.* 93, 257–273. doi: 10.1159/000144486

Markey, M. J., Main, R. P., and Marshall, C. R. (2006). In vivo cranial suture function and suture morphology in the extant fish Polypterus: implications for inferring skull function in living and fossil fish. *J. Exp. Biol.* 209, 2085–2102. doi: 10.1242/jeb.02266

Maruyama, T., Jeong, J., Sheu, T. J., and Hsu, W. (2016). Stem cells of the suture mesenchyme in craniofacial bone development, repair and regeneration. *Nat. Commun.* 7:10526. doi: 10.1038/ncomms10526

McBratney-Owen, B., Iseki, S., Bamforth, S. D., Olsen, B. R., and Morriss-Kay, G. M. (2008). Development and tissue origins of the mammalian cranial base. *Dev. Biol.* 322, 121–132. doi: 10.1016/j.ydbio.2008.07.016

McCurry, M. R., Evans, A. R., Fitzgerald, E. M. G., Adams, J. W., Clausen, P. D., and McHenry, C. R. (2017). The remarkable convergence of skull shape in crocodilians and toothed whales. *Proc. R. Soc. B* 284:1850. doi: 10.1098/rspb.2016.2348

McCurry, M. R., Mahony, M., Clausen, P. D., Quayle, M. R., Walmsley, C. W., Jessop, T. S., et al. (2015). The relationship between cranial structure, biomechanical performance and ecological diversity in varanoid lizards. *PLoS One* 10:e0130625. doi: 10.1371/journal.pone.0130625

Mehrara, B. J., Spector, J. A., Greenwald, J. A., Ueno, H., and Longaker, M. T. (2002). Adenovirus-mediated transmission of a dominant negative transforming growth factor-beta receptor inhibits in vitro mouse cranial suture fusion. *Plast. Recon. Surg.* 110, 506–514. doi: 10.1097/00006534-200208000-00022

Miller, G. S. (1923). The telescoping of the cetacean skull (with eight plates). *Smithson Misc. Coll.* 76, 1–70.

Miura, T., Perlyn, C. A., Kinboshi, M., Ogihara, N., Kobayashi-Miura, M., Morriss-Kay, G. M., et al. (2009). Mechanisms of skull suture maintenance and interdigitation. *J. Anat.* 215, 642–655. doi: 10.1111/j.1469-7580.2009.01148.x

Moazen, M., Curtis, N., O'Higgins, P., Jones, M. E. H., Evans, S. E., and Fagan, M. J. (2009). Assessment of the role of sutures in a lizard skull: a computer modelling study. *Proc. R. Soc. B* 276, 39–46. doi: 10.1098/rspb.2008.0863

Monteiro, L. R., and Lessa, L. G. (2000). Comparative analysis of cranial suture complexity in the genus *Caiman* (Crocodylia, Alligatoridae). *Rev. Brasil Biol.* 60, 689–694. doi: 10.1590/S0034-71082000000400021

Morriss-Kay, G. M. (2001). Derivation of the mammalian skull vault. *J. Anat.* 199, 143–151. doi: 10.1046/j.1469-7580.2001.19910143.x

Morriss-Kay, G. M., and Wilkie, A. O. (2005). Growth of the normal skull vault and its alteration in craniosynostosis: insights from human genetics and experimental studies. *J. Anat.* 207, 637–653. doi: 10.1111/j.1469-7580.2005.00475.x

Moss, M. L. (1957). Experimental alteration of sutural area morphology. *Anat. Rec.* 127, 569–589. doi: 10.1002/ar.1091270307

Moss, M. L., and Young, R. W. (1960). A functional approach to craniology. *Am. J. Phys. Anthropol.* 18, 281–292. doi: 10.1002/ajpa.1330180406

Nicolay, C. W., and Vaders, M. J. (2006). Cranial suture complexity in white-tailed deer (*Odocoileus virginianus*). *J. Morphol.* 267, 841–849. doi: 10.1002/jmor.10445

Noden, D. M. (1988). Interactions and fates of avian craniofacial mesenchyme. *Development* 103, 121–140.

Nunn, C. L., and Smith, K. K. (1998). Statistical analyses of developmental sequences: the craniofacial region in marsupial and placental mammals. *Am. Nat.* 152, 82–101. doi: 10.1086/286151

O'Hara, J., Ruggiero, F., Wilson, L., James, G., Glass, G., Jeelani, O., et al. (2019). Syndromic craniosynostosis: complexities of clinical care. *Mol. Syndromol.* 10, 83–97. doi: 10.1159/000495739

Opperman, L. A. (2000). Cranial sutures as intramembranous bone growth sites. *Dev. Dyn* 219, 472–485. doi: 10.1002/1097-017720009999:9999<::AID-DVDY1073<3.0.CO;2-F

Opperman, L. A., Chhabra, A., Nolen, A. A., Bao, Y., and Ogle, R. C. (1998). Dura mater maintains rat cranial sutures *in vitro* by regulating suture cell proliferation and collagen production. *J. Craniofac. Genet. Dev. Biol.* 18, 150–158.

Opperman, L. A., Gakunga, P. T., and Carlson, D. S. (2005). Genetic factors influencing morphogenesis and growth of sutures and synchondroses in the craniofacial complex. *Semin Orthod* 11, 199–208. doi: 10.1053/j.sodo.2005.07.004

Opperman, L. A., Passarelli, R. W., Morgan, E. P., Reintjes, M., and Ogle, R. C. (1995). Cranial sutures require tissue interactions with dura mater to resist osseous obliteration *in vitro*. *J. Bone Miner. Res.* 10, 1978–1987. doi: 10.1002/jbmr.5650101218

Opperman, L. A., Sweeney, T. M., Redmon, J., Persing, J. A., and Ogle, R. C. (1993). Tissue interactions with underlying dura mater inhibit osseous obliteration of developing cranial sutures. *Dev. Dyn.* 198, 312–322. doi: 10.1002/aja.1001980408

Otto, A. W. (1830). *Lehrbuch der Pathologischen Anatomie des Meuchen und der Thiere*. Berlin: Rücker.

Oudhof, H. A. J. (1982). Sutural growth. *Acta Anat.* 112, 58–68. doi: 10.1159/000145497

Panchal, J., and Uttchin, V. (2003). Management of craniosynostosis. *Plast. Reconstr. Surg.* 111, 2032–2048. doi: 10.1097/01.PRS.0000056839.94034.47

Parr, W. C. H., Wilson, L. A. B., Wroe, S., Colman, N. J., Crowther, M. S., and Letnic, M. (2016). Cranial shape and the modularity of hybridization in dingoes and dogs; hybridization does not spell the end for native morphology. *Evol. Biol.* 43, 171–187. doi: 10.1007/s11692-016-9371-x

Paterson, J. R., and Edgecombe, G. D. (2006). The Early Cambrian trilobite family Emuellidae Pocock, 1970: systematic position and revision of Australian species. *J. Paleontol.* 80, 496–513.

Persson, M., Magnusson, B., and Thilander, B. (1978). Sutural closure in rabbit and man: a morphological and histochemical study. *J. Anat.* 125, 313–321.

Pierce, S. E., Angielczyk, K. D., and Rayfield, E. J. (2009). Shape and mechanics in thalattosuchian (Crocodylomorpha) skulls: implications for feeding behaviour and niche partitioning. *J. Anat.* 215, 555–576. doi: 10.1111/j.1469-7580.2009.01137.x

Pritchard, J. J., Scott, J. H., and Girgis, F. G. (1956). The structure and development of cranial and facial sutures. *J. Anat.* 90, 73–86.

Pucek, Z. (1963). Seasonal changes in the braincase of some representatives of the genus Sorex from the Palaearctic. *J. Mammal.* 44, 523–536. doi: 10.2307/1377135

Rager, L., Hautier, L., Forasiepi, A., Goswami, A., and Sánchez-Villagra, M. R. (2014). Timing of cranial suture closure in placental mammals: phylogenetic patterns, intraspecific variation, and comparison with marsupials. *J. Morphol.* 275, 125–140. doi: 10.1002/jmor.20203

Rayfield, E. J. (2005). Using finite element analysis to investigate suture morphology: a case study using large carnivorous dinosaurs. *Anat. Rec. A Discov. Mol. Cell. Evol. Biol.* 283, 349–365. doi: 10.1002/ar.a.20168

Rice, D., Kim, H.-J., Kettunen, P., and Thesleff, I. (1998). Molecular signaling in suture development. *Acta Odontol. Scand.* 56:387. doi: 10.1080/000163598428383

Rice, D. P., Aberg, T., Chan, Y., Tang, Z., Kettunen, P. J., Pakarinen, L., et al. (2000). Integration of FGF and TWIST in calvarial bone and suture development. *Development* 12, 1845–1855.

Rice, D. P. C., Rice, R., and Thesleff, I. (2003). Molecular mechanisms in calvarial bone and suture development, and their relation to craniosynostosis. *Eur. J. Orthod.* 25, 139–148. doi: 10.1093/ejo/25.2.139

Richtsmeier, J. T., Aldridge, K., DeLeon, V. B., Panchal, J., Kane, A. A., Marsh, J. L., et al. (2006). Phenotypic integration of neurocranium and brain. *J. Exp. Zool. B. Mol. Dev. Evol.* 306, 360–378. doi: 10.1002/jez.b.21092

Roston, R. A., and Roth, V. L. (2019). Cetacean skull telescoping brings evolution of cranial sutures into focus. *Anat. Rec.* 302, 1055–1073. doi: 10.1002/ar.24079

Roth, D. A., Bradley, J. P., Levine, J. P., McMullen, H. F., McCarthy, J. G., and Longaker, M. T. (1996). Studies in cranial suture biology: part II. Role of the dura in cranial suture fusion. *Plast. Reconstr. Surg.* 97, 693–699. doi: 10.1097/00006534-199604000-00001

Sampson, S. D., Ryan, M. J., and Tanke, D. H. (1997). Craniofacial ontogeny in centrosaurine dinosaurs (Ornithischia: Ceratopsidae): Taxonomic and behavioral implications. *Zool. J. Linn. Soc.* 121, 293–337. doi: 10.1111/j.1096-3642.1997.tb00340.x

Senarath-Yapa, K., Chung, M. T., McArdle, A., Wong, V. W., Quarto, N., Longaker, M. T., et al. (2012). Craniosynostosis: molecular pathways and future pharmacologic therapy. *Organogenesis* 8, 103–113. doi: 10.4161/org.23307

Shim, K.-W., Park, E.-K., Kim, J.-S., Kim, Y.-O., and Kim, D.-S. (2016). Neurodevelopmental problems in non-syndromic craniosynostosis. *J. Korean Neurosurg. Soc.* 59, 242–246. doi: 10.3340/jkns.2016.59.3.242

Sidor, C. (2001). Simplification as a trend in synapsid cranial evolution. *Evolution* 55, 1419–1442. doi: 10.1111/j.0014-3820.2001.tb00663.x

Skrzat, J., Brzozowska, I., and Walocha, J. (2004). A preliminary study on the relationship between the complexity of the sagittal suture and cranial dimensions. *Folia Morphol. (Warsz)* 63, 43–46.

Slater, B. J., Lenton, K. A., Kwan, M. D., Gupta, D. M., Wan, D. C., and Longaker, M. T. (2008). Cranial sutures: a brief review. *Plast. Reconstr. Surg.* 121, 170e–178e. doi: 10.1097/01.prs.0000304441.99483.97

Stayton, C. T. (2005). Morphological evolution of the lizard skull: a geometric morphometrics survey. *J. Morphol.* 263, 47–59. doi: 10.1002/jmor.10288

Teng, C. S., Cavin, L., Maxson Jnr, R. E., Sánchez-Villagra, M. R., and Crump, J. G. (2019). Resolving homology in the face of shifting germ layer origins: lessons from a major skull vault boundary. *Elife* 8:e52814. doi: 10.7554/eLife.52814

Teng, C. S., Ting, M., Farmer, D. T., Brockop, M., and Maxson, R. E. (2018). Altered bone growth dynamics prefigure craniosynostosis in a zebrafish model of Saethre-Chotzen syndrome. *eLife* 7:e37024. doi: 10.7554/eLife.37024

Toussaint, N., Redhead, Y., Vidal-García, M., Lo Vercio, L., Liu, W., Fisher, E. M. C., et al. (2021). A landmark-free morphometrics pipeline for high-resolution phenotyping: application to a mouse model of Down syndrome. *Development* 148:dev188631. doi: 10.1242/dev.188631

Ubelaker, D. H., and Khosrowshahi, H. (2019). Estimation of age in forensic anthropology: historical perspective and recent methodological advances. *Forensic Sci. Res.* 4, 1–9. doi: 10.1080/20961790.2018.1549711

Usui, K., and Tokita, M. (2018). Creating diversity in mammalian facial morphology: a review of potential developmental mechanisms. *EvoDevo* 9:15. doi: 10.1186/s13227-018-0103-4

Virchow, R. (1851). Über den Cretinismus, namentlich in Franken, und über pathologische Schädelformen. *Verh. Phys. Med. Ges. Würzbg.* 2, 230–271.

Vodanović, M., Dumančić, J., Galić, I., Savić Pavičin, I., Petrovečki, M., Cameriere, R., et al. (2011). Age Estimation in archaeological skeletal remains: evaluation of four non-destructive age calculation methods. *J. Forensic Odontostomatol.* 29, 14–21.

Warren, S. M., Brunet, L. J., Harland, R. M., Economides, A. N., and Longaker, M. T. (2003). The BMP antagonist noggin regulates cranial suture fusion. *Nature* 422, 625–629. doi: 10.1038/nature01545

Warren, S. M., Walder, B., Dec, W., Longaker, M. T., and Ting, K. (2008). Confocal laser scanning microscopic analysis of collagen scaffolding patterns in cranial sutures. *J. Craniofac. Surg.* 19, 198–203. doi: 10.1097/scs.0b013e31815c8a9a

Watanabe, A., Fabre, A.-C., Felice, R. N., Maisano, J. A., Müller, J., Herrel, A., et al. (2019). Ecomorphological diversification in squamates from conserved pattern of cranial integration. *Proc. Natl. Aacd. Sci. U.S.A.* 116, 14688–14697. doi: 10.1073/pnas.1820967116

Weinzweig, J., Kirschner, R. E., Farley, A., Reiss, P., Hunter, J., Whitaker, L. A., et al. (2003). Metopic synostosis: defining the temporal sequence of normal suture fusion and differentiating it from synostosis on the basis of computed tomography images. *Plast. Reconstr. Surg.* 112, 1211–1218. doi: 10.1097/01.PRS.0000080729.28749.A3

White, H. E., Clavel, J., Tucker, A. S., and Goswami, A. (2020). A comparison of metrics for quantifying cranial suture complexity. *J. R. Soc. Interface* 17:20200476. doi: 10.1098/rsif.2020.0476

Wilk, K., Yeh, S. A., Mortensen, L. J., Ghaffarigarakani, S., Lombardo, C. M., Bassir, S. H., et al. (2017). Postnatal calvarial skeletal stem cells expressing PRX1 reside exclusively in the calvarial sutures and are required for bone regeneration. *Stem Cell Rep*. 8, 933–946. doi: 10.1016/j.stemcr.2017.03.002

Wilkie, A. O., and Morriss-Kay, G. M. (2001). Genetics of craniofacial development and malformation. *Nat. Rev. Genet.* 2, 458–468. doi: 10.1038/3507660

Wilson, L. A. B., and Sánchez-Villagra, M. R. (2009). Heterochrony and patterns of cranial suture closure in hystricognath rodents. *J. Anat.* 214, 339–354. doi: 10.1111/j.1469-7580.2008.01031.x

Wood, C. (2015). The age-related emergence of cranial morphological variation. *Forensic Sci. Int.* 251:220.e1–20. doi: 10.1016/j.forsciint.2015.03.030

Yoshida, T., Vivatbutsiri, P., Morriss-Kay, G., Saga, Y., and Iseki, S. (2008). Cell lineage in mammalian craniofacial mesenchyme. *Mech. Dev.* 125, 797–808. doi: 10.1016/j.mod.2008.06.007

Zhao, H., Feng, J., Ho, T. V., Grimes, W., Urata, M., and Chai, Y. (2015). The suture provides a niche for mesenchymal stem cells of craniofacial bones. *Nat. Cell Biol.* 17, 386–396. doi: 10.1038/ncb3139

Zhou, Y. X., Xu, X., Chen, L., Li, C., Brodie, S. G., and Deng, C.-X. (2000). A Pro250Arg substitution in mouse Fgfr1 causes increased expression of Cbfa1 and premature fusion of calvarial sutures. *Hum. Mol. Genet.* 9, 2001–2008. doi: 10.1093/hmg/9.13.2001

Zimmermann, B., Moegelin, A., de Souza, P., and Bier, J. (1998). Morphology of the development of the sagittal suture of mice. *Anat. Embrol.* 197, 155–165. doi: 10.1007/s004290050127

Conflict of Interest: The authors declare that the research was conducted in the absence of any commercial or financial relationships that could be construed as a potential conflict of interest.

frontiers in Ecology and Evolution

ORIGINAL RESEARCH
published: 24 May 2021
doi: 10.3389/fevo.2021.654846

Diversity in the Development of the Neuromuscular System of Nemertean Larvae (Nemertea, Spiralia)

*Jörn von Döhren**

Institute of Evolutionary Biology and Ecology, University of Bonn, Bonn, Germany

In studies on the development of nervous systems and musculature, fluorescent labeling of neuroactive substances and filamentous actin (*f-actin*) of muscle cells and the subsequent analysis with confocal laser scanning microscopy (CLSM), has led to a broad comparative data set for the majority of the clades of the superphylum Spiralia. However, a number of clades remain understudied, which results in gaps in our knowledge that drastically hamper the formulation of broad-scale hypotheses on the evolutionary developmental biology (EvoDevo) of the structures in question. Regarding comparative data on the development of the peptidergic nervous system and the musculature of species belonging to the spiralian clade Nemertea (ribbon worms), such considerable knowledge gaps are manifest. This paper presents first findings on fluorescent labeling of the FMRFamide-like component of the nervous system and contributes additional data on the muscle development in the presently still underrepresented larvae of palaeo- and hoplonemertean species. Whereas the architecture of the FMRFamide-like nervous system is comparably uniform between the studied representatives, the formation of the musculature differs considerably, exhibiting developmental modes yet undescribed for any spiralian species. The presented results fill a significant gap in the spiralian EvoDevo data set and thus allow for further elaboration of hypotheses on the ancestral pattern of the musculature and a prominent component of the nervous system in Nemertea. However, with respect to the variety observed, it is expected that the true diversity of the developmental pathways is still to be discovered when more detailed data on other nemertean species will be available.

Keywords: immuno-staining, neuromuscular system, development, heterochrony, Nemertea, Lophotrochozoa, evolution, EvoDevo

OPEN ACCESS

Edited by:
Fernando Casares, Andalusian Center for Developmental Biology (CABD), Spain

Reviewed by:
Conrad Helm, University of Göttingen, Germany
Jose Maria Martin-Duran, Queen Mary University of London, United Kingdom

***Correspondence:**
Jörn von Döhren
jdoehren@evolution.uni-bonn.de

Specialty section:
This article was submitted to Evolutionary Developmental Biology, a section of the journal Frontiers in Ecology and Evolution

Received: *17 January 2021*
Accepted: *26 March 2021*
Published: *24 May 2021*

Citation:
von Döhren J (2021) Diversity in the Development of the Neuromuscular System of Nemertean Larvae (Nemertea, Spiralia). Front. Ecol. Evol. 9:654846. doi: 10.3389/fevo.2021.654846

INTRODUCTION

Bilaterian animals are currently grouped into three major superphyla, Ecdysozoa, Deuterostomia, and Spiralia (Halanych et al., 1995; Aguinaldo et al., 1997; Giribet, 2002, 2016; Dunn et al., 2008, 2014; Hejnol et al., 2009; Edgecombe et al., 2011). Despite recent advances in metazoan systematics, there is no robustly supported phylogeny of Spiralia, with numerous, but sometimes contradicting tree topologies recently published (Laumer et al., 2015, 2019; Kocot et al., 2017; Marlétaz et al., 2019). Currently, it seems undisputed that Spiralia comprise at least Platyhelminthes (*sensu stricto*, i.e., to the exclusion of Acoelomorpha), and Lophotrochozoa that develop either via a typical trochophore-type larva or possess a

lophophore, a tentacle feeding apparatus that is supported by an inner coelomic cavity. Gnathifera is also often included in Spiralia (Laumer et al., 2015; Kocot, 2016; Marlétaz et al., 2019).

No other metazoan superphylum shows such an enormous diversity of morphologies as Spiralia and as a consequence, body wall musculature and nervous systems are also highly diverse (Wanninger, 2015). This diversity in morphologies and hence the body wall muscles and nervous systems is somewhat puzzling, since most members of Spiralia share a stereotypic, spiral cleavage (Boyer and Henry, 1998; Lambert, 2010; Nielsen, 2010; Martín-Durán and Marlétaz, 2020). It is characterized by a spiral arrangement of the blastomeres, with quartets of cells in a helicoidal arrangement above each other, that each have a determined fate in the future morphology of the species. The fates of the respective blastomeres are reported to be very conservative, even between phyla within Spiralia (Lambert, 2010; Martín-Durán and Marlétaz, 2020). Thus, highly diverse adult body plans result from a stereotypic, only marginally variable embryogenesis. The solution to this paradox may be that the majority of the morphological diversity observed in adult spiralian lineages results from diversification of post-embryonic development.

Post-embryonic development in the spiralian subclade Lophotrochozoa is characterized by a planktonic larval stage that more or less gradually develops into the benthic adult shape (Nielsen, 2004, 2005; Nezlin, 2010). During the time of larval life, the organism is subject to selection that shapes the larval morphology, but also has an impact on its metamorphosis to the adult body organization. Since the most promising approach to elucidating the evolution spiralian morphological diversity is seen to lie in investigating post-embryonic development, development of the musculature and nervous systems has recently gained much attention (Wanninger, 2009, 2015; Nezlin, 2010; Richter et al., 2015). Myo- and neurogenesis have been studied by fluorescent staining with phalloidin for muscles or antibodies against various neuroactive substances for subsets of the nervous system and examined with confocal microscopic setups. The most prominent spiralian clades Annelida and Mollusca are currently most extensively studied (Bleidorn et al., 2015; Wanninger and Wollesen, 2015). For the lophophorate taxa Brachiopoda, Ectoprocta, and Phoronida, detailed data on musculature and nervous system in the larval stages and comparison with the adult musculature has been obtained more recently (Santagata and Zimmer, 2002; Santagata, 2004, 2008a,b, 2011; Wanninger et al., 2005; Gruhl, 2008, 2009; Altenburger and Wanninger, 2009, 2010; Nielsen and Worsaae, 2010; Temereva and Wanninger, 2012; Temereva and Tsitrin, 2013, 2014).

Some smaller, indubitably spiralian taxa however, could not yet be consistently placed on the spiralian tree of life (Kocot et al., 2017; Laumer et al., 2019). Among the most notorious of these are Nemertea, that also primarily possess pelagic larvae (Maslakova and Hiebert, 2014). Nemertea (ribbon worms) is a comparably small phylum of worm-shaped, mostly marine animals comprising approximately 1300 species (Kajihara et al., 2008). As adults, the majority of nemertean species are photophobic predators that capture their prey with an eversible, muscular proboscis that is housed in a secondary body cavity, called rhynchocoel. Based on molecular data, three major lineages are currently recognized: Hoplonemertea, Pilidiophora, and Palaeonemertea (Andrade et al., 2012, 2014; Kvist et al., 2014). Hoplonemertea possess a proboscis that is armed with a stylet apparatus consisting of one or multiple calcareous stylets, employed to stab the prey and poison it with a species-specific cocktail of toxic substances (McDermott and Roe, 1985; Chernyshev, 2000; von Reumont et al., 2020). Pilidiophora are characterized by a specific type of larva, the pilidium (Thollesson and Norenburg, 2003; Maslakova, 2010a; Maslakova and Hiebert, 2014). Palaeonemertea, although characterized as monophyletic in the most recent phylogenetic analyses based on genome-scale datasets (Andrade et al., 2014), do not share any unambiguously derived morphological characters. Development in the palaeo- and hoplonemertean species has traditionally been described as "direct," since no explicitly larval characters had been detected (Iwata, 1960; Maslakova, 2010a; Maslakova and Hiebert, 2014). More recently however, the pelagic developmental stage of Hoplonemertea has been characterized as decidula larva, due to a transitory larval epidermis found in many representatives of this clade (Maslakova and von Döhren, 2009; Hiebert et al., 2010; Maslakova, 2010a; Maslakova and Hiebert, 2014). The ancestral larval type of Palaeonemertea has been postulated to represent a so-called hidden trochophore larva (Maslakova et al., 2004).

With respect to development of nervous system and musculature, nemertean larvae are clearly understudied. Information on the development of the nervous system of Nemertea by means of fluorescent antibody labeling and confocal microscopy is almost exclusively restricted to the serotonin immunoreactive component in about a handful of mostly pilidiophoran species and the development of the body wall musculature by fluorescent labeling with phalloidin has never been in the focus of any comparative investigation (Hay-Schmidt, 1990; Martindale and Henry, 1995; Maslakova et al., 2004; Schwartz, 2009; Chernyshev and Magarlamov, 2010; Hiebert et al., 2010; Maslakova, 2010b; von Döhren, 2011, 2015, 2016; Chernyshev et al., 2013; Hindinger et al., 2013; Beckers and von Döhren, 2015; Hiebert and Maslakova, 2015a,b; Martín-Durán et al., 2015). This study aims at a comparative description of the development of the body wall musculature and of the FMRFamide immunoreactive component, a subset of the peptidergic nervous system in several non-pilidiophoran representatives that possess the type of development that has traditionally been termed as "direct." Both hoplo- and palaeonemertean representatives were investigated. The results obtained are expected to provide additional data to trace the evolution of morphological diversity within the highly diverse superphylum Spiralia.

MATERIALS AND METHODS

Species and Collection Sites

Adult, sexually mature specimens of both sexes of *Tubulanus polymorphus* Renier, 1804 (Tubulanidae, Palaeonemertea) were collected in the intertidal zone close to the Station Biologique de Roscoff, France in July and August 2014. The animals are endobenthic and had to be dug out of the sand. After collection, the specimens were kept in running seawater at the Station. Sexually mature adult males and females of *Carinoma*

armandi (McIntosh, 1875) (Carinomidae, Palaeonemertea) were obtained by digging in the intertidal sandflat of the Anse de Pouldohan near Concarneau, France in June 2018. Animals were subsequently transported to the Institute of Evolutionary Biology and Ecology of the University of Bonn (IEZ), were they were kept in plastic aquaria filled with seawater and sand from the collection site with weakly water changes. *Carinoma mutabilis* Griffin, 1898 (Carinomidae, Palaeonemertea) males and females were found sexually mature from January to February, 2007 in the intertidal sandflat of False Bay on San Juan Island, WA, United States. They were taken to Friday Harbor Laboratories where they were kept in running seawater. *Carcinonemertes carcinophila* (Kölliker, 1845) (Monostilifera, Hoplonemertea) is ectoparasitic on the decapod crab *Carcinus maenas* (Linnaeus, 1758). The crabs were collected during cruises with the research vessel Mya in the vicinity of the AWI Wattenmeerstation in List auf Sylt, Germany in June 2012. At the AWI Wattenmeerstation, gravid *C. maenas* females were inspected for sexually mature male and female *C. carcinophila* individuals that were removed from between the egg masses of the crabs. The nemerteans were kept at 8°C in natural sea water until they were transported to the IEZ, were they were kept in large plastic petri dishes at comparable temperatures. *Amphiporus* sp. (Monostilifera, Hoplonemertea) is a yet undescribed free-living, benthic nemertean species. A formal description of this species is planned for the near future. One sexually mature female and two males were found under stones submerged in approximately 0.5 m deep water on the coast of Giglio island, Italy in June 2013. Animals were transported to the IEZ were they were kept at 18 °C in plastic aquaria with artificial sea water and medium sized stones to provide shelter from light.

Obtaining and Rearing Larvae

Larvae of palaeonemetean species were obtained by artificial fertilization from dissected oocytes that were fertilized with a diluted suspension of sperm dissected from the males. Prior to fertilization, the oocytes were placed in sterile-filtered natural seawater from the respective collection site until they round up, which is usually accomplished within 20–30 min. Zygotes were kept in sterile filtered sea water from the collection site of their parents. In the hoplonemertean species, eggs could not be artificially fertilized. In *C. carcinophila*, the eggs are shed into parchment-like gelatinous tubes. The egg strings are normally found, wrapped around the pleopods between the developing eggs of the host crab, but *C. carcinophila* females in petri dishes laid eggs after warming up the water to 18°C. In *Amphiporus* sp. the eggs were shed at night-time and were transferred to clean seawater the next morning. The containers with the larvae of *T. polymorphus* and *C. mutabilis* were cooled by placing them up to half of their height in running seawater (*T. polymorphus* 14–16°C, *C. mutabilis* at 8–10°C). Larvae of *C. armandi* were kept at 12°C, those of *C. carcinophila* and *Amphiporus* sp. at 18°C. Clean filtered seawater was replaced every 2–3 days. Although several food items were offered, e.g., quartered sea urchin embryos (to *C. mutabilis*), blue mussel oocytes (to *C. armandi*), and brine shrimp nauplii (to *Amphiporus* sp.), none of the larvae were observed to feed.

Sampling and Fixation of Larvae

The larvae were fixed at different times after fertilization (*C. mutabilis*: 1–2, 3, and 5 days; *C. armandi*: 1–3, 5, and 7 days; *T. polymorphus*: 1–4, 6, and 9 days) or egg-deposition (*C. carcinophila*: 3 and 4 days; *Amphiporus* sp.: 1–5, 7, 10, 14, and 18 days). To prevent possible muscle contraction during fixation, hatched larvae that show muscular contraction (usually from 3 days after fertilization or egg-deposition) were relaxed in a 1:1 mixture of sterile-filtered seawater and aqueous $MgCl_2$ solution of 0.33 mol l^{-1} (*C. mutabilis*) or 0.37 mol l^{-1} (remaining species) at room temperature until no muscle contractions were observed (usually after 10–15 min). Specimens were fixed in 4% (v/v) formaldehyde (prepared from 1 part of a 16% aqueous paraformaldehyde solution, EMS or VWR Chemicals, mixed with 3 parts of sterile-filtered sea water) at 18°C or at room temperature for 30 min. After fixation, larvae were washed three times for 10 min each in 0.1 M phosphate buffer saline (PBS, pH 7.4; Fisher Scientific for *C. mutabilis*, own formulation for the other species) at 18°C or at room temperature. Except for *C. mutabilis*, larvae were stored at 4–8°C in the same buffer but with 0.01% (w/v) NaN_3 (Roth) added to prevent microbial growth. In the larvae of the former species, no NaN_3 was added to the buffer for storage.

Immunohistochemistry and Fluorescent Labeling

Up to 12 larvae of *C. mutabilis* were blocked in 6% normal donkey serum (Jackson Immunoresearch) in PBS with 0.1% Triton X-100 (Fisher Scientific), hereafter referred to as 0.1% PBT for 2 h at room temperature. After washing with 5 changes of 0.1% PBT for 5 min each, larvae were incubated in rabbit-anti-FMRFamide (Immunostar) at 1:500 dilution in PBS overnight at 4°C followed by washing with three changes of 0.1% PBT for 10 min each at room temperature. Subsequently, the specimens were incubated in donkey-anti-rabbit antibody conjugated with Alexa Fluor 488 (Molecular Probes) at a dilution of 1:600 for 2 h at room temperature and afterward rinsed with three changes of PBS, each for 10 min. For immunostaining in the remaining species, depending on the size between 10 and 15 specimens were permeabilized in three changes of PBS with 0.3% Triton X-1000 (0.3% PBT) each for 10 min at room temperature. Subsequently, specimens were blocked in 10% normal goat serum (NGS, Sigma-Aldrich) in 0.3% PBT for 2 h at room temperature and afterward incubated with the primary antibodies overnight at 18°C. Antibodies used were against FMRFamide produced in rabbit (Abcam) at a dilution of 1:1000 and against acetylated α-tubulin raised in mouse (Sigma-Aldrich) at a dilution of 1:200 in 0.3% PBT with 10% NGS. In double labeling experiments, both antibodies were applied simultaneously. After incubation with primary antibodies, specimens were washed in three changes of 0.3% PBT for 10 min each at room temperature. As secondary antibodies, goat-anti-rabbit conjugated with Alexa Fluor 488, Alexa Fluor 568 or Alexa Fluor 633 and goat-anti-mouse, conjugated with Alexa Fluor 488 or Alexa Fluor 633 (Invitrogen) were used at a concentration of 1:100 to 1:400 in 0.1% PBT with 10% NGS. The specimens were incubated with the secondary antibodies for 2 h at room temperature and

subsequently washed 3 times for 10 min each in 0.1% PBT. In double labeling experiments, both antibodies, against mouse and against rabbit with different conjugated fluorophores, were applied simultaneously.

For labeling of filamentous actin (*f-actin*), larvae of *C. mutabilis* were permeabilized in three changes of PBT (10 min each), and stained with Bodipy FL phallacidin (Molecular Probes) at a dilution of 1:100 for 40 min at room temperature. After staining, larvae were rinsed three times with PBS for 10 min each. In the remaining species f-actin was labeled with phalloidin coupled to Alexa Fluor 488 or tetramethylrhodamine-isothiocyanate (TRITC) (Invitrogen) at a dilution ranging from 1:100 to 1:200 for 40 min up to 2 h. In double labeling experiments with immunostainings, phalloidin was added together with the secondary antibodies. After staining, larvae were rinsed three times each for 10 min in PBS (*C. mutabilis* larvae) or 0.1% PBT (larvae of remaining species).

Mounting, Confocal Laser Scanning Microscopy and Image Processing

All samples were mounted on coverslips coated with poly-L-lysine (Sigma-Aldrich). Larvae of *C. mutabilis* stained with antibodies against FMRFamide were mounted in Vectashield (Vector Laboratories). All larval stages of *C. carcinophila* were mounted in 90% (v/v) glycerol in PBS. The remaining larvae were quickly dehydrated in isopropanol (1 min each in 70, 85, and 95%, 2 times 100%), cleared in three changes of BABB (mixture of 1 part of benzyl alcohol and 2 parts of benzyl benzoate) for 10 min each, mounted in BABB on glass slides with several layers of 100-μm-thick adhesive tape or clay pieces as spacers, and sealed with nail polish.

To examine *C. mutabilis*, a Bio-Rad Radiance 2000 laser scanning confocal system mounted on a Nikon Eclipse E800 microscope with a 40 × 1.3 NA oil immersion objective and an excitation wavelength of λ = 488 nm (light blue) was used. Optical section thickness was set to 1 μm and images were recorded at 8-bit image depth at a resolution of 1024 × 1024 pixels. For signal detection in the remaining species a Leica TCS/SPE confocal laser scanning system mounted on a Leica DM 2500 microscope was used. Alexa Fluor 488 was excited with the 488 nm-, Alexa Fluor 568 and TRITC with the 532 nm- (green), and Alexa Fluor 633 with the 635 nm-laser line (red). All images were recorded with a 40 × 0.75 NA dry objective. For double-stained specimens the sequential excitation/detection setting was used. Stacks of images were recorded with an optical section thickness of 0.88 μm with a resolution of 1024 × 1024 pixels and an image depth of 8 bit.

Image stacks were processed with the Fiji distribution package of ImageJ by W. S. Rasband, NIH, version 1.53c (Schindelin et al., 2012; Schneider et al., 2012). To produce two dimensional images from the recorded stacks, the maximum-intensity stack-projection function was used. Images were subsequently adjusted using global contrast settings, gamma function (detailed in the figure subheadings), unsharp mask-, and remove outlier-filters. Resulting images were rotated, translated, and cropped (details of image enhancement are listed in **Supplementary Table 1**). Mounting and annotation of images and line drawings were made with Adobe Illustrator CS6. **Supplementary Videos** were produced in Fiji/ImageJ version 1.53c. The respective image series were rotated in the x- and y-axes (so that the apical pole/frontal end is oriented up in every video) and cropped using the respective commands. The image series were subjected to background subtraction (command "Subtract Background..." at default settings), global contrast adjustment (command "Enhance Contrast...", saturated pixels: 0.3% and "use stack histogram" checked, followed by command "Adjust Brightness/Contrast" with lower cut-off level set to 2), and noise reduction (command "Remove Outliers..." at default settings). After annotation of the image series the images were saved as avi-files with JPEG-compression at a frame rate of 4 *fps* (frames per second).

RESULTS

Tubulanus polymorphus (Tubulanidae, Palaeonemertea)

Post-embryonic Development

At 14–16°C, hatching in *T. polymorphus* takes place before 1 day after fertilization (*1-dpf*), resulting in spherical free-swimming developmental stages. In the majority of specimens observed, gastrulation is completed after 1 day of development and the epidermal cells are adorned with a dense coat of epidermal cilia visualized by acetylated α-tubulin-like immunoreactivity (**Figure 1A**: α-*tub-lir* at 2-dpf). The blastopore has begun to shift its position from opposite of the apical tuft to a more anterior location as it becomes the mouth opening and foregut at 2-dpf (**Figure 1A**: *fg*). The translocation of the mouth opening to more anterior continues through all observed stages; a closure of the blastopore is not observed. Additionally, at 1-dpf, an apical pit with a tuft of elongated cilia and pair of apical epidermal invaginations, each on either side of the apical pit are forming (**Figure 1A**: *at* at 2-dpf). The cilia of the apical tuft elongate to attain their maximal length at 3-dpf. The epithelium of the midgut becomes ciliated between 1- and 2-dpf and the first signals of ciliated nephridia also appear at that time (**Figure 1A**: *mg* and *pn*). In the course of further development, the larvae become more elongate and ellipsoid. General internal anatomy remains largely unchanged until 9-dpf, the oldest examined stage (**Figure 2B**). Neither the formation of the anal opening, nor the formation of a proboscis rudiment is observed until the end of the examined development. The larva of *T. polymorphus* does not possess eyes in any of the observed stages.

FMRFamide-Like Immunoreactivity

In post-gastrula stages of *T. polymorphus*, there are several more or less spherical signals of comparable size (300–400 nm in diameter) distributed over the surface of the larva. Most of the signals are located at the level of the epidermal cells, but do not reach their surface. Others are clearly superficial. No clear neurite-like signals could be observed at this time of development. The epidermis shows small, spot-like signals all over its surface, without any conspicuous aggregations detectable (**Figure 1B** at 2-dpf). These spot-like signals are very likely unspecific staining. The first distinctive FMRFamide-like immunoreactive (*RFa-lir*) signals are observable after 1-dpf. Inside the larva, there are no strong signals, although two cell-like signals, slightly dorso-lateral underneath the apical pit show

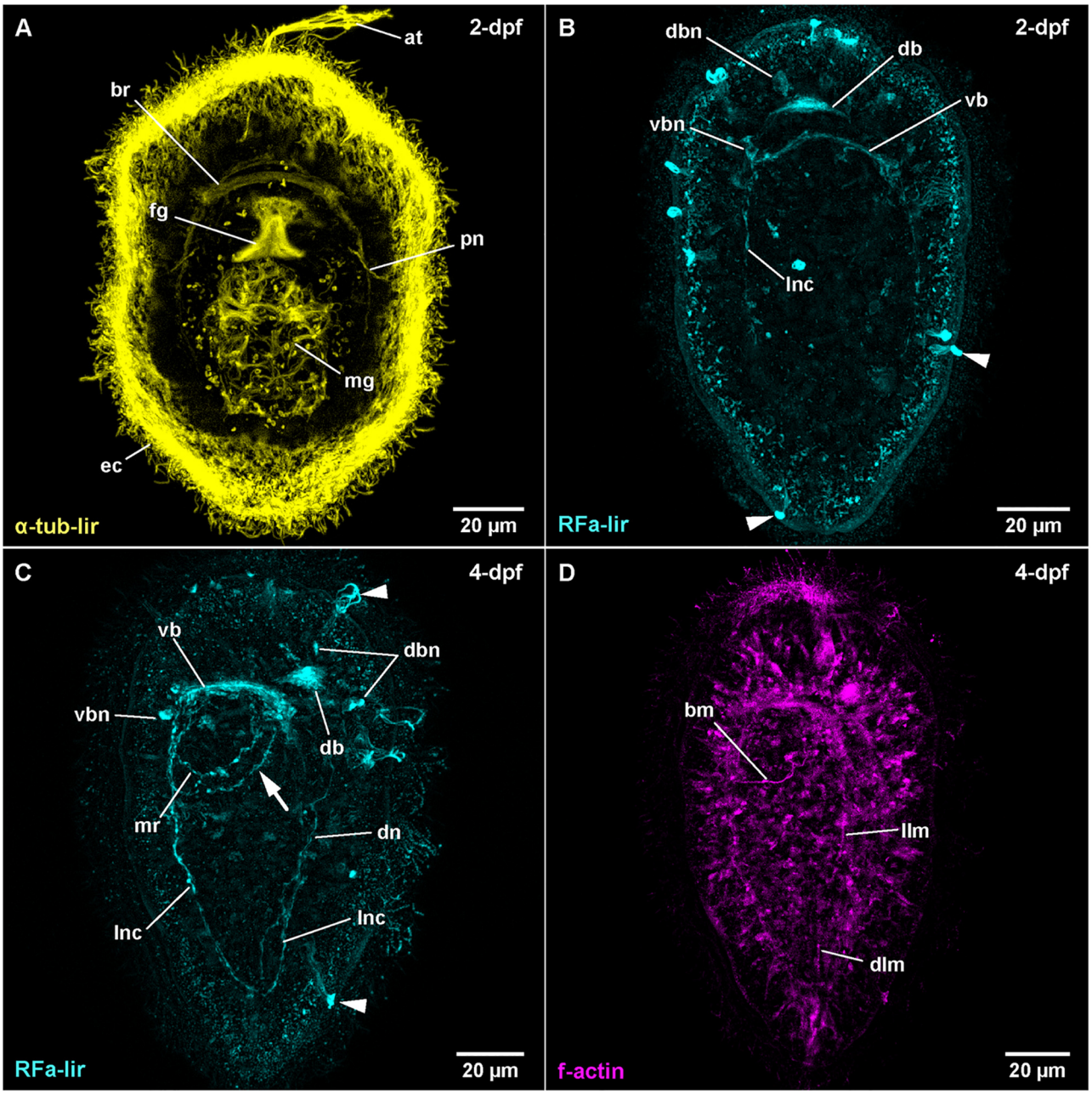

FIGURE 1 | *Tubulanus polymorphus*, (frontal is up in all images, age of larval stages indicated in top right-hand corner, dpf: days post artificial fertilization). **(A)** (γ = 0.6); projection of 31 optical sections, ventral view. **(B)** (γ = 0.8); maximum projection of 28 optical sections, dorsal view. *Arrowheads* indicate unspecific staining of epidermal gland cells. **(C)** (γ = 0.75); maximum projection of 27 optical sections, ventro-lateral view. *Arrowheads* indicate unspecific staining of epidermal gland cells, *arrow* indicates second mouth ring neurite. **(D)** (γ = 1.2); maximum projection of 14 optical sections, ventro-lateral view. at: apical tuft, bm: buccal muscle, br: brain ring, db: dorsal part of brain ring, dbn: neuron of dorsal part of brain, dlm: dorsal longitudinal muscle, dn: dorsal nerve, ec: epidermal cilia, fg: foregut, llm: lateral longitudinal muscle, lnc: lateral nerve cord, mg: midgut, mr: mouth ring neurite, pn: protonephridium, vb: ventral part of brain ring, vbn: neuron of ventral part of brain.

up slightly brighter than their surroundings. The signals seem to project distally to the apical pit and proximally seem to converge to a single signal that is oriented perpendicular to the longitudinal body axis and located slightly dorsal and anterior of the archenteron. Since this signal is in the position where the dorsal part of the brain ring is expected to form, it is interpreted as the rudiment of the dorsal part of the brain ring (**Figure 1B**: *db* at 2-dpf).

At 2-dpf, the epidermis cells still show the dot-shaped, presumably unspecific signals (**Figures 1B,C**). Inside the larva,

the neurite-like RFa-lir signals of the developing brain ring are visible (**Figure 1B**: *db* and *vb*). The strongest signals are located in the dorso-median position anterior of the developing gut, whereas the ventral brain ring is represented by a single RFa-lir neurite-like signal. On the dorsal side, there are up to 1–2 pairs of roughly spherical, dorso-laterally located and 1 medially located RFa-lir neuron-like signals (**Figure 1B**: *dbn*). Ventrally, 1–2 pairs of spherical lateral and up to three fusiform median neuron-like signals are observable in the vicinity of the brain ring neurite-like signal (**Figure 1B**: *vbn*). A bundle of few RFa-lir neurite-like signals extend from the ventral part of the brain ring bilaterally to the posterior end of the larva. These signals represent the developing lateral nerve cords (**Figure 1B**: *lnc*). Additionally, there are bright, superficial signals of a diameter of 300–400 nm observable in the epidermis, that are unevenly distributed over the entire length and circumference of the larva (**Figure 1B**: *arrowheads*). This type of signals is seen in all subsequent larval stages of *T. polymorphus* that have been investigated (**Figures 1C**, **2A**: *arrowheads*). These signals are connected to underlying, less bright fibril-like signals that fan out into the epidermis and extend through its complete width. At the level of the base of the surrounding epidermis cells, the fibril-like signals converge and thus attain a roughly pyriform, basket-like appearance. In some of these structures, similar fibril-like extensions are seen to fan out above the epidermis to the exterior (**Figure 1C**: *arrowheads* at 4-dpf). These structures are without any detectable contact to any internal, neurite-like signals observable inside the larva. Due to their similar internal and external fibrillar sub-structures, their uneven distribution and the lack of contact to the nervous system, these signals are interpreted as epidermal mucus gland cells showing unspecific staining that have partly extruded their contents in a fibrillar shape during fixation of the larvae.

During further development, the majority of developing RFa-lir nervous system-like structures have only slightly increasing in intensity. Posterior of the brain ring and between the signals of the lateral nerve cords on the ventral side of the larva, a bundle of neurites is detected to surround the mouth opening (**Figure 1C**: *mr*). The posterior semi-circle of this mouth ring neurite-bundle shows a plexus-like arrangement of its neurite-like signals. Whereas the plexus-like arrangement of the posterior semi-circle of the mouth ring neurite bundle has largely disappeared at 4-dpf, a second neurite-like signal is seen next to the posterior semi-circle of the mouth ring (**Figure 1D**: *arrow*). After 4-dpf, dorso-laterally, slightly posterior of the brain ring, 1–2 pairs of additional slightly lobate RFa-lir neuron-like signals have appeared during subsequent development (**Figure 2A**: *dbn* at 6-dpf). The dorso-lateral RFa-lir neuron-like signals posterior of the brain ring show neurite-like signals that extend from the perikarya anteriorly to the median aggregation of RFa-lir neurite-like signals of the dorsal part of the brain ring (**Supplementary File 1**). Also on the dorsal side of the larva, the first RFa-lir neurite-like signal of the longitudinally oriented dorsal nerve is forming (**Figures 1C**, **3A**: *dn*). In presumably less advanced specimens, the neurite-like signal is without connection to the dorsal part of the brain ring, whereas a connection of the

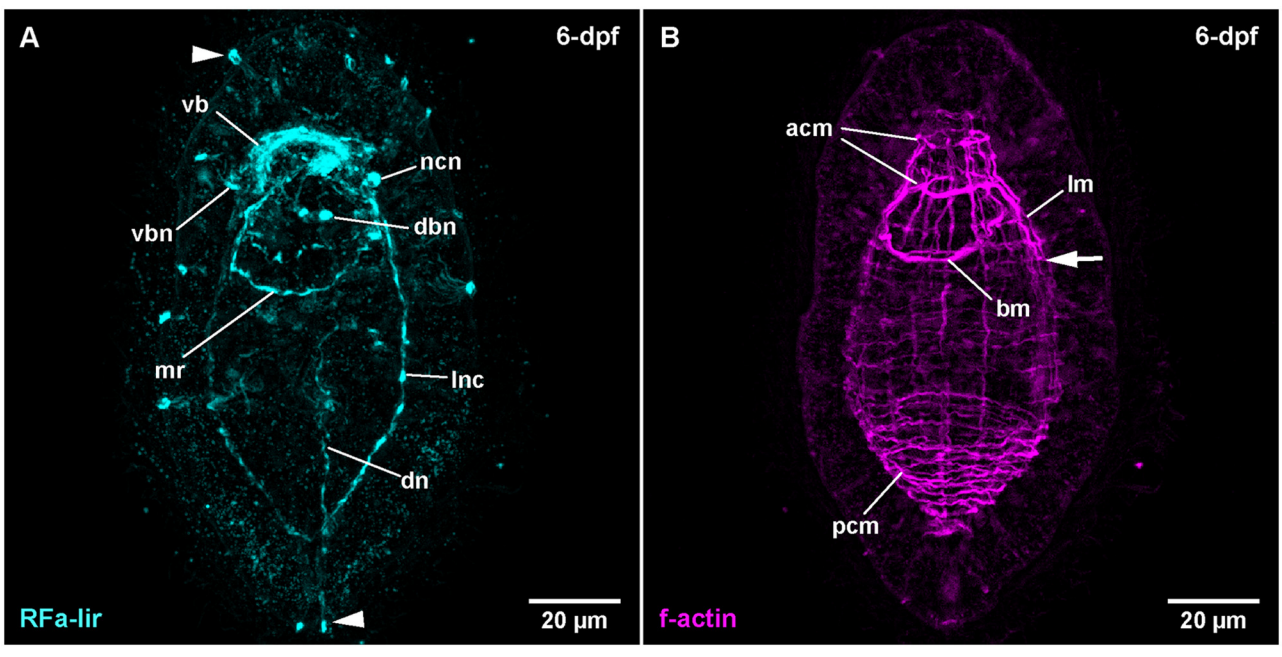

FIGURE 2 | *Tubulanus polymorphus*, (frontal is up in all images, age of larval stages indicated in top right-hand corner, dpf: days post artificial fertilization). **(A)** (γ = 0.85); maximum projection of 26 optical sections, ventro-lateral view. *Arrowheads* indicate unspecific staining of epidermal gland cells. **(B)** (γ = 0.75); same as A. *Arrow* indicates extension of lateral longitudinal muscles. acm: anterior circular muscle, bm: buccal muscle, dbn: neuron of dorsal part of brain, dn: dorsal nerve, lm: longitudinal muscle, lnc: lateral nerve cord, mr: mouth ring neurite, ncn: nerve cord neuron, pcm: posterior circular muscle, vb: ventral part of brain ring, vbn: neuron of ventral part of brain.

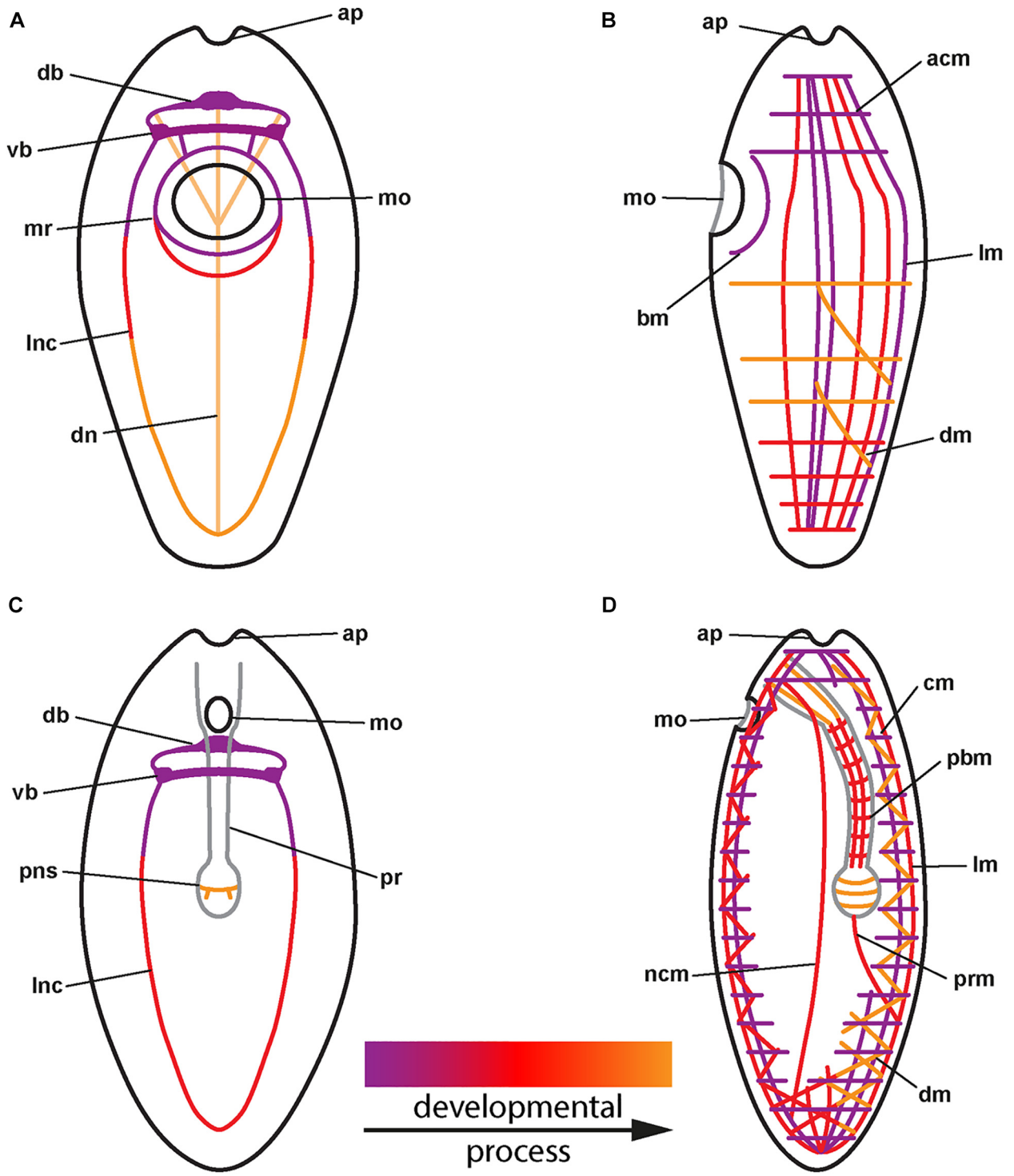

FIGURE 3 | (A) Generalized development of the nervous system in palaeonemertean species (for clarity, only neurites of main components shown). **(B)** Generalized development of the musculature in palaeonemertean species. **(C)** Generalized development of the nervous system in monostiliferan, hoplonemertean species (for clarity, only neurites of main components shown). **(D)** Generalized development of the musculature in monostiliferan, hoplonemertean species (part of the body wall muscles omitted to show internal muscular elements of proboscis and nerve cords). acm: anterior circular muscle, ap: apical pit, bm: buccal muscle, cm: circular muscle, db: dorsal part of brain ring, dm: diagonal muscle, dn: dorsal nerve, lm: longitudinal muscle, lnc: lateral nerve cord, mo: mouth opening, mr: mouth ring neurite, ncm: nerve cord muscle, pbm: proboscis muscle, pns: proboscis nervous-like signal, pr: proboscis, prm: proboscis retractor muscle, vb: ventral part of brain ring.

anterior end of the dorsal nerve neurite-like signals to the median aggregation of dorsal neurite-like signals of the brain ring is visible in presumably more advanced stages (**Figure 3A**: *dn*). Additionally, the more posteriorly located pair of dorso-lateral neuron-like signals of the brain is connected to the dorsal nerve neurite-like signal via an RFa-lir neurite-like signal that is diagonally extending from each side toward the dorsal nerve signal (**Figure 3A**–neurons not shown). Furthermore, there are up to three smaller dorso-median RFa-lir neuron-like signals detected anterior of the brain ring (**Supplementary File 1**). On the ventral side of the larva, two pairs of RFa-lir neuron-like signals have appeared in the vicinity of the brain ring and the lateral nerve cord neurite-like signals. One of them is located at the transition of the brain ring to the lateral nerve cords, the other slightly more posterior, laterally of the lateral nerve cords (**Figure 2A**: *ncn*). Posterior of the dorsal brain ring neurite-like signals, a 3rd pair of weak, dorsolateral RFa-lir neuron-like signals that is similar in shape as the existing two pairs has developed at 6-dpf (**Figure 2A**: *dbn*–only one pair visible). Anterior of the brain ring signals, on both the dorsal and the ventral side, some slender RFa-lir neuron-like signals extend in a longitudinal orientation to the anterior end of the larva. Some of the dorsally located signals are connected to the dorsal brain ring signal aggregation by forked, RFa-lir neurite-like signals, especially to the dorso-median neurite-like signal aggregation (**Supplementary File 2**). The anterior neuron-like signals are interpreted as sensory cells, their connecting neurite-like signals as the first signals of the cephalic nerves. In the oldest investigated stages (9-dpf) the dorso-median RFa-lir neuron-like signals anterior of the brain amount to up to 5, the lateral-most pair showing branching RFa-lir neurite-like signals extending from each neuron-like signal to the surface of the epidermis (data not shown).

F-Actin Labeling of Musculature

The first observable signals of muscular f-actin are observed in 4-dpf larvae. At first a single short, longitudinally oriented fiber-shaped signal is visible on the dorsal side, on the level of the mouth opening. In presumably more advanced stages of that age this first signal has elongated toward the posterior end and additional shorter longitudinally oriented signals are seen on the dorso-lateral sides of the larva, extending posterior of the mouth opening (**Figure 1D**: *dlm* and *llm*). A muscular f-actin signal running alongside the posterior rim of the mouth opening becomes apparent (**Figure 1D**: *bm*). In the same specimens, the first f-actin signals of circular muscles are formed anterior of the mouth opening and distal to the longitudinal signals (not visible in **Figure 1D**, but see **Figure 2B**: *acm* at 6-dpf).

In some more advanced specimens, the longitudinal, lateral f-actin strands extend further to the posterior end of the body and additional circular muscular f-actin signals are visible in the posterior region of the larva. By 6-dpf, more dorso-lateral longitudinal f-actin signals are seen extending along the entire length of the larva (**Figure 2B**). Additional longitudinally oriented f-actin signals are located laterally and ventro-laterally. These strands only reach to the posterior rim of the mouth opening (**Figure 2B**: *arrow*). Circular muscle signals have become more numerous, but especially in the group of signals posterior of the mouth opening, the signals are weaker anteriorly (**Figure 2B**: *pcm*). The ring-shaped signal surrounding the mouth opening is completely closed (**Figure 2B**: *bm*). During further development up to 9-dpf larvae, longitudinal signals become more numerous and seemingly more pronounced but remain confined to the dorsal, and lateral faces of the body where they are evenly spaced (**Figure 3B**). The f-actin signals of the posterior circular muscles increase in number toward the posterior end, while some of the more anteriorly located signals of this group become connected on the ventral side (data not shown).

Carinoma armandi and *Carinoma mutabilis* (Carinomidae, Palaeonemertea)

Post-embryonic Development

The water temperature during development in *C. armandi* was 12°C, whereas in *C. mutabilis*, it was in the range of 8–10°C. At 1-dpf, developmental stages of both species have hatched. In *C. armandi*, the epidermis becomes ciliated, indicated by α-tub-lir at 1-dpf. At 2-dpf, in both species an apical pit and a pair of apical invaginations are formed, one on each side of the apical pit (**Figures 4B,D**: *ap* and *li*). In *C. armandi*, the apical invaginations form slightly earlier than the apical pit. In *C. armandi*, gastrulation is completed at 2-dpf, in *C. mutabilis* at 3-dpf (**Figure 4C**). Closure of the blastopore could not be ascertained but a mouth opening if present, is not ciliated and inconspicuous. A ciliated foregut, located roughly halfway along the length of the larva, has formed in *C. armandi* at 3-dpf although it does not seem to be open to the exterior (**Figure 4D**: *fg*). The cilia of the midgut epithelium start forming at 2-dpf and become conspicuous at 3-dpf (**Figure 4D**: *mg*). In both *Carinoma* species, the lateral apical invaginations have disappeared at 5-dpf (**Figures 5A,B**). Paired, unbranched protonephridia, located one on each side of the mouth opening are detectable at 7-dpf (**Figure 5C**: *pn*). In neither of the *Carinoma* species a caudal tuft, nor the formation of the anal opening or development of the proboscis was seen during the observed period of development.

FMRFamide-Like Immunoreactivity

The earliest stage of *C. armandi*, in which internal RFa-lir signals are detectable is 2-dpf. Although, the signals observed are not stronger than the coarsely granular signals observed in the outermost layer of the large epidermis cells, the internal signals are visible against the weak autofluorescence of their surroundings (**Supplementary File 3**). Since a mouth opening is not evident in the earlier stages, it is impossible to identify whether the signals are dorsally, ventrally or laterally located. In most specimens, up to two, rarely three anteriorly located signals are detected. The signals have an elongated, sometimes pyriform outline extending from the interior with the slender part to the surface of the apical pole of the larva. The proximal portions of the signals are usually stronger. In larvae at 3-dpf, the number of signals observed in each specimen has increased to 3–6, the range indicating a sequence of appearance and subsequent

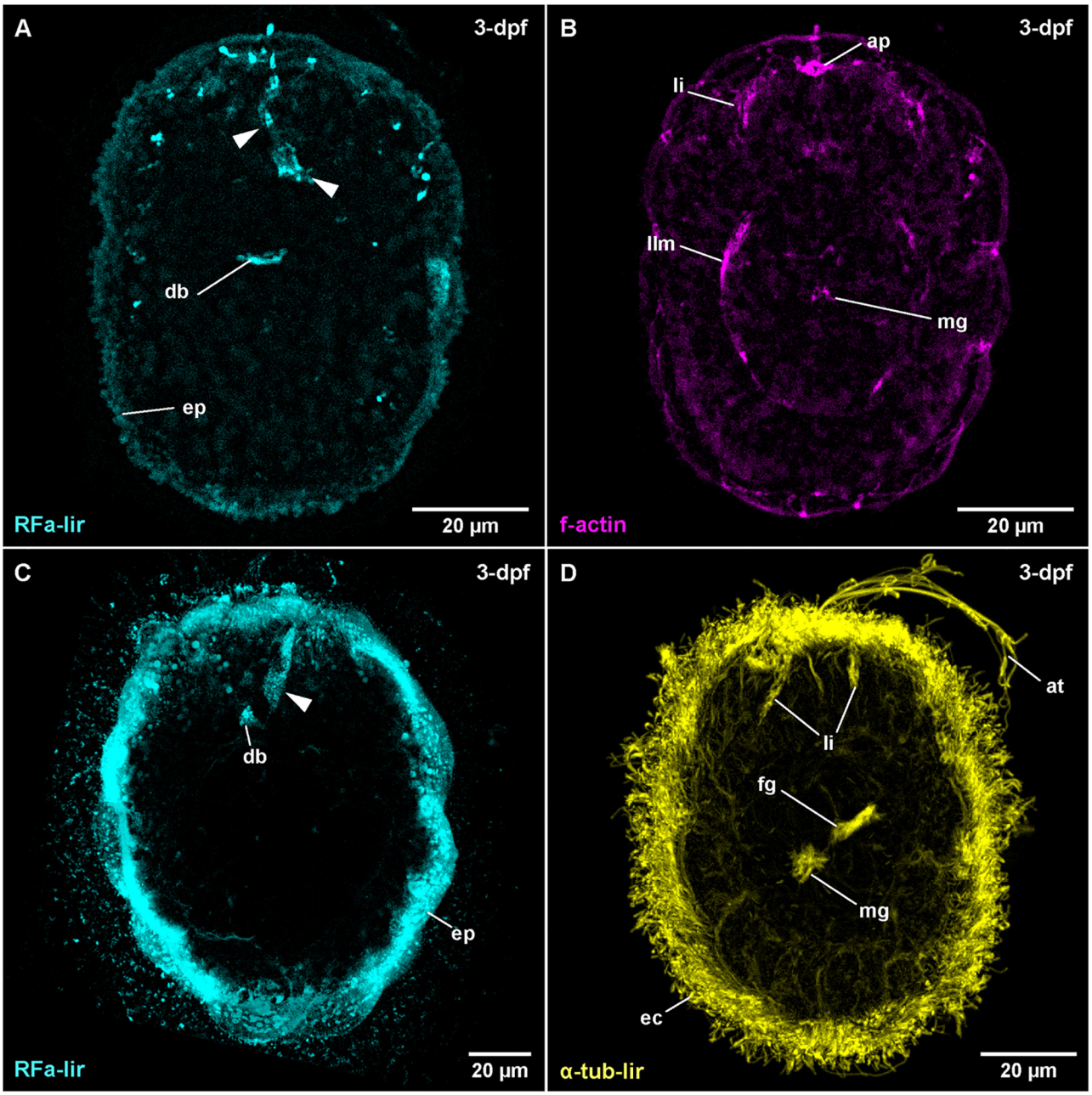

FIGURE 4 | *Carinoma* species (frontal is up in all images, age of larval stages indicated in top right-hand corner, dpf: days post artificial fertilization). **(A)** *C. armandi* (γ = 1.1); maximum projection of 11 optical sections, dorsal view. *Arrowheads* indicate different portions of transitory flask-shaped apical neuron. **(B)** *C. armandi* (γ = 1.1); same as panel **(A)** *C. mutabilis* (γ = 0.85); maximum projection of 13 optical sections, dorsal view. *Arrowheads* indicate basal portions of transitory flask-shaped apical neuron. **(D)** *C. armandi* (γ = 0.8); maximum projection of 16 optical sections, ventro-lateral view. ap: apical pit, at: apical tuft, db: dorsal part of brain ring, ec: epidermal cilia, ep: epidermis, fg: foregut, li: lateral epidermal invaginations, llm: lateral longitudinal muscle, mg: midgut.

disappearance (**Figure 4A**: *arrowheads* at 3-dpf). Interiorly, the signals usually converge on a slightly elongated signal that is oriented perpendicular to the longitudinal axis of the larva. This signal is interpreted as the first RFa-lir signal of the developing dorsal part of the brain ring (**Figure 4A**: *db*). Since by this time, the apical pit and an anterior epidermal invagination bilaterally on each side of the pit have formed, the position of the pyriform or elongated early RFa-lir signals can now be identified more precisely. The majority of signals extends from the apical pole of the larva in the vicinity of the lateral epidermal invagination or from the dorsal face between them to the dorsal brain ring rudiment, but it cannot be ruled out that few signals observed are located ventro-laterally. In *C. mutabilis* larvae at 3-dpf, up to two inconspicuous RFa-lir, fusiform, neuron-like signals are visible

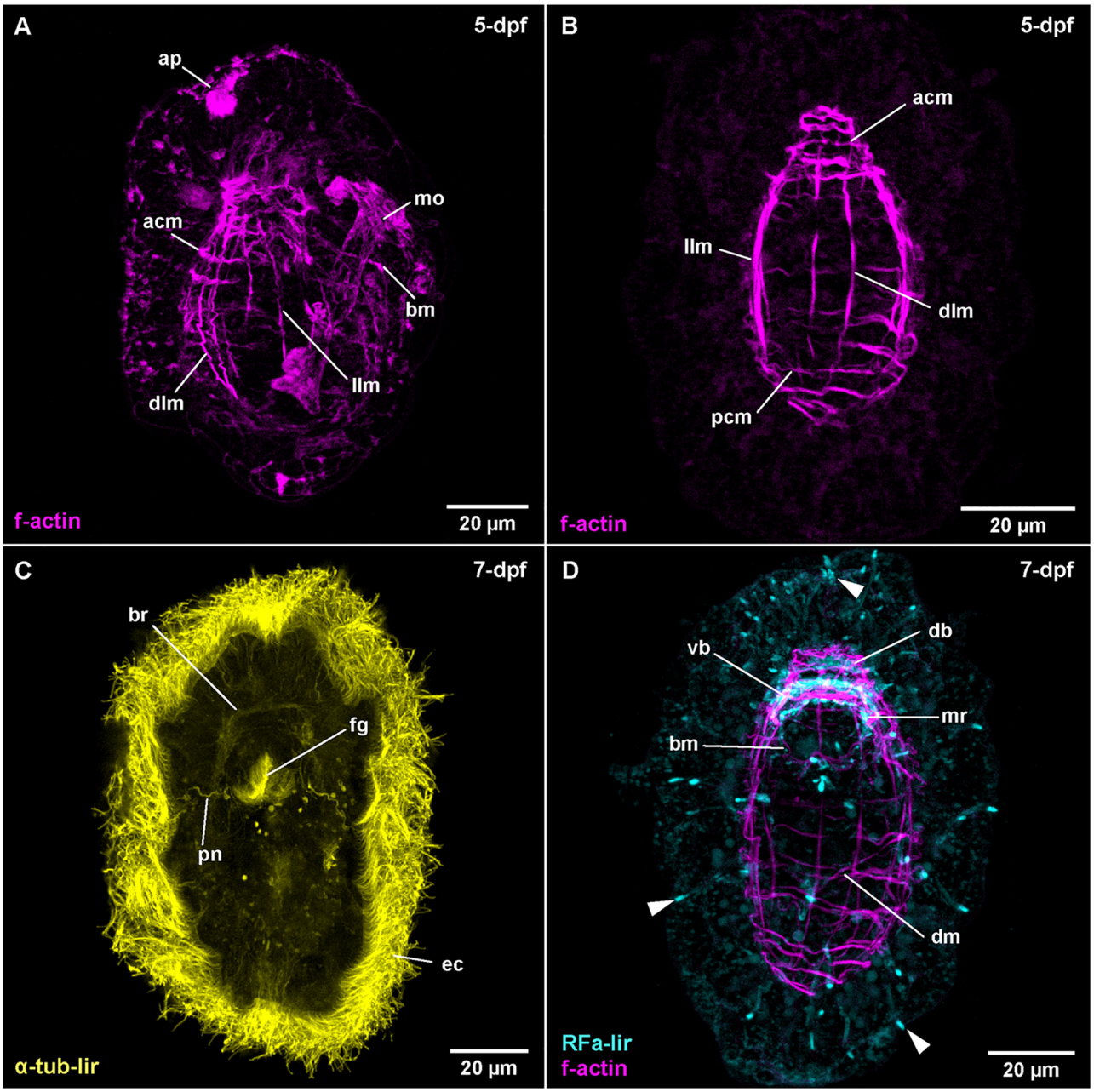

FIGURE 5 | *Carinoma* species (frontal is up in all images, age of larval stages indicated in top right-hand corner, dpf: days post artificial fertilization). **(A)** *C. mutabilis* ($\gamma = 0.9$); maximum projection of 67 optical sections, lateral view. **(B)** *C. armandi* ($\gamma = 0.8$); maximum projection of 10 optical sections, dorsal view. **(C)** *C. armandi* ($\gamma = 0.7$); maximum projection of 9 optical sections, ventral view. **(D)** *C. armandi* (RFa-lir: $\gamma = 0.7$, f-actin: $\gamma = 0.7$); maximum projection of 27 optical sections, ventral view. *Arrowheads* indicate peripheral neuron-like signals. acm: apical circular muscle, ap: apical pit, bm: buccal muscle, br: brain ring, db: dorsal part of brain ring, dlm: dorsal longitudinal muscle, dm: diagonal muscle, ec: epidermal cilia, fg: foregut, llm: lateral longitudinal muscle, mo: mouth opening, mr: mouth ring neurite, pcm: posterior circular muscle, pn: protonephridium, vb: ventral part of brain ring.

underneath the apical pole of the larva (**Figure 4C**: *arrowhead*). They converge to a third signal that is shaped like a flat cone with its tip directed apically, likely corresponding to the first rudiment of the dorsal part of the brain ring (**Figure 4C**: *db*). Thus, the observed signals are very similar to the signals observed in *C. armandi* at 2-dpf.

By 5-dpf in larvae of *C. armandi*, no pyriform apical neurons comparable to those seen in earlier stages are detectable (**Figure 5D** at 7-dpf). The RFa-lir neurite-like signals of the brain ring are now seen to form a complete ring, although the signals in the dorsal part are stronger (**Figures 3A**, **5D**: *vb* and *db* at 7-dpf). In the dorsal part there are 1 pair of dorso-lateral

and 1 median RFa-lir neuron-like signals visible, connecting to the brain ring neurite-like signals (**Supplementary File 4**). The median neuron projects a slender process into the apical pit. In the ventral part of the brain ring, there seems to be one median RFa-lir neuron-like signal connected to the brain ring neurite-like signals in some specimens (data not shown). Slightly behind the brain ring on the ventral side of the larva, a semicircle of an RFa-lir neurite-like signal anterior to the mouth opening is seen that is later completed by a posterior, albeit much weaker signal. These signals are interpreted as mouth ring neurites (**Figures 3A**, **5D**: *mr* at 7-dpf). In more elongated and therefore presumably more advanced larvae, the first weak RFa-lir neurite-like signals of the developing lateral nerve cords are observable (**Figure 3A**– not visible in maximum projection). Originating from the ventral part of the brain ring, they extend along the lateral sides of the larvae. In all parts of the body, but especially concentrated at the anterior pole and around the mouth opening, there are slender elongated RFa-lir neuron-like signals situated between the unstained epidermis cells (**Figure 5D**: *arrowheads* at 7-dpf). Although a connection to the remaining nervous system-like RFa-lir signals is not obvious, their shape and the signal strength comparable to other nervous system-like signals make a function of these cells as receptor cells of a forming peripheral nervous system likely. In the brain ring of 7-dpf larvae, some of the RFa-lir neuron-like signals show neurite-like projections to the epidermal surface (**Supplementary File 5**), further supporting the interpretation of the remaining peripheral signals as receptor cell-like structures.

F-Actin Labeling of Musculature

The first diffuse muscular f-actin signals are detected in larvae of *C. armandi* at 3-dpf (**Figure 4B**: *llm*). They comprise a pair of longitudinally oriented bundles lateral of the midgut. In more advanced stages, these signals become more pronounced and a semi-circular signal behind the posterior rim of the mouth opening is added (**Figure 3B**). By 5-dpf, the lateral f-actin strands have elongated to the anterior and posterior (**Figure 5B**: *llm*). One, later two median dorsal, longitudinal f-actin signals are also visible, extending dorsally from the anterior part of the larva to slightly posterior of the level of the mouth opening (**Figure 5B**: *dlm*). The first f-actin signals of the circular muscles are formed distal of the longitudinal signals, situated in front of and behind the mouth opening (**Figures 3B**, **5B**: *acm* and *pcm*). They seem to be more densely spaced toward the anterior and the posterior end of the larva, respectively (**Figure 5B**). In front of the mouth opening, the circular f-actin signals are completely encircling the larva, whereas the muscular f-actin signals behind the mouth opening are restricted to the dorsal part, extending laterally to the level of the lateral longitudinal muscle strands (**Figure 3B**). In presumably more advanced stages of this age, a pair of diagonally running f-actin signals extends bilaterally from the lateral longitudinal strands anteriorly on each of the dorso-lateral sides of the larva. A second pair of similar, but weaker signals is seen in some specimens more posteriorly (data not shown). These diagonally oriented signals are not addressed as diagonal muscles. Instead, they are seen as forming longitudinal muscles that have not yet assumed their final orientation parallel to the already existing longitudinal strands. The latter assumption is supported by the fact that such diagonal strands are not readily apparent in later stages (see **Figure 5D**).

In *C. mutabilis*, only 5-dpf stages were examined. At this stage, ventro-laterally located, longitudinally oriented strands composed of 2–4 fibers on both sides of the mouth opening are detected (**Figure 5A**: *llm*). A few signals reach from in front of the mouth opening posteriorly, extending along almost the complete length of the larva. Additionally, a median, longitudinal strand, composed of 3–4 paired signals extends along the dorsal side (**Figure 5A**: *dlm*). In this strand, only 1–2 fiber-signals extend the full body length. A group of circular f-actin signals is present in front of the mouth opening (**Figure 5A**: *acm*). The signals are stronger on the dorsal side, diminishing in intensity while extending around the circumference of the larva toward the ventral side. The anterior-most of the signals form complete rings around the larva, whereas the posterior signals form rings that remain open ventrally. A single muscular f-actin signal is observable running alongside the posterior rim of the mouth opening (**Figure 5A**: *bm* and *mo*).

In the oldest observed stages of *C. armandi*, at 7-dpf, the already existing signals have not changed significantly. Only the longitudinal muscle signals on the dorsal side of the larva have slightly increased in intensity and seem to be more evenly spaced. On the ventral side, a buccal muscle becomes apparent behind mouth opening (**Figure 5D**: *bm*). In the posterior half of the body, a set of diagonal signals is seen that encircles the larva in an angle of 30–40° relative to the remaining circular muscles (**Figures 3B**, **5D**: *dm*). It cannot be ruled out that these diagonal signals are derivatives of the circular muscle signals, which they are crossing on the lateral sides of the larva.

Carcinonemertes carcinophila (Monostilifera, Hoplonemertea)

Post-embryonic Development

Although of comparably small size in *C. carcinophila* the opacity of the egg caused by finely dispersed yolk vesicles prevented unambiguous findings by optical examination [transmitted light and confocal laser scanning microscopy (CLSM)] prior to 3 days after egg deposition (*3-dpd*). Since development is somewhat asynchronous even among eggs within the same egg string, some gradual differences in development could be identified when comparing several specimens. Therefore, a superficial overview on early post-embryonic development at 18°C can be given.

In the earliest observable stages at 3-dpd, gastrulation is completed and the blastopore has already closed. The epidermal cells are adorned with multiple cilia showing α-tub-lir. Some invaginations are seen on the apical pole of the developing larva (data not shown). In more advanced stages at 3-dpd, the invagination of the proboscis rudiment and, slightly more ventral, the slender foregut rudiment can be detected as an internal cavity. A connection of the foregut cavity to the midgut cavity could not be clearly seen but its existence cannot be ruled out either. In some specimens, a tuft of elongate cilia emanating from the apical pit is visible (**Figure 6B**: *at* at 4-dpd). At 4-dpd, the larvae have hatched and are pelagic. Apart from the

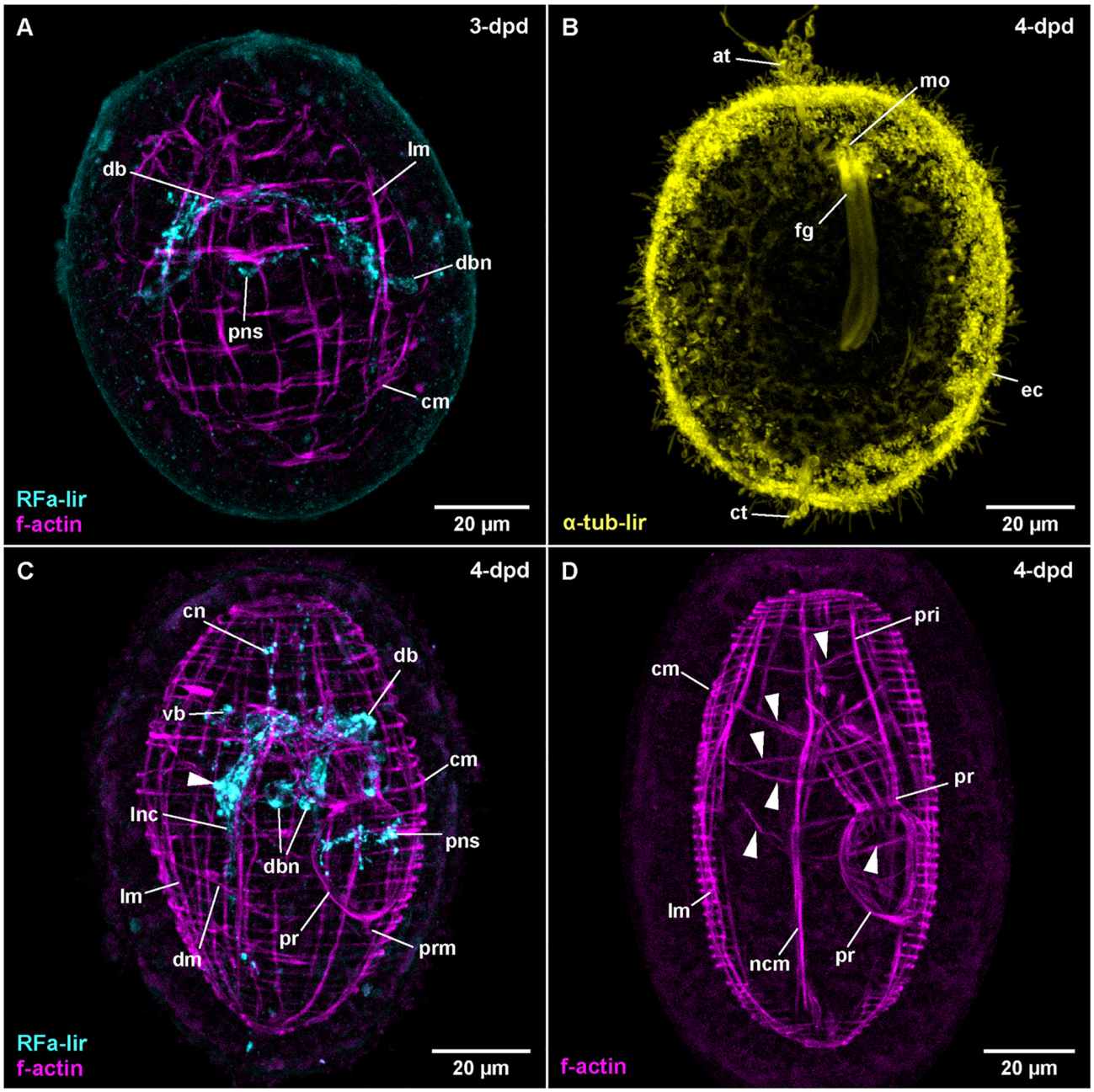

FIGURE 6 | *Carcinonemertes carcinophila* (frontal is up in all images, age of larval stages indicated in top right-hand corner, dpd: days post egg-deposition). **(A)** (RFa-lir: γ = 0.75, f-actin: γ = 0.7); maximum projection of 47 optical sections, dorsal view. **(B)** (γ = 0.6); maximum projection of 26 optical sections, ventro-lateral view. **(C)** (RFa-lir: γ = 0.8, f-actin: γ = 0.7); maximum projection of 45 optical sections, dorso-lateral view. *Arrowhead* indicates neuron-like signal in ventral part of brain ring. **(D)** (γ = 0.75); maximum projection of 21 optical sections, lateral view. *Arrowheads* indicate transversal muscle signals proximal of body wall muscle layers. at: apical tuft, cm: circular muscle, ct: caudal tuft, cn: cephalic neurite-like signal, db: dorsal part of brain ring, dbn: neuron of dorsal part of brain, dm: diagonal muscle, ec: epidermal cilia, fg: foregut, lm: longitudinal muscle, lnc: lateral nerve cord, mo: mouth opening, ncm: nerve cord muscle, pns: proboscis nervous-like signal, pr: proboscis, pri: proboscis insertion muscle, prm: proboscis retractor muscle, vb: ventral part of brain ring.

proboscis invagination and the apical pit, all other epidermal invaginations have disappeared. There is a tuft of elongated cilia emanating from the apical pit (**Figure 6B**: *at*). The foregut is open to the exterior via a mouth opening and there is a caudal tuft at the hind end of the larva visible in some specimens (**Figure 6B**: *fg*, *mo*, and *ct*). At this developmental stage, neither cilia of the midgut epithelium, nor of protonephridia are present. Furthermore, no anal opening or eyes are detected. The larvae

after 4-dpd represent the most advanced developmental stages of *C. carcinophila* studied. Further development of the larva could not be followed due to the lack of older larvae. Moreover, significant metamorphic changes in this ectoparasitic species will supposedly occur after the host, *C. maenas*, has been colonized (*cf.* Stricker and Reed, 1981 for *Carcinonemertes epialti*).

FMRFamide-Like Immunoreactivity

In *C. carcinophila*, the egg-membrane is permeable to antibodies, so that RFa-lir could be detected in developmental stages prior to hatching. In the least developed specimens examined, RFa-lir neurite-like signals can be detected in the future dorsal part of the brain ring (**Figure 6A**: *db*). Along with the neurite-like signals, up to two pairs of dorso-lateral RFa-lir brain neurons are seen (**Figure 6A**: *dbn*). In presumably more advanced stages, the first RFa-lir neurite-like signal in the proboscis rudiment is detectable (**Figure 6A**: *pns*). At this point in time, the lateral nerve cords begin to show short RFa-lir neurite-like signals (**Figure 3C**).

At 4-dpd, the RFa-lir neurite-like signals of the brain ring show it to be completely closed (**Figure 3C**: *vb* and *db*). The number of dorso-lateral neurons posterior of the brain ring has increased to three pairs (**Figure 6C**: *dbn*–only two visible on one body side). Ventral of the brain ring, two pairs of neurons are detected in its vicinity (**Figure 6C**: *arrowhead*) and there is possibly an additional pair anterior of the ventral part of the brain ring present. From the lateral sides of the ventral part of the brain ring, a paired RFa-lir neurite-like signal, presumably the first developing cephalic nerves, extends toward the anterior end of the larva (**Figure 6C**: *cn*). The RFa-lir neurite-like signals of the lateral nerve cords are elongated to the posterior end of the larva, where they connect to each other (**Figure 3C**). In the proboscis, there is a bundle of ring-shaped RFa-lir neurite-like signals in the anterior part of the bulbous region, with associated RFa-lir putative neuron-like signals, one each, ventrally and dorsally (**Figure 6C**: *pns*). In presumably more advanced stages, there seems to be a plexus of weak RFa-lir neurite-like signals underlying the epidermis in the periphery of the larva (data not shown).

F-Actin Labeling of Musculature

The first muscular f-actin signals are detected in 3-dpd stages that are still within the egg membranes. The signals constitute an unordered tangle of obliquely oriented fibers in the vicinity and anterior of the developing lateral nerve cords (as can be shown by double labeling with phalloidin and antibodies against FMRF-amide). The signals are somewhat more densely arranged in the anterior part of the body, as well as on its dorsal side. Judging from their orientation relative to the developing lateral nerve cords, the majority of these signals might be future longitudinal muscle signals, being located distal to the nerve cord signals. Anterior of the developing brain ring, some seemingly transverse signals, arguably future circular muscles are recognized (data not shown). In other still unhatched stages that are assumed to be more advanced, there are more or less evenly spaced longitudinal muscle signals arranged around the circumference of the larva (**Figure 6A**: *lm*). On the dorsal side, the longitudinal signals are more densely set than on the ventral side. Evenly spaced f-actin signals of circular muscles are distributed over the entire length of the larva, although their signals appear slightly weaker on the ventral side (**Figure 6A**: *cm*). In some of these stages the beginning of proboscis muscle development is seen as a bulbous, unordered mass of muscular f-actin signals on the dorsal side but proximal of the longitudinal muscle signals.

In 4-dpd stages, all examined specimens are hatched larvae. The longitudinal body wall muscles comprise evenly spaced signals spanning the complete length of the body that are overlain by the evenly spaced signals of the circular muscles (**Figure 6C**: *lm* and *cm*). The circular signals are also distributed along the complete length of the larva, although they are more densely set than the longitudinal signals (**Figure 6C**: *cm*). In some specimens, a few diagonally oriented f-actin signals located on the ventral side are visible (**Figure 6C**: *dm*), whereas in other, arguably more advanced larvae, the f-actin signals of the diagonal muscles are seen along most of the length of the larva, with most of the signals showing double stranded fiber zones (**Supplementary File 6**). Lateral nerve cord muscles are clearly seen at this stage, extending on the proximal side of the lateral nerve cords, anteriorly passing through the brain ring and ending on both ends of the larva among the body wall muscles (**Figures 6C**, D: *ncm*). The developing proboscis is divided into a posterior, bulbous portion that shows longitudinally oriented muscular f-actin signals only, and an anterior, funnel-shaped portion, that shows both proximal longitudinal and distal circular muscle signals (**Figures 3D**, **6D**: *pr*). Posteriorly, the bulbous portion of the proboscis is connected to the body wall longitudinal muscular signals by the short longitudinal f-actin signal of the proboscis retractor (**Figures 3D**, **6C**: *prm*). Anterior of the funnel-shaped portion, the muscular f-actin signals of the proboscis insertion are represented by a pair of ventro-lateral and a pair of dorso-lateral, longitudinal signals radiating from the anterior rim of the funnel-shaped portion of the developing proboscis the laterally to the body wall muscles (**Figures 3D**, **6D**: *pri*). The ventro-lateral pair runs more or less parallel to the anterior portion of the lateral nerve cord muscle signals. In the same stage, a series of additional transverse muscular f-actin signals are detected proximal of the longitudinal body wall muscles, in the vicinity of the proboscis and foregut (**Figure 6D**: *arrowheads*–not all muscles visible in maximum projection). From anterior to posterior these muscular signals comprise three pairs of dorso-ventral muscles, one strand on each side of the foregut and proboscis rudiment, one u-shaped muscle strand that is dorsally open, a posterior pair of dorso-ventral muscles similar to the anterior three pairs and a posterior u-shaped muscle strand that is open dorsally and forked at its dorsal ends. The function of these muscles can only be speculated about.

Amphiporus sp. (Monostilifera, Hoplonemertea)

Post-embryonic Development

Within one batch of eggs, development was observed to be somewhat asynchronous within a time range of up to 1 day. Therefore, the times of development are approximations for a water temperature of 18°C. After 1-dpd, the majority of

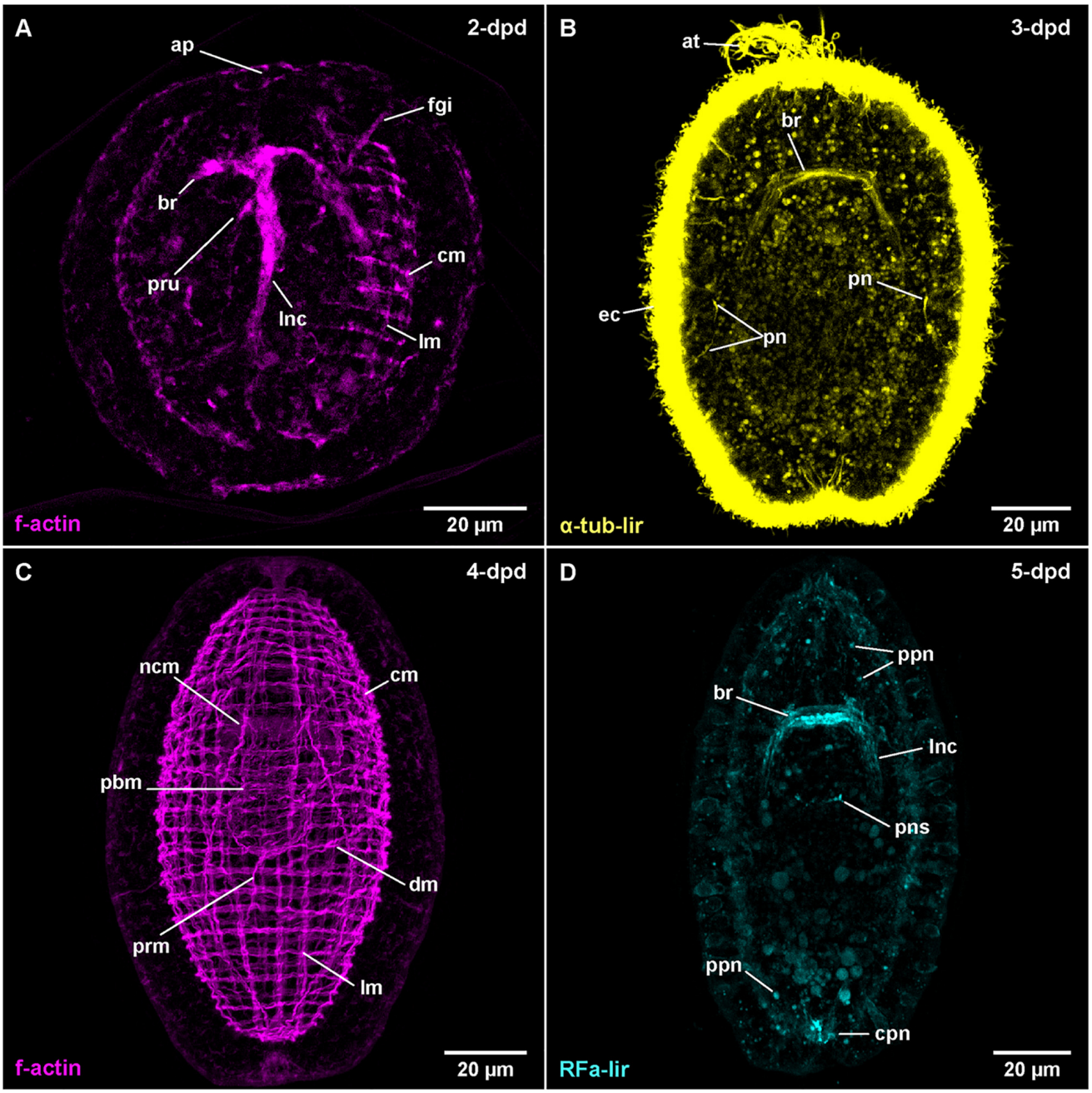

FIGURE 7 | *Amphiporus* sp. (frontal is up in all images, age of larval stages indicated in top right-hand corner, dpd: days post egg-deposition). **(A)** (γ = 1.0); maximum projection of 50 optical sections, ventro-lateral view. **(B)** (γ = 1.1); maximum projection of 15 optical sections, ventral view. **(C)** (γ = 0.7); maximum projection of 46 optical sections, dorsal view. **(D)** (γ = 1.1); maximum projection of 16 optical sections, dorsal view. at: apical tuft, br: brain ring, cm: circular muscle, cpn: caudal peripheral neuron, dm: diagonal muscle, ec: epidermal cilia, fgi: foregut invagination, lm: longitudinal muscle, lnc: lateral nerve cord, ncm: nerve cord muscle, pbm: proboscis muscle, pn: protonephridium, pns: proboscis nervous-like signal, ppn: peripheral plexus neuron, prm: proboscis retractor muscle.

developmental stages have completed gastrulation and the blastopore is closed. At one, presumably the apical pole of the larva, some epidermal invaginations have formed (data not shown). Of these epidermal invaginations, the invagination of the apical pit and, slightly more ventral and deeper, the epidermal in-folding of the developing proboscis remain visible after 2-dpd (**Figure 7A**: *ap* and *pru*). A narrow, elongate inner cavity, located anterior and slightly ventral of the forming proboscis represents the rudiment of the foregut (**Figure 7A**: *fgi*). At 3-dpd, the majority of larvae have hatched and are pelagic, spherical stages completely covered with cilia as shown by α-tub-lir (**Figure 7B** at 3-dpd). They possess a well-developed apical tuft of cilia emanating from the apical pit and a pair of eyes, situated dorso-laterally, slightly posterior of the anterior end of the larva

(data not shown). A pair of simple, unbranched protonephridia is detectable by the cilia of their nephroduct laterally on each side, halfway along the length of the larva (**Figure 7B**: *pn*). After 3-dpd, the anteriorly located, densely ciliated foregut opens to the exterior and a caudal tuft of elongated cilia at the hind-end of the larva begins to form (data not shown). The larvae survived for two additional weeks and became more elongate until they started to degenerate after 18-dpd. At that stage, the mouth opening is still independent of the proboscis pore and a stylet has also not formed yet (data not shown).

FMRFamide-Like Immunoreactivity

Although gastrulation and organogenesis already begin prior to hatching, no immunohistochemical staining could be accomplished owing to the impermeability of the egg-membranes to antibodies. The earliest result of immunohistochemical staining are therefore available for post-hatching stages later than 2-dpd. However, in the subsequent stages, the tissue has a strong autofluorescence that obscures several of the weaker signals in maximum projections of the image series.

The first RFa-lir neurite-like signals that develop are those of the brain ring (**Figure 3C**). It should be noted however, that the signals in the dorsal part of the brain ring are stronger than in the ventral part and the lateral transition from the dorsal to the ventral side of the brain ring showed especially weak signals. Due to strong autofluorescence, RFa-lir neuron-like signals could not be unambiguously identified in the brain ring in early stages. Later, at 4-dpd, a pair of small lateral and 1–3 larger median RFa-lir neuron-like signals are visible anterior of the dorsal part of the brain ring neurite-like signals (**Supplementary File 7**). The lateral nerve cords show RFa-lir neurite-like signals throughout their entire length, as well as, in more advanced stages, a connection in their posterior-most extension (**Figure 3C**). No unambiguously identifiable neuron-like signals along the lateral nerve cord neurite-like signals could be found. Additionally, a semicircular RFa-lir neurite-like signal perpendicular to the longitudinal body axis is detected in the inverted outer epithelium of the developing proboscis. It develops into a ring-shaped, RFa-lir neurite-like signal surrounding the transition zone between the anterior cylindrical and the posterior bulbous part of the developing proboscis by 5-dpd (**Figures 3C**, **7D**: *pns*).

In 5-dpd stage larvae, the overall strength of the brain ring and lateral nerve cord neurite-like signals is slightly increased (**Figure 7D**: *br* and *lnc*). From the brain ring, two pairs of RFa-lir neurite-like signals extend anteriorly, one located ventro-laterally the other dorso-laterally. Several peripheral RFa-lir neuron-like signals are observed at both the anterior, dorsal and the posterior pole of the larva, at the base of the caudal tuft (**Figure 7D**: *cpn*, **Supplementary File 8**). The posterior neuron-like signal aggregation is in close vicinity to the posterior connection of the lateral nerve cords, whereas the anterior neuron-like signal aggregation is in the position where the frontal organ is located in the adult animal. The anterior neuron-like signals are therefore interpreted as the first sensory neurons of the frontal organ. Several peripheral, neuron-like signals are irregularly distributed along the length of the larva (**Figure 7D**: *ppn*). They might represent sensory neurons of a developing peripheral plexus.

After 5-dpd, observation of the nervous system was hampered by difficulties to deliver the antibodies through the body wall musculature to the proximal components of the nervous system without severely compromising the integrity of the larva. Thus, the brain and the lateral nerve cords are comparably weakly stained. In 7-dpd larvae, the epidermis shows a strong fluorescence, so that no internal signals are visible. In the oldest stage (14-dpd), the epidermis shows less intense fluorescence revealing RFa-lir neurite-like signals of the brain ring and the lateral nerve cords (**Figure 8B**: *br* and *lnc*). Anteriorly, the brain and the posterior end of the lateral nerve cords are connected to the anterior and posterior masses of several intensely fluorescent neurite-like and a few neuron-like signals (**Figure 8B**: *fpn* and *cpn*). Both signal aggregations extend from the interior to the surface of the epidermis where they are confluent with the neurite-like signals of a peripheral plexus that extends at the base of numerous, lightly fluorescent epidermal gland cells along the entire body (**Figure 8B**: *pp*). Further development was not observed.

F-Actin Labeling of Musculature and Nervous System

The first f-actin signals labeled with phalloidin are visible in developmental stages at 2-dpd that have not yet hatched from the egg case (**Figure 7A**). The earliest signals detected do not obviously belong to developing muscles but are signals of the developing nervous system, comprising the brain ring and the first rudiments of the lateral nerve cords. In later, but still unhatched stages of this age, fluorescent signals outline a completely developed brain ring that shows stronger signal in its ventral portion and a pair of lateral nerve cords (**Figure 7A**: *br* and *lnc*). The lateral nerve cords, however, do not yet show a posterior connection. Earliest f-actin signals belonging to the body wall muscles are seen as four longitudinally oriented strands, situated in dorso- and ventro-lateral positions, two on each side of the body (data not shown). The signals of the developing longitudinal muscles are weaker in intensity than the signals of the brain and lateral nerve cords. In hatched specimens at 2-dpd, signals of the circular muscles are also detected. They are distributed along the entire length of the larvae and span its circumference on the dorsal and ventral side, thereby showing a gap above the signals of the lateral nerve cords (**Figure 7A**: *cm*, **Supplemetary File 9**). At this stage, the signals of the longitudinal muscles are more numerous but thinner and distributed over the dorsal and ventral sides of the larva (**Figure 7A**: *lm*). However, there are fewer longitudinally extending muscular f-actin signals than there are circular signals.

After 3-dpd, all examined larvae are hatched and both longitudinal and circular muscular f-actin signals are more or less evenly distributed over the larva. The signals of muscular f-actin become more pronounced on the lateral sides of the body and generally stronger than the diffuse f-actin signals of the brain ring and the lateral nerve cords. Both the longitudinal and the lateral signals of the body wall muscles are first arranged in groups of 1–3 (mostly 2) closely set fibers that are evenly spaced from the neighboring groups. The groups of circular signals are more numerous and more densely set than the groups of longitudinal signals. The signals of the longitudinal and circular muscles have significantly increased in intensity in the 4-dpd stages, with the

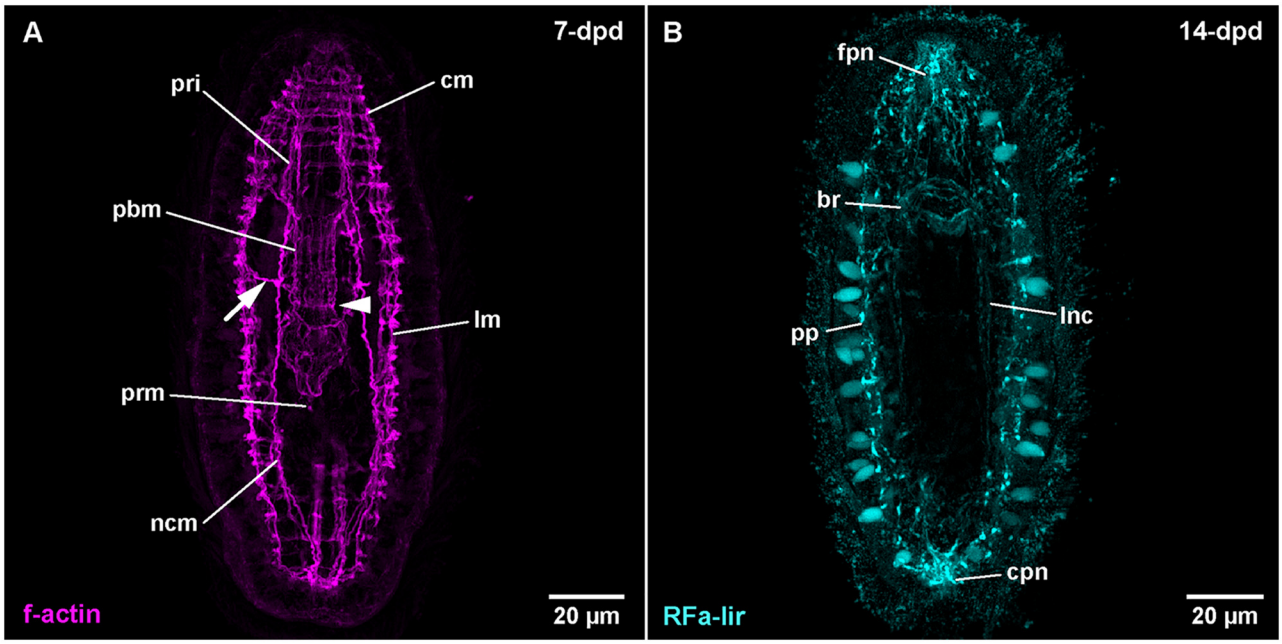

FIGURE 8 | *Amphiporus* sp. (frontal is up in all images, age of larval stages indicated in top right-hand corner, dpd: days post egg-deposition). **(A)** (γ = 0.9); maximum projection of 11 optical sections, ventral view. *Arrowhead* marks sphincter-like f-actin signal in proboscis, *arrow* marks signals extending from nerve cord muscle to body wall muscles. **(B)** (γ = 0.8); maximum projection of 13 optical sections, ventral view. br: brain ring, cm: circular muscle, cpn: caudal peripheral neuron, fpn: frontal peripheral neuron, lm: longitudinal muscle, lnc: lateral nerve cord, ncm: nerve cord muscle, pbm: proboscis muscle, pp: peripheral plexus, pri: proboscis insertion muscle, prm: proboscis retractor muscle.

former also having notably increased in numbers (**Figure 7C**: *lm* and *cm*). The grouped arrangement is still apparent as described before. Adjacent to the diffuse signals of the lateral nerve cords, on their proximal side, there is a single muscular f-actin signal on each side first detected in 3-dpd stages, the signal of the lateral nerve cord muscles, running parallelly to the lateral nerve cords and anteriorly passing through the brain ring (**Figure 7C**: *ncm* at 4-dpd). Anteriorly and posteriorly, the lateral nerve cord muscle signals end at the level of the anterior and posterior end of the body wall muscles, respectively (**Figure 7C**: *ncm*). The lateral nerve cord muscle signals increase in intensity by 4-dpd. In supposedly more advanced stages at 3-dpd and even more obvious at 4-dpd, the first diagonal f-actin signals of the body wall muscles are observed on the ventral and ventro-lateral sides between the circular and the longitudinal signals. The signals run in an angle of 30–45° to the f-actin signals of the circular muscles (**Figure 7C**: *dm*). They comprise few, widely separated fibers along the mid-body region of the larva that cross on the ventral midline in 3-dpd stages and additional weak signals present on the dorsal side of the body on the level of the posterior bulbous part of developing proboscis at 4-dpd. At this stage on the ventral and lateral sides, multiple crisscrossings of diagonal signals are seen **Supplementary File 10**.

The proboscis rudiment shows the first f-actin signals of its muscles as early as 3-dpd. They comprise few weak signals, arranged both longitudinally and circularly around the posterior, bulbous part. They become stronger during subsequent development when distinct longitudinal, some obliquely oriented, and few weak circular muscular f-actin signals around the posterior, bulbous part of the proboscis rudiment form. At the same time, the anteriorly adjacent cylindrical part shows outer circular and inner longitudinal, muscular f-actin signals (**Figures 3D**, **7C**: *pbm* at 4-dpd). One pair of longitudinal muscular f-actin signals extends in the dorsal wall of the anterior, funnel-shaped part of the proboscis, running roughly parallel to the lateral nerve cord muscle signals, which in turn run in the ventral wall of the funnel-shaped part of the developing proboscis apparatus in this body region. The former signals are tentatively addressed as developing proboscis insertion muscles (**Figure 8A**: *pri* at 7-dpd). In addition, at 4-dpf, 1–2 pairs of f-actin signals extend radially from the from the anterior rim of the cylindrical part of the developing proboscis invagination to the body wall muscles (**Supplementary File 10**). A strand of longitudinal muscular f-actin signals belonging to the developing proboscis retractor muscle, extend from the posterior end of the bulbous part of the developing proboscis to the longitudinal body wall muscle signals. It is seen to elongate during further development (**Figure 7C**: *prm*). Other muscular f-actin signals occasionally detected in younger larval stages comprise few transversally and radially oriented thin strands around the proboscis rudiment and the foregut, proximal of the inner longitudinal body wall muscles (not visible in maximum projection). In 4-dpd larvae, a series of muscular f-actin signals around the proboscis apparatus and foregut are detected. They comprise a dorsally open, u-shaped muscle that extends to the dorsal body wall muscles, two pairs of radial signals extending to the lateral body wall muscles, and one pair extending to the anterior body wall muscles. Three pairs of radial muscles are seen running to the dorsal body wall muscles

(not visible in maximum projection, but reminiscent of signals in *C. carcinophila* in **Figure 6D**: *arrowheads*).

The larvae after 4-dpd show a general increase in intensity of the muscular f-actin signals, especially of the body wall muscles. The signals of the diagonal body wall muscles are seen to also cross on the dorsal side at this developmental stage (**Supplementary File 11**). The lateral nerve cord muscle signals are now composed of at least two parallel fibrous signals (**Figure 8A**: *ncm* at 7-dpd). In larval stages at 7-dpd, apart from the muscle signals described for the preceding stages, an additional pair of longitudinal muscular f-actin signals has developed, flanking the foregut on both sided in a proximal position relative to the inner longitudinal body wall muscles (**Supplementary File 12**). In the developing proboscis, a strong ring-shaped muscular f-actin signal is seen that is delimiting the anterior and the posterior half of the middle cylindrical portion of the developing proboscis (**Figure 8A**: *arrowhead*). Occasionally, 1–2 muscular f-actin signals are seen on each side distally extending from the lateral nerve cord muscles to the longitudinal body wall muscle signals in the anterior half of the larva (**Figure 8A**: *arrow*). In successive stages, up to 14-dpd, the existing muscular signals become stronger and especially the cylindrical part of the developing proboscis apparatus becomes more muscular, thus changing its shape to become more or less dumbbell-shaped with its narrowest part being demarcated by the ring-shaped sphincter muscle formed at 7-dpd (data not shown). In the area of the proboscis insertion, additional but weaker longitudinal muscular f-actin signals fan from proximal to distal between the existing stronger longitudinal muscle signals of the proboscis insertion (data not shown). In the most advanced larvae at 18-dpd, before the larvae started to degenerate, no additional muscular systems have formed.

DISCUSSION

Novel Findings on the Development of Body-Wall Muscles and RFa-lir Nervous System

Information on the development of the musculature by means of fluorescent phalloidin labeling and examination with confocal microscopic setups is only available to some detail in the hoplonemertean species *Nemertopsis bivittata*, *Paranemertes peregrina*, and *Pantinonemertes californiensis* (Martindale and Henry, 1995; Maslakova and von Döhren, 2009; Hiebert et al., 2010). In some pilidiophoran species, such as *Maculaura* (as *Micrura*) *alaskensis*, *Lineus ruber*, *Lineus viridis*, and *Micrura wilsoni*, but also the palaeonemertean species *Carinoma tremaphoros*, data on only few stages have been published (Maslakova et al., 2004; Maslakova, 2010b; von Döhren, 2011; Hiebert and Maslakova, 2015b; Martín-Durán et al., 2015). A comparable situation is encountered in the development of the nervous system components with immuno-fluorescent methods, with the serotonin-immunoreactive (*5HT-lir*) component having been subject to more detailed analyses. Data on the development of the 5HT-lir nervous system is available for the pilidiophoran species *M. alaskensis*, *Lineus albocinctus*, as well as an unidentified pilidium-larva of the *gyrans*-type (supposedly *Micrura purpurea*) (Hay-Schmidt, 1990; Maslakova, 2010b; Hindinger et al., 2013); for the hoplonemertean species *Quasitetrastemma stimpsoni* and *P. californiensis* (Chernyshev and Magarlamov, 2010; Hiebert and Maslakova, 2015a); and for the palaeonemertean species *Carinina ochracea* (von Döhren, 2016). Data on the development of the RFa-lir component of the nervous system are scarcer, having only been published for the palaeonemertean species *C. ochracea* and the pilidium larvae of two heteronemertean Pilidiophora, *L. albocinctus* and an unidentified pilidium-larva of the *gyrans*-type, tentatively assigned to *M. purpurea* (Hay-Schmidt, 1990; Hindinger et al., 2013; von Döhren, 2016). To date, no modern investigation has focused on the joint development of body wall musculature and nervous system so that the available data comes from histological examinations only. However, the descriptions are partly contradicting (reviewed in von Döhren, 2015). The present paper reports the first data on the development of the RFa-lir component of the nervous system in two hoplonemertean representatives and significantly expands the knowledge on Palaeonemertea, with data on three additional species.

Development of the RFa-lir Nervous System Is Relatively Uniform in Nemertea but Development of the Body Wall Muscles Differs Significantly

In the examined palaeonemertean species, the first detectable muscular elements are a pair of lateral muscle bundles in the vicinity of the mouth opening in the *C. armandi* and a single short, longitudinal signal dorsally, followed soon after by a pair of lateral bundles in *T. polymorphus*. A similar sequence as in *T. polymorphus* is also suggested for *C. mutabilis*. Furthermore, a muscle ring surrounding the mouth opening becomes apparent in the larva. Subsequently in *T. polymorphus* and *C. armandi*, the muscle strands extend toward anterior and posterior and the lateral bundles seem to distribute dorsally to attain a more or less evenly spaced arrangement of muscle strands along the dorsal and the lateral sides of the body. At the same time the first circular muscle signals appear anterior of the mouth opening on the dorsal side and elongate ventro-laterally. Several additional circular signals appear on the dorsal side anterior and posterior of the first signals. Whereas the circular muscles are added almost up to the anterior tip of the larva, progress of the circular muscles posteriorly stops in front of the mouth opening and an additional region of circular muscle formation appears some distance behind the mouth opening. From here, additional circular muscles are added posteriorly and anteriorly. Data on the development of the body wall musculature in *C. tremaphoros*, although not as detailed, are largely congruent with the herein reported data: longitudinal muscles develop prior to circular muscles in a dorsal to ventral progression and no proboscis muscles are seen to develop in the early larval stage. Circular, but also diagonal muscles have been found in stages as early as 30 h of development (Maslakova et al., 2004). The early formation of the main components of the body wall muscles indicates somewhat faster development in *C. tremaphoros*. Regarding formation of longitudinal body wall muscles with dorsal longitudinal muscles formed prior to

lateral longitudinal muscles, *C. tremaphoros* seems to be more similar to *T. polymorphus* than to *C. armandi*. Outside of Nemertea, this type of body wall muscle formation, especially of the circular component, has never been reported before (*cf.* Wanninger, 2009). In the hoplonemertean species examined, formation of the longitudinal component and shortly afterward the circular component of the body wall muscles seems to be almost synchronous (Maslakova and von Döhren, 2009; Hiebert et al., 2010). In contrast to muscle development in *Amphiporus* sp., *P. peregrina*, and probably also *P. californiensis*, the muscles are not formed in their definite position in *C. carcinophila* but seem to become evenly distributed later during the course of development to constitute the definite orthogonal arrangement of circular and longitudinal muscle strands. Both the longitudinal and circular muscles are fully formed at the time of hatching. The diagonal muscles in the hoplonemertean species examined develop after hatching *in situ*; in *C. carcinophila* and *Amphiporus* sp. most likely, if not as independent entities, as derivatives of the longitudinal musculature. While the muscles of the proboscis apparatus and the lateral nerve cord muscles develop shortly after the larva has hatched in the hoplonemertean species, there is no sign of proboscis muscle development in any of the examined palaeonemertean species during the observed development.

No signs of differentiated nervous systems could be detected by immunolabelling with antibodies against FMRFamide in the newly hatched larvae of the examined palaeonemertean species. It is only later in the elongating larvae that the brain ring, the neurite bundles around the mouth opening and subsequently, the lateral nerve cords and a peripheral plexus develop. Even in the most advanced stages investigated, no trace of neuronal elements of the future proboscis apparatus was seen. In *C. ochracea*, the only other palaeonemertean species investigated for the development of the RFa-lir nervous system the sequence of formation is nearly identical. Development of the RFa-lir nervous system component is first seen in the dorsal portion of the brain ring and progresses from there to the ventral side of the larva, where the ventral portion of the brain ring forms and the lateral nerve cords develop. Also, the distribution of neuronal perikarya is essentially the same (von Döhren, 2016). The early appearance of a longitudinal RFa-lir dorsal nerve is a character *C. ochracea* shares with *T. polymorphus*, it is not seen to form in the examined *Carinoma* species, although they possess dorsal nerves as adults (Beckers et al., 2013). In both *C. carcinophila* and *Amphiporus* sp., the brain ring begins to form before hatching, although in *C. carcinophila*, like in the palaeonemertean species studied, formation of the dorsal part precedes that of the ventral part (this study and von Döhren, 2016). The lateral nerve cords are fully developed at the time of hatching in *Amphiporus* sp. and shortly after in *C. carcinophila*. Development of the proboscis nervous system, on the other hand, seems to begin earlier in *C. carcinophila*. Only the peripheral nerve plexus begins to develop after the larva has hatched in both species.

In Pilidiophora, the nervous system is described to develop with the brain ring forming prior to the development of the lateral nerve cords, and thus in a similar way as described for palaeonemertean and hoplonemertean species (reviewed in von Döhren, 2015). Development of the RFa-lir component of the peptidergic nervous system is unfortunately not detailed enough to allow for comparison of the developmental sequence (Hindinger et al., 2013). With the exception of *L. ruber* that has a derived intracapsular larval type, the development of the body wall muscles in Pilidiophora, has not been subject to detailed, comparative investigations using fluorescent staining and confocal microscopy observations (Martín-Durán et al., 2015). In *L. ruber* and *L. viridis*, the larval tissues are devoid of musculature and juvenile muscles begin to develop late, shortly before the larval envelope is shed (von Döhren, 2011; Martín-Durán et al., 2015). In the former species the first differentiated muscles are detected around the mouth opening and in the cephalic lobe, followed later by the body wall muscles and the musculature of the pharynx (Martín-Durán et al., 2015). In the various histological investigations, there seems to be some discord as to whether the longitudinal or the circular component of the body wall muscles develops first, but all studies agree in that the body wall muscles of the juvenile are formed independently of the larval musculature of the pilidium (reviewed in von Döhren, 2015). Clearly, a closer look at the development of the musculature of pilidiophoran species with immunofluorescent staining and CLSM would refine the picture and help resolve the prevailing contradiction in the descriptions.

Heterochronic Effects in Neuromuscular System-Development Might Be Correlated With Morphological Diversity in the Adults

The diversity in the development of muscles and nervous system in the investigated nemertean species differs most strikingly in the degree of differentiation of the respective organ systems at the time of hatching. In palaeonemertean larvae, the first muscular and RFa-lir nervous elements are formed in the larva after hatching. The main difference between the two palaeonemertean species examined lies in the timing of development of the body wall musculature. Relative to the developing RFa-lir nervous system, development of the body wall muscles starts considerably later in *T. polymorphus* than in *Carinoma* species (this study and Maslakova et al., 2004). Presently, it remains unclear whether this difference represents an acceleration in *C. armandi* or a deceleration in *T. polymorphus*. In hoplonemertean larvae, the timing of development of the respective organ systems is rather different. According to published results on *P. peregrina* and *P. californiensis*, the main components of the body wall muscles develop in the early pelagic larval stage after hatching (Maslakova and von Döhren, 2009; Hiebert et al., 2010), whereas in *C. carcinophila* and *Amphiporus* sp., most of the body wall musculature have already formed before the larva hatches. With the nearly synchronous mode of muscle formation, the only true difference between the herein described species on the one hand and *P. peregrina* and *P. californiensis* on the other hand, seems to be the time of hatching, that is delayed in *Amphiporus* sp. and *C. carcinophila*. For the development of the RFa-lir component of the peptidergic nervous system in Hoplonemertea, there was no detailed-enough comparative data available prior to this investigation. In the palaeonemertean species *C. ochracea*, *T. polymorphus* and the *Carinoma* species, the RFa-lir component

of the brain ring and the lateral longitudinal nerve cords develop after the larvae have hatched (this stuy and von Döhren, 2016). In *C. carcinophila* and *Amphiporus* sp. on the other hand, the RFa-lir component is already beginning to differentiate before hatching. Further investigations in other hoplonemertean species will have to show whether the onset of the formation of the RFA-lir component of the nervous system similarly coincides with onset of muscle formation or starts earlier, as seen in *T. polymorphus*.

Irrespective of the developmental progress at hatching, development of the neuromuscular system in Hoplonemertea shows a heterochronic shift compared to Palaeonemertea and Pilidiophora. The components of the proboscis muscles and nervous system, which are clearly adult structures, form before or soon after hatching in Hoplonemertea (this study and Maslakova and von Döhren, 2009; Chernyshev and Magarlamov, 2010; Hiebert et al., 2010; Hiebert and Maslakova, 2015a). A general acceleration of development in Hoplonemertea compared to Palaeonemertea and Pilidiophora and thus considerably shorter time needed for metamorphosis in hoplonemertean species, has long been known for Nemertea, (Iwata, 1960). Interestingly, morphological diversity with respect to the nervous system and musculature seems to be negatively correlated with the duration of post-embryonic development. Hoplonemertean larvae, in which development is accelerated, show comparably uniform adult neuromuscular morphologies. In palaeonemertean and pilidiophoran species, formation of juvenile structures takes much longer (Iwata, 1960; Maslakova, 2010b; Beckers et al., 2015). On the other hand, morphological diversity of musculature and nervous system, e.g., proboscis musculature and brain anatomy, is much higher in these lineages (Chernyshev, 2010, 2015; Beckers et al., 2013, 2018; Beckers, 2015). It remains to be shown if this different diversity observed is due to developmental timing or if acceleration of the formation of prospective adult structures in Hoplonemertea was only made possible because of relatively uniform morphology in the first place.

No Transitory Muscle or RFa-lir Nervous System Elements Are Detected in Palaeo- or Hoplonemertean Larvae

In recent years, employing fluorescent and immunofluorescent methods to follow the development of spiralian larvae has led to an enormous increase of comparative data in a number of clades, foremost in Annelida and Mollusca, but also in Lophophorata, Entoprocta, and Platyhelminthes (Temereva, 2012; Temereva and Wanninger, 2012; Temereva and Tsitrin, 2013, 2014; Sonnleitner et al., 2014; Audino et al., 2015; Bleidorn et al., 2015; Scherholz et al., 2015; Wanninger, 2015; Wanninger and Wollesen, 2015; Kristof et al., 2016; Sun et al., 2019). However, whereas patterns are emerging in the more well-studied clades, others, such as Nemertea, remained largely unknown from a comparative perspective.

Among Lophotrochozoa (*s. str.*), the most prevalent type of larva is the trochophore-type larva that has therefore been suggested to represent the ancestral lophotrochozoan larval form (Marlow et al., 2014; Nielsen, 2018; Malakhov et al., 2019; Wang et al., 2020). With comparably few, arguably derived exceptions, the trochophore-type larva and its presumably related forms, such as the actinotrocha-larva of Phoronida, and the different larval-types of Brachiopoda, Ectoprocta, and Entoprocta, show certain comparable, and hence assumingly homologous, muscular and neural structures (Wanninger, 2008, 2009; Nielsen, 2012, 2013, 2015). They comprise: (1) the prototroch muscle ring, a ring muscle underlying the prototroch (an equatorial band of cells adorned with differentially elongated, compound cilia); (2) the trochal neurite (bundle), a neurite or neurite-bundle that runs alongside the prototroch ring muscle; and (3) the apical organ comprising a group of cells, some with apical extensions that project into the apical pit or in its vicinity. The apical organ is minimally composed of a small to moderate number of flask-shaped 5HT-lir and a small number of RFa-lir cells (Wanninger, 2008). All of these structures are considered larval, since they commonly develop early in development and disappear later, during metamorphosis. In Nemertea, the pilidium has been, until more recently, assumed to represent the larval type that is homologous to the trochophore-type larva. Therefore, the nervous and muscular elements of the apical pit and the marginal band in the pilidium and the trochophore-type larva were interpreted as homologous (Nielsen, 2005, 2012). However, molecular phylogenetic analyses have clearly shown that the pilidium is restricted to the taxon Pilidiophora, which in turn represents a derived clade within Nemertea (Thollesson and Norenburg, 2003; Andrade et al., 2014). Therefore, it is more parsimonious that the pilidium larva is not the ancestral larval form of Nemertea. As a consequence, musculature and nervous system of the pilidium are most likely not homologous to respective structures in the trochophore-like larval type (Maslakova and Hiebert, 2014).

The absence of elaborated larval structures, such as the prototroch in larvae of Palaeonemertea and Hoplonemertea is reflected by the development of the nervous system and body-wall muscles. Whereas the first muscular element to develop in most lophotrochozoan larvae is the larval prototroch muscle ring (Wanninger, 2009; Bleidorn et al., 2015), the first muscles to develop in nemertean larvae are the longitudinal muscles of the body wall (this study and Maslakova et al., 2004; Maslakova and von Döhren, 2009; Hiebert et al., 2010; von Döhren, 2015). The circular muscles anterior of the mouth opening that develop subsequently in palaeonemertean species are different from the prototroch muscle ring of trochophore-type larvae in that they are located a noticeable distance away from the mouth opening instead of adjacent to the mouth opening as in most feeding trochophore-type larvae. Additionally, they are, unlike the prototroch muscle ring, obviously not transitory muscles (this study). Neither in hoplonemertean nor in palaeonemertean larvae, RFa-lir trochal neurites have been observed (this study and von Döhren, 2016). The brain ring in Palaeonemertea is seen to form from putative neuroblasts presumably originating from the apical pit and later the paired lateral nerve cords develop from its ventral portion. A similar sequence of development is described for the 5HT-lir component of the nervous system, although development starts in the ventral portion of the brain ring (von Döhren, 2016). The identity of the brain ring as a

non-larval structure becomes evident from its position in the hoplonemertean larvae, in which it surrounds the developing proboscis and, at the same time, is located posterior to the mouth opening; an arrangement that is identically found in adults of Hoplonemertea (Maslakova and von Döhren, 2009; Beckers et al., 2018). The early developing ring-shaped brain is thus clearly different and not comparable with the trochal neurites or neurite bundles of trochophore-type larvae.

Although an apical pit with an apical tuft of cilia is present in the trochophore-type larva as well as in all planktonic larval types of nemerteans, the respective expressions of RFa-lir neurons are clearly different. In many trochophore-type larvae, the apical organ neurons show RFa-lir early in development and the RFa-lir component of the brain develops later in close vicinity to the apical neurons (Wanninger, 2009). In nemertean larvae, no comparably clear signal of RFa-lir expressing apical neurons is detectable. In larvae of the examined palaeonemertean species, faint signals are seen instead, that have disappeared when the first clear signals of the future dorsal part of the RFa-lir component of the brain ring are visible (this study). Due to their faint and very short expression, these signals are interpreted as yet undifferentiated RFa-lir brain neurons that invade the larva from the apical pit and its vicinity. They are thus most likely identical to the first clearly visible RFa-lir neuron-like signals of the dorsal brain ring. Although this does not preclude the RFa-lir apical neurons of the trochophore-type larva from being homologous to the faint early RFa-lir signals in palaeonemertean larvae as neuroblasts, their respective developmental fate cannot be considered truly homologous. Later developing peripheral RFa-lir neurons with presumably sensory function in both palaeonemertean and hoplonemertean larvae should be interpreted as components of the developing peripheral plexus, that is also present in the adults and therefore not a transitory larval trait homologous to the early apical neurons of lophotrochozoan larvae.

CONCLUSION

Details on the developmental diversity in Nemertea are only starting to become known. However, some interesting aspects are emerging that deserve to be pursued in the future–in Nemertea but also beyond:

(1) Most of within clade morphological diversity in Nemertea seems to result from post-embryonic development. Future research needs to concentrate on the mechanisms that generate the morphological diversity.
(2) Acceleration of development seems to be correlated with decreasing morphological diversity in Hoplonemertea. It remains to be investigated, which is the cause and which is the result and whether this correlation also holds true on a larger scale.
(3) The hypothetical, ancestral nemertean larva seems to lack strictly larval structures in the investigated neuromuscular system components. Whether this lack is ancestral or derived with respect to the assumingly ancestral trochophore-type larva of Lophotrochozoa can only be answered when a robust placement of Nemertea within the phylogeny of Spiralia is available.

DATA AVAILABILITY STATEMENT

The original contributions presented in the study are included in the article/**Supplementary Material**, further inquiries can be directed to the corresponding author.

AUTHOR CONTRIBUTIONS

The author confirms being the sole contributor of this work and has approved it for publication.

FUNDING

The work at Friday Harbor Laboratories was financially supported by a German Research Council-grant (DFG: Ba 2015/11-1) and the work at the Station Biologique de Roscoff was made possible with financial support by the ASSEMBLE Marine program of the EU ("Comparative development in Nemerteans").

ACKNOWLEDGMENTS

I would like to gratefully acknowledge the staff of the Friday Harbor Laboratories, and especially S. A. Maslakova for assistance with collecting and fertilizing of *Carinoma mutabilis* and rearing, staining and imaging of the larvae of this species. I would also like to express my gratitude to the staff of the Station de Biologie Marine de Concarneau, for offering hospitality during the collecting trips for *Carinoma armandi*, the staff of the Wattenmeerstation of the AWI Bremerhaven in List auf Sylt, including the crew of the research vessel "Mya" for providing laboratory facilities and conducting collecting cruises for *Carcinonemertes carcinophila*, and the staff of the Station Biologique de Roscoff for providing equipment and laboratory facilities for collecting and fertilizing *Tubulanus polymorphus* and rearing the larvae of this species. I would also like to thank T. Bartolomaeus for helping to collect several of the included species and C. Müller from the Institute of Evolutionary Biology and Ecology of the University of Bonn for staining and imaging of larvae of *Amphiporus* sp., *C. armandi*, *C. carcinophila*, and *T. polymorphus*. The editor and the reviewers are gratefully acknowledged for helpful comments.

SUPPLEMENTARY MATERIAL

The Supplementary Material for this article can be found online at: https://www.frontiersin.org/articles/10.3389/fevo.2021.654846/full#supplementary-material

Supplementary Table 1 | Adjustments of CLSM-stacks made with Fiji (ImageJ version 1.53c).

Supplementary File 1 | fly-through video of image stack of *Tubulanus polymorphus* 4-dpf, same as in **Figure 1C**.

Supplementary File 2 | fly-through video of image stack of *Tubulanus polymorphus* 6-dpf, same as in **Figure 2A**.

Supplementary File 3 | fly-through video of image stack of *Carinoma armandi* 2-dpf, RFa-lir, frontal is up.

Supplementary File 4 | fly-through video of image stack of *Carinoma armandi* 5-dpf, RFa-lir of specimen in **Figure 5B**.

Supplementary File 5 | fly-through video of image stack of *Carinoma armandi* 7-dpf, RFa-lir of specimen in **Figure 5D**.

Supplementary File 6 | fly-through video of image stack of *Carcinonemertes carcinophila* 4-dpd, f-actin stain of specimen in **Figure 6C**.

Supplementary File 7 | fly-through video of image stack of *Amphiporus* sp. 4-dpd, RFa-lir of specimen in **Figure 7C**.

Supplementary File 8 | fly-through video of image stack of *Amphiporus* sp. 5-dpd, same as **Figure 7D**.

Supplementary File 9 | fly-through video of image stack of *Amphiporus* sp. 2-dpd, same as **Figure 7A**.

Supplementary File 10 | fly-through video of image stack of *Amphiporus* sp. 4-dpd, same as **Figure 7C**.

Supplementary File 11 | fly-through video of image stack of *Amphiporus* sp. 5-dpd, f-actin stain of specimen in **Figure 7D**.

Supplementary File 12 | fly-through video of image stack of *Amphiporus* sp. 7-dpd, same as **Figure 8A**.

REFERENCES

Aguinaldo, A. M. A., Turbeville, J. M., Linford, L. S., Rivera, M. C., Garey, J. R., Raff, R. A., et al. (1997). Evidence for a clade of nematodes, arthropods and other moulting animals. *Nature* 387, 489–493. doi: 10.1038/387489a0

Altenburger, A., and Wanninger, A. (2009). Comparative larval myogenesis and adult myoanatomy of the rhynchonelliform (articulate) brachiopods *Argyrotheca cordata, A. cistellula*, and *Terebratalia transversa*. *Front. Zool.* 6:3. doi: 10.1186/1742-9994-6-3

Altenburger, A., and Wanninger, A. (2010). Neuromuscular development in *Novocrania anomala*: evidence for the presence of serotonin and a spiralian-like apical organ in lecithotrophic brachiopod larvae. *Evol. Dev.* 12, 16–24. doi: 10.1111/j.1525-142X.2009.00387.x

Andrade, S. C. S., Montenegro, H., Strand, M., Schwartz, M. L., Kajihara, H., Norenburg, J. L., et al. (2014). A transcriptomic approach to ribbon worm systematics (Nemertea): resolving the pilidiophora problem. *Mol. Biol. Evol.* 31, 3206–3215. doi: 10.1093/molbev/msu253

Andrade, S. C. S., Strand, M., Schwartz, M., Chen, H., Kajihara, H., von Döhren, J., et al. (2012). Disentangling ribbon worm relationships: multi-locus analysis supports traditional classification of the phylum Nemertea. *Cladistics* 28, 141–159. doi: 10.1111/j.1096-0031.2011.00376.x

Audino, J. A., Marian, J. E. A. R., Kristof, A., and Wanninger, A. (2015). Inferring muscular ground patterns in Bivalvia: myogenesis in the scallop *Nodipecten nodosus*. *Front. Zool.* 12:34. doi: 10.1186/s12983-015-0125-x

Beckers, P. (2015). The nervous systems of Pilidiophora (Nemertea). *Zoomorphology* 134, 1–24. doi: 10.1007/s00435-014-0246-3

Beckers, P., and von Döhren, J. (2015). "Nemertea (Nemertini)," in *Structure and Evolution of Invertebrate Nervous Systems*, eds A. Schmidt-Rhaesa, S. Harzsch, and G. Purschke (Oxford: Oxford University Press), 148–165.

Beckers, P., Loesel, R., and Bartolomaeus, T. (2013). The nervous systems of basally branching Nemertea (Palaeonemertea). *PLoS One* 8:e66137. doi: 10.1371/journal.pone.0066137

Beckers, P., Bartolomaeus, T., and von Döhren, J. (2015). Observations and experiments on the biology and life history of *Riseriellus occultus* (Heteronemertea: Lineidae). *Zoolog. Sci.* 32, 531–546. doi: 10.2108/zs140270

Beckers, P., Krämer, D., and Bartolomaeus, T. (2018). The nervous systems of Hoplonemertea (Nemertea). *Zoomorphology* 137, 473–500. doi: 10.1007/s00435-018-0414-y

Bleidorn, C., Helm, C., Weigert, A., and Aguado, M. T. (2015). "Annelida," in *Evolutionary Developmental Biology of Invertebrates Vol. 2: Lophotrochozoa (Spiralia)*, ed. A. Wanninger (Wien: Springer), 193–230.

Boyer, B. C., and Henry, J. Q. (1998). Evolutionary modifications of the spiralian developmental program. *Integr. Comp. Biol.* 38, 621–633. doi: 10.1093/icb/38.4.621

Chernyshev, A. V. (2000). Food and feeding behavior of the nemertean *Tortus tokmakovae*. *Russ. J. Mar. Biol.* 26, 120–123. doi: 10.1007/BF02759525

Chernyshev, A. V. (2010). Confocal laser scanning microscopy analysis of the phalloidin-labelled musculature in nemerteans. *J. Nat. Hist.* 44, 2287–2302. doi: 10.1080/00222933.2010.504890

Chernyshev, A. V. (2015). CLSM analysis of the phalloidin-stained muscle system of the nemertean proboscis and rhynchocoel. *Zoolog. Sci.* 32, 547–560. doi: 10.2108/zs140267

Chernyshev, A. V., Astakhova, A. A., Dautov, S. S., and Yushin, V. V. (2013). The morphology of the apical organ and adjacent epithelium of *pilidium prorecurvatum*, a pelagic larva of an unknown heteronemertean (Nemertea). *Russ. J. Mar. Biol.* 39, 116–124. doi: 10.1134/S106307401302003x

Chernyshev, A. V., and Magarlamov, T. Y. (2010). The first data on the nervous system of hoplonemertean larvae (Nemertea, Hoplonemertea). *Dokl. Biol. Sci.* 430, 48–50. doi: 10.1134/S001249661001

Dunn, C. W., Giribet, G., Edgecombe, G. D., and Hejnol, A. (2014). Animal phylogeny and its evolutionary implications. *Annu. Rev. Ecol. Evol. Syst.* 45, 371–395. doi: 10.1146/annurev-ecolsys-120213-091627

Dunn, C. W., Hejnol, A., Matus, D. Q., Pang, K., Browne, W. E., Smith, S. A., et al. (2008). Broad phylogenomic sampling improves resolution of the animal tree of life. *Nature* 452, 745–749. doi: 10.1038/nature06614

Edgecombe, G. D., Giribet, G., Dunn, C. W., Hejnol, A., Kristensen, R. M., Neves, R. C., et al. (2011). Higher-level metazoan relationships: recent progress and remaining questions. *Org. Divers. Evol.* 11, 151–172. doi: 10.1007/s13127-011-0044-4

Giribet, G. (2002). Current advances in the phylogenetic reconstruction of metazoan evolution. A new paradigm for the cambrian explosion? *Mol. Phylogenet. Evol.* 24, 345–357. doi: 10.1016/S1055-7903(02)00206-3

Giribet, G. (2016). New animal phylogeny: future challenges for animal phylogeny in the age of phylogenomics. *Org. Divers. Evol.* 16, 419–426. doi: 10.1007/s13127-015-0236-4

Gruhl, A. (2008). Muscular systems in gymnolaemate bryozoan larvae (Bryozoa: Gymnolaemata). *Zoomorphology* 127, 143–159. doi: 10.1007/s00435-008-0059-3

Gruhl, A. (2009). Serotonergic and FMRFamidergic nervous systems in gymnolaemate bryozoan larvae. *Zoomorphology* 128, 135–156. doi: 10.1007/s00435-009-0084-x

Halanych, K. M., Bacheller, J. D., Aguinaldo, A. M., Liva, S. M., Hillis, D. M., and Lake, J. A. (1995). Evidence from 18S ribosomal DNA that the lophophorates are protostome animals. *Science* 267, 1641–1643. doi: 10.1126/science.7886451

Hay-Schmidt, A. (1990). Catecholamine-containing, serotonin-like and neuropeptide FMRFamide-like immunoreactive cells and processes in the nervous system of the pilidium larva (Nemertini). *Zoomorphology* 109, 231–244. doi: 10.1007/BF00312190

Hejnol, A., Obst, M., Stamatakis, A., Ott, M., Rouse, G. W., Edgecombe, G. D., et al. (2009). Assessing the root of bilaterian animals with scalable phylogenomic methods. *Proc. R. Soc. B Biol. Sci.* 276, 4261–4270. doi: 10.1098/rspb.2009.0896

Hiebert, L. S., and Maslakova, S. A. (2015a). Expression of *Hox, Cdx*, and *Six3/6* genes in the hoplonemertean *Pantinonemertes californiensis* offers insight into the evolution of maximally indirect development in the phylum Nemertea. *Evodevo* 6:26. doi: 10.1186/s13227-015-0021-7

Hiebert, T. C., and Maslakova, S. A. (2015b). Larval development of two NE Pacific pilidiophoran nemerteans (Heteronemertea; Lineidae). *Biol. Bull.* 229, 265–275.

Hiebert, L. S., Gavelis, G., von Dassow, G., and Maslakova, S. A. (2010). Five invaginations and shedding of the larval epidermis during development of the hoplonemertean *Pantinonemertes californiensis* (Nemertea: Hoplonemertea). *J. Nat. Hist.* 44, 2331–2347. doi: 10.1080/00222933.2010.504893

Hindinger, S., Schwaha, T., and Wanninger, A. (2013). Immunocytochemical studies reveal novel neural structures in nemertean pilidium larvae and provide

evidence for incorporation of larval components into the juvenile nervous system. *Front. Zool.* 10:31. doi: 10.1186/1742-9994-10-31

Iwata, F. (1960). Studies on the comparative embryology of nemerteans with special reference to their interrelationships. *Publ. Akkeshi Mar. Biol. Stn.* 10, 1–55.

Kajihara, H., Chernyshev, A. V., Sun, S.-C., Sundberg, P., and Crandall, F. B. (2008). Checklist of nemertean genera and species published between 1995 and 2007. *Species Divers.* 13, 245–274. doi: 10.12782/specdiv.13.245

Kocot, K. M. (2016). On 20 years of Lophotrochozoa. *Org. Divers. Evol.* 16, 329–343. doi: 10.1007/s13127-015-0261-3

Kocot, K. M., Struck, T. H., Merkel, J., Waits, D. S., Todt, C., Brannock, P. M., et al. (2017). Phylogenomics of lophotrochozoa with consideration of systematic error. *Syst. Biol.* 66, 256–282. doi: 10.1093/sysbio/syw079

Kristof, A., de Oliveira, A. L., Kolbin, K. G., and Wanninger, A. (2016). Neuromuscular development in Patellogastropoda (Mollusca: Gastropoda) and its importance for reconstructing ancestral gastropod bodyplan features. *J. Zool. Syst. Evol. Res.* 54, 22–39. doi: 10.1111/jzs.12112

Kvist, S., Laumer, C. E., Junoy, J., and Giribet, G. (2014). New insights into the phylogeny, systematics and DNA barcoding of Nemertea. *Invertebr. Syst.* 28, 287–308. doi: 10.1071/IS13061

Lambert, J. D. (2010). Developmental patterns in spiralian embryos. *Curr. Biol.* 20, R72–R77. doi: 10.1016/j.cub.2009.11.041

Laumer, C. E., Bekkouche, N., Kerbl, A., Goetz, F., Neves, R. C., Sørensen, M. V., et al. (2015). Spiralian phylogeny informs the evolution of microscopic lineages. *Curr. Biol.* 25, 2000–2006. doi: 10.1016/j.cub.2015.06.068

Laumer, C. E., Fernández, R., Lemer, S., Combosch, D., Kocot, K. M., Riesgo, A., et al. (2019). Revisiting metazoan phylogeny with genomic sampling of all phyla. *Proc. R. Soc. B Biol. Sci.* 286:20190831. doi: 10.1098/rspb.2019.0831

Malakhov, V. V., Bogomolova, E. V., Kuzmina, T. V., and Temereva, E. N. (2019). Evolution of metazoan life cycles and the origin of pelagic larvae. *Russ. J. Dev. Biol.* 50, 303–316. doi: 10.1134/S1062360419060043

Marlétaz, F., Peijnenburg, K. T. C. A., Goto, T., Satoh, N., and Rokhsar, D. S. (2019). A new spiralian phylogeny places the enigmatic arrow worms among gnathiferans. *Curr. Biol.* 29, 312–318.e3. doi: 10.1016/j.cub.2018.11.042

Marlow, H., Tosches, M. A., Tomer, R., Steinmetz, P. R., Lauri, A., Larsson, T., et al. (2014). Larval body patterning and apical organs are conserved in animal evolution. *BMC Biol.* 12:7. doi: 10.1186/1741-7007-12-7

Martín-Durán, J. M., and Marlétaz, F. (2020). Unravelling spiral cleavage. *Development* 147:dev181081. doi: 10.1242/dev.181081

Martín-Durán, J. M., Vellutini, B. C., and Hejnol, A. (2015). Evolution and development of the adelphophagic, intracapsular Schmidt's larva of the nemertean *Lineus ruber*. *Evodevo* 6:28. doi: 10.1186/s13227-015-0023-5

Martindale, M. Q., and Henry, J. Q. (1995). Modifications of cell fate specification in equal-cleaving nemertean embryos - alternate patterns of spiralian development. *Development* 121, 3175–3185.

Maslakova, S. A. (2010a). The invention of the pilidium larva in an otherwise perfectly good spiralian phylum Nemertea. *Integr. Comp. Biol.* 50, 734–743. doi: 10.1093/icb/icq096

Maslakova, S. A. (2010b). Development to metamorphosis of the nemertean pilidium larva. *Front. Zool.* 7:30. doi: 10.1186/1742-9994-7-30

Maslakova, S. A., and Hiebert, T. C. (2014). From trochophore to pilidium and back again- a larva's journey. *Int. J. Dev. Biol.* 58, 585–591. doi: 10.1387/ijdb.140090sm

Maslakova, S. A., and von Döhren, J. (2009). Larval development with transitory epidermis in *Paranemertes peregrina* and other hoplonemerteans. *Biol. Bull.* 216, 273–292. doi: 10.2307/25548160

Maslakova, S. A., Martindale, M. Q., and Norenburg, J. L. (2004). Vestigial prototroch in a basal nemertean, *Carinoma tremaphoros* (Nemertea; Palaeonemertea). *Evol. Dev.* 6, 219–226. doi: 10.1111/j.1525-142X.2004.04027.x

McDermott, J. J., and Roe, P. (1985). Food, feeding behavior and feeding ecology of nemerteans. *Am. Zool.* 25, 113–125. doi: 10.1093/icb/25.1.113

Nezlin, L. (2010). The golden age of comparative morphology: laser scanning microscopy and neurogenesis in trochophore animals. *Russ. J. Dev. Biol.* 41, 381–390. doi: 10.1134/S1062360410060056

Nielsen, C. (2004). Trochophora Larvae: cell-Lineages, ciliary bands, and body regions. 1. Annelida and Mollusca. *J. Exp. Zool. Part B Mol. Dev. Evol.* 302, 35–68. doi: 10.1002/jez.b.20001

Nielsen, C. (2005). Trochophora larvae: cell-lineages, ciliary bands and body regions. 2. Other groups and general discussion. *J. Exp. Zool. Part B Mol. Dev. Evol.* 304, 401–447. doi: 10.1002/jez.b.21050

Nielsen, C. (2010). Some aspects of spiralian development. *Acta Zool.* 91, 20–28. doi: 10.1111/j.1463-6395.2009.00421.x

Nielsen, C. (2012). How to make a protostome. *Invertebr. Syst.* 26, 25–40. doi: 10.1071/IS11041

Nielsen, C. (2013). Life cycle evolution: was the eumetazoan ancestor a holopelagic, planktotrophic gastraea? *BMC Evol. Biol.* 13:171. doi: 10.1186/1471-2148-13-171

Nielsen, C. (2015). Larval nervous systems: true larval and precocious adult. *J. Exp. Biol.* 218, 629–636. doi: 10.1242/jeb.109603

Nielsen, C. (2018). Origin of the trochophora larva. *R. Soc. Open Sci.* 5:180042. doi: 10.1098/rsos.180042

Nielsen, C., and Worsaae, K. (2010). Structure and occurrence of cyphonautes larvae (Bryozoa, Ectoprocta). *J. Morphol.* 271, 1094–1109. doi: 10.1002/jmor.10856

Richter, S., Stach, T., and Wanninger, A. (2015). "Perspective — nervous system development in bilaterian larvae: testing the concept of 'primary larvae," in *Structure and Evolution of Invertebrate Nervous Systems*, eds A. Schmidt-Rhaesa, S. Harzsch, and G. Purschke (Oxford: Oxford University Press), 313–324.

Santagata, S. (2004). Larval development of *Phoronis pallida* (Phoronida): implications for morphological convergence and divergence among larval body plans. *J. Morphol.* 259, 347–358. doi: 10.1002/jmor.10205

Santagata, S. (2008a). Evolutionary and structural diversification of the larval nervous system among marine bryozoans. *Biol. Bull.* 215, 3–23. doi: 10.2307/25470679

Santagata, S. (2008b). The morphology and evolutionary significance of the ciliary fields and musculature among marine bryozoan larvae. *J. Morphol.* 269, 349–364. doi: 10.1002/jmor.10592

Santagata, S. (2011). Evaluating neurophylogenetic patterns in the larval nervous systems of brachiopods and their evolutionary significance to other bilaterian phyla. *J. Morphol.* 272, 1153–1169. doi: 10.1002/jmor.10975

Santagata, S., and Zimmer, R. L. (2002). Comparison of the neuromuscular systems among actinotroch larvae: systematic and evolutionary implications. *Evol. Dev.* 4, 43–54. doi: 10.1046/j.1525-142x.2002.01056.x

Scherholz, M., Redl, E., Wollesen, T., Todt, C., and Wanninger, A. (2015). From complex to simple: myogenesis in an aplacophoran mollusk reveals key traits in aculiferan evolution. *BMC Evol. Biol.* 15:201. doi: 10.1186/s12862-015-0467-1

Schindelin, J., Arganda-Carreras, I., Frise, E., Kaynig, V., Longair, M., Pietzsch, T., et al. (2012). Fiji: an open-source platform for biological-image analysis. *Nat. Methods* 9, 676–682. doi: 10.1038/nmeth.2019

Schneider, C. A., Rasband, W. S., and Eliceiri, K. W. (2012). NIH Image to ImageJ: 25 years of image analysis. *Nat. Methods* 9, 671–675. doi: 10.1038/nmeth.2089

Schwartz, M. L. (2009). *Untying a Gordian Knot of Worms: Systematics and Taxonomy of the Pilidiophora (Phylum Nemertea) from Multiple Data Sets*. [Doctor of Philosophy dissertation]. George Washington University, Washington, DC.

Sonnleitner, B., Schwaha, T., and Wanninger, A. (2014). Inter- and intraspecific plasticity in distribution patterns of immunoreactive compounds in actinotroch larvae of Phoronida (Lophotrochozoa). *J. Zool. Syst. Evol. Res.* 52, 1–14. doi: 10.1111/jzs.12043

Stricker, S. A., and Reed, C. G. (1981). Larval morphology of the nemertean *Carcinonemertes epialti* (Nemertea: Hoplonemertea). *J. Morphol.* 169, 61–70. doi: 10.1002/jmor.1051690106

Sun, X., Zheng, Y., Yu, T., Wu, B., Liu, Z., Zhou, L., et al. (2019). Developmental dynamics of myogenesis in Yesso Scallop *Patinopecten yessoensis*. *Comp. Biochem. Physiol. Part B Biochem. Mol. Biol.* 228, 51–60. doi: 10.1016/j.cbpb.2018.11.004

Temereva, E. N. (2012). Ventral nerve cord in *Phoronopsis harmeri* larvae. *J. Exp. Zool. Part B Mol. Dev. Evol.* 318, 26–34. doi: 10.1002/jez.b.21437

Temereva, E. N., and Tsitrin, E. B. (2013). Development, organization, and remodeling of phoronid muscles from embryo to metamorphosis (Lophotrochozoa: Phoronida). *BMC Dev. Biol.* 13:14. doi: 10.1186/1471-213X-13-14

Temereva, E. N., and Tsitrin, E. B. (2014). Development and organization of the larval nervous system in *Phoronopsis harmeri*: new insights into phoronid phylogeny. *Front. Zool.* 11:3. doi: 10.1186/1742-9994-11-3

Temereva, E., and Wanninger, A. (2012). Development of the nervous system in *Phoronopsis harmeri* (Lophotrochozoa, Phoronida) reveals both deuterostome- and trochozoan-like features. *BMC Evol. Biol.* 12:121. doi: 10.1186/1471-2148-12-121

Thollesson, M., and Norenburg, J. L. (2003). Ribbon worm relationships: a phylogeny of the phylum Nemertea. *Proc. Biol. Sci.* 270, 407–415. doi: 10.1098/rspb.2002.2254

von Döhren, J. (2011). The fate of the larval epidermis in the Desor-larva of *Lineus viridis* (Pilidiophora, Nemertea) displays a historically constrained functional shift from planktotrophy to lecithotrophy. *Zoomorphology* 130, 189–196. doi: 10.1007/s00435-011-0131-2

von Döhren, J. (2015). "Nemertea," in *Evolutionary Developmental Biology of Invertebrates Vol. 2: Lophotrochozoa (Spiralia)*, ed. A. Wanninger (Wien: Springer Verlag), 155–192. doi: 10.1007/978-3-7091-1871-9

von Döhren, J. (2016). Development of the nervous system of *Carinina ochracea* (Palaeonemertea, Nemertea). *PLoS One* 11:e0165649. doi: 10.1371/journal.pone.0165649

von Reumont, B. M., Lüddecke, T., Timm, T., Lochnit, G., Vilcinskas, A., von Döhren, J., et al. (2020). Proteo-transcriptomic analysis identifies potential novel toxins secreted by the predatory, prey-piercing ribbon worm *Amphiporus lactifloreus*. *Mar. Drugs* 18:407. doi: 10.3390/MD18080407

Wang, J., Zhang, L., Lian, S., Qin, Z., Zhu, X., Dai, X., et al. (2020). Evolutionary transcriptomics of metazoan biphasic life cycle supports a single intercalation origin of metazoan larvae. *Nat. Ecol. Evol.* 4, 725–736. doi: 10.1038/s41559-020-1138-1

Wanninger, A. (2008). Comparative lophotrochozoan neurogenesis and larval neuroanatomy: recent advances from previously neglected taxa. *Acta Biol. Hung.* 59(Suppl.), 127–136. doi: 10.1556/ABiol.59.2008.Suppl.21

Wanninger, A. (2009). Shaping the things to come: Ontogeny of lophotrochozoan neuromuscular systems and the tetraneuralia concept. *Biol. Bull.* 216, 293–306. doi: 10.1086/BBLv216n3p293

Wanninger, A. (2015). Morphology is dead - long live morphology! Integrating MorphoEvoDevo into molecular EvoDevo and phylogenomics. *Front. Ecol. Evol.* 3:54. doi: 10.3389/fevo.2015.00054

Wanninger, A., and Wollesen, T. (2015). "Mollusca," in *Evolutionary Developmental Biology of Invertebrates Vol. 2: Lophotrochozoa (Spiralia)*, ed. A. Wanninger (Wien: Springer), 1–289. doi: 10.1007/978-3-7091-1871-9

Wanninger, A., Koop, D., and Degnan, B. M. (2005). Immunocytochemistry and metamorphic fate of the larval nervous system of *Triphyllozoon mucronatum* (Ectoprocta: Gymnolaemata: Cheilostomata). *Zoomorphology* 124, 161–170. doi: 10.1007/s00435-005-0004-7

Conflict of Interest: The author declares that the research was conducted in the absence of any commercial or financial relationships that could be construed as a potential conflict of interest.

frontiers in Cell and Developmental Biology

REVIEW
published: 10 June 2021
doi: 10.3389/fcell.2021.653792

Function and Evolution of Nuclear Receptors in Environmental-Dependent Postembryonic Development

Jan Taubenheim†, Constantin Kortmann and Sebastian Fraune**

Zoology and Organismic Interactions, Heinrich Heine University Düsseldorf, Düsseldorf, Germany

OPEN ACCESS

Edited by:
Nico Posnien, University of Göttingen, Germany

Reviewed by:
Vincent Laudet, Okinawa Institute of Science and Technology Graduate University, Japan
Markus Friedrich, Wayne State University, United States
François Bonneton, Université Claude Bernard Lyon 1, France

***Correspondence:**
Jan Taubenheim
j.taubenheim@iem.uni-kiel.de
Sebastian Fraune
fraune@hhu.de

†Present address:
Jan Taubenheim, Medical Systems Biology, Institute for Experimental Medicine, UKSH Kiel, Kiel, Germany

Specialty section:
This article was submitted to Evolutionary Developmental Biology, a section of the journal Frontiers in Cell and Developmental Biology

Received: *15 January 2021*
Accepted: *06 May 2021*
Published: *10 June 2021*

Citation:
Taubenheim J, Kortmann C and Fraune S (2021) Function and Evolution of Nuclear Receptors in Environmental-Dependent Postembryonic Development. Front. Cell Dev. Biol. 9:653792. doi: 10.3389/fcell.2021.653792

Nuclear receptors (NRs) fulfill key roles in the coordination of postembryonal developmental transitions in animal species. They control the metamorphosis and sexual maturation in virtually all animals and by that the two main environmental-dependent developmental decision points. Sexual maturation and metamorphosis are controlled by steroid receptors and thyroid receptors, respectively in vertebrates, while both processes are orchestrated by the ecdysone receptor (EcR) in insects. The regulation of these processes depends on environmental factors like nutrition, temperature, or photoperiods and by that NRs form evolutionary conserved mediators of phenotypic plasticity. While the mechanism of action for metamorphosis and sexual maturation are well studied in model organisms, the evolution of these systems is not entirely understood and requires further investigation. We here review the current knowledge of NR involvement in metamorphosis and sexual maturation across the animal tree of life with special attention to environmental integration and evolution of the signaling mechanism. Furthermore, we compare commonalities and differences of the different signaling systems. Finally, we identify key gaps in our knowledge of NR evolution, which, if sufficiently investigated, would lead to an importantly improved understanding of the evolution of complex signaling systems, the evolution of life history decision points, and, ultimately, speciation events in the metazoan kingdom.

Keywords: nuclear receptor (NR), thyroid hormone, ecdysone, estrogen, metamorphosis, sexual maturation

THE NUCLEAR RECEPTOR FAMILY

Metazoans depend, unlike unicellular organisms, on regulative mechanisms to coordinate different tissues and cells. Nuclear receptors (NRs) mediate this coordination and provide a direct link between extracellular signaling molecules and the transcriptional response by recognizing special DNA sequences, the hormone response elements (HREs). NRs form a family of metazoan proteins that regulate fundamental biological processes like cell proliferation, development, metabolism, and reproduction (Laudet, 1997; Fahrbach et al., 2012; Sever and Glass, 2013), while integrating environmental inputs, which renders them key molecules for phenotypic plasticity (Gilbert and Epel, 2015).

Nuclear receptors respond to small, mostly hydrophobic molecules. These include hormones, produced in special tissues, endogenous or exogenous metabolites, or xenobiotics, which are

detrimental to the organism (Escriva et al., 2004). Ligands for the receptors can thereby enter the cell either by diffusion due to their hydrophobic nature or by active transport *via* specific transporter (Schweizer et al., 2014; Okamoto et al., 2018). After entering the cell, the ligands are recognized by their NR, which are able to mediate transcriptional regulation upon binding (Sever and Glass, 2013). However, the ligands' action might be complemented by recognition of membrane receptors, which are often associated with non-transcriptomic regulations (Filardo and Thomas, 2012). As soon as the NRs are activated by their ligand, they regulate the transcription of target genes.

Most importantly, NRs are involved in virtually all major postembryonal developmental steps in metazoans. We will here review the current knowledge of NR involvement in major life history changes, mainly morphogenesis, in multicellular animals and try to draw conclusions on the evolution of these developmental steps. Furthermore, we will stress the importance of NRs for phenotypic plasticity by the integration of environmental signals into the developmental pathways lying beneath these postembryonal morphological adaptations.

Structure of Nuclear Receptors

Nuclear receptors consist of up to four domains that fulfill different modular functions (**Figure 1**). The C-domain, also referred to as DNA-binding domain (DBD) is stabilized by two zinc fingers, necessary for identification and binding to specific response elements in the DNA (Kumar and Thompson, 1999). The E-domain includes the ligand-binding domain (LBD) and enables the NRs to regulate the transcription after ligand binding. The C-terminal part of the LBD contains an activation function 2 (AF-2) subdomain and enhances the ligand-dependent transcription by binding to coactivation factors (Wärnmark et al., 2003). The A/B-domain, or N-terminal domain, is variable and comprises an activation function-1 motif (AF-1) in most NR proteins that may induce a ligand-independent transcription. The diverse D-domain is often referred to as "hinge" due to its function as a connector between DBD and LBD (Fahrbach et al., 2012).

Nuclear receptors developed diverse structural mechanisms to stabilize the active conformation together with the ligand (Germain et al., 2006). Usually, a heat shock protein dissociates from the receptor upon ligand binding, which enables homo- or heterodimerization with other NRs and is accompanied with translocation into the nucleus for cytosolic NRs. Furthermore, ligands change the conformation of the AF-2 domain by binding to the NR's allosteric center, which supports the binding of NRs with additional coactivators and inhibits association of corepressors (Sever and Glass, 2013). Hence, the possibility to form the active conformation is important to activate expression of target genes and therefore for the NR's function (Kumar and Thompson, 1999).

EVOLUTION OF NRs

Understanding the evolution of NRs will help to decipher the evolution of different life history (e.g., larval-adult stage vs. direct development) as the developmental processes are regulated by members of the NR family. Thus, it also has direct implication for our understanding of the evolution of new species, because NRs regulate key functions for integration of environmental and endogenous signals into developmental processes and are crucial for correct timing of developmental transitions. Looking at the diversity of animal species, it is striking that seemingly members of all major clades of metazoan life use NRs to regulate these developmental transitions, although different members of the NR family take part. However, the evolutionary origin of NRs lies at the base of metazoan life and is not an inherited feature of earlier single cell evolution (Bridgham et al., 2010; **Figure 2**).

The sponge *Amphimedon queenslandica* contains only two members of the NR family, both belonging to the NR2 subfamily (the same as RXR, see below) (Bridgham et al., 2010; **Figure 2**). From here, there exist mainly two different scenarios of NRs' diversification. A first theory, based on initial phylogenetic analyses, assumed that the ancestral NR functioned as a constitutive transcription factor without binding a ligand. The receptors descendants acquired the capability to bind ligands secondarily and independently, at different times in evolution (Escriva et al., 2000; Fahrbach et al., 2012). This theory is supported by the fact that NRs are binding structurally different ligands in the same subfamily and the orphan receptors (receptors without a known ligand) are widely spread out in the phylogenetic tree. This implies that there is no connection between the evolutionary relationships of NRs and the origin of their ligands. For example, the evolutionary closely related receptors of subfamily I, the thyroid hormone receptors (TRs), the retinoic acid receptors (RARs), the peroxisome proliferator-activated receptors (PPARs), and the vitamin D receptors (VDRs), bind to ligands that derive from entirely different biosynthetic pathways (Escriva et al., 2000). Furthermore, the RARs (NR1) and the retinoid X receptors (RXR; NR2) are evolutionary less related but bind to the same ligand (retinoid acid), which resembles independent convergent evolution (Escriva et al., 2000). This makes sense in the light of evolutionary constraints, which were placed on the LBD of NRs. Many extant NRs function as metabolic sensors, regulating metabolism and thus have to integrate signals, which are specific to the nutrition of the organism (Garcia et al., 2018). This in turn implies that early evolution of NRs was also associated with metabolic regulation. While the metabolic network regulated by the ancient DBD was relatively fixed, nutritional input could change easily during exploration of new ecological niches of the organism. Thus, the DBD was constrained to regulate the metabolic network, while the LBD had to be flexible and maybe was aquired several times independently during evolution of the ligand binding feature of the NRs.

An alternative scenario implies that the ancient NRs may have been lipid sensors, which are receptors with relatively low affinity for a range of hydrophobic molecules like hemes, retinoids, steroids, fatty acids, eicosanoids, and other lipids, that are ingested with nutrition. In fact, the two NRs expressed in the sponge *A. queenslandica* bind long chained fatty acids like palmitic acid (Bridgham et al., 2010). The low

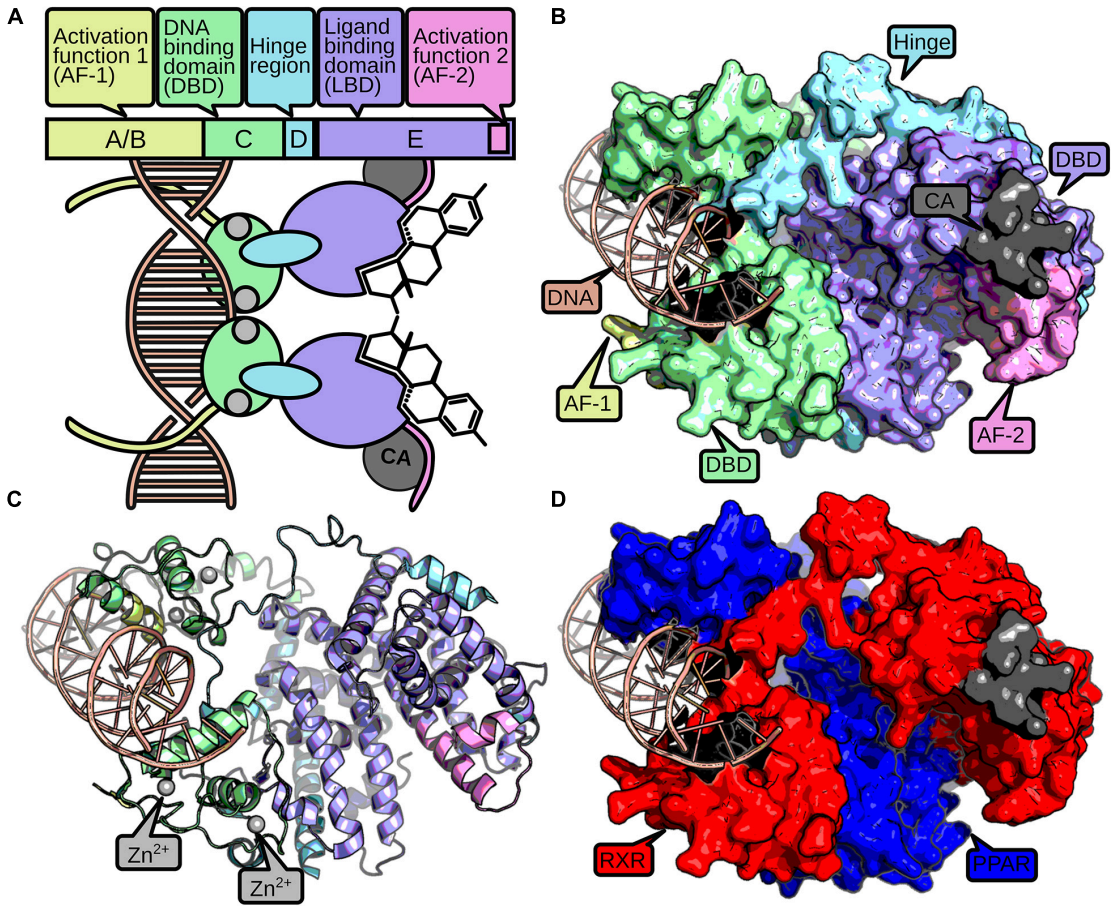

FIGURE 1 | The structure of a nuclear receptor is defined by up to five domains. The AF-1 domain (yellow) can mediate ligand-independent transcriptional regulation. The DBD consists of two zinc-finger domains (green), which are stabilized by zinc ions (gray). The zinc-finger domains recognize and bind to specific DNA-binding sites (red). A hinge region (blue) connects the DBD and the LBD (purple). The LBD usually binds a small hydrophobic ligand, which induces dimerization and a conformational change in the AF-2 domain (pink). Active AF-2 stabilizes the binding to the DNA by recruiting coactivators (CA, dark gray) and mediates transcriptional activity. A schematic representation of a NR homodimer is displayed in **(A)**, while a surface and cartoon representation of an RXR-PPAR heterodimer crystallization (PDB: 3DZY) (Chandra et al., 2008) is given in **(B,C)**, respectively, following the same color scheme as above. For better discrimination of the two dimers, **(D)** displays PPAR in blue and RXR in red.

affinity binding contrasts them to hormonal receptors that have a high affinity for very specific compounds. During evolution, these multipurpose lipid sensors presumably lost the ligand-based regulation of transcriptional activation secondarily by duplications and neofunctionalization to become what is known as orphan receptors today (Markov and Laudet, 2011). Other receptors specialized to bind particular molecules with a very high affinity and formed hormone specific receptors (Markov and Laudet, 2011). The existence of liganded NRs in early branching phyla underlines this theory and several studies identified different liganded NRs in basal metazoans (Keay and Thornton, 2009; Bridgham et al., 2010; Novotný et al., 2017; Khalturin et al., 2018). Hence, both theories have their reasoning and it seems obvious that LBD and DBD of the receptors show different evolutionary trajectories, given their different subjection to evolutionary constraints. It thus might appear on the molecular level that the two domains evolved as two separate genes. In fact, ancient NRs might have been a product of the fusion of LBD and DBD proteins, as for instance early branching Ctenophora NRs consist only of a LBD but contain no DBD (Reitzel et al., 2011).

Interestingly, although a metazoan innovation, NRs are able to function in nonmetazoan contexts: transfection of NRs into yeast or plants yielded functional receptors, which were able to control transcription (although containing species specific DBDs) (Metzger et al., 1988; Schena and Yamamoto, 1988; Schena et al., 1991). This indicates that NRs evolved bounded to already present regulatory cellular protein interactions, which were adapted to facilitate transcriptional regulation.

In early branching metazoans, at least seven NR subfamilies (NR1–7) with several groups and members exist (Nuclear Receptors Nomenclature Committee, 1999), suggesting a rapid expansion of the family during early metazoan evolution (Bertrand et al., 2004). It is possible to discern two periods of diversification through gene duplication by comparison of

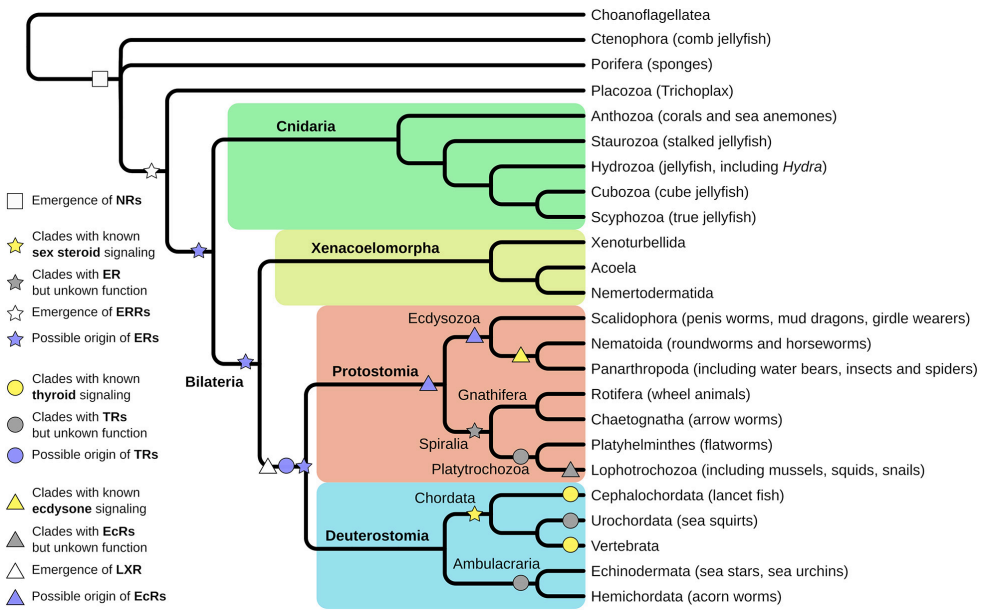

FIGURE 2 | Evolution of nuclear receptors (NRs) starts at the base of metazoan life. Porifera are the first animal clade where functional NRs emerged (white square). *Trichoplax* evolved an estrogen-related receptor (ERR), an orphan receptor, and close homolog to the estrogen receptor (ER) (white star). Evolution of a ligand-binding ER is proposed before the split of Protostomia and Deuterostomia, thus is located either in the Cnidarian or the Xenacoelomorpha lineage (purple star). Experimental support for ligand-binding ERs has been found in Annelida and Rotifers, thus in the Sprialia lineage within the Protostomia (gray star). Fully described and functional estrogen signaling exists in Vertebrata and Cephalochordata, thus in the Chordata lineage (yellow star). Homologs for thyroid receptors (TRs) have been identified in Lophotrochozoa, Urochordata, and Ambulacraria (gray circles) but were functionally characterized only in Cephalochordata and Vertebra (yellow circles). However, emergence of the TR was proposed at the base of Protostomia and Deuterostomia (purple circle). Ecdysone receptor (EcR) signaling has been functionally described in Panarthropoda and to some extent in Nematoida (yellow triangle) but homologs have been identified in different Lophotrochozoa (gray triangle). Hence, the emergence of EcR can be presumed at the base of Protostomia, but at least in the Ecdysozoan clade (purple triangles). The closely related LXR receptor is assumed to have emerged at the base of Protostomia and Deuterostomia (white triangle).

different taxa, e.g., arthropods and vertebrates (Escriva et al., 1998; Nuclear Receptors Nomenclature Committee, 1999):

i. The first diversification occurred before the split of Deuterostomia/Protostomia. This led to the appearance of the seven families and their receptors.
ii. The second split created the paralogous groups (e.g., TRα and β, RARα, β, and γ) within the families after bilaterian/pre-bilaterian division, especially in vertebrates.

This pattern is also visible in other gene families like Hox or Ets transcription factors (Escriva et al., 2004). Retinoic acid receptors (RARs and RXRs) regulate the Hox gene transcription in vertebrates, thereby implying a connection between the homeotic genes, that determine the cell identity in the developing embryo, and the NRs, which regulate the cell-to-cell communication (Escriva et al., 1998). Additionally, synteny analysis of the CYP enzymes revealed that the metazoan seeding cluster for the CYP diversity is located close to the Hox gene cluster. CYP enzymes are involved in almost all NR ligand synthesis processes and are virtually always targets of NR regulation, thus form a strong interaction partner in the NR-mediated processes (see below). This might explain the parallel evolution of *hox* genes and CYP enzymes and thus the coevolution of different NRs, Hox, and CYP enzymes (Nelson et al., 2013).

STEROID RECEPTORS SIGNALING

Function of Steroid Receptors

One of the most profound postembryonal developmental transitions in all animals is sexual maturation. Sex determination and maturation are processes, which are highly dependent on sex steroids—androgens, estrogens, and progestogens in vertebrates. These hormones have pleiotropic effects on the individual organism, starting from behavioral changes (Frankl-Vilches and Gahr, 2018), to sexual maturation like gonad development (Hamilton et al., 2017; Fuentes and Silveyra, 2019) and development of secondary sexual traits (Ogino et al., 2018).

The developmental differences upon the stimulation of NRs in the estrogen and ketosteroid receptor subfamily (NR3 subfamily) by steroids are very diverse and species specific, ranging from special appendages in viviparous fish to vocal organ development in amphibians to the development of secondary sexual features in humans (Ogino et al., 2018). To mention all these differences in the sexual development in vertebrate species would go beyond the scope of this review, as sexual development is a highly species specific trait and has been reviewed elsewhere (Valenzuela, 2008; Ogino et al., 2018). However, all these effects are regulated by NRs, which bind a highly specific (nanomolar affinity) steroidal ligand comprising two ER (ERα and ERβ), an androgen (AR), and a progesterone receptor (PR) (Baker, 2019). Of these, the two ERs

and the AR play the major roles in postembryonal development by mediation of the development of sex-specific phenotypes and behavior. Steroid signaling is thereby orchestrated by a range of environmental and developmental cues, which again, are highly species specific. Vertebrates include day length and/or body size information to time puberty with season and food availability (Leka-Emiri et al., 2017; Paul et al., 2018; Hanlon et al., 2020), which are the most common sources for environmentally induced variation (phenotypic plasticity).

However, sexual maturation is also associated with the reduction of growth in vertebrates. Usually, the sexual developmental switch is induced after a critical size/weight threshold is reached and the environmental conditions allow for sexual maturation (Hyun, 2013; Leka-Emiri et al., 2017; Hanlon et al., 2020). This in turn causes a cease of growth in the organism and sexual maturation determines the final body size. From an evolutionary perspective, it resembles a switch for resource allocation: from investment in growth to investment in reproduction. This is a delicate switch and highly dependent on the environment as detrimental conditions can cause either increase of developmental speed to reach sexual maturity and ensure offspring before death, or it leads to the deceleration of growth in order to endure unfavorable conditions and postpone development. Larger body sizes are generally associated with higher survival, larger harem sizes, and higher fecundity, but it comes to the expense of higher resource demand, longer developmental times, and more time in potentially vulnerable larval stages (Blanckenhorn, 2000; Kingsolver and Huey, 2008).

Evolution of Steroid Receptors

The complete NR3 subfamily of NRs consists of estrogen related receptors (ERR, NR3B), 3-ketosteroid receptors (NR3C, containing gluco- and mineralocorticoid, progesterone, and androgen receptors) and estrogen receptors (NR3A). However, the full set of receptors is only present in vertebrates. A genome duplication event in the common ancestors of Gnathostoma (sharks are the first split within the clade) facilitated the diversification of a single steroid receptor (SR) into today's known receptors for corticosteroids, androgens, progesterones, and aldosterones (Baker, 2019), while an ancestral ER/ERR diversified into the extant ERs and ERRs.

Before further discussion on the topic, we should clarify, that hereafter we use the term ER and ERR within the Protostomia and pre-Bilateria clades, which could be misleading as defining correct orthology is a difficult task. We consider all homologs of the NR3 subfamily as orthologs to either ER or ERR and used the terms depending on the suggested orthology and/or the function of the receptor in the organism. However, correct naming of NR3 receptors in invertebrates is controversial (Markov et al., 2008) and we want explicitly state that orthology to ketosteroid receptors might be just as probable, despite our choice of terminology.

The evolution of sex SRs in invertebrate species is less clear today and especially the origin of estrogen signaling is under debate. Evolutionary earliest evidence for NR3 members can be found in Placozoa where an ERR was identified in *Trichoplax adhaerens* that clusters as an outgroup to vertebrate ERs (Baker, 2008; Novotný et al., 2017; **Figure 2**). Furthermore, some cnidarian species seem to have retained this receptor, e.g., in *Hydra* (Khalturin et al., 2018), although in others cnidarians like *Nematostella vectensis*, no NR3 subfamily member was identified (Reitzel and Tarrant, 2009). Additionally, an ERR was annotated in the genome of *Hofstenia miamia* (Gehrke et al., 2019), a Xenacoelomorpha [forms a bilaterian sister group to all Deuterostomia and Protostomia (Rouse et al., 2016; Cannon et al., 2016; **Figure 2**]. The physiological function of these genes and whether they were able to bind a steroid (or other) ligand is unclear to date. However, investigation of the function of these receptors might be rewarding, as knowledge about the metamorphic events in Cnidaria are currently lacking, but seem coordinated by NR signaling (Fuchs et al., 2014).

Within the Protostomia, ERs, and ERRs can be found in Lophotrochozoa (**Figure 2**). There is evidence for functional sex SRs in three classes of mollusks: Bivalvia, Gastropoda, and Cephalopoda (Köhler et al., 2007). In contrast to vertebrate ERs, they are not activated by estrogen but mediate transcription constitutively. The mollusks ER's LBD's allosteric switch became possibly stuck in the agonist position and leads to constitutive transcription (Keay and Thornton, 2009). Although various publications exist where steroids (especially those also active in vertebrates) are reported to influence developmental timing and number of gonads in mollusks and that enzymatic functionality is present (Ketata et al., 2008; Fernandes et al., 2011), there is considerable critique on these reports (Scott, 2012, 2013; Minakata and Tsutsui, 2016; Fodor et al., 2020). It is thus not quite clear, whether Molluska employ steroids to control sexual maturation.

However, ERs that are sensitive to estrogen and endocrine disruptors have been found in annelida, the sister phylum of mollusks (Keay and Thornton, 2009). Keay and Thornton isolated and characterized the NRs from two annelids, *Platynereis dumerilii* and *Capitella capitata*, which are orthologs of mollusk and vertebrate ERs. The annelid ERs show the same functions as vertebrate ERs in estrogen sensitivity and specificity. They recognize classic estrogen responsive elements and activate transcription at low doses of estrogen. Estrogen is produced by the annelids themselves and is therefore not only an environmental factor. The hormones regulate the provisioning of oocytes with vitellogenin during female reproduction and the ERs mediate these effects (Keay and Thornton, 2009). This was a surprising finding, as the estrogen signaling was thought to be a mere vertebrate specific feature.

These results are complemented by studies in rotifers, a sister group to Platytrochozoa (comprising Platyhelminthes and Lophotrochozoa) (**Figure 2**). In a phylogenetic study, an ER homolog has been identified in different *Brachionus* species (Kim et al., 2017). Furthermore, biochemical studies identified steroid derivatives, a functional progesterone, and an estrogen receptor of the NR3 subfamily in *Brachionus manjavacas* (Stout et al., 2010; Jones et al., 2017). Both seem to be associated with sexual reproduction, leading to the assumption that rotifers employ an estrogen-like signaling pathway to coordinate their reproductive processes.

Within the Platyhelminthes, no NRs of NR3 subfamily could be identified. Thus, this class of proteins seems to have been lost in this phylum (Wu and LoVerde, 2019; **Figure 2**).

In Ecdysozoa, an ERR has been identified (Bridgham et al., 2010; Fahrbach et al., 2012). It is involved in the downstream regulation of the EcR (see below), but seems not involved in hormonal recognition (Tennessen et al., 2011; Beebe et al., 2020), despite being an integrator of environmental signals (Li et al., 2013) and regulator of metabolism (Beebe et al., 2020).

Taken together, the presence of NR3-family members in Mollusks, Annelida, Rotifers, and Ecdysozoa implies the evolution of the prototype receptor for the vertebrate estrogen in a common ancestor of Protostomia and Deuterostomia. Several questions remain: was the ancestral receptor able to bind a steroid ligand, and are extant receptors in early branching metazoans? And is the extant receptor involved in major developmental processes?

Within the Deuterostomia invertebrates, nearly nothing is known about steroid signaling. There have been some suggestive publications on sex steroid effects in Echinodermata (Köhler et al., 2007), but there is no link to an active NR, or receptor in general (Silvia et al., 2015). The same is true for Tunicata, which seem to regulate sexual maturity mainly through peptidergic signaling (Tello et al., 2005; Matsubara et al., 2019). The best studied NR3 members are those of Cephalochordata. In Branchiostoma, a fully functional SR next to an ER without ligand binding capacity was identified (Callard et al., 2011; **Figure 2**). It seems likely that all other vertebrate SRs including the functional estrogen receptor diversified from these two genes.

Differences in presence and absence of receptors in different phyla and differences of ligand-binding activity, if a receptor is present, promoted a series of studies, which tried to infer the ancestral state of the receptor and its ligand by using phylogenetic maximum likelihood approaches. This ancestral sequence reconstruction is based on statistical support for most likely amino-acid compositions (or reactions leading to a ligand) of the respective protein/molecule of interest. These can then be cloned and heterologously expressed (or synthesized) to experimentally explore biochemical and signaling properties. For example, an ancestral SR was inferred using inactive lophotrochozoan sequences, but was able to bind steroid derivatives (Thornton, 2003). Furthermore, the ancestral steroid ligand could be reconstructed and is able to bind and activate an ancestral receptor (Markov et al., 2017), although in micromolar range, which is weaker compared to hormones. Additionally, these studies contributed to our understanding how transcription factor binding specificity to its recognition DNA sequence (McKeown et al., 2014) and ligand-receptor specificity evolved (Eick et al., 2012). Both need predominantly mutations to inhibit specific binding in order to escape an evolutionary trap, which is formed by the already present function of the protein. Otherwise, newly gained functions would readily interfere with (vital) present functions of the receptor. In case of the ligand recognition function of the receptor: specificity is achieved by excluding ligands with missing features, rather than recognizing all features of a given ligand for NRs (Eick et al., 2012). This might also explain the broad ranges of xenobiotics recognized by different NRs and the final evolution of highly sensitive hormone receptors (which acquired more feature recognition sites). Finally, these results all point to the evolution of steroid binding SR, which were derived from less-specific ligand binding NRs, which diversified and specified during evolution in the different clades.

However, although our knowledge is quite deep in certain details of SR evolution, experimental evidence of the function is missing in many phyla. The Lophotrochozoan clade in particular seems to hold much information about the evolution of ERs as functional as well as nonfunctional ERs exist. Similar is true for the evolution of the promiscuous NR, which forms the ancestor to all other ERs. Neither a definitive protein, ligand, nor function have been identified or studied in extant organisms in one of the sister groups to the Protostomia-Deuterostomia. Exploration of these animal clades, however, contains important functional information about regulation and consequences of activation of this receptor, which is needed to understand the evolutionary constraints of the molecular changes in the ERs.

THYROID RECEPTOR SIGNALING

Function of Thyroid Receptors

Thyroid hormones are the major players for induction of metamorphosis in vertebrates (Laudet, 2011) and control many metabolic functions in human (Mullur et al., 2014). The function of this signaling cascade is well understood in vertebrate systems, where basically all poikilotherm species undergo a metamorphic event in their life history controlled by TH signaling. This event is often associated with dramatic morphological and physiological changes, for example, the transition from tadpoles to juvenile frogs, or the transition from benthic blind lamprey larva to pelagic sighted juvenile individuals. It can, however, be more subtle as in fish, where still some debate exists, whether the morphological changes resemble a real metamorphosis (Campinho, 2019).

Amphibian transition from aquatic, mostly herbivore tadpoles to terrestrial, carnivore adults is thereby a textbook example of larva-to-adult metamorphosis. It is one of the best studied postembryonal developmental processes in the vertebrate clade, especially in the clawed frog *Xenopus laevis*. The metamorphosis in *Xenopus* is mediated by TRs (TRα, NR1A1; TRβ, NR1A2) and a peak of the thyroid hormone (TH, here T3 and T4), which coincides with the development of the thyroid gland in the tadpole. The thyroid gland produces the T4 hormone, which is biologically less active. It first has to be converted to biological active T3 or is inactivated by Deiodinases (D1–3, D1, and D2 produce T3, while D3 deactivates T4 and T3) in a tissue specific manner, resulting in differential response to circulatory TH release in different tissues (Mullur et al., 2014).

Tissue specific responses to TH cause a resorption of the tail, growth of the limbs and remodeling of the intestine and nervous system, among other tissue adaptations. Interestingly, TRα and TRβ have contrary functions: while TRα induces growth and cell proliferation in tissues like brain, limb buds, and skin upon TH binding, TRβ causes apoptosis and proteolysis in tail and gills (Mourouzis et al., 2020). However, the metamorphosis of

amphibians is not a spontaneous process. It is dependent on the corticotropin releasing hormone (CRH) in the hypothalamus of the tadpole, which induces the release of TSH in the pituitary and consequently induces the TH production in the thyroid gland (Laudet, 2011; **Figure 3**). This process is dependent on the environmental factors like presence of predators or pond drying and integrates with the general stress response of the animals *via* cortisol (Denver, 2009; Laudet, 2011). In that regard, CRH is not only regulating the TSH release but also the ACTH release in the pituitary, which, as a consequence, additionally regulates cortisol levels in *Xenopus* (**Figure 3**) leading to de- or acceleration of the development depending on the animal's developmental stage (Denver, 2009; Laudet, 2011).

Apart from the reoccurring pattern of environmental integration of important developmental steps *via* NR-driven processes, anuran species harbor another interesting feature: nonmetamorphic species. These frogs hatch as small adult variants and skip the tadpole stage. However, it seems that the nonmetamorphic frog *Eleutherodactylus coqui* goes through a morphogenesis-like transition *in ovo*, induced partly by maternal addition of TH to the egg (Laudet, 2011; Laslo et al., 2019). The same seems to be true for different fish and salamander species, which show no obvious metamorphosis (Laudet, 2011). This finding has evolutionary consequences, as it poses the question, whether other nonmetamorphic vertebrates completely lost a larval stage on the ontological level, undergo metamorphosis during embryogenesis by provision of maternal hormones or undergo a cryptic postembryonal metamorphosis. For example, in humans, TH concentrations are correlated with size and growth during embryonic development and are maternally provisioned during the first 4 weeks (Forhead and Fowden, 2014). After that point, it is mostly endogenously produced by the embryo, which resembles the sequence of events in *E. coqui* during embryogenesis. To answer the question regarding the evolution of direct and larval development, it is pivotal to understand the evolution of molecular key regulators in metamorphic events, like NRs.

The molecular implementation of TH activation and release is generally the same for all species: upon environmental and developmental cues, which are received in the hypothalamus, a peptidergic releasing hormone activates the associated pituitary gland (**Figure 3**). The pituitary releases a thyroid stimulating hormone (TSH) and thus induces TH production in the thyroid gland/endostyle where the signal is received. The TH is released into the circulation and recognized by NRs in target tissues, where it induces tissue specific effects. This axis of regulation is called hypothalamus-pituitary-thyroid axis (HPT-axis) and although the general pattern is the same in all vertebrates, species specific differences in this regulation exist. The metamorphic event is generally associated with a sharp and rather sudden increase in free TH-serum levels leading to induction of larva-to-adult transitions (Laudet, 2011).

The implementation of the releasing hormone in the hypothalamus differs in vertebrate species (**Figure 3**). While mammals and birds use a specific thyroid releasing hormone (Manzon and Manzon, 2017; Lazcano et al., 2020), amphibians predominantly employ a corticotropin (CRH)-like peptide (Laudet, 2011; Lazcano et al., 2020). For fish, contradicting

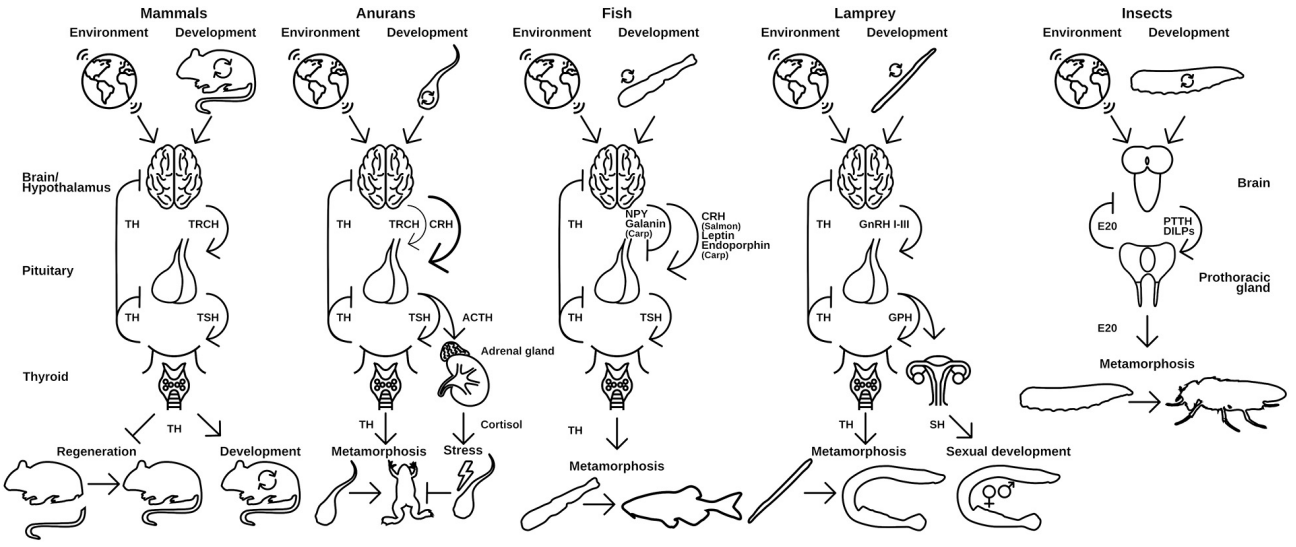

FIGURE 3 | Hypothalamus-pituitary-thyroid axis in different vertebrates use distinct releasing hormones to regulate TH release. Environmental and developmental signals control the release of releasing peptide hormones from the brain, which initiates the release of thyroid-stimulating hormones (TSH) from the pituitary gland. TSH in turn activates the production and release of TH from the thyroid. Released TH initiates and regulates metamorphic events in the animal. A similar regulation is seen in insects and the release of ecdysone (E20). PTTH and DILPS are produced in the brain after developmental and environmental cues, which induce the production of E20 in the PG. TRCH, thyroid releasing hormone; TSH, thyroid-stimulating hormone; CRH, corticotropin-releasing hormone; ACTH, adrenocorticotropic hormone; NPY, neuropeptide Y; GnRH, gonadotropin-releasing hormone; GPH, gonadal pituitary hormones; SH, sex hormones; PTTH, prothoracictropic hormone; DILP, *Drosophila* insulin-like peptides. Parts of the figures were derived from www.phylopic.org and www.svgrepo.com/page/licensing and are public domain or licensed under CC0 1.0.

reports in different species exist, but it seems that the major teleost clades developed specific implementations of the releasing hormone signaling. While Salmonidae seem to also use CRH (Campinho, 2019), Cyprinidae use a combination of leptins, endorphins (both activating), neuropeptide Y, and Galanin (both inhibiting) to control their TH release. Cyclostomes use three different gonadal releasing hormones (GnRHI-III) to regulate the release of TH (Manzon and Manzon, 2017).

Cyclostomata form the sister group to all other vertebrates and are the earliest branching phyla within the Vertebrata (Kuraku and Kuratani, 2006; Miyashita et al., 2019). Extant species of the cyclostomes comprise lampreys and hagfish. Lampreys show metamorphosis from eyeless, filter feeding and benthic living larva to mostly parasitic, pelagic juveniles (Manzon and Manzon, 2017). The transition between larvae and juveniles is controlled by TH signaling, which is in its basics the same as in anurans.

However, a divergence in TH action is present as the TH concentration rises throughout the larval stage followed by a sharp decline that induces the metamorphosis (Leatherland et al., 1990; Youson et al., 1994; Manzon and Manzon, 2017). Hence, the pattern of TH induced metamorphosis has clearly evolved before the emergence of Vertebrata.

In Cyclostomata, the metamorphic event is dependent on two environmental factors: temperature and population densities. While low temperatures inhibit metamorphosis in general, it is the change from cold to warmer temperatures (probably as sensor for seasonal changes) which induces metamorphosis (Leatherland et al., 1990; Holmes and Youson, 1994; Youson et al., 1994). High population densities, however, prevent metamorphosis as it reduces growth of the larvae since a critical size/weight (called conditioning factor in fisheries biology) is needed before metamorphosis is induced (Manzon and Manzon, 2017). Food is generally not a limiting factor and it is unclear why growth is hampered in high populations of lamprey, despite a chemical signal secreted in the water column was suspected (Rodriguez-Munoz et al., 2003). How these environmental cues are integrated in the thyroid signaling pathway is not clear to date, but the molecular signatures associated with this signal integration promises to unravel core mechanisms of developmental plasticity in the vertebrate clade.

In mammals, TH action in development takes place predominantly during embryogenesis, where it promotes growth and maturing of the organs, apart from regulating diverse metabolic functions in the embryo to ensure timely and full development at birth (Forhead and Fowden, 2014; Mourouzis et al., 2020). It has delicate functions in the developing nervous system where minor changes in the concentration of TH during embryogenesis can have impact on the final IQ of humans (Sachs and Buchholz, 2017). Postnatally, THR regulates growth and maturation of muscle and bone, leading to short stature if disturbed after birth. In hyperthyroid conditions, this is caused by rapid skeletal growth and premature fusion of the growth plates in bones, while hypothyroidism causes delayed bone maturation with lower bone mineralization and general skeletal dysplasia (Mourouzis et al., 2020). However, the most pronounced effect of TH in mammalian postnatal development is the loss of regenerative capacity, which coincides with terminal differentiation of myoblasts to myocytes (Lee et al., 2014) and with a peak of TH at birth in human and roughly 7 days after birth in mouse (Wu and LoVerde, 2019). Axon regeneration in the mouse brain is active for the first week after birth, and external addition of TH or removal is reducing and extending this plasticity respectively (Avci et al., 2012). Similarly, heart regeneration is possible in newborn mice but this capability is lost after the TH peak at around 7 days (Hirose et al., 2019). The same authors associated regeneration capacity and thermal regulation through TH in phylogeny as well as ontogeny and propose a tradeoff between regeneration capabilities vs. high and regulated body temperature (Hirose et al., 2019). However, it seems that genetic determination of resource allocation to reproduction and differentiated tissue might be the main cause of loss of regeneration in mice, as poikilotherm anurans are also unable to regenerate the heart after metamorphosis, which is TH induced (Marshall et al., 2019). On the other hand, regenerative capabilities of another mammalian (thus homeotherm) species, *Acomys* (spiny mice), is much higher, speaking against a general rule of homeotherm-regeneration trade-off (Maden, 2018; Sandoval and Maden, 2020). Furthermore, it has been suggested that TH peaks coincide with becoming independent of parental care in mammals and sauropsids (Holzer and Laudet, 2013). Altricial (self autonomous at birth/hatching) species of birds and mammals show a peak of TH at birth/hatching. In contrast precocial (dependence on parental care at birth/hatching) species show a smoother increase in TH hormones during postembryonic development, which coincides with active thermoregulation, end of weaning and autonomous feeding (McNabb et al., 1984; Castro et al., 1986; Richardson et al., 2002; McNabb, 2006). Thus, TH peaks are associated with a "larva"-juvenile transition in homeotherm vertebrates and resembles the remnants of a metamorphosis element during postembryonic development.

Another important finding for TH signaling in homeotherm vertebrates was the control of seasonal gonadal development in Japanese quail to mediate optimally timed reproduction. The photoperiod is measured by TSH expression in the pars tubularis of the hypothalamus and controls the expression of deiodinases (D2 and D3) in the mediobasal hypothalamus, thereby increasing local T3 concentrations about 10-fold. This local TH increase causes a morphological change in the axon terminals of GnRH producing neurons, which end there and increase their production and secretion of GnRH. This in turn increases the production of sex hormones and leads to temporal gonadal growth to orchestrate reproduction with the seasonal changes of light (Nakayama and Yoshimura, 2018). A similar axis of photoperiodic changes in local TH production was observed in melatonin proficient mice and suggests a similar regulation of seasonal developmental adjustments in mammals (Nakayama and Yoshimura, 2018). The effects of TH signaling due to different photoperiods can thereby be context specific, as for example two closely related vole species adapt seasonal strategies (growth vs. fast reproduction) in contrary direction, although both

effects are regulated through the TH-signaling pathway (van Rosmalen et al., 2020).

Evolution of Thyroid Receptors

Within vertebrates, the genes for the TRs diversified before the split of the gnathostome lineage and thus TRs and RXRs resemble the evolution of SR (see above) as their major diversification event is occurring at the genome duplication event during Teleost evolution (Escriva et al., 2002).

Cyclostomes are the evolutionary first branching animals within the vertebrate group. Although their TR and RXR repertoire is the same as in other vertebrates (two TR homologs and three RXR homologs), this seems to be due to convergent evolution. The sequences for both receptors cluster in monophyletic groups as outgroups to the rest of the vertebrate receptors (Escriva et al., 2002; Manzon et al., 2014). This might explain the difference in control of metamorphosis by TH (see above). However, it is interesting to see that the general signaling pattern evolved before the integration of developmental events in vertebrates, so that the TH signaling is important for metamorphosis, but the signal transduction can be implemented fundamentally differently (increase vs. decrease of TH). This hints to the importance of integrated cues within the TH-signaling, which are crucial for correct timing of postembryonal developmental events.

Outside vertebrates, there is clear evidence of TR signaling in Cephalochordata, which controls the metamorphosis in these animals through a single TR (Paris et al., 2008, 2010; **Figure 2**). The TR has the uncommon ligand Tiratricol (TRIAC), which is a derivative of T3 (Paris et al., 2008) and is effectively deactivated by endogenous deiodinases (Klootwijk et al., 2011). The TRIAC synthesis requires an additional enzymatic step, indicating that TH-signaling evolved by reducing the biochemical processes on the synthesis of the hormone. Interestingly, the synthesis of active TH resembles again a breakdown process (deamination and decarboxylation, diodination in vertebrates), similar to the production of active steroid hormones. It seems that this is a general pattern for the evolution of NR ligands and makes sense in the light of NR evolution, as NRs turn from rather promiscuous receptors for a variety of compounds, which regulate metabolism and detoxification, to highly specific hormone receptors. It indicates that the active hormone evolves as a byproduct of already available biosynthetic pathways.

Within the other Deuterostomia, less is known about the evolution of TH-signaling. Tunicates and Echinoderm genomes contain a TR and form outgroups to the vertebrate clade, with echinoderm receptors showing more homology to vertebrate sequences (Ollikainen et al., 2006). This divergence is also reflected in the binding pocket for the ligand in these receptors, leading to the initial conclusion that classical TH are not able to bind in these animals (Ollikainen et al., 2006). Still, members of both clades are responsive to exogenous addition of TH in terms of acceleration of metamorphosis and development, show increase in TH levels before metamorphosis and expression of TRs (Taylor and Heyland, 2017). However, some of the echinoderm species seem to not produce TH by themselves (Chino et al., 1994), while others do (Heyland et al., 2004). The molecular actions of TH and the generality, that they are developmentally relevant in these species, is thus still unclear and needs further investigation (**Figure 2**).

Within the Protostomia, TRs have been identified in platyhelminths (Wu and LoVerde, 2019) and mollusks (Fukazawa et al., 2001; Huang et al., 2015; Wang et al., 2019; Li et al., 2020; **Figure 2**). Functional knockdown or knockout of the TR in the abalone *Haliotis diversicolor* and the oyster *Crassostrea gigas* reduced the proportion of metamorphic animals, indicating a role of thyroid signaling in postembryonal development in mollusks (Wang et al., 2019; Li et al., 2020). It was previously shown that after external administration of T4, metamorphosis could be induced in other species of abalone (Fukazawa et al., 2001) and that the oyster TR is responsive to TH treatment *in vivo*, although not *in vitro* (Fukazawa et al., 2001). However, the TR expression is peaking during the gastrulation of *C. gigas,* but shows only low expression during metamorphosis, speaking against a function in metamorphosis (Vogeler et al., 2016). Taken together, these results indicate a regulative function of TH in mollusk metamorphosis, although the effects are not as conclusive as in vertebrates.

Despite the findings in mollusks and the presence in platyhelminths, no TR could be identified in other Protostomia species. The presence of a TR in mollusks, however, implies a common ancestor in the pre-bilaterian lineage. This ancestral TR has been retained in Deuterostomia, Molluska, and Platyhelminthes but has probably been lost in the other Protostomia clades. In turn, this means that Annelida, Gnathifera, and Ecdysozoa have lost the TR independently, indicating a less vital role of TR in the urbilaterian ancestor of these animals (**Figure 2**). Given the fact that thyroid-like molecules are common in marine environments and that these are easily integrated into the food chain of the animals (Holzer et al., 2017; Markov et al., 2018), it is likely that the ancestral TR served as a nutrient sensor to control metabolism. During evolution, this sensory function might have become less important, which leads to either the loss of the signaling pathway, or the neofunctionalization to serve as a hormone-integrating metabolic and developmental function.

In Cnidaria, an RXR plays a major role in the transition from asexual reproduction of sessile polyps to sexual reproduction in pelagic medusae called strobilation of *Aurelia aurita* (Fuchs et al., 2014). In the same study, the authors identified a peptidergic ligand, which is the inducer of strobilation, while 9-cis-RA seems to be a strong coactivator (Fuchs et al., 2014). However, the dimerization partner for RXR is still elusive in this process and to date it is unknown how the peptide ligand is recognized in this strobilation event. However, the peptide inducing strobilation comprises WSRRRWL with the tryptophane residues being the inducing agent, as could be shown by chemical analogons (Fuchs et al., 2014). This is a striking similarity to the TH, which is derived from another aromatic amino acid—tyrosine. Hence, it might be possible that the putative cnidarian receptor and the TR have a common ancestor, which recognized peptidergic ligands.

ECDYSONE RECEPTOR SIGNALING

Evolution of Thyroid Receptors

Postembryonal development in Ecdysozoa is determined by several stages of larval development, which is accompanied with cuticle shedding to allow growth. Regulation of this growth period is necessary to attain the species specific body sizes and is associated with the onset of sexual maturity (Mirth and Shingleton, 2012). Thus, morphogenesis and sexual maturation coincides in insects and are not separate developmental steps, as in vertebrates, although they may be differentially regulated. In insects, this regulation is mediated by the production of ecdysone (20-hydroxecdysone and derivates) and juvenile hormone (JH) (Hiruma and Kaneko, 2013; Liu et al., 2018). The former is produced in pulses throughout the larval development and determines transitions between the different larval instars, while the latter is predominantly produced in the larval stages. If JH levels drop, ecdysone induces pupariation leading to fixation of final body size and sexual maturity (Mirth and Shingleton, 2012). While ecdysone is recognized by an NR, namely, the EcR (member of the LXR/NR1H group), JH is bound by methropen tolerant (met, a basic-helix-loop-helix PAS domain receptor/AhR homolog, which is functionally very similar to NRs) (Hiruma and Kaneko, 2013; Dubrovsky and Bernardo, 2014). The actions of both hormones are thus integrated at the genetic level. Ultraspiracle (USP, member of the RXR/NR2B group) serves as the coreceptor of EcR (Yao et al., 1992, 1993; Jones and Sharp, 1997).

The production of ecdysone is controlled by two main components: insulin-like peptides (ILPs) (Colombani, 2005) and PTTH (Shimell et al., 2018). Thereby, PTTH is responsive to ILP signals from imaginal disks to facilitate allometry and damage repair (Colombani et al., 2015; Garelli et al., 2015; Vallejo et al., 2015; Jaszczak et al., 2016). Additionally, ILP signals coordinate the integration of the nutritional state to PTTH and the ecdysone signaling (Faunes and Larraín, 2016). For pupariation, the larva needs to attain a certain weight (critical weight) to safely make the progression to the adult fly. The correct size at pupariation is monitored by the corpora allata, the production tissue of PTTH (Mirth et al., 2005; Shimell et al., 2018). Furthermore, PTTH integrates light signaling and photo periods to coordinate developmental timing to circadian rhythms (Mirth et al., 2005; Shimell et al., 2018) and forms a feed-forward loop with ecdysone signaling in the brain (Christensen et al., 2020). ILPs do not only act through the PTTH axis to mediate their effect on the ecdysone but are able to directly control the ecdysone production in the prothoracic gland (PG) (Colombani, 2005). ILPs signaling is regulated by extrinsic signals like temperature (Li and Gong, 2015) and nutrition (Hyun, 2013; Lee et al., 2018), which in turn influences the developmental timing in insects. PTTH and ILP are regulated by a complex network of neuronal signals mediated by neuropeptides and sense the mentioned extrinsic signals (Koyama et al., 2020). Interestingly, the signals of PTTH and ILP need priming of the PG by activin, a TGF-β member, before they are able to induce ecdysone production (Gibbens et al., 2011). Furthermore, other environmental factors like oxygen are integrated in the ecdysone signaling (Callier and Nijhout, 2011), rendering it a highly environmentally dependent decision point for postembryonal development adjusting life history traits to the given environment.

Remarkably, the EcR itself induces expression of E75 (Rev-ERB/NR1 subfamily), E78 (Rev-ERB/NR1 subfamily), DHR3 (ROR/NR1 subfamily), FTZ-F1 (SF-1/NR5 subfamily), DHR39 (SF-1/NR5 subfamily), and DHR4 (GCNF/NR6 subfamily) upon activation by ecdysone—all belonging to the NR class of transcription factors. These factors control and execute correct molting and pupariation, next to other essential functions during embryonic development (Richards, 1997).

Caenorhabditis elegans possesses an alternative steroid signaling pathway that involves dafachronic acid (DA) and its receptor dauer formation 12 (DAF12, LXR/NR1 subfamily member) (Fielenbach and Antebi, 2008), a closely related NR to EcR. DAF12 regulates the occurrence of an additional senescent larval state, dauer diapause, and thereby developmental timing, reproductive maturation, metabolism, and lifespan. Dauer formation is initiated upon detrimental environmental conditions, such as starvation, high temperature, or high aggregation of worms (Fielenbach and Antebi, 2008), which prevents the synthesis of DA (Motola et al., 2006). Many (if not all) of the environmental cues are transduced by two main signaling cascades—the insulin and the TGF-β pathway—which form the most important regulators for DA in *C. elegans* (Fielenbach and Antebi, 2008). Dauer forms are resistant to all kinds of environmental stresses and can extend lifespan up to 3–6 months. Once the environmental conditions become more favorable, *C. elegans* resumes its development to sexual maturation and reproduction (Fielenbach and Antebi, 2008). The regulation, the mode of action, and the signaling outcome is thus very similar to the ecdysone system in insects and might resemble an evolutionary special case of *C. elegans*, where DA replaced the generic ecdysone (Gáliková et al., 2011) thereby regulating genes homologous to the EcR downstream genes (Gissendanner et al., 2004).

Evolution of Ecdysone Receptors

The ecdysone signaling pathway is one of the best understood hormonal pathways in invertebrate species, not least because of *Drosophila melanogaster*'s role as a pivotal model organism (Koelle et al., 1991). Within the Ecdysozoa, the number of isoforms differ in the different clades. While *Locusta* inherits only one isoform, *Drosophila* expresses three isoforms with different function, although expressed from a single locus (Truman and Riddiford, 2002).

Ecdysone receptor is uniformly found in most ecdysozoan species, except to the nematode *C. elegans* (Schumann et al., 2018), which lacks EcR and USP genes. However, the NRs, which are downstream of the EcR in insects and that are usually involved in molting, exist and have similar functions in *C. elegans* as well (Gissendanner et al., 2004). Hence, the loss of ecdysone and its receptor might be very specific to *C. elegans*.

Interestingly, DAF12, the DA receptor of *C. elegans* is similarly closely related to the EcR, but seems to have been evolved only

in a rather *C. elegans* specific clade (Sluder, 2001). At least filarial nematodes possess a functional ecdysone signaling, indicating the EcR ancestry in nematodes (Tzertzinis et al., 2010; Mhashilkar et al., 2016). However, the definitive evolutionary trajectory of EcR in the nematode lineage remains to be clarified.

While the expression of EcR seems to be an ancestral state of Ecdysozoa, the enzymes for the synthesis of ecdysone (so-called Halloween genes) are not found in all subclades and species. There is a stepwise evolution of ecdysone producing CYP450 enzymes: Nematoda and Priapulida do not contain any of these genes, while Tardigrada and Onychophora express a *sad* gene. In the Panarthropoda, the genes *spook*, *disembodied*, and *shadow* are additionally found. From there, the additional expression of *phantom*, *spookiest*, and *spok* are found in a stepwise addition in Myriapoda (centipedes), Crustacea, and Hexapoda (Schumann et al., 2018). It is thus interesting to see whether and how other ecdysone derivatives are produced in other animal clades within the Ecdysozoa. It might elucidate the evolution of Ecdysone signaling in the Ecdysozoa and by that will provide valuable information to the evolution of a steroid ligand in all animals.

It has long been thought that ecdysone signaling was a first insect, later ecdysozoan invention only (Sluder, 2001; Hyde et al., 2019), but newer studies found EcRs outside the Ecdysozoa. Annelida, Molluska (Lophotrochozoa), and Platyhelminthes contain an EcR homolog in their genome, although not much is known of the function of this receptor in these species (Laguerre and Veenstra, 2010; Vogeler et al., 2014; Kaur et al., 2015). There is an upregulation of EcR to the onset of metamorphosis in the mollusk *C. gigas* (Vogeler et al., 2016) but apart from that, functional studies are lacking.

The EcR is closely related to the liver X receptor (LXR) in humans and even more closely to the one found in *Ciona intestinalis*, which indicates a common ancestry of the two receptors (Truman and Riddiford, 2002; **Figure 2**). Both receptors are known to bind steroid ligands, while the deuterostome LXR is involved in metabolic regulation for cholesterol and binds oxysterol (Lehmann et al., 1997; Yoshikawa et al., 2001), EcR evolved into a major determinant of postembryonal development in arthropods binding ecdysone. The common ancestry, however, indicates a function of steroid-binding NRs before the split of Deuterostomia and Protostomia. It would be highly interesting to investigate the nature and the regulatory function of such a receptor to elucidate the evolution of steroid signaling. Was the hormone function of steroids acquired in insects or lost in deuterostomes?

RETINOID X RECEPTORS—IMPORTANT CORECEPTOR OF NRs IN POSTEMBRYONAL DEVELOPMENT

Retinoid X receptors have a special role during the signaling of different NRs, because they form the heterodimerization partner for many of the NRs and hence enable their signaling. RXR-heterodimers are formed with TR, VDR, RAR, PPAR, LXR, farnesyl X receptor (FXR), pregnane X receptor (PXR), or constitutive androstane receptor (CAR)—all NR1 subfamily members (Desvergne, 2007; Evans and Mangelsdorf, 2014). RXR are thereby able to bind a variety of endogenous and natural occurring compounds, including 9-cis retinoic acid (9-cis RA), linoleic acid (and other unsaturated fatty acids), and phytanic acid (Dominguez et al., 2017). These compounds are all readily available as nutrients and RXR therefore is an important hub for the integration of nutritional information into metabolic and developmental pathways. However, despite the name of the receptor, there is considerable doubt on the physiological relevance of 9-cis RA as ligand for RXR (Mic et al., 2003; Calleja, 2006; Dawson and Xia, 2012) and it seems more probable that 9-cis-13,14-dihydroretinoic acid is an endogenous ligand (Rühl et al., 2015), while various fatty acid ligands obtained through the diet might be relevant RXR ligands (Dominguez et al., 2017).

Depending on the interaction partner, liganded RXR either activate signaling or enhance it. The dimerization partners can be classified in permissive and nonpermissive. Hence, ligand binding in either of the dimers is sufficient to activate signaling (permissive), or signaling is activated only if the dominant partner (not RXR) is liganded (nonpermissive) (Germain et al., 2002; Desvergne, 2007). Interestingly, this classification coincides with the specificity and binding affinity strength of the ligand to the receptor. Nonpermissive NRs are highly specific for their ligand, hence exhibit a strong binding affinity. Nonpermissive receptors include TR, VDR, and RAR. They fulfill crucial developmental signaling and recognize endogenous hormones. Additional binding of a ligand to the RXR generally enhances the signaling strength, thus forms an option for modulating the signaling outcome (Germain et al., 2002).

Nonpermissive signaling seems crucial already in evolutionary early branching organisms like Cnidaria, where it promotes strobilation in *A. aurita* (Fuchs et al., 2014). In *T. adhaerens*, the supplementation of 9-cis RA in the food modulates growth and shape, which is recognized by the RXR (Novotný et al., 2017). The fly RXR homolog *usp* is the binding partner of the EcR (Yao et al., 1992; Yao et al., 1993). Although 9-cis RA seems not to be a relevant ligand for *usp* (Oro et al., 1990), correct formation of the ligand binding pocket in *usp* is necessary for normal larva to adult transition in *Drosophila*, thus Usp mediates another control point for correct development (Jones et al., 2013). In vertebrates, TR-RXR dimer mediate morphogenesis and specific inhibitors/activators for RXR are able to abrogate/enhance precocious metamorphosis under T3 treatment (Mengeling et al., 2018). Given the range of RXR ligands and its modulating role in metamorphosis, it is very likely that RXR has a function in coordination of major developmental steps to the nutritional state of the organism. However, the current data shows only insufficiently if and how RXR relay this information to developmental decisions.

Peroxisome proliferator-activated receptor, LXR, FXR, and PXR are permissive NRs and exhibit a broader range of possible ligands with a much lower binding affinity for them. However, they play important roles in detoxification and regulation of metabolism (Desvergne, 2007; Duniec-Dmuchowski et al., 2007; Lim and Huang, 2008).

THE ROLE OF CYP ENZYMES IN NR REGULATION AND FUNCTION

Cytochrome P450 proteins are a class of oxidizing enzymes, which have a broad range of substrates. They play a pivotal role in metabolizing hydrophobic molecules by oxygenation and thus render them more hydrophilic for subsequent function in metabolism and signaling (Danielson, 2002).

CYP enzyme activity is closely regulated in the interplay with NRs. On the one hand, most of the ligands of the NRs are synthesized by at least one CYP enzyme (Miller, 1988; Cheng et al., 2004; Motola et al., 2006), while on the other hand many, if not all NRs regulate the expression of CYP enzymes after activation (Honkakoski and Negishi, 2000). This tight interaction forms feedback mechanisms within the regulation of NRs and renders CYP enzymes extremely important for environmental signal integration. They form key regulatory steps for the production or catabolism of hormones, which control developmental decision points (Miller, 1988; Cheng et al., 2004; Gilbert, 2004; Motola et al., 2006; Catharine Ross and Zolfaghari, 2011).

Although tightly integrated in the NR network, CYP enzymes appeared earlier in evolution than NRs and are present in all kingdoms of life (Danielson, 2002; Nelson, 2018) in contrast to NRs, which can be found only in metazoans (Bridgham et al., 2010). The ancestral function for CYPs was not necessarily associated with metabolism of xenobiotics but rather part of the physiological metabolism (Bridgham et al., 2010). In extant species, most of the CYP enzymes are involved in either metabolization of xenobiotics or the production of structural or signal molecules (Sezutsu et al., 2013) and can be functionally distinguished into environmental response genes or physiological metabolic regulators (Sezutsu et al., 2013).

In metazoans, CYP enzymes can be roughly classified into 10–11 major classes, so-called clans: CYP-clan 2, 3, 4, 7, 19, 20, 26, 46, 51, 74, and mito (-chondrial) (Gotoh, 2012; Nelson et al., 2013). These have evolved mainly by gene duplication events, which led to blooming of some of the clans with many similar enzymes and a broad range of substrates (Nelson et al., 2013). However, clans that contain genes, which are associated with hormone synthesis are usually small, with only one or a few members, indicating more evolutionary constraints for these genes (Thomas, 2007). Furthermore, these clans are generally rather derived and appeared late in evolution, like the enzymes for the steroid synthesis, which can only be found in phyla leading to vertebrates (Gotoh, 2012) or ecdysone-producing enzymes in Arthropoda (Markov et al., 2009).

In general, CYP enzymes belong to the fastest evolving genes and there is not a single residue conserved across this group of genes (Danielson, 2002; Sezutsu et al., 2013) and even the number of members in the different clans, as well as the number of clans present in the different phyla is highly variable (Nelson et al., 2013). Even developmental important genes like CYP307, which is involved in ecdysone production of arthropods, are highly unstable. Several paralogues of CYP307 were independently lost and gained within the arthropod clade (Sezutsu et al., 2013) and it exemplifies that the genetic plasticity can cause the adaption of developmental processes to the environment on the genetic level.

FROM ENVIRONMENTAL SENSOR TO DEVELOPMENTAL DETERMINANT

It is worth mentioning that it is no coincidence that the NRs form these conserved signaling molecules, which regulate postembryonal developmental transitions. A main evolutionary argument for distinct life cycles in organisms has been the separation of ecological niches in larval and adult forms (Holstein and Laudet, 2014). The timing of the transitions between these two states crucially depends on two factors: the developmental state of the larva and the environmental conditions. Is the larva not developed well enough (too small in most of the cases), it will not survive the transition, because energy reserves are not sufficient to facilitate the tissue remodeling during metamorphosis (De Moed et al., 1999; Laudet, 2011; Gokhale and Shingleton, 2015). On the other hand, if environmental conditions are unfavorable for the transition, the animal might mature in an environment inappropriate for sexual reproduction. This integration of environmental cues into developmental pathways has been termed phenotypic plasticity and was determined to be a major driver of evolution (West-Eberhard, 2003; Gilbert and Epel, 2015).

The first checkpoint is generally closely regulated by endogenous control of the metabolism and growth factors like mTOR or insulin signaling (Gokhale and Shingleton, 2015). The second factor—environment—is less well defined and is highly specific to the respective organism and can range from various cues like population densities (Golden and Riddle, 1982; Zwaal et al., 1997), temperature (Leatherland et al., 1990; Kingsolver and Huey, 2008; Fuchs et al., 2014; Politis et al., 2018), photoperiod (Nakayama and Yoshimura, 2018), or bacterial status (Hadfield, 2011). Integration of these diverse signals necessitates the evolutionary flexibility of NRs and the associated CYP enzymes both in terms of ligand and substrate recognition, respectively. This is especially true for organisms without a functional nervous system (basically Placozoa and Porifera) as there is no special tissue dedicated to the recognition for extrinsic signals. During evolution, the flexibility was early integrated, first into the control of metabolism (Bridgham et al., 2010) and later into developmental pathways (Novotný et al., 2017; **Figure 4**). Once integrated into the developmental pathways, the NRs were evolutionary fixed and thus relatively stable in their function to form the transitional switch. However, with the evolution of the nervous system as an even more flexible system for environmental integration emerged, allowing direct physiological responses (Arendt et al., 2016). However, this freed the original ligand of the NR from evolutionary restrictions and enabled the organism to neofunctionalize the ligand-binding properties (Markov and Laudet, 2011; **Figure 4**). The neuronal signals were again integrated in the production

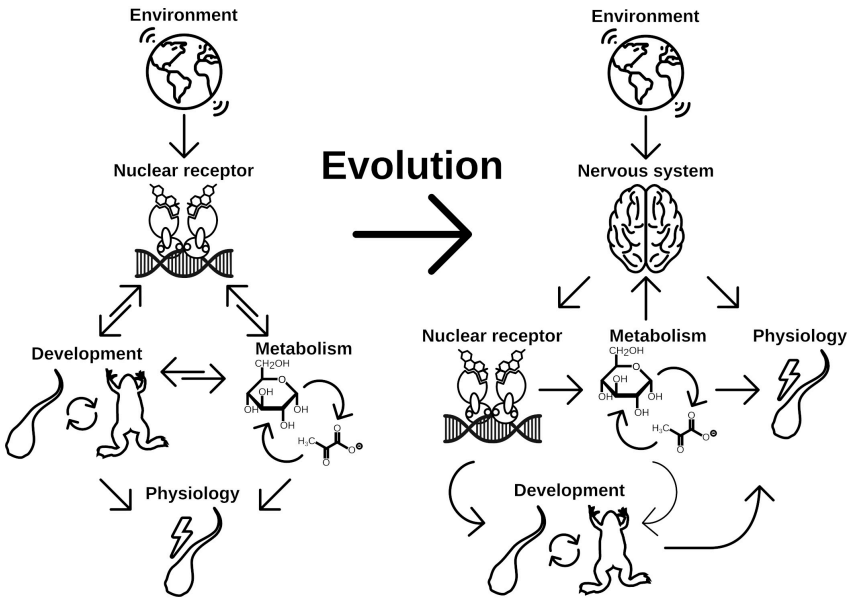

FIGURE 4 | Evolution of NRs as central point for developmental switch control is a consequence of early implementation of physiology regulation. Physiological response to different environmental cues were initially controlled by two main regulation routes, metabolism and life history changes. While changes in metabolism is the immediate response to given conditions, developmental switches control the time point of ecological niche changes. Both routes might be directly controlled by NRs in early branching animals, which renders the NRs a central element for phenotypic plasticity. With evolution of the nervous system, the evolutionary constrains on the NRs for direct control of physiology has been lifted. Consequently evolution of hormone signaling was enabled, which controls developmental processes independent of direct environmental inputs. Environmental cues are recognized by the nervous system, which eventually controls hormone signaling (thus NR signaling) and at the same time is able to directly control aspects of physiology of the organism. It thus adds another layer of environmental signal processing to facilitate more fine grained and at the same time more flexible control of physiology and life history decisions, which increases the phenotypic plasticity of the organism.

of NR ligands controlling the developmental switches, which is reflected in the HPT of vertebrates and the corpora allata—pituitary gland axis in insects, which are strikingly similar (**Figures 3**, **4**).

Although this argumentation is sound in itself, experimental evidence lacks for such a scenario. It would be interesting to further investigate the mechanisms of life history changes in early emerging animals, such as Porifera, Placozoa, and Cnidaria (Bosch et al., 2014). Hereby, Cnidaria take an extraordinary role, as they developed a rudimentary nerve cell system, which forms the prototype for nervous system functions for all other animals (Klimovich and Bosch, 2018). There are intricate interactions between the nervous system of *Hydra* and its associated microbiome (Augustin et al., 2017; Murillo-Rincon et al., 2017). and we have shown that the microbiome controls developmental programs *via* Wnt (Taubenheim et al., 2020). It thus seems that the cnidarian nervous system is able to integrate environmental signals, like the associated bacteria, into developmental pathways. Similarly, Wnt and TGF-β include temperature and metabolic information *via* insulin signaling to control body size in *Hydra* due to timing of asexual reproduction (Mortzfeld et al., 2019). That again links back to resource allocation between reproduction and growth. It is highly analogous to the control of maturation in insects *via* ecdysone or in vertebrates *via* estrogen. Hence, it would not be surprising to see an NR controlling the switch between growth and reproduction in Cnidaria, which would elucidate the evolutionary trajectories of NR signaling in pre-Bilateria. Given the fact that *A. aurita* controls sexual maturation (strobilation) *via* an RXR associated process (Fuchs et al., 2014), it is indeed very likely.

Furthermore, elucidation of ligands for NRs in early emerging metazoa would be interesting, because it would shape our notion on how hormonal ligands and their synthesis pathway evolve. It seems less surprising that the synthesis pathways for the functional hormonal ligands resemble catabolic processes like in estrogen production (Payne and Hales, 2004), activation of TH (deiodination) or the ecdysone production, a multiple oxidated cholesterol derivative and typical for detoxification of xenobiotics (Liska, 1998). Steroid derivatives emerged at least twice independently during evolution (Markov et al., 2009), probably because of diverse possibilities to modify the steroid backbone and its conformation (Brueggemeier and Li, 2010).

Taken together, it is rather a consequence of evolutionary constraints, than coincidence that NRs are central to major postembryonal developmental processes. However, ancestral functionality, the integration of the diverse environmental, as well as intrinsic cues into these pathways, may it be due to sensory neurons or the signaling by growth or metabolic factors, is insufficiently understood across the animal tree of life. To study these systems in non-model organisms, especially on the brink of evolution of nerve systems and bilaterality, promises insights in the evolution of different

life histories. In turn, this promises nothing less than to understand a major driver of ecological adaptation, animal diversity, and the mechanisms of speciation.

AUTHOR CONTRIBUTIONS

JT and CK reviewed the literature. JT, CK, and SF wrote the manuscript. JT and SF supervised and conceptualized the project. All authors contributed to the article and approved the submitted version.

ACKNOWLEDGMENTS

We thank Claudia Taubenheim for fruitful discussions as well as for carefully reading and editing the manuscript.

REFERENCES

Arendt, D., Tosches, M. A., and Marlow, H. (2016). From nerve net to nerve ring, nerve cord and brain — evolution of the nervous system. *Nat. Rev. Neurosci.* 17, 61–72. doi: 10.1038/nrn.2015.15

Augustin, R., Schröder, K., Murillo Rincón, A. P., Fraune, S., Anton-Erxleben, F., Herbst, E. M., et al. (2017). A secreted antibacterial neuropeptide shapes the microbiome of Hydra. *Nat. Commun.* 8:698. doi: 10.1038/s41467-017-00625-1

Avci, H. X., Lebrun, C., Wehrlé, R., Doulazmi, M., Chatonnet, F., Morel, M. P., et al. (2012). Thyroid hormone triggers the developmental loss of axonal regenerative capacity via thyroid hormone receptor 1 and kruppel-like factor 9 in Purkinje cells. *Proc. Natl. Acad. Sci.U.S.A.* 109, 14206–14211. doi: 10.1073/pnas.1119853109

Baker, M. E. (2008). Trichoplax, the simplest known animal, contains an estrogen-related receptor but no estrogen receptor: implications for estrogen receptor evolution. *Biochem. Biophys. Res. Commun.* 375, 623–627. doi: 10.1016/j.bbrc.2008.08.047

Baker, M. E. (2019). Steroid receptors and vertebrate evolution. *Mol. Cell. Endocrinol.* 496:110526. doi: 10.1016/j.mce.2019.110526

Beebe, K., Robins, M. M., Hernandez, E. J., Lam, G., Horner, M. A., and Thummel, C. S. (2020). *Drosophila* estrogen-related receptor directs a transcriptional switch that supports adult glycolysis and lipogenesis. *Genes Dev.* 34, 701–714. doi: 10.1101/gad.335281.119

Bertrand, S., Brunet, F. G., Escriva, H., Parmentier, G., Laudet, V., and Robinson-Rechavi, M. (2004). Evolutionary genomics of nuclear receptors: from twenty-five ancestral genes to derived endocrine systems. *Mol. Biol. Evol.* 21, 1923–1937. doi: 10.1093/molbev/msh200

Blanckenhorn, W. U. (2000). The evolution of body size: what keeps organisms small? *Q. Rev. Biol.* 75, 385–407. doi: 10.1086/393620

Bosch, T. C. G., Adamska, M., Augustin, R., Domazet-Loso, T., Foret, S., Fraune, S., et al. (2014). How do environmental factors influence life cycles and development? An experimental framework for early-diverging metazoans: prospects & overviews. *BioEssays* 36, 1185–1194. doi: 10.1002/bies.201400065

Bridgham, J. T., Eick, G. N., Larroux, C., Deshpande, K., Harms, M. J., Gauthier, M. E., et al. (2010). Protein evolution by molecular tinkering: diversification of the nuclear receptor superfamily from a ligand-dependent ancestor. *PLoS Biol.* 8:e1000497. doi: 10.1371/journal.pbio.1000497

Brueggemeier, R. W., and Li, P. K. (2010). "Fundamentals of steroid chemistry and biochemistry," in *Burger's Medicinal Chemistry and Drug Discovery*, ed. D. J. Abraham (Hoboken, NJ: John Wiley & Sons, Inc), bmc053.

Callard, G. V., Tarrant, A. M., Novillo, A., Yacci, P., Ciaccia, L., Vajda, S., et al. (2011). Evolutionary origins of the estrogen signaling system: insights from amphioxus. *J. Steroid Biochem. Mol. Biol.* 127, 176–188. doi: 10.1016/j.jsbmb.2011.03.022

Calleja, C. (2006). Genetic and pharmacological evidence that a retinoic acid cannot be the RXR-activating ligand in mouse epidermis keratinocytes. *Genes Dev.* 20, 1525–1538. doi: 10.1101/gad.368706

Callier, V., and Nijhout, H. F. (2011). Control of body size by oxygen supply reveals size-dependent and size-independent mechanisms of molting and metamorphosis. *Proc. Natl. Acad. Sci. U.S.A.* 108, 14664–14669. doi: 10.1073/pnas.1106556108

Campinho, M. A. (2019). Teleost metamorphosis: the role of thyroid hormone. *Front. Endocrinol.* 10:383. doi: 10.3389/fendo.2019.00383

Cannon, J. T., Vellutini, B. C., Smith, J., Ronquist, F., Jondelius, U., and Hejnol, A. (2016). Xenacoelomorpha is the sister group to Nephrozoa. *Nature* 530, 89–93. doi: 10.1038/nature16520

Castro, M. I., Alex, S., Young, R. A., Braverman, L. E., and Emerson, C. H. (1986). Total and free serum thyroid hormone concentrations in fetal and adult pregnant and Nonpregnant Guinea Pigs. *Endocrinology* 118, 533–537. doi: 10.1210/endo-118-2-533

Catharine Ross, A., and Zolfaghari, R. (2011). Cytochrome P450s in the regulation of cellular retinoic acid metabolism. *Annu. Rev. Nutr.* 31, 65–87. doi: 10.1146/annurev-nutr-072610-145127

Chandra, V., Huang, P., Hamuro, Y., Raghuram, S., Wang, Y., Burris, T. P., et al. (2008). Structure of the intact PPAR-γ–RXR-α nuclear receptor complex on DNA. *Nature* 456, 350–356. doi: 10.1038/nature07413

Cheng, J. B., Levine, M. A., Bell, N. H., Mangelsdorf, D. J., and Russell, D. W. (2004). Genetic evidence that the human CYP2R1 enzyme is a key vitamin D 25-hydroxylase. *Proc. Natl. Acad. Sci. U.S.A.* 101, 7711–7715. doi: 10.1073/pnas.0402490101

Chino, Y., Saito, M., Yamasu, K., Suyemitsu, T., and Ishihara, K. (1994). Formation of the adult rudiment of sea urchins is influenced by thyroid hormones. *Dev. Biol.* 161, 1–11. doi: 10.1006/dbio.1994.1001

Christensen, C. F., Koyama, T., Nagy, S., Danielsen, E. T., Texada, M. J., Halberg, K. A., et al. (2020). Ecdysone-dependent feedback regulation of prothoracicotropic hormone controls the timing of developmental maturation. *Development* 147:dev188110. doi: 10.1242/dev.188110

Colombani, J. (2005). Antagonistic actions of ecdysone and insulins determine final size in *Drosophila*. *Science* 310, 667–670. doi: 10.1126/science.1119432

Colombani, J., Andersen, D. S., Boulan, L., Boone, E., Romero, N., Virolle, V., et al. (2015). Drosophila Lgr3 couples organ growth with maturation and ensures developmental stability. *Curr. Biol.* 25, 2723–2729. doi: 10.1016/j.cub.2015.09.020

Danielson, B. S. P. P. B. (2002). The cytochrome P450 superfamily: biochemistry, evolution and drug metabolism in humans. *Curr. Drug Metab.* 3, 561–597. doi: 10.2174/1389200023337054

Dawson, M. I., and Xia, Z. (2012). The retinoid X receptors and their ligands. *Biochim. Biophys. Acta BBA - Mol. Cell Biol. Lipids* 1821, 21–56. doi: 10.1016/j.bbalip.2011.09.014

De Moed, G. H., Kruitwagen, C. L. J. J., De Jong, G., and Scharloo, W. (1999). Critical weight for the induction of pupariation in Drosophila melanogaster: genetic and environmental variation. *J. Evol. Biol.* 12, 852–858. doi: 10.1046/j.1420-9101.1999.00103.x

Denver, R. J. (2009). Stress hormones mediate environment-genotype interactions during amphibian development. *Gen. Comp. Endocrinol.* 164, 20–31. doi: 10.1016/j.ygcen.2009.04.016

Desvergne, B. (2007). "RXR: from partnership to leadership in metabolic regulations," in *Vitamins & Hormones*, ed. G. Litwack (Amsterdam: Elsevier), 1–32.

Dominguez, M., Alvarez, S., and de Lera, A. R. (2017). Natural and structure-based RXR ligand scaffolds and their functions. *Curr. Top. Med. Chem.* 17, 631–662. doi: 10.2174/1568026616666160617072521

Dubrovsky, E. B., and Bernardo, T. J. (2014). "The juvenile hormone receptor and molecular mechanisms of juvenile hormone action," in *Advances in Insect Physiology*, ed. S. Simpson (Amsterdam: Elsevier), 305–388.

Duniec-Dmuchowski, Z., Ellis, E., Strom, S. C., and Kocarek, T. A. (2007). Regulation of CYP3A4 and CYP2B6 expression by liver X receptor agonists. *Biochem. Pharmacol.* 74, 1535–1540. doi: 10.1016/j.bcp.2007.07.040

Eick, G. N., Colucci, J. K., Harms, M. J., Ortlund, E. A., and Thornton, J. W. (2012). Evolution of minimal specificity and promiscuity in steroid hormone receptors. *PLoS Genet.* 8:e1003072. doi: 10.1371/journal.pgen.1003072

Escriva, H., Bertrand, S., and Laudet, V. (2004). The evolution of the nuclear receptor superfamily. *Essays Biochem.* 40, 11–26. doi: 10.1042/bse0400011

Escriva, H., Delaunay, F., and Laudet, V. (2000). Ligand binding and nuclear receptor evolution. *BioEssays News Rev. Mol. Cell. Dev. Biol.* 22, 717–727. doi: 10.1002/1521-1878(200008)22:8<717::AID-BIES5>3.0.CO;2-I

Escriva, H., Langlois, M.-C., Mendonca, R. L., Pierce, R., and Laudet, V. (1998). Evolution and diversification of the nuclear receptor superfamilya. *Ann. N. Y. Acad. Sci.* 839, 143–146. doi: 10.1111/j.1749-6632.1998.tb10747.x

Escriva, H., Manzon, L., Youson, J., and Laudet, V. (2002). Analysis of lamprey and hagfish genes reveals a complex history of gene duplications during early vertebrate evolution. *Mol. Biol. Evol.* 19, 1440–1450. doi: 10.1093/oxfordjournals.molbev.a004207

Evans, R. M., and Mangelsdorf, D. J. (2014). Nuclear receptors, RXR, and the big bang. *Cell* 157, 255–266. doi: 10.1016/j.cell.2014.03.012

Fahrbach, S. E., Smagghe, G., and Velarde, R. A. (2012). Insect nuclear receptors. *Annu. Rev. Entomol.* 57, 83–106. doi: 10.1146/annurev-ento-120710-100607

Faunes, F., and Larraín, J. (2016). Conservation in the involvement of heterochronic genes and hormones during developmental transitions. *Dev. Biol.* 416, 3–17. doi: 10.1016/j.ydbio.2016.06.013

Fernandes, D., Loi, B., and Porte, C. (2011). Biosynthesis and metabolism of steroids in molluscs. *J. Steroid Biochem. Mol. Biol.* 127, 189–195. doi: 10.1016/j.jsbmb.2010.12.009

Fielenbach, N., and Antebi, A. (2008). C. elegans dauer formation and the molecular basis of plasticity. *Genes Dev.* 22, 2149–2165. doi: 10.1101/gad.1701508

Filardo, E. J., and Thomas, P. (2012). Minireview: G protein-coupled estrogen receptor-1, GPER-1: its mechanism of action and role in female reproductive cancer, renal and vascular physiology. *Endocrinology* 153, 2953–2962. doi: 10.1210/en.2012-1061

Fodor, I., Urbán, P., Scott, A. P., and Pirger, Z. (2020). A critical evaluation of some of the recent so-called 'evidence' for the involvement of vertebrate-type sex steroids in the reproduction of mollusks. *Mol. Cell. Endocrinol.* 516:10949. doi: 10.1016/j.mce.2020.110949

Forhead, A. J., and Fowden, A. L. (2014). Thyroid hormones in fetal growth and prepartum maturation. *J. Endocrinol.* 221, R87–R103. doi: 10.1530/JOE-14-0025

Frankl-Vilches, C., and Gahr, M. (2018). Androgen and estrogen sensitivity of bird song: a comparative view on gene regulatory levels. *J. Comp. Physiol. A* 204, 113–126. doi: 10.1007/s00359-017-1236-y

Fuchs, B., Wang, W., Graspeuntner, S., Li, Y., Insua, S., Herbst, E. M., et al. (2014). Regulation of polyp-to-jellyfish transition in aurelia aurita. *Curr. Biol.* 24, 263–273. doi: 10.1016/j.cub.2013.12.003

Fuentes, N., and Silveyra, P. (2019). "Estrogen receptor signaling mechanisms," in *Advances in Protein Chemistry and Structural Biology*, ed. R. Donev (Amsterdam: Elsevier), 135–170.

Fukazawa, H., Hirai, H., Hori, H., Roberts, R. D., Nukaya, H., Ishida, H., et al. (2001). Induction of abalone larval metamorphosis by thyroid hormones. *Fish. Sci.* 67, 985–988. doi: 10.1046/j.1444-2906.2001.00351.x

Gáliková, M., Klepsatel, P., Senti, G., and Flatt, T. (2011). Steroid hormone regulation of C. elegans and *Drosophila* aging and life history. *Exp. Gerontol.* 46, 141–147. doi: 10.1016/j.exger.2010.08.021

Garcia, M., Thirouard, L., Sedès, L., Monrose, M., Holota, H., Caira, F., et al. (2018). Nuclear receptor metabolism of bile acids and Xenobiotics: a coordinated detoxification system with impact on health and diseases. *Int. J. Mol. Sci.* 19:3630. doi: 10.3390/ijms19113630

Garelli, A., Heredia, F., Casimiro, A. P., Macedo, A., Nunes, C., Garcez, M., et al. (2015). Dilp8 requires the neuronal relaxin receptor Lgr3 to couple growth to developmental timing. *Nat. Commun.* 6:8732. doi: 10.1038/ncomms9732

Gehrke, A. R., Neverett, E., Luo, Y. J., Brandt, A., Ricci, L., Hulett, R. E., et al. (2019). Acoel genome reveals the regulatory landscape of whole-body regeneration. *Science* 363:eaau6173. doi: 10.1126/science.aau6173

Germain, P., Iyer, J., Zechel, C., and Gronemeyer, H. (2002). Co-regulator recruitment and the mechanism of retinoic acid receptor synergy. *Nature* 415, 187–192. doi: 10.1038/415187a

Germain, P., Staels, B., Dacquet, C., Spedding, M., and Laudet, V. (2006). Overview of nomenclature of nuclear receptors. *Pharmacol. Rev.* 58, 685–704. doi: 10.1124/pr.58.4.2

Gibbens, Y. Y., Warren, J. T., Gilbert, L. I., and O'Connor, M. B. (2011). Neuroendocrine regulation of *Drosophila* metamorphosis requires TGF/Activin signaling. *Development* 138, 2693–2703. doi: 10.1242/dev.063412

Gilbert, L. I. (2004). Halloween genes encode P450 enzymes that mediate steroid hormone biosynthesis in *Drosophila* melanogaster. *Mol. Cell. Endocrinol.* 215, 1–10. doi: 10.1016/j.mce.2003.11.003

Gilbert, S. F., and Epel, D. (2015). *Ecological Developmental Biology: The Environmental Regulation of Development, Health, and Evolution*, Second Edn. Sunderland, MA: Sinauer Associates, Inc.

Gissendanner, C. R., Crossgrove, K., Kraus, K. A., Maina, C. V., and Sluder, A. E. (2004). Expression and function of conserved nuclear receptor genes in Caenorhabditis elegans. *Dev. Biol.* 266, 399–416. doi: 10.1016/j.ydbio.2003.10.014

Gokhale, R. H., and Shingleton, A. W. (2015). Size control: the developmental physiology of body and organ size regulation: the developmental physiology of size control. *Wiley Interdiscip. Rev. Dev. Biol.* 4, 335–356. doi: 10.1002/wdev.181

Golden, J., and Riddle, D. (1982). A pheromone influences larval development in the nematode Caenorhabditis elegans. *Science* 218, 578–580. doi: 10.1126/science.6896933

Gotoh, O. (2012). Evolution of cytochrome P450 genes from the viewpoint of genome informatics. *Biol. Pharm. Bull.* 35, 812–817. doi: 10.1248/bpb.35.812

Hadfield, M. G. (2011). Biofilms and marine invertebrate larvae: what bacteria produce that larvae use to choose settlement sites. *Annu. Rev. Mar. Sci.* 3, 453–470. doi: 10.1146/annurev-marine-120709-142753

Hamilton, K. J., Hewitt, S. C., Arao, Y., and Korach, K. S. (2017). "Estrogen hormone biology," in *Current Topics in Developmental Biology*, ed. G. Schatten (Amsterdam: Elsevier), 109–146.

Hanlon, C., Ramachandran, R., Zuidhof, M. J., and Bédécarrats, G. Y. (2020). Should I lay or should i grow: photoperiodic versus metabolic cues in chickens. *Front. Physiol.* 11:707. doi: 10.3389/fphys.2020.00707

Heyland, A., Reitzel, A. M., and Hodin, J. (2004). Thyroid hormones determine developmental mode in sand dollars (Echinodermata: Echinoidea). *Evol. Dev.* 6, 382–392. doi: 10.1111/j.1525-142X.2004.04047.x

Hirose, K., Payumo, A. Y., Cutie, S., Hoang, A., Zhang, H., Guyot, R., et al. (2019). Evidence for hormonal control of heart regenerative capacity during endothermy acquisition. *Science* 364, 184–188. doi: 10.1126/science.aar2038

Hiruma, K., and Kaneko, Y. (2013). Hormonal regulation of insect metamorphosis with special reference to juvenile hormone biosynthesis. *Curr. Topics Dev. Biol.* 103, 73–100.

Holmes, J. A., and Youson, J. H. (1994). Fall condition factor and temperature influence the incidence of metamorphosis in sea lampreys, Petromyzon marinus. *Can. J. Zool.* 72, 1134–1140. doi: 10.1139/z94-151

Holstein, T. W., and Laudet, V. (2014). Life-history evolution: at the origins of metamorphosis. *Curr. Biol.* 24, R159–R161. doi: 10.1016/j.cub.2014.01.003

Holzer, G., and Laudet, V. (2013). "Thyroid hormones and postembryonic development in amniotes," in *Current Topics in Developmental Biology*, ed. G. Schatten (Amsterdam: Elsevier), 397–425.

Holzer, G., Roux, N., and Laudet, V. (2017). Evolution of ligands, receptors and metabolizing enzymes of thyroid signaling. *Mol. Cell. Endocrinol.* 459, 5–13. doi: 10.1016/j.mce.2017.03.021

Honkakoski, P., and Negishi, M. (2000). Regulation of cytochrome P450 (CYP) genes by nuclear receptors. *Biochem. J.* 347:321. doi: 10.1042/0264-6021:3470321

Huang, W., Xu, F., Qu, T., Zhang, R., Li, L., Que, H., et al. (2015). Identification of thyroid hormones and functional characterization of thyroid hormone receptor in the pacific oyster crassostrea gigas provide insight into evolution of the thyroid hormone system. *PLoS One* 10:e0144991. doi: 10.1371/journal.pone.0144991

Hyde, C. J., Elizur, A., and Ventura, T. (2019). The crustacean ecdysone cassette: a gatekeeper for molt and metamorphosis. *J. Steroid Biochem. Mol. Biol.* 185, 172–183. doi: 10.1016/j.jsbmb.2018.08.012

Hyun, S. (2013). Body size regulation and insulin-like growth factor signaling. *Cell. Mol. Life Sci.* 70, 2351–2365. doi: 10.1007/s00018-013-1313-5

Jaszczak, J. S., Wolpe, J. B., Bhandari, R., Jaszczak, R. G., and Halme, A. (2016). Growth Coordination During *Drosophila* melanogaster Imaginal disc regeneration is mediated by signaling through the relaxin receptor Lgr3

in the prothoracic gland. *Genetics* 204, 703–709. doi: 10.1534/genetics.116.193706

Jones, B. L., Walker, C., Azizi, B., Tolbert, L., Williams, L. D., and Snell, T. W. (2017). Conservation of estrogen receptor function in invertebrate reproduction. *BMC Evol. Biol.* 17:65. doi: 10.1186/s12862-017-0909-z

Jones, G., and Sharp, P. A. (1997). Ultraspiracle: an invertebrate nuclear receptor for juvenile hormones. *Proc. Natl. Acad. Sci. U.S.A.* 94, 13499–13503. doi: 10.1073/pnas.94.25.13499

Jones, G., Teal, P., Henrich, V. C., Krzywonos, A., Sapa, A., Wozniak, M., et al. (2013). Ligand binding pocket function of *Drosophila* USP is necessary for metamorphosis. *Gen. Comp. Endocrinol.* 182, 73–82. doi: 10.1016/j.ygcen.2012.11.009

Kaur, S., Jobling, S., Jones, C. S., Noble, L. R., Routledge, E. J., and Lockyer, A. E. (2015). The nuclear receptors of biomphalaria glabrata and lottia gigantea: implications for developing new model organisms. *PLoS One* 10:e0121259. doi: 10.1371/journal.pone.0121259

Keay, J., and Thornton, J. W. (2009). Hormone-activated estrogen receptors in annelid invertebrates: implications for evolution and endocrine disruption. *Endocrinology* 150, 1731–1738. doi: 10.1210/en.2008-1338

Ketata, I., Denier, X., Hamza-Chaffai, A., and Minier, C. (2008). Endocrine-related reproductive effects in molluscs. *Comp. Biochem. Physiol. Part C Toxicol. Pharmacol.* 147, 261–270. doi: 10.1016/j.cbpc.2007.11.007

Khalturin, K., Billas, I. M. L., Chebaro, Y., Reitzel, A. M., Tarrant, A. M., Laudet, V., et al. (2018). NR3E receptors in cnidarians: a new family of steroid receptor relatives extends the possible mechanisms for ligand binding. *J. Steroid Biochem. Mol. Biol.* 184, 11–19. doi: 10.1016/j.jsbmb.2018.06.014

Kim, D. H., Kim, H. S., Hwang, H. J., Kim, H. J., Hagiwara, A., Lee, J. S., et al. (2017). Genome-wide identification of nuclear receptor (NR) genes and the evolutionary significance of the NR1O subfamily in the monogonont rotifer Brachionus spp. *Gen. Comp. Endocrinol.* 252, 219–225. doi: 10.1016/j.ygcen.2017.06.030

Kingsolver, J. G., and Huey, R. B. (2008). Size, temperature, and fitness: three rules. *Evol. Ecol. Res.* 10, 251–268.

Klimovich, A. V., and Bosch, T. C. G. (2018). Rethinking the role of the nervous system: lessons from the hydra holobiont. *BioEssays* 40:1800060. doi: 10.1002/bies.201800060

Klootwijk, W., Friesema, E. C. H., and Visser, T. J. (2011). A Nonselenoprotein from amphioxus deiodinates triac but not T3: is triac the primordial bioactive thyroid hormone? *Endocrinology* 152, 3259–3267. doi: 10.1210/en.2010-1408

Koelle, M. R., Talbot, W. S., Segraves, W. A., Bender, M. T., Cherbas, P., and Hogness, D. S. (1991). The *drosophila* EcR gene encodes an ecdysone receptor, a new member of the steroid receptor superfamily. *Cell* 67, 59–77. doi: 10.1016/0092-8674(91)90572-G

Köhler, H.-R., Kloas, W., Schirling, M., Lutz, I., Reye, A. L., Langen, J. S., et al. (2007). Sex steroid receptor evolution and signalling in aquatic invertebrates. *Ecotoxicology* 16, 131–143. doi: 10.1007/s10646-006-0111-3

Koyama, T., Texada, M. J., Halberg, K. A., and Rewitz, K. (2020). Metabolism and growth adaptation to environmental conditions in *Drosophila*. *Cell. Mol. Life Sci.* 77, 4523–4551. doi: 10.1007/s00018-020-03547-2

Kumar, R., and Thompson, E. B. (1999). The structure of the nuclear hormone receptors. *Steroids* 64, 310–319. doi: 10.1016/S0039-128X(99)00014-8

Kuraku, S., and Kuratani, S. (2006). Time scale for cyclostome evolution inferred with a phylogenetic diagnosis of hagfish and lamprey cDNA Sequences. *Zoolog. Sci.* 23, 1053–1064. doi: 10.2108/zsj.23.1053

Laguerre, M., and Veenstra, J. A. (2010). Ecdysone receptor homologs from mollusks, leeches and a polychaete worm. *FEBS Lett.* 584, 4458–4462. doi: 10.1016/j.febslet.2010.10.004

Laslo, M., Denver, R. J., and Hanken, J. (2019). Evolutionary conservation of thyroid hormone receptor and deiodinase expression dynamics in ovo in a direct-developing frog, Eleutherodactylus coqui. *Front. Endocrinol.* 10:307. doi: 10.3389/fendo.2019.00307

Laudet, V. (1997). Evolution of the nuclear receptor superfamily: early diversification from an ancestral orphan receptor. *J. Mol. Endocrinol.* 19, 207–226. doi: 10.1677/jme.0.0190207

Laudet, V. (2011). The origins and evolution of vertebrate metamorphosis. *Curr. Biol.* 21, R726–R737. doi: 10.1016/j.cub.2011.07.030

Lazcano, I., Rodríguez Rodríguez, A., Uribe, R. M., Orozco, A., Joseph-Bravo, P., and Charli, J.-L. (2020). Evolution of thyrotropin-releasing factor extracellular communication units. *Gen. Comp. Endocrinol.* 305:113642. doi: 10.1016/j.ygcen.2020.113642

Leatherland, J. F., Hilliard, R. W., Macey, D. J., and Potter, I. C. (1990). Changes in serum thyroxine and triiodothyronine concentrations during metamorphosis of the Southern Hemisphere Lamprey Geotria australis, and the effect of propylthiouracil, triiodothyronine and environmental temperature on serum thyroid hormone concentrations of ammocoetes. *Fish Physiol. Biochem.* 8, 167–177. doi: 10.1007/BF00004444

Lee, G. J., Han, G., Yun, H. M., Lim, J. J., Noh, S., Lee, J., et al. (2018). Steroid signaling mediates nutritional regulation of juvenile body growth via IGF-binding protein in *Drosophila*. *Proc. Natl. Acad. Sci. U.S.A.* 115, 5992–5997. doi: 10.1073/pnas.1718834115

Lee, J.-W., Kim, N.-H., and Milanesi, A. (2014). Thyroid hormone signaling in muscle development, repair and metabolism. *J. Endocrinol. Diabetes Obes.* 2:1046.

Lehmann, J. M., Kliewer, S. A., Moore, L. B., Smith-Oliver, T. A., Oliver, B. B., Su, J. L., et al. (1997). Activation of the nuclear receptor lxr by oxysterols defines a new hormone response pathway. *J. Biol. Chem.* 272, 3137–3140. doi: 10.1074/jbc.272.6.3137

Leka-Emiri, S., Chrousos, G. P., and Kanaka-Gantenbein, C. (2017). The mystery of puberty initiation: genetics and epigenetics of idiopathic central precocious puberty (ICPP). *J. Endocrinol. Invest.* 40, 789–802. doi: 10.1007/s40618-017-0627-9

Li, Q., and Gong, Z. (2015). Cold-sensing regulates *Drosophila* growth through insulin-producing cells. *Nat. Commun.* 6:10083. doi: 10.1038/ncomms10083

Li, Y., Padmanabha, D., Gentile, L. B., Dumur, C. I., Beckstead, R. B., and Baker, K. D. (2013). HIF- and Non-HIF-regulated hypoxic responses require the estrogen-related receptor in *Drosophila* melanogaster. *PLoS Genet.* 9:e1003230. doi: 10.1371/journal.pgen.1003230

Li, Y.-F., Cheng, Y. L., Chen, K., Cheng, Z. Y., Zhu, X., Liang, X., et al. (2020). Thyroid hormone receptor: a new player in epinephrine-induced larval metamorphosis of the hard-shelled mussel. *Gen. Comp. Endocrinol.* 287:113347. doi: 10.1016/j.ygcen.2019.113347

Lim, Y.-P., and Huang, J. (2008). Interplay of Pregnane X receptor with other nuclear receptors on gene regulation. *Drug Metab. Pharmacokinet* 23, 14–21. doi: 10.2133/dmpk.23.14

Liska, D. J. (1998). The detoxification enzyme systems. *Altern. Med. Rev. J. Clin. Ther.* 3, 187–198.

Liu, S., Li, K., Gao, Y., Liu, X., Chen, W., Ge, W., et al. (2018). Antagonistic actions of juvenile hormone and 20-hydroxyecdysone within the ring gland determine developmental transitions in *Drosophila*. *Proc. Natl. Acad. Sci. U.S.A.* 115, 139–144. doi: 10.1073/pnas.1716897115

Maden, M. (2018). The evolution of regeneration – where does that leave mammals? *Int. J. Dev. Biol.* 62, 369–372. doi: 10.1387/ijdb.180031mm

Manzon, L. A., Youson, J. H., Holzer, G., Staiano, L., Laudet, V., and Manzon, R. G. (2014). Thyroid hormone and retinoid X receptor function and expression during sea lamprey (Petromyzon marinus) metamorphosis. *Gen. Comp. Endocrinol.* 204, 211–222. doi: 10.1016/j.ygcen.2014.05.030

Manzon, R. G., and Manzon, L. A. (2017). Lamprey metamorphosis: thyroid hormone signaling in a basal vertebrate. *Mol. Cell. Endocrinol.* 459, 28–42. doi: 10.1016/j.mce.2017.06.015

Markov, G. V., and Laudet, V. (2011). Origin and evolution of the ligand-binding ability of nuclear receptors. *Mol. Cell. Endocrinol.* 334, 21–30. doi: 10.1016/j.mce.2010.10.017

Markov, G. V., Girard, J., Laudet, V., and Leblanc, C. (2018). Hormonally active phytochemicals from macroalgae: a largely untapped source of ligands to deorphanize nuclear receptors in emerging marine animal models. *Gen. Comp. Endocrinol.* 265, 41–45. doi: 10.1016/j.ygcen.2018.06.004

Markov, G. V., Gutierrez-Mazariegos, J., Pitrat, D., Billas, I. M. L., Bonneton, F., Moras, D., et al. (2017). Origin of an ancient hormone/receptor couple revealed by resurrection of an ancestral estrogen. *Sci. Adv.* 3:e1601778. doi: 10.1126/sciadv.1601778

Markov, G. V., Tavares, R., Dauphin-Villemant, C., Demeneix, B. A., Baker, M. E., and Laudet, V. (2009). Independent elaboration of steroid hormone signaling

pathways in metazoans. *Proc. Natl. Acad. Sci. U.S.A.* 106, 11913–11918. doi: 10.1073/pnas.0812138106

Markov, G., Lecointre, G., Demeneix, B., and Laudet, V. (2008). The 'street light syndrome', or how protein taxonomy can bias experimental manipulations. *BioEssays* 30, 349–357. doi: 10.1002/bies.20730

Marshall, L. N., Vivien, C. J., Girardot, F., Péricard, L., Scerbo, P., Palmier, K., et al. (2019). Stage-dependent cardiac regeneration in Xenopus is regulated by thyroid hormone availability. *Proc. Natl. Acad. Sci. U.S.A.* 116, 3614–3623. doi: 10.1073/pnas.1803794116

Matsubara, S., Shiraishi, A., Osugi, T., Kawada, T., and Satake, H. (2019). The regulation of oocyte maturation and ovulation in the closest sister group of vertebrates. *eLife* 8:e49062. doi: 10.7554/eLife.49062

McKeown, A. N., Bridgham, J. T., Anderson, D. W., Murphy, M. N., Ortlund, E. A., and Thornton, J. W. (2014). Evolution of DNA specificity in a transcription factor family produced a new gene regulatory module. *Cell* 159, 58–68. doi: 10.1016/j.cell.2014.09.003

McNabb, F. M. A. (2006). Avian thyroid development and adaptive plasticity. *Gen. Comp. Endocrinol.* 147, 93–101. doi: 10.1016/j.ygcen.2005.12.011

McNabb, F. M. A., Lyons, L. J., and Hughes, T. E. (1984). Free thyroid hormones in altricial (Ring Doves) versus precocial (Japanese Quail) Development. *Endocrinology* 115, 2133–2136. doi: 10.1210/endo-115-6-2133

Mengeling, B. J., Goodson, M. L., and Furlow, J. D. (2018). RXR ligands modulate thyroid hormone signaling competence in young Xenopus laevis tadpoles. *Endocrinology* 159, 2576–2595. doi: 10.1210/en.2018-00172

Metzger, D., White, J. H., and Chambon, P. (1988). The human oestrogen receptor functions in yeast. *Nature* 334, 31–36. doi: 10.1038/334031a0

Mhashilkar, A. S., Vankayala, S. L., Liu, C., Kearns, F., Mehrotra, P., Tzertzinis, G., et al. (2016). Identification of ecdysone hormone receptor agonists as a therapeutic approach for treating filarial infections. *PLoS Negl. Trop. Dis.* 10:e0004772. doi: 10.1371/journal.pntd.0004772

Mic, F. A., Molotkov, A., Benbrook, D. M., and Duester, G. (2003). Retinoid activation of retinoic acid receptor but not retinoid X receptor is sufficient to rescue lethal defect in retinoic acid synthesis. *Proc. Natl. Acad. Sci. U.S.A.* 100, 7135–7140. doi: 10.1073/pnas.1231422100

Miller, W. L. (1988). Molecular biology of steroid hormone synthesis. *Endocr. Rev.* 9, 295–318. doi: 10.1210/edrv-9-3-295

Minakata, H., and Tsutsui, K. (2016). Oct-GnRH, the first protostomian gonadotropin-releasing hormone-like peptide and a critical mini-review of the presence of vertebrate sex steroids in molluscs. *Gen. Comp. Endocrinol.* 227, 109–114. doi: 10.1016/j.ygcen.2015.07.011

Mirth, C. K., and Shingleton, A. W. (2012). Integrating body and organ size in drosophila: recent advances and outstanding problems. *Front. Endocrinol.* 3:49. doi: 10.3389/fendo.2012.00049

Mirth, C., Truman, J. W., and Riddiford, L. M. (2005). The role of the prothoracic gland in determining critical weight for metamorphosis in *Drosophila* melanogaster. *Curr. Biol.* 15, 1796–1807. doi: 10.1016/j.cub.2005.09.017

Miyashita, T., Coates, M. I., Farrar, R., Larson, P., Manning, P. L., Wogelius, R. A., et al. (2019). Hagfish from the Cretaceous Tethys Sea and a reconciliation of the morphological–molecular conflict in early vertebrate phylogeny. *Proc. Natl. Acad. Sci. U.S.A.* 116, 2146–2151. doi: 10.1073/pnas.1814794116

Mortzfeld, B. M., Taubenheim, J., Klimovich, A. V., Fraune, S., Rosenstiel, P., and Bosch, T. C. G. (2019). Temperature and insulin signaling regulate body size in Hydra by the Wnt and TGF-beta pathways. *Nat. Commun.* 10:3257. doi: 10.1038/s41467-019-11136-6

Motola, D. L., Cummins, C. L., Rottiers, V., Sharma, K. K., Li, T., Li, Y., et al. (2006). Identification of ligands for DAF-12 that govern dauer formation and reproduction in C. elegans. *Cell* 124, 1209–1223. doi: 10.1016/j.cell.2006.01.037

Mourouzis, I., Lavecchia, A. M., and Xinaris, C. (2020). Thyroid hormone signalling: from the dawn of life to the bedside. *J. Mol. Evol.* 88, 88–103. doi: 10.1007/s00239-019-09908-1

Mullur, R., Liu, Y.-Y., and Brent, G. A. (2014). Thyroid hormone regulation of metabolism. *Physiol. Rev.* 94, 355–382. doi: 10.1152/physrev.00030.2013

Murillo-Rincon, A. P., Klimovich, A., Pemöller, E., Taubenheim, J., Mortzfeld, B., Augustin, R., et al. (2017). Spontaneous body contractions are modulated by the microbiome of Hydra. *Sci. Rep.* 7:15937. doi: 10.1038/s41598-017-16191-x

Nakayama, T., and Yoshimura, T. (2018). Seasonal rhythms: the role of thyrotropin and thyroid hormones. *Thyroid* 28, 4–10. doi: 10.1089/thy.2017.0186

Nelson, D. R. (2018). Cytochrome P450 diversity in the tree of life. *Biochim. Biophys. Acta BBA - Proteins Proteomics* 1866, 141–154. doi: 10.1016/j.bbapap.2017.05.003

Nelson, D. R., Goldstone, J. V., and Stegeman, J. J. (2013). The cytochrome P450 genesis locus: the origin and evolution of animal cytochrome P450s. *Philos. Trans. R. Soc. B Biol. Sci.* 368:20120474. doi: 10.1098/rstb.2012.0474

Novotný, J. P., Chughtai, A. A., Kostrouchová, M., Kostrouchová, V., Kostrouch, D., Kaššák, F., et al. (2017). Trichoplax adhaerens reveals a network of nuclear receptors sensitive to 9- cis -retinoic acid at the base of metazoan evolution. *PeerJ.* 5:e3789. doi: 10.7717/peerj.3789

Nuclear Receptors Nomenclature Committee, (1999). A unified nomenclature system for the nuclear receptor superfamily. *Cell* 97, 161–163. doi: 10.1016/S0092-8674(00)80726-6

Ogino, Y., Tohyama, S., Kohno, S., Toyota, K., Yamada, G., Yatsu, R., et al. (2018). Functional distinctions associated with the diversity of sex steroid hormone receptors ESR and AR. *J. Steroid Biochem. Mol. Biol.* 184, .38–46. doi: 10.1016/j.jsbmb.2018.06.002

Okamoto, N., Viswanatha, R., Bittar, R., Li, Z., Haga-Yamanaka, S., Perrimon, N., et al. (2018). A Membrane transporter is required for steroid hormone uptake in *Drosophila*. *Dev. Cell* 47, 294–305.e7. doi: 10.1016/j.devcel.2018.09.012

Ollikainen, N., Chandsawangbhuwana, C., and Baker, M. E. (2006). Evolution of the thyroid hormone, retinoic acid, ecdysone and liver X receptors. *Integr. Comp. Biol.* 46, 815–826. doi: 10.1093/icb/icl035

Oro, A. E., McKeown, M., and Evans, R. M. (1990). Relationship between the product of the *Drosophila* ultraspiracle locus and the vertebrate retinoid X receptor. *Nature* 347, 298–301. doi: 10.1038/347298a0

Paris, M., Escriva, H., Schubert, M., Brunet, F., Brtko, J., Ciesielski, F., et al. (2008). Amphioxus postembryonic development reveals the homology of chordate metamorphosis. *Curr. Biol.* 18, 825–830. doi: 10.1016/j.cub.2008.04.078

Paris, M., Hillenweck, A., Bertrand, S., Delous, G., Escriva, H., Zalko, D., et al. (2010). Active metabolism of thyroid hormone during metamorphosis of amphioxus. *Integr. Comp. Biol.* 50, 63–74. doi: 10.1093/icb/icq052

Paul, M. J., Probst, C. K., Brown, L. M., and de Vries, G. J. (2018). Dissociation of puberty and adolescent social development in a seasonally breeding species. *Curr. Biol.* 28, 1116–1123.e2. doi: 10.1016/j.cub.2018.02.030

Payne, A. H., and Hales, D. B. (2004). Overview of steroidogenic enzymes in the pathway from cholesterol to active steroid hormones. *Endocr. Rev.* 25, 947–970. doi: 10.1210/er.2003-0030

Politis, S. N., Servili, A., Mazurais, D., Zambonino-Infante, J. L., Miest, J. J., Tomkiewicz, J., et al. (2018). Temperature induced variation in gene expression of thyroid hormone receptors and deiodinases of European eel (Anguilla anguilla) larvae. *Gen. Comp. Endocrinol.* 259, 54–65. doi: 10.1016/j.ygcen.2017.11.003

Reitzel, A. M., and Tarrant, A. M. (2009). Nuclear receptor complement of the cnidarian Nematostella vectensis: phylogenetic relationships and developmental expression patterns. *BMC Evol. Biol.* 9:230. doi: 10.1186/1471-2148-9-230

Reitzel, A. M., Pang, K., Ryan, J. F., Mullikin, J. C., Martindale, M. Q., Baxevanis, A. D., et al. (2011). Nuclear receptors from the ctenophore Mnemiopsis leidyi lack a zinc-finger DNA-binding domain: lineage-specific loss or ancestral condition in the emergence of the nuclear receptor superfamily? *EvoDevo* 2:3. doi: 10.1186/2041-9139-2-3

Richards, G. (1997). "The ecdysone regulatory cascades in *Drosophila*," in *Advances in Developmental Biology (1992)*, ed. P. Wassarman (Amsterdam: Elsevier), 81–135.

Richardson, S. J., Aldred, A. R., Leng, S. L., Renfree, M. B., Hulbert, A. J., and Schreiber, G. (2002). Developmental profile of thyroid hormone distributor proteins in a marsupial, the Tammar Wallaby *Macropus eugenii*. *Gen. Comp. Endocrinol.* 125, 92–103. doi: 10.1006/gcen.2001.7729

Rodriguez-Munoz, R., Nicieza, A. G., and Brana, F. (2003). Density-dependent growth of Sea Lamprey larvae: evidence for chemical interference. *Funct. Ecol.* 17, 403–408. doi: 10.1046/j.1365-2435.2003.00744.x

Rouse, G. W., Wilson, N. G., Carvajal, J. I., and Vrijenhoek, R. C. (2016). New deep-sea species of Xenoturbella and the position of Xenacoelomorpha. *Nature* 530, 94–97. doi: 10.1038/nature16545

Rühl, R., Krzyżosiak, A., Niewiadomska-Cimicka, A., Rochel, N., Szeles, L., Vaz, B., et al. (2015). 9-cis-13,14-dihydroretinoic acid is an endogenous retinoid acting as RXR ligand in mice. *PLoS Genet.* 11:e1005213. doi: 10.1371/journal.pgen.1005213

Sachs, L. M., and Buchholz, D. R. (2017). Frogs model man: *In vivo* thyroid hormone signaling during development: SACHS and BUCHHOLZ. *Genesis* 55:e23000. doi: 10.1002/dvg.23000

Sandoval, A. G. W., and Maden, M. (2020). Regeneration in the spiny mouse, Acomys, a new mammalian model. *Curr. Opin. Genet. Dev.* 64, 31–36. doi: 10.1016/j.gde.2020.05.019

Schena, M., and Yamamoto, K. (1988). Mammalian glucocorticoid receptor derivatives enhance transcription in yeast. *Science* 241, 965–967. doi: 10.1126/science.3043665

Schena, M., Lloyd, A. M., and Davis, R. W. (1991). A steroid-inducible gene expression system for plant cells. *Proc. Natl. Acad. Sci. U.S.A.* 88, 10421–10425. doi: 10.1073/pnas.88.23.10421

Schumann, I., Kenny, N., Hui, J., Hering, L., and Mayer, G. (2018). Halloween genes in panarthropods and the evolution of the early moulting pathway in Ecdysozoa. *R. Soc. Open Sci.* 5:180888. doi: 10.1098/rsos.180888

Schweizer, U., Johannes, J., Bayer, D., and Braun, D. (2014). Structure and function of thyroid hormone plasma membrane transporters. *Eur. Thyroid J.* 3, 143–153. doi: 10.1159/000367858

Scott, A. P. (2012). Do mollusks use vertebrate sex steroids as reproductive hormones? Part I: critical appraisal of the evidence for the presence, biosynthesis and uptake of steroids. *Steroids* 77, 1450–1468. doi: 10.1016/j.steroids.2012.08.009

Scott, A. P. (2013). Do mollusks use vertebrate sex steroids as reproductive hormones? II. Critical review of the evidence that steroids have biological effects. *Steroids* 78, 268–281. doi: 10.1016/j.steroids.2012.11.006

Sever, R., and Glass, C. K. (2013). Signaling by nuclear receptors. *Cold Spring Harb. Perspect. Biol.* 5:a016709. doi: 10.1101/cshperspect.a016709

Sezutsu, H., Le Goff, G., and Feyereisen, R. (2013). Origins of P450 diversity. *Philos. Trans. R. Soc. B Biol. Sci.* 368:20120428. doi: 10.1098/rstb.2012.0428

Shimell, M., Pan, X., Martin, F. A., Ghosh, A. C., Leopold, P., O'Connor, M. B., et al. (2018). Prothoracicotropic hormone modulates environmental adaptive plasticity through the control of developmental timing. *Development* 145:dev159699. doi: 10.1242/dev.159699

Silvia, M., Paolo, T., Nobile, M., Denise, F., Cinta, P., and Michela, S. (2015). Unraveling estradiol metabolism and involvement in the reproductive cycle of non-vertebrate animals: the sea urchin model. *Steroids* 104, 25–36. doi: 10.1016/j.steroids.2015.08.008

Sluder, A. (2001). Nuclear receptors in nematodes: themes and variations. *Trends Genet.* 17, 206–213. doi: 10.1016/S0168-9525(01)02242-9

Stout, E. P., La Clair, J. J., Snell, T. W., Shearer, T. L., and Kubanek, J. (2010). Conservation of progesterone hormone function in invertebrate reproduction. *Proc. Natl. Acad. Sci. U.S.A.* 107, 11859–11864. doi: 10.1073/pnas.1006074107

Taubenheim, J., Willoweit-Ohl, D., Knop, M., Franzenburg, S., He, J., Bosch, T. C. G., et al. (2020). Bacteria- and temperature-regulated peptides modulate β-catenin signaling in Hydra. *Proc. Natl. Acad. Sci. U.S.A.* 117, 21459–21468. doi: 10.1073/pnas.2010945117

Taylor, E., and Heyland, A. (2017). Evolution of thyroid hormone signaling in animals: Non-genomic and genomic modes of action. *Mol. Cell. Endocrinol.* 459, 14–20. doi: 10.1016/j.mce.2017.05.019

Tello, J. A., Rivier, J. E., and Sherwood, N. M. (2005). Tunicate gonadotropin-releasing hormone (GnRH) peptides selectively activate ciona intestinalis GnRH receptors and the green monkey type II GnRH receptor. *Endocrinology* 146, 4061–4073. doi: 10.1210/en.2004-1558

Tennessen, J. M., Baker, K. D., Lam, G., Evans, J., and Thummel, C. S. (2011). The *Drosophila* estrogen-related receptor directs a metabolic switch that supports developmental growth. *Cell Metab.* 13, 139–148. doi: 10.1016/j.cmet.2011.01.005

Thomas, J. H. (2007). Rapid birth–death evolution specific to xenobiotic cytochrome P450 genes in vertebrates. *PLoS Genet.* 3:e67. doi: 10.1371/journal.pgen.0030067

Thornton, J. W. (2003). Resurrecting the ancestral steroid receptor: ancient origin of estrogen signaling. *Science* 301, 1714–1717. doi: 10.1126/science.1086185

Truman, J. W., and Riddiford, L. M. (2002). Endocrine insights into the evolution of metamorphosis in insects. *Annu. Rev. Entomol.* 47, 467–500. doi: 10.1146/annurev.ento.47.091201.145230

Tzertzinis, G., Egaña, A. L., Palli, S. R., Robinson-Rechavi, M., Gissendanner, C. R., Liu, C., et al. (2010). Molecular evidence for a functional ecdysone signaling system in Brugia malayi. *PLoS Negl. Trop. Dis.* 4:e625. doi: 10.1371/journal.pntd.0000625

Valenzuela, N. (2008). Sexual development and the evolution of sex determination. *Sex. Dev.* 2, 64–72. doi: 10.1159/000129691

Vallejo, D. M., Juarez-Carreño, S., Bolivar, J., Morante, J., and Dominguez, M. (2015). A brain circuit that synchronizes growth and maturation revealed through Dilp8 binding to Lgr3. *Science* 350:aac6767. doi: 10.1126/science.aac6767

van Rosmalen, L., van Dalum, J., Hazlerigg, D. G., and Hut, R. A. (2020). Gonads or body? Differences in gonadal and somatic photoperiodic growth response in two vole species. *bioRxiv [Preprint]* doi: 10.1101/2020.06.12.147777

Vogeler, S., Bean, T. P., Lyons, B. P., and Galloway, T. S. (2016). Dynamics of nuclear receptor gene expression during Pacific oyster development. *BMC Dev. Biol.* 16:33. doi: 10.1186/s12861-016-0129-6

Vogeler, S., Galloway, T. S., Lyons, B. P., and Bean, T. P. (2014). The nuclear receptor gene family in the Pacific oyster, Crassostrea gigas, contains a novel subfamily group. *BMC Genomics* 15:369. doi: 10.1186/1471-2164-15-369

Wang, G., Zhang, L., Xu, J., Yin, C., Zhang, Z., and Wang, Y. (2019). The roles of thyroid hormone receptor and T3 in metamorphosis of Haliotis diversicolor. *J. Oceanol. Limnol.* 37, 745–758. doi: 10.1007/s00343-019-7359-y

Wärnmark, A., Treuter, E., Wright, A. P. H., and Gustafsson, J. -Å (2003). Activation functions 1 and 2 of nuclear receptors: molecular strategies for transcriptional activation. *Mol. Endocrinol.* 17, 1901–1909. doi: 10.1210/me.2002-0384

West-Eberhard, M. J. (2003). *Developmental Plasticity and Evolution*. Oxford: Oxford University Press.

Wu, W., and LoVerde, P. T. (2019). Nuclear hormone receptors in parasitic Platyhelminths. *Mol. Biochem. Parasitol.* 233:111218. doi: 10.1016/j.molbiopara.2019.111218

Yao, T.-P., Forman, B. M., Jiang, Z., Cherbas, L., Chen, J. D., McKeown, M., et al. (1993). Functional ecdysone receptor is the product of EcR and Ultraspiracle genes. *Nature* 366, 476–479. doi: 10.1038/366476a0

Yao, T.-P., Segraves, W. A., Oro, A. E., McKeown, M., and Evans, R. M. (1992). *Drosophila* ultraspiracle modulates ecdysone receptor function via heterodimer formation. *Cell* 71, 63–72. doi: 10.1016/0092-8674(92)90266-F

Yoshikawa, T., Shimano, H., Amemiya-Kudo, M., Yahagi, N., Hasty, A. H., Matsuzaka, T., et al. (2001). Identification of Liver X receptor-retinoid X receptor as an activator of the sterol regulatory element-binding protein 1c gene promoter. *Mol. Cell. Biol.* 21, 2991–3000. doi: 10.1128/MCB.21.9.2991-3000.2001

Youson, J. H., Plisetskaya, E. M., and Leatherland, J. F. (1994). Concentrations of insulin and thyroid hormones in the serum of landlocked sea lampreys (Petromyzon marinus) of three larval year classes, in larvae exposed to two temperature regimes, and in individuals during and after metamorphosis. *Gen. Comp. Endocrinol.* 94, 294–304. doi: 10.1006/gcen.1994.1086

Zwaal, R. R., Mendel, J. E., Sternberg, P. W., and Plasterk, R. H. (1997). Two neuronal G proteins are involved in chemosensation of the Caenorhabditis elegans Dauer-inducing pheromone. *Genetics* 145, 715–727.

Conflict of Interest: The authors declare that the research was conducted in the absence of any commercial or financial relationships that could be construed as a potential conflict of interest.

frontiers in Ecology and Evolution

ORIGINAL RESEARCH
published: 17 November 2021
doi: 10.3389/fevo.2021.660546

Conserved and Divergent Aspects of Plasticity and Sexual Dimorphism in Wing Size and Shape in Three Diptera

*Micael Reis†, Natalia Siomava†‡, Ernst A. Wimmer and Nico Posnien**

Department of Developmental Biology, Göttingen Center for Molecular Biosciences (GZMB), Johann-Friedrich-Blumenbach-Institute of Zoology and Anthropology, University Göttingen, Göttingen, Germany

OPEN ACCESS

Edited by:
Lauren Sumner-Rooney, University of Oxford, United Kingdom

Reviewed by:
Darija Lemić, University of Zagreb, Croatia
Renata Bažok, University of Zagreb, Croatia

***Correspondence:**
Nico Posnien
nposnie@gwdg.de

†These authors have contributed equally to this work and share first authorship

‡Present address:
Natalia Siomava, College of Health Sciences, Abu Dhabi University, Abu Dhabi, United Arab Emirates

Specialty section:
This article was submitted to Evolutionary Developmental Biology, a section of the journal Frontiers in Ecology and Evolution

Received: *29 January 2021*
Accepted: *29 October 2021*
Published: *17 November 2021*

Citation:
Reis M, Siomava N, Wimmer EA and Posnien N (2021) Conserved and Divergent Aspects of Plasticity and Sexual Dimorphism in Wing Size and Shape in Three Diptera. Front. Ecol. Evol. 9:660546. doi: 10.3389/fevo.2021.660546

The ability of powered flight in insects facilitated their great evolutionary success allowing them to occupy various ecological niches. Beyond this primary task, wings are often involved in various premating behaviors, such as the generation of courtship songs and the initiation of mating in flight. These specific functions imply special adaptations of wing morphology, as well as sex-specific wing morphologies. Although wing morphology has been extensively studied in *Drosophila melanogaster* (Meigen, 1830), a comprehensive understanding of developmental plasticity and the impact of sex on wing size and shape plasticity is missing for other Diptera. Therefore, we raised flies of the three Diptera species *Drosophila melanogaster*, *Ceratitis capitata* (Wiedemann, 1824) and *Musca domestica* (Linnaeus, 1758) at different environmental conditions and applied geometric morphometrics to analyze wing shape. Our data showed extensive interspecific differences in wing shape, as well as a clear sexual wing shape dimorphism in all three species. We revealed an impact of different rearing temperatures on wing shape in all three species, which was mostly explained by plasticity in wing size in *D. melanogaster*. Rearing densities had significant effects on allometric wing shape in *D. melanogaster,* while no obvious effects were observed for the other two species. Additionally, we did not find evidence for sex-specific response to different rearing conditions in *D. melanogaster* and *C. capitata*, while a male-specific impact of different rearing conditions was observed on non-allometric wing shape in *M. domestica*. Overall, our data strongly suggests that many aspects of wing morphology underly species-specific adaptations and we discuss potential developmental and functional implications of our results.

Keywords: Diptera, wing shape, geometric morphometrics, sexual shape dimorphism, allometry, *Drosophila melanogaster*, *Ceratitis capitata*, *Musca domestica*

INTRODUCTION

Natural variation in size and shape of animal body parts is often the result of adaptation to an ever-changing environment. Insect wings are an excellent model to study organ size and shape because insects are the only group of arthropods that developed the ability of a powered flight. This adaptation allowed them to occupy various ecological niches, including air, and contributed

to the morphological diversity and great ecological success of the entire class. Flying helps insects to surmount long distances in a relatively short time, facilitating basic tasks, such as finding mating partners and food resources. In line with these crucial functions, wing size has been shown to be highly variable between (Houle et al., 2003; Salcedo et al., 2019) and within species (Coyne and Beecham, 1987; Imasheva et al., 1994; James et al., 1995, 1997; van't Land et al., 1999; Zwaan et al., 2000; Alves and Bélo, 2002; Hoffmann and Shirriffs, 2002; Bai et al., 2016; Rohner et al., 2019). Most of our current understanding of intraspecific variation in wing size is based on extensive work in *Drosophila melanogaster* (Meigen, 1830). For instance, longitudinal (Coyne and Beecham, 1987; Imasheva et al., 1994; James et al., 1997; Zwaan et al., 2000) and altitudinal (Pitchers et al., 2013; Klepsatel et al., 2014) clines in wing size have been observed on all continents studied to date with positive correlations between wing size and latitude and altitude, respectively. The analysis of latitudinal clines in conjunction with laboratory experiments showed that temperature is a major environmental factor affecting wing size (Cavicchi et al., 1985; Partridge et al., 1994a; James et al., 1995; van't Land et al., 1999; Zwaan et al., 2000). The effect of temperature on wing size can be further modulated by other environmental factors. Wing length, for example, reacts more to changes in rearing temperature under limited food conditions (de Moed et al., 1997). Overall, this data obtained from *D. melanogaster* revealed that natural variation in wing size is caused by a combination of the genetic and environmental factors.

Variation in organ size must be accompanied by shape changes to retain fully functional properties. As shown for wing size, latitudinal and altitudinal clines for wing shape have been observed in *D. melanogaster* and environmental factors, such as temperature, have profound effects on wing shape (Gilchrist et al., 2000; Debat et al., 2003, 2009; Pitchers et al., 2013). Advances in geometric morphometrics methodology to quantify shape variation nowadays allow analyzing size and shape independently to study the allometric effect on wing shape (Bookstein, 1996; Bitner-Mathé and Klaczko, 1999; Debat et al., 2003; Mitteroecker and Gunz, 2009; Klingenberg, 2016). Such analyses revealed that natural variation in *D. melanogaster* wing shape is predominantly caused by differences in wing size (i.e., strong allometric component of shape variation) (Gilchrist et al., 2000; Debat et al., 2003). Strong allometric effects on wing shape as well as similar clinal patterns and plastic responses to different temperature regimes have been observed in other insects, such as sepsid flies (Rohner et al., 2019) and grasshoppers (Bai et al., 2016). These findings suggests that wing size and shape must be well-coordinated during development. Indeed, in *D. melanogaster* both aspects of wing morphology are regulated by similar patterning and differentiation processes during larval and pupal wing imaginal disc development (Day and Lawrence, 2000; Matamoro-Vidal et al., 2015; Testa and Dworkin, 2016). However, despite this tight connection between wing size and shape, laboratory crosses in *D. melanogaster* showed that wing size variation is shaped by directional selection, while wing shape shows signs of optimizing selection (Gilchrist and Partridge, 2001). Similarly, experimental evolution of *D. subobscura* (Collin, 1936) at three different temperature regimes for 81 generations revealed clear effects of temperature adaptation on wing shape, while wing size was not affected (Santos et al., 2006). These results suggest that wing size and shape are under different selection pressures and may be less functionally connected than expected. Support for this notion also comes from studies in other insects, such as the Muscidae *Polietina orbitalis* (Stein, 1904; Alves et al., 2016) and Australian populations of *D. serrata* (Malloch, 1927; Hoffmann and Shirriffs, 2002) where wing shape varies independently from wing size. Data from different insects, thus, revealed contrasting results with respect to the impact of wing size on wing shape in different environmental conditions. To test whether allometric aspects of wing shape in different rearing conditions are indeed species-specific or rather conserved among insects, interspecific comparisons with comparable experimental designs are needed. We have previously shown that the size of different body parts, including the wings, vary in response to different rearing temperatures and densities in the three Diptera species *D. melanogaster*, the Mediterranean fruit fly *Ceratitis capitata* (Wiedemann, 1824) and the housefly *Musca domestica* (Linnaeus, 1758; Siomava et al., 2016). Therefore, we used these three species to reveal conserved and species-specific effects of different rearing temperatures and densities on allometric aspects of wing shape.

In modern insects, wings became engaged in other essential processes, such as mating. For instance, numerous fruit flies, such as *D. melanogaster* and *C. capitata* use their wings to perform courtship songs, reflecting the size and vigor of males to help females choosing the right mating partner (Keiser et al., 1973; Burk and Webb, 1983; Webb et al., 1983; Partridge et al., 1987). Some insects mate in the air during flight (Wilkinson and Johns, 2005), while others, such as *M. domestica* initiate the mating process in flight but always land prior to copulation (Murvosh et al., 1964). These different behaviors in combination with intersexual food competition and various reproductive roles of the wing pose a constant selective pressure resulting in pronounced sexual dimorphism in wing size and shape in insects (Gidaszewski et al., 2009; de Camargo et al., 2015). In addition to sexual wing size dimorphism (Siomava et al., 2016), *D. melanogaster* exhibits a clear wing shape dimorphism with male wings being broader than female wings (Bitner-Mathé and Klaczko, 1999; Gilchrist et al., 2000; Gidaszewski et al., 2009). Given that males of *C. capitata* produce courtship songs like *D. melanogaster*, it is not surprising that similar trends in wing size and shape have been observed in this species (Siomava et al., 2016; Pieterse et al., 2017; Lemic et al., 2020). Wing size (Siomava et al., 2016; Cortés-Suarez et al., 2021) and shape (Rohner, 2020; Cortés-Suarez et al., 2021) are also sexually dimorphic in *M. domestica*. Since this species does not produce songs, but relies on the initiation of mating in flight, it remains to be tested, whether sexual differences in wing shape reflect this mating behavior in comparison to song-producing Diptera, such as *D. melanogaster* and *C. capitata*. In addition to sexual dimorphisms in wing morphology, data from *D. melanogaster* showed that plastic responses of wing shape to different rearing temperatures is sex-specific because opposite shape changes were observed in males and females (Aytekin et al., 2009). However, in

the other two species it is still unknown whether plasticity in wing shape is sexually dimorphic. Therefore, we studied plasticity in wing morphology in different Diptera species to reveal conserved and divergent features of sexual size and shape dimorphisms.

In this study, we applied geometric morphometrics to comprehensively describe and compare plasticity in wing shape in *C. capitata, D. melanogaster*, and *M. domestica*. Furthermore, we asked whether plasticity in allometric and non-allometric wing shape were sexually dimorphic in the three species. We found clear evidence for sexual shape dimorphism in all three species with major contribution of wing size on shape differences in *D. melanogaster*. Different rearing temperatures had a strong effect on total and non-allometric wing shape in all three species, while density effects were most pronounced in *D. melanogaster*. Eventually, we did not find strong arguments for sexual dimorphism in response to the different rearing conditions, although *M. domestica* males showed slightly stronger differences than females. We identified highly variable regions, the radio-medial (r-m) crossvein, the R2 + 3 radial vein and the basal-medial-cubital (bm-cu) crossvein, which changed similarly among the three species in response to various larval densities and temperature regimes. Overall, we reveal mostly species-specific aspects of plasticity and sexual dimorphism in wing morphology, and we discuss developmental and functional implications of our results.

MATERIALS AND METHODS

Fly Species

All experiments were performed using three different fly species (**Figure 1A**; Siomava et al., 2016). We used the highly inbred laboratory strain *Drosophila melanogaster* w1118, which was kept at 18°C on standard food (400 g of malt extract, 400 g of corn flour, 50 g of soy flour, 110 g of sugar beet syrup, 51 g of agar, 90 g of yeast extract, 31.5 ml of propionic acid, and 7.5 g of Nipagin dissolved in 40 ml of Ethanol, water up to 5 l). The other two flies were *Musca domestica* wild type ITA1 collected in Italy, Altavilla Silentia in 2013 (Y. Wu and L. Beukeboom, GELIFES, Netherlands) and *Ceratitis capitata* wild type Egypt II (IAEA). The *M. domestica* strain was reared at room temperature (RT) (22 ± 2°C) on food composed by 500 g of wheat bran, 75 g of wheat flour, 60 g of milk powder, 25 g of yeast extract, 872 ml of water, and 18.85 ml of Nipagin (2.86 g of Nipagin in 10 ml of Ethanol). Adult *M. domestica* flies were provided with sugar water. *C. capitata* were kept at 28°C, 55 ± 5% RH on a diet composed by 52.5 g of yeast extract, 52.5 g of carrot powder, 2 g of Sodium benzoate, 1.75 g of agar, 2.25 ml of 32% HCl, and 5 ml of Nipagin (2.86 g of Nipagin in 10 ml of Ethanol), water up to 500 ml for larvae. For adult flies, we used a 1:3 mixture of sugar and yeast extract.

Treatment of Experimental Groups

To generate a range of sizes for each species, we varied two environmental factors known to influence overall body size – temperature and density. Prior to the experiment, *D. melanogaster* flies were placed at 25°C for two days. On the third day, flies were moved from vials into egg-collection chambers and provided with apple-agar plates. After several hours, we started egg collection by removing apple-agar plates with laid eggs once per hour. Collected plates were kept at 25°C for 24 h to allow embryonic development to complete. Freshly hatched first-instar larvae were transferred into 50 ml vials with 15 ml of fly food. Three vials containing 25 larvae each (low density) and three vials with 300 larvae each (high density) were moved to 18°C; the second set of six vials with the same densities was left at 25°C.

Ceratitis capitata flies were kept at 28°C and allowed to lay eggs through a net into water. Every hour, eggs were collected and transferred to the larval food. After 22 h, first-instar larvae were transferred into small Petri dishes (diameter 55 mm) with 15 ml of the larval food in three densities: 25 (low density), 100 (medium density), or 300 (high density) larvae per plate. Two plates of each density were moved to 18°C. The second set of six plates was left at 28°C for further development.

Eggs of *M. domestica* were collected in the wet larval food at RT and after 24 h, all hatched larvae were removed from food. Only larvae hatched within the next hour were transferred into 50 ml vials with 5 g of food. Collection of larvae was repeated several times to obtain two experimental sets with three replicates of three experimental densities 10 (low density), 20 (medium density), or 40 (high density) larvae. One set of nine vials was moved to 18°C, the other was left at RT.

After pupation, individuals of *C. capitata* and *M. domestica* were collected from the food and kept until eclosion in vials with a wet sponge, which was refreshed every other day.

The experimental temperature regimes were chosen for the following reasons. *D. melanogaster* is known to survive in the range 10 to 33°C, but flies remain fertile at 12 to 30°C with the optimum at 25°C (Hoffmann, 2010). Reproduction temperatures in *C. capitata* range from 14°C to 30°C with the optimum at 28°C (Duyck and Quilici, 2002; Navarro-Campos et al., 2011). *M. domestica* flies survive at 10 to 35°C (Hewitt, 1914) with the optimum between 24 and 27°C (Hafez, 1948; Chun-Hsung, 2012). The low temperature for our experiment was chose as the one above the survival and fertile minimums for all three species – 18°C. The warm temperature was aimed to be optimal for each species.

Data Collection

For each combination of temperature and density, we randomly picked 8 to 24 (median: 12.5) flies for *C. capitata*, 20 to 31 (median: 23) flies for *D. melanogaster* and 5 to 15 (median: 8) flies for *M. domestica*. Both wings were dissected, embedded in *Roti*®-Histokitt II (Roth, Buchenau) on a microscope slide, and photographed under the Leica MZ16 FA stereo microscope with the Q Imaging Micro Publisher 5.0 RTV Camera.

Wing shape was analyzed using landmark-based geometric morphometric methods (Rohlf, 1990; Bookstein, 1991). We digitized 10 anatomically homologous landmarks on wings of the three species (**Figure 1A**). The landmarks were the following [nomenclature is given after (Colless and McAlpine, 1991)]: 1, branching point of veins R_1 and R_S (base of R_{2+3} and R_{4+5}); 2, branching point of veins R_{2+3} and R_{4+5}; 3, intersection of

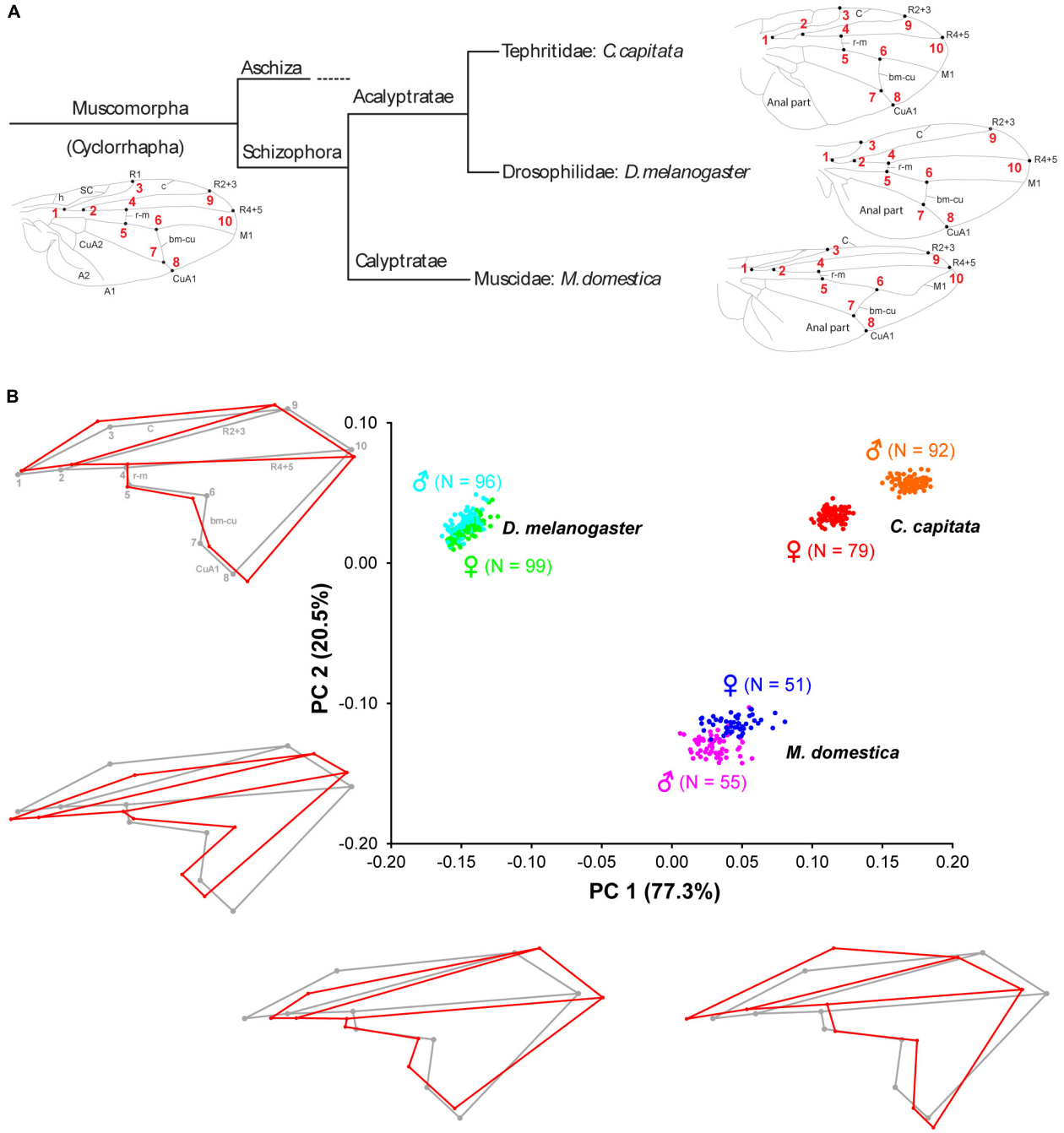

FIGURE 1 | Schematic overview of the phylogenetic relationships Muscomorpha and interspecific wing shape variation *D. melanogaster, C. capitata*, *and M. domestica*. **(A)** Homologous landmarks 1–10 in *C. capitata*, *D. melanogaster*, and *M. domestica* are shown as black points with the respective number in red. A, anal vein; bm-cu, basal-madial-cubital crossvein; CuA, anterior cubital vein; C, costal vein; h, humeral crossvein; M, medial vein; R, radial veins; r-m, radio-medial crossvein; SC, subcosta. Branch lengths of the tree do not indicate evolutionary time or distance. **(B)** Wing shape variation between *D. melanogaster*, *C. capitata,* and *M. domestica*. Principal Component Analysis of shape (PC1 and PC2). The red wireframes depict shape changes along the main axes of variation (PC1: –0.2, 0.2; PC2: –0.2, 0.1) relative to the gray wireframes (0 for both axes). The amount of variation explained by each PC is shown in brackets and the number of individuals analyzed for each sex is provided next to each species.

veins C and R_1; 4, intersection of vein R_{4+5} and crossvein *r-m* (anterior crossvein); 5, intersection of crossvein *r-m* and vein M_{1+2}; 6, intersection of vein M_{1+2} and crossvein *i-m* (posterior crossvein); 7, intersection of crossvein *i-m* and vein M_{3+4}; 8, intersection of M_{3+4} and the wing margin; 9, intersection of veins C and R_{2+3}; 10, intersection of veins C and R_{4+5}.

Procrustes Superimposition and Interspecies Comparison

Wing images were digitized using tpsUtil and tpsDig2 (Rohlf, 2015) to obtain raw *x* and *y* landmark coordinates. Using superimposition methods, it is possible to register landmarks of a sample to a common coordinate system in three steps: translating all landmark configurations to the same centroid, scaling all configurations to the same centroid size, and rotating all configurations until the summed squared distances between the landmarks and their corresponding sample average is a minimum scaling (Slice, 2005; Mitteroecker et al., 2013). To follow these three steps, we applied the generalized Procrustes analysis (GPA) (Dryden and Mardia, 1998; Slice, 2005) as implemented in MorphoJ (version 1.06d) (Klingenberg, 2011). The wings were aligned by principal axes, the mean configuration of landmarks was computed, and each wing was projected to a linear shape tangent space. The coordinates of the aligned wings were the Procrustes coordinates. To evaluate wing asymmetry, we used the R package Geomorph (v. 3.3.1) (Adams et al., 2021) to partition shape variation by individuals, side (directional asymmetry) and the interaction between individual and side (fluctuating asymmetry). Procrustes ANOVA was used to evaluate statistical significance. Since we obtained no evidence for fluctuating asymmetry for all species (**Supplementary Table 1**), we averaged the coordinates for the right and left wings for further analyses. Next, we used Type III Procrustes ANOVA (with Randomization of null model residuals and 1,000 permutations) as implemented in Geomorph (v. 3.3.1) (Adams et al., 2021) to determine the effect of the species, sex, temperature, and density as well as potential interactions between these explanatory variables and shape (**Table 1**). Temperature and density values were re-labeled as low, high, or intermediate to allow the comparison between species. To visualize the main components of shape variation, we performed a principal component analysis (PCA) and generated wireframes using MorphoJ (version 1.06d) (**Figure 1B**).

Intraspecific Sexual Dimorphism and Effects of Rearing Conditions

Since most of the variation in shape was explained by differences between species (see section "Results"), we split the analysis to further evaluate the effects of sex, rearing temperature, and density as well as potential interactions on wing shape within each species using Procrustes ANOVA in Geomorph (v. 3.3.1) (**Supplementary Table 2**). Magnitudes of sexual shape dimorphism were estimated using the discriminant function analysis (DFA) and expressed in units of Procrustes distance using MorphoJ (version 1.06d). DFA identifies shape features that differ the most between groups relative to within groups and it can only be applied to contrast two experimental groups. Therefore, we used this method to define sexual shape dimorphism (males and females), as well as effects of the rearing temperature (high and low) and density (high and low) in each species. Wing shape changes were visualized using wireframe graphs. To test for the significance of the observed differences, we ran a permutation test with 1,000 random permutations (Good, 1994) for each test using MorphoJ (version 1.06d).

Estimation of the Non-allometric Component of Shape

To evaluate the impact of wing size on shape variation, we estimated wing centroid size (WCS) that was computed from raw data of landmarks and measured as the square root of the sum of squared deviations of landmarks around their centroid (Bookstein, 1996; Dryden and Mardia, 1998; Slice, 2005) in MorphoJ (version 1.06d). The wing images were taken at different magnifications to account for the different body sizes of the three species. *C. capitata* wings were takes at a 1,280 × 960 resolution, *M. domestica* at a 2,560 × 1,920 resolution and for *D. melanogaster* images with both resolutions were obtained. Therefore, the WCS values were corrected for differences in magnification and resolution among photos before being used as covariate. The effects of sex, temperature, density, and their interactions on WCS was tested using Type III ANOVA for each species.

Since a Type III Procrustes ANOVA for all three species including WCS as covariate revealed significant interaction between species and WCS (**Supplementary Table 3**, sheet "All Species_total"), we estimated the non-allometric shape component for each species independently. The non-allometric Procrustes coordinates were obtained as the residuals of the multiple regression of WCS onto the Procrustes coordinates pooling the samples by sex, temperature, and density, as implemented in MorphoJ (version 1.06d) (Klingenberg, 2011, 2016). To evaluate the success of the size correction, we ran a Type II ANOVA testing for additive effects of explanatory variables prior to and after the size correction. This analysis revealed that WCS had no impact on wing shape after size correction (**Supplementary Table 3**, compare sheets "*_total" to "*_non-allometric"), suggesting that the approach accounted for most of the impact of size on shape. Note that species-specific Type III Procrustes ANOVAs including WCS as covariate revealed significant interactions for *C. capitata* and *D. melanogaster* (**Supplementary Table 3**, sheets "C. capitata_total," "D. melanogaster_total"), suggesting complex relationships between wing size and shape. Since the regression approach to estimate allometry across all explanatory variables (i.e., sex, temperature, and density) assumes similar slopes of within-group regressions (Gidaszewski et al., 2009; Klingenberg, 2016), we analyzed those regressions in more detail. Although the directions of within-group regressions (i.e., regression scores of the regression of Procrustes coordinates onto WCS pooled by sex, temperature, and density) were comparable (**Figure 3**), type III ANOVA testing for interactions of explanatory variables partially resulted in significant interactions in *C. capitata* and *D. melanogaster* (**Supplementary Table 4**), suggesting some significant differences in slopes. Therefore, the distinction between allometric and non-allometric shape differences may not be fully accurate. However, due to a lack of a better method,

TABLE 1 | Effects of species, sex, temperature, density, and their interactions on total wing shape tested by Type III Procrustes ANOVA.

	Df	SS	MS	R^2	*F*	*Z*	*P*-value
Spec	2	0.844	0.422	0.081	1260.417	8.506	***0.001***
Sex	1	0.027	0.027	0.003	80.926	7.175	***0.001***
Temp	1	0.000	0.000	0.000	1.285	0.646	0.261
Dens	2	0.001	0.000	0.000	1.399	0.957	0.168
Spec:Sex	2	0.036	0.018	0.003	54.078	9.158	***0.001***
Spec:Temp	2	0.004	0.002	0.000	5.356	4.178	***0.001***
Sex:Temp	1	0.000	0.000	0.000	0.897	0.106	0.471
Spec:Dens	2	0.003	0.001	0.000	3.701	3.253	***0.001***
Sex:Dens	2	0.001	0.000	0.000	1.313	0.815	0.205
Temp:Dens	2	0.001	0.000	0.000	1.061	0.266	0.408
Spec:Sex:Temp	2	0.001	0.000	0.000	1.476	1.183	0.128
Spec:Sex:Dens	2	0.002	0.001	0.000	2.551	2.387	***0.005***
Spec:Temp:Dens	2	0.001	0.001	0.000	1.560	1.264	0.110
Sex:Temp:Dens	2	0.001	0.000	0.000	0.753	−0.530	0.700
Spec:Sex:Temp:Dens	2	0.001	0.001	0.000	1.537	1.245	0.107

Significant effects and interactions at P ≤ 0.01 are provided as bold-italic P-values. spec, species; temp, temperature; dens, density; Df, degree of freedom; SS, sum of squares; MS, mean squares.

we decided to proceed with the analysis and to interpret the results cautiously. The amount of shape variation explained by wing centroid size was estimated by obtaining R^2 for the linear model describing the pooled regression (i.e., the unique curve after pooling the data by groups: centered_reg_scores ∼centered_WCS).

Magnitudes of non-allometric shape differences for each explanatory variable and for sex-specific effects of different temperature and density conditions were estimated using DFA as described before. Since wing size and shape of intermediate densities for *C. capitata* and *M. domestica* overlapped with the high- and low-density conditions, respectively (**Figure 3**), we restricted the detailed shape analysis to the extreme values.

RESULTS

Wing Shape Variation in Dipteran Species

To characterize wing shape variation among *Ceratitis capitata*, *Drosophila melanogaster*, and *Musca domestica*, we applied geometric morphometrics based on 10 landmarks (**Figure 1A**). Procrustes ANOVA revealed that most of the shape variance was caused by differences among species (**Table 1**). This result was also reflected by the principal component analysis (PCA) which clearly distinguished the three species with the first two principal components (PCs) accounting for almost 98% of the variation (**Figure 1B**). The main shape difference along PC1 (77.3% of the variation) reflected the ratio between the proximal and distal parts of the wing as well as wing length. The wireframe graphs showed that *C. capitata* wings were broad in the proximal part (landmarks 1–5) and narrow in the distal part (landmarks 6–10), while *D. melanogaster* wings showed the opposite pattern with the proximal part being heavily compressed along the anterior-posterior axis. *M. domestica* had an intermediate morphology being, however, more similar to *C. capitata* (**Figure 1B**, wireframe graphs along PC1). PC2 explained 20.5% of the variation mainly accounting for the ratio between the length and width of the whole wing. *C. capitata* and *D. melanogaster* showed wider and shorter wings, while *M. domestica* showed more elongated wings (**Figure 1B**, wireframe graphs along PC2). Together, we found evidence for extensive wing shape variation among *C. capitata*, *D. melanogaster*, and *M. domestica*.

Sexual Dimorphism in Wing Shape

Our interspecific shape analysis revealed a clear sexual shape dimorphism which was most pronounced for *C. capitata* (**Figure 1B** and **Table 1**). The extreme sexual shape dimorphism in *C. capitata* and the observation that males and females occupy different relative positions along PC1 compared to *D. melanogaster* and *M. domestica* likely explain the significant interaction between species and sex (**Table 1**). Species-specific Procrustes ANOVA for all three species revealed that within-species shape variation was affected independently by sex and rearing conditions (i.e., temperature and density, see below) (**Supplementary Table 2**). Therefore, we split the analysis by species and ran a DFA to determine the total shape differences caused by sex (**Figures 2A–C**). For all three species we found a highly significant sexual shape dimorphism (**Figures 2A–C**). Male wings were broader than those of females in *C. capitata* (**Figure 2A**) and *D. melanogaster* (**Figure 2B**), while the opposite trend was observed in *M. domestica* (**Figure 2C**). Wings of *C. capitata* females were slightly longer than male wings (**Figure 2A**) and in *D. melanogaster* and *M. domestica* male wings were longer (**Figures 2B,C**). The radio-medial crossvein (r-m) defined by landmarks 4 and 5 was different between males and females in *C. capitata* (**Figure 2A**). In *D. melanogaster* we observed clear sexual differences in the radial vein R2 + 3 defined by landmarks 2 and 9 and in the basal-madial-cubital crossvein (bm-cu) defined by landmarks 6 and 7 (**Figure 2B**). In summary,

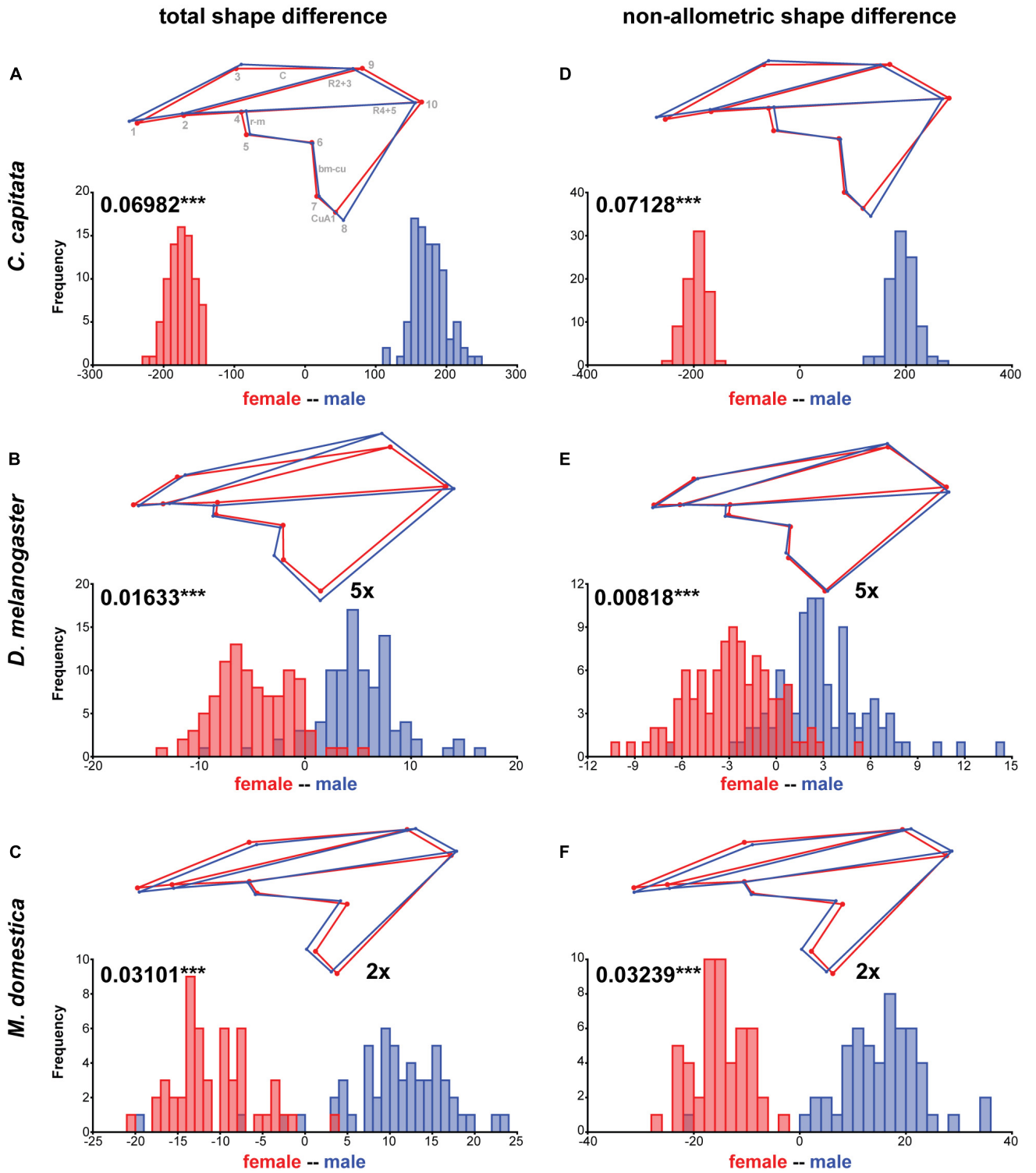

FIGURE 2 | Total and non-allometric sexual shape dimorphism. Summary of discriminant function analyses for total **(A–C)** and non-allometric **(D–F)** shape differences between females and males. The wireframes represent differences between female (red) and male (blue) average wing shapes. The scale factor is provided next to the wireframes. The magnitude of sexual shape dimorphism is indicated in units of Procrustes distance with the corresponding *p*-values based on 1,000 random permutations (***$P \leq 0.001$). Histograms with the distributions of the discriminant scores show shape separation into two distinct groups for each species. See also **Supplementary Table 5** for details.

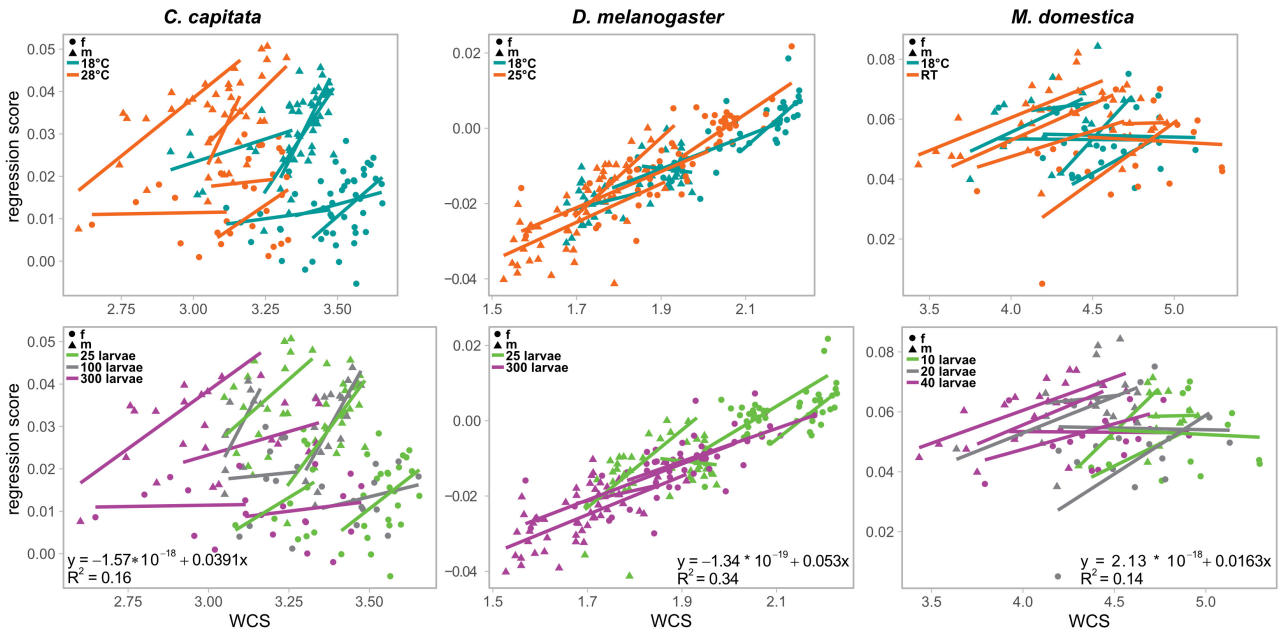

FIGURE 3 | Relationship of the shape component that is most associated with wing size and wing centroid size. Scatterplots showing the relationship of the regression score (i.e., regression of wing centroid size onto Procrustes coordinates pooled by sex, temperature, and density) and wing centroid size (WCS). Linear regression lines were fitted for each category to illustrate the allometric relationships in detail. In the upper row, the data is color coded by the different rearing temperatures and in the lower row, the data is color coded by the different rearing temperatures. Equations and corresponding R^2 values in the plots of the lower row represent pooled regressions for all data combined for each species. f, females; m, male.

we found a clear total sexual shape dimorphism in all three studied species.

Influence of Sexual Size Dimorphisms on Wing Shape

Since sex had a significant influence on wing size in all three species (**Table 2**, see also **Figure 3**) (see Siomava et al., 2016 for independent wing size measures) we next asked how much of the shape differences between sexes was explained by differences in wing size. Wing size explained 16% and 14% of wing shape variation in *C. capitata* and *M. domestica*, respectively (**Figure 3**). Wing shape was more clearly associated with differences in wing size in *D. melanogaster* (34%; **Figure 3**). To analyze the non-allometric shape differences between sexes in more detail, we accounted for wing size (Klingenberg, 2016; see section "Materials and Methods" for details). A species-specific DFA using the non-allometric shape component revealed significant sexual shape dimorphism for all three species (**Figures 2D–F**). This observation was confirmed by a Procrustes ANOVA (**Supplementary Table 2**). In line with the minor impact of wing size on wing shape, the extant of the total compared to the non-allometric sexual shape dimorphism was very similar in *C. capitata* and *M. domestica* (**Figures 2D,F**). Accordingly, the differences in shape decreased after size correction in *D. melanogaster* (**Figure 2E**). Specifically, differences in the length and the width of the wings were largely reduced in the non-allometric shape component. These results suggest that major difference between sexes observed in *C. capitata* and *M. domestica* can be explained by the non-allometric shape component, while wing size differences contribute to the sexual shape dimorphism in *D. melanogaster*.

Effect of Different Rearing Conditions on Wing Shape

To evaluate the effect of wing size on shape in the three species in more detail, we raised flies at different temperatures and densities. The Procrustes ANOVA for all three species revealed significant interactions between species and density and temperature, respectively (**Table 1**), suggesting species-specific effects of the rearing conditions on wing shape. Density had significant effects on wing size in all three species, while temperature affected only *D. melanogaster* and *C. capitata* (**Table 2**). Since temperature and density contributed additively to wing shape differences (**Supplementary Table 2**), we therefore split the analyses by species and performed species-specific DFA to study the total shape differences caused by different rearing temperatures (**Figures 4A–C**) and densities (**Figure 5A**), respectively. Additionally, we calculated the non-allometric component of shape (see section "Materials and Methods" for details) and analyzed the differences using DFA (**Figures 4D–F** for temperature and **Figure 5B** for density).

In accordance with the species-specific Procrustes ANOVA testing for effects of rearing conditions on total wing shape variation (**Supplementary Table 2**), the DFA clearly assigned wings to one of the two rearing temperatures (**Figures 4A–C**). The most obvious effect of different rearing temperatures on wing

TABLE 2 | Effects of sex, temperature, density, and their interactions on wing centroid size tested by Type III ANOVA.

	C. capitata				*D. melanogaster*				*M. domestica*			
	SS	**Df**	***F***	***P*-value**	**SS**	**Df**	***F***	***P*-value**	**SS**	**Df**	***F***	***P*-value**
Intercept	1608,3	1	192139,8	***< 0.001***	677,69	1	114561,7	***< 0.001***	1800,26	1	25808,9	***<0.001***
Sex	0,45	1	54,3	***< 0.001***	2,81	1	475,5	***<0.001***	1,17	1	16,8	***<0,001***
Temp	3,42	1	408,9	***<0.001***	0,74	1	124,8	***<0.001***	0	1	0,034	0,854
Dens	2,2	2	131,4	***<0.001***	1,71	1	288,6	***<0.001***	5,1	2	36,6	***<0.001***
Sex:Temp	0,04	1	4,4	***0,038***	0	1	0,8	0,363	0,01	1	0,15	0,702
Sex:Dens	0	2	0,2	0,82	0,03	1	5,6	***0,0186***	0,01	2	0,08	0,922
Temp:Dens	0,04	2	2,5	0,085	0,01	1	1,15	0,286	0,61	2	4,34	***0,016***
Sex:Temp:Dens	0,01	2	0,4	0,65	0,02	1	2,9	0,092	0,1	2	0,7	0,501
Residuals	1,33	159			1,11	187			6,56	94		

Significant effects and interactions at P ≤ 0.05 are provided as bold-italic P-values. temp, temperature; dens, density; Df, degree of freedom; SS, sum of squares.

shape was observed in *D. melanogaster* (**Figure 4B**). Wings of *D. melanogaster* flies raised at higher temperatures were wider in the distal-central region defined by landmarks 7–9 and distally shortened (i.e., displacement of landmark 10) (**Figure 4B**). The distal contraction remained after size correction, while the width was much less affected (**Figure 4E**). This observation suggests that temperature-dependent plasticity in wing width is predominantly caused by differences in wing size. Different rearing temperatures also affected distal-central wing width in *C. capitata* (**Figure 4A**) and *M. domestica* (**Figure 4C**). Narrower wings were observed at higher temperatures in *M. domestica*, while wings were narrower at lower temperatures in *C. capitata* (**Figures 4A,C**). *M. domestica* wings were longer at higher rearing temperatures (i.e., displacement of landmark 10) (**Figure 4C**). Only minor changes were present between total and non-allometric shape differences in *C. capitata*, suggesting that temperature-dependent size differences had small effects on wing shape in this species. In line with non-significant effects of temperature on wing size (**Table 2**), we observed no differences between the allometric and non-allometric shape in *M. domestica* (**Figures 4D,F**), In all three species, we observed temperature-dependent plasticity in the placement of the radio-medial (r-m) crossveins (defined by landmarks 4 and 5), the basal-medial-cubital (bm-cu) crossveins (defined by landmarks 6 and 7), the radial vein R2 + 3 (defined by landmarks 2 and 9) and the anterior cubital (CuA1) veins (defined by landmarks 7 and 8) (**Figure 4**).

As suggested by the Procrustes ANOVA (**Supplementary Table 2**), the DFA showed that different rearing densities only significantly affected total wing shape in *D. melanogaster* (**Figure 5A** and **Supplementary Table 5**). Wings of flies raised at high densities were wider in the central-distal region (defined by landmarks 7–9) and elongated (i.e., displaced landmark 10) (**Figure 5A**). We observed plasticity in the placement of the basal-medial-cubital (bm-cu) crossveins (defined by landmarks 6 and 7), the anterior cubital (CuA1) veins (defined by landmarks 7 and 8), the radial vein R2 + 3 (defined by landmarks 2 and 9) and the costal (C) vein (defined by landmarks 3 and 9) (**Figure 5A**). All these differences were gone after size correction (**Figure 5B**), suggesting that wing shape differences in response to rearing densities were predominantly associated with variation in size. The displacement of landmark 3 was consistent in both analyses (compare **Figures 5A,B**), implying that this region of the wing may be affected by different rearing densities independent of wing size. Despite a weak effect of density on *C. capitata* wing shape in our Procrustes ANOVA (**Supplementary Table 2**), the DFA did not reveal significant shape differences for flies raised at high and low densities (**Supplementary Table 5**). The same was true for *M. domestica*, supporting the Procrustes ANOVA results (**Supplementary Table 2**). Note that we observed significant differences in wing shape at different rearing densities after size correction in *C. capitata* and *M. domestica* in our Procrustes ANOVA (**Supplementary Table 2**) and in the DFA (**Supplementary Table 5**).

In summary, we showed that different rearing temperatures had a profound effect on wing shape *D. melanogaster* and minor effects were observed in *C. capitata* and *M. domestica*. Variation in rearing densities only clearly affected wing shape in *D. melanogaster*.

Sexual Dimorphism in Response to Rearing Conditions

Since the non-allometric component of shape was consistently affected by different rearing conditions (**Supplementary Tables 2**, **5**), we next asked for each species, whether a sexual dimorphism in response to different rearing temperatures and densities exists. In all three species, we did not observe significant interactions between sex and rearing conditions in our Procrustes ANOVA of size corrected shape variables (**Supplementary Table 2**). Accordingly, in *C. capitata* and *D. melanogaster* a DFA revealed very similar non-allometric shape differences between high and low temperatures (**Supplementary Figure 1** and **Supplementary Table 5**) and densities (**Supplementary Figure 2** and **Supplementary Table 5**), respectively, for both sexes. Despite insignificant interaction terms in the Procrustes ANOVA the effect of interactions between sex and rearing conditions was up to 9 times higher in *M. domestica* compared to the other two species (see sum of squares in **Supplementary Table 2**; "*_non-allometric"-sheets). Interestingly, the DFA revealed a significant effect of temperature (**Figures 6A,B**

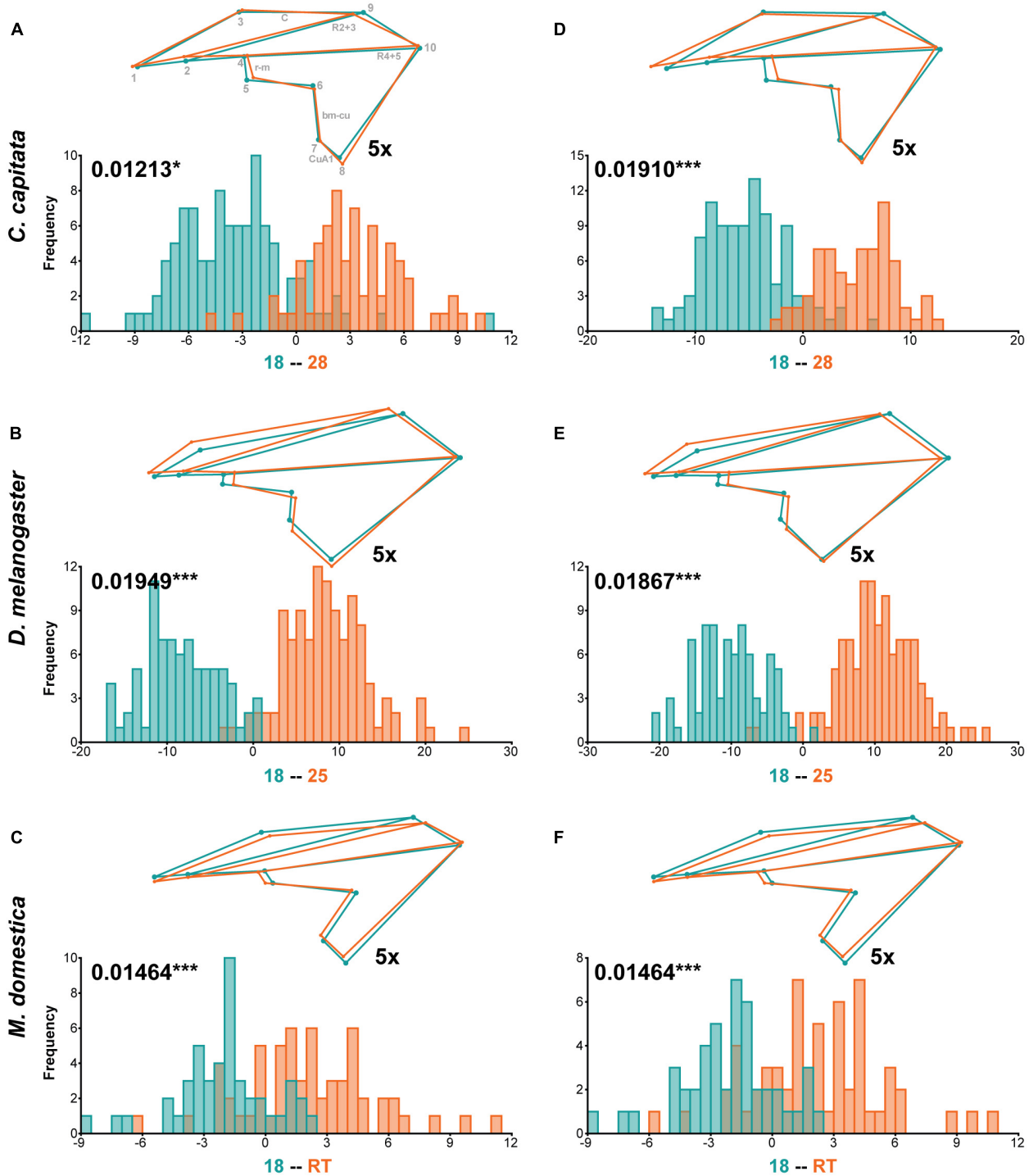

FIGURE 4 | Total and non-allometric shape differences due to different rearing temperatures. Summary of discriminant function analyses for total **(A–C)** and non-allometric **(D–F)** shape differences for flies raised at different temperatures. The wireframes represent differences between the low temperature (turquoise) and high temperature (orange) average wing shapes. The scale factor is provided next to the wireframes. The magnitude of shape variation is indicated in units of Procrustes distance with the corresponding *p*-values based on 1,000 random permutations (*$P \leq 0.05$ and ***$P \leq 0.001$). Histograms with the distributions of the discriminant scores show shape separation into two distinct groups for each species. See also **Supplementary Table 5** for details.

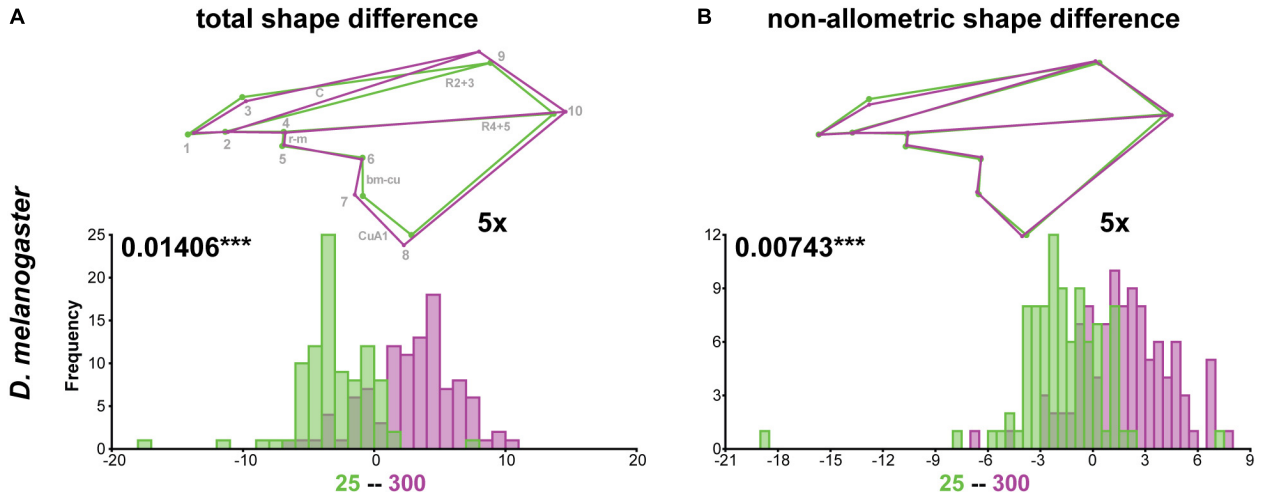

FIGURE 5 | Total and non-allometric shape differences in *D. melanogaster* due to different rearing densities. Summary of discriminant function analyses for total **(A)** and non-allometric **(B)** shape differences for flies raised at different densities. The wireframes represent differences between the low density (green) and high density (purple) average wing shapes. The scale factor is provided next to the wireframes. The magnitude of shape variation is indicated in units of Procrustes distance with the corresponding *p*-values based on 1,000 random permutations (***$P \leq 0.001$). Histograms with the distributions of the discriminant scores show shape separation into two distinct groups for each species. See also **Supplementary Table 5** for details.

and **Supplementary Table 5**) and density (**Figures 6C,D** and **Supplementary Table 5**) on non-allometric shape differences in males, while females were unaffected.

In summary, we found no evidence for a sexual dimorphism in the response to different rearing conditions in *C. capitata* and *D. melanogaster*. In contrast, we found indications for a sexual dimorphism in the non-allometric shape differences between extreme rearing temperatures and densities in *M. domestica*.

DISCUSSION

Wing morphology is thought to be a highly adaptive trait because wings facilitate basic tasks, such as finding food and mating partners (e.g., Wootton, 1992; Le Roy et al., 2019). In some insects, wings are engaged in mating behaviors. For instance, males of *D. melanogaster* and *C. capitata* generate species-specific courtship songs by fast and repetitive wing movements and females judge the size and vigor of a potential mating partner by the intensity of this buzzing (Burk and Webb, 1983; Sivinski et al., 1984; Webb et al., 1984; Churchill-Stanland et al., 1986; Partridge et al., 1987). In other fly species, such as *M. domestica*, the mating process is initiated during flight by an attack of a male against the female (i.e., mating strike). A successful mating strike usually results in the immediate landing and start of copulation (Murvosh et al., 1964). In line with these different behaviors, our interspecific PCA separated *C. capitata* and *D. melanogaster* (courtship songs) from *M. domestica* (mating strike) along PC2 that explained about 20% of the shape variation and captured differences in the ratio of wing width and wing length. Hence, the longer and narrower wings of *M. domestica* might be under selection for better flight performance (Alves and Bélo, 2002; Shyy et al., 2013), while the shorter and rounder wings of *D. melanogaster* and *C. capitata* seem to be better suited to displace more air for repeated buzzing (Burk and Webb, 1983; Webb et al., 1983; Wheeler et al., 1988; Talyn and Dowse, 2004; de Souza et al., 2015). Despite this potential link between interspecific wing shape differences and mating behavior, our data revealed that all three species were equally separated along PC1 that captured wing width along the proximal-distal axis and explained about 77% of the variation. Therefore, different mating behaviors (i.e., courtship songs vs. mating strike) are not the predominant driver for interspecific wing shape differences and many other species-specific adaptations must be at play. For instance, interspecific differences in absolute body size and shape and general flying behaviors influence selection on wing size and shape.

In the following we discuss our major findings on plasticity and sexual dimorphism in wing size and wing shape across three Diptera species with an emphasis on conserved and divergent aspects of variation in wing morphology.

Species-Specific and Conserved Aspects of Plastic Response to Different Rearing Conditions

We raised flies at different temperature and density regimes and analyzed the impact on wing size, wing shape and the relationship of both. Overall, we revealed a few common, but mostly species-specific patterns of plastic responses.

Plasticity in Response to Rearing Temperature

The most consistent results were obtained for different rearing temperatures that affected wing size in *D. melanogaster* and *C. capitata* and wing shape in all three species. The temperature impact on wing size is consistent with previous observations

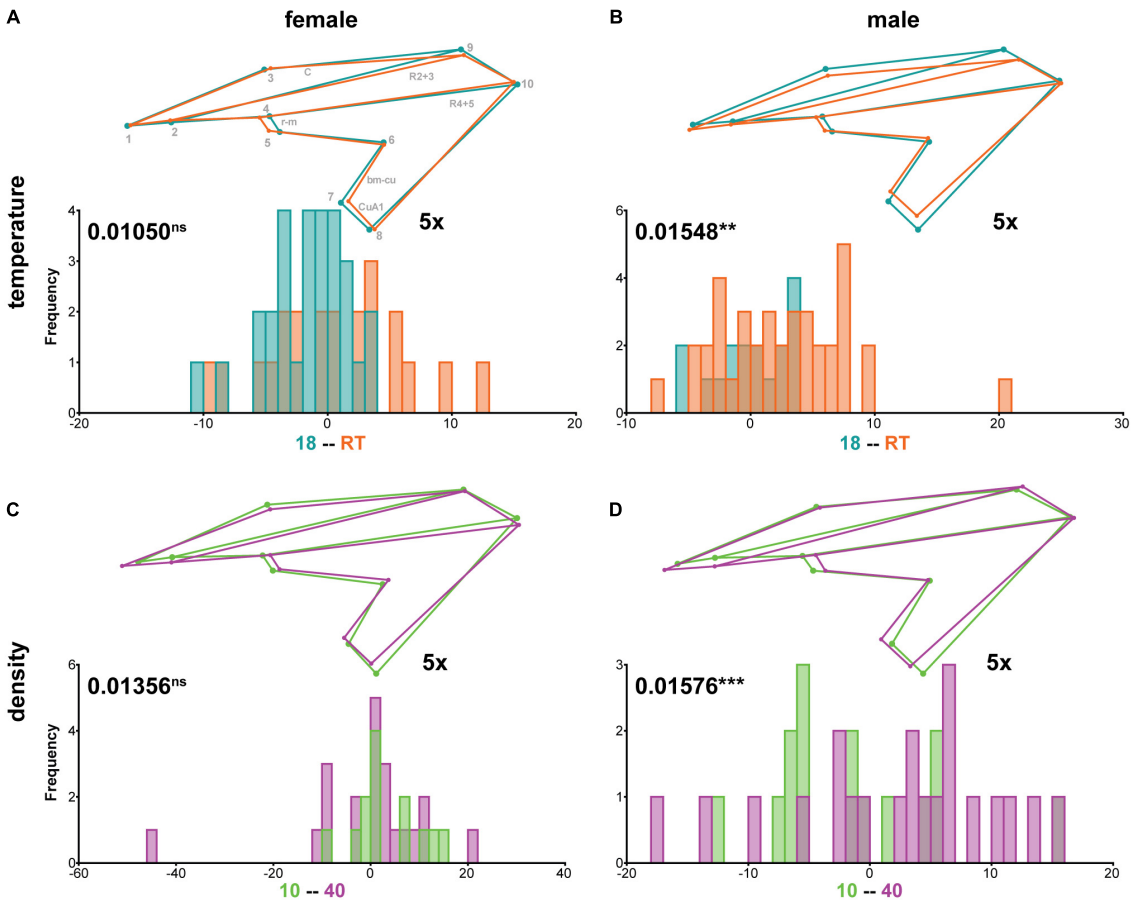

FIGURE 6 | Sex-specific non-allometric shape differences due to different rearing temperatures and densities in *M. domestica*. Summary of discriminant function analyses for non-allometric shape differences for flies raised at different temperatures **(A,B)** or densities **(C,D)**. The wireframes represent differences between the low temperature (turquoise) and high temperature (orange) **(A,B)** and the low density (green) and high density (purple) **(C,D)** average wing shapes, respectively. The scale factor is provided next to the wireframes. The magnitude of shape variation is indicated in units of Procrustes distance with the corresponding *p*-values based on 1,000 random permutations ($^{ns}P > 0.05$; $^{**}P \leq 0.01$; and $^{***}P \leq 0.001$). Histograms with the distributions of the discriminant scores show shape separation into two distinct groups for each species. See also **Supplementary Table 5** for details.

in these two species (Cavicchi et al., 1985; Partridge et al., 1994a; James et al., 1995; van't Land et al., 1999; Zwaan et al., 2000; Navarro-Campos et al., 2011) and the general trend that insects develop larger body sizes and wings in at lower temperatures (Bergmann, 1847; Ray, 1960). A previous study of natural *M. domestica* populations in South America found a positive correlation between latitude and wing size in females (Alves and Bélo, 2002). Since such latitudinal clines are often related to variable temperatures, the complete lack of association between wing size and rearing temperature in our work is a bit surprising. A potential explanation could be that the higher temperature (i.e., room temperature of 22–25°C) in our experiment could be lower than optimal for the Italian *M. domestica* strain used here (Siomava et al., 2016) and we may not have covered the entire range of optimal rearing temperatures. However, the discrepancy could also be a real biological pattern because two very different *M. domestica* populations are being compared. Support for this notion comes from an analysis of thermal plasticity in the two sepsid fly species *Sepsis fulgens* (Meigen, 1826) and *Sepsis punctum* (Fabricius, 1794) which share comparable geographic distributions and ecological niches, but still exhibited opposite clinal patterns of wing size (Rohner et al., 2019). Thermal plasticity in wing shape was most obvious in wing width since wings of flies raised at higher temperatures were generally wider in *D. melanogaster* and *C. capitata* and narrower in *M. domestica*. We detected a slightly stronger plasticity in proximal landmarks in *D. melanogaster*, which is in contrast to previous data that revealed a strong response of the distal wing region to different temperatures (Debat et al., 2003). This discrepancy could partially be due to the more moderate temperature range used in our study (18–25°C) because the lower temperature of 12–14°C used by Debat et al. (2003) is already stressful as for instance wing size variation increases at 13°C (Bubliy and Loeschcke, 2002).

Plasticity in Response to Rearing Density

Besides temperature, environmental factors related to nutrition levels and/or quality influence organ size and shape. For instance,

in the wasp *Ephedrus persicae* (Froggatt, 1904) that parasitizes aphids, wing size and shape depends on the type of host (Bogdanović et al., 2009). Different density regimes, inducing competition for nutrition levels, clearly affected wing size in all three studied species, a common trend previously observed in *D. melanogaster* (Bitner-Mathé and Klaczko, 1999; Siomava et al., 2016) and in *C. capitata* and *M. domestica* (Siomava et al., 2016). Data from *C. capitata* natural strains strongly suggests that these laboratory experiments elicit ecologically relevant plasticity because body and wing size in *C. capitata* depends on the sugar content of the host fruits on which larvae develop (Krainacker et al., 1987; Navarro-Campos et al., 2011). An association of wing shape variation with the host fruit has also been observed in this species (Pieterse et al., 2017). Since different rearing densities in our experiment reflect variable nutrient quantities with constant composition and we did not observe density related wing shape effects in *C. capitata*, the shape variation induced by different host fruits may be the result of nutrient quality rather than quantity. In contrast, the plasticity in wing shape in *D. melanogaster* observed in this work is most likely a result of nutrient quantity. It will be interesting in future controlled laboratory experiments to test how nutrient quality and quantity affect wing size and shape.

Species-Specific Scaling Relationships

We observed the most obvious differences among species with respect to allometric shape differences. Overall, we could assign about 34% of shape variation in *D. melanogaster* to variation in wing size. This trend went down to 16% and 13% in *C. capitata* and *M. domestica*, respectively. Intriguingly, our data showed that scaling relationships were uniform in *D. melanogaster* across all groups (i.e., sex, temperature and density), while very complex scaling relationships, partially with significant interaction terms, were observed for the other two species (see **Figure 3**). These complex scaling relationships may have influenced our regression approach to partition total shape variation into an allometric and a non-allometric component (Gidaszewski et al., 2009; Klingenberg, 2016). For example, in some cases we found significant differences in the non-allometric shape component despite insignificant total shape differences (e.g., compare **Figures 4A,B** for *C. capitata*). While this rather counterintuitive finding could be an artifact, we confirmed that the size correction indeed removed the effect of centroid size on wing shape variation. Moreover, a study in the *Leporinus cylindriformis* (Borodin, 1929) group of ray-finned fishes revealed that the distinction of species based on geometric morphometrics data was facilitated by the inclusion of size correction (Sidlauskas et al., 2011), suggesting that indeed relevant aspects of shape variation could be recovered. To clarify this aspect further, more accurate estimates of within-group scaling relationships are needed because the number of flies for each subgroup (i.e., a certain sex at a specific rearing temperature and density, respectively) was rather low in our nested experimental design.

The different scaling relationships among species could be caused by complex interactions between temperature and density regimes applied during our experiments as artificial thermal selection experiments in *D. melanogaster* revealed effects on resource intake and management and thus the ability to accept different resource levels (Bochdanovits and de Jong, 2003). For instance, while cold adapted flies process food resources more efficiently resulting in better larval survival when raised in low density regimes, they show lower larval survival at higher larval density (Partridge et al., 1994b, 1995). Moreover, the rearing regimes applied for *C. capitata* and *M. domestica* may have been more in the stressful range compared to *D. melanogaster*. In the latter species, increased variation in wing size has been observed at higher density (Imasheva and Bubliy, 2003) and at stressful low temperatures (13°C) (Bubliy and Loeschcke, 2002), showing that environmental factors do not only affect morphology of the individual, but also the level of interindividual phenotypic variability. Genetic factors may also play a role in defining the species-specific scaling relationships observed in our data as the interindividual genetic diversity could be different between the three species studied here. We used a highly inbred laboratory strain of *D. melanogaster* (>20 years inbreeding) and more recently collected wildtype strains of *C. capitata* and *M. domestica*, respectively. For instance, the Italian *M. domestica* strain used for our work was established as laboratory culture only 1–2 years prior to the experiments (Siomava et al., 2016). Since mutations affecting thermal plasticity in wing development have been identified in *D. melanogaster* (Debat et al., 2009), it is likely that more such mutations segregate in the more recently collected and thus less inbred species. However, more "plasticity loci" segregating in *C. capitata* and *M. domestica* cannot fully explain our observations, since this hypothesis implies that these two species should show the most pronounced plastic responses. In contrast, we found the most obvious responses of wing size and shape to different rearing conditions in *D. melanogaster*. Therefore, the species-specific scaling relationships must be caused by additional processes. While it is generally accepted that variation in organ size entails shape changes (Debat et al., 2003; Klingenberg, 2016), the level of this coupling could be variable among species. Our *D. melanogaster* data confirms previous findings in this species that processes regulating wing size and shape are highly coordinated during development (Day and Lawrence, 2000; Matamoro-Vidal et al., 2015; Testa and Dworkin, 2016), while partially different processes could be at play in the other two species.

An interesting approach to learn more about the developmental basis of coordinated size and shape regulation may be to study the cellular basis of the observed plasticity. Data in *D. melanogaster* (Zwaan et al., 2000; Klepsatel et al., 2014) and *D. subobscura* (Calboli et al., 2003) revealed that different clinal patterns of wing size variation can be caused by differences in cell number or cell size, while wing size variation induced by different temperature conditions seems to be predominantly driven by variation in cell size (reviewed in Arendt, 2007). Artificial selection for different wing shapes (i.e., rounded vs. elongated wings) in *D. melanogaster* resulted in flies with different wing shapes, but comparable wing sizes (Menezes et al., 2013; Torquato et al., 2014). Rounder wings have more cells than elongated wings, while the cell size does not seem to contribute to the differences (Torquato et al., 2014).

Intriguingly, complex interactions between environmental factors have been observed in *D. melanogaster* since wing length and cell size reacts more to changes in rearing temperature under limited food conditions, while cell number seems to be unaffected (de Moed et al., 1997). Therefore, the cellular basis of size and shape differences can be differentially shaped by various environmental factors. Overall, based on our species comparison we propose that the general capacity for plastic development and the processes affecting scaling relationships can be uncoupled and evolve independently. Future experiments testing whether plasticity in wing morphology in different insects is caused by variation in cell size or cell number will help formulating thorough developmental hypotheses.

Conserved Aspects of Plastic Shape Variation

Our shape analysis revealed a high level of variation in the positioning of the r-m (landmarks 4 and 5), R2 + 3 (landmarks 2 and 9), CuA1 (landmarks 7 and 8), and bm-cu (landmarks 6 and 7) veins in all treatment groups in all three species. These distal and posterior wing regions were also shown to be most variable across 25 *Drosophila* species (Houle et al., 2003) and between inbred strains from one *D. melanogaster* population (Matamoro-Vidal et al., 2015; Pitchers et al., 2019). Interestingly, our data showed that variation in these wing regions was predominantly caused by variation in wing size. Similar results were obtained for different *Drosophila* species as well (Cavicchi et al., 1991; Bitner-Mathé et al., 1995; Baylac and Penin, 1998; Haas and Tolley, 1998), suggesting that the development of these veins may be a hotspot for the integration of wing size variation (Cavicchi et al., 1985; Guerra et al., 1997; Pezzoli et al., 1997; Baylac and Penin, 1998). Moreover, the recurrent variation in similar wing regions implies that the development of those wing veins may be highly coordinated. It will therefore be interesting to study the cellular and molecular mechanisms underlying plasticity in wing morphology in different species to test whether the same or different developmental mechanisms are responsible for the observed patterns.

Sexual Dimorphism in Wing Morphology

In accordance with previous observations (Bitner-Mathé and Klaczko, 1999; Gilchrist et al., 2000; Gidaszewski et al., 2009; de Camargo et al., 2015; Siomava et al., 2016; Pieterse et al., 2017; Lemic et al., 2020; Rohner, 2020; Cortés-Suarez et al., 2021), we detected a clear sexual dimorphism in wing size and shape in all three species, which was most pronounced in *C. capitata*. Sexual dimorphism in wing shape is most likely functionally relevant because it is widespread in insects (Cowley et al., 1986; Pretorius, 2005; Bogdanović et al., 2009; Gidaszewski et al., 2009; Ribak et al., 2009; Allen et al., 2011; Benítez et al., 2011; de Camargo et al., 2015; Gallesi et al., 2015; Virginio et al., 2015; Lorenz et al., 2017; Rodríguez and Liria, 2017; Pajač Živković et al., 2018). In *C. capitata* and *D. melanogaster*, males and females differed mostly in wing width. Males of both species had wider wings in favor of more efficient buzzing during courtship (Burk and Webb, 1983; Webb et al., 1983; Wheeler et al., 1988; Talyn and Dowse, 2004; de Souza et al., 2015). A correlation between male wing shape and mating success has been established in *C. capitata* because males with wider wings copulated more often successfully (de Souza et al., 2015). Interestingly, males with elongated wings have a higher mating success in *D. melanogaster* (Menezes et al., 2013), showing that intra-sex variation in wing shape are caused by species-specific processes. Indeed, both species differ in the frequency and quality of their courtship song (Cowling and Burnet, 1981; Burk and Webb, 1983; Briceño et al., 2002; Rybak et al., 2002). In contrast to *C. capitata* and *D. melanogaster*, we found the most obvious sexual differences in *M. domestica* in wing length. The slightly elongated wings in males may increase flying efficiency and could be linked to the mating strike (Murvosh et al., 1964; Alves and Bélo, 2002).

Among the three studied species we observed different effects of wing size on sex-specific wing shape. Exclusion of the allometric coefficient clearly decreased the sexual shape dimorphism in *D. melanogaster*, suggesting that most of the observed shape differences could be explained by differences in wing size. In contrast, sex had only a minor effect on wing size in *C. capitata* and *M. domestica* (Siomava et al., 2016) and accordingly, the impact of the allometric component on wing shape was weak. Species-specific sexual dimorphism in scaling relationships were also observed in five schizophoran Diptera (Rohner, 2020) and in Sphingidae moths, where up to 60% of the shape variation could be explained by wing size differences (de Camargo et al., 2015). An extreme example has been observed in the aphid parasitoid *Ephedrus persicae,* where male wings are twice as large as female wings although females have generally larger body sizes. In this species, only 5% of the sexual shape differences can be explained by wing size (Bogdanović et al., 2009), suggesting that exaggerated male wing size may be more advantageous than sex-specific wing shape. All this data implies that sexual dimorphisms in wing shape scaling may reflect species-specific adaptations rather than conserved patterns across insects.

Since sexually dimorphic organs have been shown to grow disproportionally with body size in one sex in response to environmental cues (Teder and Tammaru, 2005; Bonduriansky, 2007; Lavine et al., 2015; Siomava et al., 2016), we tested for sexually dimorphic patterns of plasticity. We did not find evidence for a sexual dimorphism in the response to different rearing temperatures and densities in all three studied species. It is important to note that our experimental design is particularly limited with respect to this question because the number of individuals in each relevant group (i.e., split by sex, density and temperature) is very low and we might not have the statistical power to detect any general trends. However, our DFA implies that non-allometric shape differences between extreme rearing temperatures and densities observed in *M. domestica* may be restricted to males. This trend contradicts a previous observation in this species that showed a significant positive correlation between wing size and wing width with latitude specifically in females of different populations from South America (Alves and Bélo, 2002). This discrepancy could be explained by the use of an Italian strain in our experiments. Future experiments addressing

these specific questions should be performed to obtain more conclusive results.

CONCLUSION

In summary, our morphometric analysis of wing morphology in three Diptera species revealed various species-specific aspects of plasticity and sexual dimorphism in wing size and shape. Such analyses allow identifying interesting species to further study the developmental and genetic underpinnings of the observed wing morphology and link these to species-specific ecological and behavioral adaptations.

DATA AVAILABILITY STATEMENT

The original contributions presented in the study are included in the article/**Supplementary Material**. Raw wing images, landmark files, R scripts, and MorphoJ project files are available in an online repository (https://doi.org/10.25625/BXZHAF).

AUTHOR CONTRIBUTIONS

MR, NS, EW, and NP conceptualized the research. NS performed all fly experiments. MR and NS conducted data analysis and data visualization. NS, NP, and MR wrote the original draft. NP administered the project. All authors revised the manuscript.

FUNDING

This work has been funded by a German Academic Exchange Service (DAAD) fellowship number 91540915 to NS, Göttingen Graduate School for Neurosciences, Biophysics, and Molecular Biosciences (GGNB), and Volkswagen Foundation (project number: 85 983 to NP).

ACKNOWLEDGMENTS

We thank Y. Wu and L. Beukeboom for providing *M. domestica* flies. We also thank reviewers whose constructive suggestions improved the manuscript.

SUPPLEMENTARY MATERIAL

The Supplementary Material for this article can be found online at: https://www.frontiersin.org/articles/10.3389/fevo.2021.660546/full#supplementary-material

REFERENCES

Adams, D. C., Collyer, M. L., Kaliontzopoulou, A., and Baken, E. (2021). *Geomorph: Software for Geometric Morphometric Analyses. R Package Version 3.3.2*.

Allen, C. E., Zwaan, B. J., and Brakefield, P. M. (2011). Evolution of sexual dimorphism in the Lepidoptera. *Annu. Rev. Entomol.* 56, 445–464. doi: 10.1146/annurev-ento-120709-144828

Alves, S. M., and Bélo, M. (2002). Morphometric variations in the housefly, *Musca domestica* (L.) with latitude. *Genetica* 115, 243–251. doi: 10.1023/A:1020685727460

Alves, V. M., Moura, M. O., and de Carvalho, C. J. (2016). Wing shape is influenced by environmental variability in *Polietina orbitalis* (Stein) (Diptera: Muscidae). *Rev. Bras. Entomol.* 60, 150–156. doi: 10.1016/j.rbe.2016.02.003

Arendt, J. (2007). Ecological correlates of body size in relation to cell size and cell number: patterns in flies, fish, fruits and foliage. *Biol. Rev. Camb. Philos. Soc.* 82, 241–256. doi: 10.1111/j.1469-185X.2007.00013.x

Aytekin, S., Aytekin, A. M., and Alten, B. (2009). Effect of different larval rearing temperatures on the productivity (R o) and morphology of the malaria vector *Anopheles superpictus* Grassi (Diptera: Culicidae) using geometric morphometrics. *J. Vector Ecol.* 34, 32–42. doi: 10.1111/j.1948-7134.2009.00005.x

Bai, Y., Dong, J.-J., Guan, D.-L., Xie, J.-Y., and Xu, S.-Q. (2016). Geographic variation in wing size and shape of the grasshopper *Trilophidia annulata* (Orthoptera: Oedipodidae): morphological trait variations follow an ecogeographical rule. *Sci. Rep.* 6:32680. doi: 10.1038/srep32680

Baylac, M., and Penin, X. (1998). Wing static allometry in *Drosophila simulans* males (Diptera, Drosophilidae) and its relationships with developmental compartments. *Acta Zool. Acad. Sci. Hung.* 44, 97–112.

Benítez, H., Parra, L., Sepulveda, E., and Sanzana, M. (2011). Geometric perspectives of sexual dimorphism in the wing shape of Lepidoptera: the case of *Synneuria* sp. (Lepidoptera: Geometridae). *J. Entomol. Res. Soc.* 13, 53–60.

Bergmann, C. (1847). *Über die Verhältnisse der Wärmeökonomie der Thiere zu ihrer Grösse*. Göttingen: Göttinger Studien, Vandenhoeck & Ruprecht.

Bitner-Mathé, B. C., and Klaczko, L. B. (1999). Plasticity of *Drosophila melanogaster* wing morphology: effects of sex, temperature and density. *Genetica* 105, 203–210. doi: 10.1023/a:1003765106652

Bitner-Mathé, B. C., Peixoto, A. A., and Klaczko, L. B. (1995). Morphological variation in a natural population of *Drosophila mediopunctata*: altitudinal cline, temporal changes and influence of chromosome inversions. *Heredity* 75(Pt 1), 54–61. doi: 10.1038/hdy.1995.103

Bochdanovits, Z., and de Jong, G. (2003). Experimental evolution in *Drosophila melanogaster*: interaction of temperature and food quality selection regimes. *Evolution* 57, 1829–1836. doi: 10.1111/j.0014-3820.2003.tb00590.x

Bogdanović, A. M., Ivanović, A., Tomanović, Ž, Žikić, V., Starý, P., and Kavallieratos, N. G. (2009). Sexual dimorphism in *Ephedrus persicae* (Hymenoptera: Braconidae: Aphidiinae): intraspecific variation in size and shape. *Can. Entomol.* 141, 550–560. doi: 10.4039/n09-029

Bonduriansky, R. (2007). Sexual selection and allometry: a critical reappraisal of the evidence and ideas. *Evolution* 61, 838–849. doi: 10.1111/j.1558-5646.2007.00081.x

Bookstein, F. L. (1991). *Morphometric Tools for Landmark Data: Geometry and Biology*. Cambridge: Cambridge University Press.

Bookstein, F. L. (1996). Biometrics, biomathematics and the morphometric synthesis. *Bull. Math. Biol.* 58, 313–365. doi: 10.1007/BF02458311

Briceño, R. D., Eberhard, W. G., Vilardi, J. C., Liedo, P., and Shelly, T. E. (2002). Variation in the intermittent buzzing songs of male medflies (Diptera: Tephritidae) associated with geography, mass-rearing, and courtship success. *Fla. Entomol.* 85, 32–40. doi: 10.1653/0015-4040(2002)085[0032:vitibs]2.0.co;2

Bubliy, O. A., and Loeschcke, V. (2002). Effect of low stressful temperature on genetic variation of five quantitative traits in *Drosophila melanogaster*. *Heredity* 89, 70–75. doi: 10.1038/sj.hdy.6800104

Burk, T., and Webb, J. C. (1983). Effect of male size on calling propensity, song parameters, and mating success in Caribbean fruit flies, *Anastrepha suspensa* (Loew) (Diptera: Tephritidae). *Ann. Entomol. Soc. Am.* 76, 678–682. doi: 10.1093/aesa/76.4.678

Calboli, F. C. F., Gilchrist, G. W., and Partridge, L. (2003). Different cell size and cell number contribution in two newly established and one ancient body size

cline of *Drosophila subobscura*. *Evolution* 57, 566–573. doi: 10.1111/j.0014-3820.2003.tb01548.x

Cavicchi, S., Giorgi, G., Natali, V., and Guerra, D. (1991). Temperature-related divergence in experimental populations of *Drosophila melanogaster*. III. Fourier and centroid analysis of wing shape and relationship between shape variation and fitness. *J. Evol. Biol.* 4, 141–159.

Cavicchi, S., Guerra, D., Giorgi, G., and Pezzoli, C. (1985). Temperature-related divergence in experimental populations of *Drosophila melanogaster*. I. Genetic and developmental basis of wing size and shape variation. *Genetics* 109, 665–689. doi: 10.1093/genetics/109.4.665

Chun-Hsung, C. (2012). *Method for Breeding Musca Domestica. US 2012/0132140 A1*.

Churchill-Stanland, C., Stanland, R., Wong, T. T. Y., Tanaka, N., McInnis, D. O., and Dowell, R. V. (1986). Size as a factor in the mating propensity of Mediterranean fruit flies, *Ceratitis capitata* (Diptera: Tephritidae), in the laboratory. *J. Econ. Entomol.* 79, 614–619. doi: 10.1093/jee/79.3.614

Colless, D. H., and McAlpine, D. K. (1991). "Diptera (flies)," in *Insects of Australia*, ed. I. D. Naumann (Collingwood, VIC: CSIRO Publishing), 717–786.

Cortés-Suarez, L., Durango, Y. S., and Gómez, G. F. (2021). Sexual dimorphism in the wing geometry of *Musca domestica* L. (Diptera: Muscidae) from Colombia. *Rev. Soc. Entomol. Arg.* 80, 81–88. doi: 10.25085/rsea.800109

Cowley, D. E., Atchley, W. R., and Rutledge, J. J. (1986). Quantitative genetics of *Drosophila melanogaster*. I. Sexual dimorphism in genetic parameters for wing traits. *Genetics* 114, 549–566. doi: 10.1093/genetics/114.2.549

Cowling, D. E., and Burnet, B. (1981). Courtship songs and genetic control of their acoustic characteristics in sibling species of the *Drosophila melanogaster* subgroup. *Anim. Behav.* 29, 924–935. doi: 10.1016/S0003-3472(81)80030-9

Coyne, J. A., and Beecham, E. (1987). Heritability of two morphological characters within and among natural populations of *Drosophila melanogaster*. *Genetics* 117, 727–737. doi: 10.1093/genetics/117.4.727

Day, S. J., and Lawrence, P. A. (2000). Measuring dimensions: the regulation of size and shape. *Development* 127, 2977–2987. doi: 10.1242/dev.127.14.2977

de Camargo, W. R. F., de Camargo, N. F., Corrêa, D. C. V., de Camargo, A. J. A., and Diniz, I. R. (2015). Sexual dimorphism and allometric effects associated with the wing shape of seven moth species of Sphingidae (Lepidoptera: Bombycoidea). *J. Insect Sci.* 15, 107. doi: 10.1093/jisesa/iev083

de Moed, G. H., de Jong, G., and Scharloo, W. (1997). Environmental effects on body size variation in *Drosophila melanogaster* and its cellular basis. *Genet. Res.* 70, 35–43. doi: 10.1017/S0016672397002930

de Souza, J. M. G. A., de Lima-Filho, P. A., Molina, W. F., de Almeida, L. M., de Gouveia, M. B., de Macêdo, F. P., et al. (2015). Wing morphometry and acoustic signals in sterile and wild males: implications for mating success in *Ceratitis capitata*. *ScientificWorldJournal* 2015:526969. doi: 10.1155/2015/526969

Debat, V., Bégin, M., Legout, H., and David, J. R. (2003). Allometric and nonallometric components of *Drosophila* wing shape respond differently to developmental temperature. *Evolution* 57, 2773–2784. doi: 10.1111/j.0014-3820.2003.tb01519.x

Debat, V., Debelle, A., and Dworkin, I. (2009). Plasticity, canalization, and developmental stability of the *Drosophila* wing: joint effects of mutations and developmental temperature. *Evolution* 63, 2864–2876. doi: 10.1111/j.1558-5646.2009.00774.x

Dryden, I. L., and Mardia, V. K. (1998). *Statistical Shape Analysis*. Chichester: John Wiley & Sons Ltd.

Duyck, P. F., and Quilici, S. (2002). Survival and development of different life stages of three *Ceratitis* spp. (Diptera: Tephritidae) reared at five constant temperatures. *Bull. Entomol. Res.* 92, 461–469. doi: 10.1079/ber2002188

Gallesi, M. M., Mobili, S., Cigognini, R., Hardersen, S., and Sacchi, R. (2015). Sexual dimorphism in wings and wing bands of *Sympetrum pedemontanum* (Müller in Allioni 1776). *Zoomorphology* 134, 531–540. doi: 10.1007/s00435-015-0280-9

Gidaszewski, N. A., Baylac, M., and Klingenberg, C. P. (2009). Evolution of sexual dimorphism of wing shape in the *Drosophila melanogaster* subgroup. *BMC Evol. Biol.* 9:110. doi: 10.1186/1471-2148-9-110

Gilchrist, A. S., Azevedo, R. B. R., Partridge, L., and O'higgins, P. (2000). Adaptation and constraint in the evolution of *Drosophila melanogaster* wing shape. *Evol. Dev.* 2, 114–124. doi: 10.1046/j.1525-142x.2000.00041.x

Gilchrist, A. S., and Partridge, L. (2001). The contrasting genetic architecture of wing size and shape in *Drosophila melanogaster*. *Heredity* 86, 144–152. doi: 10.1046/j.1365-2540.2001.00779.x

Good, P. (1994). *Permutation Tests: A Practical Guide to Resampling Methods for Testing Hypotheses*. New York, NY: Springer.

Guerra, D., Pezzoli, M. C., Giorgi, G., Garoia, F., and Cavicchi, S. (1997). Developmental constraints in the *Drosophila* wing. *Heredity* 79(Pt 6), 564–571. doi: 10.1038/hdy.1997.200

Haas, H. L., and Tolley, K. A. (1998). Geographic variation of wing morphology in three Eurasian populations of the fruit fly, *Drosophila lummei*. *J. Zool.* 245, 197–203. doi: 10.1111/j.1469-7998.1998.tb00087.x

Hafez, M. (1948). A simple method for breeding the house-fly, *Musca domestica*, L., in the laboratory. *Bull. Entomol. Res.* 39:385. doi: 10.1017/S0007485300022483

Hewitt, C. G. (1914). *The House-Fly, Musca Domestica Linn.: Its Structure, Habits, Development, Relation to Disease and Control*. Cambridge: Cambridge University Press.

Hoffmann, A. A. (2010). Physiological climatic limits in *Drosophila*: patterns and implications. *J. Exp. Biol.* 213, 870–880. doi: 10.1242/jeb.037630

Hoffmann, A. A., and Shirriffs, J. (2002). Geographic variation for wing shape in *Drosophila serrata*. *Evolution* 56, 1068–1073. doi: 10.1111/j.0014-3820.2002.tb01418.x

Houle, D., Mezey, J., Galpern, P., and Carter, A. (2003). Automated measurement of *Drosophila* wings. *BMC Evol. Biol.* 3:25. doi: 10.1186/1471-2148-3-25

Imasheva, A. G., and Bubliy, O. A. (2003). Quantitative variation of four morphological traits in *Drosophila melanogaster* under larval crowding. *Hereditas* 138, 193–199. doi: 10.1034/j.1601-5223.2003.01727.x

Imasheva, A. G., Bubli, O. A., and Lazebny, O. E. (1994). Variation in wing length in Eurasian natural populations of *Drosophila melanogaster*. *Heredity* 72(Pt 5), 508–514. doi: 10.1038/hdy.1994.68

James, A. C., Azevedo, R. B., and Partridge, L. (1995). Cellular basis and developmental timing in a size cline of *Drosophila melanogaster*. *Genetics* 140, 659–666. doi: 10.1093/genetics/140.2.659

James, A. C., Azevedo, R. B., and Partridge, L. (1997). Genetic and environmental responses to temperature of *Drosophila melanogaster* from a latitudinal cline. *Genetics* 146, 881–890. doi: 10.1093/genetics/146.3.881

Keiser, I., Kobayashi, R. M., Chambers, D., and Schneider, E. L. (1973). Relation of sexual dimorphism in the wings, potential stridulation, and illumination to mating of oriental fruit flies, melon flies, and Mediterranean fruit flies in Hawaii. *Ann. Entomol. Soc. Am.* 66, 937–941. doi: 10.1093/aesa/66.5.937

Klepsatel, P., Gáliková, M., Huber, C. D., and Flatt, T. (2014). Similarities and differences in altitudinal versus latitudinal variation for morphological traits in *Drosophila melanogaster*. *Evol. Int. J. Organ. Evol.* 68, 1385–1398. doi: 10.1111/evo.12351

Klingenberg, C. P. (2011). MorphoJ: an integrated software package for geometric morphometrics. *Mol. Ecol. Resour.* 11, 353–357. doi: 10.1111/j.1755-0998.2010.02924.x

Klingenberg, C. P. (2016). Size, shape, and form: concepts of allometry in geometric morphometrics. *Dev. Genes Evol.* 226, 113–137. doi: 10.1007/s00427-016-0539-2

Krainacker, D. A., Carey, J. R., and Vargas, R. I. (1987). Effect of larval host on life history traits of the Mediterranean fruit fly, *Ceratitis capitata*. *Oecologia* 73, 583–590. doi: 10.1007/BF00379420

Lavine, L., Gotoh, H., Brent, C. S., Dworkin, I., and Emlen, D. J. (2015). Exaggerated trait growth in insects. *Annu. Rev. Entomol.* 60, 453–472. doi: 10.1146/annurev-ento-010814-021045

Le Roy, C., Debat, V., and Llaurens, V. (2019). Adaptive evolution of butterfly wing shape: from morphology to behaviour. *Biol. Rev. Camb. Philos. Soc.* 94, 1261–1281. doi: 10.1111/brv.12500

Lemic, D., Benítez, H. A., Bjeliš, M., Órdenes-Claveria, R., Ninčević, P., Mikac, K. M., et al. (2020). Agroecological effect and sexual shape dimorphism in medfly *Ceratitis capitata* (Diptera: Tephritidae) an example in Croatian populations. *Zool. Anz.* 288, 118–124. doi: 10.1016/j.jcz.2020.08.005

Lorenz, C., Almeida, F., Almeida-Lopes, F., Louise, C., Pereira, S. N., Petersen, V., et al. (2017). Geometric morphometrics in mosquitoes: what has been measured? *Infect. Genet. Evol.* 54, 205–215. doi: 10.1016/j.meegid.2017.06.029

Matamoro-Vidal, A., Salazar-Ciudad, I., and Houle, D. (2015). Making quantitative morphological variation from basic developmental processes: where are we? The case of the *Drosophila* wing. *Dev. Dyn.* 244, 1058–1073. doi: 10.1002/dvdy.24255

Menezes, B. F., Vigoder, F. M., Peixoto, A. A., Varaldi, J., and Bitner-Mathé, B. C. (2013). The influence of male wing shape on mating success in *Drosophila melanogaster*. *Anim. Behav.* 85, 1217–1223. doi: 10.1016/j.anbehav.2013.03.008

Mitteroecker, P., and Gunz, P. (2009). Advances in geometric morphometrics. *Evol. Biol.* 36, 235–247. doi: 10.1007/s11692-009-9055-x

Mitteroecker, P., Gunz, P., Windhager, S., and Schaefer, K. (2013). A brief review of shape, form, and allometry in geometric morphometrics, with applications to human facial morphology. *Hystrix Ital. J. Mammal.* 24, 59–66.

Murvosh, C. M., Fye, R. L., and Labrecque, G. C. (1964). Studies on the mating behavior of the house fly, *Musca domestica* L. *Ohio J. Sci.* 64, 264–271.

Navarro-Campos, C., Martínez-Ferrer, M. T., Campos, J. M., Fibla, J. M., Alcaide, J., Bargues, L., et al. (2011). The influence of host fruit and temperature on the body size of adult *Ceratitis capitata* (Diptera: Tephritidae) under laboratory and field conditions. *Environ. Entomol.* 40, 931–938. doi: 10.1603/EN10302

Pajač Živković, I., Lemic, D., Mešić, A., Barić, B., Órdenes, R., and Benítez, H. A. (2018). Effect of fruit host on wing morphology in *Drosophila suzukii* (Diptera: Drosophilidae): a first view using geometric morphometrics. *Entomol. Res.* 48, 262–268. doi: 10.1111/1748-5967.12278

Partridge, L., Barrie, B., Barton, N. H., Fowler, K., and French, V. (1995). Rapid laboratory evolution of adult life-history traits in *Drosophila melanogaster* in response to temperature. *Evol. Int. J. Organ. Evol.* 49, 538–544. doi: 10.1111/j.1558-5646.1995.tb02285.x

Partridge, L., Barrie, B., Fowler, K., and French, V. (1994b). Thermal evolution of pre-adult life history traits in *Drosophila melanogaster*. *J. Evol. Biol.* 7, 645–663. doi: 10.1046/j.1420-9101.1994.7060645.x

Partridge, L., Barrie, B., Fowler, K., and French, V. (1994a). Evolution and development of body size and cell size in *Drosophila melanogaster* in response to temperature. *Evol. Int. J. Organ. Evol.* 48, 1269–1276. doi: 10.1111/j.1558-5646.1994.tb05311.x

Partridge, L., Ewing, A., and Chandler, A. (1987). Male size and mating success in *Drosophila melanogaster*: the roles of male and female behaviour. *Anim. Behav.* 35, 555–562. doi: 10.1016/S0003-3472(87)80281-6

Pezzoli, M. C., Guerra, D., Giorgi, G., Garoia, F., and Cavicchi, S. (1997). Developmental constraints and wing shape variation in natural populations of *Drosophila melanogaster*. *Heredity* 79(Pt 6), 572–577. doi: 10.1038/hdy.1997.201

Pieterse, W., Benítez, H. A., and Addison, P. (2017). The use of geometric morphometric analysis to illustrate the shape change induced by different fruit hosts on the wing shape of *Bactrocera dorsalis* and *Ceratitis capitata* (Diptera: Tephritidae). *Zool. Anz. J. Comp. Zool.* 269, 110–116. doi: 10.1016/j.jcz.2017.08.004

Pitchers, W., Nye, J., Márquez, E. J., Kowalski, A., Dworkin, I., and Houle, D. (2019). A multivariate genome-wide association study of wing shape in *Drosophila melanogaster*. *Genetics* 211, 1429–1447. doi: 10.1534/genetics.118.301342

Pitchers, W., Pool, J. E., and Dworkin, I. (2013). Altitudinal clinal variation in wing size and shape in African *Drosophila melanogaster*: one cline or many? *Evol. Int. J. Organ. Evol.* 67, 438–452. doi: 10.1111/j.1558-5646.2012.01774.x

Pretorius, E. (2005). Using geometric morphometrics to investigate wing dimorphism in males and females of Hymenoptera – a case study based on the genus *Tachysphex* Kohl (Hymenoptera: Sphecidae: Larrinae). *Aust. J. Entomol.* 44, 113–121. doi: 10.1111/j.1440-6055.2005.00464.x

Ray, C. (1960). The application of Bergmann's and Allen's rules to the poikilotherms. *J. Morphol.* 106, 85–108. doi: 10.1002/jmor.1051060104

Ribak, G. A., Pitts, M. L., Wilkinson, G. S., and Swallow, J. G. (2009). Wing shape, wing size, and sexual dimorphism in eye-span in stalk-eyed flies (Diopsidae). *Biol. J. Linn. Soc.* 98, 860–871. doi: 10.1111/j.1095-8312.2009.01326.x

Rodríguez, J. N., and Liria, J. (2017). Sexual wing shape dimorphism in *Piophila casei* (Linnaeus, 1758 Diptera: Piophilidae). *Indian J. Forensic Med. Toxicol.* 11, 217–221. doi: 10.5958/0973-9130.2017.00100.1

Rohlf, F. (2015). The tps series of software. *Hystrix Ital. J. Mammal.* 26, 1–4. doi: 10.4404/hystrix-26.1-11264

Rohlf, F. J. (1990). Morphometrics. *Annu. Rev. Ecol. Syst.* 21, 299–316. doi: 10.1146/annurev.es.21.110190.001503

Rohner, P. T. (2020). Evolution of multivariate wing allometry in schizophoran flies (Diptera: Schizophora). *J. Evol. Biol.* 33, 831–841. doi: 10.1111/jeb.13613

Rohner, P. T., Roy, J., Schäfer, M. A., Blanckenhorn, W. U., and Berger, D. (2019). Does thermal plasticity align with local adaptation? An interspecific comparison of wing morphology in sepsid flies. *J. Evol. Biol.* 32, 463–475. doi: 10.1111/jeb.13429

Rybak, F., Aubin, T., Moulin, B., and Jallon, J.-M. (2002). Acoustic communication in *Drosophila melanogaster* courtship: are pulse- and sine-song frequencies important for courtship success? *Can. J. Zool.* 80, 987–996. doi: 10.1139/z02-082

Salcedo, M. K., Hoffmann, J., Donoughe, S., and Mahadevan, L. (2019). Computational analysis of size, shape and structure of insect wings. *Biol. Open* 8:bio040774. doi: 10.1242/bio.040774

Santos, M., Brites, D., and Laayouni, H. (2006). Thermal evolution of pre-adult life history traits, geometric size and shape, and developmental stability in *Drosophila subobscura*. *J. Evol. Biol.* 19, 2006–2021. doi: 10.1111/j.1420-9101.2006.01139.x

Shyy, W., Aono, H., Kang, C., and Liu, H. (2013). *An Introduction to Flapping Wing Aerodynamics*. Cambridge: Cambridge University Press.

Sidlauskas, B. L., Mol, J. H., and Vari, R. P. (2011). Dealing with allometry in linear and geometric morphometrics: a taxonomic case study in the *Leporinus cylindriformis* group (Characiformes: Anostomidae) with description of a new species from Suriname. *Zool. J. Linn. Soc.* 162, 103–130. doi: 10.1111/j.1096-3642.2010.00677.x

Siomava, N., Wimmer, E. A., and Posnien, N. (2016). Size relationships of different body parts in the three dipteran species *Drosophila melanogaster*, *Ceratitis capitata* and *Musca domestica*. *Dev. Genes Evol.* 226, 245–256. doi: 10.1007/s00427-016-0543-6

Sivinski, J., Burk, T., and Webb, J. C. (1984). Acoustic courtship signals in the Caribbean fruit fly, *Anastrepha suspensa* (Loew). *Anim. Behav.* 32, 1011–1016. doi: 10.1016/S0003-3472(84)80214-6

Slice, D. E. (2005). "Modern morphometrics," in *Modern Morphometrics in Physical Anthropology*, ed. D. E. Slice (New York, NY: Plenum Publishers), 1–45.

Talyn, B. C., and Dowse, H. B. (2004). The role of courtship song in sexual selection and species recognition by female *Drosophila melanogaster*. *Anim. Behav.* 68, 1165–1180. doi: 10.1016/j.anbehav.2003.11.023

Teder, T., and Tammaru, T. (2005). Sexual size dimorphism within species increases with body size in insects. *Oikos* 108, 321–334. doi: 10.1111/j.0030-1299.2005.13609.x

Testa, N. D., and Dworkin, I. (2016). The sex-limited effects of mutations in the EGFR and TGF-β signaling pathways on shape and size sexual dimorphism and allometry in the *Drosophila* wing. *Dev. Genes Evol.* 226, 159–171. doi: 10.1007/s00427-016-0534-7

Torquato, L. S., Mattos, D., Matta, B. P., and Bitner-Mathé, B. C. (2014). Cellular basis of morphological variation and temperature-related plasticity in *Drosophila melanogaster* strains with divergent wing shapes. *Genetica* 142, 495–505. doi: 10.1007/s10709-014-9795-0

van't Land, J., van Putten, P., Zwaan, B., Kamping, A., and van Delden, W. (1999). Latitudinal variation in wild populations of *Drosophila melanogaster*: heritabilities and reaction norms. *J. Evol. Biol.* 12, 222–232. doi: 10.1046/j.1420-9101.1999.00029.x

Virginio, F., Oliveira Vidal, P., and Suesdek, L. (2015). Wing sexual dimorphism of pathogen-vector culicids. *Parasit. Vectors* 8:159. doi: 10.1186/s13071-015-0769-6

Webb, J. C., Calkins, C. O., Chambers, D. L., Schwienbacher, W., and Russ, K. (1983). Acoustical aspects of behavior of Mediterranean fruit fly, *Ceratitis capitata*: analysis and identification of courtship sounds. *Entomol. Exp. Appl.* 33, 1–8. doi: 10.1111/j.1570-7458.1983.tb03224.x

Webb, J. C., Sivinski, J., and Litzkow, C. (1984). Acoustical behavior and sexual success in the Caribbean fruit fly, *Anastrepha suspensa* (Loew) (Diptera: Tephritidae). *Environ. Entomol.* 13, 650–656. doi: 10.1093/ee/13.3.650

Wheeler, D. A., Fields, W. L., and Hall, J. C. (1988). Spectral analysis of *Drosophila* courtship songs: *D. melanogaster*, *D. simulans*, and their interspecific hybrid. *Behav. Genet.* 18, 675–703. doi: 10.1007/BF01066850

Wilkinson, G., and Johns, P. M. (2005). "Sexual selection and the evolution of mating systems in flies," in *The Biology of the Diptera*, eds D. Yeates, and B. M. Weigmann (New York, NY: Columbia University Press), 312–339.

Wootton, R. J. (1992). Functional morphology of insect wings. *Annu. Rev. Entomol.* 37, 113–140. doi: 10.1146/annurev.en.37.010192.000553

Zwaan, B. J., Azevedo, R. B., James, A. C., van 't Land, J., and Partridge, L. (2000). Cellular basis of wing size variation in *Drosophila melanogaster*: a comparison of latitudinal clines on two continents. *Heredity* 84(Pt 3), 338–347. doi: 10.1046/j.1365-2540.2000.00677.x

Conflict of Interest: The authors declare that the research was conducted in the absence of any commercial or financial relationships that could be construed as a potential conflict of interest.

Advantages of publishing in Frontiers

OPEN ACCESS
Articles are free to read for greatest visibility and readership

FAST PUBLICATION
Around 90 days from submission to decision

HIGH QUALITY PEER-REVIEW
Rigorous, collaborative, and constructive peer-review

TRANSPARENT PEER-REVIEW
Editors and reviewers acknowledged by name on published articles

Frontiers
Avenue du Tribunal-Fédéral 34
1005 Lausanne | Switzerland

Visit us: www.frontiersin.org
Contact us: frontiersin.org/about/contact

REPRODUCIBILITY OF RESEARCH
Support open data and methods to enhance research reproducibility

DIGITAL PUBLISHING
Articles designed for optimal readership across devices

FOLLOW US
@frontiersin

IMPACT METRICS
Advanced article metrics track visibility across digital media

EXTENSIVE PROMOTION
Marketing and promotion of impactful research

LOOP RESEARCH NETWORK
Our network increases your article's readership